THE ROLE OF GENE POLYMORPHISM IN MODULATING THE IMMUNE RESPONSES AGAINST TROPICAL INFECTIOUS DISEASES

EDITED BY: Adriana Malheiro, David Courtin, Eduardo Antonio Donadi and Rajendranath Ramasawmy
PUBLISHED IN: Frontiers in Immunology and Frontiers in Cellular and Infection Microbiology

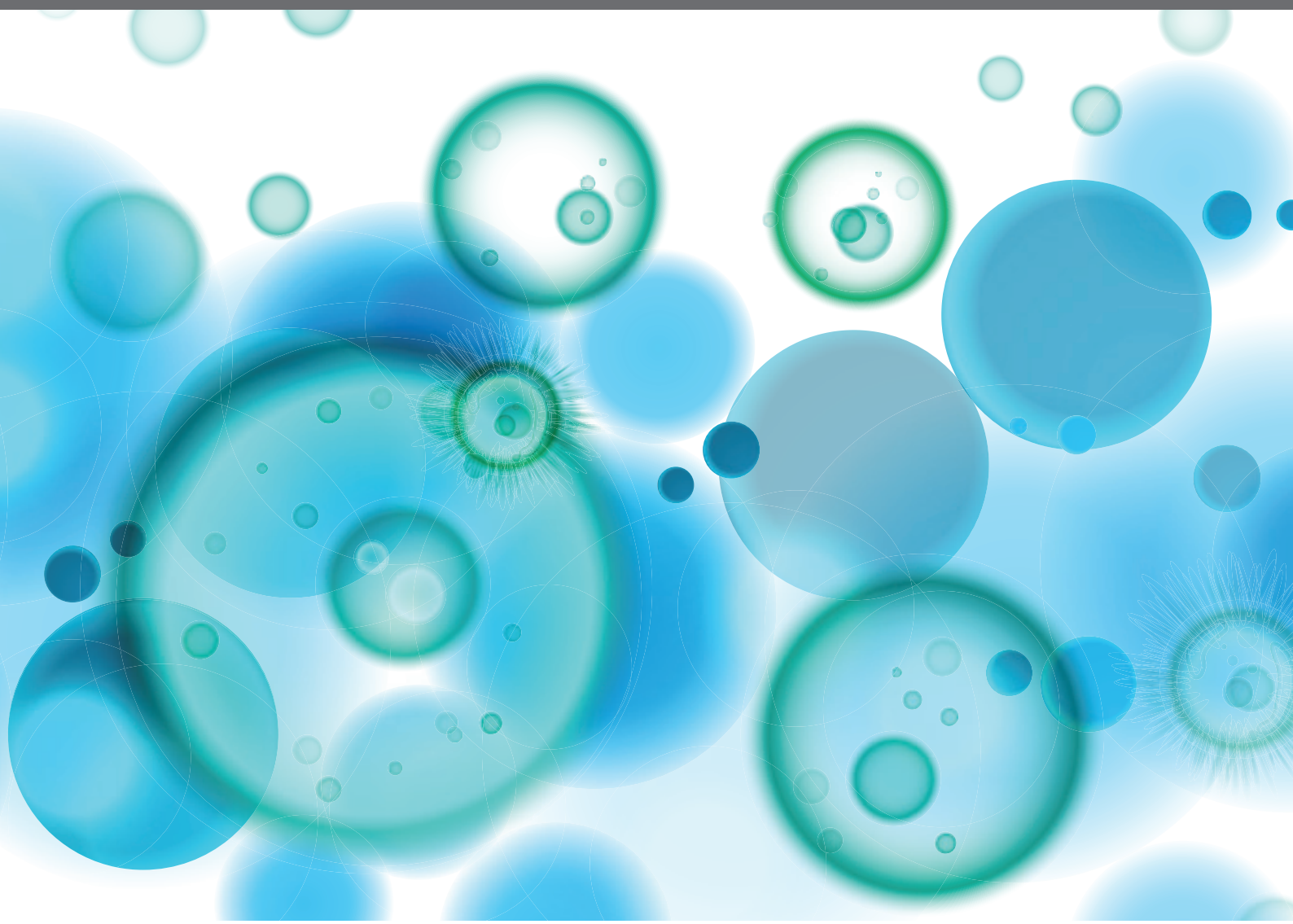

frontiers Research Topics

frontiers

ISSN 1664-8714
ISBN 978-2-88971-382-0
DOI 10.3389/978-2-88971-382-0

About Frontiers

Frontiers is more than just an open-access publisher of scholarly articles: it is a pioneering approach to the world of academia, radically improving the way scholarly research is managed. The grand vision of Frontiers is a world where all people have an equal opportunity to seek, share and generate knowledge. Frontiers provides immediate and permanent online open access to all its publications, but this alone is not enough to realize our grand goals.

Frontiers Journal Series

The Frontiers Journal Series is a multi-tier and interdisciplinary set of open-access, online journals, promising a paradigm shift from the current review, selection and dissemination processes in academic publishing. All Frontiers journals are driven by researchers for researchers; therefore, they constitute a service to the scholarly community. At the same time, the Frontiers Journal Series operates on a revolutionary invention, the tiered publishing system, initially addressing specific communities of scholars, and gradually climbing up to broader public understanding, thus serving the interests of the lay society, too.

Dedication to Quality

Each Frontiers article is a landmark of the highest quality, thanks to genuinely collaborative interactions between authors and review editors, who include some of the world's best academicians. Research must be certified by peers before entering a stream of knowledge that may eventually reach the public - and shape society; therefore, Frontiers only applies the most rigorous and unbiased reviews.
Frontiers revolutionizes research publishing by freely delivering the most outstanding research, evaluated with no bias from both the academic and social point of view. By applying the most advanced information technologies, Frontiers is catapulting scholarly publishing into a new generation.

What are Frontiers Research Topics?

Frontiers Research Topics are very popular trademarks of the Frontiers Journals Series: they are collections of at least ten articles, all centered on a particular subject. With their unique mix of varied contributions from Original Research to Review Articles, Frontiers Research Topics unify the most influential researchers, the latest key findings and historical advances in a hot research area! Find out more on how to host your own Frontiers Research Topic or contribute to one as an author by contacting the Frontiers Editorial Office: frontiersin.org/about/contact

THE ROLE OF GENE POLYMORPHISM IN MODULATING THE IMMUNE RESPONSES AGAINST TROPICAL INFECTIOUS DISEASES

Topic Editors:
Adriana Malheiro, Federal University of Amazonas, Brazil
David Courtin, Institut de Recherche Pour le Développement (IRD), France
Eduardo Antonio Donadi, University of São Paulo, Brazil
Rajendranath Ramasawmy, Universidade Nilton Lins, Brazil

Citation: Malheiro, A., Courtin, D., Donadi, E. A., Ramasawmy, R., eds. (2021). The Role of Gene Polymorphism in Modulating the Immune Responses Against Tropical Infectious Diseases. Lausanne: Frontiers Media SA. doi: 10.3389/978-2-88971-382-0

Table of Contents

05 ***Editorial: The Role of Gene Polymorphisms in Modulating the Immune Responses Against Tropical Infectious Diseases***
Adriana Malheiro, Rajendranath Ramasawmy, David Courtin and Eduardo Antonio Donadi

08 ***The* SAMHD1 *rs6029941 (A/G) Polymorphism Seems to Influence the HTLV-1 Proviral Load and IFN-Alpha Levels***
Maria Alice Freitas Queiroz, Ednelza da Silva Graça Amoras, Tuane Carolina Ferreira Moura, Carlos Araújo da Costa, Maisa Silva de Sousa, Sandra Souza Lima, Ricardo Ishak and Antonio Carlos Rosário Vallinoto

14 ***Polymorphisms in Genes Affecting Interferon-γ Production and Th1 T Cell Differentiation are Associated With Progression to Chagas Disease Cardiomyopathy***
Amanda Farage Frade-Barros, Barbara Maria Ianni, Sandrine Cabantous, Cristina Wide Pissetti, Bruno Saba, Hui Tzu Lin-Wang, Paula Buck, José Antonio Marin-Neto, André Schmidt, Fabrício Dias, Mario Hiroyuki Hirata, Marcelo Sampaio, Abílio Fragata, Alexandre Costa Pereira, Eduardo Donadi, Virmondes Rodrigues, Jorge Kalil, Christophe Chevillard and Edecio Cunha-Neto

26 ***Corrigendum: Polymorphisms in Genes Affecting Interferon-γ Production and Th1 T Cell Differentiation are Associated With Progression to Chagas Disease Cardiomyopathy***
Amanda Farage Frade-Barros, Barbara Maria Ianni, Sandrine Cabantous, Cristina Wide Pissetti, Bruno Saba, Hui Tzu Lin-Wang, Paula Buck, José Antonio Marin-Neto, André Schmidt, Fabrício Dias, Mario Hiroyuki Hirata, Marcelo Sampaio, Abílio Fragata, Alexandre Costa Pereira, Eduardo Donadi, Virmondes Rodrigues, Jorge Kalil, Christophe Chevillard and Edecio Cunha-Neto

27 ***Association of IL-10 Gene Polymorphism With IL-10 Secretion by CD4 and T Regulatory Cells in Human Leprosy***
Mohammad Tarique, Huma Naz, Chaman Saini, Mohd Suhail, Hari Shankar, Neena Khanna and Alpana Sharma

35 ***Polymorphism in the Promoter Region of the* IL18 *Gene and the Association With Severity on Paracoccidioidomycosis***
Paula Keiko Sato, Felipe Delatorre Busser, Flávia Mendes da Cunha Carvalho, Alexandra Gomes dos Santos, Aya Sadahiro, Constancia Lima Diogo, Adriana Satie Gonçalves Kono, Maria Luiza Moretti, Olinda do Carmo Luiz and Maria Aparecida Shikanai-Yasuda

46 ***Combining Host Genetics and Functional Analysis to Depict Inflammasome Contribution in Tuberculosis Susceptibility and Outcome in Endemic Areas***
Dhêmerson Souza De Lima, Caio C. B. Bomfim, Vinícius N. C. Leal, Edione C. Reis, Jaíne L. S. Soares, Fernanda P. Fernandes, Eduardo P. Amaral, Flavio V. Loures, Mauricio M. Ogusku, Maria R. D'Imperio Lima, Aya Sadahiro and Alessandra Pontillo

63 ***A Specific* IL6 *Polymorphic Genotype Modulates the Risk of* Trypanosoma cruzi *Parasitemia While* IL18*,* IL17A*, and* IL1B *Variant Profiles and HIV Infection Protect Against Cardiomyopathy in Chagas Disease***
Alexandra Gomes dos Santos, Elieser Hitoshi Watanabe, Daiane Tomomi Ferreira, Jamille Oliveira, Érika Shimoda Nakanishi, Claudia Silva Oliveira, Edimar Bocchi, Cristina Terra Gallafrio Novaes, Fatima Cruz, Noemia Barbosa Carvalho, Paula Keiko Sato, Edite Hatsumi Yamashiro-Kanashiro, Alessandra Pontillo, Vera Lucia Teixeira de Freitas, Luiz Fernando Onuchic and Maria Aparecida Shikanai-Yasuda

78 ***Structural Modeling and Molecular Dynamics of the Immune Checkpoint Molecule HLA-G***
Thais Arns, Dinler A. Antunes, Jayvee R. Abella, Maurício M. Rigo, Lydia E. Kavraki, Silvana Giuliatti and Eduardo A. Donadi

91 ***Susceptibility to* Plasmodium falciparum *Malaria: Influence of Combined Polymorphisms of IgG3 Gm Allotypes and Fc Gamma Receptors IIA, IIIA, and IIIB***
Abdou Khadre Dit Jadir Fall, Celia Dechavanne, Audrey Sabbagh, Evelyne Guitard, Jacqueline Milet, André Garcia, Jean-Michel Dugoujon, David Courtin and Florence Migot-Nabias

106 ***The Genetics of Human Schistosomiasis Infection Intensity and Liver Disease: A Review***
Estelle M. Mewamba, Oscar A. Nyangiri, Harry A. Noyes, Moses Egesa, Enock Matovu and Gustave Simo

121 **CCR5 *Promoter Polymorphisms Associated With Pulmonary Tuberculosis in a Chinese Han Population***
Shuyuan Liu, Nannan Liu, Hui Wang, Xinwen Zhang, Yufeng Yao, Shuqiong Zhang and Li Shi

131 ***Single-Nucleotide Variants in the AIM2 – Absent in Melanoma 2 Gene (rs1103577) Associated With Protection for Tuberculosis***
Mariana Brasil de Andrade Figueira, Dhêmerson Souza de Lima, Antonio Luiz Boechat, Milton Gomes do Nascimento Filho, Irineide Assumpção Antunes, Joycenéa da Silva Matsuda, Thaís Rodrigues de Albuquerque Ribeiro, Luana Sousa Felix, Ariane Senna Fonseca Gonçalves, Allyson Guimarães da Costa, Rajendranath Ramasawmy, Alessandra Pontillo, Mauricio Morishi Ogusku and Aya Sadahiro

141 ***Increased PD-1 Level in Severe Cervical Injury is Associated With the Rare Programmed Cell Death 1 (*PDCD1*) rs36084323 A Allele in a Dominant Model***
Mauro César da Silva, Fernanda Silva Medeiros, Neila Caroline Henrique da Silva, Larissa Albuquerque Paiva, Fabiana Oliveira dos Santos Gomes, Matheus Costa e Silva, Thailany Thays Gomes, Christina Alves Peixoto, Maria Carolina Valença Rygaard, Maria Luiza Bezerra Menezes, Stefan Welkovic, Eduardo Antônio Donadi and Norma Lucena-Silva

frontiers in Immunology

EDITORIAL
published: 22 July 2021
doi: 10.3389/fimmu.2021.714237

Editorial: The Role of Gene Polymorphisms in Modulating the Immune Responses Against Tropical Infectious Diseases

Adriana Malheiro[1,2]*, *Rajendranath Ramasawmy*[3,4], *David Courtin*[5] *and Eduardo Antonio Donadi*[6]

[1] Departamento de Parasitologia, Programa de Pós-graduação em Imunologia Básica e Aplicada, Universidade Federal do Amazonas, Manaus, Brazil, [2] Fundação Hospitalar de Hematologia e Hemoterapia do Amazonas, Laboratório de Genômica-Rede Regesam, Manaus, Brazil, [3] Faculdade de Medicina, Universidade Nilton Lins, Manaus, Brazil, [4] Fundacão de Medicina Tropical-Doutor Heitor Vieira Dourado, Manaus, Brazil, [5] UMR 261 MERIT, Université de Paris, Institut de Recherche pour le Développement (IRD), Paris, France, [6] Division of Clinical Immunology, Department of Medicine, Ribeirão Preto Medical School, University of São Paulo (USP), Ribeirão Preto, Brazil

Keywords: infectious diseases, HLA, immune response, gene polymorphism, tropical diseases

Editorial on the Research Topic

The Role of Gene Polymorphisms in Modulating the Immune Responses Against Tropical Infectious Diseases

OPEN ACCESS

Edited and reviewed by:
Ian Marriott,
University of North Carolina at Charlotte, United States

***Correspondence:**
Adriana Malheiro
malheiroadriana@yahoo.com.br

Specialty section:
This article was submitted to Microbial Immunology, a section of the journal Frontiers in Immunology

Received: *24 May 2021*
Accepted: *05 July 2021*
Published: *22 July 2021*

Citation:
Malheiro A, Ramasawmy R, Courtin D and Donadi EA (2021) Editorial: The Role of Gene Polymorphisms in Modulating the Immune Responses Against Tropical Infectious Diseases. Front. Immunol. 12:714237. doi: 10.3389/fimmu.2021.714237

Immune responses against pathogens can be modulated by T and B regulatory cells, surface-bound and soluble immune checkpoint molecules, neutralizing antibodies and antibody receptors, soluble mediators produced during the immune response, and intracellular molecules, among others. Immune checkpoint molecules may promiscuously inhibit several types of cells of the immune system. For example, HLA-G may inhibit the function of T, B, natural killer, and antigen presenting, cells upon ligation with specific receptors on immune cells. The description of the in *silico* structures of the membrane-bound and of the soluble HLA-G1 and G5 isoforms (shown on the cover page and in the related article) is important to understand the docking of HLA-G with its major receptors (Arns et al.). Other immune checkpoint molecules may specifically inhibit a single or a group of lymphocyte subsets after cell activation, including programmed cell death protein-1 (PD-1). Immune responses against pathogens may be further modulated by the presence of nucleotide variation in genes responsible for the immune responses. In this Research Topic, nucleotide variants in genes associated with the control of the adaptive and innate immune responses are reported in viral, bacterial, fungal, and protozoan infections.

Interaction of PD-1 (*PDCD1* gene) with its ligands (PD-L1 and PD-L2) inhibits cellular immune responses and maintains the balance between activation and tolerance. The study of the *PDCD1* -606G>A (rs36084323) promoter region polymorphism in cervical lesions caused by high-risk human papillomavirus revealed that the mutant -606A allele is associated with increased protein and gene expression, irrespective of lesion severity. Additionally, a differential *PDCD1* expression was observed according to the severity of the lesion, indicating that the virus may escape immune control by regulating PD1 (da Silva et al.).

Cytophilic IgG antibodies bind to Fc gamma receptors (FcgR) expressed at the surface of immune cells, and genetic variability at the IgG heavy chain constant region and in FcgR may

modulate the susceptibility to malaria infections. The study of the variability in the *FcgR* (*FcgRIIA*, *FcgRIIIA*, *FcgRIIIB NA1/NA2*) genes in Beninese children revealed that carriers the G3m24 single allotype and the G3m5,6,10,11,13,14,24 phenotype were independently associated with risk for malaria infection. In addition, several combinations of the *FcgRIIA, FcgRIIIA*, and *FcgRIIIB* polymorphisms and the IgG G3m allotypes were also associated with susceptibility to malaria, particularly in conditions of high intensity of exposure to mosquito bites, emphasizing the importance of cytophilic IgG1 and IgG3 isotypes in protection against *Plasmodium falciparum* malaria (Fall et al.).

Cytokine/chemokine gene diversity was evaluated in Chagas disease, paracoccidioidomycosis, leprosy, and tuberculosis. In Brazilian Chagasic patients, 35 Tag single nucleotide polymorphisms along the *IL12B*, *IL10*, *IFNG* and *IL4* cytokine genes were evaluated in patients exhibiting chronic cardiomyopathy and in asymptomatic patients. Only, the *IL12* (rs2546893G, rs919766C) and *IL10* (rs3024496C) alleles were associated with an increased risk for cardiomyopathy development (Frade-Barros et al.). Additionally, the promoter region *IL6* −174CG (rs1800795) genotype was associated with decreased risk for *Trypanosoma cruzi* detection whereas the *IL17A* −152AA (rs2275913), *IL18* −607AA (rs1946518), *IL1B* -31TC (rs1143627) genotypes and the HIV co-infection were associated with reduced risk for developing cardiomyopathy or severe cardiac dysfunction (dos Santos et al.). In Brazilian paracoccidiodomycosis patients, evaluation of cytokine and cytokine receptor genes (*IL12A, IL18* and *IFNGR1*) revealed that the *IL18* -607A allele was associated with susceptibility for the acute and chronic multifocal forms, whereas the *IL18* -607C allele was associated with protection against the unifocal chronic form (Sato et al.). The *IL10* polymorphism were studied in Indian patients presenting lepromatous leprosy. The promoter region *IL10* -819TT (rs1800871) and -1082GG (rs1800896) genotypes were overrepresented in patients, and the -819TT genotype was associated with an increased number of IL-10-producing CD4 and Treg cells, and increased skin expression of IL-10, supporting a significant role for IL-10 in disease pathogenesis (Tarique et al.).

Eight variants located in the promoter region of the chemokine receptor *CCR5* gene were investigated in Han Chinese patients infected with *Mycobacterium tuberculosis* (Mtb). The rs2734648-G at single or double doses and the rs1799987-AA genotype were associated with susceptibility to tuberculosis or pulmonary tuberculosis. Haplotype analysis of the eight variants revealed that the CCR5 rs2227010A-rs2856758A-rs2734648G-rs1799987G-rs1799988T-rs41469351C-rs1800023G-rs1800024C haplotype increased susceptibility to tuberculosis and pulmonary tuberculosis (Liu et al.). This study sheds light on the importance of CCR5 in the regulation, recruitment, and activation of macrophages. An increase in the expression of CCR5 might be detrimental and lead to the development of TB.

Considering that host innate immune genes may shape susceptibility to pathogens, inflammasome gene polymorphisms (nucleotide-binding oligomerization domain-like receptor pyrin domain containing-3 (*NLRP3)* C>G rs10754558, nucleotide-binding oligomerization domain-like receptor-CARD domain-containing protein 4 (*NLRC4)* G>C rs479333, absent in 28 melanoma 2 *(AIM2)* T>C rs1103577, Caspase-Activation and Recruitment Domain-8 (*CARD8*) T>C rs2009373, and cathepsin B (*CTSB)* A>C rs1692816) were evaluated in tuberculosis in two Brazilian studies. The gain-of-function *NLRP3* GG (rs10754558) genotype was associated with increased IL-1ß production when stimulated with Mtb compared to non-carriers, representing an important sensor for Mtb virulence, whereas the presence of at least one lost-of-function *NLRC4* C (rs479333) allele was associated with extra-pulmonary tuberculosis (De Lima et al.). The *AIM2* CC (rs1103577) genotype was associated with increased risk for pulmonary tuberculosis development, since patients carrying this genotype exhibited high levels of IL-1β. The *CTSB* gene (rs1692816) was associated with reduced risk for extra-pulmonary manifestations (Figueira et al.). These studies highlight the importance of inflammasomes in the development of TB and suggest that individuals predisposed to high levels of IL-1β production were more susceptible to the development of TB.

An innate immune retroviral restriction factor was also studied. The Sterile Alpha Motif (SAM) and Histidine-Aspartic (HD) domain-containing protein 1 (*SAMHD1)* gene is a dNTPase that prevents the synthesis of double-stranded DNA, impairing viral replication cycle and viral integration into the cell genome. The G allele of the *SAMHD1* A>G (rs6029941) 3' untranslated region (3'UTR) polymorphism was associated with a higher pro-viral load and lower levels of IFN-α in human T-cell lymphotropic virus type 1 (HTLV1) infected patients from the Brazilian Amazon area, suggesting that microRNAs may differentially target this polymorphic site (Queiroz et al.).

This study identifies individual that carry the G allele and produce low levels of IFN-α as having higher proviral load during HTLV1 infection. Furthermore, a possible influence of microRNA acting in this region may regulate the expression of the gene.

Finally, a review article, focusing on the role of genetic factors in schistosomiasis, identified several major quantitative trait *loci* (QTL), including *Schistosoma mansoni*, susceptibility/resistance region 1 (SM1) located in the region (5q31-q33) that are associated with parasite burden. This region harbors several genes of the Th2 immune response. A second QTL (SM2, 6q22-q23) was associated with the intensity of liver fibrosis. QTLs interspersed in SM1 and SM2 regions, were related to genes of the Th17 profile (Mewamba et al.). This review demonstrates the importance of the host genetic background in the controlling of the parasite.

Altogether, this series of papers describe the differential impact of nucleotide variation in genes related to the control of the innate and/or adaptive immune response against infectious diseases. Variations observed in exonic regions may modify protein function, whereas polymorphisms observed at the regulatory regions (promoter and 3'UTR) may impact gene expression. Accordingly, this series provides evidence that nucleotide variation in genes associated with the control of the immune response against tropical infectious diseases impacts

pathogen escape from the specific immune response, disease pathogenesis, and disease morbidity.

AUTHOR CONTRIBUTIONS

All authors contributed to the article and approved the submitted version. For the elaboration of the editorial paper, all contributed with the writing and revisions.

Conflict of Interest: The authors declare that the research was conducted in the absence of any commercial or financial relationships that could be construed as a potential conflict of interest.

frontiers in Cellular and Infection Microbiology

ORIGINAL RESEARCH
published: 25 May 2020
doi: 10.3389/fcimb.2020.00246

The *SAMHD1* rs6029941 (A/G) Polymorphism Seems to Influence the HTLV-1 Proviral Load and IFN-Alpha Levels

Maria Alice Freitas Queiroz[1], Ednelza da Silva Graça Amoras[1], Tuane Carolina Ferreira Moura[1], Carlos Araújo da Costa[2], Maisa Silva de Sousa[2], Sandra Souza Lima[1], Ricardo Ishak[1] and Antonio Carlos Rosário Vallinoto[1]*

[1] Laboratory of Virology, Institute of Biological Sciences, Federal University of Pará, Belém, Brazil, [2] Laboratory of Cellular and Molecular Biology, Tropical Medicine Center, Federal University of Pará, Belém, Brazil

SAMHD1, a host dNTPase, acts as a retroviral restriction factor by degrading the pool of nucleotides available for the initial reverse transcription of retroviruses, including HTLV-1. Polymorphisms in the *SAMDH1* gene may alter the enzymatic expression and influence the course of infection by the virus. The present study investigated the effect of polymorphisms on HTLV-1 infection susceptibility and on progression to disease in 108 individuals infected by HTLV-1 (47 symptomatic and 61 asymptomatic) and 100 individuals in a control group. *SAMHD1* rs6029941 (G/A) genotyping and HTLV-1 proviral load measurements were performed using real-time PCR and plasma IFN-α was measured by ELISA. Polymorphism frequency was not associated with HTLV-1 infection susceptibility or with the presence of symptoms. The proviral load was significantly higher in symptomatic individuals with the G allele ($p = 0.0143$), which presented lower levels of IFN-α ($p = 0.0383$). *SAMHD1* polymorphism is associated with increased proviral load and reduced levels of IFN-α in symptomatic patients, and may be a factor that contributes to the appearance of disease symptoms.

Keywords: HTLV-1, SAMHD1, polymorphism, IFN-α, symptomatic

OPEN ACCESS

Edited by:
Rachel L. Roper, The Brody School of Medicine at East Carolina University, United States

Reviewed by:
Alan G. Goodman, Washington State University, United States
Chloé Journo, Université de Lyon, France

****Correspondence:***
Maria Alice Freitas Queiroz
alicefarma@hotmail.com

Specialty section:
This article was submitted to Virus and Host, a section of the journal Frontiers in Cellular and Infection Microbiology

Received: *20 February 2020*
Accepted: *29 April 2020*
Published: *25 May 2020*

Citation:
Queiroz MAF, Amoras ESG, Moura TCF, da Costa CA, Sousa MS, Lima SS, Ishak R and Vallinoto ACR (2020) The SAMHD1 rs6029941 (A/G) Polymorphism Seems to Influence the HTLV-1 Proviral Load and IFN-Alpha Levels. Front. Cell. Infect. Microbiol. 10:246. doi: 10.3389/fcimb.2020.00246

INTRODUCTION

HTLV-1 is responsible for the development of HTLV-1-associated myelopathy/tropical spastic paraparesis (HAM/TSP) and adult T-cell leukemia/lymphoma (ATLL) and is associated with other inflammatory syndromes, such as rheumatoid arthritis, dermatitis, and uveitis, in addition to autoimmune diseases (Quaresma et al., 2015). However, most infected individuals do not develop symptoms, and parameters for evaluating the clinical outcome of each carrier remain undefined (Bangham et al., 2015). Therefore, several studies have investigated factors, mainly genetic factors that can elucidate the course of HTLV-1 infection in the onset of infection-related symptoms (Talledo et al., 2010; Assone et al., 2018; Vallinoto et al., 2019).

SAMHD1 is a deoxynucleotide triphosphate triphosphohydrolase (dNTPase) that acts as an intrinsic factor of retroviral restriction, degrading the pool of nucleotides available for the initial reverse transcription, limiting the replication of retroviruses, including HTLV-1 (van Montfoort et al., 2014). Blocking this step prevents the synthesis of double-stranded DNA and disrupts the later stages of the viral replication cycle, including nuclear translocation and integration of DNA into the genome of the host cell (Sze et al., 2013b).

Genetic variations in the *SAMDH1* gene may alter the expression of the enzyme and influence the course of viral infection. A polymorphism in the *SAMHD1* 3′-UTR region, rs6029941 (A/G), seems to alter enzyme expression, where the A allele is associated with higher levels of *SAMHD1* expression and the G polymorphic allele is associated with lower levels (Zhu et al., 2018). In this regard, individuals infected by HTLV-1 with reduced SAMHD1 levels may have a greater proviral load, whereas increased enzyme expression may reduce viral replication and activate a potent type I IFN response, which would enable infection control (van Montfoort et al., 2014). The aim of the present study was to evaluate the effect of the *SAMHD1* polymorphism rs6029941 (A/G) on the proviral load and the development of symptoms of HTLV-1-associated diseases.

MATERIALS AND METHODS

Study Population and Sample Collection

The present study included blood samples from 108 individuals infected with HTLV-1 (22 clinically diagnosed with HAM/TSP, 18 with rheumatic manifestations, 3 with dermatitis, 1 with uveitis, 3 with more than one diagnosis and 61 asymptomatic) treated at the Tropical Medicine Center outpatient clinic of the Federal University of Pará. The patients were of both sexes, were older than 18 years of age and had not been treated with glucocorticoids. The control group included 100 individuals at risk of infection but not infected with the HTLV-1/2, HIV-1, hepatitis B or C, *Chlamydia trachomatis* or syphilis viruses, to compare polymorphism frequencies.

A 10 mL blood sample was collected by intravenous puncture using a vacutainer system containing ethylenediaminetetraacetic acid as an anticoagulant. The samples were centrifuged and separated into plasma and a leukocyte mass. The leukocyte samples were used to extract genomic DNA for analysis of the SAMHD1 rs6029941 (A/G) polymorphism and quantification of the proviral load.

DNA Extraction

DNA was extracted from peripheral blood leukocytes using the Puregene kit (Gentra Systems, Minneapolis, MN, USA) according to the manufacturer's protocol, which included cell lysis, protein precipitation, and DNA precipitation and rehydration. DNA was quantified using a Qubit® 2.0 fluorometer (Life Technologies, Carlsbad, CA, USA) and Qubit™ DNA assay kit reagents (Life Technologies, Carlsbad, CA, USA), following the protocol recommended by the manufacturer.

Quantification of HTLV-1 Proviral Load

Proviral load was quantified using a quantitative real-time PCR using three target sequences, synthesized through the TaqMan® system (Life Technologies, Foster City, CA, USA), according to a previously described protocol (Tamegão-Lopes et al., 2006). Samples containing 5 mL of whole blood were collected for leukocyte DNA extraction, followed by relative quantification using real-time PCR. The results were subsequently adjusted for the absolute proviral quantity, based on leukocyte counts per μL, and expressed as proviral DNA copies/μL.

Genotyping of *SAMHD*1 rs6029941 (A/G)

The polymorphism, located in the UTR3′ region of the gene, was genotyped by real-time PCR using a StepOnePLUS™Real-Time PCR System. The reaction consisted of a commercial assay (C__29973868_10) containing primers and specific TaqMan® probes for amplification of the target sequence (Thermo Fisher, Carlsbad, California, USA). The reaction contained 1× MasterMix, H_2O, 20× C_11537906_20 assay buffer and 50 ng of DNA, which was subjected to the following cycling conditions: 10 min at 95°C and 40 cycles of 15 s at 95°C and 1 min at 60°C.

Quantification of Plasma IFN-α

Plasma IFN-α was measured by the enzyme-linked immunosorbent assay (ELISA) Invitrogen Human IFN alpha ELISA Kit (ThermoFisher, Carlsbad, CA, USA), which uses specific monoclonal antibodies to detect the cytokine and followed the manufacturer's instructions.

Statistical Analysis

The genotype frequencies were estimated by direct count. The allele frequency was calculated using the formula: F = 2 × number of homozygous individuals + number of heterozygous individuals/total number of individuals. The sum of the two alleles must equal 1. This is the standard form of scientific literature in the field of genetics to describe allele frequencies (the allele frequency described in the table not corresponding to "*n*" and %).

Differences between genotype frequencies observed in the investigated groups were calculated by the χ^2 (chi-square) test. The proviral load and plasma IFN-α were compared between groups using the non-parametric Kruskal-Wallis and Mann-Whitney test. All tests were performed using BioEstat 5.3 software. Associations with $p < 0.05$ were considered statistically significant.

RESULTS

The distributions of the allele and genotype frequencies of the rs6029941 (A>G) polymorphism were similar between individuals infected with HTLV-1 and the control group, with a higher frequency of the polymorphic allele (*SAMDH1**G) in individuals with the virus, but without statistical significance (**Table 1**). Among the infected individuals, no statistically significant difference was observed between the asymptomatic group and the patients with different symptom manifestations (including patients with HAM/TSP, rheumatic manifestations, dermatitis, and uveitis) (**Table 1**).

The proviral load test was performed only on 47 samples and the plasma measurement of IFN-α in 52 samples from individuals infected with HTLV-1, because not all samples were viable for these tests.

The median of proviral load was higher in individuals infected carrying the polymorphic allele (AA: 33.95, AG: 270.1 and GG: 424.2), and significant difference was observed between wild-type and polymorphic genotypes, AG and GG (**Figure 1A**; $p = 0.0100$ and $p = 0.0010$, respectively). In contrast, median IFN-α levels were lower in individuals with polymorphic genotypes

TABLE 1 | Genotype and allele frequencies of *SAMHD1* rs6029941 (A>G) polymorphism among HTLV-1 carriers and in the control group and among asymptomatic and symptomatic HTLV-1 carriers.

Genotypes and alleles	HTLV-1 *n* = 108 *n* (%)	Control *n* = 100 *n* (%)	*p***	Asymptomatic *n* = 61 *n* (%)	Symptomatic *n* = 47 *n* (%)	*p***
AA	48 (33.3)	52 (52.0)	0.3339	25 (41.0)	23 (48.9)	0.5236
AG	41 (50.0)	37 (40.0)		26 (42.6)	15 (31.9)	
GG	19 (16.7)	11 (11.0)		10 (16.4)	09 (19.2)	
*A	0.63	0.71	0.2925	0.62	0.64	0.8836
*G	0.37	0.29		0.38	0.36	

*n, number of individuals. **Chi-square test. *allele.*

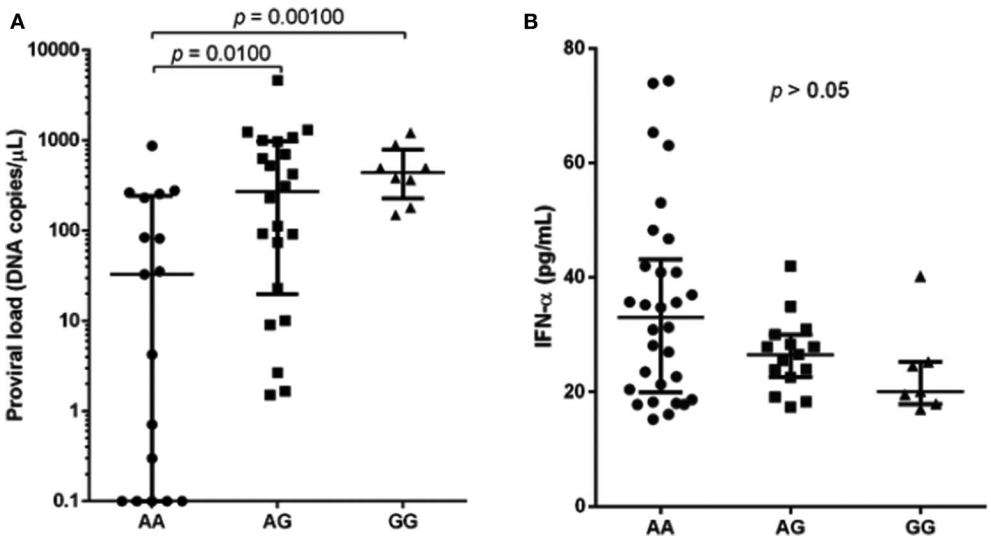

FIGURE 1 | Proviral load **(A)** and IFN-α levels **(B)** among HTLV-1 infected individuals with different genotypes for the SAMHD1 rs6029941 (A > G) polymorphism. Kruskal-Wallis test.

(AA: 33.04, AG: 26.52 and GG: 20.10) but without statistical significance (**Figure 1B**; $p = 0.1246$).

Analyzes of proviral load and IFN-alpha levels were performed among individuals with wild genotype (AA), related to greater expression of SAMHD1, compared to individuals with genotypes expressing the polymorphic allele (*G) in homo and heterozygosis (AG and GG), which are associated with reduced expression of the restriction factor. The viral load was significantly higher in symptomatic individuals with polymorphic genotypes, $p = 0.0143$ (**Figure 2A**), who had lower levels of IFN-α, $p = 0.0383$ (**Figure 2B**). Analysis of the asymptomatic group showed higher median levels of proviral load in individuals with polymorphic genotypes, although it is not statistically significant (**Figure 2C**). There was no difference in IFN-α levels (**Figure 2D**).

DISCUSSION

Restriction factors are important components of innate immunity that recognize specific patterns of retroviruses and inhibit viral replication. The main restriction factors associated with the inhibition of retroviruses include APOBEC3, TRIM5α, Tetherin, and SAMHD1 (Wilkins and Gale, 2010). The SAMHD1 enzyme restricts infection by degrading the pool of nucleotides available for viral reverse transcription. Furthermore, SAMHD1 undergoes specific conformational changes that promote signaling for the production of type I interferon and the expression of proinflammatory cytokines by the infected cell (van Montfoort et al., 2014).

In the present study, the frequency of the *SAMHD1* rs6029941 (A/G) polymorphism was not associated with infection susceptibility or with the presence of HTLV-1-related symptoms. These results may be related to the small sample size used in the study. Although the Amazon region is endemic for HTLV-2 infection, found mainly in the indigenous population (Ishak et al., 2003; Braço et al., 2019), the prevalence of HTLV-1 is low, approximately 0.9% among blood donors (Catalan-Soares et al., 2005). However, the sample size of the study corresponds to the number of patients who are attending the outpatient clinic at the Center for Tropical Medicine at the Federal University of

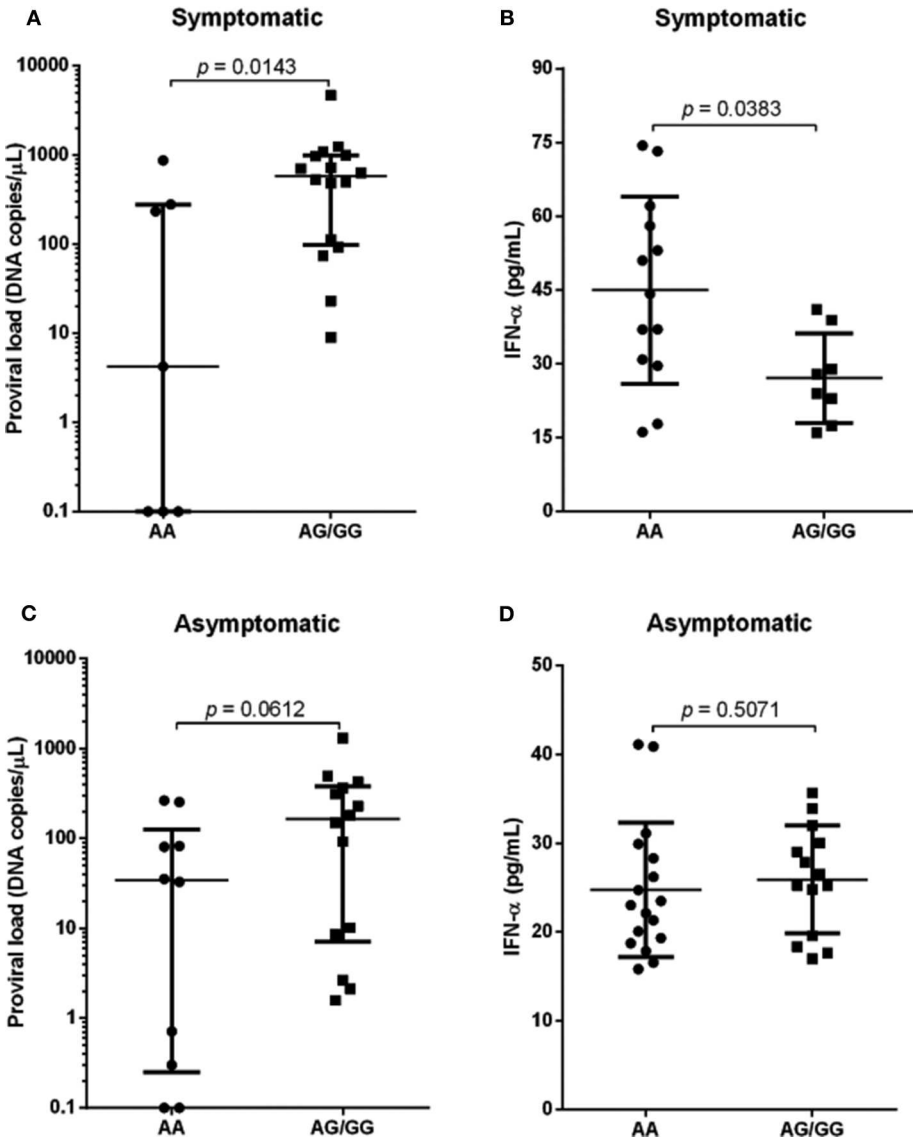

FIGURE 2 | Proviral load and IFN-α levels among individuals with different genotypes for the SAMHD1 rs6029941 (A>G) polymorphism according to the presence **(A,B)** and absence of symptoms **(C,D)**. Mann-Whitney test.

Pará, a place that monitors patients diagnosed with HTLV-1 in the city of Belém.

Another possibility of the lack of association of the frequency of *SAMHD1* rs6029941 (A/G) polymorphism with the symptoms of the diseases is that it may not be associated with the development of symptoms of all types of diseases associated with HTLV-1, because, although they are of inflammatory etiology, they activate different immunological mechanisms (Quaresma et al., 2015). Thus, these data show that frequency analysis alone is not sufficient to determine the influence of polymorphism on the development of HTLV-1 infection. To better assess this relationship, the levels of proviral load and IFN-α were analyzed, and the results showed that polymorphism could act as a possible factor that would contribute to the complex manifestations of the symptoms of the disease.

There was an association between the *SAMHD1* rs6029941 (A/G) polymorphism and variations in the HTLV-1 proviral load. The GG polymorphic genotype, related to lower enzyme levels (Zhu et al., 2018), was associated with a higher proviral load in individuals infected with HTLV-1, regardless of the presence or absence of infection-related symptoms. These results corroborate recent data indicating that this polymorphism reduces SAMHD1 gene expression (Zhu et al., 2018) because reduced SAMHD1 levels favor HTLV-1 replication, which results in an increased proviral load.

The AA genotype, which conferred greater expression of *SAMHD1*, was associated with lower levels of proviral load, which may be related to better control of HTLV-1 replication. Higher levels of SAMHD1 would restrict infection by degradation of the nucleotides pool for reverse transcription. Although

it has been demonstrated that HTLV does not appear to be affected by SAMHD1, this finding could be related to a possible escape mechanism of the virus to the restriction factor (Gramberg et al., 2013). However, Sze et al. (2013a) observed that SAMHD1 inhibited reverse transcription in monocytes infected with HTLV-1, leading to the formation of reverse transcription intermediates, responsible for inducing apoptosis and limiting infection. Although the present study did not evaluate a specific type of cells, the results suggest that the polymorphism could favor escape mechanisms of the virus against the control of the innate immune system, influencing the evolution of the infection.

Mutations in the *SAMHD1* gene may alter enzyme synthesis and result in uncontrolled inflammatory responses, mainly mediated through the increased production of type I IFN (Rice et al., 2009). Mutations in the *SAMHD1* gene are associated with an autoimmune disorder through the irregular response of type I IFN, which characterizes Aicardi-Goutières syndrome, in which there is marked production of IL-12 and TNF-α (White et al., 2017).

An important aspect that needs to be considered is the genetic background of the population analyzed in this study, which results from interethnic crossbreeding of Europeans, Indians, and Africans (Santos et al., 2009). Therefore, these preliminary data seem to suggest that the *SAMHD1* rs6029941 (A/G) polymorphism may influence HTLV-1 infection in the evaluated tri-hybrid population. However, because this is the first study that investigated the association of polymorphism in HTLV-1 infection, it will also be necessary to analyze its relationship in other different infected ethnic groups to determine its relevance in other populations.

The choice of the SAMHD1 rs6029941 polymorphism (A/G) was based on its influence on changes in gene expression and because it has not yet been evaluated for HIV and HTLV infection. Although the frequency of polymorphism is not associated with the presence of disease symptoms, it was associated with a higher proviral burden in symptomatic patients, and patients without symptoms, also had higher levels. Possibly, the polymorphism, related to the lower expression of SAMHD1, could promote less inhibition of reverse transcription, leading to the formation of few reverse transcription intermediates (RTIs) and low type I interferon production, resulting in a more productive infection, with a high proviral load (van Montfoort et al., 2014).

The findings found in the present study suggest that only *SAMHD1* rs6029941 (A/G) polymorphism is not able to induce the progression and worsening of the infection, but it would act as a factor that could increase the proviral load and contribute to the appearance of symptoms. Other studies, including the follow-up of asymptomatic patients with polymorphism, may better clarify its influence on the development of symptoms associated with HTLV-1.

In summary, the results suggest that the *SAMHD1* rs6029941 (A/G) polymorphism is associated with increased HTLV-1 proviral load and lower levels of IFN-α in symptomatic patients. Thus, the polymorphism could contribute to the development of the symptoms of the disease.

DATA AVAILABILITY STATEMENT

The datasets used and analyzed during the current study are available from the corresponding author on reasonable requests from a qualified researcher.

ETHICS STATEMENT

The studies involving human participants were reviewed and approved by the Research Ethics Committee of the Health Science Institute of the Federal University of Pará (protocol no. 2872434/2018). The patients/participants provided their written informed consent to participate in this study.

AUTHOR CONTRIBUTIONS

MQ and EA designed the study. TM, CC, and MS provided technical assistance and executed the experiments. MQ, EA, SL, and AV analyzed and interpreted the date. MQ, RI, and AV wrote the manuscript with input from all authors. All authors read and approved the final manuscript.

FUNDING

This study was funded by the National Council for Scientific and Technological Development (CNPq; #301869/2017-0), the CAPES/PRO-AMAZONIA program (23038000732/2013-09), and the Federal University of Pará (PROPESP/PAPQ 2018).

REFERENCES

Assone, T., Malta, F. M., Bakkour, S., Montalvo, L., Paiva, A. M., Smid, J., et al. (2018). Polymorphisms in HLA-C and KIR alleles are not associated with HAM/TSP risk in HTLV-1-infected subjects. *Virus Res.* 244, 71–74. doi: 10.1016/j.virusres.2017.11.010

Bangham, C. R., Araujo, A., Yamano, Y., and Taylor, G. P. (2015). HTLV-1-associated myelopathy/tropical spastic paraparesis. *Nat. Rev. Dis. Primers* 1:15012. doi: 10.1038/nrdp.2015.23

Braço, I. L. J., de Sá, K. S. G., Waqasi, M., Queiroz, M. A. F., da Silva, A. N. R., Cayres-Vallinoto, I. M. V., et al. (2019). High prevalence of human T-lymphotropic virus 2 (HTLV-2) infection in villages of the Xikrin tribe (Kayapo), Brazilian Amazon region. *BMC Infect. Dis.* 19:459. doi: 10.1186/s12879-019-4041-0

Catalan-Soares, B., Carneiro-Proietti, A. B. F., and Proietti, F. A. (2005). Interdisciplinary HTLV Research Group. Heterogeneous geographic distribution of human T-cell lymphotropic viruses I and II (HTLV-I / II): serological screening prevalence rates in blood donors from large urban areas in Brazil. *Cad. Saúde Pública* 21, 926–931. doi: 10.1590/S0102-311X2005000300027

Gramberg, T., Kahle, T., Bloch, N., Wittmann, S., Müllers, E., Daddacha, W., et al. (2013). Restriction of diverse retroviruses by SAMHD1. *Retrovirology* 10:26. doi: 10.1186/1742-4690-10-26

Ishak, V. A. C. R., Azevedo, V. N., and Guimarães Ishak, M. O. (2003). Epidemiological aspects of retrovirus (HTLV) infection among Indian populations in the Amazon Region of Brazil. *Cad. Saúde Pública* 19, 901–914. doi: 10.1590/S0102-311X2003000400013

Quaresma, J. A., Yoshikawa, G. T., Koyama, R. V., Dias, G. A., Fujihara, S., and Fuzii, H. T. (2015). HTLV-1, immune response and autoimmunity. *Viruses* 8:E5. doi: 10.3390/v8010005

Rice, G. I., Bond, J., Asipu, A., Brunette, R. L., Manfield, I. W., Carr, I. M., et al. (2009). Mutations involved in Aicardi-Goutières syndrome implicate SAMHD1 as regulator of the innate immune response. *Nat. Genet.* 41, 829–832. doi: 10.1038/ng.373

Santos, N. P., Ribeiro-Rodrigues, E. M., Ribeiro-Dos-Santos, A. K., Pereira, R., Gusmão, L., Amorim, A., et al. (2009). Assessing individual interethnic admixture and population substructure using a 48-insertion-deletion (INSEL) ancestry-informative marker (AIM) panel. *Hum. Mutat.* 31, 184–190. doi: 10.1002/humu.21159

Sze, A., Belgnaoui, S. M., Olagnier, D., Lin, R., Hiscott, J., and van Grevenynghe, J. (2013a). Host restriction factor SAMHD1 limits human T cell leukemia virus type 1 infection of monocytes via STING-mediated apoptosis. *Cell Host Microbe* 14, 422–434. doi: 10.1016/j.chom.2013.09.009

Sze, A., Olagnier, D., Lin, R., van Grevenynghe, J., and Hiscott, J. (2013b). SAMHD1 host restriction factor: a link with innate immune sensing of retrovirus infection. *J. Mol. Biol.* 425, 4981–4994. doi: 10.1016/j.jmb.2013.10.022

Talledo, M., López, G., Huyghe, J. R., Verdonck, K., Adaui, V., González, E., et al. (2010). Evaluation of host genetic and viral factors as surrogate markers for HTLV-1-associated myelopathy/tropical spastic paraparesis in Peruvian HTLV-1-infected patients. *J. Med. Virol.* 82, 460–466. doi: 10.1002/jmv.21675

Tamegão-Lopes, B. P., Rezende, P. R., Maradei-Pereira, L. M., and de Lemos, J. A. (2006). HTLV-1 and HTLV-2 proviral load: a simple method using quantitative real-time PCR. *Rev. Soc. Bras. Med. Trop.* 39, 548–552. doi: 10.1590/S0037-86822006000600007

Vallinoto, A. C. R., Cayres-Vallinoto, I., Freitas Queiroz, M. A., Ishak, M. O. G., and Ishak, R. (2019). Influence of immunogenetic biomarkers in the clinical outcome of HTLV-1 infected persons. *Viruses* 11:974. doi: 10.3390/v11110974

van Montfoort, N., Olagnier, D., and Hiscott, J. (2014). Unmasking immune sensing of retroviruses: interplay between innate sensors and host effectors. *Cytokine Growth Factor Rev.* 25, 657–668. doi: 10.1016/j.cytogfr.2014.08.006

White, T. E., Brandariz-Nuñez, A., Martinez-Lopez, A., Knowlton, C., Lenzi, G., Kim, B., et al. (2017). A SAMHD1 mutation associated with aicardi-goutières syndrome uncouples the ability of SAMHD1 to restrict HIV-1 from its ability to downmodulate type I interferon in humans. *Hum. Mutat.* 38, 658–668. doi: 10.1002/humu.23201

Wilkins, C., and Gale, M. Jr. (2010). Recognition of viruses by cytoplasmic sensors. *Curr. Opin. Immunol.* 22, 41–47. doi: 10.1016/j.coi.2009.12.003

Zhu, K. W., Chen, P., Zhang, D. Y., Yan, H., Liu, H., Cen, L. N., et al. (2018). Association of genetic polymorphisms in genes involved in Ara-C and dNTP metabolism pathway with chemosensitivity and prognosis of adult acute myeloid leukemia (AML). *J. Transl. Med.* 16:90. doi: 10.1186/s12967-018-1463-1

Conflict of Interest: The authors declare that the research was conducted in the absence of any commercial or financial relationships that could be construed as a potential conflict of interest.

frontiers in Immunology

ORIGINAL RESEARCH
published: 07 July 2020
doi: 10.3389/fimmu.2020.01386

Polymorphisms in Genes Affecting Interferon-γ Production and Th1 T Cell Differentiation Are Associated With Progression to Chagas Disease Cardiomyopathy

Amanda Farage Frade-Barros[1,2,3,4,5], Barbara Maria Ianni[1], Sandrine Cabantous[3], Cristina Wide Pissetti[6], Bruno Saba[7], Hui Tzu Lin-Wang[7], Paula Buck[1], José Antonio Marin-Neto[8], André Schmidt[8], Fabrício Dias[8], Mario Hiroyuki Hirata[9], Marcelo Sampaio[7], Abílio Fragata[7], Alexandre Costa Pereira[1], Eduardo Donadi[8], Virmondes Rodrigues[6], Jorge Kalil[1,2,5], Christophe Chevillard[10†] and Edecio Cunha-Neto[1,2,4†]*

[1] Heart Institute (InCor), University of São Paulo School of Medicine (FMUSP), São Paulo, Brazil, [2] Institute for Investigation in Immunology (iii), INCT, São Paulo, Brazil, [3] Aix-Marseille Université, INSERM, GIMP UMR_S906, Marseille, France, [4] Division of Clinical Immunology and Allergy, University of São Paulo School of Medicine, São Paulo, Brazil, [5] Bioengineering Program, Instituto Tecnológico, Universidade Brasil, São Paulo, Brazil, [6] Laboratory of Immunology, Universidade Federal Do Triângulo Mineiro (UFTM), Uberaba, Brazil, [7] Laboratório de Investigação Molecular em Cardiologia, Instituto de Cardiologia Dante Pazzanese (IDPC), São Paulo, Brazil, [8] School of Medicine of Ribeirão Preto (FMRP), University of São Paulo, Ribeirão Preto, Brazil, [9] Department of Clinical and Toxicological Analyses, Faculty of Pharmaceutical Sciences, University of São Paulo (USP), São Paulo, Brazil, [10] Aix Marseille Université, INSERM, TAGC Theories and Approaches of Genomic Complexity, UMR_1090, Marseille, France

Background: Chagas disease, caused by the protozoan *Trypanosoma cruzi*, is endemic in Latin America. Thirty percent of infected individuals develop chronic Chagas cardiomyopathy (CCC), an inflammatory dilated cardiomyopathy that is the most important clinical consequence of *T. cruzi* infection, while the others remain asymptomatic (ASY). IFN-γ and IFN-γ-producing Th1-type T cells are increased in peripheral blood and CCC myocardium as compared to ASY patients, while the Th1-antagonizing cytokine IL-10 is more expressed in ASY patients. Importantly IFN-γ-producing Th1-type T cells are the most frequent cytokine-producing T cell subset in CCC myocardium, while expression of Th1-antagonizing cytokines IL-10 and IL-4 is unaltered. The control of IFN-γ production by Th1-type T cells may be a key event for progression toward CCC. A genetic component to disease progression was suggested by the familial aggregation of cases and the association of gene polymorphisms with CCC development. We here investigate the role of gene polymorphisms (SNPs) in several genes involved in the control of IFN-γ production and Th1 T cell differentiation in CCC development.

Methods: We studied a Brazilian population including 315 CCC cases and 118 ASY subjects. We assessed 35 Tag SNPs designed to represent all the genetic information contained in the *IL12B, IL10, IFNG*, and *IL4* genes.

Results: We found 2 *IL12* SNPs (rs2546893, rs919766) and a trend of association for a *IL10* SNP (rs3024496) to be significantly associated with the ASY group. these associations were confirmed by multivariate analysis and allele tests. The rs919766C,

OPEN ACCESS

Edited by:
Paul Laszlo Bollyky, Stanford University, United States

Reviewed by:
Javier Martin, Instituto de Parasitología y Biomedicina López-Neyra (IPBLN), Spain
Clara Isabel González, Industrial University of Santander, Colombia

***Correspondence:**
Amanda Farage Frade-Barros
amanda.frade@universidadebrasil.edu.br

† These authors have contributed equally to this work

Specialty section:
This article was submitted to Microbial Immunology, a section of the journal Frontiers in Immunology

Received: *21 March 2020*
Accepted: *29 May 2020*
Published: *07 July 2020*

Citation:
Farage Frade-Barros A, Ianni BM, Cabantous S, Pissetti CW, Saba B, Lin-Wang HT, Buck P, Marin-Neto JA, Schmidt A, Dias F, Hirata MH, Sampaio M, Fragata A, Pereira AC, Donadi E, Rodrigues V, Kalil J, Chevillard C and Cunha-Neto E (2020) Polymorphisms in Genes Affecting Interferon-γ Production and Th1 T Cell Differentiation Are Associated With Progression to Chagas Disease Cardiomyopathy. Front. Immunol. 11:1386. doi: 10.3389/fimmu.2020.01386

12rs2546893G, and rs3024496C alleles were associated to an increase risk to CCC development.

Conclusions: Our data show that novel polymorphisms affecting *IL12B* and *IL10*, but not *IFNG* or *IL4* genes play a role in genetic susceptibility to CCC development. This might indicate that the increased Th1 differentiation and IFN-γ production associated with CCC is genetically controlled.

Keywords: Chagas disease, cardiomyopathy, susceptibility, IL12, IL 10, IFN, IL4

INTRODUCTION

Chagas disease (American trypanosomiasis) is caused by the protozoan *Trypanosoma cruzi* (*T. cruzi*) and mainly transmitted by the reduviid arthropod vector. It is endemic in Latin America, where an estimated 8 million people are infected (https://www.cdc.gov/parasites/chagas/index.html). Imported disease is increasingly recognized as an emerging problem in the USA and Europe due to immigration from Latin America (https://www.who.int/chagas/disease/en/). Decades after acute infection, 20–30% of the patients develop chronic Chagas disease cardiomyopathy (CCC), where heart tissue inflammation and remodeling, fibrosis, electrical and structural abnormalities often lead to life-threatening heart failure and arrhythmia (1). Five to 10% of infected individuals develop digestive disease, with denervation and dilation of the digestive tract. The remaining two-thirds of infected individuals remain asymptomatic (ASY) and free from symptomatic disease for life (2). Heart failure due to CCC has a worse prognosis, with 50% shorter survival when compared to like ischemic, idiopathic and hypertensive cardiomyopathies (3, 4). The pathogenic determinants of differential disease progression have not yet been completely elucidated.

The finding that 30% of Chagas disease patients develop CCC suggested the participation of genetics in differential disease progression. In addition, familial aggregation of CCC cases has been described (5), and a significant number of genetic polymorphisms has been associated with CCC development. A recent literature search found ca. 150 case-control genetic association studies addressing polymorphisms in 76 genes, which disclosed 62 SNPs from 44 genes to be associated with CCC, mostly related to immunology and inflammation. From those, a much smaller number of SNPs were associated with CCC severity (ventricular dysfunction) (6–8).

Many of these SNPs are related to pathogen resistance and disease tolerance genes—those related to direct control of parasitism or to reduction of tissue damage, respectively (7). Chagas disease is associated with increased production of inflammatory cytokines; IFN-γ is a major pathogen resistance gene and plays a major role in the disease; *T. cruzi* infection of mice genetically deficient of IFNG leads to uncontrolled parasitism and 100% mortality (9, 10). While it is a key player in pathogen protection, excessive levels lead to increased inflammation and tissue damage during the acute phase as well as CCC (7). During acute infection, *T. cruzi* pathogen-associated molecular patterns (PAMPs) trigger innate immunity (3, 11, 12) leading to the release of proinflammatory cytokines and chemokines, including IL-12 and IL-18, the major drivers of differentiation of IFN-γ-producing *T. cruzi*–specific Th1 T cells which migrate to sites of *T. cruzi*-induced inflammation (13, 14). IFNγ is then produced at high levels, inducing production of microbicidal and potentially tissue-damaging reactive oxygen and nitrogen species that kill intracellular *T. cruzi*. This leads to the control—but not complete elimination—of parasitism, establishing a low-grade chronic persistent infection by *T. cruzi*. On the other hand, cytokines that are able to modulate excessive IFN-γ production/Th1 T cell differentiation can modulate tissue damage in the acute phase of infection. Mice genetically deficient in disease tolerance genes IL10 (15), IL4 (16) and IL27b/Ebi3 (17), factors known to limit Th1 T cell differentiation and IFNγ production (17–20) display increased inflammation and may die early. Animals who keep a balance between inflammatory Th1 and anti-inflammatory cytokines may survive and progress to the chronic phase. As a result of persistent infection, both CCC and ASY chronic Chagas disease patients produce higher levels of IFNγ than seronegative controls (21, 22), but those who develop Chagas cardiomyopathy display a particularly strong Th1-type immune response with increased numbers of IFN-γ-producing Th1 cells in peripheral blood mononuclear cells (PBMC) (19, 20, 22, 23) and decreased IFNγ -modulating factors IL-10, IL-27b/Ebi3, and Treg cells (17–20). Accordingly, CCC patients displayed increased plasma levels of IFNγ while levels of IL-10 are reduced when compared to ASY individuals (24–26). These data suggest that the cytokine balance can modulate progression to CCC development. Indeed, CCC hearts display a prominent IFNγ -producing T-cell dependent myocarditis. IFNγ is the most highly expressed cytokine in CCC myocardium (27), and mononuclear cells producing this cytokine are abundant in CCC heart (12, 14, 22). mRNA expression IL-10 and other Th1-antagonizing cytokines and cell types (Treg and Th2) was low or undetectable in CCC heart tissue. This indicates that the Th1 infiltrate in CCC myocardium is essentially unopposed by regulatory cells or cytokines, and subject to little regulation (27). The failure to regulate Th1 responses and IFNγ production may thus be one key immune defect of patients who progress to CCC. This creates a paradox, in that IFNγ is essential for control of parasitism in acute and chronic Chagas disease, but at the same time causes tissue damage (7).

Cytokine gene polymorphisms may contribute to the control of Th1 T cell differentiation/IFN-γ production. Previous studies have assessed the association of SNPs in cytokines important for regulation of IFN-γ responses with CCC. For *IFNG*, no

SNP was found to be associated with CCC when compared to ASY after comparison for multiple testing (28). Likewise, *IL4* SNP case-control studies between CCC and ASY failed to show associations, but may have been underpowered, with only110 and 260 total Chagasic patients, respectively (29, 30). A promoter polymorphism in *IL12B* +1188 (rs3212227) was found to be associated with CCC in an Colombian population (31). The SNP IL10-1082 (rs1800896) was shown to be functional (32) and was associated to CCC in a Brazilian population comparing ASY individuals vs. CCC (33). On a Brazilian population, the frequency of the polymorphic rs1800896A allele (associated with lower expression of IL-10) was higher in the asymptomatic group than in the cardiac group. On the other hand, Florez et al. compared CCC ($n = 130$) to ASY ($n = 130$) cases in a Colombian population. Florez et al. failed to show associations in the genotypes and allele frequencies neither in *IL10* SNPs *IL10*-1082 (rs1800896) nor in the additional SNPs *IL10*-819 (rs1800871) and *IL10*-592 (rs1800872). It is possible that this lack of association in our study is was due to a small sample size or to epistasis between IL-10 and MHC.

Since the previous studies had some limitations, i.e., focused on selected polymorphisms, failed to be replicated in other populations, or lacked appropriate statistical power, we here comprehensively assessed the role of polymorphisms in these genes on CCC progression. For that matter we here performed a thorough genetic study focusing on 35 polymorphisms of *IL4, IL12B, IL10*, and *IFNG* using the Tag SNP approach, which represent all the genetic information contained in the mentioned genes, in a larger cohort ($n = 433$) of Brazilian Chagas disease patients, including CCC patients with or without ventricular dysfunction as well as asymptomatic patients. With the tag SNP approach, we could both replicate the study of previously investigated SNPs as well as novel polymorphisms. This way, we could perform a more sensitive assessment of the contribution of genetic variants in prognosis to CCC either confirming or finding additional associated SNPs in the mentioned genes. In addition, our experimental design allowed the study of possible interactions between polymorphisms in different cytokines.

METHODS

Ethical Standard

Written informed consent was obtained from all the patients, in accordance with the guidelines of the various internal review boards of all the involved institutions. The protocol was also approved by the INSERM Internal Review Board and the Brazilian National Ethics in Research Commission (CONEP). All the patients enrolled in this study were over 21 years old. Investigations were conformed to the principles outlined in the declaration of Helsinki.

Diagnostic Criteria

The diagnostic criteria for Chagas disease included the detection of antibodies against *T. cruzi* in at least two of three independent serological tests (EIA [Hemobio Chagas; Embrabio São Paulo], indirect immunofluorescence assays [IFA-immunocruzi; Biolab Merieux], and indirect hemagglutination tests [Biolab Merieux]) (34). All Chagas disease patients underwent standard electrocardiography and echocardiography. Echocardiography was performed at the hospital, with a Sequoia model 512 echocardiograph with a broad-band transducer. Left ventricular dimensions and regional and global function, including the recording of left ventricular ejection fraction (LVEF), were evaluated with a two-dimensional, M-mode approach, in accordance with the recommendations of the American Society of Echocardiography. ASY subjects had no electrocardiography and echocardiography changes. CCC patients presented typical conduction abnormalities (right bundle branch block and/or left anterior division hemiblock) (35). CCC patients with significant left ventricular systolic dysfunction (LVEF $< 40\%$) were classified as having severe CCC, whereas those with no significant ventricular dysfunction (LVEF $\geq 40\%$) were classified as having moderate CCC. We selected 40% as arbitrary cutoff value that has been previously used to define significant ventricular dysfunction by our group and others (36–38).

Study Population for Polymorphism Analysis

The CCC and ASY patients were born and raised in rural areas of Sao Paulo, Minas Gerais and Bahia states and enrolled in one of the study centers (Incor, FMUSP, FMRP, UFTM, IDPC). Patients with digestive forms were excluded of this study. Patients were classified as ASY ($n = 118$) or as having CCC ($n = 315$). ASY individuals were used as the control subjects for this study because they were from the same areas of endemicity as the patients with CCC, had encountered the parasite and had tested seropositive for T. cruzi infection, but the infection had not progressed to CCC. Here, the Case/Control ratio, which is 0.375, illustrate the difficulty to enroll real ASY subjects. For our association study, if we are fixing the significant level to 0.05, the disease prevalence to 30%, the disease allele Frequency to 0.2 and the genotype relative risk to 1.5, the expected power of our association study reaches 0.895.

Of 315 patients with CCC, 106 (42 men [39.6%] and 64 women [60.4%]) showed no significant ventricular dysfunction (LVEF $\geq 40\%$) and were thus classified as having moderate CCC, whereas 199 (144 men [72.4%] and 55 women [27.6%]) had severe ventricular dysfunction (LVEF $< 40\%$) and were classified as having severe CCC. Data for left ventricular ejection fraction were missing for 10 patients with CCC. So, when we compared moderate patients to severe patients, these 10 individuals were excluded from the analysis. Regarding progression of the ASY cases to CCC, the yearly progression rate –regardless of age group- is ca. 1–2%/year. The average age of Subjects with asymptomatic form was above 55 years. Taking into account that they were all born in endemic areas before vector transmission was interrupted, it is likely that in most if not all cases vector-borne infection occurred in early childhood. The odds that a significant number of such mature patients convert to CCC, and that this thwarts our statistical calculation is rather low; however, this is a pitfall of all cross sectional studies on diseases that display progression.

Blood Samples and DNA Preparation

For each subject, 5–15 ml of blood were collected in EDTA tubes. Genomic DNA was isolated on a silica-membrane according to the manufacturer's protocol (QIAamp DNA Blood Max Kit, Qiagen, Hilden, Germany).

SNP Selection

Tag single nucleotide polymorphisms (SNPs) were selected on the basis on Ensembl Release GRCh38 for the Caucasian and Yoruba reference populations. Tag SNPs were selected within a region extending 5 kb on either side of the candidate gene. The minor allele frequency (MAF) cut off value was arbitrarily set at 20% (so the markers characterized by a MAF <20% were excluded from the analysis by lack of power). In each reference population, the markers with MAF > 20% are included in different blocks of correlation (based on the r^2 values). For each correlation block in the gene, one marker was selected and considered as a Tag SNP. Indeed, markers located in the same block of correlation yielded the same genetic information in association studies. Tag SNPs characterized by a MAF over 20% on at least one reference population were selected. These Tag SNPs were thus defined to gather all the genetic information from each candidate gene. we selected a total of 35 Tag SNPs: sixteen tag SNPs for *IL12B*, six tag SNPs for *IL10*, six for *IFNG* and seven tag SNPs for *IL4*.

SNP Genotyping

Most of the genotyping was done with the Golden Gate genotyping assay (Illumina, San Diego, USA). In some cases, genotyping assays were performed with the *Taq*Man system (Applied Biosystems, Foster City, USA) according to the manufacturer's instructions. Genotyes are available on request.

Statistical Analysis

SPSS Statistics software v. 17.0 (IBM, Armonk, USA) was used for statistical analyses. We performed stepwise binary logistic regression analysis on the whole population, to analyse the relationship between the probability of an individual to develop chronic Chagas cardiomyopathy and the main covariates (sex and polymorphisms). Sex was considered as a binary covariate. In our stepwise binary logistic regression analysis, genotypes were considered as binary covariates. Indeed, for each polymorphism we had two alleles (A frequent one; a rare one). So, we obtained three genotypes (AA, Aa, and aa). In our stepwise binary logistic regression analysis, genotypes were considered as binary covariates. So, we performed three different analyses (Analysis 1: AA vs. Aa + aa (we supposed that the a allele is dominant); Analysis 2: AA + aa vs. Aa (we supposed that the heterozygote carriers are different from the homozygote ones); Analysis 3: AA + Aa vs. aa (we supposed that the A allele is dominant).

In multivariate analyses, several polymorphisms and gender were included as covariates. All the covariates are analyzed in the same time. In a stepwise approach, the worse associated covariate (non-significant) is removed and the analysis is run again up to keep only significant associated covariates.

An investigation of a candidate gene should test many SNPs individually for association. However, such multiple testing will increase the false-positive (type I error) rate under nominal significance thresholds ($\alpha = 0.05$). So, we applied the Holm-Bonferroni sequential correction for multiple testing (39).

RESULTS

We conducted a study focusing on the *IL12B, IL10, IFNG*, and *IL4* genes. 35 Tag SNPs were selected (**Supplementary Table 1**). 97.8% markers were genotyped successfully on our cohort including ASY subjects ($n = 118$) and CCC patients ($n = 315$). The genotype distribution of each SNP is summarized in **Supplementary Table 2**. All the SNPs were in Hardy-Weinberg equilibrium on the ASY individuals considered as control subjects. Of the 118 ASY subjects, 45.3% were male, whereas in the CCC patients group, this percentage reaches 61.3%. The difference in sex distribution between the groups was significant ($p = 1.21E-4$; OR = 2.126; 95%CI: 1.450–3.12). It is well-known that male patients infected with T. cruzi have a higher risk of progression to CCC than female patients. Of 315 patients with CCC, 106 (42 men [39.6%] and 64 women [60.4%]) showed no significant ventricular dysfunction and were thus classified as having moderate CCC, whereas 199 (144 men [72.4%] and 55 women [27.6%]) had severe ventricular dysfunction and were classified as having severe CCC.

Polymorphisms rs2546893G/A, rs919766A/C in and Around the *IL12B* Gene Are Associated to an Increased Risk of CCC

Fourteen on sixteen tag SNPs for the IL12B gene were genotyped successfully. *IL-12B* genotype data are shown in **Tables 1**, **2**. All these markers are located in intronic region of IL12B gene. In the CCC subjects group, 269 (86.8%) subjects carried the rs2546893G/G or G/A genotypes whereas 79 (73.8%) of the ASY carried these genotypes ($p = 0.002$; OR = 1.548; 95%CI: 1.176–2.037 (see **Table 1**). These data suggest that rs2546893G/G or G/A genotypes are associated to an increased susceptibility to CCC.

For the rs919766A/C polymorphism, 107 (34.7%) CCC subjects carried the C/C or A/C genotypes vs. 17 (15.9%) for the ASY group ($p = 0.001$; OR = 1.653; 95%CI: 1.241–2.198). For the rs1003199C/T polymorphism, 276 (88.7%) CCC subjects carried the C/C or C/T genotypes vs. 285 (78.7%) for the ASY group. This difference was significant ($p = 0.005$; OR = 1.522; 95%CI: 1.134–2.045). For the rs11574790C/T polymorphism, 95 (30.5%) CCC subjects carried the C/T or T/T genotypes vs. 17 (15.7%) for the ASY group ($p = 0.006$; OR = 1.497; 95%CI: 1.124–1.996). For the rs2569253T/C polymorphism, 256 (87.46%) CCC subjects carried the T/T or T/C genotypes vs. 81 (79.4%) for the ASY ($p = 0.039$; OR = 1.371; 95%CI: 1.015–1.852). After performing a correction for multiple testing using the Bonferroni methods, the two main polymorphisms (rs919766 and rs25466893) remain significant (corrected *p*-values were 0.014 and 0.026, respectively).

In a multivariate analysis, including these five polymorphisms and gender as covariates, the gender ($p = 0.004$; OR = 2.036; 95% CI: 1.249–3.318) and two markers (rs2546893: $p = 0.005$;

TABLE 1 | Association studies between CCC and ASY including as covariates the gender and the polymorphisms (genotype associations and allelic tests).

GENE	Tag SNP	Genotype groups	Association test
IL12B	rs2546890	GG vs. GA + AA	$p = 0.103$; OR = 1.231; 95%CI: 0.959–1.579
		MAF	ASY MAF(A) = 46.6%; CCC MAF(A) = 40.9%
		Allelic test	Chi-square = 2.11 and $p = 0.15$
	rs730691	GG vs. GA	$p = 0.441$; OR = 1.274; 95%CI: 0.688–2.358
		MAF	ASY MAF(A) = 9.1%; CCC MAF(A) = 11.1%
		Allelic test	Chi-square = 0.56 and $p = 0.46$
	rs2546893	GG + GA vs. AA	$p = 0.002$; OR = 1.548; 95%CI: 1.176–2.037
		MAF	ASY MAF(A) = 45.8%; CCC MAF(A) = 35.0%
		Allelic test	Chi-square = 7.89 and $p = 0.005$
	rs1003199	CC + CT vs. TT	$p = 0.005$; OR = 1.522; 95%CI: 1.134–2.045
		MAF	ASY MAF(T) = 43.1%; CCC MAF(T) = 35.9%
		Allelic test	Chi-square = 3.54 and $p = 0.06$
	rs3181216	TT vs. TA + AA	$p = 0.702$; OR = 1.047; 95%CI: 0.829–1.321
		MAF	ASY MAF(A) = 21.6%; CCC MAF(A) = 21.8%
		Allelic test	Chi-square = 0.001 and $p = 0.97$
	rs2569253	TT + TC vs. CC	$p = 0.039$; OR = 1.371; 95%CI: 1.015–1.852
		MAF	ASY MAF(C) = 40.7%; CCC MAF(C) = 35.3%
		Allelic test	Chi-square = 1.87 and $p = 0.17$
	rs2853694	AA vs. AC + CC	$p = 0.382$; OR = 1.105; 95%CI: 0.884–1.381
		MAF	ASY MAF(C) = 34.7%; CCC MAF(C) = 32.7%
		Allelic test	Chi-square = 0.28 and $p = 0.60$
	rs919766	AA vs. AC + CC	$p = 0.001$; OR = 1.653; 95%CI: 1.241–2.198
		MAF	ASY MAF(C) = 8.9%; CCC MAF(C) = 19.3%
		Allelic test	Chi-square = 36.67 and $p < 0.00001$
	rs2853696	GG vs. GA + AA	$p = 0.981$; OR = 1.003; 95%CI: 0.759–1.328
		MAF	ASY MAF(A) = 10.6%; CCC MAF(A) = 10.6%
		Allelic test	Chi-square = 0.002 and $p = 0.097$
	rs11574790	CC vs. CT + TT	$p = 0.006$; OR = 1.497; 95%CI: 1.124–1.996
		MAF	ASY MAF(T) = 8.3%; CCC MAF(T) = 16.6%
		Allelic test	Chi-square = 8.78 and $p = 0.03$
	rs3212227	AA vs. AC + CC	$p = 0.973$; OR = 1.004; 95%CI: 0.803–1.254
		MAF	ASY MAF(C) = 31.1%; CCC MAF(C) = 31.0%
		Allelic test	Chi-square = 0.001 and $p = 0.97$
	rs1368439	TT vs. TG + GG	$p = 0.735$; OR = 1.048; 95%CI: 0.800–1.373
		MAF	ASY MAF(G) = 11.2%; CCC MAF(G) = 10.5%
		Allelic test	Chi-square = 0.073 and $p = 0.79$
	rs6870828	AA vs. AG + GG	$p = 0.754$; OR = 1.040; 95%CI: 0.814–1.328
		MAF	ASY MAF(G) = 39.4%; CCC MAF(G) = 40.6%
		Allelic test	Chi-square = 0.086 and $p = 0.77$
	rs6859018	CC vs. CT + TT	$p = 0.603$; OR = 1.093; 95%CI: 0.782–1.527
		MAF	ASY MAF(T) = 33.0%; CCC MAF(T) = 32.5%
		Allelic test	Chi-square = 0.018 and $p = 0.89$
IL10	rs1800890	TT vs. TA + AA	$p = 0.636$; OR = 1.055; 95%CI: 0.845–1.318
		MAF	ASY MAF(A) = 26.4%; CCC MAF(A) = 24.7%
		Allelic test	Chi-square = 0.25 and $p = 0.62$
	rs1800896	AA + AG vs. GG	$p = 0.013$; OR = 1.527; 95%CI: 1.092–2.137
		MAF	ASY MAF(G) = 36.9%; CCC MAF(G) = 32.7%
		Allelic test	Chi-square = 1.24 and $p = 0.27$
	rs1800871	CC + TT vs. CT	$p = 0.059$; OR = 1.246; 95%CI: 0.992–1.566
		MAF	ASY MAF(T) = 35.3%; CCC MAF(T) = 35.3%
		Allelic test	Chi-square = 0.0001 and $p = 0.99$

(Continued)

TABLE 1 | Continued

GENE	Tag SNP	Genotype groups	Association test
	rs1518111	GG + AA vs. GA	$p = 0.104$; OR = 1.208; 95%CI: 0.962–1.516
		MAF	ASY MAF(A) = 32.4%; CCC MAF(A) = 34.2%
		Allelic test	Chi-square = 0.24 and $p = 0.62$
	rs3024496	TT + TC vs. CC	$p = 0.031$; OR = 1.437; 95%CI: 1.033–2.000
		MAF	ASY MAF(C) = 40.3%; CCC MAF(C) = 35.0%
		Allelic test	Chi-square = 1.89 and $p = 0.17$
	rs6673928	CC vs. CA	$p = 0.329$; OR = 2.141; 95%CI: 0.464–9.885
		MAF	ASY MAF(A) = 1.3%; CCC MAF(A) = 0.6%
		Allelic test	Chi-square = 0.95 and $p = 0.33$
IFNG	rs2069705	TT vs. TC + CC	$p = 0.337$; OR = 1.12; 95%CI: 0.89–1.41
		MAF	ASY MAF(C) = 39.6%; CCC MAF(C) = 37.9%
		Allelic test	Chi-square = 0.20 and $p = 0.66$
	rs1861494	AA vs. AG + GG	$p = 0.057$; OR = 1.24; 95%CI: 0.99–1.55
		MAF	ASY MAF(G) = 24.3%; CCC MAF(G) = 18.8%
		Allelic test	Chi-square = 3.21 and $p = 0.07$
	rs2069718	CC + CT vs. TT	$p = 0.183$; OR = 1.18; 95%CI: 0.92–1.52
		MAF	ASY MAF(C) = 48.2%; CCC MAF(C) = 52.4%
		Allelic test	Chi-square = 1.16 and $p = 0.28$
	rs2069727	AA + AG vs. GG	$p = 0.232$; OR = 1.22; 95%CI: 0.88–1.70
		MAF	ASY MAF(G) = 36.4%; CCC MAF(G) = 38.9%
		Allelic test	Chi-square = 0.45 and $p = 0.50$
	rs3181035	GG vs. GA + AA	$p = 0.371$; OR = 1.12; 95%CI: 0.88–1.42
		MAF	ASY MAF(A) = 17.0%; CCC MAF(A) = 13.7%
		Allelic test	Chi-square = 1.38 and $p = 0.24$
IL4	rs2070874	CC vs. CT + TT	$p = 0.481$; OR = 1.08; 95%CI: 0.87–1.34
		MAF	ASY MAF(T) = 27.0%; CCC MAF(T) = 27.9%
		Allelic test	Chi-square = 0.07 and $p = 0.79$
	rs2227284	AA + AC vs. CC	$p = 0.268$; OR = 1.15; 95%CI: 0.90–1.46
		MAF	ASY MAF(C) = 53.2%; CCC MAF(C) = 48.2%
		Allelic test	Chi-square = 1.62 and $p = 0.20$
	rs2243261	GG vs. GT + TT	$p = 0.651$; OR = 1.10; 95%CI: 0.74–1.63
		MAF	ASY MAF(T) = 3.8%; CCC MAF(T) = 4.6%
		Allelic test	Chi-square = 0.26 and $p = 0.61$
	rs2243268	AA vs. AC + CC	$p = 0.467$; OR = 1.08; 95%CI: 0.86–1.38
		MAF	ASY MAF(C) = 20.0%; CCC MAF(C) = 21.2%
		Allelic test	Chi-square = 0.15 and $p = 0.70$
	rs2243274	GG + GA vs. AA	$p = 0.423$; OR = 1.15; 95%CI: 0.82–1.60
		MAF	ASY MAF(A) = 31.2%; CCC MAF(A) = 35.8%
		Allelic test	Chi-square = 1.53 and $p = 0.22$
	rs2243290	CC + CA vs. AA	$p = 0.352$; OR = 1.21; 95%CI: 0.81–1.82
		MAF	ASY MAF(A) = 23.7%; CCC MAF(A) = 24.8%
		Allelic test	Chi-square = 0.12 and $p = 0.73$
	rs2406539	AA vs. AT + TT	$p = 0.570$; OR = 1.19; 95%CI: 0.65–2.17
		MAF	ASY MAF(T) = 7.5%; CCC MAF(T) = 9.2%
		Allelic test	Chi-square = 0.60 and $p = 0.44$

MAF, Minor Allelic frequency.

OR = 1.536; 95% CI: 1.139–2.070; rs919766: $p = 0.014$; OR = 1.477; 95% CI: 1.081–2.020) remained significantly associated. The three other markers were excluded from the best model. Allelic tests confirmed the association of these two IL12 markers. The rs919766C allele ($p < 0.00001$) and the rs2546893G allele ($p = 0.005$) were associated to an increase risk to CCC development.

The same analysis was performed between the ASY subjects and severe CCC patients. The same polymorphisms were

TABLE 2 | Association studies between CCC with a left ventricular ejection fraction value under 0.4% and ASY including as covariates the gender and the polymorphism one by one.

GENE	Tag SNP		Association tests
IL12B	rs2546890	GG vs. GA + AA	$p = 0.121$; OR = 1.23; 95%CI: 0.95–1.61
		MAF	ASY MAF(A) = 46.6%; SEV CCC MAF(A) = 378%
		Allelic test	Chi-square = 4.30 and $p = 0.04$
	rs730691	GG vs. GA	$p = 0.407$; OR = 1.33; 95%CI: 0.68–2.58
		MAF	ASY MAF(A) = 9.1%; SEV CCC MAF(A) = 12.0%
		Allelic test	Chi-square = 0.91 and $p = 0.34$
	rs2546893	GG + GA vs. AA	$p = 0.001$; OR = 1.69; 95%CI: 1.23–2.34
		MAF	ASY MAF(A) = 45.8%; SEV CCC MAF(A) = 32.8%
		Allelic test	Chi-square = 9.84 and $p = 0.002$
	rs1003199	CC + CT vs. TT	$p = 0.013$; OR = 1.52; 95%CI: 1.09–2.13
		MAF	ASY MAF(T) = 43.123.7%; SEV CCC MAF(T) = 34.8%
		Allelic test	Chi-square = 3.98 and $p = 0.05$
	rs3181216	TT vs. TA + AA	$p = 0.430$; OR = 1.11; 95%CI: 0.86–1.43
		MAF	ASY MAF(A) = 23.7%; SEV CCC MAF(A) = 24.8%
		Allelic test	Chi-square = 0.80 and $p = 0.37$
	rs2569253	TT + CC vs. TC	$p = 0.036$; OR = 1.45; 95%CI: 1.02–2.05
		MAF	ASY MAF(C) = 40.7%; SEV CCC MAF(C) = 34.3%
		Allelic test	Chi-square = 2.33 and $p = 0.13$
	rs2853694	AA vs. AC + CC	$p = 0.360$; OR = 1.12; 95%CI: 0.88–1.43
		MAF	ASY MAF(C) = 34.7%; SEV CCC MAF(C) = 30.2%
		Allelic test	Chi-square = 1.34 and $p = 0.25$
	rs919766	AA vs. AC + CC	$p = 0.007$; OR = 1.49; 95%CI: 1.11–1.98
		MAF	ASY MAF(C) = 8.9%; SEV CCC MAF(C) = 20.7%
		Allelic test	Chi-square = 13.91 and $p = 0.0002$
	rs2853696	GG vs. GA + AA	$p = 0.649$; OR = 1.27; 95%CI: 0.45–3.56
		MAF	ASY MAF(A) = 10.6%; SEV CCC MAF(A) = 9.5%
		Allelic test	Chi-square = 0.21 and $p = 0.64$
	rs11574790	CC vs. CT + TT	$p = 0.026$; OR = 1.39; 95%CI: 1.04–1.86
		MAF	ASY MAF(T) = 8.3%; SEV CCC MAF(T) = 18.3%
		Allelic test	Chi-square = 10.98 and $p = 0.0009$
	rs3212227	AA vs. AC + CC	$p = 0.631$; OR = 1.06; 95%CI: 0.83–1.35
		MAF	ASY MAF(C) = 31.1%; SEV CCC MAF(C) = 31.9%
		Allelic test	Chi-square = 0.04 and $p = 0.84$
	rs1368439	TT vs. TG + GG	$p = 0.547$; OR = 1.09; 95%CI: 0.82–1.47
		MAF	ASY MAF(G) = 11.2%; SEV CCC MAF(G) = 9.9%
		Allelic test	Chi-square = 0.24 and $p = 0.62$
	rs6870828	AA + AG vs. GG	$p = 0.181$; OR = 1.28; 95%CI: 0.89–1.82
		MAF	ASY MAF(G) = 39.4%; SEV CCC MAF(G) = 42.4%
		Allelic test	Chi-square = 0.48 and $p = 0.49$
	rs6859018	CC vs. CT + TT	$P = 0.898$; OR = 1.02; 95%CI: 0.80–1.29
		MAF	ASY MAF(T) = 33.0%; SEV CCC MAF(T) = 34.3%
		Allelic test	Chi-square = 0.10 and $p = 0.75$
IL10	rs1800890	TT vs. TA + AA	$p = 0.181$; OR = 1.22; 95%CI: 0.91–1.63
		MAF	ASY MAF(A) = 26.4%; SEV CCC MAF(A) = 24.0%
		Allelic test	Chi-square = 0.44 and $p = 0.51$
	rs1800896	AA + AG vs. GG	$p = 0.097$; OR = 1.38; 95%CI: 0.94–2.01
		MAF	ASY MAF(G) = 36.9%; SEV CCC MAF(G) = 33.4%
		Allelic test	Chi-square = 0.74 and $p = 0.39$
	rs1800871	CC + TT vs. CT	$p = 0.041$; OR = 1.30; 95%CI: 1.01–1.66
		MAF	ASY MAF(T) = 35.3%; SEV CCC MAF(T) = 34.1%
		Allelic test	Chi-square = 6.18 and $p = 0.01$

(Continued)

TABLE 2 | Continued

GENE	Tag SNP		Association tests
	rs1518111	GG + AA vs. GA	$p = 0.067$; OR = 1.26; 95%CI: 0.98–1.61
		MAF	ASY MAF(A) = 32.4%; SEV CCC MAF(A) = 32.6%
		Allelic test	Chi-square = 0.001 and $p = 0.97$
	rs3024496	TT + TC vs. CC	$p = 0.036$; OR = 1.49; 95%CI: 1.03–2.16
		MAF	ASY MAF(C) = 40.3%; SEV CCC MAF(C) = 35.2%
		Allelic test	Chi-square = 1.55 and $p = 0.21$
	rs6673928	CC vs. CA	$p = 0.432$; OR = 2.12; 95%CI: 0.33–13.83
		MAF	ASY MAF(A) = 1.3%; SEV CCC MAF(A) = 0.5%
		Allelic test	Chi-square = 1.12 and $p = 0.29$
IFNG	rs2069705	TT vs. TC + CC	$p = 0.333$; OR = 1.13; 95%CI: 0.88–1.46
		MAF	ASY MAF(C) = 39.6%; SEV CCC MAF(C) = 37.1%
		Allelic test	Chi-square = 0.38 and $p = 0.54$
	rs1861494	AA vs. AG + GG	$p = 0.067$; OR = 1.26; 95%CI: 0.98–1.61
		MAF	ASY MAF(G) = 24.3%; SEV CCC MAF(G) = 17.0%
		Allelic test	Chi-square=4.88 and p=0.03
	rs2069718	CC + CT vs. TT	$p = 0.147$; OR = 1.23; 95%CI: 0.93–1.63
		MAF	ASY MAF(T) = 51.8%; SEV CCC MAF(T) = 46.7%
		Allelic test	Chi-square = 1.47 and $p = 0.22$
	rs2069727	AA + AG vs. GG	$p = 0.254$; OR = 1.23; 95%CI: 0.86–1.75
		MAF	ASY MAF(G) = 36.4%; SEV CCC MAF(G) = 39.5%
		Allelic test	Chi-square = 0.60 and $p = 0.44$
	rs3181035	GG vs. GA + AA	$p = 0.440$; OR = 1.11; 95%CI: 0.85–1.45
		MAF	ASY MAF(A) = 17.0%; SEV CCC MAF(A) = 13.4%
		Allelic test	Chi-square = 1.46 and $p = 0.23$
IL4	rs2070874	CC vs. CT + TT	$p = 0.274$; OR = 1.14; 95%CI: 0.90–1.45
		MAF	ASY MAF(T) = 27.0%; SEV CCC MAF(T) = 30.8%
		Allelic test	Chi-square = 1.07 and $p = 0.30$
	rs2227284	AA + AC vs. CC	$p = 0.059$; OR = 1.30; 95%CI: 0.99–1.72
		MAF	ASY MAF(C) = 53.2%; SEV CCC MAF(C) = 43.3%
		Allelic test	Chi-square = 5.48 and $p = 0.02$
	rs2243261	GG vs. GT + TT	$p = 0.841$; OR = 1.05; 95%CI: 0.68–1.62
		MAF	ASY MAF(T) = 3.8%; SEV CCC MAF(T) = 4.8%
		Allelic test	Chi-square = 0.34 and $p = 0.56$
	rs2243268	AA vs. AC + CC	$p = 0.159$; OR = 1.20; 95%CI: 0.93–1.55
		MAF	ASY MAF(C) = 20.0%; SEV CCC MAF(C) = 23.8%
		Allelic test	Chi-square = 1.20 and $p = 0.27$
	rs2243274	GG + GA vs. AA	$p = 0.225$; OR = 1.25; 95%CI: 0.87–1.80
		MAF	ASY MAF(A) = 31.2%; SEV CCC MAF(A) = 38.4%
		Allelic test	Chi-square = 3.16 and $p = 0.08$
	rs2243290	CC + CA vs. AA	$p = 0.842$; OR = 1.04; 95%CI: 0.68–1.61
		MAF	ASY MAF(A) = 23.7%; SEV CCC MAF(A) = 27.2%
		Allelic test	Chi-square = 0.91 and $p = 0.34$
	rs2406539	AA vs. AT + TT	$p = 0.538$; OR = 1.23; 95%CI: 0.64–2.35
		MAF	ASY MAF(T) = 7.5%; SEV CCC MAF(T) = 10.0%
		Allelic test	Chi-square = 1.05 and $p = 0.30$

These association tests are genotype association and allelic tests.
SEV CCC, Severe CCC.

associated, in univariate analysis, to an increased risk to develop severe chronic cardiomyopathy (rs2546893G/A: $p = 0.001$; OR = 1.706; 95%CI: 1.236–2.353; rs919766A/C: $p = 0.001$; OR = 1.672; 95%CI: 1.231–2.267; rs1003199C/T: $p = 0.013$; OR = 1.531; 95%CI: 1.236–2.353; rs2569253T/C: $p = 0.037$; OR = 1.445; 95%CI: 1.022–2.041; rs11574790C/T: $p = 0.004$; OR =

1.562; 95%CI: 1.151–2.123) (see **Table 2**). After correction for multiple testing the polymorphism rs2546893 remains significant (corrected p-value = 0.014) and the polymorphism rs919766 is borderline (corrected p-value = 0.091). In a multivariate analysis, the gender and the two polymorphisms remained significantly associated (rs2546893G/A: $p = 0.005$; OR = 1.667; 95% CI: 1.170–2.375; rs919766A/C: $p = 0.024$; OR = 1.471; 95%CI: 1.051–2.058; gender: $p = 2.25 \times 10^{-5}$; OR = 3.261; 95% CI: 1.888–5.632). the allelic tests confirmed that the rs2546893G allele ($p < 0.002$) and the rs919766C allele ($p = 0.0002$) were associated to an increase risk to severe CCC. None of the studied *IL12B* markers discriminated moderate from severe CCC patient groups.

Polymorphism rs3024496T/C Around the *IL10* Gene Is Showing a Trend of Association to CCC

Six tag SNPs were genotyped for the *IL10* gene. **Table 1** shows comparison between CCC and ASY, while **Table 2** shows comparison of severe CCC and ASY. For the rs1800896A/G polymorphism, 282 (91.9%) CCC subjects carried the A/A or A/G genotypes vs. 90 (84.1%) for the ASY ($p = 0.013$; OR = 1.527; 95%CI: 1.092–2.137). The same result was obtained when the analysis was restricted to severe CCC vs. ASY ($p = 0.028$; OR = 1.536; 95%CI: 1.047–2.252) (see **Table 2**). For the rs3024496T/C polymorphism, 284 (91.3%) CCC subjects carried the T/T or T/C genotypes vs. 92 (84.3%) for the ASY ($p = 0.031$; OR = 1.437; 95%CI: 1.033–2.000) (see **Table 1**). The same result was obtained when the analysis was restricted to severe CCC vs. ASY ($p = 0.049$; OR = 1.462; 95%CI: 1.002–2.132) (see **Table 2**). For the rs1800871 marker, we found a significant association when severe CCC patients were compared the ASY subjects ($p = 0.035$; OR = 1.311; 95%CI: 1.019–1.686). No association was found for this last marker in the comparison between ASY and the whole CCC group (see **Table 1**). After correction for multiple testing, the polymorphism rs1800896A/G and rs3024496T/C has shown only trends of association (rs1800896A/G: corrected p-value = 0.078). The allelic tests reach the same trends of association (rs3024496C $p = 0.17$ and rs1800896G $p = 0.27$).

Based on the results of the multivariate analysis, we had an association between CCC and ASY with two SNPs located in the IL12B gene (rs2546893 and rs919766) and one polymorphism in the IL10 gene (rs3024496). Subjects carrying the three susceptibility genotypes [rs2546893(GG or GA) + rs919766(CC or AC) + rs3024496(TT or TC)] have a higher risk (OR = 2.68) to develop CCC. In contrast, subjects carrying the resistant genotypes (rs2546893AA + r919766AA + rs3024496CC) have a lower risk [OR = 4.48 (1/0.223)] to develop CCC (**Table 3**).

No Clear Evidence of Association Was Detected for Tag Polymorphisms in the *IFNG* and *IL4* Genes

Six tag SNPs were genotyped for the *IFNG* gene. For the rs1861494 A/G polymorphism, a trend of association was detected. Indeed, 202 (64.7%) CCC subjects carried the A/A genotype vs. 62 (54.9%) for the ASY ($p = 0.057$; OR = 1.24; 95%CI: 0.99–1.55) (see **Supplementary Table 2**). The same trend appeared on severe cases ($p = 0.067$; OR = 1.26; 95%CI: 0.98–1.61) (see **Table 2**). Seven tag SNPs into the *IL4* gene were genotyped on our whole study population (see **Supplementary Table 2**). Comparisons between ASY and CCC patients disclosed no significant associations (see **Tables 1**, **2**).

DISCUSSION

Association studies of cytokine gene polymorphisms in Chagas disease frequently include a small number of patients, and are often not replicated in different studies or ethnical groups. The present study was designed to determine whether SNPs in *IL12B, IL10, IFNG* and *IL4,* key genes involved in the promotion and control of Th1 differentiation and IFN-g production to *T. cruzi*, are associated with Chagas disease outcome. For that, we used a larger population and performed a comprehensive assessment of 35 Tag SNPs covering all the genetic information

TABLE 3 | Genotype combination analysis based on the following polymorphisms (rs2546893/rs919766/rs3024496).

Genotype combinations	IL12 rs2546893	IL12 rs919766	IL10 rs3024496	CCC	ASY	Total	% in ASY	% in CCC	Ratio CCC/ASY	p-value	Odds Ratio	95% C.I. for EXP(B)
1 S1 S2 S3	GG + GA	CC + AC	TC + CC	89	14	103	**14%**	**86%**	**6.36**	0.0006	2.677	1.468–4.838
2 S1 S2 R3	GG + GA	CC + AC	CC	9	3	12	**25%**	**75%**	**3.00**	0.6340	1.028	0.2758
3 S1 R2 S3	GG + GA	AA	TC + CC	149	46	195	**24%**	**76%**	**3.24**	0.1963	1.217	0.7777–1.928
4 R1 S2 S3	AA	AC + CC	TC + CC	6	0	6	**0%**	**100%**	**X**	0.1688	X	X
5 S1 R2 R3	GG + GA	AA	CC	13	11	24	**46%**	**54%**	**1.18**	0.0058	0.3483	0.1434–0.7776
6 R1 S2 R3	AA	AC + CC	CC	1	0	1	**0%**	**100%**	**X**	0.7450	X	X
7 R1 R2 S3	AA	AA	TC + CC	29	25	54	**46%**	**54%**	**1.16**	<0.0001	0.3320	0.1834–0.6135
8 R1 R2 R3	AA	AA	CC	2	3	5	**60%**	**40%**	**0.67**	0.1075	0.2230	0.0393–1.110

R, Resistant genotype; S, Susceptibility genotype; SNP 1 = rs2546893/SNP2 = rs919766/SNP3 = rs3024496.

Bold value indicates % ASY, Percentage of ASY subjects carrying the genotype combination; % CCC, Percentage of CCC subjects carrying the genotype combination Ratio; CCC/ASY, Ratio between these two percentage.

of the mentioned genes. We found significant associations of genotypes and alleles of *IL12B* and *IL10* with increased risk to CCC progression.

For the *IL12B* gene region, in a multivariate analysis, two SNPs were significantly associated to disease (rs2546893G/A, rs919766A/C). The rs919766C and rs2546893G alleles were associated to an increase risk to CCC development. Interestingly, these two markers are located 5 to 13 kb away from the rs3212227 polymorphism (*IL12B* 3′UTR region), that was previously associated to Chagas cardiomyopathy (31). Our results are consistent as these 3 markers are in linkage disequilibrium ($D^{'} = 0.99$) on the African (Yoruba) reference population and the markers rs919766 and rs3212227 are in strong linkage disequilibrium ($D^{'} = 0.99$) on the European reference population.

For the *IL10* gene, the rs3024496 polymorphism (located in the 3′UTR region), and rs1800896 polymorphism (located in the promoter region) have shown trends of association to susceptibility to cardiomyopathy. The rs3024496C and rs1800896G alleles were more frequent in patients. Our data are consistent with the previous study that showed that the marker (IL10-1082 known as rs1800896 too) was previously associated with development of CCC (33). Costa et al. have shown that the A allele has been associated with lower IL-10 expression in disease and lower left ventricular ejection fraction values in CCC (33). The two markers (rs3024496 and rs1800896) are in strong linkage disequilibrium on the European reference population ($D^{'} = 1$) and on the Yoruba population ($D^{'} = 0.83$).

Three SNPs in the *IL10* gene (the two rs3024496, rs1800896 mentioned above, plus rs1800871) detected trends of association. A study performed on a Brazilian population infected by *Leishmania braziliensis* has shown that these markers are correlated (r^2 value >0.8) (40). So, from one Brazilian sub population to another one, the associated marker may change (due to light allelic frequency variation) or population stratification. However, the associated marker is coming from the same correlation block.

We did not find any significant association with SNPs from the *IFNG* and *IL4* genes. This is in agreement with Arnez et al. who studied some of these same SNPs (rs2070874, rs2227284, rs2243268, rs2243274, rs2243290 in an Bolivian population (29), and Flórez et al. who studied one SNP not tested by our group (rs2243250) in a Colombian population, failing to find any association (30). Taken together, these results suggest that we do not have evidence that polymorphisms in or within the IFN gene control the expression of this key cytokine for the pathogenic process.

During *T. cruzi* infection, once the inflammatory process starts, IFN-γ will be produced by Th1 cells and act as a prime inflammatory cytokine in different pathways of the immune system, such as upregulating MHC class I and class II molecules, suppressing Th2 immune responses by antagonism of IL-4 production, inducing high levels of antigen presentation and activating macrophages (41). Moreover, CCC patients have an increased peripheral production of IFN-γ and TNF-α when compared to patients with the asymptomatic/indeterminate form. On the other hand, IFN-γ has direct effects on cardiomyocytes and perhaps other cells of the myocardium (34). At this level we can speculate that the existence of functional or pathogenic variants in or within the IFN gene will have a too strong deleterious effect that will be lethal. So, the genetic control of the human susceptibility to cardiomyopathy mainly target genes that are involved in the regulation of this TH1 response, such as *IL12B* and *IL10* genes.

On the other hand, our data confirmed the involvement of *IL12B* and *IL10* in the control of susceptibility to human Chagas cardiomyopathy. The *IL10* polymorphism has been described as a functional polymorphism. It remains to be tested whether the *IL12B* polymorphism and linked SNPs are functional as well. Taking into account the effects of both cytokines on Th1 T cell differentiation and IFNγ production, it can be hypothesized that this is linked to the increased number of IFNγ producing Th1 T cells in the peripheral blood and heart tissue of CCC patients. Our study and others have identified several genes in the control of human susceptibility to chronic disease. However, each gene is characterized by a low odds ratio, implying a small contribution in Chagas disease infection. However, the combination of the several genetic markers increases the protection from disease development, with individual odds ratio around 1.5, to ca. 4.5 in patients carrying all the protection genotypes in all three loci. The identification of more genetic markers for CCC will provide information for pathogenesis as well as therapeutic targets. Identifying early or causal predictive genetic factors for the clinical progression of the disease is essential for clarifying the pathogenesis and defining appropriate treatment modalities.

DATA AVAILABILITY STATEMENT

The datasets presented in this study can be found in online repositories. The names of the repository/repositories and accession number(s) can be found in the article/**Supplementary Material**.

ETHICS STATEMENT

The studies involving human participants were reviewed and approved by The INSERM Internal Review Board, The Brazilian National Ethics in Research Commission (CONEP). The patients/participants provided their written informed consent to participate in this study.

AUTHOR CONTRIBUTIONS

JK, EC-N, and CC: study design. AF-B and SC: experiments. AF-B, BI, CP, BS, HL-W, PB, JM-N, AS, FD, MH, MS, AF, AP, ED, VR, JK, CC, and EC-N: manuscript preparation. All authors contributed to the article and approved the submitted version.

FUNDING

This work was supported by the Institut National de la Santé et de la Recherche Médicale (INSERM), Aix-Marseille University (Direction des Relations Internationales), the ARCUS II PACA Brésil program, CNPq (the Brazilian National Research Council), FAPESP (São Paulo State Research Funding Agency-Brazil), and the National Institute of Health (P50 AI098461-02 and U19AI098461-06; to EC-N). EC-N and CC were recipient for an international program funded either by the French ANR and the Brazilian FAPESP agencies (Br-Fr-chagas). AF-B hold fellowships from the São Paulo State Research Funding Agency, FAPESP. EC-N and JK have received a Council for Scientific and Technological Development—CNPq productivity award. CC was a recipient of a temporary professor position supported by the French consulate in Brazil and the University of São Paulo (USP).

ACKNOWLEDGMENTS

We are thankful for the access to the genotyping platform (Denis Milan, Cecile Donnadieu, and Frederic Martins).

SUPPLEMENTARY MATERIAL

The Supplementary Material for this article can be found online at: https://www.frontiersin.org/articles/10.3389/fimmu.2020.01386/full#supplementary-material

REFERENCES

1. Bocchi EA, Bestetti RB, Scanavacca MI, Cunha Neto E, Issa VS. Chronic chagas heart disease management: from etiology to cardiomyopathy treatment. *J Am Coll Cardiol*. (2017) 70:1510–24. doi: 10.1016/j.jacc.2017.08.004
2. Coura JR, Borges-Pereira J. Chagas disease. What is known and what should be improved: a systemic review. *Rev Soc Bras Med Trop*. (2012) 45:286–96. doi: 10.1590/S0037-86822012000300002
3. Barbosa AP, Cardinalli Neto A, Otaviano AP, Rocha BF, Bestetti RB. Comparison of outcome between Chagas cardiomyopathy and idiopathic dilated cardiomyopathy. *Arq Bras Cardiol*. (2011) 97:517–25. doi: 10.1590/S0066-782X2011005000112
4. Bestetti RB, Muccillo G. Clinical course of Chagas' heart disease: a comparison with dilated cardiomyopathy. *Int J Cardiol*. (1997) 60:187–93. doi: 10.1016/S0167-5273(97)00083-1
5. Zicker F, Smith PG, Netto JC, Oliveira RM, Zicker EM. Physical activity, opportunity for reinfection, and sibling history of heart disease as risk factors for Chagas' cardiopathy. *Am J Trop Med Hyg*. (1990) 43:498–505. doi: 10.4269/ajtmh.1990.43.498
6. Acosta-Herrera M, Strauss M, Casares-Marfil D, Martin J. Genomic medicine in Chagas disease. *Acta Trop*. (2019) 197:105062. doi: 10.1016/j.actatropica.2019.105062
7. Chevillard C, Nunes JPS, Frade AF, Almeida RR, Pandey RP, Nascimento MS, et al. Disease tolerance and pathogen resistance genes may underlie *Trypanosoma cruzi* persistence and differential progression to chagas disease cardiomsyopathy. *Front Immunol*. (2018) 9:2791. doi: 10.3389/fimmu.2018.02791
8. Strauss M, Acosta-Herrera M, Alcaraz A, Casares-Marfil D, Bosch-Nicolau P, Lo Presti MS, et al. Association of IL18 genetic polymorphisms with Chagas disease in Latin American populations. *PLoS Negl Trop Dis*. (2019) 13:e0007859. doi: 10.1371/journal.pntd.0007859
9. Cunha-Neto E, Chevillard C. Chagas disease cardiomyopathy: immunopathology and genetics. *Mediators Inflamm*. (2014) 2014:683230. doi: 10.1155/2014/683230
10. Michailowsky V, Silva NM, Rocha CD, Vieira LQ, Lannes-Vieira J, Gazzinelli RT. Pivotal role of interleukin-12 and interferon-gamma axis in controlling tissue parasitism and inflammation in the heart and central nervous system during *Trypanosoma cruzi* infection. *Am J Pathol*. (2001) 159:1723–33. doi: 10.1016/S0002-9440(10)63019-2
11. Bilate AM, Cunha-Neto E. Chagas disease cardiomyopathy: current concepts of an old disease. *Rev Inst Med Trop Sao Paulo*. (2008) 50:67–74. doi: 10.1590/S0036-46652008000200001
12. Reis MM, Higuchi Mde L, Benvenuti LA, Aiello VD, Gutierrez PS, Bellotti G, et al. An *in situ* quantitative immunohistochemical study of cytokines and IL-2R+ in chronic human chagasic myocarditis: correlation with the presence of myocardial *Trypanosoma cruzi* antigens. *Clin Immunol Immunopathol*. (1997) 83:165–72. doi: 10.1006/clin.1997.4335
13. Muller U, Kohler G, Mossmann H, Schaub GA, Alber G, Di Santo JP, et al. IL-12-independent IFN-gamma production by T cells in experimental Chagas' disease is mediated by IL-18. *J Immunol*. (2001) 167:3346–53. doi: 10.4049/jimmunol.167.6.3346
14. Rocha Rodrigues DB, dos Reis MA, Romano A, Pereira SA, Teixeira Vde P, Tostes S, et al. *In situ* expression of regulatory cytokines by heart inflammatory cells in Chagas' disease patients with heart failure. *Clin Dev Immunol*. (2012) 2012:361730. doi: 10.1155/2012/361730
15. Holscher C, Mohrs M, Dai WJ, Kohler G, Ryffel B, Schaub GA, et al. Tumor necrosis factor alpha-mediated toxic shock in *Trypanosoma cruzi*-infected interleukin 10-deficient mice. *Infect Immun*. (2000) 68:4075–83. doi: 10.1128/IAI.68.7.4075-4083.2000
16. Soares MP, Gozzelino R, Weis S. Tissue damage control in disease tolerance. *Trends Immunol*. (2014) 35:483–94. doi: 10.1016/j.it.2014.08.001
17. Medina TS, Oliveira GG, Silva MC, David BA, Silva GK, Fonseca DM, et al. Ebi3 prevents *Trypanosoma cruzi*-induced myocarditis by dampening IFN-gamma-driven inflammation. *Front Immunol*. (2017) 8:1213. doi: 10.3389/fimmu.2017.01213
18. Araujo FF, Gomes JA, Rocha MO, Williams-Blangero S, Pinheiro VM, Morato MJ, et al. Potential role of CD4+CD25HIGH regulatory T cells in morbidity in Chagas disease. *Front Biosci*. (2007) 12:2797–806. doi: 10.2741/2273
19. Cunha-Neto E, Kalil J. Heart-infiltrating and peripheral T cells in the pathogenesis of human Chagas' disease cardiomyopathy. *Autoimmunity*. (2001) 34:187–92. doi: 10.3109/08916930109007383
20. Gomes JA, Bahia-Oliveira LM, Rocha MO, Martins-Filho OA, Gazzinelli G, Correa-Oliveira R. Evidence that development of severe cardiomyopathy in human Chagas' disease is due to a Th1-specific immune response. *Infect Immun*. (2003) 71:1185–93. doi: 10.1128/IAI.71.3.1185-1193.2003
21. Ribeirao M, Pereira-Chioccola VL, Renia L, Augusto Fragata Filho A, Schenkman S, Rodrigues MM. Chagasic patients develop a type 1 immune response to Trypanosoma cruzi trans-sialidase. *Parasite Immunol*. (2000) 22:49–53. doi: 10.1046/j.1365-3024.2000.00260.x
22. Abel LC, Rizzo LV, Ianni B, Albuquerque F, Bacal F, Carrara D, et al. Chronic Chagas' disease cardiomyopathy patients display an increased IFN-gamma response to *Trypanosoma cruzi* infection. *J Autoimmun*. (2001) 17:99–107. doi: 10.1006/jaut.2001.0523
23. Gomes JA, Bahia-Oliveira LM, Rocha MO, Busek SC, Teixeira MM, Silva JS, et al. Type 1 chemokine receptor expression in Chagas' disease correlates with morbidity in cardiac patients. *Infect Immun*. (2005) 73:7960–6. doi: 10.1128/IAI.73.12.7960-7966.2005
24. Ferreira RC, Ianni BM, Abel LC, Buck P, Mady C, Kalil J, et al. Increased plasma levels of tumor necrosis factor-alpha in asymptomatic/"indeterminate" and Chagas disease cardiomyopathy patients. *Mem Inst Oswaldo Cruz*. (2003) 98:407–11. doi: 10.1590/S0074-02762003000300021
25. Sousa GR, Gomes JA, Fares RC, Damasio MP, Chaves AT, Ferreira KS, et al. Plasma cytokine expression is associated with cardiac morbidity in chagas disease. *PLoS ONE*. (2014) 9:e87082. doi: 10.1371/journal.pone.0087082

26. Talvani A, Rocha MO, Ribeiro AL, Correa-Oliveira R, Teixeira MM. Chemokine receptor expression on the surface of peripheral blood mononuclear cells in Chagas disease. *J Infect Dis*. (2004) 189:214–20. doi: 10.1086/380803
27. Nogueira LG, Santos RH, Fiorelli AI, Mairena EC, Benvenuti LA, Bocchi EA, et al. Myocardial gene expression of T-bet, GATA-3, Ror-gammat, FoxP3, and hallmark cytokines in chronic Chagas disease cardiomyopathy: an essentially unopposed TH1-type response. *Mediators Inflamm*. (2014) 2014:914326. doi: 10.1155/2014/914326
28. de Alba-Alvarado M, Salazar-Schettino PM, Jimenez-Alvarez L, Cabrera-Bravo M, Garcia-Sancho C, Zenteno E, et al. Th-17 cytokines are associated with severity of *Trypanosoma cruzi* chronic infection in pediatric patients from endemic areas of Mexico. *Acta Trop*. (2018) 178:134–41. doi: 10.1016/j.actatropica.2017.11.009
29. Alvarado Arnez LE, Venegas EN, Ober C, Thompson EE. Sequence variation in the IL4 gene and resistance to *Trypanosoma cruzi* infection in Bolivians. *J Allergy Clin Immunol*. (2011) 127:279–82, 282 e1–3. doi: 10.1016/j.jaci.2010.10.026
30. Florez O, Martin J, Gonzalez CI. Interleukin 4, interleukin 4 receptor-alpha and interleukin 10 gene polymorphisms in Chagas disease. *Parasite Immunol*. (2011) 33:506–11. doi: 10.1111/j.1365-3024.2011.01314.x
31. Zafra G, Morillo C, Martin J, Gonzalez A, Gonzalez CI. Polymorphism in the 3′ UTR of the IL12B gene is associated with Chagas' disease cardiomyopathy. *Microbes Infect*. (2007) 9:1049–52. doi: 10.1016/j.micinf.2007.04.010
32. Turner DM, Williams DM, Sankaran D, Lazarus M, Sinnott PJ, Hutchinson IV. An investigation of polymorphism in the interleukin-10 gene promoter. *Eur J Immunogenet*. (1997) 24:1–8. doi: 10.1111/j.1365-2370.1997.tb00001.x
33. Costa GC, da Costa Rocha MO, Moreira PR, Menezes CA, Silva MR, Gollob KJ, et al. Functional IL-10 gene polymorphism is associated with Chagas disease cardiomyopathy. *J Infect Dis*. (2009) 199:451–4. doi: 10.1086/596061
34. Cunha-Neto E, Dzau VJ, Allen PD, Stamatiou D, Benvenutti L, Higuchi ML, et al. Cardiac gene expression profiling provides evidence for cytokinopathy as a molecular mechanism in Chagas' disease cardiomyopathy. *Am J Pathol*. (2005) 167:305–13. doi: 10.1016/S0002-9440(10)62976-8
35. Jorge MT, Macedo TA, Janones RS, Carizzi DP, Heredia RA, Acha RE. Types of arrhythmia among cases of American trypanosomiasis, compared with those in other cardiology patients. *Ann Trop Med Parasitol*. (2003) 97:139–48. doi: 10.1179/000349803235001561
36. Januzzi JL Jr. Natriuretic peptides, ejection fraction, and prognosis: parsing the phenotypes of heart failure. *J Am Coll Cardiol*. (2013) 61:1507–9. doi: 10.1016/j.jacc.2013.01.039
37. van Veldhuisen DJ, Linssen GC, Jaarsma T, van Gilst WH, Hoes AW, Tijssen JG, et al. B-type natriuretic peptide and prognosis in heart failure patients with preserved and reduced ejection fraction. *J Am Coll Cardiol*. (2013) 61:1498–506. doi: 10.1016/j.jacc.2012.12.044
38. Nogueira LG, Santos RH, Ianni BM, Fiorelli AI, Mairena EC, Benvenuti LA, et al. Myocardial chemokine expression and intensity of myocarditis in Chagas cardiomyopathy are controlled by polymorphisms in CXCL9 and CXCL10. *PLoS Negl Trop Dis*. (2012) 6:e1867. doi: 10.1371/journal.pntd.0001867
39. Holm S. A simple sequentially rejective multiple test procedure. *Scand J Stat*. (1979) 6:65–70.
40. Salhi A, Rodrigues V Jr, Santoro F, Dessein H, Romano A, Roberto Castellano L, et al. Immunological and genetic evidence for a crucial role of IL-10 in cutaneous lesions in humans infected with Leishmania braziliensis. *J Immunol*. (2008) 180:6139–48. doi: 10.4049/jimmunol.180.9.6139
41. Schroder K, Hertzog PJ, Ravasi T, Hume DA. Interferon-gamma: an overview of signals, mechanisms and functions. *J Leukoc Biol*. (2004) 75:163–89. doi: 10.1189/jlb.0603252

Conflict of Interest: The authors declare that the research was conducted in the absence of any commercial or financial relationships that could be construed as a potential conflict of interest.

frontiers in Immunology

CORRECTION
published: 09 September 2020
doi: 10.3389/fimmu.2020.593759

Corrigendum: Polymorphisms in Genes Affecting Interferon-γ Production and Th1 T Cell Differentiation Are Associated With Progression to Chagas Disease Cardiomyopathy

Amanda Farage Frade-Barros[1,2,3,4,5], Barbara Maria Ianni[1], Sandrine Cabantous[3], Cristina Wide Pissetti[6], Bruno Saba[7], Hui Tzu Lin-Wang[7], Paula Buck[1], José Antonio Marin-Neto[8], André Schmidt[8], Fabrício Dias[8], Mario Hiroyuki Hirata[9], Marcelo Sampaio[7], Abílio Fragata[7], Alexandre Costa Pereira[1], Eduardo Donadi[8], Virmondes Rodrigues[6], Jorge Kalil[1,2,5], Christophe Chevillard[10†] and Edecio Cunha-Neto[1,2,4†]*

[1] Heart Institute (InCor), University of São Paulo School of Medicine (FMUSP), São Paulo, Brazil, [2] Institute for Investigation in Immunology (iii), INCT, São Paulo, Brazil, [3] Aix-Marseille Université, INSERM, GIMP UMR_S906, Marseille, France, [4] Division of Clinical Immunology and Allergy, University of São Paulo School of Medicine, São Paulo, Brazil, [5] Bioengineering Program, Instituto Tecnológico, Universidade Brasil, São Paulo, Brazil, [6] Laboratory of Immunology, Universidade Federal Do Triângulo Mineiro (UFTM), Uberaba, Brazil, [7] Laboratório de Investigação Molecular em Cardiologia, Instituto de Cardiologia Dante Pazzanese (IDPC), São Paulo, Brazil, [8] School of Medicine of Ribeirão Preto (FMRP), University of São Paulo, Ribeirão Preto, Brazil, [9] Department of Clinical and Toxicological Analyses, Faculty of Pharmaceutical Sciences, University of São Paulo (USP), São Paulo, Brazil, [10] Aix Marseille Université, INSERM, TAGC Theories and Approaches of Genomic Complexity, UMR_1090, Marseille, France

Keywords: Chagas disease, cardiomyopathy, susceptibility, IL12, IL 10, IFN, IL4

OPEN ACCESS

Approved by:
Frontiers Editorial Office, Frontiers Media SA, Switzerland

****Correspondence:***
Amanda Farage Frade-Barros
amanda.frade@universidadebrasil.edu.br

† These authors have contributed equally to this work

Specialty section:
This article was submitted to Microbial Immunology, a section of the journal Frontiers in Immunology

Received: *12 August 2020*
Accepted: *12 August 2020*
Published: *09 September 2020*

Citation:
Farage Frade-Barros A, Ianni BM, Cabantous S, Pissetti CW, Saba B, Lin-Wang HT, Buck P, Marin-Neto JA, Schmidt A, Dias F, Hirata MH, Sampaio M, Fragata A, Pereira AC, Donadi E, Rodrigues V, Kalil J, Chevillard C and Cunha-Neto E (2020) Corrigendum: Polymorphisms in Genes Affecting Interferon-γ Production and Th1 T Cell Differentiation Are Associated With Progression to Chagas Disease Cardiomyopathy. Front. Immunol. 11:593759. doi: 10.3389/fimmu.2020.593759

A Corrigendum on

Polymorphisms in Genes Affecting Interferon-γ Production and Th1 T Cell Differentiation Are Associated With Progression to Chagas Disease Cardiomyopathy
by Farage Frade-Barros, A. F., Ianni, B. M., Cabantous, S., Pissetti, C. W., Saba, B., Lin-Wang, H. T., et al. (2020). Front. Immunol. 11:1386. doi: 10.3389/fimmu.2020.01386

In the original article, we neglected to include the funding from the National Institute of Health (P50 AI098461-02 and U19AI098461-06) to EC-N.

The authors apologize for this error and state that this does not change the scientific conclusions of the article in any way. The original article has been updated.

frontiers in Immunology

ORIGINAL RESEARCH
published: 06 August 2020
doi: 10.3389/fimmu.2020.01974

Association of IL-10 Gene Polymorphism With IL-10 Secretion by CD4 and T Regulatory Cells in Human Leprosy

Mohammad Tarique[1†], Huma Naz[2†], Chaman Saini[1], Mohd Suhail[3,4], Hari Shankar[5], Neena Khanna[6] and Alpana Sharma[1]*

[1] Department of Biochemistry, All India Institute of Medical Sciences (AIIMS), New Delhi, India, [2] Centre for Interdisciplinary Research in Basic Sciences, Jamia Millia Islamia, New Delhi, India, [3] King Fahd Medical Research Center, King Abdulaziz University, Jeddah, Saudi Arabia, [4] Department of Medical Laboratory Technology, Faculty of Applied Medical Sciences, King Abdulaziz University, Jeddah, Saudi Arabia, [5] Parasite-Host Biology Group, ICMR – National Institute of Malaria Research, New Delhi, India, [6] Department of Dermatovenerology, All India Institute of Medical Sciences (AIIMS), New Delhi, India

OPEN ACCESS

Edited by:
Rajendranath Ramasawmy, Universidade Nilton Lins, Brazil

Reviewed by:
Ken Oestreich, The Ohio State University, United States
Margarida Saraiva, Universidade do Porto, Portugal

***Correspondence:**
Alpana Sharma
dralpanasharma@gmail.com

†Present address:
Mohammad Tarique, Department of Surgery, University of Miami, Miami, FL, United States
Huma Naz, Department of Anesthesiology, University of Miami, Miami, FL, United States

Specialty section:
This article was submitted to Microbial Immunology, a section of the journal Frontiers in Immunology

Received: 16 May 2020
Accepted: 21 July 2020
Published: 06 August 2020

Citation:
Tarique M, Naz H, Saini C, Suhail M, Shankar H, Khanna N and Sharma A (2020) Association of IL-10 Gene Polymorphism With IL-10 Secretion by CD4 and T Regulatory Cells in Human Leprosy. Front. Immunol. 11:1974. doi: 10.3389/fimmu.2020.01974

Leprosy is a chronic bacterial disease caused by *Mycobacterium leprae*. Cytokines are known to play vital role as a peacekeeper during inflammatory and other immunocompromised conditions such as leprosy. This study has tried to bridge the gap of information on cytokine gene polymorphisms and its potential role in the pathogenesis of leprosy. Interleukin-10 (IL-10) is an immunosuppressive cytokine, found to be elevated in leprosy that accounted for the suppression of host's immune system by regulating the functions of other immune cells. T helper cells and T regulatory (Tregs) cells are the major source of IL-10 in lepromatous leprosy patients. In this study, we have documented the association of IL-10 cytokine gene polymorphism with the disease progression. A total of 132 lepromatous leprosy patients and 120 healthy controls were analyzed for IL-10 cytokine gene polymorphisms using PCR-SSP assay and flow cytometry was used to analyze IL-10 secretion by CD4 and Tregs in various genotype of leprosy patients. The frequencies of IL-10 (-819) TT and IL-10 (-1082) GG genotypes were significantly higher in leprosy patients as compared to healthy controls. This observation advocates that these genotypes were associated with the susceptibility and development of the disease. In addition, flow cytometry analysis demonstrated an increased number of IL-10 producing CD4 and Treg cells in IL-10 (819) TT genotype compared to CT and CC genotypes. These observations were further supported by immunohistochemical studies. Therefore, we can conclude that IL-10 cytokine gene polymorphisms by affecting its production can determine the predilection and progression of leprosy in the study population.

Keywords: cytokines, gene polymorphisms, leprosy, interleukin-10, regulatory T-cells, helper T-cells

INTRODUCTION

Leprosy is a bacterial disease caused by *Mycobacterium leprae* (*M. leprae*), which mainly affects macrophages and Schwann cells from the peripheral nerves. It offers an ideal model to study the host pathogen interaction and immune dysregulation in human because each clinical form of the disease is accompanied with the diverse levels of immunological alterations during

M. leprae infection (1). Leprosy disease is mainly classified into two forms, paucibacillary (PB) and multibacillary (MB). PB pole is associated with a strong cell-mediated immunity (CMI), and it is relatively resistant to the pathogens and localized infections. While, MB pole is characterized by the defective cell-mediated immune response comprising foamy macrophages in the dermis due to very high number of bacilli accompanied with the lesions all over the body parts. In between two poles of the disease, borderline forms of tuberculoid and lepromatous disease are laid which are immunologically unstable (2–4).

Cytokines play a vital role in activating host-pathogen interaction and in the immunopathogenesis of leprosy (2). PB form of the disease commencement correlates with Th1 (IL-2, IL-12, TNF-α, IFN-γ) cytokines with a localized infection but vigorous cell mediated immune response; whereas, MB form is associated with a Th2 and Th3 cytokine (IL-10, TGF-β, IL-4) response, presence of local skin lesions, prominent antibody production, but very weak CMI response (5). IL-10 and TGF-β appeared as the sole factor puts forth an anti-proliferative effect on Th1 and Th2 cells by perturbing the differentiation of either Th1 or Th2 cells and inhibition of pro-inflammatory cytokine production, that eventually result into the progression of Th3 immune response (6, 7). Our laboratory have previously reported the association of increased levels of IL-10 in lepromatous leprosy patients with high bacterial load of *M. leprae* and suppressed immune system of the host (2, 6). Furthermore, an increased frequency of IL-35 producing Tregs was observed in lepromatous leprosy patients, which is associated with the disease severity (8). Treg cells plays vital role in leprosy pathogenesis and fate of these cells also depends on cytokine milieu. This is supported from our previous study that explored the changes in the plasticity of Tregs under the influence of IL-12 and IL-23 treatment (9). Besides Tregs, another immunosuppressive population of γδ T cells plays an important role in the pathogenesis of leprosy (10, 11). IL-10, secreted by monocytes/macrophage, T cell subsets (Th2, Tregs) and B regulatory cells shows immune regulatory effects in case of human leprosy (12). IL-10-producing regulatory B cells transformed T effector cells into Tregs, thus enhanced regulatory T cells functions in human leprosy. Also, high levels of IL-10 are reported in lepromatous polar form compared with tuberculoid polar form and a low TNF-α/IL-10 ratio was found associated with disease progression (13). Single nucleotide polymorphisms (SNPs) are thought to be one of the most abundant causes of genomic variation in humans. The presence of SNPs in a gene can create differences in the structure and functions of a coded protein (14). Some SNPs are vital for the susceptibility and outcome of leprosy (13). Studies on IL-10 gene polymorphisms at −819 and −1082 positions within the promoter region have shown disease susceptibility and resistance between populations (15–17). Reports suggests that polymorphisms of the IL-10 promoters at positions −1082 (G/A), −819 (C/T), and −592 (C/A) are associated with the resistance against leprosy in Brazilian (18), Indian groups (15) and Columbian population (19).

Although cytokine gene polymorphism is associated with the susceptibility and resistance of a disease, but its association with cytokine production is not well studied. Therefore, the goal of current study is to investigate the association of IL-10 cytokine gene polymorphisms with Th and Treg cells mediated production of IL-10 and its association with the susceptibility and progression of leprosy in Indian population.

MATERIALS AND METHODS

Patients and Controls

A total of 132 leprosy patients (71 males, 61 females) with bacteriological index (BI) 2–6 and 120 healthy controls were recruited from Department of Dermatovenerology, AIIMS, New Delhi, India (**Table 1**). The study was approved by the Institute Ethics Committee, All India Institute of Medical Sciences (AIIMS), New Delhi. Patients and age matched healthy volunteers were recruited after obtaining their informed consent. All patients were without any history of mycobacterial, HIV or any other infection and belonging to the same geographical region as the patients were included and healthy controls.

Genotyping of SNPs for Cytokine Genes

Ten milliliters blood from each leprosy patients and healthy control was collected. 5 mL of blood in heparinized vials were subjected to DNA isolation and PCR–SSP assay, while and another 5 ml collected for IL-10 ELISA and flowcytometry. DNA was extracted by using phenol–chloroform method and stored at −80°C till further use. DNA was quantified by NanoDrop1000 spectrophotometer (Thermo Scientific NanoDrop 1000; NanoDrop Technologies, Wilmington, DE, United States) and samples having 260/280 ratio in the range of 1.82–1.86 were used for the PCR–SSP analysis. Subsequently, DNA was subjected to PCR amplification using Cytokine CTS–PCR–SSP Tray Kit (Heidelberg, Germany, United Kingdom) according to manufacturer's instructions and data was analyzed as described in earlier report (16) (**Supplementary Figure S1**).

ELISA

IL-10 cytokine level was quantified by ELISA (Ready Set Go, eBioscience, San Diego, CA, United States) as per manufacturer's instructions. Serum samples were tested in duplicates in a 96-wells plate (Nunc, Rochester, NY, United States) precoated with biotin conjugated anti-human antibodies IL-10. Protocol was followed according to the manufacturer's instructions and optical density of each well was measured at 450 nm.

TABLE 1 | Characteristics of the study population.

	Leprosy patients (*n* = 132)	Controls (*n* = 120)
Age (years)	***n* (%)**	***n* (%)**
Mean	38.4 ± 15.3	32.2 ± 13.1
Gender		
Male	71 (53.8)	74 (61.7)
Female	61 (46.2)	46 (38.3)

Leprosy patients were classified according to Ridley–Jopling classification.

PBMCs Isolation and Flow Cytometry

Blood samples were layered on ficoll-hypaque (Sigma Aldrich, United States), and mononuclear cells were isolated by centrifugation at 1,500 rpm for 25 min. Cells were washed thrice in sterile phosphate buffer saline (PBS) by centrifugation at 1,500 rpm for 10 min. Washed cells were resuspended in RPMI 1640 along with 10% fetal calf serum (Gibco, CA, United States) and cell viability and enumeration were estimated by 0.2% trypan blue using hemocytometer. 1×10^6 cells/ml were stimulated with *M. leprae* sonicated antigen (10 μg/ml) kindly provided by Dr. P. J. Brennan of Colorado State University. All the cultures were stimulated with IL-2, anti-CD3/CD28. After stimulation, cultures were incubated in 5% CO_2 incubator at 37°C for 48 h. After 48 h, cultured cells were harvested and stained with surface antibodies Alexa Fluor 488 Mouse Anti-Human CD4 (RPA-T4), APC-Cy7 Mouse Anti-Human CD25 (Clone: M-A251) for 60 min at 4°C in the dark. After surface staining, cells were incubated with intracellular staining buffer for 15 min at room temperature; cells were washed twice and permeabilized with 1X permeabilization buffer (eBioscience, United States) 30 min at room temperature. The cells were washed twice, resuspended in staining buffer, and incubated with PE Rat Anti-Human IL-10 (Clone: JES3-19F1). Staining was performed according to the specifications of the manufacturer. All the antibodies were obtained from BD Biosciences, San Diego, CA, United States. The cells were fixed in 400 μl of 2% paraformaldehyde and stored at 4°C. For intracellular staining, cultures were incubated with Protein Transport Inhibitor containing Monensin (BD Golgi Stop) for 4 h prior to harvest to block the secretion of cytokines. The data were collected using FACS Canto flow cytometer (BD Biosciences, United States) and analyzed cytometry along with isotype controls of phycoerythrin (PE mouse IgG1), Alexa Fluor 488 (mouse IgG1), APC Cy7 (mouse IgG1) using FlowJo software. Details of gating strategy are provided in **Supplementary Figure S2**.

Immunohistochemistry (IHC)

Five micrometer thick formalin fixed paraffin embedded tissues were cut by rotary microtome (Leica Biosystems Nussloch, Germany, United Kingdom). The sections were picked-up on poly L-lysine (Sigma Aldrich, St. Louis, MO, United States) coated glass slides and stored at room temperature. Rabbit anti human IL-10 antibody (Abcam, CA, United Kingdom) was used in the dilution of 1:100. Briefly, sections were first deparaffinized, followed by rehydration and blocking of endogenous peroxidase activity by 3% H_2O_2 and antigen-retrieval with Tris-EDTA (pH-9.0) buffer. The sections were incubated with 1% albumin for 1 h for blocking. After three washes with PBS, sections were incubated with anti-human IL-10 overnight at 4°C in humidified chamber. The sections were again subjected to three washes of PBS followed by incubation with secondary antibody anti rabbit IgG (VECTASTAIN® ABC-HRP Kit) for 30 min. Color was developed using diaminobenzidine (DAB1) chromogen system. Positive and negative stained cells were counted under the microscope using Image Pro express 6.0 software (Media cybernetics, United States) and percentage calculated from multiple fields.

Statistical Analysis

Genotype frequencies were obtained through direct counting. Data was analyzed using statistical software Graph-Pad Prism (San Diego, CA, United States). All categorical variables were expressed in *n* (%) and continuous variables were expressed in Mean ± SD. ANOVA was applied to compare the continuous variables between multiple groups; whereas *t*-test was applied to compare the two groups. Proportions of categorical variables among groups were compared using chi-Square test. Logistic regression analysis was used to calculate the Odds Ratio (OR). A *p*-value of <0.05 was considered to be statistically significant.

RESULTS

Association Between IL-10 (-819) CT/TT Genotypes With Leprosy Susceptibility

Mutations occurred more often in the IL-10 (anti-inflammatory cytokine) promoter gene than in the TNF-α (pro-inflammatory) promoter gene in all leprosy groups (18). Genotype distribution for IL-10 −819 (*C/T at −819: rs1800871)* are shown in **Table 2**. A significantly higher frequency of −819 TT genotype was observed in leprosy patients (59.8%) as compared to healthy controls (27.5%) ($p < 0.0001$, OR = 0.25, 95% CI 0.149–0.432). Contrasting to this, leprosy patients (7.6%) had significantly lower frequency of −819 CC genotype than the control subjects (20.8%) ($p = 0.002$, OR = 3.21, 95% CI 1.47–7.01). Genotype distribution analysis also revealed that 32.6% of leprosy patients and 51.7% of control subjects had −819 CT genotype ($p = 0.002$, OR = 2.21, 95% CI 1.31–3.68). These results demonstrate that substitution of C allele by T allele make the individuals susceptible toward the leprosy disease. As shown in **Table 2**, TT genotype has higher bacteriological index (BI: 4.2-6) as compared to the CC genotype (BI: 3-4). These data corelates BI with TT genotypes and pointing out that TT genotypes are susceptible and CC genotypes are resistance toward the *M. leprae* infection.

TABLE 2 | Distribution of IL-10 (*C/T at −819: rs1800871*) genotypes in leprosy patients and control subjects.

SNPs	Genotype	Controls	Patients	BI	OR (*P*-value)	CI
IL10-^{819}	CC	25 (20.8)	10 (7.6)	3.0–4.0	3.21 (0.002**)	1.470–7.011
	CT	62 (51.7)	43 (32.6)	2.5–4.5	2.21 (0.002**)	1.328–3.687
	TT	33 (27.5)	79 (59.8)	4.5–6.0	0.25 (<0.0001****)	0.149–0.432

*χ^2 test with contingency table for genotype between leprosy patients and control subjects, bacteriological index (BI), odds ratio (OR), p** > 0.005; p**** > 0.0005 and confidence interval (CI).*

TABLE 3 | Distribution of IL-10 (*G/A at −1082: rs1800896*) genotypes in leprosy patients and control subjects.

SNPs	Genotype	Controls	Patients	BI	OR (*P*-value)	CI
IL10-^{1082}	GG	11 (9.2)	34 (25.8)	4.8–6.0	0.29 (0.0006***)	0.140–0.605
	GA	49 (40.8)	50 (37.9)	3.0–4.5	1.13 (0.6987)	0.682–1.878
	AA	60 (50.0)	48 (36.5)	2.0–3.2	1.75 (<0.0289*)	1.057–2.897

*χ^2 test with contingency table for genotype between leprosy patients and control subjects, bacteriological index (BI), odds ratio (OR), *p < 0.05; ***p < 0.0005 and confidence interval (CI).*

Association Between IL-10 (-1082) GA/GG Genotypes and Leprosy Susceptibility and Resistance

Notably, a significantly higher frequency of the homozygous −1082 GG (*G/A at −1082: rs1800896)* genotype was observed when leprosy patients were compared with control subjects (25.8 vs. 9.2%) ($p = 0.0006$, OR = 0.29, 95% CI 0.139–0.605). Moreover, frequency of homozygous GA genotype was lower compared between leprosy patients and healthy controls at −1082GA position. We found a lower frequency in patient group (37.9%) compared to control group (40.8%) ($p = 0.698$, OR = 1.13, 95% CI 0.682–1.88). When leprosy patients (36.5%) were compared with controls (50%) at −1082AA position, significant difference was observed ($p = 0.03$, OR = 1.75, 95% CI 1.05–2.89) (**Table 3**). Higher bacteriological index (4.8–6) in GG genotype as compared to AA genotype (2–3.2) indicates its susceptibility toward leprosy as compared to AA genotype that showed resistance.

819TT Genotypes Are Higher Producer of T Helper Cells ($CD4^+IL\text{-}10^+$) IL-10 in Leprosy Patients

IL-10 is an anti-inflammatory cytokine produced by several immune cells like monocytes and macrophages, T cells, Treg cells as well as Breg cells (20). To find out the association of cytokine gene polymorphism with IL-10 production by T helper cells, we performed flowcytometry using CD4 and IL-10 antibodies. As shown in **Figures 1C,D**, IL-10 production by $CD4^+$ was affected by cytokine gene polymorphism at −819 position. IL-10 levels produced by CD4 cells were significantly higher in TT genotype as compared to CC genotype. CT genotype was also higher producer of IL-10 as compared to CC genotype, but lower than the TT genotype. These results suggest that the substitution of C by T allele does affect the IL-10 production by CD4 cells in leprosy patients. Increased IL-10 levels in serum of TT bearing genotype at IL-10^{-819} position as compared to CC genotype in leprosy patients further complemented these results (**Figures 1A,B**).

Increased Production of IL-10 in −819TT Genotypes by T Regulatory Cells ($CD4^+CD25^+IL\text{-}10^+$) in Leprosy Patients

To identify the frequency of Treg cells in various (CC, CT, TT) genotypes at −819 position in leprosy patients, immunophenotyping was done by using CD4, CD25 markers (**Figure 2A**) in PBMCs isolated from leprosy patients. Treg cells was profoundly augmented in TT genotype as compared to CC and CT genotypes in leprosy patients (**Figures 2A,B**). Increased Treg population in TT genotype patients suggested their important role in the host immune suppression observed in TT genotypes. To evaluate the functional enrichment of Treg cells in various genotypes (CC, CT and TT) in leprosy patients, we measured intracellular IL-10 production by flow cytometry (**Figure 2C**), using PBMCs derived from leprosy patients. Percentage of IL-10 producing Treg cells (CD4 + CD25 +) was significantly higher among TT genotypes in leprosy patients (**Figures 2C,D**) compared to that of CC and CT genotypes of leprosy patients ($P = 0.0003$). The augmentation of IL-10 producing Treg cells in TT genotypes directs their suppressive role by releasing IL-10. We also observed the simmiler pattern of IL-10 production by $CD4^+CD25^-$ cells in various genotypes (CC, CT and TT) of leprosy patients (**Figures 2E,F**).

Higher Expression of IL-10 in the Skin of IL-10 (-819) TT Genotype of Leprosy Patients

Expression of the IL-10 also measured in skin of leprosy patients bearing TT and CC genotypes at −819 position. The expression of the IL-10, was also significantly higher in the TT genotypes of leprosy patients as compared to CC genotype (**Figures 3A,B**). This again highlights that IL-10 producing immune cells are possibly recruited at the lesioned sites (which is more in TT genotype) of leprosy patients, where they facilitate their characteristic suppressive action. These results suggested that cytokine gene polymorphism at −819 position are associated with IL-10 production in leprosy patients and makes more susceptible toward leprosy.

DISCUSSION

During leprosy, there is a full-blown systemic activation of immune responses. As a result, leprosy is escorted by altered immune and imbalanced cytokine responses, which ultimately leads to excessive inflammation. Cytokines modulates the immune response of a host but cytokine gene polymorphism affects the cytokine production. This is the underlying reason to the distinct individual-specific immune responses. The idea behind studying the cytokine polymorphism in leprosy patients was: hypothetically a change either in regulatory region (promoter) or coding region is expected to modulate the expression of cytokines. A specific genotype either may result in low or high production of respective cytokine, which in turn could eventually alter the direction of immune response.

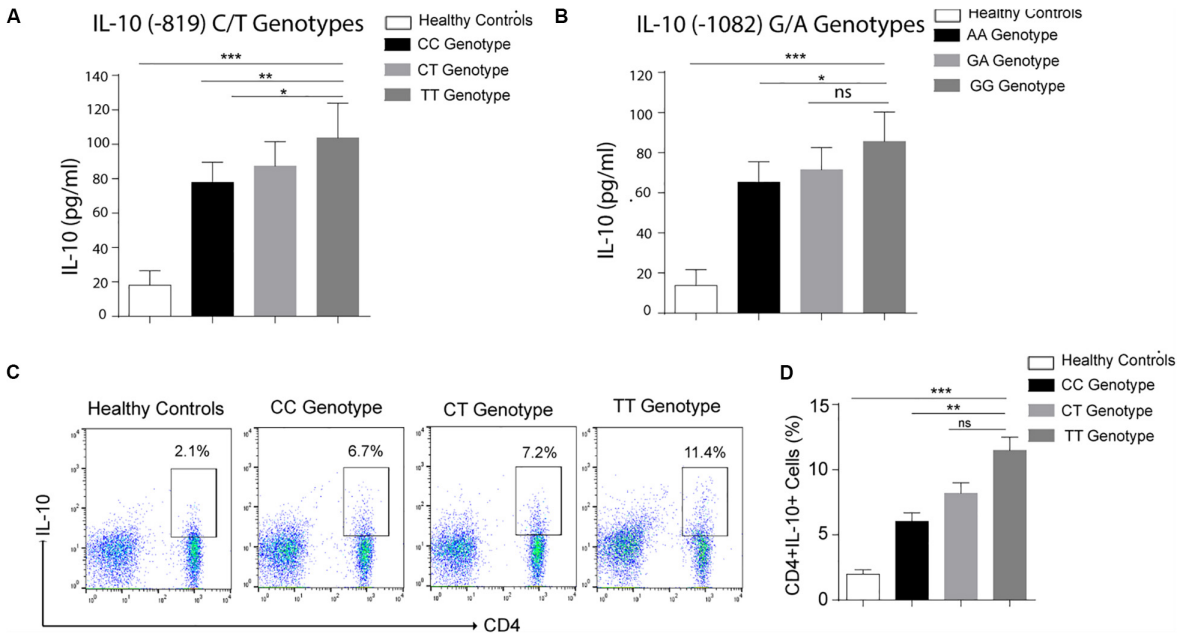

FIGURE 1 | Graph plot is showing IL-10 level in the serum of leprosy patients produced by various genotypes **(A)** Healthy controls (HCs), −819 CC, CT and TT genotypes **(B)** Healthy controls (HCs), 1082 AA, GA, and GG genotypes. **(C)** Representative FACS plot showing enumeration of T helper cell producing IL-10 ($CD4^+IL\text{-}10^+$) frequency in peripheral blood mononuclear cells isolated from leprosy patients with various genotypes (-819CC, CT and TT) and healthy controls (HCs) cultured with *M. leprae* sonicated antigen for 48 h. **(D)** Graph Plots are showing total interleukin-10 (IL-10) producing $CD4^+$ cells by various genotype (-819CC, CT and TT) in leprosy patients (n = 10) and healthy controls (HCs),Mean ± SD values are shown in each set while p value <0.05 was considered significant. 100,000 cells were acquired and analyzed by flow cytometry. Data analysis was performed with flowjo software. Statistical analysis was done using ANOVA test (*$p < 0.05$; **$p < 0.005$; ***$p < 0.0005$).

Increased IL-10 production has been observed in leprosy patients and up-regulation of IL-10 is a vital mechanism in the suppression of T cell-driven immune response (21). SNPs in IL-10 in the distal and the proximal regions are formed of haplotypes in the promoter gene, and such haplotypes were found to be associated with differential secretion of IL-10 cytokine (22). Our present data demonstrates that IL-10 −819 TT genotype frequency was greater among the leprosy patients than the control subjects. Frequency of GG genotype at IL-10 −1082 position was also higher in the leprosy patients as compared to healthy control. These results corroborate with our previous findings (16) and it has also been reported that the individuals in Brazilian population bearing IL10 −819 CC genotype were resistant to leprosy (18). Our results are further confirming the results of earlier findings that −819T allele and −819TT genotype were associated with leprosy susceptibility (17) in Indian population. These findings suggested that substitution of C by T at −819 in IL-10 promotor may be involved in differential cell mediated immune response in leprosy patients. It may also influence on the production of IL-10 levels as well as makes the individual susceptible toward leprosy. Moreover, a study by Malhotra et al. (17) suggested that −819TT and −1082GG are the most frequent genotype associated with susceptibility of leprosy. In our study, homozygous IL-10 −1082 GG genotype was significantly higher in leprosy patients compared to the controls, due to the predominance of G allele suggesting an impact for allele G in leprosy susceptibility. Similar findings have been observed by other groups, where they found that the extended genotype 1082GG, 819TT was associated with leprosy susceptibility (15). Moreover, another study by Pereira et al. demonstrated that −1082G/G genotype reinforced the results, indicating that the combination carrying −819TT and −1082G/G was associated with leprosy susceptibility (23).

To evaluate the association of cytokine gene polymorphism on its function, we tested leprosy patients and quantified IL-10 levels in various genotype −819 C/T and −1082 G/A. We observed elevated levels of IL-10 in −819TT and −1082GG genotypes in the serum of leprosy patients as compared to other genotypes. Thus, −819TT and −1082GG bearing genotypes were high IL-10 producers. These findings brought up a new direction to understand the pathogenesis of leprosy. These sustained high levels of IL-10 are necessary to lead leprosy to a chronic and T cells unresponsive state. Leprosy patient presents a state where genetic mosaicism is associated with cytokine production that dictates various immune reactions, resulting to ambiguous interpretations linked with the different clinical outcomes. IL-10 produced by various immune cells such as Tregs, Th2, Bregs and other cells suppresses the immune system of host and responsible for T cell anergy in leprosy patients (24–26). We want to address the source of IL-10 production by various genotypes in leprosy patients. To answer this, we have evaluated the expression of IL-10 in T helper and Treg cells of leprosy patients. Remarkably, IL-10 −819 TT and IL-10 −1082 GG genotypes were

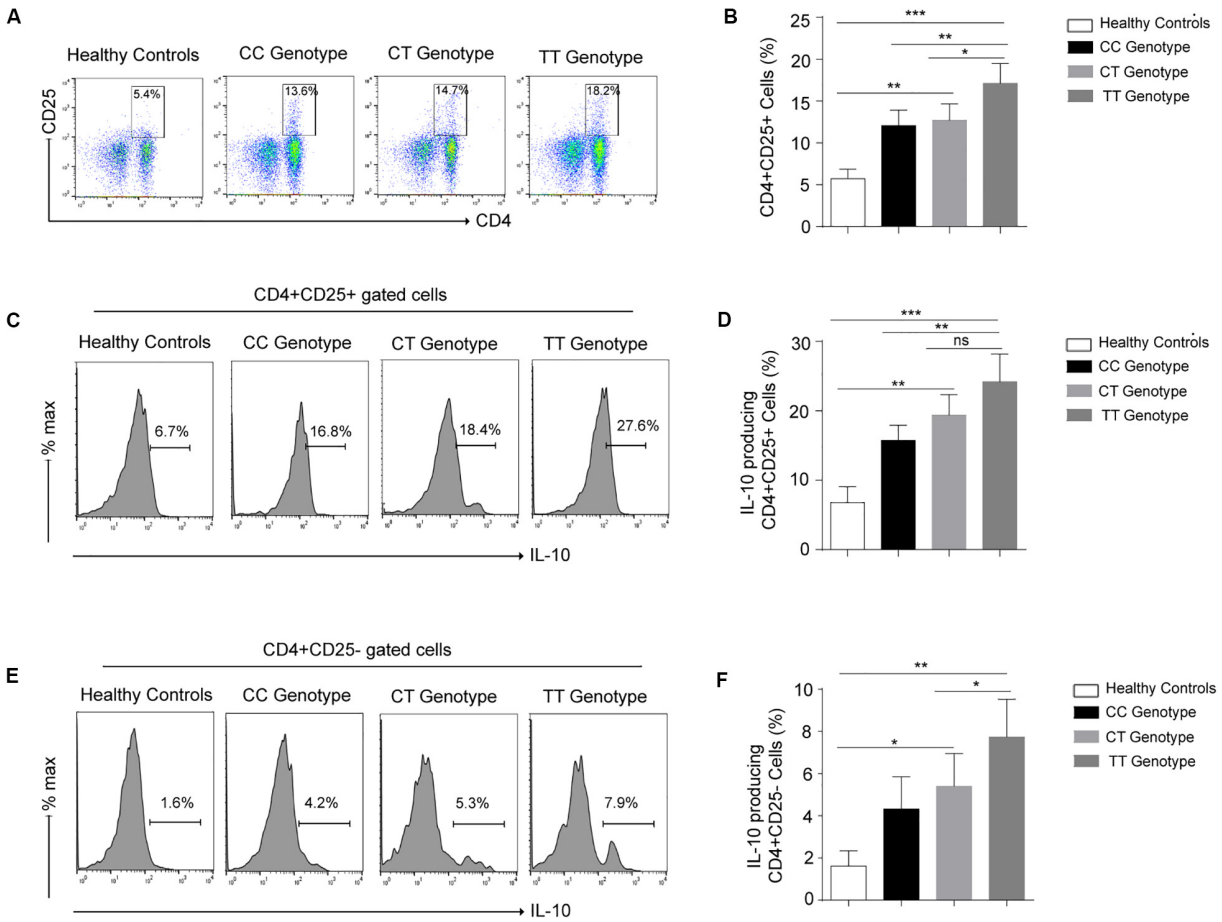

FIGURE 2 | (A) Representative cartoon showing T regulatory cells ($CD4^+CD25^+$) cells in peripheral blood mononuclear cells (PBMCs) isolated from peripheral blood of various genotypes (-819CC, CT and TT) of leprosy patient ($n = 10$) and healthy controls (HCs). **(B)** Graph plot is showing the percentage of T regulatory cells ($CD4^+CD25^+$) in various genotypes (-819CC, CT and TT) in leprosy patients and healthy controls (HCs). **(C)** Representative histogram showing expression of IL-10 in Treg ($CD4^+CD25^+$) cells in PBMCs isolated from peripheral blood of various genotypes of leprosy patient and healthy controls (HCs). **(D)** Graph plot is showing expression of IL-10 in Tregs in leprosy patients by various genotype and healthy controls (HCs). **(E)** Representative histogram showing secreation of IL-10 by ($CD4^+CD25^-$) cells in PBMCs isolated from peripheral blood of various genotypes of leprosy patient and healthy controls (HCs). **(F)** Graph plot is showing production of IL-10 by ($CD4^+CD25^-$) cells in leprosy patients by various genotype and healthy controls (HCs). Mean ± SD values are shown in each set while p value <0.05 was considered significant. 100,000 cells were acquired and analyzed by flow cytometry. Data analysis was performed with flowjo software. Statistical analysis was done using ANOVA test (*$p < 0.05$; **$p < 0.005$; ***$p < 0.0005$).

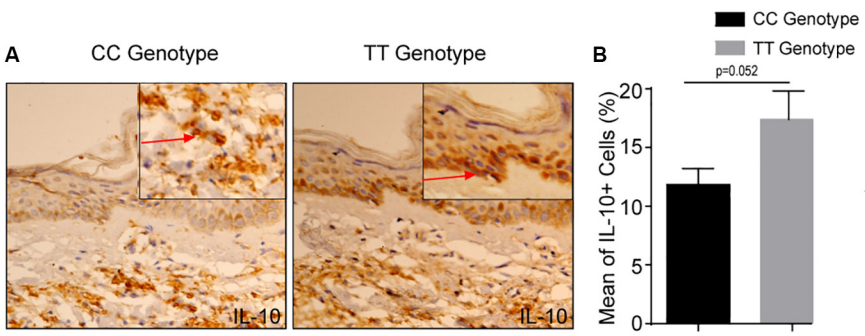

FIGURE 3 | (A) Increased IL-10 + cells in −819TT genotype in leprosy skin lesions. Immunohistochemistry on representative skin lesions from CC and TT genotypes of leprosy patients ($n = 5$). **(B)** Graph diagram showing increase of cells with IL-10^+ in TT genotype of leprosy patients as compared to CC genotype at −819 position. Bars indicate Mean ± SD of positive cells of 1,000 total cells. Statistical analysis was done using Student's t-test for unpaired samples (*$p < 0.05$).

appeared as high producer of IL-10 by T helper as well as T regulatory cells. Increased level of IL-10 was found to be logical and supported our previous reports (12, 16). This data designates that high amount of IL-10 in the microenvironment suppresses the host immune system, that eventually may help in expansion of *M. leprae* continually in leprosy patients, as high bacteriological index correlates with high level of IL-10 in −819TT and −1082 GG genotypes. Therefore, it can be inferred here that the patients with −819TT and −1082 GG genotypes are bearing higher risks of the growth of *M. leprae*.

Since leprosy is a chronic inflammatory disease and its severity is associated to the host immune response, and the level of IL-10 production can be vital to define disease outcome. Our data point-outs the conclusive association of the −819TT and −1082 GG genotypes with the susceptibility of leprosy and suggests that these polymorphisms have remarkable role in higher production of IL-10 by T helper and T regulatory cells.

DATA AVAILABILITY STATEMENT

The datasets presented in this study can be found in online repositories. The names of the repository/repositories and accession number(s) can be found in the article/ **Supplementary Material**.

ETHICS STATEMENT

The studies involving human participants were reviewed and approved by The Institute Ethics Committee, All India Institute of Medical Sciences (AIIMS), New Delhi, India (IESC/T-417/01.11.2013). The patients/participants provided their written informed consent to participate in this study.

AUTHOR CONTRIBUTIONS

MT, HN, and CS designed experiments. MT, HS, and CS performed experiments and analyzed the data. MT, HN, and MS wrote the manuscript. NK contributed to clinical diagnosis. AS, HS, and CS critically reviewed the manuscript. All authors discussed the results and contributed to the final manuscript and reviewed manuscript.

SUPPLEMENTARY MATERIAL

The Supplementary Material for this article can be found online at: https://www.frontiersin.org/articles/10.3389/fimmu.2020.01974/full#supplementary-material

REFERENCES

1. Ridley DS, Jopling WH. Classification of leprosy according to immunity. A five-group system. *Int J Lepr Other Mycobact Dis.* (1966) 34:255–73.
2. Tarique M, Saini C, Naz H, Naqvi RA, Khan FI, Sharma A. Fate of T cells and their secretory proteins during the progression of leprosy. *Curr Protein Pept Sci.* (2018) 19:889–99. doi: 10.2174/1389203718666170829120729
3. Saini C, Tarique M, Rai R, Siddiqui A, Khanna N, Sharma A. T helper cells in leprosy: an update. *Immunol Lett.* (2017) 184:61–6. doi: 10.1016/j.imlet.2017.02.013
4. Yamamura M, Uyemura K, Deans RJ, Weinberg K, Rea TH, Bloom BR, et al. Defining protective responses to pathogens: cytokine profiles in leprosy lesions. *Science.* (1991) 254:277–9. doi: 10.1126/science.1925582
5. Alcais A, Mira M, Casanova JL, Schurr E, Abel L. Genetic dissection of immunity in leprosy. *Curr Opin Immunol.* (2005) 17:44–8. doi: 10.1016/j.coi.2004.11.006
6. Kumar S, Naqvi RA, Khanna N, Pathak P, Rao DN. Th3 immune responses in the progression of leprosy via molecular cross-talks of TGF-beta. CTLA-4 and Cbl-b. *Clin Immunol.* (2011) 141:133–42. doi: 10.1016/j.clim.2011.06.007
7. Saini C, Ramesh V, Nath I. Increase in TGF-beta secreting CD4(+)CD25(+) FOXP3(+) T regulatory cells in anergic lepromatous leprosy patients. *PLoS Negl Trop Dis.* (2014) 8:e2639. doi: 10.1371/journal.pntd.0002639
8. Tarique M, Saini C, Naqvi RA, Khanna N, Rao DN. Increased IL-35 producing Tregs and CD19(+)IL-35(+) cells are associated with disease progression in leprosy patients. *Cytokine.* (2017) 91:82–8. doi: 10.1016/j.cyto.2016.12.011
9. Tarique M, Saini C, Naqvi RA, Khanna N, Sharma A, Rao DN. IL-12 and IL-23 modulate plasticity of FoxP3(+) regulatory T cells in human Leprosy. *Mol Immunol.* (2017) 83:72–81. doi: 10.1016/j.molimm.2017.01.008
10. Saini C, Tarique M, Ramesh V, Khanna N, Sharma A. Gammadelta T cells are associated with inflammation and immunopathogenesis of leprosy reactions. *Immunol Lett.* (2018) 200:55–65. doi: 10.1016/j.imlet.2018.07.005
11. Tarique M, Naqvi RA, Ali R, Khanna N, Rao DN. CD4(+) TCRgammadelta(+) FoxP3(+) cells: an unidentified population of immunosuppressive cells towards disease progression leprosy patients. *Exp Dermatol.* (2017) 26:946–8. doi: 10.1111/exd.13302
12. Tarique M, Naz H, Kurra SV, Chaman S, Raza AN, Reeta R, et al. Interleukin-10 producing regulatory B cells transformed CD4(+)CD25(-) into tregs and enhanced regulatory T Cells function in human leprosy. *Front Immunol.* (2018) 9:1636. doi: 10.3389/fimmu.2018.01636
13. Cardoso CC, Pereira AC, De Sales Marques C, Moraes MO. Leprosy susceptibility: genetic variations regulate innate and adaptive immunity, and disease outcome. *Future Microbiol.* (2011) 6:533–49. doi: 10.2217/fmb.11.39
14. Suh Y, Vijg J. SNP discovery in associating genetic variation with human disease phenotypes. *Mutat Res.* (2005) 573:41–53. doi: 10.1016/j.mrfmmm.2005.01.005
15. Moraes MO, Pacheco AG, Schonkeren JJ, Vanderborght PR, Nery JAC, Santos AR, et al. Interleukin-10 promoter single-nucleotide polymorphisms as markers for disease susceptibility and disease severity in leprosy. *Genes Immun.* (2004) 5:592–5. doi: 10.1038/sj.gene.6364122
16. Tarique M, Naqvi RA, Santosh KV, Kamal VK, Khanna N, Rao DN. Association of TNF-alpha-(308(GG)), IL-10(-819(TT)), IL-10(-1082(GG)) and IL-1R1(+1970(CC)) genotypes with the susceptibility and progression of leprosy in North Indian population. *Cytokine.* (2015) 73:61–5. doi: 10.1016/j.cyto.2015.01.014
17. Malhotra D, Darvishi K, Sood S, Swarkar S, Chander G, Vineet R, et al. IL-10 promoter single nucleotide polymorphisms are significantly associated with resistance to leprosy. *Hum Genet.* (2005) 118:295–300. doi: 10.1007/s00439-005-0042-8
18. Santos AR, Suffys PN, Vanderborght PR, Milton OM, Leila MMV, Pedro HC, et al. Role of tumor necrosis factor-alpha and interleukin-10 promoter gene polymorphisms in leprosy. *J Infect Dis.* (2002) 186:1687–91. doi: 10.1086/345366
19. Cardona-Castro N, Sanchez-Jimenez M, Rojas W, Bedoya-Berrio G. IL-10 gene promoter polymorphisms and leprosy in a Colombian population sample. *Biomedica.* (2012) 32:71–6. doi: 10.7705/biomedica.v32i1.386
20. Okeke EB, Uzonna JE. The pivotal role of regulatory T cells in the regulation of innate immune cells. *Front Immunol.* (2019) 10:680. doi: 10.3389/fimmu.2019.00680

21. Misra N, Selvakumar M, Singh S, Bharadwaj M, Ramesh V, Misra RS, et al. Monocyte derived IL 10 and PGE2 are associated with the absence of Th 1 cells and in vitro T cell suppression in lepromatous leprosy. *Immunol Lett.* (1995) 48:123–8. doi: 10.1016/0165-2478(95)02455-7
22. Gibson AW, Edberg JC, Wu J, Westendorp RG, Huizinga TW, Kimberly RP. Novel single nucleotide polymorphisms in the distal IL-10 promoter affect IL-10 production and enhance the risk of systemic lupus erythematosus. *J Immunol.* (2001) 166:3915–22. doi: 10.4049/jimmunol.166.6.3915
23. Pereira AC, Brito-de-Souza VN, Cardoso CC, Dias-Baptista IMF, Parelli FPC, Venturini J, et al. Genetic, epidemiological and biological analysis of interleukin-10 promoter single-nucleotide polymorphisms suggests a definitive role for −819C/T in leprosy susceptibility. *Genes Immun.* (2009) 10:174–80. doi: 10.1038/gene.2008.97
24. Stewart CA, Metheny H, Iida N, Loretta S, Miranda H, Folkert S, et al. Interferon-dependent IL-10 production by Tregs limits tumor Th17 inflammation. *J Clin Invest.* (2013) 123:4859–74. doi: 10.1172/JCI65180
25. Akdis CA, Blaser K. Mechanisms of interleukin-10-mediated immune suppression. *Immunology.* (2001) 103:131–6. doi: 10.1046/j.1365-2567.2001.01235.x
26. Saini C, Kumar P, Tarique M, Sharma A, Ramesh V. Regulatory T cells antagonize proinflammatory response of IL-17 during cutaneous tuberculosis. *J Inflamm Res.* (2018) 11:377–88. doi: 10.2147/JIR.S172878

Conflict of Interest: The authors declare that the research was conducted in the absence of any commercial or financial relationships that could be construed as a potential conflict of interest.

frontiers in Immunology

ORIGINAL RESEARCH
published: 01 October 2020
doi: 10.3389/fimmu.2020.542210

Polymorphism in the Promoter Region of the *IL18* Gene and the Association With Severity on Paracoccidioidomycosis

Paula Keiko Sato [1,2†], Felipe Delatorre Busser [1,2†], Flávia Mendes da Cunha Carvalho [1,3‡], Alexandra Gomes dos Santos [1,3], Aya Sadahiro [4], Constancia Lima Diogo [1,2], Adriana Satie Gonçalves Kono [5], Maria Luiza Moretti [6], Olinda do Carmo Luiz [7] and Maria Aparecida Shikanai-Yasuda [1,2,3*]*

[1] Laboratory of Medical Investigation in Immunology (LIM48), Faculdade de Medicina, Hospital das Clínicas, University of São Paulo, São Paulo, Brazil, [2] Institute of Tropical Medicine, Faculdade de Medicina, University of São Paulo, São Paulo, Brazil, [3] Department of Infectious and Parasitic Diseases, Faculdade de Medicina, University of São Paulo, São Paulo, Brazil, [4] Department of Parasitology, Instituto de Ciências Biológicas, Federal University of Amazonas, Manaus, Brazil, [5] Infectious Diseases Division, Hospital das Clínicas, University of São Paulo, São Paulo, Brazil, [6] Faculdade de Ciências Médicas, Hospital das Clínicas, State University of Campinas, Campinas, Brazil, [7] Department of Preventive Medicine, Faculdade de Medicina, University of São Paulo, São Paulo, Brazil

Paracoccidioidomycosis (PCM) is an important endemic, systemic disease in Latin America caused by *Paracoccidioides* spp. This mycosis has been associated with high morbidity and sequels, and its clinical manifestations depend on the virulence of the infecting strain, the degree and type of immune response, infected tissues, and intrinsic characteristics of the host. The T helper(Th)1 and Th17/Th22 cells are related to resistance and control of infection, and a Th2/Th9 response is associated with disease susceptibility. In this study, we focused on interleukin(IL)-12p35 (*IL12A*), IL-18 (*IL18*), and IFN-γ receptor 1 (*IFNGR1*) genetic polymorphisms because their respective roles have been described in human PCM. Real-time PCR was employed to analyze *IL12A* -504 G/T (rs2243115), *IL18* -607 C/A (rs1946518), and *IFNGR1* -611 A/G (rs1327474) single nucleotide polymorphisms (SNP). One hundred forty-nine patients with the acute form (AF), multifocal chronic (MC), or unifocal chronic (UC) forms of PCM and 110 non-PCM individuals as a control group were included. In the unconditional logistic regression analysis adjusted by ethnicity and sex, we observed a high risk of the *IL18* -607 *A*-allele for both AF [$p = 0.015$; OR = 3.10 (95% CI: 1.24–7.77)] and MC groups [$p = 0.023$; OR = 2.61 (95% CI: 1.14–5.96)] when compared with UC. The *IL18* -607 *A*-allele associated risk for the AF and MC groups as well as the protective role of the *C*-allele in UC are possibly linked to higher levels of IL-18 at different periods of the course of the disease. Therefore, a novel role of *IL18* -607 C/A SNP is shown in the present study, highlighting its importance in the outcome of PCM.

Keywords: paracoccidioidomycosis, *Paracoccidioides* spp., single nucleotide polymophism, IL18, IL12A, IFNGR1, clinical forms of paracoccidioidomycosis

OPEN ACCESS

Edited by:
Adriana Malheiro, Federal University of Amazonas, Brazil

Reviewed by:
Yean Kong Yong, Xiamen University Malaysia, Malaysia
Anamelia Lorenzetti Bocca, University of Brasilia, Brazil

***Correspondence:**
Paula Keiko Sato
paula.s@hc.fm.usp.br
Maria Aparecida Shikanai-Yasuda
masyasuda@yahoo.com.br

[†] These authors have contributed equally to this work

[‡] Present address:
Flávia Mendes da Cunha Carvalho, Structural Biology Unit, Laboratory of Medical Investigation in Immunopathology of Schistosomiasis and Other Parasitoses (LIM06), Faculdade de Medicina, Hospital das Clínicas, University of São Paulo, São Paulo, Brazil

Specialty section:
This article was submitted to Microbial Immunology, a section of the journal Frontiers in Immunology

Received: *11 March 2020*
Accepted: *21 August 2020*
Published: *01 October 2020*

Citation:
Sato PK, Busser FD, Carvalho FMC, Gomes dos Santos A, Sadahiro A, Diogo CL, Kono ASG, Moretti ML, Luiz OC and Shikanai-Yasuda MA (2020) Polymorphism in the Promoter Region of the IL18 Gene and the Association With Severity on Paracoccidioidomycosis. Front. Immunol. 11:542210. doi: 10.3389/fimmu.2020.542210

INTRODUCTION

Paracoccidioidomycosis (PCM) is one of the main endemic, systemic mycoses in Latin America, and it is caused by the thermally dimorphic fungi of the *Paracoccidioides brasiliensis* (*P. brasiliensis*) complex (*Paracoccidioides* spp.) and *Paracoccidioides lutzii*. PCM is associated with high morbidity and sequels; however, because it is not a compulsorily notified disease in Brazil, the actual data are based on reports of epidemiological surveys, case series, hospitalization, and mortality data (1). It is endemic in the southeast, central west, and south regions of Brazil and estimated at 0.71–2.70/100,000 inhabitants/year (2). Epidemic areas have been reported in the western Brazilian areas with a mean incidence of 9.4/100,000 and peaks of 37–39/100,000 inhabitants (3).

The inhalation of conidia of *Paracoccidioides* spp. can result in infection without symptoms, acute or chronic disease, or in sequelae. The clinical manifestations depend on the virulence of the infecting strain, the degree and type of immune response, infected tissues, and intrinsic characteristics of the host (4).

Some components of the innate immunity, such as neutrophils, dendritic cells, toll-like receptors, dectin-1, myeloid differentiation primary response 88 (MyD88), and NOD-like receptor P3 (NLRP3) inflammasome, have been evaluated in both experimental and human PCM (5–10). However, it is the adaptive response to *P. brasiliensis* that has been extensively studied with a well-established murine model and characterization of clinical forms of PCM by T helper (Th) responses and antibodies (11).

The acute form of PCM shows a mixed Th2/Th9 response: increased levels of IL-4, IL-5, IL-9, IL-10, TGF-β, and IL-27; low production of IFN-γ and TNF-α; and high levels of specific IgG4 and IgE antibodies. On the other hand, the chronic form presents a Th17/Th22 profile with high production of IL-17 and IL-22 and also secreting Th1-type cytokines, such as IFN-γ, TNF-α, and IL-2 as well as variable levels of IL-10 and IL-4 and increased levels of specific IgG1 antibodies (12, 13). Therefore, the Th2/Th9 responses can be associated with susceptibility to PCM, and the presence of Th1 and Th17/Th22 cells can contribute to more mild clinical manifestations with the axis IFN-γ/IL-12 directly associated with protection and control of the infection (11–16).

The high-affinity binding of IL-12 to its receptor results in the differentiation of naïve CD4 T cells into Th1 lymphocytes, which are the major producers of IFN-γ, alongside NK cells. In the presence of IL-12, IL-18 also stimulates the production of IFN-γ, inducing a Th1-mediated immune response; in the absence of IL-12, IL-18 can stimulate a Th2 response (17, 18).

Higher levels of IL-18 and sTNF-RII are described in the acute form of PCM when compared with the chronic form and controls, and IL-12 is also higher in patients than in controls (19). The same group reports higher levels of IL-18 during treatment and lower levels after antifungal treatment (20). As the disease is more severe in the acute form with high IL-18 levels, the authors suggest that this cytokine could be a useful marker of PCM severity.

Previous studies on murine PCM have shown that IL-12 and IL-18 secretions are associated with innate immunity factors. MyD88-deficient mice show a more severe disease after 8 weeks of infection with low levels of IL-12, and a protective role in murine pulmonary PCM was shown in the NLRP3 inflammasome, associated with IL-1β and IL-18 secretion and expansion of Th1 and Th17 cells and suppressive control of T-reg cells (7, 21).

The mechanisms controlling these effects are unclear, but reports on genetic background in both human and experimental disease have been shedding light on this matter. For instance, an autosomal dominant gene has been associated with resistance in murine PCM (22), and in human disease, reports show the influence of the human leukocyte antigen (HLA) in both susceptibility and outcomes. The HLA class I, HLA-B13, was found in a higher proportion in PCM patients compared to controls as well as a higher frequency of HLA-A9 in patients with the progressive pulmonary form (23). In parallel, increased risk of PCM development was associated with the presence of HLA-B40, which was found more in patients than in controls (24, 25). In 2011, the class II-HLA-DRB1*11 allele was reported in a higher frequency in patients with the more benign clinical presentation of this disease, the unifocal chronic (UC) form (26). Moreover, PCM patients were shown to have a higher proportion of the non-expressed C4B allele, C4B*Q0, of deficient C4 isotypes, suggesting to the authors a possible influence of different C4 isotype and allotype frequencies in the course of infection (27).

In addition, an enzyme phenotype (GLO-1 phenotype of glyoxalase I) was associated with PCM infection represented by a positive intradermic reaction, and a possible relationship with HLA antigens deserves further discussion because there is a close linkage between the GLO phenotype and HLA (28).

Our group and others have been studying single nucleotide polymorphisms (SNPs) and different mutations on cytokines and receptor genes. For instance, the inherited mutation Leu77Phe on the IL-12 receptor β1 subunit (IL-12Rβ1) gene (*IL12RB1*) associated with its loss of function and complete deficiency, resulting in a severe, acute form of PCM (29). Moreover, in Brazilian patients with PCM, reports of polymorphisms on IL-4 and IL-12Rβ1 genes have shown the relevance of *IL4* -590 C/T and *IL12RB1* 641 A/G SNPs in association with infection or clinical forms, contributing to a better understanding of the immunopathogenesis of this disease (30, 31).

Polymorphisms on the IFN-γ gene have also been described in infectious diseases, such as toxoplasmosis, tegumentar leishmaniasis, and PCM, and no association between alleles or genotypes and these diseases was observed (31–35). Furthermore, it is also necessary to consider that the expression of the IFN-γ receptor could be interfering in the axis IL-12/IFN-γ because its deficiency was already described in the more disseminated forms of histoplasmosis, coccidioidomycosis, mycobacteriosis, and disseminated BCG infection (36–39). This deficient expression could be associated with a mutation in the IFN-γ receptor 1 gene, such as the *IFNGR1* -611 A/G SNP, which has been associated with strong promoter activity and with decreased risk of pulmonary tuberculosis (40, 41).

IL-12p70, the bioactive form of IL-12, is a heterodimer of two subunits: p35 (encoded by the *IL12A* gene) and p40 (encoded by the *IL12B* gene). No association was found between *IL12B* +1188

A/C SNP and PCM (31). SNPs in the *IL12A* gene, on the other hand, have not yet been explored in this mycosis.

Studies show an association of *IL18* -607 C/A SNP (rs1946518) with protection or risk in several infections (42–45). However, as with the *IL12A* -504 G/T (rs2243115) and the *IFNGR1* -611 A/G (rs1327474) SNPs, there are still no studies associating this genetic polymorphism with systemic fungal infections.

Considering the interaction between IL-18, IL-12, and IFN-γ and the genetic aspects possibly involved in susceptibility to PCM and the lack of studies on this disease, the present study aimed to analyze the *IL18* -607 C/A (rs1946518), *IL12A* -504 G/T (rs2243115), and *IFNGR1* -611 A/G (rs1327474) SNPs, for the first time to our knowledge, in a cohort of Brazilian patients with PCM, also presenting a brief review of studies on these SNPs in infectious diseases.

MATERIALS AND METHODS

Subjects

A total of 149 patients with PCM from the General Infirmary and Systemic Mycosis Outpatient Clinic from the Infectious Diseases Division (Hospital das Clínicas, Faculdade de Medicina, University of São Paulo—HCFMUSP, São Paulo, SP, Brazil) were included in the study (**Table 2**). Thirty-nine patients had the acute form of PCM (AF) and 110 had the chronic form (CF); 93 had the multifocal chronic form (MC) and 17 had the UC form. This classification was performed according to Franco et al. (46). UC includes only patients with mild, restricted disease to the skin, mucosae, or lymph nodes without lung or cerebral involvement. The control group (CO) included 110 non-PCM subjects. The study protocol was approved by the ethics committee of HCFMUSP (CAPPesq 10273; Plataforma Brasil 123334/2013), and all subjects gave written informed consent in accordance with the Declaration of Helsinki.

The inclusion criteria were (a) patients with PCM: identification of *Paracoccidioides* spp. by mycological and/or histopathological examination and/or presence of anti-*P. brasiliensis* serum antibodies (titers ≥32 on counterimmunoelectrophoresis test) at the moment of enrollment or proven in the past; and (b) CO: individuals considered healthy without a previous history of the disease, not sensitized in lymphoproliferation assays against the 43-kDa glycoprotein of *P. brasiliensis*, and absence of serum anti-*P. brasiliensis* antibodies (by immunodiffusion test). Subjects with comorbidities, such as neoplasia and other acute or chronic systemic infectious diseases, were excluded.

DNA Extraction

Genomic DNA was obtained from peripheral blood leukocytes by the salt precipitation method (DTAB/CTAB; dodecyl trimethyl ammonium bromide/cetyltrimethyl ammonium bromide, both from Sigma-Aldrich, Merck, St. Louis, MO, USA) as previously described (47). The concentration and purity of the extracted DNA were evaluated by a UV spectrophotometer (Nanodrop LITE, Thermo Fisher Scientific, Carlsbad, CA, USA).

Detection of SNPs

The SNPs in the IL-12p35 (*IL12A* -504 G/T, rs2243115), IL-18 (*IL18* -607 C/A, rs1946518), and IFN-γ receptor 1 (*IFNGR1* -611 A/G, rs1327474) genes were investigated by real-time PCR using specific oligonucleotides and probes labeled with VIC (wild allele) or FAM (mutated allele) fluorochromes and TaqMan™ Genotyping Master Mix (all from Molecular Probes, Thermo Fisher Scientific, Carlsbad CA, USA). The assays and results were performed and analyzed with the StepOne Plus Real Time PCR System and software (Applied Biosystems, Thermo Fisher Scientific, Foster City, CA, USA).

Statistical Analysis

The deviations from the Hardy–Weinberg equilibrium and the distribution of genotypic and allelic frequencies of the SNPs on *IL12A*, *IL18*, and *IFNGR1* genes in the studied population were evaluated by Pearson's χ^2 test. To estimate the risk of patients with AF, MC, and UC PCM associated with genotypes and alleles, odds ratios (ORs) and 95% confidence intervals (95% CIs) were calculated as approximations of relative risk using unconditional logistic regression analysis. For ordered variables, tests for linear trend were done by categorizing the exposure variables and entering the scores as continuous. To verify the strength of association between the final events, we performed univariate and multivariate logistic analyses adjusted by ethnicity and sex with the STATA 14.0 software (StataCorp, College Station, TX, USA), and p-values ≤0.05 were considered statistically significant.

RESULTS

Considering the plausible role of genetic background in human PCM, we summarize all previously reported SNPs or mutations on immune-related genes and their main results on Brazilian patients in **Table 1**. Eight SNPs or mutations on DC-SIGN, HLA, IL-4, IL-10, IL-12Rβ1, and Vitamin D receptor genes were found to have an association with risk, outcome, or clinical forms of PCM. As the SNPs of this study had not yet been evaluated on PCM patients, we also compiled previous reports on the *IL18* (-607 C/A, rs1946518 and -137 G/C, rs187238), *IL12A* (-504 G/T, rs2243115), and *IFNGR1* (-611 A/G, rs13277474) SNPs and their association with diverse infectious diseases (**Supplementary Tables 1**–**3**, respectively).

This study evaluated the *IL18* -607 C/A, *IL12A* -504 G/T, and *IFNGR1* -611 A/G SNPs in 149 patients with the AF and CF of PCM and 110 control individuals (CO). The CF group is subclassified as MC and UC forms. There were no statistically significant differences between cases and controls in the distribution of ethnic groups or sex (data not shown). Regarding the different groups of patients (AF, MC, and UC), no differences in ethnic distribution were found ($p = 0.476$). However, in the univariate analysis of sex distribution, there was a significant difference between these groups with a male majority on a ratio of 17.6 in the MC group (**Table 2**).

Genotypic frequencies for the three evaluated SNPs were in Hardy–Weinberg equilibrium (data not shown). The distribution of genotypic and allelic frequencies of *IL12A* -504 G/T, *IL18* -607 C/A, and *IFNGR1* -611 A/G SNPs among patients and controls

TABLE 1 | Polymorphisms on immune-related genes in Brazilian patients with PCM.

Structure (gene)	Mutation (rs)	Main results	References
CTLA-4 (*CTLA4*)	−318 C/T and +49 A/G[a]	• No differences between patients and controls	(48)
DC-SIGN (*DCSIGN*)	rs4804803	• Genotype *DCSIGN-GG* on patients with oral PCM ($p = 0.032$)	(49)
FCγ-RIIa (*FCGR2A*)	rs1801274	• No differences between patients and controls	(49)
HLA (*HLA*)	HLA-DRB1 and HLA-DQB1 alleles[a]	• *HLA-DRB1*11* allele associated with UC form of PCM ($p = 0.039$)	(26)
IFN-γ (*IFNG*)	+874 T/A[a]	• No differences between patients and controls	(35)
	+874 T/A (rs2430561)	• No differences between patients and controls	(31)
		• No differences between clinical forms of PCM	
IL-4 (*IL4*)	−590 T/C[a]	• Patients with *C*-allele produce more IL-4 than those with *T*-allele ($p < 0.05$)	(35)
		• No differences between patients and controls	(30)
	Intron-3 microsatellite *RP1*/*RP2*[a]	• Genotypes *RP2*/*RP2* on patients and *RP1*/*RP1* on controls (with low IL-4 expression): $p = 0.0042$	(30)
IL-10 (*IL10*)	−1082 G/A[a]	• Genotypes *IL10-GG* on patients and *IL10-AA* on controls ($p = 0.0218$)	(34)
IL-12p40 (*IL12B*)	+1188 A/C (rs3212227)	• No differences between patients and controls	(31)
		• No differences between clinical forms of PCM	
IL-12Rβ1 (*IL12RB1*)	230 T/C Leu77Phe[a]	• Inherited IL-12Rβ1 deficiency leading to acute form of PCM	(29)
	641 A/G (rs11575834)	• No differences between patients and controls	(31)
		• Male patients: Genotype *IL12RB1-AA* on MC form and *IL12RB1-AG* on UC form ($p = 0.048$)	
JAK1	rs11208534	• No differences between patients and controls	(49)
TNF-α (*TNFA*)	−308 G/A[a]	• No differences between patients and controls	(34)
	rs1800629	• No differences between patients and controls	(49)
Vitamin D Receptor (*VDR*)	rs7975232	• Genotype *VDR-CC* ($p < 0.001$) and *C*-allele ($p = 0.027$) on patients	(49)

[a]*rs not informed or not applicable.*

TABLE 2 | Distribution (*n*), sex (M = Male; F = Female) and ethnicity (W = White; B = Black) ratio, and *p*-values among the groups of patients with acute, multifocal chronic and unifocal chronic forms of PCM.

Clinical forms of PCM	*n*	Sex ratio (M/F)	*p*	Ethnicity ratio (W/B)	*p*
Acute	39	1.8 (25/14)	0.000	1.2 (12/10)	0.476
Multifocal chronic	93	17.6 (88/5)		2.1 (57/27)	
Unifocal chronic	17	2.4 (12/5)		2.5 (10/4)	

and among AF and CF groups is shown in **Table 3**. We found no statistical significances in the univariate analysis of genotypic frequencies in the codominant, dominant, and recessive models nor in the distribution and frequencies of alleles.

In **Table 4**, we show the distribution of genotypic and allelic frequencies of *IL12A* -504 G/T, *IL18* -607 C/A, and *IFNGR1* -611 A/G SNPs among the groups of patients with the different clinical forms of PCM, analyzed by unconditional logistic regression with adjustments for ethnicity and sex. The comparison between AF, MC, and UC genotypic distribution did not result in a statistical difference.

Regarding the allelic distribution and frequencies of *IL18* -607 C/A SNP, unconditional logistic regression with adjustments for ethnicity and sex shows significant differences between AF and UC [$p = 0.015$; OR = 3.1 (95% CI: 1.24–7.77)] with a higher frequency of the *A*-allele in AF (53.8%) than in UC (26.5%) (**Tables 4**, **5**). The same is observed in the comparison between MC and UC [$p = 0.023$; OR = 2.61 (95% CI: 1.14–5.96)]. Concerning alleles of *IL12A* -504 G/T and *IFNGR1* -611 A/G SNPs, no statistical differences were found. Furthermore, **Table 5** shows the statistical data on sex and ethnicity as covariates of *IL18* -607 C/A SNP in the distribution of genotypes and alleles. There was a significant difference of sex distribution between AF and MC with a higher proportion of women in AF ($p = 0.000$); this is the opposite of the comparison between MC and UC, in which the proportion of female patients is significantly lower in the MC group ($p < 0.015$). This same effect occurred with the codominant, dominant, recessive, and allelic analyses, confirming and detailing the data of **Table 2**. There were no differences regarding sex distribution between AF and UC, and ethnicity had no statistically significant effect as a covariate in this analysis.

DISCUSSION

Genetic studies are relevant to understanding the mechanisms involved in the pathogenesis of diseases (50, 51). Some genetic polymorphisms are shown to directly interfere in cytokine expression, therefore directing the immune response of the host and possibly influencing the outcome of the disease.

TABLE 3 | Genotypic and allelic distributions and frequencies of *IL12A* -504 G/T, *IL18* -607 C/A, and *IFNGR1* -611 A/G SNPs, values of Odds Ratio (OR) and 95% Confidence Interval (95% CI) among the groups of Controls ($n = 110$) and Patients ($n = 149$), and among the groups of patients with Acute ($n = 39$) and Chronic (Multifocal + Unifocal) forms of PCM ($n = 110$).

SNP	Genotypes	Alleles	Groups—*n* (%)			Clinical forms of PCM—*n* (%)		
			Controls	Patients	OR (95% CI)	Acute	Chronic	OR (95% CI)
IL12A -564 G/T	GG		2 (1.8)	2 (1.3)	1.0	1 (2.6)	1 (0.8)	1.0
	GT		28 (25.5)	40 (26.9)	1.43 (0.19–10.76)	13 (33.4)	27 (24.6)	0.48 (0.03–8.32)
	TT		80 (72.7)	107 (71.8)	1.34 (0.18–9.7)	25 (64.0)	82 (74.6)	0.3 (0.02–5.05)
		G	32 (14.5)	44 (14.8)	1.0	15 (19.2)	29 (13.2)	1.0
		T	188 (85.5)	254 (85.2)	0.98 (0.6–1.61)	63 (80.8)	191 (86.8)	0.63 (0.32–1.26)
IL18 -607 C/A	CC		29 (26.4)	44 (29.5)	1.0	10 (25.7)	34 (30.9)	1.0
	CA		60 (54.5)	68 (45.6)	0.75 (0.42–1.34)	16 (41.0)	52 (47.3)	1.05 (0.43–2.58)
	AA		21 (19.1)	37 (24.8)	1.16 (0.57–2.37)	13 (33.3)	24 (21.8)	1.84 (0.7–4.89)
		C	118 (53.6)	156 (52.3)	1.0	36 (46.2)	120 (54.5)	1.0
		A	102 (46.4)	142 (47.7)	1.05 (0.74–1.49)	42 (53.8)	100 (45.5)	1.4 (0.83–2.35)
IFNGR1 -611 A/G	AA		14 (12.8)	21 (14.1)	1.0	4 (10.3)	17 (15.5)	1.0
	AG		47 (43.1)	66 (44.3)	0.93 (0.43–2.03)	19 (48.7)	47 (42.7)	0.58 (0.17–1.96)
	GG		48 (44.0)	62 (41.6)	0.86 (0.4–1.87)	16 (41.0)	46 (41.8)	0.67 (0.2–2.3)
		A	75 (34.4)	108 (36.2)	1.0	27 (34.6)	81 (36.8)	1.0
		G	143 (65.6)	190 (63.8)	0.92 (0.64–1.33)	51 (65.4)	139 (63.2)	1.1 (0.64–1.89)

In the present study, we investigated the possible association between the *IL12A* -504 G/T, *IL18* -607 C/A, and *IFNGR1* -611 A/G SNPs in Brazilian patients with PCM and disease susceptibility. The distribution of genotypes and alleles of the *IL12A* -504 G/T SNP was similar in all evaluated comparisons on our study. Although this SNP was related to immune responses against rubella vaccination and HBV and protection in tuberculosis, we did not observe a clear association with PCM (52–54).

As for *IFNGR1* -611 A/G SNP, genotypic and allelic distributions were similar in all evaluated comparisons, confirmed by unconditional logistic regression analysis (adjusted for sex and race). The absence of association with risk or protection reported here is similar to the data reported in tuberculosis and liver fibrosis progression due to recurrent hepatitis C (55–58). An association between tuberculosis and the *IFNGR1* -611 A/G and -56 T/C haplotype was observed by Bullak-Kardum et al. (41). In fact, the promoter activity is supposed to be stronger in -611 A/G than -56 T/C, and the variant *A* is estimated to decrease the binding of GATA-1 and TFIID factors to this site (40, 58). Because previous associations with risk or protection have been described in other SNPs, further studies should include the *IFNGR1* -611 A/G SNP.

In our analysis of the *IL18* -607 C/A SNP, we found no differences on allelic and genotypic distributions between patients and controls or between AF and CF groups of patients. On the other hand, the adjustment for sex and ethnicity in the unconditional regression logistic analysis confirmed the presence of the *A*-allele as a risk factor for the AF and MC groups when compared to the UC group.

The association of the *A*-allele/*AA*-genotype and higher risk is shown in various infectious diseases, such as chronic hepatitis B in Thailand and in India, gingivitis in the Czech Republic, pulmonary tuberculosis in China, Chagas disease in Colombia (mainly driven by rs360719), and infection by the hepatitis C virus in Egypt (37, 43, 52–62). Similarly to our results, the mutant allele/genotype of *IL18* -607 C/A is also associated with more severe outcomes in other infectious diseases: higher virus shedding of the severe acute respiratory syndrome-associated (SARS) coronavirus in Taiwan, lipodystrophy syndrome on HIV-positive Brazilian individuals, immune restoration disease on HIV–tuberculosis coinfected Indian patients, bacterial infections after liver transplantation in China, and hepatitis C–related hepatocellular carcinoma in Egypt (63–67).

The effect of the *A*-allele/*AA*-genotype on PCM and other infectious diseases could be explained by changes in IL-18 levels introduced by this mutant allele in the -607 position. In effect, the IL-18 human gene is composed of six exons and five introns with three very well-known SNPs in the promoter region: -656 G/T (rs1946519), -607 C/A (rs1946518), and -137 G/C (rs187238). Two of these positions, -607 and -137, are thought to be nuclear factor binding sites for cAMP responsive element binding protein and H4TF-1 nuclear factor, respectively, and mutation on both sites can affect the IL-18 levels (50).

The -607 *C*-allele/*CC*-genotype carriage has been associated with higher levels of IL-18 in the serum and/or of mRNA expression (50, 66, 68–70). In our study, we found higher *C*-allele carriage on patients with the UC form of PCM (73.5%), whereas the AF and MC groups (with 46.2 and 51.1% of *C*-allele carriage, respectively) had already been reported to have higher serum IL-18 levels than those from the former group (19, 20).

We hypothesize that the higher *C*-allele carriage on patients with the UC form of PCM may induce higher IL-18 levels at the early stages of infection, determining increased

TABLE 4 | Genotypic and allelic distributions and frequencies of *IL12A* -504 G/T, *IL18* -607 C/A, and *IFNGR1* -611 A/G SNPs, values of Odds Ratio (OR) and 95% Confidence Interval (95% CI) adjusted for sex and race by unconditional logistic regression analysis among the groups of patients with Acute (AF, $n = 39$), Multifocal Chronic (MC, $n = 93$) and Unifocal Chronic (UC, $n = 17$) forms of PCM.

SNP	Model	Genotypes	Alleles	Clinical Forms of PCM—*n* (%)			AF vs. MC[a]	AF vs. UC[b]	MC vs. UC[c]
				AF	MC	UC	OR (95% CI)	OR (95% CI)	OR (95% CI)
IL12A -504 G/T	Codominant	GG		1 (2.6)	1 (1.1)	0 (0.0)	1		
		GT		13 (33.4)	21 (22.6)	6 (35.3)	0.62 (0.04–10.78)	—	—
		TT		25 (64.0)	71 (76.3)	11 (64.7)	0.35 (0.02–5.84)	—	—
	Dominant	GG		1 (2.6)	1 (1.1)	0 (0.0)	1		
		GT + TT		38 (97.4)	92 (98.9)	17 (100.0)	0.41 (0.03–6.78)	—	—
	Recessive	GG + GT		14 (36.0)	22 (23.7)	6 (35.3)	1	1	1
		TT		25 (64.0)	71 (76.3)	11 (64.7)	0.55 (0.25–1.24)	0.97 (0.3–3.2)	1.76 (0.58–1.76)
			G	15 (19.2)	23 (12.4)	6 (17.6)	1	1	1
			T	63 (80.8)	163 (87.6)	28 (82.4)	0.59 (0.29–1.21)	0.90 (0.32–2.56)	1.52 (0.47–4.06)
IL18 -607 C/A	Codominant	CC		10 (25.7)	26 (28.0)	8 (47.1)	1		
		CA		16 (41.0)	43 (46.2)	9 (52.9)	0.97 (0.38–2.45)	—	—
		AA		13 (33.3)	24 (25.8)	0 (0.0)	1.41 (0.52–3.80)	—	—
	Dominant	CC		10 (25.7)	26 (28.0)	8 (47.1)	1	1	1
		CA + AA		29 (74.3)	67 (72.0)	9 (52.9)	1.13 (0.48–2.63)	2.58 (0.78–8.5)	2.29 (0.80–6.58)
	Recessive	CC + CA		27 (66.7)	69 (74.2)	17 (100.0)	1		
		AA		13 (33.3)	24 (25.8)	0 (0.0)	1.38 (0.63–3.11)	—	—
			C	36 (46.2)	95 (51.1)	25 (73.5)	1	1	1
			A	42 (53.8)	91 (48.9)	9 (26.5)	1.19 (0.69–2.07)	3.10 (1.24–7.77)	2.61 (1.14–5.96)
IFNGR1 -611 A/G	Codominant	AA		16 (41.0)	39 (41.9)	7 (41.2)	1	1	1
		AG		19 (48.7)	37 (39.8)	10 (58.8)	2.82 (0.84–9.52)	0.84 (0.2–3.52)	0.64 (0.19–2.18)
		GG		4 (10.3)	17 (18.3)	0 (0.0)	0.39 (0.03-4.22)	—	—
	Dominant	AA		16 (41.0)	39 (41.9)	7 (41.2)	1	1	1
		AG + GG		23 (59.0)	54 (85.1)	10 (58.8)	1.95 (0.61–6.22)	0.97 (0.24–3.92)	0.98 (0.29–3.25)
	Recessive	AA + AG		35 (89.7)	76 (81.7)	17 (100.0)	1		
		GG		4 (10.3)	17 (18.3)	0 (0.0)	0.23 (0.02–2.20)	—	—
			A	51 (65.4)	115 (61.8)	24 (70.6)	1	1	1
			G	27 (34.6)	71 (38.2)	10 (29.4)	0.86 (0.49–1.49)	1.27 (0.53–3.04)	1.48 (0.67–3.38)

[a] *Reference for AF vs. MC = MC.*
[b] *Reference for AF vs. UC = UC.*
[c] *Reference for MC vs. UC = UC.*

TABLE 5 | Association studies between the groups of patients with Acute (AF), Multifocal Chronic (MC), and Unifocal Chronic (UC) forms of PCM including sex, ethnicity, and the *IL18* -607 C/A SNP as covariates and results of *p*-values, Odds Ratio (OR), and 95% Confidence Interval (95% CI).

Covariates of *IL18* -607 C/A SNP	Comparisons								
	AF vs. MC[c]			AF vs. UC[d]			MC vs. UC[e]		
	p-value	OR	95% CI	*p*-value	OR	95% CI	*p*-value	OR	95% CI
Sex[a]	0.000	12.63	3.64–43.81	0.484	1.74	0.37–8.18	0.020	0.16	0.35–0.76
Ethnicity[b]	0.433	1.54	0.52–4.55	0.350	2.12	0.44–10.31	0.517	1.56	0.40–6.00
CC vs. CA vs. AA	0.546	1.25	0.60–2.62	0.070	3.06	0.91–10.27	0.164	1.89	0.77–4.65
Sex[a]	0.000	12.58	3.64–43.50	0.393	1.89	0.44–8.16	0.015	0.151	0.03–0.70
Ethnicity[b]	0.420	1.56	0.53–4.64	0.399	1.85	0.59–9.16	0.600	1.42	0.38–5.36
CC vs. CA + AA	0.755	1.13	0.48–2.63	0.769	2.58	0.78–8.5	0.724	2.29	0.80–6.58
Sex[a]	0.000	12.39	3.58–42.98	0.609	1.52	0.31–7.50	0.018	0.15	0.03–0.72
Ethnicity[b]	0.402	1.59	0.53–4.75	0.699	1.63	0.47–8.00	0.364	1.88	0.48–7.36
CC + CA vs. AA	0.569	1.38	0.63–3.11		Omitted			Omitted	
Sex[a]	0.000	12.6	3.64–43.80	0.484	1.74	0.37–8.31	0.020	0.16	0.03–0.76
Ethnicity[b]	0.430	1.54	0.52–0.30	0.350	2.12	0.44–10.31	0.517	1.56	0.40–6.00
C vs. A	0.528	1.19	0.69–2.07	0.015	3.10	1.24–7.77	0.023	2.61	1.14–5.96

[a] *Reference for sex = male.*
[b] *Reference for ethnicity = white.*
[c] *Reference for AF vs. MC = MC.*
[d] *Reference for AF vs. UC = UC.*
[e] *Reference for MC vs. UC = UC.*

levels of IFN-γ and a more efficient cellular response that controls fungal dissemination and the consequential tissular inflammation. In parallel, previous work in our lab shows that phytohemagglutinin-stimulated cells from *IL18* -607 *C*-allele-unifocal patients apparently produce more IFN-γ than *C*-allele carriers from the acute or the chronic multifocal groups, although without statistically significant difference (unpublished data). However, because both infection and disease in humans are recognized in a later and undefined period after fungal entrance, those initial events can only be evaluated in experimental PCM and have been elegantly shown in deficient mice models. The intravenous infection of IL-18-deficient mice (*IL-18*$^{-/-}$) with *P. brasiliensis* yeast cells resulted in a higher fungal burden in the lungs compared with wild-type (WT) animals and absence of granuloma formation (71). Furthermore, *P. brasiliensis* intratracheally infected mice deficient for NLRP3 inflammasome components (*Nlrp3*$^{-/-}$, *Casp1/11*$^{-/-}$, *Asc*$^{-/-}$) as well as deficient for the ATP receptor (*P2x7r*$^{-/-}$) also had a higher fungal burden in their lungs and liver; predominance of CD4^{+}IL-4^{+}, CD4^{+}TGF-β^{+}, and T-reg cells; a lower number of pulmonary PMN cells; and less IL-18 and IL-1β compared with their WT controls (7).

In this context, it is possible that patients with the less severe UC form of PCM present a more balanced IL-18/IL-12/IFN-γ axis, resulting in more localized and milder clinical manifestations compared with the other groups, in which the higher IL-18 levels are accompanied by other immunomodulating cytokines. The more severe form of PCM, the acute form, has been characterized by IL-4 with IL-18 inducing a Th2 immune response (high levels of IL-4, IL-5, and IL-13), by IL-4 and TGF-β inducing a Th9 pattern (high levels of IL-9), and both Th2 and Th9 inhibiting the Th1 response. Patients with chronic PCM were previously shown to have a mixed immune response of Th1 (IL-12 and IL-18 leading to IFN-γ production), Th17 (induced by IL-18, IL-1 and IL-23), and Th22 (induced by IL-18, IL-1, IL-23, and IL-21), which result in heterogeneous clinical symptoms (12, 13, 20).

In our study, the UC group included only patients with mild and restricted disease to the skin, mucosae, or lymph nodes. The exclusion of patients with lung involvement was based on the possible misclassification of MC patients who are more prone to develop pulmonary lesions. Although these criteria resulted in fewer patients in the UC group, it also revealed specific immunogenetic characteristics, such as the association of a more favorable outcome with the *IL18* -607 *C*-allele in the present study and the *IL12RB1* 641 *AG*-genotype and the HLA-DRB1*11 allele carriage, previously reported by our group (26, 31).

Additionally, the association of the *IL18* -607 *A*-allele with the more severe forms of PCM described herein collaborates with previous reports on different genes emphasizing the influence of genetic background on the outcome of this mycosis. The *GG*-genotype of *IL10* -1082 G/A SNP, the *RP2/RP2*-genotype of the intron-3 microsatellite polymorphism of the *IL4* gene, the *AA*-genotype of *IL12RB1* 641 A/G SNP, the *GG*-genotype of the *DCSIGN* rs4804803 A/G SNP, and the *CC*-genotype of the *VDR* rs7975232 A/C SNP have all been previously associated with susceptibility or the more severe outcome in PCM (26, 29–31, 34, 35, 49). In parallel, HLA class I antigens and the GLO-1 phenotype of the glyoxalase enzyme have been associated with the progression of disease (pulmonary form) or infection (23–25, 27, 28).

We reinforce that our present data and all the genetic associations previously described may be considered in the same context of association of autosomal gene dominance with resistance in murine PCM, which is a model that reproduces several characteristics of the human disease (22).

The comparison between patients and controls in our study shows a greater number of male than female subjects, particularly in the MC group. As previously described, there has been a male predominance among cases of chronic PCM (72–74). This mycosis manifests more frequently in male farmers who are constantly working in direct contact with the soil where *Paracoccidioides* spp. probably occurs (1). In addition, infected women are less likely to manifest the chronic form because of the putative role of estrogen (17-β-estradiol) as a protective factor that impairs conidia transformation into yeast form during murine infection (75–77). Although this effect has been less commonly registered in human PCM, epidemiological data reported in Brazil show that the disease is rare in adult females (4.3%) and usually occurring in the menopausal period (91.3%) (78). Contrarily, it has been demonstrated that 17-β-estradiol can exert an anti-inflammatory role by decreasing TNF-α and IL-6 while increasing IL-4 levels, which further results in a Th2 response (79). In oral PCM lesions, a positive correlation between the amount of estradiol receptors and the fungal burden was observed only in female patients (80). These recent findings may explain the more even distribution of the acute form of PCM among sexes, and the higher frequency of females in UC and lower in MC could be evidence of protection for women in developing the more severe chronic form of the disease.

Possible limitations in our study are the inclusion of only one health center, mixed ethnic groups in the Brazilian population, and lack of detection of IL-18 levels and functional analyses. Although reflecting the distribution of PCM in endemic areas, our cohort with a low number of patients with the UC form is also a limitation for further inquiry.

In summary, our study did not show an association between PCM and the evaluated *IL12A* and *IFNGR1* SNPs or between the acute and chronic forms or between multifocal and unifocal chronic forms. For the *IL18* -607 C/A SNP, no association was shown with infection or among acute and chronic forms. However, we show an association between the *IL18* -607 *A*-allele and the more severe clinical forms of PCM, acute and multifocal chronic forms, when compared to the UC form, the less severe form of this disease, associated with the *IL18* -607 *C*-allele. To the best of our knowledge, this is the first study that evaluates the association between *IL12A*, *IFNGR1*, and *IL18* SNPs and PCM.

The present data suggest a novel role of *IL18* -607 C/A SNP as a contributor to a more favorable outcome of this disease, potentially leading to a more balanced and more efficient cellular response for the control of fungal dissemination at the early stages of infection in UC. Furthermore, our work highlights the need for new studies with other SNPs on the *IL18* gene and on other components of the immune response for a better understanding of the pathophysiology and the clinical expression of PCM.

DATA AVAILABILITY STATEMENT

The datasets generated for this study are available on request to the corresponding author.

ETHICS STATEMENT

The studies involving human participants were reviewed and approved by Research and Ethics Committee of Hospital das Clínicas, Faculdade de Medicina, University of São Paulo - HCFMUSP, São Paulo, SP, Brazil (CAPPesq 10273; Plataforma Brasil 123334/2013). The patients/participants provided their written informed consent to participate in this study.

AUTHOR CONTRIBUTIONS

PS and MS-Y conceived and designed the experiments. MM and AK contributed with samples and patient selection. PS, FB, FC, CD, and AS performed the experiments. PS, AG, and OL analyzed the data. PS, FB, AG, FC, and MS-Y wrote the paper and/or performed bibliographic revision. PS, MS-Y, MM, AK, FB, FC, CD, AS, AG, and OL approved the paper. All authors contributed to the article and approved the submitted version.

FUNDING

This work was supported by grants from Fundação de Amparo à Pesquisa do Estado de São Paulo (FAPESP 2012/25192-7) and Fundação Faculdade de Medicina. The funders had no role in study design, data collection and analysis, decision to publish, or preparation of the manuscript. FC was supported by grants from the Coordenação de Aperfeiçoamento de Pessoal de Nível Superior (CAPES), and FB was supported by grants from FAPESP (2014/07801-1).

ACKNOWLEDGMENTS

We thank Nídia P. O. Silva and Eron L. dos Santos for their contribution on DNA extraction of some of the samples and Marcia A. Ferreira, Carlos Jose Quinteiro, and Rodolfo E. Fujimori for providing older articles.

SUPPLEMENTARY MATERIAL

The Supplementary Material for this article can be found online at: https://www.frontiersin.org/articles/10.3389/fimmu.2020.542210/full#supplementary-material

REFERENCES

1. Martinez R. New trends in paracoccidioidomycosis epidemiology. *J Fungi.* (2017) 3:1. doi: 10.3390/jof3010001
2. Martinez R. Epidemiology of paracoccidioidomycosis. *Rev Inst Med Trop São Paulo.* (2015) 57:11–20. doi: 10.1590/S0036-46652015000700004
3. Vieira G de D, Alves T da C, Lima SM, Camargo LM, Sousa CM. Paracoccidioidomycosis in a western Brazilian Amazon State: clinical-epidemiologic profile and spatial distribution of the disease. *Rev Soc Bras Med Trop.* (2014) 47:63–8. doi: 10.1590/0037-8682-0225-2013
4. Benard G. An overview of the immunopathology of human paracoccidioidomycosis. *Mycopathologia.* (2008) 165:209–21. doi: 10.1007/s11046-007-9065-0
5. Calich VL, Costa TA, Felonato M, Arruda C, Bernardino S, Loures FV, et al. Innate immunity to *Paracoccidioides brasiliensis* infection. *Mycopathologia.* (2008) 165:223–36. doi: 10.1007/s11046-007-9048-1
6. Calich VL, Pina A, Felonato M, Bernardino S, Costa TA, Loures FV. Toll-like receptors and fungal infections: the role of TLR2, TLR4 and MyD88 in paracoccidioidomycosis. *FEMS Immunol Med Microbiol.* (2008) 53:1–7. doi: 10.1111/j.1574-695X.2008.00378.x
7. Feriotti C, de Araújo EF, Loures FV, da Costa TA, Galdino NAL, Zamboni DS, et al. NOD-like receptor P3 inflammasome controls protective Th1/Th17 immunity against pulmonary paracoccidioidomycosis. *Front Immunol.* (2017) 10:786. doi: 10.3389/fimmu.2017.00786
8. Jannuzzi GP, de Almeida JRF, Amarante-Mendes GP, Romera LMD, Kaihami GH, Vasconcelos JR, et al. TLR3 is a negative regulator of immune responses against *Paracoccidioides brasiliensis*. *Front Cell Infect Microbiol.* (2019) 8:426. doi: 10.3389/fcimb.2018.00426
9. Rodrigues DR, Fernandes RK, Balderramas H de A, Penitenti M, Bachiega TF, Calvi SA, et al. Interferon-gamma production by human neutrophils upon stimulation by IL-12, IL-15 and IL-18 and challenge with *Paracoccidioides brasiliensis*. *Cytokine.* (2014) 69:102–9. doi: 10.1016/j.cyto.2014.05.009
10. de Castro LF, Longhi LNA, Paião MR, Justo-Júnior ADS, de Jesus MB, Blotta MHSL, et al. NLRP3 inflammasome is involved in the recognition of *Paracoccidioides brasiliensis* by human dendritic cells and in the induction of Th17 cells. *J Infect.* (2018) 77:137–44. doi: 10.1016/j.jinf.2018.03.004
11. Calich VL, Vaz CA, Burger E. Immunity to *Paracoccidioides brasiliensis* infection. *Res Immunol.* (1998) 149:407–500. doi: 10.1016/S0923-2494(98)80764-5
12. Oliveira SJ, Mamoni RL, Musatti CC, Papaiordanou PM, Blotta MH. Cytokines and lymphocyte proliferation in juvenile and adult forms of paracoccidioidomycosis: comparison with infected and non-infected controls. *Microbes Infect.* (2002) 4:139–44. doi: 10.1016/S1286-4579(01)01521-0
13. de Castro LF, Ferreira MC, Silva RM, Blotta MHSL, Longhi LN, Mamoni RL. Characterization of immune response in human paracoccidioidomycosis. *J Infect.* (2013) 67:470–85. doi: 10.1016/j.jinf.2013.07.019
14. Calich VLG, Mamoni RL, Loures FV. Regulatory T cells in paracoccidioidomycosis. *Virulence.* (2018) 1:1–12. doi: 10.1080/21505594.2018.1483674
15. Benard G, Romano CC, Cacere CR, Juvenale M, Mendes-Giannini MJ, Duarte AJ. Imbalance of IL-2, IFN-gamma and IL-10 secretion in the immunosuppression associated with human paracoccidioidomycosis. *Cytokine.* (2001) 13:248–52. doi: 10.1006/cyto.2000.0824
16. Romano CC, Mendes-Giannini MJS, Duarte AJS, Benard G. The role of interleukin-10 in the differential expression of interleukin-12p70 and its β2 receptor on patients with active or treated paracoccidioidomycosis and healthy infected subjects. *Clin Immunol.* (2005) 114:86–94. doi: 10.1016/j.clim.2004.09.005
17. Nakanishi K, Yoshimoto T, Tsutsui H, Okamura H. Interleukin-18 is a unique cytokine that stimulates both Th1 and Th2 responses depending on its cytokine milieu. *Cytokine Growth Factor Rev.* (2001) 12:53–72. doi: 10.1016/S1359-6101(00)00015-0
18. Samarani S, Allam O, Sagala P, Aldabah Z, Jenabian MA, Mehraj V, et al. Imbalanced production of IL-18 and its antagonist in human diseases, and its implications for HIV-1 infection. *Cytokine.* (2016) 82:38–51. doi: 10.1016/j.cyto.2016.01.006
19. Corvino CL, Mamoni RL, Fagundes GZ, Blotta MH. Serum interleukin-18 and soluble tumour necrosis factor receptor 2 are associated with disease severity in patients with paracoccidioidomycosis. *Clin Exp Immunol.* (2007) 147:483–90. doi: 10.1111/j.1365-2249.2006.03308.x
20. Alves ABRM, David MA, de Castro LF, da Silva RM, Longhi LNA, Blotta MHSL, et al. Differential production of interleukin-1 family cytokines (IL-1β, IL-18, IL-33 and IL-37) in patients with paracoccidioidomycosis: correlation with clinical form and antifungal therapy. *Med Mycol.* (2018) 56:332–43. doi: 10.1093/mmy/myx050
21. Loures FV, Pina A, Felonato M, Feriotti C, de Araújo EF, Calich VL. MyD88 signaling is required for efficient innate and adaptive immune responses to *Paracoccidioides brasiliensis* infection. *Infect Immun.* (2011) 79:2470–80. doi: 10.1128/IAI.00375-10
22. Calich VL, Burger E, Kashino SS, Fazioli RA, Singer-Vermes LM. Resistance to *Paracoccidioides brasiliensis* in mice is controlled by a single dominant autosomal gene. *Infect Immun.* (1987) 55:1919–23. doi: 10.1128/IAI.55.8.1919-1923.1987
23. de Restrepo FM, Restrepo M, Restrepo A. Blood groups and HLA antigens in paracoccidioidomycosis. *Sabouraudia.* (1983) 21:35–9. doi: 10.1080/00362178385380061
24. Lacerda GB, Arce-Gomez B, Telles Filho FQ. Increased frequency of HLA-B40 in patients with paracoccidioidomycosis. *J Med Vet Mycol.* (1988) 26:253–6. doi: 10.1080/02681218880000351
25. Goldani LZ, Monteiro CM, Donadi EA, Martinez R, Voltarelli JC. HLA antigens in Brazilian patients with paracoccidioidomycosis. *Mycopathologia.* (1991) 114:89–91. doi: 10.1007/BF00436427
26. Sadahiro A, Roque AC, Shikanai-Yasuda MA. Generic human leukocyte antigen class II (DRB1 and DQB1) alleles in patients with paracoccidioidomycosis. *Med Mycol.* (2007) 45:35–40. doi: 10.1080/13693780600999132
27. de Messias IJ, Reis A, Brenden M, Queiroz-Telles F, Mauff G. Association of major histocompatibility complex class III complement components C2, BF, and C4 with Brazilian paracoccidioidomycosis. *Complement Inflamm.* (1991) 8:288–93. doi: 10.1159/000463198
28. Balarin MA, Freire-Maia DV. The association between glyoxalase I and paracoccidioidomycosis infection. *Rev Soc Bras Med Trop.* (1993) 26:141–3. doi: 10.1590/S0037-86821993000300002
29. Moraes-Vasconcelos D, Grumach AS, Yamaguti A, Andrade MEB, Fieschi C, Beaucoudrey L, et al. *Paracoccidioides brasiliensis* disseminated disease in a patient with inherited deficiency in the beta1 subunit of the interleukin (IL)-12/IL-23 receptor. *Clin Infect Dis.* (2005) 41:e31–7. doi: 10.1086/432119
30. Mendonça MS, Peraçolli TS, Silva-Vergara ML, Ribeiro SC, Oliveira RF, Mendes RP, et al. High interleukin-4 expression and interleukin-4 gene polymorphisms are associated with susceptibility to human paracoccidioidomycosis. *Mem Inst Oswaldo Cruz.* (2015) 110:781–5. doi: 10.1590/0074-02760150197
31. Carvalho FM, Busser FD, Freitas VL, Furucho CR, Sadahiro A, Kono AS, et al. Polymorphisms on *IFNG*, *IL12B* and *IL12RB1* genes and paracoccidioidomycosis in the Brazilian population. *Infect Genet Evol.* (2016) 43:245–51. doi: 10.1016/j.meegid.2016.05.025
32. Neves E de S, Curi AL, Albuquerque MC, Palhano-Silva CS, Silva LB, Bueno WF, et al. Genetic polymorphism for IFN-γ +874 T/A in patients with acute toxoplasmosis. *Rev Soc Bras Med Trop.* (2012) 45:751–60. doi: 10.1590/S0037-86822012000600020
33. Matos GI, Covas CJF, Bittar RC Gomes-Silva A, Marques F, Maniero VC, et al. *IFNG* +874 T/A polymorphism is not associated with American tegumentary leishmaniasis susceptibility but can influence *Leishmania* induced IFN-γ production. *BMC Infec Dis.* (2007) 7:33. doi: 10.1186/1471-2334-7-33
34. Bozzi A, Pereira PP, Reis BS, Goulart MI, Pereira MC, Pedroso EP, et al. Interleukin-10 and tumor necrosis factor-alpha single nucleotide gene polymorphism frequency in paracoccidioidomycosis. *Hum Immunol.* (2006) 67:931–9. doi: 10.1016/j.humimm.2006.07.014
35. Bozzi A, Reis BS, Pereira PP, Pedroso EP, Goes AM. Interferon-gamma and interleukin-4 single nucleotide gene polymorphisms in Paracoccidioidomycosis. *Cytokine.* (2009) 48:212–7. doi: 10.1016/j.cyto.2009.07.011
36. Jouanguy E, Dupuis S, Pallier A, Döffinger R, Fondanèche MC, Fieschi C, et al. In a novel form of IFN-gamma receptor 1 deficiency, cell surface receptors fail to bind IFN-gamma. *J Clin Invest.* (2000) 105:1429–36. doi: 10.1172/JCI9166

37. Zerbe CS, Holland SM. Disseminated histoplasmosis in persons with interferon-γ receptor 1 deficiency. *Clin Infect Dis.* (2005) 41:e38–41. doi: 10.1086/432120
38. Vinh DC, Masannat F, Dzioba RB, Galgianai JN, Holland SM. Refractory disseminated coccidioidomycosis & mycobacteriosis in interferon-γ receptor deficiency. *Clin Infect Dis.* (2009) 49:e62–5. doi: 10.1086/605532
39. Marazzi MG, Chapgier A, Defilippi A, Pistioia V, Mangini S, Savioli C, et al. Disseminated *Mycobacterium scrofulaceum* infection in a child with interferon-γ receptor 1 deficiency. *Int J Infect Dis.* (2010) 14:167–70. doi: 10.1016/j.ijid.2009.03.025
40. Rosenzweig SD, Schäffer AA, Ding L, Sullivan R, Enyedi B, Yim JJ, et al. Interferon-gamma receptor 1 promoter polymorphisms: population distribution and functional implications. *Clin Immunol.* (2004) 112:113–9. doi: 10.1016/j.clim.2004.03.018
41. Bulat-Kardum L, Etokebe GE, Knezevic J, Balen S, Matakovic-Mileusnic N, Zaputovic L, et al. Interferon-gamma receptor-1 gene promoter polymorphisms (G-611A; T-56C) and susceptibility to tuberculosis. *Scand J Immunol.* (2006) 63:142–50. doi: 10.1111/j.1365-3083.2005.01694.x
42. Anyona SB, Kempaiah P, Raballah E, Ouma C, Were T, Davenport GC, et al. Functional promoter haplotypes of interleukin-18 condition susceptibility to severe malarial anemia and childhood mortality. *Infect Immun.* (2011) 79:4923–32. doi: 10.1128/IAI.05601-11
43. Han M, Yue J, Lian YY, Zhao YL, Wang HX, Liu LR. Relationship between single nucleotide polymorphism of interleukin-18 and susceptibility to pulmonary tuberculosis in the Chinese Han population. *Microbiol Immunol.* (2011) 55:388–93. doi: 10.1111/j.1348-0421.2011.00332.x
44. Hirankarn N, Manonom C, Tangkijvanich P, Poovorawan Y. Association of interleukin-18 gene polymorphism (-607A/A genotype) with susceptibility to chronic hepatitis B virus infection. *Tissue Antigens.* (2007) 70:160–3. doi: 10.1111/j.1399-0039.2007.00865.x
45. Haas SL, Weiss C, Bugert P, Gundt J, Witt H, Singer MV, et al. Interleukin 18 promoter variants (−137G>C and −607C>A) in patients with chronic hepatitis C: association with treatment response. *J Clin Immunol.* (2009) 29:620–8. doi: 10.1007/s10875-009-9302-z
46. Franco M, Montenegro MR, Marques RS, Dillon L. Host-parasite relationship in Paracoccidioidomycosis. *J Med Vet Mycol.* (1987) 25:5–9. doi: 10.1080/02681218780000021
47. Gustincich S, Manfioletti G, Del Sal GS, Schneider G, Carninci PA. A fast method for high quality genomic DNA extraction from whole human blood. *Biotechniques.* (1991) 11:298–302.
48. Lozano VF, Lins TC, Teixeira MM, Vieira RG, Blotta MHS, Goes AM, et al. Polymorphism analysis of the CTLA-4 gene in paracoccidioidomycosis patients. *Mem Inst Oswaldo Cruz.* (2011) 106:220–6. doi: 10.1590/S0074-02762011000200017
49. Alves Pereira Neto T, Costa Pereira AA, Costa Hanemann JA, Coelho LFL, Malaquias LCC. *DC-SIGN* and *VDR* polymorphisms are associated with chronic form of paracoccidioidomycosis with oral manifestations. *Mycoses.* (2019) 62:186–92. doi: 10.1111/myc.12866
50. Giedraitis V, He B, Huang WX, Hillert J. Cloning and mutation analysis of the human IL-18 promoter: a possible role of polymorphisms in expression regulation. *J Neuroimmunol.* (2001) 112:146–52. doi: 10.1016/S0165-5728(00)00407-0
51. Cao W, Luo LL, Chen WW, Liang L, Zhang RR, Zhao YL, et al. Polymorphism in the *EREG* gene confers susceptibility to tuberculosis. *BMC Med Genet.* (2019) 20:7. doi: 10.1186/s12881-018-0729-z
52. Dhiman N, Haralambieva IH, Vierkant RA, Pankratz VS, Ryan JE, Jacobson RM, et al. Predominant inflammatory cytokine secretion pattern in response to two doses of live rubella vaccine in healthy vaccinees. *Cytokine.* (2010) 50:24–9. doi: 10.1016/j.cyto.2009.12.002
53. Pan L, Zhang W, Liang Z, Wu X, Zhu X, Li J, et al. Association between polymorphisms of the cytokine and cytokine receptor genes and immune response to hepatitis B vaccination in a Chinese Han population. *J Med Virol.* (2012) 84:26–33. doi: 10.1002/jmv.22251
54. Wang J, Tang S, Shen H. Association of genetic polymorphisms in the *IL12-IFNG* pathway with susceptibility to and prognosis of pulmonary tuberculosis in a Chinese population. *Eur J Clin Microbiol Infect Dis.* (2010) 29:1291–5. doi: 10.1007/s10096-010-0985-0
55. Awomoyi AA, Nejentsev S, Richardson A, Hull J, Koch O, Podinovskaia M, et al. No association between interferon-gamma receptor-1 gene polymorphism and pulmonary tuberculosis in a Gambian population sample. *Thorax.* (2004) 59:291–4. doi: 10.1136/thx.2003.013029
56. Velez DR, Hulme WF, Myers JL, Weinberg JB, Levesque MC, Stryjewskiet ME, et al. *NOS2A*, *TLR4*, and *IFNGR1* interactions influence pulmonary tuberculosis susceptibility in African-Americans. *Hum Genet.* (2009) 126:643–53. doi: 10.1007/s00439-009-0713-y
57. Shin JG, Park BL, Kim LH, Namgoong S, Kim JO, Chang HS, et al. Association study of polymorphisms in interferon-γ receptor genes with the risk of pulmonary tuberculosis. *Mol Med Rep.* (2015) 12:1568–78. doi: 10.3892/mmr.2015.3544
58. Falleti E, Fabris C, Toniutto P, Fontanini E, Cussigh A, Caldato M, et al. Genetic polymorphisms of inflammatory cytokines and liver fibrosis progression due to recurrent hepatitis C. *Interferon Cytokine Res.* (2007) 27:239–46. doi: 10.1089/jir.2006.0062
59. Karra VK, Gumma PK, Chowdhury SJ, Ruttala R, Polipalli SK, Chakravarti A, et al. IL-18 polymorphisms in hepatitis B virus related liver disease. *Cytokine.* (2015) 73:277–82. doi: 10.1016/j.cyto.2015.02.015
60. Vokurka J, Klapusová L, Pantuckova P, Kukletova M, Kukla L, Holla LI. The association of MMP-9 and IL-18 gene promoter polymorphisms with gingivitis in adolescents. *Arch Oral Biol.* (2009) 54:172–8. doi: 10.1016/j.archoralbio.2008.09.002
61. Leon Rodriguez DA, Carmona FD, Echeverría LE, González CI, Martin J. *IL18* gene variants influence the susceptibility to Chagas disease. *PLoS Negl Trop Dis.* (2016) 10:e0004583. doi: 10.1371/journal.pntd.0004583
62. Estfanous SZK, Ali SA, Seif SM, Soror SHA, Abdelaziz DHA. Inflammasome genes' polymorphisms in Egyptian chronic hepatitis c patients: influence on vulnerability to infection and response to treatment. *Mediators Inflamm.* (2019) 2019:3273645. doi: 10.1155/2019/3273645
63. Chen WJ, Yang JY, Lin JH, Fann CSJ, Osyetrov V, King CC, et al. Nasopharyngeal shedding of severe acute respiratory syndrome-associated coronavirus is associated with genetic polymorphisms. *Clin Infect Dis.* (2006) 42:1561–9. doi: 10.1086/503843
64. Castelar L, Silva MM, Castelli EC, Deghaide NHS, Mendes-Junior CT, Machado AA, et al. Interleukin-18 and interferon-gamma polymorphisms in Brazilian human immunodeficiency virus-1-infected patients presenting with lipodystrophy syndrome. *Tissue Antigens.* (2010) 76:126–30. doi: 10.1111/j.1399-0039.2010.01471.x
65. Affandi JS, Kumar M, Agarwal U, Singh S, Price P. The search for a genetic factor associating with immune restoration disease in HIV patients co-infected with *Mycobacterium tuberculosis*. *Dis Markers.* (2013) 34:445–9. doi: 10.1155/2013/246017
66. Shi BJ, Yu XY, Li H, Xing TH, Fan JW, Wang PW, et al. Association between donor and recipient interleukin-18 gene polymorphisms and the risk of infection after liver transplantation. *Clin Invest Med.* (2017) 40:E176–87. doi: 10.25011/cim.v40i5.28623
67. Bakr NM, Awad A, A Moustafa E. Association of genetic variants in the interleukin-18 gene promoter with risk of hepatocellular carcinoma and metastasis in patients with hepatitis C virus infection. *IUBMB Life.* (2018) 70:165–74. doi: 10.1002/iub.1714
68. Sakai K, Kita M, Sawai N, Shiomi S, Sumida Y, Kanemasa K, et al. Levels of interleukin-18 are markedly increased in *Helicobacter pylori*-infected gastric mucosa among patients with specific *IL18* genotypes. *J Infect Dis.* (2008) 197:1752–61. doi: 10.1086/588196
69. Rezaeifar A, Eskandari-Nasab E, Moghadampour M, Kharazi-Nejad E, Hasani SSA, Asadi-Saghandi A, et al. The association of interleukin-18 promoter polymorphisms and serum levels with duodenal ulcer, and their correlations with bacterial CagA and VacA virulence factors. *Scand J Infect Dis.* (2013) 45:584–92. doi: 10.3109/00365548.2013.794301
70. Hasan FT, Naif HM. Association of gene polymorphisms and serum levels of IL-18 with the susceptibility to infection with hepatitis B virus. *J Infect Dis Med.* (2017) 2:3. doi: 10.4172/2576-1420.1000117
71. Ketelut-Carneiro N, Silva GK, Rocha FA, Milanezi CM, Cavalcanti-Neto FF, Zamboni DS, et al. IL-18 triggered by the Nlrp3 inflammasome induces host

innate resistance in a pulmonary model of fungal infection. *J Immunol.* (2015) 194:4507–17. doi: 10.4049/jimmunol.1402321
72. Blotta MHSL, Mamoni RL, Oliveira SJ, Nouér SA, Papaiordanou PMO, Goveia A, et al. Endemic regions of paracoccidioidomycosis in Brazil: a clinical and epidemiologic study of 584 cases in the southeast region. *Am J Trop Med Hyg.* (1999) 61:390–4. doi: 10.4269/ajtmh.1999.61.390
73. Belissimo-Rodrigues F, Machado AA, Martinez R. Paracoccidioidomycosis epidemiological features of 1000-cases series from a hyperendemic area on the Southeast of Brazil. *Am J Trop Med Hyg.* (2011) 85:546–50. doi: 10.4269/ajtmh.2011.11-0084
74. Shikanai-Yasuda MA, Mendes RP, Colombo AL, Queiroz-Telles F, Kono ASG, Paniago AMM, et al. Brazilian guidelines for the clinical management of paracoccidioidomycosis. *Rev Soc Bras Med Trop.* (2017) 50:715–40. doi: 10.1590/0037-8682-0230-2017
75. Aristizabal BH, Clemons KV, Stevens DA, Restrepo A. Morphological transition of *Paracoccidioides brasiliensis* conidia to yeast cells: *in vivo* inhibition in females. *Infect Immun.* (1998) 66:5587–91. doi: 10.1128/IAI.66.11.5587-5591.1998
76. Pinzan CF, Ruas LP, Casabona-Fortunato AS, Carvalho FC, Roque-Barreira MC. Immunological basis for the gender differences in murine *Paracoccidioides brasiliensis* infection. *PLoS ONE.* (2010) 5:e10757. doi: 10.1371/journal.pone.0010757
77. Shankar J, Wu TD, Clemons VK, Monteiro JP, Mirels LF, Stevens DA. Influence of 17-beta-estradiol on gene expression of *Paracoccidioides* during mycelia-to-yeast transition. *PLoS ONE.* (2011) 6:e28402. doi: 10.1371/journal.pone.0028402
78. Severo LC, Roesch EW, Oliveira EA, Rocha MM, Londero AT. Paracoccidioidomycosis in women. *Rev Iberoam Micol.* (1998) 15:88–9.
79. Santos RS, de Fatima LA, Frank AP, Carneiro EM, Clegg DJ. The effects of 17 alpha-estradiol to inhibit inflammation *in vitro*. *Biol Sex Differ.* (2017) 8:30. doi: 10.1186/s13293-017-0151-9
80. Caixeta CA, de Carli ML, Ribeiro Júnior NV, Sperandio FF, Nonogaki S, Nogueira DA, et al. Estrogen receptor-α correlates with higher fungal cell number in oral paracoccidioidomycosis in women. *Mycopathologia.* (2018) 183:785–91. doi: 10.1007/s11046-018-0272-7

Conflict of Interest: The authors declare that the research was conducted in the absence of any commercial or financial relationships that could be construed as a potential conflict of interest.

frontiers in Immunology

ORIGINAL RESEARCH
published: 21 October 2020
doi: 10.3389/fimmu.2020.550624

Combining Host Genetics and Functional Analysis to Depict Inflammasome Contribution in Tuberculosis Susceptibility and Outcome in Endemic Areas

*Dhêmerson Souza De Lima[1], Caio C. B. Bomfim[2], Vinícius N. C. Leal[1], Edione C. Reis[1], Jaíne L. S. Soares[1], Fernanda P. Fernandes[1], Eduardo P. Amaral[2], Flavio V. Loures[3], Mauricio M. Ogusku[4], Maria R. D'Imperio Lima[2], Aya Sadahiro[5] and Alessandra Pontillo[1]**

[1] Laboratório de Imunogenética, Departamento de Imunologia, Instituto de Ciências Biomédicas, Universidade de São Paulo, São Paulo, Brazil, [2] Laboratório de Imunologia das Doenças Infecciosas, Departamento de Imunologia, Instituto de Ciências Biomédicas, Universidade de São Paulo, São Paulo, Brazil, [3] Instituto de Ciência e Tecnologia, Universidade Federal de São Paulo, São José dos Campos, Brazil, [4] Laboratório de Micobacteriologia, Instituto Nacional de Pesquisas da Amazônia, Manaus, Brazil, [5] Departamento de Parasitologia, Universidade Federal do Amazonas, Manaus, Brazil

OPEN ACCESS

Edited by:
David Courtin,
Institut de Recherche pour le Développement (IRD), France

Reviewed by:
Andre G. Loxton,
South African Medical Research Council, South Africa
Claudia A. S. Lage,
Federal University of Rio de Janeiro, Brazil

***Correspondence:**
Alessandra Pontillo
alepontillo@usp.br

Specialty section:
This article was submitted to Microbial Immunology, a section of the journal Frontiers in Immunology

Received: 09 May 2020
Accepted: 25 August 2020
Published: 21 October 2020

Citation:
Souza De Lima D, Bomfim CCB, Leal VNC, Reis EC, Soares JLS, Fernandes FP, Amaral EP, Loures FV, Ogusku MM, Lima MRD'I, Sadahiro A and Pontillo A (2020) Combining Host Genetics and Functional Analysis to Depict Inflammasome Contribution in Tuberculosis Susceptibility and Outcome in Endemic Areas. Front. Immunol. 11:550624. doi: 10.3389/fimmu.2020.550624

The interplay between *M. tuberculosis* (Mtb) and humans is multifactorial. The susceptibility/resistance profile and the establishment of clinical tuberculosis (TB) still remains elusive. The gain-of-function variant rs10754558 in the *NLRP3* gene (found in 30% of the world population) confers protection against the development of TB, indicating a prominent role played by NLRP3 inflammasome against Mtb. Through genotype-guided assays and various Mtb strains (BCG, H37Rv, Beijing-1471, MP287/03), we demonstrate that Mtb strains activate inflammasome according to the NLRP3/IL-1ß or NLRC4/IL18 preferential axis. *NLRP3* and *NLRC4 g*enetic variants contribute to the presentation of TB. For the first time, we have shown that loss-of-function variants in *NLRC4* significantly contribute to the development of extra-pulmonary TB. The analysis of inflammasome activation in a cohort of TB patients and their "household contacts" (CNT) revealed that plasma IL-1ß/IFN-α ratio lets us distinguish patients from Mtb-exposed-but-healthy individuals from an endemic region. Moreover, NLRP3 inflammasome seemed "exhausted" in TB patients compared to CNT, indicating a more efficient activation of inflammasome in resistant individuals. These findings suggest that inflammasome genetics as well as virulence-dependent level of inflammasome activation contribute to the onset of a susceptible/resistant profile among Mtb-exposed individuals.

Keywords: tuberculosis, inflammasome, genetics, NLRP3, Nlrc4

INTRODUCTION

Tuberculosis (TB) is caused by a *Mycobacterium tuberculosis* (Mtb) infection. Only 5–10% of Mtb-infected individuals develop active TB and, in the majority of cases, the bacteria is either eliminated or remains in a latent state (1, 2). The cross-talk among host, pathogen and environment determines the outcome of an infection (3).

Host innate immune genes have been recently taken into account to explain how the first host/pathogen contact could shape one's subsequent response to Mtb (resistance vs. susceptibility). After accessing the host airways, Mtb is phagocyted by alveolar macrophages which initiate an innate immune response that leads to pathogen eradication, with the occasional contribution of an adaptive cell-mediated response (mainly driven by interferon (IFN)-γ) (4). Alternatively, a chronic inflammatory process begins with Mtb persistance in the lung and that may result in tissue damage through the formation of granulomas and lung fibrosis. In more severe infections, a dramatic lung parenchyma destruction occurs (5, 6). As such, the host innate immune response and further tissue inflammation could either be beneficial or detrimental in the fight against Mtb, possibly due to a delicate balance among several mediators.

Recently, Mayer Barber et al. showed that the plasma level of interleukin (IL)-1ß, type I IFN (IFN-I) and prostaglandin (PG)-E2—among several other inflammatory mediators—characterized the clinical presentation (severe vs. mild) of Mtb infections in TB patients (7), suggesting that a fine-tune regulation of innate immune response is crucial for TB outcomes.

Inflammasome is a cytosolic multi-protein complex that mediates the maturation and release of IL-1β and IL-18 (8). Pathogen- or damage-associated molecular patterns (PAMPs and DAMPs, respectively) activate the inflammasome through a group of cytosolic pathogen recognition receptors (PRRs), including NLRP1, NLRP3, NLRC4, NAIP, AIM2, and pyrin (8, 9). During infection, pathogens carry or inject PAMPs into cell cytosol and/or induce damage and break into the host homeostasis through the release of DAMPs. These are detected by inflammasome sensors, which in turn can recruit the adaptor molecule ASC and the effector molecule caspase-1, which is responsible for the maturation of IL-1ß and IL-18. Moreover, caspase-1 can mediate the cleavage of the pore-forming protein gasdermin D, leading to pro-inflammatory active cell death called pyroptosis (8).

Inflammasome activation constitutes a very efficient and rapid mechanism for host defense against pathogens. In this case, the inflammation is triggered either by leukocyte recruitment, *via* IL-1ß and IL-18 or by the destruction of the pathogen *niche* and inflammation amplification through pyroptosis. However, pathogen-induced response may be excessive with inflammasome-mediated tissue damage or, on the other hand, pathogens may evade host detection and/or inflammasome activation itself (9).

In murine bone marrow-derived macrophages, Mtb activates inflammasome through NLRP3 (10, 11) and mice lacking NLRP3 showed a reduced IL-1β production in response to an Mtb infection (12), suggesting that this sensor is crucial to trigger an animal response to this bacteria.

Besides being one of the most studied inflammasome sensors, researchers still have not completely demonstrated how NLRP3 is activated, as it responds to several PAMPs and DAMP, such as bacterial lipopolysaccharide (LPS), bacterial secretion systems, bacterial toxins, viral proteins, nucleic acids, increased extracellular concentration of ATP and alarmins (released by dead cells), organic and inorganic crystal or fibers (i.e., uric acid, cholesterol, ß-amyloid). Scientific evidence indicate that PAMPs and DAMPs activate NLRP3 through the induction of cytosolic alterations, such as K+ efflux, mediated by membrane pore-forming toxins or the binding of extracellular ATP to the purinergic receptor P2X7; or even in the case of damage in cell organelles (mitochondria or lysosome) with the consequent release of their contents, including reactive oxygen species, mitochondrial DNA or lysosomal cathepsins (8). As NLRP3 can be activated by such a plethora of signals, it is strongly regulated at several levels, including transcription and post-transcriptional events, including the feed-back mechanism induced by nitric oxide (NO), interferons and PGE2 (13–15).

Intriguingly, Mtb not only induces NLRP3 inflammasome activation but also the production of NO and IFN-I in mice (16). Accordingly, Wasserman et al. have shown that in THP-1, the human monocytic cell line, Mtb H37Rv triggers both NLRP3 and AIM2 inflammasome activation and IFN-1 production, most likely as an escape mechanism (17). In TB patients, the relative balance between the serum level of IL-1ß, IFN-I, and PGE-2 allows for classification according to disease severity (7). Altogether, these findings suggest that correct NLRP3 inflammasome activation can certainly contribute to bacterial clearance.

We previously reported the protective gain-of-function effect of a Single Nucleotide Variant (SNV) in the *NLRP3* 3'UTR region (rs10754558; found in about 30% of the world population) against the development of pulmonary TB (18). This led us to hypothesize genes coding factors taking part in the inflammasome assembling and function, which directly influences the IL-1ß and/or IL-18 production, could affect the outcome of an Mtb infection, therefore determining either the susceptibility and/or the prognosis for a TB patients.

In this study, we proposed a model of host/pathogen interplay including host inflammasome genetics, Mtb aggressiveness and inflammasome response rate, to evaluate the relative contribution of each parameter in individual TB susceptibility and outcome.

MATERIALS AND METHODS

Cohort for Cellular Assays

Three groups of adult volunteers were recruited for the *in vitro* study: healthy donors (HD) from TB non-endemic area, TB patients and their household contacts from TB endemic area. Thirty unrelated healthy volunteers from the metropolitan area of São Paulo (SP, Brazil) were recruited at the Blood Bank of "Oswaldo Cruz" hospital. Twenty-seven unrelated adults recently diagnosed with active pulmonary TB were recruited at the Reference Centre for Sanitary Pneumology "Cardoso Fontes" (Manaus, AM, Brazil). Twenty-seven unrelated adults in daily contact with TB patients ("household contacts") but without TB symptoms and negative for Mtb detection tests were included in the study as Mtb-exposed TB negative individuals. Diagnosis of active pulmonary TB is based on the evaluation of clinical symptoms together with Mtb detection tests: sputum smears analyses (19, 20) and/or GeneXpert MTB/RIF tests (*Cepheid*). Main characteristics of the volunteers recruited for the study are presented in **Table 1.**

Cohort for Genotyping Study

Genomic DNA from 352 unrelated TB patients and 288 healthy adults (without clinical signs or symptoms of TB) from the Brazilian State of Amazonas (not indigenous people from the Amazon forest) was used for the genetic association study. Diagnosis of TB is based on the evaluation of clinical symptoms together with Mtb detection tests, as above mentioned. Main characteristics of this cohort are presented in **Table 2**.

Mycobacterial Culture Conditions and Preparation for Cell Infection

Non-virulent Bacillus Calmette-Guerin (BCG), common virulent H37Rv and hyper-virulent Beijing 1471 (Bj) and MP287/03 (MP) mycobacterium strains were used in this study. *M. tuberculosis* H37Rv and Beijing 1471, *M. bovis strains* Bacillus Calmette-Guerin and MP287/03 were sourced from the laboratory of Professor Maria Regina D'Imperio Lima (Department of Immunology, Institute of Biomedical Sciences, University of São Paulo). Mtb were grown at 37°C, either in 7H9 medium (*Difco*) supplemented with 10% albumin-dextrose-catalase (ADC, *Middlebrook*) or on 7H10 agar plates supplemented with 10% oleic acid-albumin-dextrose-catalase (OADC, *Middlebrook*). Bacteria were grown to the exponential phase (optical density at 600 nm, OD_{600}, of 0.1), washed once in a 7H9 medium, and resuspended in 7H9 to an OD_{600}, of 1—equivalent to 2 x 10^8 bacilli/ml for BCG, 1 x10^7 bacilli/mL for H37Rv and Bj, 2 x 10^7 for MP. The required volume for Mtb bacterial suspension was then added to the cell culture medium for infection of human monocyte-derived macrophages (MDM) at a multiplicity of infection (MOI) of 0.033. This MOI was selected after pilot experiments as the minimum MOI capable of activating IL-1ß production in MDM. We avoided using a higher MOI in an attempt to mimic natural infection in humans (21). For colony formation unit (CFU) assays, infected MDM were lysed and serial dilutions were plated in a complete agar medium. After 21 days, bacterial growth in MDM was evaluated by CFU counting.

TABLE 1 | Characteristics of the individuals recruited for the cellular assays.

Characteristics	HD (*n* = 30)	TB (*n* = 27)	CNT (*n* = 27)
State of origin	SP	AM	AM
Age, years (Mean ± SD)	45 ± 13	51 ± 11	52 ± 12
Male/Female, *n* (%)	14/16 (46.7/54.3)	16/11 (59/41)	11/16 (41/59)
BCG vaccinated, *n* (%)	30 (100)	27 (100)	27 (100)
TST+, *n* (%)	0	5 (18.6)	3 (11.1)
IGRA+, *n* (%)	n.d.	12 (44.4)	13 (48.1)
Mtb detection test +, *n* (%)	n.d.	27 (100)	0
Mtb detection test in sputum smear +, *n* (%)	n.d.	13 (50)	0

State of origin in Brazil, mean age, gender distribution and BCG vaccination are reported for the three groups of studied individuals: healthy donors (HD; n = 30), TB patients (TB; n = 27) and contacts (CNT; n = 27). Positive results for TST test, IGRA, Mtb detection test as well as s Mtb detection test in the sputum smear were indicated for the TB patients and contacts.

SP, São Paulo State; AM, Amazonas State; n: number of individuals; SD, standard deviation; %, percentage; BCG, Bacillus Calmette Guerin; TST, Tuberculin Skin Test or Mantoux test; IGRA, Interferon Gamma Release Assay; Mtb, Mycobacterium tuberculosis.

TABLE 2 | General characteristics of the TB cohort for genotyping study.

Characteristics	TB (*n* = 288)	ETB (*n* = 64)	HD (*n* = 288)
Gender			
Male, *n* (%)	193 (67.0%)	30 (47.0%)	155 (46.4%)
Female, *n* (%)	95 (33.0%)	34 (53.0%)	133 (53.6%)
Mean age ± SD	38.2 ± 13.2	33.0 ± 13.02	35.8 ± 12.0
BCG–vaccinated			
Yes, *n* (%)	212 (73.6%)	55 (86.0%)	180 (62.5%)
No, *n* (%)	25 (8.70%)	9 (14.0%)	36 (12.5%)
Data not available, *n* (%)	51 (17.7%)		72 (25.0%)

Mean age, gender distribution and BCG vaccination are reported for the three groups of studied individuals from the Brazilian State of Amazonas: healthy donors (HD; n = 288), pulmonary TB (TB; n = 288) and extra-pulmonary (ETB; n = 64).

MDM Generation and *in-vitro* Infection

Peripheral blood mononuclear cells (PBMC) were isolated from donor blood using the Ficoll-Paque® density gradient centrifugation (*GE Healthcare, Biosciences*). Monocytes were separated from total PBMC by plastic adherence and cultivated at 0.4 × 10^6 cells/mL in RPMI-1640 (*Gibco, ThermoFisher Scientific*), supplemented with 10% fetal bovine serum (FBS; *Gibco*) and 25 ng/mL monocyte colony stimulating factor (M-CSF; *PreproTech*) for 5 days at 37°C in 5% CO_2 atmosphere to obtain MDM. Monocytes-to-MDM differentiation was confirmed by flow cytometry analyses of the CD14 and CD68 surface markers (**Supplementary File 1**). MDM were infected with H37Rv, Bj, MP, and BCG strains at MOI 0.033 for 3 h, washed, and then cultivated for 24 h. In some experiments. MDM were treated with 10 μM parthenolide (PTD; *Sigma-Adrich*), a general inhibitor of inflamamsome (22); or 10 μM MCC-950 (*InvivoGen*), a specific inhibitor of NLRP3 (23); or 10 μM CA074-Me (CA074; *Merck*), an inhibitor of intracellular cathepsin B; or 10 μM of cytocalasin-D (Cyt-D; *Sigma-Aldrich*), an inhibitor of actin polymerization which impairs phagocytosis. PTD, MCC-950, and Ca074 were added to MDM cultures for 1 h prior to bacterial infection. Cyt-D was added to MDM cultures during *in vitro* infection. In some experiments, 1 mM ATP (*Sigma-Aldrich*) was added at the end of treatment for another 15 min. The treatment with 1 μg/mL LPS (*E. coli* strain O111:B4; *Sigma-Aldrich*) for 24 h and 1 mM ATP for another 15 min were used as positive control for NLRP3 inflammasome activation (24, 25). For CFU assays, 10 ng/mL of recombinant human IL-1ß (rh-IL-1ß; *Peptotech*) or 10 μM PTD were added to the culture. Inflammasome activation was analyzed by IL-1ß and IL-18 release in the culture supernatants, 'cleaved/activated caspase-1 and "speck" formation.

Cytokines Quantification

IL-1ß, IL-18, IFN-ß, and TNF levels in serum and culture supernatants were measured using commercial

ELISA Kits (*Biolegend, R&D Systems*) according to the manufacturer's instructions.

Caspase-1 Activity Assay

The detection of caspase-1 activity in MDM FAM-FLICA® Caspase-1 Assay Kit (*Immunochemistry Technologies*) and flow cytometry, according to the manufacturer's instructions. Briefly, 2 x 10^5 MDM were stimulated according to the above-mentioned protocol, and then incubated with the fluorescent inhibitor probe FAM-YVAD-FMK for 1 h at 37°C, 5% CO_2. The samples were then washed, incubated with Live/Dead Fixable Cell Stain Kit (*Thermo Fisher Scientific*), and analyzed by flow cytometry. The caspase-1 activity was expressed as percentage of FAM-FLICA positive (+) live cells.

Cell Cytotoxicity

Cell cytotoxicity was assessed by the quantification of Lactate dehydrogenase (LDH) release in supernatants using the LDH Cytotoxicity Assay Kit (*ThermoFisher Scientific*), according to the manufacturer's protocol. The cytotoxicity is expressed as percentage of LDH release relative to the positive control (Triton).

"Specks" Formation

Inflammasome complex assembly was evaluated by the detection of "specks" formation using immunofluorescence microscopy. MDM were fixed and permeabilized with Cytofix/Cytoperm reagent (*BD Biosciences*) for 30 min at 37°C and 5% CO_2 and incubated with primary antibody for NLRP3 (1:100 mouse anti-human NLRP3, *Abram*) and/or NLRC4 (1:200 rabbit anti-human NLRC4; *Biolegend*) overnight at room temperature. Fluorescent secondary antibodies (Alexa 488-conjugated goat-anti-mouse IgG1, or Alexa 647-conjugated goat-anti-rabbit IgG1; *Thermofisher Scientific)* were then added for 1 h. 4',6-Diamidine-2'-phenylindole dihydrochloride (DAPI; *Sigma-Aldrich*) was used for nuclear counterstaining. Image acquisition was performed at the microscope facility at the Laboratory of Cellular Biology from the Butantan Institute (São Paulo, SP, Brazil) using a DMi8 confocal laser scanning microscope equipped with a digital camera DFC310 FX (Leica). The counting of NLRP3+ and NLRC4+ *specks* in MDM was performed manually by observing speck formation within the cells in 10 fields (26).

Inflammasome' Genes Expression Analysis

Total RNA was isolated from 0.4 × 10^6 MDM using the RNAqueous-Micro kit (*Ambion, Thermo Fisher Scientific*), according to the manufacturer's protocol, and quantified using Nanodrop N-1000 (*Agilent*). Total RNA was converted into cDNA using Superscript III RT kit and random primers (I*nvitrogen, Thermo Fisher Scientific*). *NLRP3* (*Hs00366465*), *NLRC4* (*Hs00368367*), *IL1B* (hs01555410), and *IL18 (Hs01038788*) genes were amplified using TaqMan® gene-specific assays (*Applied Biosystems, Thermo Fisher Scientific*) and qPCR on the QuantStudio 3.0 Real-Time PCR equipment (*Applied Biosystems*). The QuantStudio 3.0 software was used to obtain cycle threshold values (Ct) for relative gene expression analysis according to the Fold Change (FC) method (27). Raw expression data (Ct) were normalized with the expression of the house-keeping gene glyceraldehyde-3-phosphate dehydrogenase/*GAPDH* (*Hs02758991; TaqMan® assay*) (ΔCt), and the FC was calculated comparing stimulated and unstimulated (UN) conditions ($FC=2^{--\Delta\Delta Ct}$; $\Delta\Delta Ct = \Delta Ct_{stimulated} - \Delta Ct_{UN}$). Alternatively, basal (constitutive) gene expression was calculated as $2^{-\Delta Ct}$.

SNVs Genotyping

NLRP3 rs10754558 C>G and *NLRC4* rs479333 G>C single nucleotide variants were selected based on their known functional effect, and elevated minor allele frequency (MAF) in the general population (0.30 and 0.49 respectively, from *www.ensembl.org*). *NLRP3* rs10754558 is a 3'UTR variant previously associated with increased *NLRP3* mRNA stability and supposed augmented inflammasome activation (28). *NLRC4* rs479333 is an intronic polymorphism which negatively affects *NLRC4* expression (29) and serum IL-18 level (30). They were genotyped in the TB cohort with TaqMan®-type allele-specific commercial assays (*Applied Biosystems*) and qPCR on the QuantStudio 3.0 Real-Time PCR equipment. The QuantStudio 3.0 software was used for allelic discrimination.

Data Analysis

All data were collected and analyzed from at least three independent experiments. A normality test was applied to the data, and a parametric or non-parametric analysis was used accordingly to compare two or more data sets, as specified for each graph. The level of significance was $p < 0.05$. Calculations were performed using the statistical software package GraphPad Prism (v8.01). Genotyping data were analyzed through multivariate analysis according to the general linear model (GLM) using the package SNPassoc and R-project. Bonferroni correction for multiple comparisons (2 SNVs) required a $p < 0.025$ (0.05/2).

RESULTS

M. tuberculosis Induces Inflammasome Activation and IL-1ß Production Plays a Major Role in Bacterial Restriction *in vitro* as Well as *in vivo*

Mtb triggers NLRP3 inflammasome in mice (10–12), as well as in some *in-vitro* models of human macrophages (17, 31, 32); however, the multiplicity of infection (MOI) implied is always high (1–10 or more) compared to what expected during natural infection (<<1) (21).

Considering this, we first investigated whether the common virulent reference strain Mtb H37Rv activates the inflammasome at a physiologic MOI. For this, we measured cytokine production and caspase-1 activation at a MOI of 0.033 in Mtb-infected monocyte-derived macrophages (MDM).

At this MOI, H37Rv was also able to induce a significant release of inflammasome cytokines IL-1ß (**Figure 1A**) and IL-18

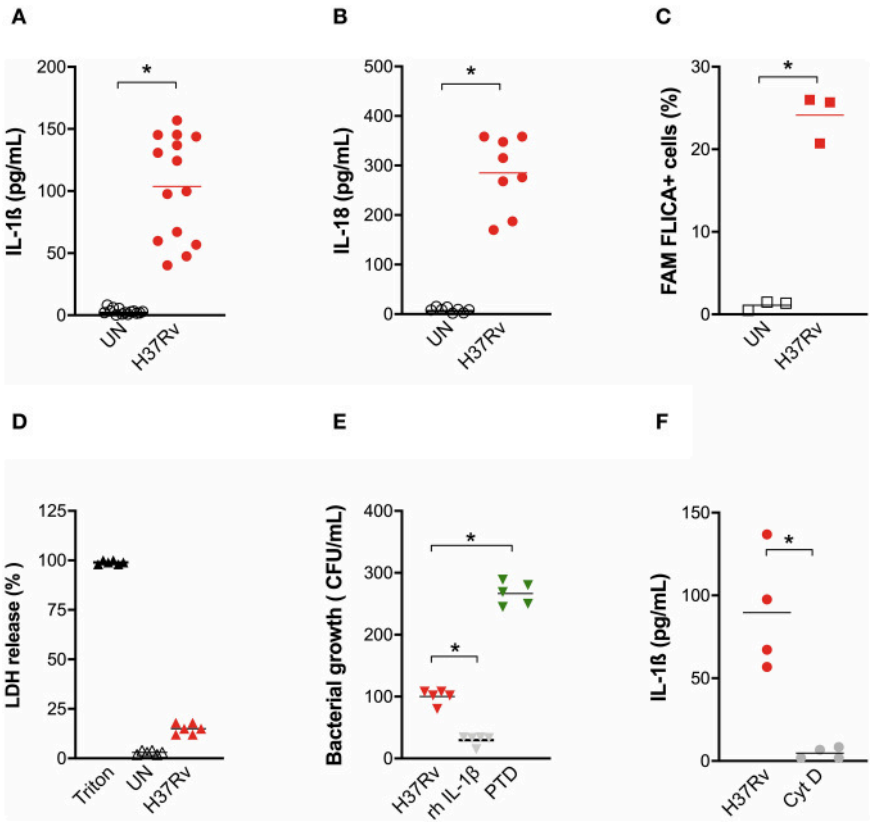

FIGURE 1 | *M. tuberculosis* strain H37Rv induces inflammasome activation in human MDM and IL-1ß production plays a major role in bacterial restriction. The healthy donors' monocyte-derived macrophages (MDM; $n = 14$) were challenged with the *M. tuberculosis* (Mtb) strain H37Rv (MOI: 0.033) for 3 h, then washed and cultured for 24 h. The release of IL-1ß ($n = 14$) **(A)** and IL-18 ($n = 8$) **(B)** was measured in culture supernatants of untreated (UN) and infected (H37Rv) MDM. Cells were harvested for an analysis of caspase-1 activity by a FAM-FLICA® assay and flow cytometry from three independent experiments. The percentage of FAM-FLICA+ cells was reported for H37Rv-infected (H37Rv) and untreated (UN) MDM **(C)**. Lactate Dehydrogenase (LDH) liberation was measured in culture supernatants in three independent experiments. Data are expressed as a percentage in respect to the positive control (Triton, 100% cell lysis) **(D)**. The healthy donors' MDM ($n = 5$) were infected with Mtb H37Rv (MOI: 0.033) for 3 h in the presence of exogenous recombinant human IL-1ß (rh-IL-1ß) or parthenolide (PTD; 10 μM), then lysed. Serial dilutions were plated in a complete agar medium. Bacterial growth was evaluated after 21 days by counting colony formation units (CFU) **(E)**. The healthy donors' MDM ($n = 4$) were infected with Mtb H37Rv (MOI: 0.033) for 3 h in the presence of cytochalasin D (Cyt D; 10 μM), then washed and cultured for 24 h. The release of IL-1ß was measured at the end of incubation in infected MDM (H37Rv) and infected MDM in the presence of a phagocytosis inhibitor (Cyt D) **(F)**. Individual data are reported with their mean. The Mann–Whitney test was used to compare treated and untreated groups **(A–C,F)**. The Kruskall–Wallis test followed by a Bonferroni post-test were used to compare H37Rv, rh-IL-1ß, and PTD groups **(E)**. Differences with a $p < 0.05$ were considered statistically significant (*).

(**Figure 1B**) from MDM, which was accompanied by the increase of caspase-1 cleavage (**Figure 1C**) but not by a significant release of LDH (**Figure 1D**), suggesting the induction of the canonical pathway of inflammasome activation, but without high rates of pyroptosis.

Little is known about a possible function of IL-18 against mycobacteria, while IL-1ß plays a role in macrophages phagocytosis (33) Therefore, we performed a bacterial growth assay in Mtb-infected MDM in the presence of exogenous recombinant IL-1ß or pre-treated with the inflammasome inhibitor parthenolide (PTD). H37Rv bacterial growth was significantly inhibited by IL-1ß (70.2% CFU inhibition). At the same time, a significant increase of Mtb growth was observed when PTD was added to cultures (160% CFU increase) (**Figure 1E**). H37Rv-driven inflammasome activation seems to be direct, as the inhibition of mycobacterial phagocytosis completely abolished IL-1ß production (**Figure 1F**).

These data emphasize that the activation of inflammasome and IL-1β production are mandatory for Mtb containment.

NLRP3 Contributes to Inflammasome Activation by the *Mtb* Common Virulence Strain H37Rv in Human MDM

As our previous results pointed out the protective role of a gain-of-function genetic variant in *NLRP3* (rs10754558) (18), and given the central role of this receptor in the mouse model of Mtb infection as well (10–12), we next asked whether the observed activation of inflammasome complex by Mtb H37Rv in MDM could be dependent on NLRP3. The

formation of *specks* indicates the activation of inflammasome and also allows for the visualization of a mounted complex platform, including the activated sensor (26). Thus, we subsequently replicated MDM infection with Mtb H37Rv to confirm NLRP3 participation in inflammasome responses. To do so, cells were stained using specific antibodies and samples analyzed at the end of infection assay under a fluorescence microscope. A significant increase of NLRP3+ specks were detected in Mtb-infected MDM compared to untreated cells (**Figures 2A,B**).

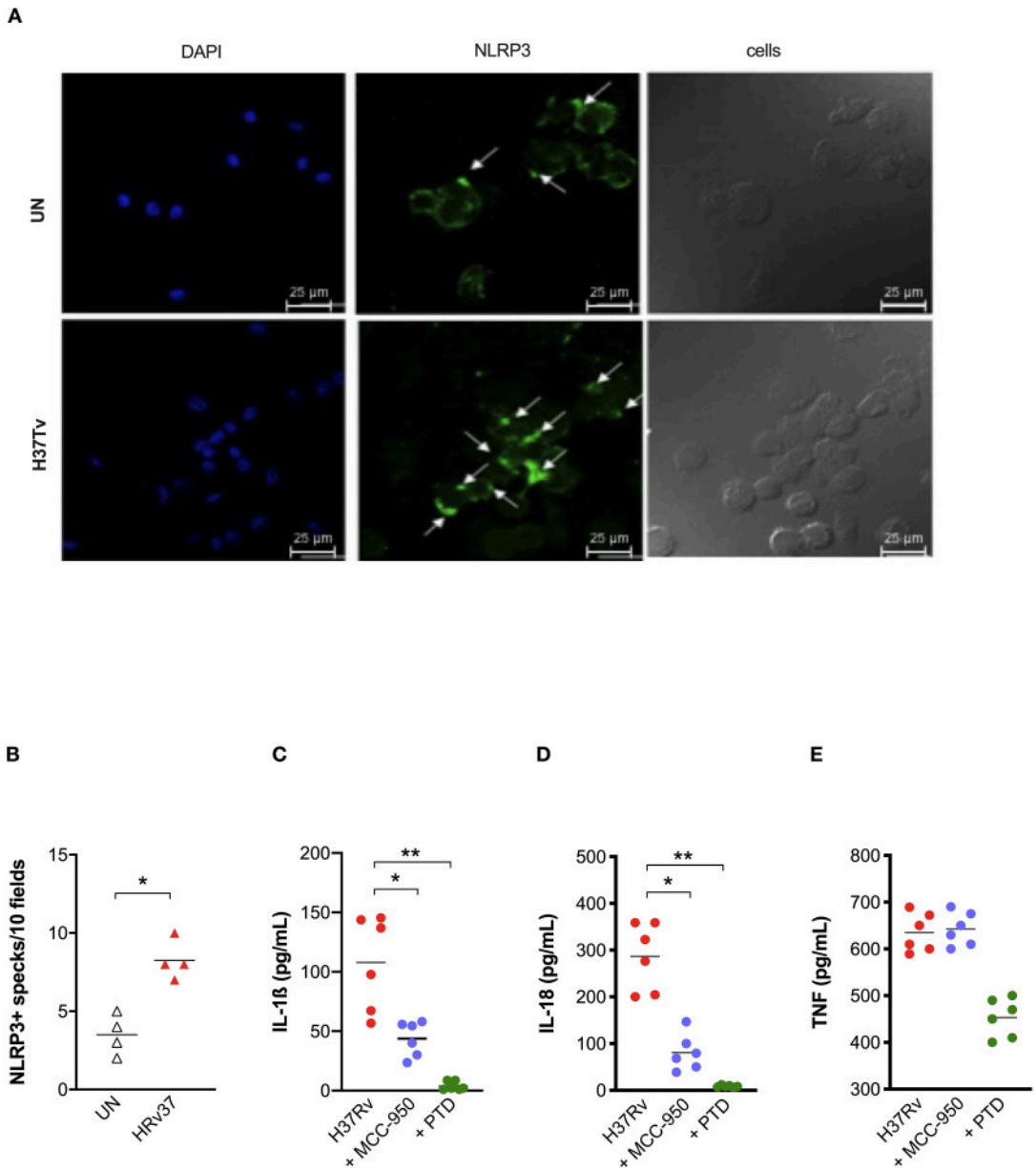

FIGURE 2 | NLRP3 contributes to inflammasome activation by *Mtb* H37Rv in human MDM. The healthy donors' monocyte-derived macrophages (MDM; $n = 4$) were cultivated (0.08×10^6) in 16-well chamber slides (*Thermo Fisher Scientific*), challenged with *M. tuberculosis* (Mtb) H37Rv (MOI: 0.033) for 3 h, then washed and cultured for 24 h. Mouse anti-human NLRP3 and a fluorescent secondary antibody (Alexa 488-conjugated goat-anti-mouse IgG1) were used to label NLRP3. DAPI was used to counterstain the nuclei. NLRP3+ speck formation in untreated (UN) and infected MDM (H37Rv) was analyzed using fluorescence microscopy. A representative experiment was reported. Arrows indicated NLRP3+ specks. **(A)**. The number of NLRP3+ specks was manually counted for each independent experiment **(B)**. The healthy donors' monocyte-derived macrophages (MDM; $n = 6$) were treated with 10 µM MCC-950 or 10 µM parthenolide (PTD) 1 h before infection with *M. tuberculosis* H37Rv (MOI: 0.033) for 3 h, then washed and cultured for 24 h. The release of IL-1ß **(C)**, IL-18 **(D)**, and TNF **(E)** was measured in culture supernatants. Individual data are reported with their mean. The Mann–Whitney test was used to compare treated and untreated groups **(B)**. The Kruskall–Wallis test followed by a Bonferroni post-test were used to compare H37Rv, MCC-950 and PTD groups **(C–E)**. Differences with a $p < 0.05$ were considered statistically significant (*). **$p < 0.001$.

Next, we applied another approach, based on the use of known chemical inhibitors, to confirm NLRP3 involvement in the response. IL-1ß and IL-18 release was measured in Mtb infected-MDM and pre-treated with the NLRP3 inhibitor MCC-950 (10 μM) (23). As a positive control of inhibition, we also pre-treated MDM with the general inflammasome inhibitor parthenolide (PTD; 10 μM) (22). As expected, PTD entirely abolished cytokines production, while MCC-950 significantly reduced, but not completely abrogated, the release of IL-1ß (**Figure 2C**) and IL-18 (**Figure 2D**) in infected-MDM (48.7 and 71.7% inhibition, respectively). The secretion of a non-inflammasome-dependent pro-inflammatory cytokine, TNF, was not significantly affected by the use of inhibitors (**Figure 2E**).

Altogether, these findings corroborate previous data about the importance of NLRP3 in macrophage' response against virulent Mtb (10–12, 17, 31, 32), including at physiologic condition of infection (MOI: 0.033), and support the protective effect observed for *NLRP3* rs10754558 against the development of active pulmonary TB (18).

TB Patients Present an Impaired NLRP3 Response and IL-1ß Release

In order to better understand the relative contribution of inflammasome activation and IL-1ß release in Mtb infection *in vivo*, we analyzed IL-1ß, IL-18, IFN-α, and TNF levels in the plasma of patients recently diagnosed with active pulmonary TB (TB) and their "household contacts" (CNT) from an endemic TB area (Brazilian State of Amazonas). A group of healthy donors from a non-endemic area (São Paulo, SP, Brazil) was also included. All cytokines, with the exception of IL-18, were up-regulated in TB and CNT individuals with respect to HD (**Figures 3A–D**). Of note, a significant difference was observed in the plasma level of IL-1ß (**Figure 3A**) and IFN-α (**Figure 3C**) between the TB and the CNT groups. The IL-1ß concentration is significantly lower in the TB than in the CNT samples, while the IFN-α level increased in the TB compared to the CNT sample (**Figures 3A,C**).

These results emphasize that the TB patients presented an imbalance between IL-1ß and IFN-α, as suggested from animal models and *in-vitro* assays (17). These results also show that "household contacts" from endemic areas are characterized by a different plasma cytokine profile compared to TB patients or to the general population from non-endemic TB areas. In part, our findings also correspond with Mayer-Barber et al. (7), even if the unbalance was described specifically for severe TB vs. mild form of the disease in that study.

When we performed a canonical correlation between plasma IL-1ß levels and sputum positivity for Mtb, we observed that the IL-1ß level inversely correlated with the Mtb positive sputum, leading us to clearly separate the CNT and TB groups (**Figure 3E**). This once more confirms that the production of IL-1ß is an important contributing factor for Mtb infection control, and that this response could be measured systemically.

Next, taking in account the role of NLRP3 in the IL-1ß release by Mtb-infected MDM and the fact that IFN-I is a known inhibitor of NLRP3 (31), we questioned whether the imbalance between IL-1ß and IFN-α, observed in the plasma of TB patients could be related to an impairment of NLRP3 inflammasome.

In an attempt to respond to this tricky question, we first compared the constitutive expression of *NLRP3*, *CASP1*, *IL1B*, and *IL18* in MDM from the TB patients, their household contacts (CNT) and heathy donors from a non-endemic region (HD); however, no significant difference resulted among the groups (**Figure 3F**).

We then treated MDM with 1 μg/mL of LPS for 24 h—with or without the further addition of 1 mM ATP for 15 min—and compared the IL-1ß release among the TB, CNT and HD groups. In cells with normal NLRP3, the addition of ATP significantly increased the LPS-induced release of IL-1ß (24). As expected, ATP boosted IL-1ß release in LPS-treated MDM from HD, and intriguingly also from CNT; however, it did not significantly affect the cytokine release in LPS-treated MDM from TB patients (**Figure 3G**).

This unresponsiveness of MDM seems to be, at least in part, due to the poor induction of *NLRP3* and *IL1B* expression in TB-treated cells, compared to MDM from HD or CNT (**Figure 3H**). This condition could be a consequence of high IFN-α production, which possibly prevents NLRP3 inflammasome response (13).

Altogether, these results demonstrate that recently diagnosed TB patients present defective NLRP3 inflammasome and IL-1ß release and, conversely, increased IFN-α production, which can be at least in part responsible for NLRP3 inhibition. Moreover, for the first time to our knowledge, we showed that exposed but healthy subjects ("household contacts") display an inflammasome response similar to non-exposed healthy donors, allowing us to hypothesize that "Mtb-resistant" individuals may have an IL-1ß production that is better able to counteract IFN-I induction by mycobacteria.

Inhibition of Cathepsin Activity Abolished IL-1ß and IL-18 Release Suggesting the Contribution of NLRC4 in Inflammasome Activation by Mtb H37Rv

Among typical NLRP3 activation pathways, P2X7-mediaded K+ efflux and lysosomal cathepsins release have been reported as possible mechanisms for an inflammasome activation by mycobacteria (11, 34). To investigate the contribution of these two mechanisms in our model, exogenous ATP (1 mM) or Ca074-Me (10 μg/mL) were added for 15 min after or 1 h before Mtb infection, respectively. As a positive control for NLRP3 activation, MDM were also stimulated with 1 μg/mL of LPS for 24 h with or without 1 mM ATP for another 15 min (24).

Exogenous ATP did not significantly alter inflammasome cytokine production in H37Rv-treated MDM, or in LPS-treated ones (**Figures 4A,B**), suggesting that, at least in this model, ATP did not amplify mycobacterial stimulation as previously observed in mice (34). On the other hand, the inhibitor of lysosomal cathepsin activity Ca074-Me completely abolished IL-1ß and IL-18 release (96.7 and 97% of inhibition, respectively) (**Figures 4A,B**), reinforcing previous findings about the role of lysosomal cathepsins release in inflammasome activation by mycobacteria (11).

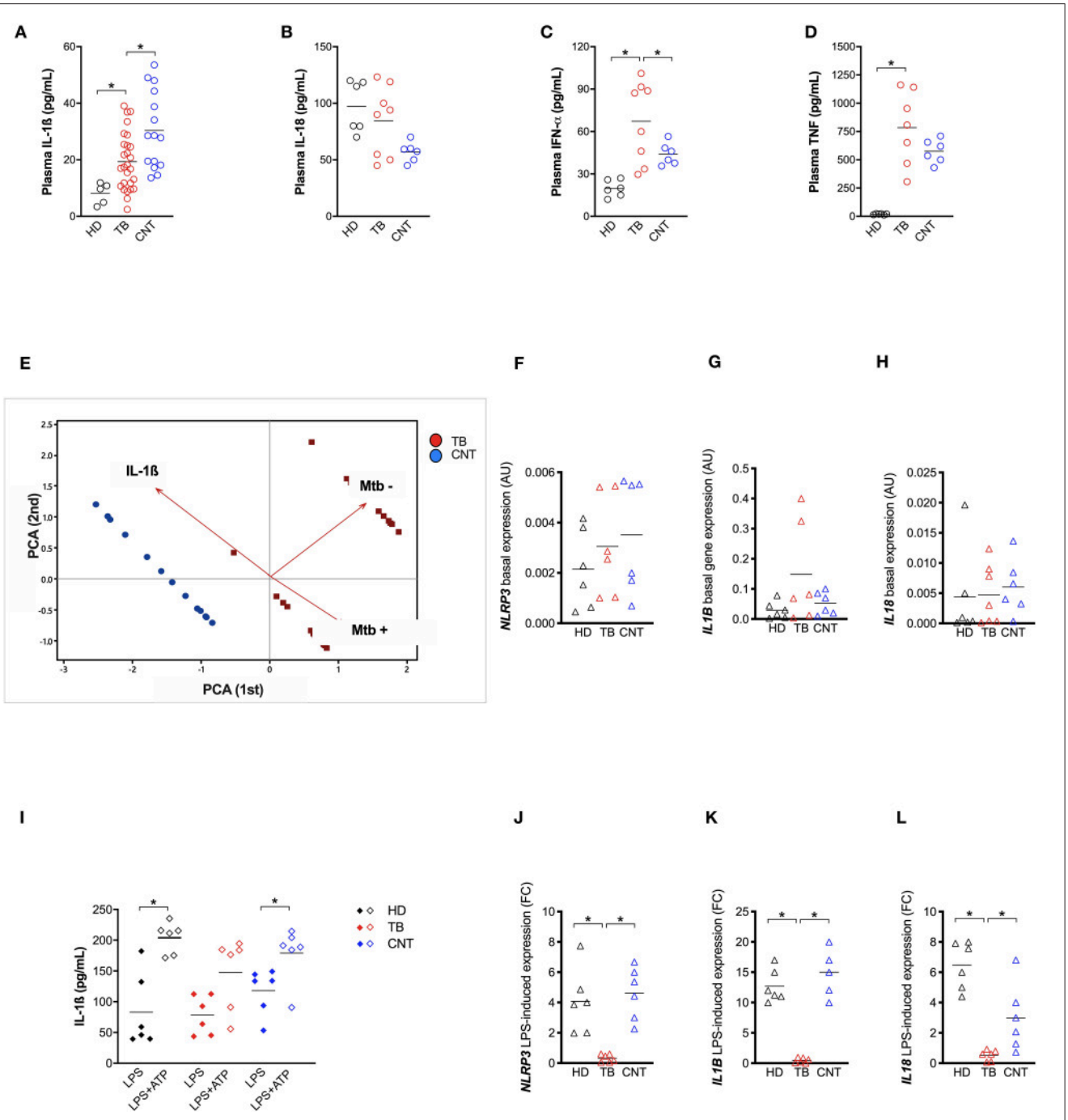

FIGURE 3 | TB patients present an impaired NLRP3 inflammasome response. IL-1ß **(A)** level were measured in plasma from recently diagnosed untreated TB patients (TB; $n = 27$) and some of their "household contacts" (CNT; $n = 15$) from an endemic TB area (Manaus, metropolitan region, AM) and from healthy donors in a non-endemic area (São Paulo metropolitan region, SP) (HD; $n = 5$). IL-18 **(B)**, IFN-a **(C)**, and TNF **(D)** dosage was executed in a group of samples (HD, $n = 6$; TB, $n = 8$; CNT, $n = 6$). **(E)** A Principal Components (PC) analysis was executed including the plasma level of IL-1ß, a mycobacteria count in a sputum analysis and a diagnosis of TB (TB or CNT). Monocyte-derived macrophages (MDM) were isolated from HD ($n = 6$), TB patients ($n = 6$), and CNT ($n = 6$) and challenged with 1 μg/mL of LPS for 24 h (LPS), or 1 μg/mL of LPS for 24 h plus 1 mM of ATP for another 15 min (LPS+ATP). Cells were lysed for RNA isolation and expression analysis. The release of IL-1ß was measured in culture supernatants. **(F–H)** Basal expression of *NLRP3, IL1B*, and *IL18* genes were analyzed in untreated MDM using gene-specific Taqman® assays and qPCR. Row target gene expression was normalized by the expression of the *GAPDH* house-keeping gene (ΔCt). Relative expression was calculated as $2^{-\Delta Ct}$. Data are expressed as arbitrary units (AU). **(I)** IL-1ß was measured in culture supernatants of treated MDM. **(J–L)** LPS-induced expression of *NLRP3, IL1B*, and *IL18* genes were analyzed in treated MDM using gene-specific Taqman® assays and qPCR. Row target gene expression was normalized by the expression of *GAPDH* house-keeping gene (ΔCt). Modulation of gene expression was calculated as Fold Change (FC = $2^{--\Delta\Delta C}$) in respect to untreated (UN) cells. Individual data are reported with their mean. The Mann–Whitney test was used to compare two groups. The Kruskall–Wallis test followed by a Bonferroni post-test were used to compare more than two groups. Differences with a $p < 0.05$ were considered statistically significant (*).

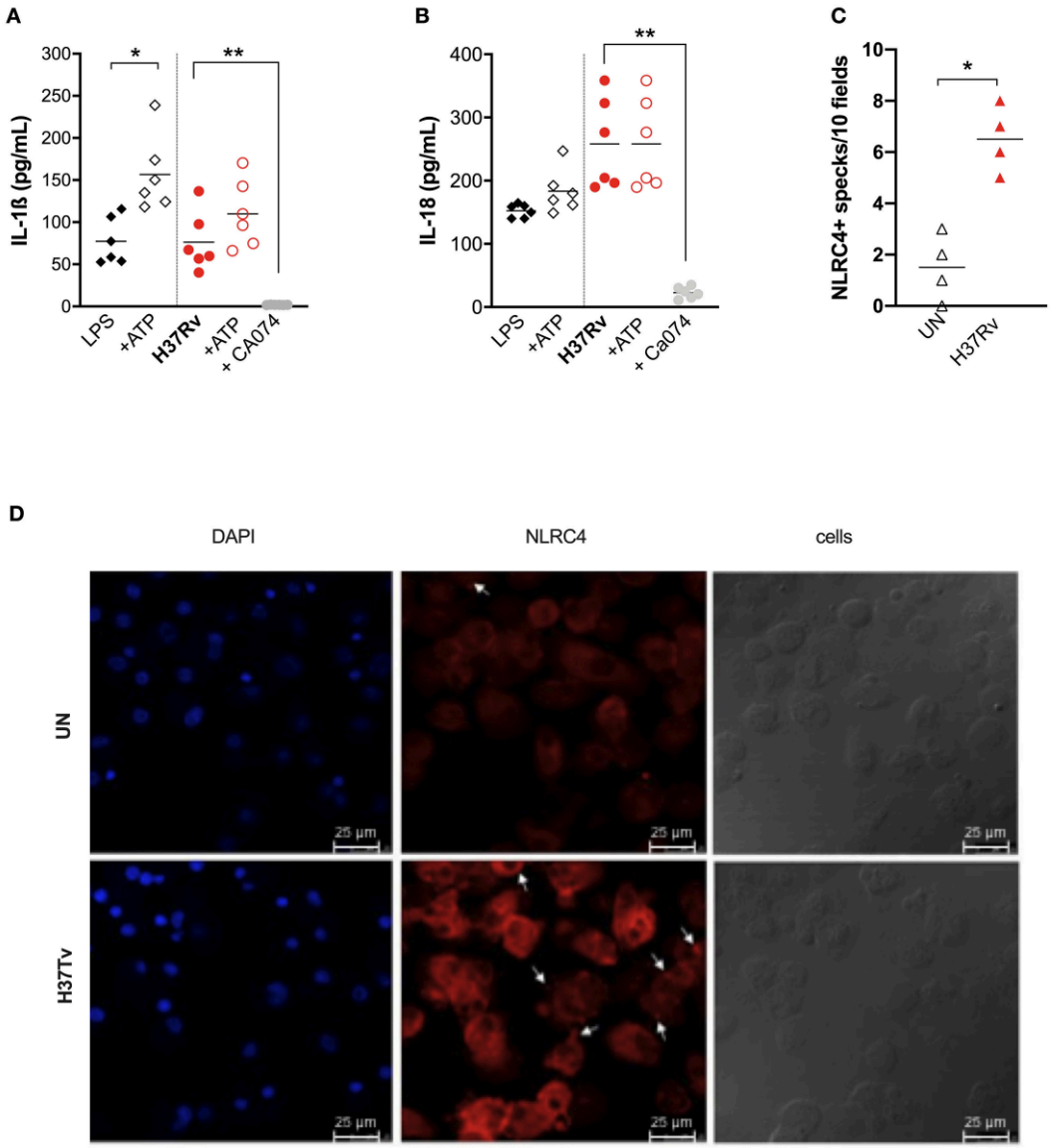

FIGURE 4 | Cathepsins activity is the major mechanism for inflammasome activation by *M. tuberculosis* H37Rv in human MDM, triggering NLRP3 and NLRC4. The healthy donors' monocyte-derived macrophages (MDM; $n = 6$) were treated or not with Ca074-Me (Ca074; 10 µM) before the infection with *M. tuberculosis* H37Rv (MOI: 0.033) for 3 h, then washed and cultured for 24 h. ATP (1 mM) was eventually added for another 15 min in H37Rv-infected MDM. The stimulation of MDM using LPS (1 µg/mL) for 24 h with or without ATP (1 mM) was included as a positive control for NLRP3 inflammasome activation. The release of IL-1ß **(A)** and IL-18 **(B)** was measured in culture supernatants. Healthy donors' monocyte-derived macrophages (MDM; $n = 4$) were cultivated (0.08×10^6) in 16-well chamber slides (*Thermo Fisher Scientific*), challenged with *M. tuberculosis* H37Rv (MOI: 0.033) for 3 h, then washed and cultured for 24 h. Rabbit anti-human NLRC4 and fluorescent secondary antibody (Alexa 647-conjugated goat-anti-rabbit IgG1) were used to label NLRC4. DAPI was used to counterstain the nuclei. NLRC4+ speck formation in untreated (UN) and infected MDM (H37Rv) was analyzed using fluorescence microscopy. The number of NLRPC+ specks was manually counted for each independent experiment **(C)**. A representative experiment was reported. Arrows indicated NLRC4+ specks. **(D)** Individual data are reported with their mean. The Kruskall–Wallis test followed by a Bonferroni post-test were used to compare more than two groups **(A,B)**. The Mann–Whitney test was used to compare treated and untreated groups **(C)**. Differences with a $p < 0.05$ were considered statistically significant (*). **$p < 0.001$.

Taking into account the discrepancy between the only partial reduction in inflammasome activation by MCC-950 (**Figures 2A,B**), the complete inhibition by Ca074-Me (**Figures 4A,B**), and the fact that cathepsin release activates another complex receptor, the NLRC4 (35), we hypothesized that this molecule could also be involved in the macrophage response to Mtb. To visualize the NLRC4 participation in inflammasome activation, we once again performed MDM infection with Mtb H37Rv assays and stained the specks using specific antibodies. Samples were observed under a fluorescence microscope. A

significant increase in the number of NLRC4+ specks was observed in Mtb-infected MDM compared to untreated cells (**Figures 4C,D**).

These findings show that lysosomal cathepsins represent the main pathway for NLRP3 triggering by H37Rv, and maybe also for NLRC4, a receptor which is poorly investigated in TB and pulmonary diseases.

Genetic Variants in *NLRP3* and *NLRC4* Genes Distinctively Affect the Host Response to *M. tuberculosis* Infection and Outcome

Once confirming the central role exerted by NLRP3 in the inflammasome activation and host response against virulent Mtb, we next investigated the contribution of the TB protective *NLRP3* variant rs10754558 (18) on this response.

For this purpose, IL-1ß and IL-18 release from Mtb-challenged HD MDM was compared in carriers and non-carriers of the variant. As expected, individuals carrying the gain-of-function rs10754558 C>G variant in homozygosis (G/G) produced more IL-1ß when stimulated with the Mtb H37Rv than non-carriers (**Figure 5A**), confirming that NLRP3 is a crucial inflammasome sensor for Mtb. Moreover, in the presence of high levels of NLRP3 (28), macrophages respond to Mtb processing a larger amount of IL-1ß. Intriguingly, the IL-18 release in Mtb-treated HD MDM was not significantly affected by this SNV (**Figure 5B**). Then we performed the genotype-guided analysis with plasma cytokines levels in TB patients TB patients carrying rs10754558 G/G displayed an increased level of IL-1ß compared to non-carriers (**Figure 5C**), emphasizing that the effect of the NLRP3 gain-of-function variant against Mtb is detectable also *in vivo*. The SNV did not affect the inflammasome-dependent cytokine TNF (**Supplementary File 2A**).

In our previous genotyping analysis (18), we did not include the *NLRC4* gene. At that time, genetic association studies did not refer to *NLRC4* as an important locus for Mtb infection. Only recently, it was reported that *NLRC4* SNVs may affect the outcome of TB in chronically infected HIV patients (36). As our *in vitro* results indicate the participation of NLRC4 in

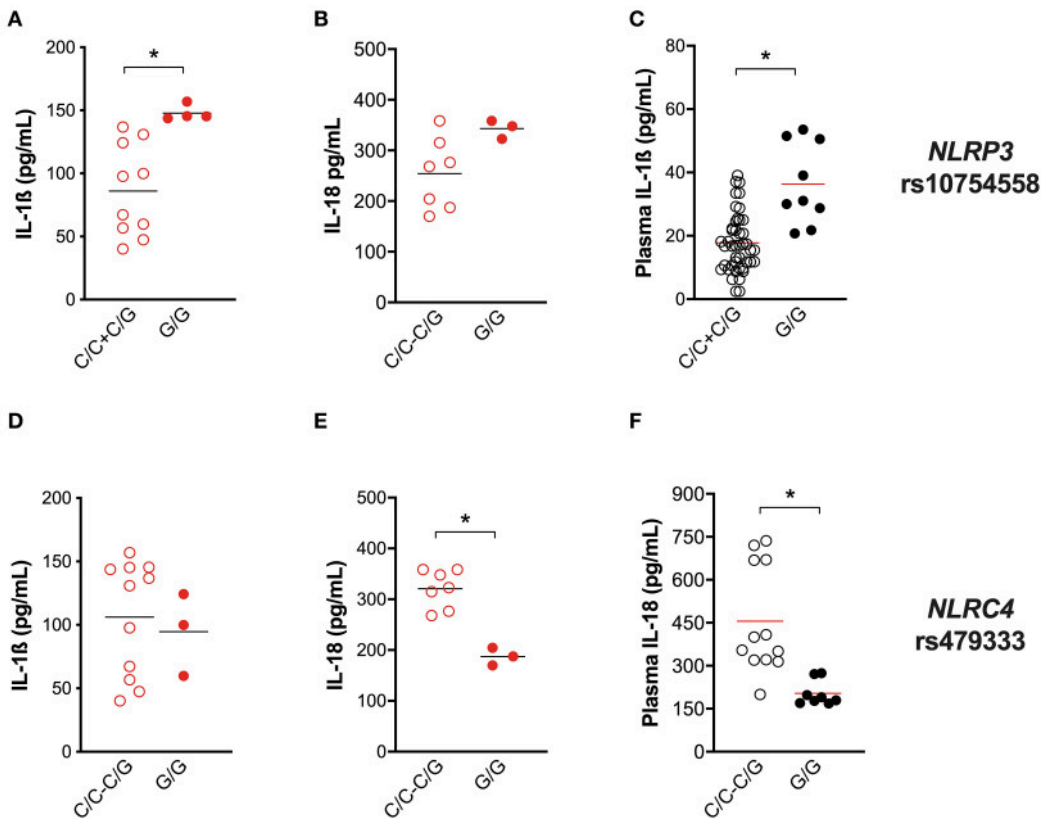

FIGURE 5 | Genetic variants in *NLRP3* and *NLRC4* genes affect host response to *M. tuberculosis*. The healthy donors' monocyte-derived macrophages (MDM; $n = 14$) were treated with *M. tuberculosis* H37Rv (MOI: 0.033) for 3 h, then washed and cultured for 24 h. The IL-1ß and IL-18 level was measured in culture supernatants at the end of experiment ($n = 14$ and 8, respectively), and in the plasma of TB patients ($n = 27$ and 20, respectively). *NLRP3* rs10754558 and *NLRC4* rs479333 SNVs were genotyped in the genomic DNA of healthy donors and TB patients. IL-1ß and IL-18 release data were then grouped by individual *NLRP3* rs10754558 genotype into homozygotes for the minor G allele (G/G) and the others (C/C+C/G), according to a recessive model of inheritance for the minor allele **(A–C)**; or by individual *NLRC4* rs479333 genotype into homozygotes for the minor C allele (C/C) and the others (G/G+G/C) according to a recessive model of inheritance for the minor allele **(D–F)**. Individual data are reported with their mean. The Mann–Whitney test was used to compare the groups. Differences with a $p < 0.05$ were considered statistically significant (*).

inflammasome activation by virulent Mtb (**Figure 4**), we selected a known functional variant in *NLRC4* (rs479333 G>C; found in 45% of the general population) and performed a genotype-guided analysis. The loss-of-function rs479333 variant did not affect IL-1ß in our *in-vitro* model of infection (**Figure 5D**), but was associated with a lower level of IL-18 both *in vitro* (**Figure 5E**) and *in vivo* (TB patients' plasma) (**Figure 5F**). The SNV did not affect the inflammasome-independent cytokine TNF (**Supplementary File 2B**).

These findings functionally demonstrate the effect of *NLRP3* rs10754558 SNV on TB protection (18), emphasizing the key role of NLRP3 in the first contact host/mycobacteria. Moreover, they suggest that *NLRC4* genetics may also affect Mtb/host interplay, even if in a different way.

Trying to assess whether *NLRC4 r*s479333 can represent a susceptibility factor for TB, we performed an association study in a case/control cohort of TB. A multivariate analysis was first executed comparing *NLRC4 r*s479333 and *NLRP3* rs10754558 distribution between TB patients and healthy donors. Then, to detect the possible effect on clinical presentation, we compared SNVs distribution in TB patients with pulmonary and with extra-pulmonary forms. The results are presented in **Table 3**.

As we have previously shown (18), *NLRP3* rs10754558 represents a protective factor against TB susceptibility, being more frequent in controls (G/G: 0.13) than in patients (0.04). On the other side, and for the first time to our knowledge, we observed that the loss-of-function variants in *NLRC4* (rs479333), which did not affect susceptibility to TB *per se* ($p_{adj} = 0.658$), results significantly less frequent in patients with the more severe form of infection (extra-pulmonary TB) compared to pulmonary TB, according to a dominant model of inheritance for the minor C allele (G/C+C/C: 0.40 vs. 0.61) (**Table 3**).

This genetic approach was not only useful for supporting the previously published association of the *NLRP3* rs10754558 variant with Mtb infection (18), but also for revealing that *NLRC4* could be another genetic factor important for the outcome of infection. It is interesting to emphasize that the two studied SNVs (rs10754558 and rs479333) principally affect one or the other inflammasome cytokine in Mtb-infected MDM (IL-1ß and IL-18, respectively), suggesting the distinct contribution of the mediators in TB.

Mtb Strains of Different Virulence and the Host's Genetic Background Shape NLRP3 Inflammasome Response to Mycobacteria

As the development of active TB is the complex outcome of several factors, including genetics, environment and pathogen biology (3), the next step was to evaluate the impact of Mtb phenotype on the inflammasome activation together with the host's genetic background. For this purpose, and considering the emergence of TB patients with a severe presentation caused by hyper-virulent strains (37, 38), MDM were challenged with different strains of mycobacteria: BCG and MP287/03 (MP) non-virulent and hyper-virulent strains from *M bovis* respectively; and the hyper-virulent strain Beijing-1471 (Bj) from *M. tuberculosis*. IL-1ß and IL-18 release was compared with the common virulent strain H37Rv, also from *M. tuberculosis*.

H37Rv and Bj strains induced a similar amount of IL-1ß, but higher than MP, providing to be a poor IL-1ß producer. BCG was the major inductor of IL-1ß, leading to about a 3-fold increase in cytokine compared to H37Rv or Bj (**Figure 6A**). This difference among BCG, H37Rv, and Bj was not as important in the case of IL-18 production, even if BCG tends to induce a higher amount of cytokine, especially when compared to H37Rv (**Figure 6B**). MP was able to induce significant IL-18 release compared to untreated MDM, even if in a lower amount compared to other strains (**Figure 6B**). Of note, the production of TNF was similar in all conditions (**Figure 6C**), as well as the LDH release (**Figure 6D**).

To depict the relative contribution of NLRP3 in sensing distinct Mtb strains, we performed assays in the presence of the NLRP3 specific inhibitor MCC-950 or the general inhibitor PTD. MCC-950 inhibited about half of IL-1ß and IL-18 production in H37Rv-, Bj-, and BCG-treated -MDM. Due to the low production of IL-18 induced by MP the inhibition rate observed for MCC-950 was not statistically significant ($p = 0.08$) (**Figures 6E,F**). As expected, PTD completely abolished IL-1ß and IL-18 production in all the conditions (**Figures 6E,F**).

The pattern of IL-1ß and IL-18 release by MDM was distinct depending on the Mtb strain, and these differences may be related to the different ability of Mtb strains to induce inflammasome genes expression (**Figure 6G**). In terms of cytokine production, BCG promotes the highest expression of

TABLE 3 | Association results for SNVs in inflammasome-encoding genes in the TB cohort from the Brazilian State of Amazonas.

Gene SNV ID	Effect	Genotypes	HD ($n = 288$)	TB ($n = 352$)	p_{adj} OR_{adj} (95%CI)	PTB ($n = 288$)	ETB ($n = 64$)	p_{adj} OR_{adj} (95%CI)
NLRP3 rs10754558	GoF	C/C	0.52	0.65	**0.003** 0.16 (1.02–1.29)	0.68	0.62	0.475 0.96 (0.64–3.56)
		C/G	0.35	0.31		0.27	0.34	
		G/G	0.13	0.04		0.05	0.04	
NLRC4 rs479333	LoF	G/G	0.66	0.49	0.658 0.78 (0.25–2.43)	0.39	0.60	**0.0006** 0.20 (1.92–13.16)
		C/G	0.20	0.31		0.39	0.23	
		C/C	0.14	0.20		0.22	0.17	

Gene symbol, variant identification number (SNV ID), genotypes frequencies for patients with active pulmonary TB (PTB) extra-pulmonary (ETB) and healthy donors (HD), GLM p-value (p), odds ratio (OR) and 95% confidence interval (CI) are reported adjusted for sex and age (p_{adj}, OR_{adj}). Statistically significant results after Bonferroni correction are indicated in bold characters.

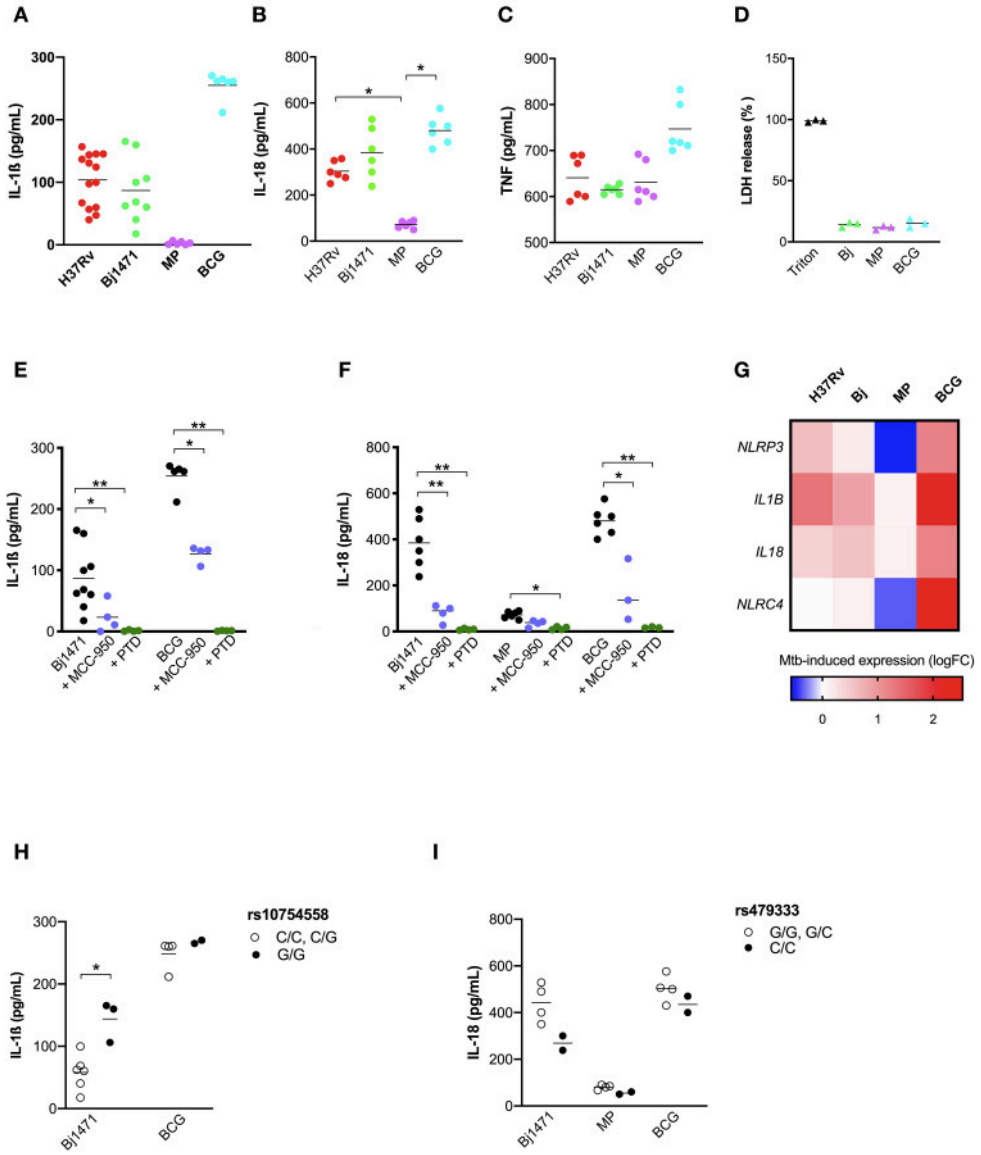

FIGURE 6 | Mtb strains of different virulence and host genetic background shaped the inflammasome response to mycobacteria. The healthy donors' monocyte-derived macrophages (MDM) were treated with 10 μM MCC-950 or 10 μM parthenolide (PTD) 1 h before infection with *M. tuberculosis* (MOI: 0.033) H37Rv ($n = 14$), Beijin-1470 (Bj-1470; $n = 9$), MP287/03 (MP; $n = 6$) and *Bacillus Calmette Guerin* (BCG; $n = 6$) for 3 h, then washed and cultured for 24 h. The release of IL-1ß **(A)**, IL-18 **(B)**, TNF **(C),** and LDH **(D)** was measured in culture supernatants. Dosage for IL-1ß was executed for all samples, while for IL-18 and TNF in six samples, for LDH in three sample. Cytokines and LDH release were compared among different Mtb strains. Cells were lysed for RNA isolation and gene expression analysis. *NLRP3* rs10754558 and *NLRC4* rs479333 SNVs were genotyped in the genomic DNA of healthy donors. The effect of MCC-950 and PTD on inflammasome activation in infected MDM was analyzed by the meaning of IL-1ß **(E)** and IL-18 **(F)** release. Mtb-induced expression of *NLRP3, NLRC4, IL1B,* and *IL18* genes in H37Rv-, Bj-1470-, MP- and BCG-infected MDM was calculated as $2^{-\Delta\Delta Ct}$ (fold-change, FC) and reported as $\log_2$FC in a heat-map graph **(G).** IL-1ß release data were grouped by individual *NLRP3* rs10754558 genotype into homozygotes for the minor G allele (G/G) and the others (C/C+C/G), according to a recessive model of inheritance for the minor allele **(H)**. IL-18 release data were grouped by *NLRC4* rs479333 genotype into homozygotes for the minor C allele (C/C) and the others (G/G+G/C) according to a recessive model of inheritance for the minor allele **(I)**. Individual data are reported with their mean. The Kruskall-Wallis test followed by a Bonferroni post-test were used to compare groups **(A–F)**. The Mann-Whitney test was used to compare two groups **(H,I)**. Differences with a $p < 0.05$ were considered statistically significant (*). **$p < 0.001$.

the 4 analyzed genes *(NLRP3, NLRC4, IL1B*, and *IL18*), and MP the lowest.

Finally, to assess the contribution of host genetics on the inflammasome activation toward different Mtb strains, we performed genotype-guided assays for the two functional variants *NLRP3 r*s10754558, and *NLRC4* rs479333. Despite the limited number of tested samples ($n = 12$), MDM from donors carrying the gain-of-function *NLRP3* variant (G/G) responded

to Beijin-1470 and BCG strains, producing a higher level of IL-1ß compared to MDM from non-carriers (C/C+C/G) (**Figure 6H**).

At the same time, and contrary to what was observed for H37Rv-treated MDM, the loss-of-function variant *NLRC4* rs479333 did not significantly affect IL-18 release in MDM challenged with BCG. Beijin-1470 or MP287/03 (**Figure 6I**).

This last set of experiments demonstrated that different strains of Mtb display a unique capacity to induce inflammasome activation at a rather physiologic condition (MOI: 0.033) with virulence (non-virulent more than virulent) playing a greater role than the type of bacteria (*M.bovis* BCG more than *M.bovis* MP287/03; *M. tuberculosis* H37Rv similar to *M. tuberculosis* Beijin-1470). Moreover, we showed that host genetics may affect the inflamamsome activation rate toward different Mtb strains, especially for *NLRP3* rs10754558 SNV—once again corroborating the important role of inflammasome genetics in individual responses to mycobacteria.

DISCUSSION

Extensive efforts have been made to better understand the mechanisms involved in Mtb/host interactions and how this complex interplay may determine resistance vs. susceptibility to Mtb and the development of TB. Innate immunity and first-line immune responses, including inflammasome and related cytokines, have recently been taken into account as important determinants in TB outcomes. Notwithstanding, our knowledge of the mechanisms underlying progression of Mtb infections and the development of the active disease in humans is not yet fully understood, in part due to the lack of appropriate models of study, and also due to the difficulty of interpreting complex genetics, immunologic, and microbiologic interactions.

Starting from our previous genetic data (18), we designed a study for the contemporary evaluation of how inflammasome genetics and Mtb phenotype affect inflammasome activation in primary human monocytes-derived macrophages, in turn contributing to individual responses to Mtb and/or to Mtb-susceptibility vs. resistance establishment.

Our findings show that the common virulent strain H37Rv induces NLRP3 inflammasome activation (but not pyroptosis) in human macrophages and that IL-1ß is mandatory for bacterial containment (**Figures 1**, **2**). These findings corroborate previous studies in murine and human macrophages (10–12, 17, 31, 32); however, it is important to mention that in those studies, the MOI level was very high (10 or higher), while we decided to infect cells with an MOI level that was as physiologic as possible (0.033). This protective response can be modulated by host genetics, as macrophages from individuals carrying the gain-of-function rs10754558 in *NLRP3* produce significantly more IL-1ß than non-carriers (**Figure 5A**), as well as by the type of Mtb strain, as non-virulent BCG strains trigger a large amount of cytokine while the hyper-virulent MP287/03 none at all (**Figure 6A**). These data support the protective effect observed for *NLRP3* rs10754558 against the development of active pulmonary TB (18).

Trying to better understand how the host/mycobacteria interplay acts *in vivo*, we analyzed the plasma levels of inflammasome cytokines, IFN-α and TNF in a group of recently diagnosed TB patients (before treatment) and their "household contacts"—representing a group of exposed but healthy subjects. As expected, responder individuals ("household contacts") presented a higher level of IL-1ß, suggesting that their inflammasome is functioning well (**Figure 3**). On the contrary, susceptible individuals (TB patients) were characterized by an imbalance between IL-1ß and IFN-α, a known inhibitor of NLRP3 inflammasome (13). This concept of fine tuning between innate immune mediators was previously proposed by Mayer-Barber et al. (7), referring to the severity of the TB presentation; however, our study demonstrates that a "good" inflammasome activation is determinant for Mtb resistance in exposed population such as endemic TB areas. Intriguingly, TB patients also appeared to be less prone to an efficient response against PAMPs/DAMPs, as suggested by impaired NLRP3 activation by common stimuli (**Figure 3**). A similar impairment of NLRP3 was first reported in the dendritic cells of HIV patients (39), which are also characterized by elevated IFN-I levels, emphasizing a common inhibitory mechanism mediated by the antiviral mediator. Wassermann and colleagues aptly demonstrated that Mtb evolved some strategies to by-pass inflammasome activation, one being to activate pathways leading to IFN production (17).

According to Amaral et al. (11), H37Rv also activates the inflammasome in human macrophages through lysosomal damage and cathepsins release, as demonstrated by the complete inhibition of cytokine release by Ca074-Me (**Figures 4A,B**). However, the discrepancy between the dramatic effect of Ca074-Me and only partial inhibition obtained with the NLRP3 specific inhibitor MCC-950 (23) led us to hypothesize the contribution of another pathway for inflammasome activation. Besides NLRP3, other inflammasome receptors, such as the NLRC4, have been shown to contribute to the host's response to intracellular bacteria (9). Differently from NLRP3, NLRC4 can either directly recognizes bacterial patterns, such as flagellin (40), or be activated by lysosomal cathepsins release, at least in mice (35). The role of NLRC4 in TB remains elusive because it has been poorly investigated in TB and pulmonary diseases. Microscopic visualization of inflammasome aggregates ("specks"), allowed us to observe NLRC4 in the mounted complex, suggesting that it can contribute to macrophages response against Mtb; however, further investigation will be needed to better depict the role of this molecule in TB pathogenesis.

Through a genetic approach and genotype-guided assay, for the first time to our knowledge, we found a significant association between NLRC4 and the outcome of TB in an endemic area. The loss-of-function variant rs479333 in the *NLRC4* gene (minor allele frequency, 49%; from ensembl.org) was less frequent in patients with extra-pulmonary TB than in patients with pulmonary disease (**Table 3**). This SNV, previously associated to reduced *NLRC4* transcription (29) and diminished plasma level of IL-18 (30), was associated with a lower release of IL-18

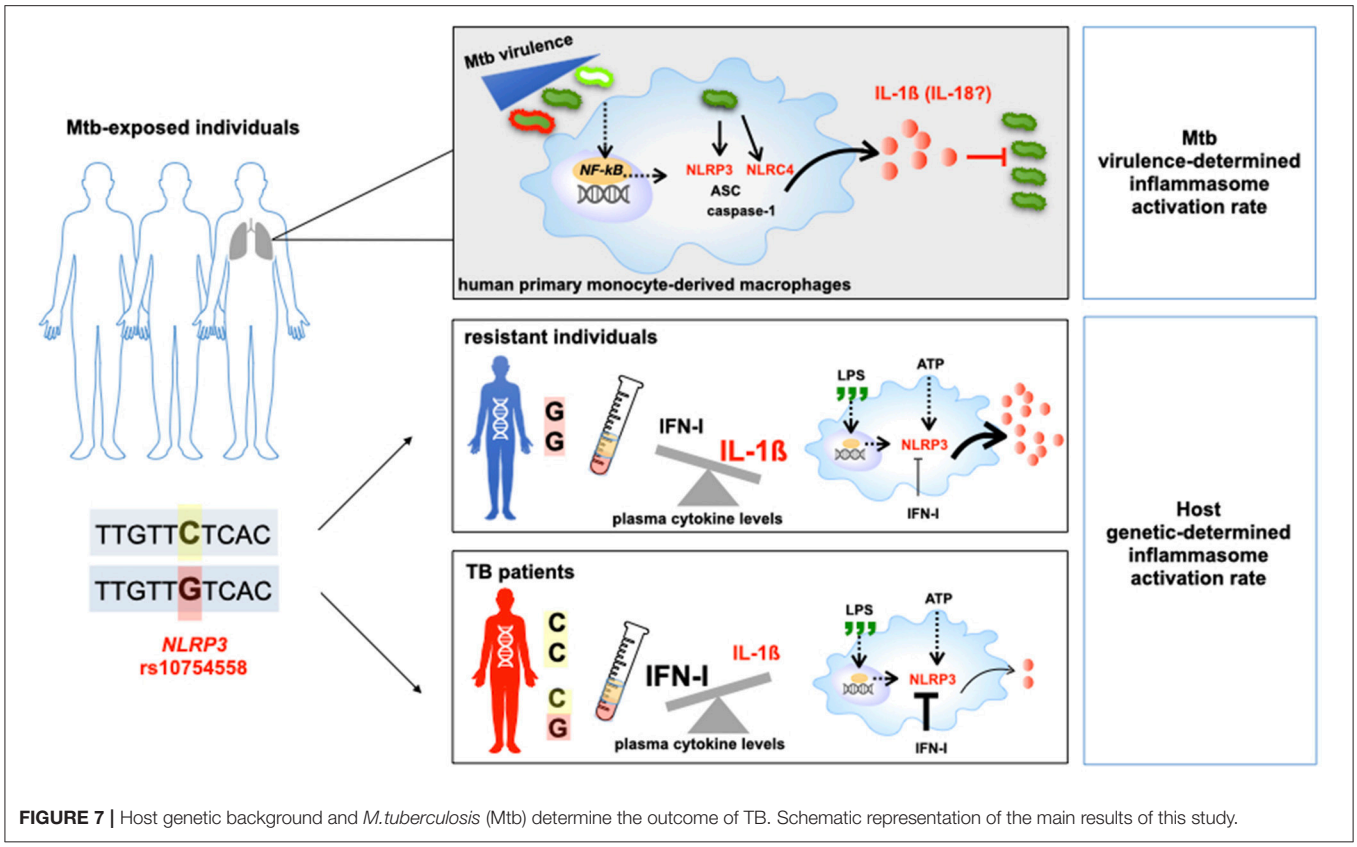

FIGURE 7 | Host genetic background and *M.tuberculosis* (Mtb) determine the outcome of TB. Schematic representation of the main results of this study.

in H37Rv-challenged MDM as well as the plasma level of the cytokine (**Figures 5E,F**), reinforcing its loss-of-function effect at both local and systemic levels.

We would like to emphasize that our data reveal two situations in Mtb/host interplay: one characterized by the preferential NLRP3/IL-1ß axis and another by NLRC4/IL18 axis. The first exerts a central role in first host/pathogen contact and in mycobacterial containment while the other is apparently more important in the outcome of Mtb infection. As we know, IL-1ß and IL-18 assume distinct roles within immune response. While IL-1ß is mainly involved in endothelium and phagocytes activation, IL-18 is involved in epithelium homeostasis and CD4+ T lymphocytes polarization toward Th1 IFN-γ-producer cells.

Considering the importance of IFN-γ-producer cells in typical TB granuloma formation, we therefore hypothesize that individuals with a defective NLRC4/IL18 axis are not able to effectively contain mycobacteria within granulomas, leading to eventual extra-pulmonary dissemination. Accordingly, at least in HIV-infected patients, the expression of *NLRC4* significantly increased in the blood of individuals with a more severe form of TB (41). Moreover, it is interesting to remember that loss-of-function SNVs in *NLRC4* have been found in HIV patents with severe TB (36) and in patients with cystic fibrosis affected by severe lung infections (42), reinforcing the important and poorly investigated role of NLRC4 in lung immunity and pulmonary diseases.

Mtb strains induce inflammasome activation in a "virulence-dependent" way. The non-virulent strain BCG promotes a dramatic inflammasome activation compared to common virulent (H37R) and rare hyper-virulent (Beijing 1471, MP287/03) strains, suggesting that Mtb virulence evolved together with some mechanism of inflammasome escape (17), and corroborating once more the importance of inflammasome activation in the immune response against Mtb.

Of note, the pattern of IL-1ß and IL-18 release is not identical in Mtb-challenged MDM (**Figure 6**), being IL-18 levels higher than IL-1ß for all tested strains. Moreover, IL-1ß production appears to be more virulence-dependent than IL-18. These findings suggest that Mtb could activate several and distinct inflammasome pathways (i.e., NLRP3/IL-1ß or NLRC4/IL-18 axis) compared to a unique PAMP, such as LPS, and these pathways could alternatively process IL-1ß or IL-18, as previously proposed (8, 9). The different level of inflammasome activation in response to distinct Mtb strains has also been observed in the murine model of infection, showing that MP287/03 is a poor inducer of IL-1ß both *in vivo* and *in vitro* compared to H37Rv or Beijing; IL-18 was not, however, evaluated in these models (34).

Masters et al. (43) proposed that the difference in the level of inflammasome activation by distinct Mtb strains is due to the virulence factor *Zmp1*. Interestingly, this group has also noted that MP287/03, which does not express *Zmp1*, activates inflammasome through NLRC4. In our assays, MP287/03 induced IL-18 but not IL-1ß. However, this Mtb strain is

not able to trigger NLRC4, nor NLRP3 expression (**Figure 6**). Consequently, we cannot conclude whether Mtb strains which preferentially induce IL-18 do so through NLRC4. Nevertheless, taking into account the long co-evolution period of Mtb and humans, it would not be surprising that several inflammasome sensors could contribute to mycobacterial defense, as it was demonstrated for NLRP3 and AIM2 (17).

In conclusion, for the first time, our findings show the intricate interaction among inflammasome genetics, Mtb virulence and the resultant inflammasome activation profile at the local (*in vitro* model) as well at the systemic (plasma) level. According to our hypothesis, during the first host/pathogen contact, the Mtb activates a strong inflammasome response in term of IL-1ß as well as IL-18, especially for non-virulent strain BCG and the common virulent one, H37Rv. This response is mediated by the NLRP3/IL-1ß axis in a cathepsin-dependent way, and the gain-of-function variant in NLRP3 contributes to the elevated production of IL-1ß, which in turn is specifically responsible for bacterial containment.

In-vitro assays and genetic association data support the involvement of the NLRC4/IL18 pathway in individual responses to mycobacteria and determine the outcome of an Mtb infection as well as TB severity. These original findings highlight that the same pathogen could activate inflammasome-dependent cleavages of cytokine pro-forms based on events that are not yet fully understood, such as a bacterial strain (i.e., MP287/03), distinct steps of the disease (i.e., first host/pathogen contact, or response to the pathogen in an individual with an established infection), or even based on an individual's genetic background (**Figure 7**).

DATA AVAILABILITY STATEMENT

The raw data supporting the conclusions of this article will be made available by the authors, without undue reservation, to any qualified researcher.

ETHICS STATEMENT

This study was approved by the Human Research Ethics Committee of the Institute of Biomedical Sciences (ICB) of the University of São Paulo (USP) (CEPSH reference number: 51780715.8.0000.5467) and the Institute of Biological Sciences (ICB) of the Federal University of Amazonas (UFAM) (reference number: 57978916.3.0000.5020). All human participants provided written informed consent and all clinical investigations were conducted according to the principles expressed in the Declaration of Helsinki. The patients/participants provided their written informed consent to participate in this study.

AUTHOR CONTRIBUTIONS

DS and AP: conceived, designed experiments, wrote the article, and conducted statistical analyse. AS and MO: selected and collected TB patients and household contacts. MO: performed microbiologic analysis. DS and CB: performed MDM experiments. EA and CB: standardized *Mycobacterial* culture and infection. DS and VL: performed the immunofluorescence experiments. ER: performed flow-cytometry experiments. FF and JS: executed ELISA, performed RNA isolation, and gene expression analyse. DS, AP, FL, MO, AS, and ML: discussed the results. All authors contributed to the article and approved the submitted version.

FUNDING

This project was supported by Fundação de Amparo à Pesquisa do Estado de São Paulo (FAPESP) (Grant Nos: 2015/23395-6, 2015/50650-7, and 2015/20432-8). DS had a Ph.D. fellowship from Fundação de Amparo à Pesquisa do Estado do Amazonas (FAPEAM); CB, VL, ER, and FF have a post-graduation fellowship from FAPESP; JS received a Master Degree fellowship from CAPES. ML and AP received a CNPq research fellowship. The funders had no role in the study design, data collection, analysis, decision to publish, or preparation of the manuscript of this study.

ACKNOWLEDGMENTS

We are very grateful to the Oswaldo Cruz Hospital Blood Bank Service (São Paulo, SP, Brazil) and to the Reference Center for Sanitary Pneumology Clínica Cardoso Fontes (Manaus, AM, Brazil) for the recruitment of healthy donors and TB patients and their household contacts, respectively. We would like to thank Professor Mario Hiroyuki Hirata (Departamento de Análises Clínicas e Toxicológicas, Universidade de São Paulo/USP), Professor Niels Olsen Saraiva Câmara (Departamento de Imunologia, Instituto de Ciências Biomédicas/ICB, USP). Dr. Telma Miyuki Oshiro (Laboratório de Investigação Médica-56, Faculdade de Medicina, USP), Professor Karina Ramalho Bortoluci (Laboratório de Imunologia Molecular, Universidade Federal de São Paulo/UNIFESP), Dr. Eliana Faquin de Lima Mauro e Alexsander Seixas de Souza (Instituto Butantan, São Paulo), Prof. Aya Sadahiro' group (ICB, Universidade Federal do Amazonas/UFAM).

SUPPLEMENTARY MATERIAL

The Supplementary Material for this article can be found online at: https://www.frontiersin.org/articles/10.3389/fimmu.2020.550624/full#supplementary-material

REFERENCES

1. Bellamy R. Genetics and pulmonary medicine. 3. Genetic susceptibility to tuberculosis in human populations. *Thorax*. (1998) 53:588–93. doi: 10.1136/thx.53.7.588
2. Forrellad MA, Klepp LI, Gioffré A, Sabio y García J, Morbidoni HR, de la Paz Santangelo M, et al. Virulence factors of the *Mycobacterium tuberculosis* complex. *Virulence*. (2013) 4:3–66. doi: 10.4161/viru.22329
3. O'Garra A, Redford PS, McNab FW, Bloom CI, Wilkinson RJ, Berry MP. The immune response in tuberculosis. *Annu Rev*

Immunol. (2013) 31:475–527. doi: 10.1146/annurev-immunol-032712-095939
4. Cooper AM. Cell-mediated immune responses in tuberculosis. *Annu Rev Immunol*. (2009) 27:393–422. doi: 10.1146/annurev.immunol.021908.132703
5. Collins AC, Cai H, Li T, Franco LH, Li XD, Nair VR, et al. Cyclic GMP-AMP Synthase Is an Innate Immune DNA Sensor for *Mycobacterium tuberculosis*. *Cell Host Microbe.* (2015) 17:820–8. doi: 10.1016/j.chom.2015.05.005
6. Watson RO, Manzanillo PS, Cox JS. Extracellular *M. tuberculosis* DNA targets bacteria for autophagy by activating the host DNA-sensing pathway. *Cell.* (2012) 150:803–15. doi: 10.1016/j.cell.2012.06.040
7. Mayer-Barber KD, Andrade BB, Oland SD, Amaral EP, Barber DL, Gonzales J, et al. Host-directed therapy of tuberculosis based on interleukin-1 and type I interferon crosstalk. *Nature.* (2014) 511:99–103. doi: 10.1038/nature13489
8. Mathur A, Hayward JA, Man SM. Molecular mechanisms of inflammasome signaling. *J Leukoc Biol.* (2018) 103:233–57.
9. Hayward JA, Mathur A, Ngo C, Man SM. Cytosolic recognition of microbes and pathogens: inflammasomes in action. *Microbiol Mol Biol Rev.* (2018) 82:e00015–18. doi: 10.1128/MMBR.00015-18
10. Jamwal SV, Mehrotra P, Singh A, Siddiqui Z, Basu A, Rao KV. Mycobacterial escape from macrophage phagosomes to the cytoplasm represents an alternate adaptation mechanism. *Sci Rep.* (2016) 6:23089. doi: 10.1038/srep23089
11. Amaral EP, Riteau N, Moayeri M, Maier N, Mayer-Barber KD, Pereira RM, et al. Lysosomal cathepsin release is required for NLRP3-inflammasome activation by *Mycobacterium tuberculosis* in infected macrophages. *Front Immunol.* (2018) 9:1427. doi: 10.3389/fimmu.2018.01427
12. Mishra BB, Moura-Alves P, Sonawane A, Hacohen N, Griffiths G, Moita LF, et al. *Mycobacterium tuberculosis* protein ESAT-6 is a potent activator of the NLRP3/ASC inflammasome. *Cell Microbiol.* (2010) 12:1046–63. doi: 10.1111/j.1462-5822.2010.01450.x
13. Guarda G, Braun M, Staehli F, Tardivel A, Mattmann C, Förster I, et al. Type I interferon inhibits interleukin-1 production and inflammasome activation. *Immunity.* (2011) 34:213–23. doi: 10.1016/j.immuni.2011.02.006
14. Sokolowska M, Chen LY, Liu Y, Martinez-Anton A, Qi HY, Logun C, et al. Prostaglandin E2 inhibits NLRP3 inflammasome activation through EP4 Receptor and intracellular cyclic AMP in Human Macrophages. *J Immunol.* (2015) 194:5472–87. doi: 10.4049/jimmunol.1401343
15. Latz E, Xiao TS, Stutz A. Activation and regulation of the inflammasomes. *Nat Rev Immunol.* (2013) 13:397–411. doi: 10.1038/nri3452
16. Briken V, Ahlbrand SE, Shah S. *Mycobacterium tuberculosis* and the host cell inflammasome: a complex relationship. *Front Cell Inform Microb.* (2013) 3:62. doi: 10.3389/fcimb.2013.00062
17. Wassermann R, Gulen MF, Sala C, Perin SG, Lou Y, Rybniker J, et al. *Mycobacterium tuberculosis* differentially activates cGAS- and inflammasome-dependent intracellular immune responses through ESX-1. *Cell Host Microbe.* (2015) 17:799–810. doi: 10.1016/j.chom.2015.05.003
18. Souza de Lima D, Ogusku MM, Sadahiro A, Pontillo A. Inflammasome genetics contributes to the development and control of active pulmonary tuberculosis. *Infect Genet Evol.* (2016) 41:240–4. doi: 10.1016/j.meegid.2016.04.015
19. Salem JI, Marója MD, Carvalho FF, Lima MO, Litaiff LR, Cardoso MS, et al. Valor relativo do exame direto, após concentração e por cultivo de escarro no diagnóstico bacteriológico da tuberculose pulmonar no Amazonas. *J.Pneumol.* (1990) 16:133–6. Available online at: https://pesquisa.bvsalud.org/portal/resource/pt/lil-94374
20. Salem JI, Carvalho CM, Ogusku MM, Maia R, Ruffino-Neto A. PKO - Alternative method for isolating mycobacteria from sputum. *Acta Amazonica.* (2007) 37:419–24. doi: 10.1590/S0044-59672007000300013
21. Kaufmann SH. How can immunology contribute to the control of tuberculosis? *Nat Rev Immunol.* (2001) 1:20–30. doi: 10.1038/35095558
22. Juliana C, Fernandes-Alnemri T, Wu J, Datta P, Solorzano L, Yu JW, et al. Anti-inflammatory compounds parthenolide and Bay 11-7082 are direct inhibitors of the inflammasome. *J Biol Chem.* (2010) 285:9792–802. doi: 10.1074/jbc.M109.082305
23. Coll RC, Robertson AA, Chae JJ, Higgins SC, Muñoz-Planillo R, Inserra MC, et al. A small-molecule inhibitor of the NLRP3 inflammasome for the treatment of inflammatory diseases. *Nat Med.* (2015) 21:248–55. doi: 10.1038/nm.3806
24. Gattorno M, Tassi S, Carta S, Delfino L, Ferlito F, Pelagatti MA, et al. Pattern of interleukin-1beta secretion in response to lipopolysaccharide and ATP before and after interleukin-1 blockade in patients with CIAS1 mutations. *Arthritis Rheum.* (2007) 56:3138–48. doi: 10.1002/art.22842
25. Mariathasan S, Weiss DS, Newton K, McBride J, O'Rourke K, Roose-Girma M, et al. Cryopyrin activates the inflammasome in response to toxins and ATP. *Nature.* (2006) 440:228–32. doi: 10.1038/nature04515
26. Stutz A, Horvath GL, Monks BG, LatzE. ASC speck formation as a readout for inflammasome activation. *Methods Mol Biol.* (2013) 1040:91–101. doi: 10.1007/978-1-62703-523-1_8
27. Schmittgen TD, Livak KJ. Analyzing real-time PCR data by the comparative C(T) method. *Nat Protoc.* (2008) 3:1101–8. doi: 10.1038/nprot.2008.73
28. Hitomi Y1, Ebisawa M, Tomikawa M, Imai T, Komata T, Hirota T, et al. Associations of functional NLRP3 polymorphisms with susceptibility to food-induced anaphylaxis and aspirin-induced asthma. *J Allergy Clin Immunol.* (2009) 124:779–85.e6. doi: 10.1016/j.jaci.2009.07.044
29. Zeller T, Haase T, Müller C, Riess H, Lau D, Zeller S, et al. Molecular characterization of the NLRC4 expression in relation to interleukin-18 levels. *Circ Cardiovasc Genet.* (2015) 8:717–26. doi: 10.1161/CIRCGENETICS.115.001079
30. Matteini AM, Li J, Lange EM, Tanaka T, Lange LA, Tracy RP, et al. Novel gene variants predict serum levels of the cytokines IL-18 and IL-1ra in older adults. *Cytokine.* (2014) 65:10–6. doi: 10.1016/j.cyto.2013.10.002
31. Welin A, Eklund D, Stendahl O, Lerm M. Human Macrophages Infected With a High Burden of ESAT-6-expressing *M. tuberculosis* Undergo caspase-1- And Cathepsin B-independent Necrosis. *Plos ONE.* (2011) 6:e20302. doi: 10.1371/journal.pone.0020302
32. Eklund D1, Welin A, Andersson H, Verma D, Söderkvist P, Stendahl O, et al. Human gene variants linked to enhanced NLRP3 activity limit intramacrophage growth of Mycobacterium tuberculosis. *J Infect Dis.* (2014) 1:209:749–53. doi: 10.1093/infdis/jit572
33. Schenk M, Fabri M, Krutzik SR, Lee DJ, Vu DM, Sieling PA, et al. Interleukin-1β triggers the differentiation of macrophages with enhanced capacity to present mycobacterial antigen to T cells. *Immunology.* (2014) 141:174–80. doi: 10.1111/imm.12167
34. Amaral EP, Ribeiro SC, Lanes VR, Almeida FM, de Andrade MR, Bomfim CC, et al. Pulmonary infection with hypervirulent mycobacteria reveals a crucial role for the P2X7 receptor in aggressive forms of tuberculosis. *PLoS Pathog.* (2014) 10:e1004188. doi: 10.1371/journal.ppat.1004188
35. Lage SL, Buzzo CL, Amaral EP, Matteucci KC, Massis LM, Icimoto MY, et al. Cytosolic flagellin-induced lysosomal pathway regulates inflammasome-dependent and -independent macrophage responses. *Proc Natl Acad Sci USA.* (2013) 110:E3321–30. doi: 10.1073/pnas.1305316110
36. Ravimohan S, Maenetje P, Auld SC, Ncube I, Mlotshwa M, Chase W, et al. A Common NLRC4 gene variant associates with inflammation and pulmonary function in human immunodeficiency virus and tuberculosis. *Clin Infect Dis.* (2019) 22:ciz898. doi: 10.1093/cid/ciz898
37. Lasunskaia E1, Ribeiro SC, Manicheva O, Gomes LL, Suffys PN, Mokrousov I, et al. Emerging multidrug resistant *Mycobacterium tuberculosis* strains of the Beijing genotype circulating in Russia express a pattern of biological properties associated with enhanced virulence. *Microbes Infect.* (2010) 12:467–75. doi: 10.1016/j.micinf.2010.02.008
38. Rocha VC, de Figueiredo SC, Rosales CA, de Hildebrand e Grisi Filho JH, Keid LB, Soares RM, et al. Molecular discrimination of *Mycobacterium bovis* in São Paulo, Brazil. *Vector Borne Zoonotic Dis.* (2013) 13:17–21. doi: 10.1089/vbz.2012.1035
39. Pontillo A, Silva LT, Oshiro TM, Finazzo C, Crovella S, Duarte AJ. HIV-1 induces NALP3-inflammasome expression and interleukin-1β secretion in dendritic cells from healthy individuals but not from HIV-positive patients. *AIDS.* (2012) 26:11–8. doi: 10.1097/QAD.0b013e32834d697f
40. Zhao Y, Yang J, Shi J, Gong YN, Lu Q, Xu H, et al. The NLRC4 inflammasome receptors for bacterial flagellin and type III secretion apparatus. *Nature.* (2011) 477:596–600. doi: 10.1038/nature10510

41. Gebremicael G, Kassa D, Quinten E, Alemayehu Y, Gebreegziaxier A, Belay Y, et al. Host gene expression kinetics during treatment of tuberculosis in HIV-coinfected individuals is independent of highly active antiretroviral therapy. *J Infect Dis.* (2018) 218:1833–46. doi: 10.1093/infdis/jiy404
42. Iannitti RG, Napolioni V, Oikonomou V, De Luca A, Galosi C, Pariano M, et al. IL-1 receptor antagonist ameliorates inflammasome-dependent inflammation in murine and human cystic fibrosis. *Nat Commun.* (2016) 7:10791. doi: 10.1038/ncomms10791
43. Master SS, Rampini SK, Davis AS, Keller C, Ehlers S, Springer B, et al. Mycobacterium tuberculosis prevents inflammasome activation. *Cell Host Microbe.* (2008) 3:224–32. doi: 10.1016/j.chom.2008.03.003

Conflict of Interest: The authors declare that the research was conducted in the absence of any commercial or financial relationships that could be construed as a potential conflict of interest.

frontiers in Immunology

ORIGINAL RESEARCH
published: 22 October 2020
doi: 10.3389/fimmu.2020.521409

A Specific *IL6* Polymorphic Genotype Modulates the Risk of *Trypanosoma cruzi* Parasitemia While *IL18*, *IL17A*, and *IL1B* Variant Profiles and HIV Infection Protect Against Cardiomyopathy in Chagas Disease

Alexandra Gomes dos Santos[1†], Elieser Hitoshi Watanabe[2†], Daiane Tomomi Ferreira[3], Jamille Oliveira[1], Érika Shimoda Nakanishi[3], Claudia Silva Oliveira[1], Edimar Bocchi[4], Cristina Terra Gallafrio Novaes[5], Fatima Cruz[4], Noemia Barbosa Carvalho[5], Paula Keiko Sato[3], Edite Hatsumi Yamashiro-Kanashiro[3,6], Alessandra Pontillo[7], Vera Lucia Teixeira de Freitas[1,3], Luiz Fernando Onuchic[2] and Maria Aparecida Shikanai-Yasuda[1,3*]*

[1] Department of Infectious and Parasitic Diseases, Faculdade de Medicina, University of São Paulo, São Paulo, Brazil, [2] Department of Medicine, Divisions of Molecular Medicine and Nephrology, Faculdade de Medicina, University of São Paulo, São Paulo, Brazil, [3] Laboratory of Immunology (LIM 48), Hospital das Clínicas, Faculdade de Medicina, University of São Paulo, São Paulo, Brazil, [4] Heart Institute, Hospital das Clínicas, Faculdade de Medicina, University of São Paulo, São Paulo, Brazil, [5] Division of Infectious Diseases, Hospital das Clinicas, Faculdade de Medicina, University of São Paulo, São Paulo, Brazil, [6] Instituto de Medicina Tropical, University of São Paulo, São Paulo, Brazil, [7] Departament of Immunology, Instituto de Ciências Biomédicas (ICB), University of São Paulo, São Paulo, Brazil

OPEN ACCESS

Edited by:
David Courtin,
Institut de recherche pour le développement (IRD), France

Reviewed by:
Thomas Jacobs,
Bernhard Nocht Institute for Tropical Medicine (BMITM), Germany
Fabrício C. Dias,
University of São Paulo, Brazil
Celso Teixeira Mendes-Junior,
University of São Paulo, Brazil

***Correspondence:**
Luiz Fernando Onuchic
lonuchic@usp.br
Maria Aparecida Shikanai-Yasuda
masyasuda@yahoo.com.br

[†]These authors have contributed equally to this work

Specialty section:
This article was submitted to Microbial Immunology, a section of the journal Frontiers in Immunology

Received: 18 December 2019
Accepted: 24 September 2020
Published: 22 October 2020

Citation:
Gomes dos Santos A, Watanabe EH, Ferreira DT, Oliveira J, Nakanishi ES, Oliveira CS, Bocchi E, Novaes CTG, Cruz F, Carvalho NB, Sato PK, Yamashiro-Kanashiro EH, Pontillo A, de Freitas VLT, Onuchic LF and Shikanai-Yasuda MA (2020) A Specific IL6 Polymorphic Genotype Modulates the Risk of Trypanosoma cruzi Parasitemia While IL18, IL17A, and IL1B Variant Profiles and HIV Infection Protect Against Cardiomyopathy in Chagas Disease. Front. Immunol. 11:521409. doi: 10.3389/fimmu.2020.521409

Background: Chagas disease caused by *Trypanosoma cruzi* (*T. cruzi*) affects approximately six million individuals worldwide. Clinical manifestations are expected to occur due to the parasite persistence and host immune response. Herein we investigated potential associations between *IL1B*, *IL6*, *IL17A*, or *IL18* polymorphism profiles and cardiomyopathy or *T. cruzi* parasitemia, as well as the impact of HIV infection on cardiopathy.

Methods: Two hundred twenty-six patients and 90 control individuals were analyzed. *IL1B* rs1143627 T>C, *IL6* rs1800795 C>G, *IL17A* rs2275913 G>A, *IL18* rs187238 C>G, and *IL18* rs1946518 C>A SNVs were analyzed by real-time PCR and *T. cruzi* parasitemia by PCR.

Results: Our data revealed association between a cytokine gene polymorphism and parasitemia never previously reported. The *IL6* rs1800795 CG genotype lowered the risk of positive parasitemia (OR = 0.45, 95% CI 0.24–0.86, P = 0.015). Original findings included associations between *IL17A* rs2275913 AA and *IL18* s1946518 AA genotypes with decreased risk of developing cardiomyopathy (OR = 0.27, 95% CI 0.07–0.97, P = 0.044; and OR = 0.35, 95% CI 0.14–0.87, P = 0.023, respectively). *IL18* rs1946518 AA and *IL1B* rs1143627 TC were associated with reduced risk for

cardiomyopathy severity, including NYHA (New York Heart Association) class ≥ 2 (OR = 0.21, 95% CI 0.06–0.68, P = 0.009; and OR = 0.48, 95% CI 0.24–0.95, P = 0.036, respectively) and LVEF (left ventricular ejection fraction) <45% for *IL18* rs1946518 AA (OR = 0.22, 95% CI 0.05–0.89, P = 0.034). A novel, unexpected protective effect of HIV infection against development/progression of cardiomyopathy was identified, based on a lower risk of developing cardiopathy (OR = 0.48, 95% CI 0.23–0.96, P = 0.039), NYHA class ≥ 2 (OR = 0.15, 95% CI 0.06–0.39, P < 0.001), and LVEF < 45% (OR = 0.03, 95% CI 0.00–0.25, P = 0.001). Digestive involvement was negatively associated with NYHA ≥ 2 and LVEF < 45% (OR = 0.20, 95% CI 0.09–0.47, P < 0.001; and OR = 0.24, 95% CI 0.09–0.62, P = 0.004, respectively).

Conclusions: Our data support a protective role of *IL17A* AA, *IL18* AA, and *IL1B* TC genotypes against development/progression of cardiomyopathy and a modulatory effect of the *IL6* CG genotype on the risk of parasitemia in Chagas disease. Notably, HIV infection was shown to protect against development/progression of cardiopathy, potentially associated with a synergistic effect of HIV and highly active antiretroviral therapy (HAART), attenuating a Th1-mediated response in the myocardium. This proposed hypothesis requires confirmation, however, in larger and more comprehensive future studies.

Keywords: *T. cruzi* parasitemia, cardiomyopathy, Chagas disease, HIV, *IL1 B*, *IL6*, *IL17 A* and *IL18* polymorphisms

INTRODUCTION

Chagas disease, a potentially life-threatening illness caused by the protozoan *Trypanosoma cruzi* (*T. cruzi*) and endemic in Latin America, affects approximately 6 million individuals worldwide. The natural course of the infection comprises acute and chronic phases. A clinically relevant acute form is observed in only 1/30 infected people, including fever, adenopathy, palpebral or legs edema and/or hepatosplenomegaly and, less often, myocarditis and meningoencephalitis. In the chronic phase, on the other hand, ~30% of the patients develop the cardiac form, expressed as arrhythmia, heart failure, and/or thromboembolic events. The chronic phase also includes a digestive form, which comprises dysphagia and/or constipation in 10–15% of the cases and, in ~5% of them, a cardio-digestive form. The indeterminate form, in turn, represented by asymptomatic patients with normal electrocardiogram and thorax and digestive tract X-rays, constitutes the most frequent chronic form, affecting 60–70% of the referred group (1, 2).

Chagas cardiopathy is a major cause of cardiovascular-related mortality within the 30–50-year age range in Latin American endemic areas (1, 3). Previous studies have recognized the fundamental role of host features in Chagas disease pathophysiology, revealing different immunological profiles in patients affected and not affected by cardiopathy (4). While the development of cardiopathy has been linked to a Th1 response in heart tissue associated with mononuclear cell infiltrate, cardiomyocyte damage, and fibrosis, a Th2 response predominates in the indeterminate form (5, 6). Reports of higher levels/expression of IL-6, IL1β, TNFα, and IFNγ in the cardiac form (7, 8) and IL6 and/IL1β or C-reactive protein in the cardiac and/or cardio-digestive forms (9, 10) support a potential role for such cytokines in the adaptative immune response at heart tissue damaging process. IL6 and IL1β could be considered, therefore, a marker of cardiac lesion. In contrast, the finding of higher plasma levels of IL17A directly associated with better systolic function in the indeterminate form suggests a protective role for this cytokine against the development of clinically relevant chronic Chagas cardiopathy, despite inverse association with diastolic performance indices (11, 12).

Previous studies in patients with indeterminate and cardiac forms suggested a role for T reg cells in the modulation of inflammatory immune responses associated with the cardiac form (6, 13). Increased number of Foxp3+, CD25+, CD4+ T cells, T reg cells that stimulate secretion of IL-17 A, IL-10, and granzyme B, was observed in the indeterminate form, in association with less inflammation and better myocardium function. In contrast, more pronounced immune responses to the parasite, associated with higher levels of inflammatory cytokines and myocardial lesion, correlated with higher densities of IL6+, IFNγ+, TNFα+, CTLA4+ T reg cells. Such findings suggest a role for T reg cells in controlling the exacerbated immune response and morbidity as well as mortality in *T. cruzi* infection, likely by stimulating Th17 cells and modulating killing effector cells (14).

An important role in the control of cardiac inflammatory lesions and remodeling has been proposed for IL18 (15, 16). This cytokine stimulates IFNγ expression independently of IL12, allowing an IL18-IFNγ cross-talk at the myocardium level during *T. cruzi* infection (17). IL18 upregulation and correlation between IL18 messenger RNA (mRNA) and IFNγ expression have in fact been reported in human Chagas heart tissue (6, 18).

T. cruzi parasitemia is another major factor implicated in the progression of chronic Chagas cardiopathy, even if intermittent and low at this disease stage (19–22). Available reports, however, are controversial on this point (23–25). Cytokines have also been shown to control *T. cruzi* parasitic burden and myocardial inflammatory lesions in both chronic and acute phases of murine infection. In chronic infection induced with the Colombian strain in *IL18*-KO mice, a significant reduction in the myocardium parasitic load was observed (26). Acute infections of *IL17A*-KO mice, on the other hand, were associated with lack of activation of immune-related cells that are critical for the killing of *T. cruzi* (27) and with increased mortality and higher-degree myocarditis. Variable parasitic loads were detected, however, depending on the mouse line and the parasite strain (27, 28). This finding unraveled a protective effect of IL17 A, evinced by the association between better cardiac function and higher plasma levels of IL17A in patients without cardiomyopathy (11, 12). In addition, in acute murine infection IL6 was shown to drive the survival of *T. cruzi* infected cardiomyocytes. IL6-KO mice lack the innate immunity crucial for host survival and rapidly die with high levels of IL1 β and inflammatory products, a process reverted by adding recombinant IL6 (29). This finding suggests a critical role for IL6 in modulating inflammatory lesions. Due to the modulating effect of IL6 on Chagas disease cardiomyopathy, the data on human disease likely represent a less severe degree of this inflammation (7, 10).

In immunosupressed patients with HIV infection, elevated IL18 serum concentrations have been reported to influence both Aids and the course of associated infections (30). Interestingly, whereas Chagas disease reactivation does not occur in immunocompetent subjects, this illness natural history is changed in HIV infected patients, being associated with increased morbidity and mortality (31).

As part of the genetic assessment of cytokine roles in Chagas disease, single nucleotide variants (SNVs) associated with various cytokine genes have been previously analyzed in *T. cruzi* infection and cardiopathy progression. No significant association involving the *IL6* SNV rs1800795 −174 C>G was identified in Colombia (32), in a context where the G allele has been associated with higher IL6 levels (33, 34) and patients with heart Chagas disease have been found to present higher IL6 levels (7, 10). Positive findings, in turn, included association between increased risk of cardiomyopathy and the CT haplotype for the *IL1B* −31 T>C and +3954 C>T (rs1143634, synonymous coding sequence variant) polymorphisms in Colombia (35). The possible proinflammatory nature of this haplotype (35) is unclear, since the *IL1B* −31 T allele has been associated with increased IL1β secretion (36), and other haplotype TCT, for *IL1B* −511 C>T, *IL1B* −31 T>C, and *IL1B* +3954 C>T, in turn, has been considered a proinflammatory haplotype, with a predominant role of *ILB* −511 C>T (37). Moreover, association between cardiomyopathy and the *IL1B* +5810 G>A (rs1143633, intronic SNV) G allele and GG genotype was also identified, despite no established effect of this allele or genotype on IL1β production (35). It is possible, however, that other biological effects or linkage disequilibrium with other polymorphisms related to functional significance may exist. By comparing seronegative individuals with seropositive cardiac patients in Colombia, a study suggested protection against *T. cruzi* infection and development of cardiopathy for patients that carry the C allele of *IL17A* rs8193036 C>T (promoter SNV) (38). These data were *a priori* not expected, since the C allele has been associated with lower IL17A mRNA expression (39) and previous reports revealed a role of IL17A in resistance to *T. cruzi* in infected mice (27) and higher IL17A levels in patients with no cardiopathy (11, 12). It should be noted, however, that this study conducted with Colombian patients shows that the *IL17A* rs8193036 SNV is probably in linkage disequilibrium with some causative variant that modulates IL17A production (38). This investigation also found no association between the *IL17A* rs7747909 G>A 3' UTR SNV and Chagas cardiopathy and between two other *IL17A* promoter SNVs (rs4711998 and rs3819024) or *IL17A* rs2275913 and heart disease, in a context where the latter A allele is associated with increased IL17 A levels (40, 41). A previous study, in turn, reported association of the *IL17A* rs2275913 G>A (promoter SNV) A allele and AA genotype with chronic cardiomyopathy in Brazil (42). This observation disagrees with previous studies that detected association between higher IL17A levels and absence of cardiomyopathy (11, 12) and are not in line with the often reported association between the A allele and increased IL17A levels (40, 41). Associations between *T. cruzi* infection and the *IL18* rs187238 C>A (promoter SNV) C, rs360719 A>G (promoter SNV) G, rs2043055 A>G (intronic SNV) A, and rs1946518 C>A (promoter SNV) A alleles were also found in Colombia, a finding mainly driven by the rs360719 G allele (43). Of note, this observation was confirmed in a larger cohort in Latin America (44). Importantly, another study detected association between the rs360719 G carrier status and higher serum IL18 mRNA expression in healthy individuals (45) while an additional report revealed increased IL18 mRNA expression at the myocardium level in Chagas disease cardiomyopathy (18). In addition, the *IL18* rs2043055 G allele was found to associate with absence of cardiomyopathy in Colombia (44). In Brazil the *IL18* rs2043055 AG genotype was more frequent in patients with a moderate than a severe cardiac phenotype. This study also suggested that it is possibly that this intronic SNV is in linkage disequilibrium with another variant functionally relevant (46). This SNV, however, has not yet been shown to affect IL18 production.

While meaningful progress has been made in linking cytokine gene polymorphisms to Chagas disease mechanisms, associations between cytokine-related SNVs with different clinical scenarios of this disease remain largely limited. Establishing their consequences in the corresponding cytokine circulating and local levels, moreover, as well as their implications on specific biological pathways at the host environment, comprise even more complexes problems to be addressed. In spite of such challenges, thoughtful and well supported hypotheses can be made to progressively add pieces to this ongoing puzzle. In this context, association studies

involving appropriate cytokine-related SNVs and strategic immune-affected medical conditions, in one side, and key Chagas phenotypes, on the other side, should be encouraged as potentially significant contributors to the comprehension of this disease pathogenesis.

Facing the biological and clinical scenarios just described, in the current study we investigated potential associations between SNVs linked to *IL1B*, *IL6*, *IL17A*, or *IL18* and the risks of positive *T. cruzi* parasitemia or development/progression of cardiomyopathy. With the assumption that immunocompromised conditions frequently associated with Chagas disease could potentially bring key mechanistic and clinical insights to the understanding of this illness, we also analyzed possible associations involving HIV infection and Chagas disease phenotypes. Surprisingly, our data revealed that positiveness for HIV protected against the development and/or progression of cardiomyopathy. We also describe novel associations between specific *IL18*, *IL17A*, and *IL1B* variant profiles and the risk of cardiomyopathy as well as between a specific *IL6* polymorphic genotype and the risk of positive *T. cruzi* parasitemia.

PATIENTS, MATERIALS, AND METHODS

Study Subjects

Our cohort included 206 patients with Chagas disease: 78 from the Heart Institute of Hospital das Clínicas da Faculdade de Medicina, University of São Paulo (HCFMUSP), and 129 from the Infectious Diseases Division of HCFMUSP, 49 of whom with HIV co-infection. These 49 cases were followed at Serviço de Extensão e Atendimento aos Paciente com Infecção por HIV/Aids of the same Division. All participants were adults. The diagnosis of trypanosomiasis was based on the 2nd Brazilian Guidelines for Chagas Diseases (1). Two positive tests of the following ones, therefore, were used to establish the diagnosis: ELISA—enzyme linked immunosorbent assay, indirect immunofluorescence, and hemagglutination (47). All patients from the Infectious Diseases Division with positive epidemiology were sent to the HIV/Aids Clinic, where HIV infection was confirmed by ELISA and immunoblot (31). Patients from the Heart Institute were tested for HIV as previously described (31). When included in the current protocol, 26 of the 49 HIV patients were not on regular HAART therapy or had therapeutic failure due to antiretroviral resistance (three patients). In 23 of them, the median viral load was 14,000 (2,618–100,000, 25th–75th percentiles) DNA viral copies/μl while the median CD4 count was 340 (93–510) cells/mm^3. Data from 23 patients under HAART for 1 to >5 years showed a median viral load of 0.0 (0.0–0.0) DNA viral copies/μl. In these 23 patients, the median CD4 count was 631 (439–715) cells/mm^3.

The patients underwent electrocardiography, echocardiography, and thorax, esophagus, and colon radiological examinations, being then classified within one of the clinical forms of Chagas disease (1). Individuals without signs and symptoms and with no alteration in the mentioned tests were classified as having the indeterminate form (n = 51), patients with abnormalities suggestive of Chagas disease on electrocardiography or on dynamic electrocardiography and without digestive involvement as with the cardiac form (n = 96), the cases with abnormal findings on esophagus and/or colon without Chagas cardiac manifestation as presenting the digestive form (n = 32). Twenty-seven patients presented both digestive and cardiac alterations, constituting the cardio-digestive group. Cardiac involvement was detected in 123 patients (cardiac and cardiac/digestive forms) while heart disease was not identified in 83 patients, a group composed of individuals with the indeterminate and digestive forms.

Patients with cardiomyopathy were evaluated for heart failure according to the New York Heart Association (NYHA) classification (48), which includes the following criteria: class 1. Patients with cardiac disease without limitation of physical activity; class 2. Patients with cardiac disease with mild limitation of physical activity and symptomatic in routine physical activity; class 3. Patients with cardiac disease with marked limitation of physical activity and symptomatic in less than ordinary physical activity; and class 4. Patients with cardiac disease and unable to carry any physical activity without discomfort, symptoms may be present even at rest. For the purposes of our study, however, Chagas patients were classified according to two different scenarios related to their cardiac status, being divided in two groups in each of the cases: A) based on the NYHA classification/absence of cardiopathy—group 1: patients without cardiopathy (no CA) and with mild cardiopathy (NYHA 1), and group 2: patients with more severe cardiopathy (NYHA ≥ 2); and B) Based on the left ventricular ejection fraction (LVEF) yielded by echocardiography—group 1: patients with LVEF ≥ 45%, and group 2: patients with LVEF < 45%.

The control group for the SNV analyses consisted of 90 healthy individuals with negative serological tests for *T. cruzi* antigens. Controls and patients comprised a total population of 296 individuals, including 149 females and 147 males: 215 white and 73 non-white. This classification was not available for eight control individuals. Among the 206 patients included in this study, 135 were classified within these groups according to self-declaration; 71 of them, in turn, following a distinct institutional policy, were classified according to their government-issued identification document or by the hospital employee who processed their hospital registration.

Ethics Statement

The present study was approved by the Ethics Committee for Research Project Analysis of Hospital das Clínicas da Faculdade de Medicina da Universidade de São Paulo (HCFMUSP), São Paulo, Brazil (CAPPesq 0174/11). All subjects gave written informed consent in accordance with the Declaration of Helsinki.

Evaluation of Parasitemia

Patients' peripheral blood samples were collected in EDTA (ethylenediaminetetraacetic acid) tubes. DNA extraction was performed using the QIAmp DNA Mini Kit (Qiagen). DNA concentration and purity were analyzed with a

spectrophotometer. The parasitemia status was determined employing a qualitative polymerase chain reaction (PCR) performed with the S35/S36 primers designed to the kinetoplastic DNA of *T. cruzi* (Invitrogen, Thermo Fisher Scientific, Carlsbad, CA, USA), as previously described (49).

DNA Extraction and Genotyping

In most patients genomic DNA was extracted from peripheral blood samples using the QIAampTM DNA Mini Kit (Qiagen, Hilden, Germany). For the cases the DNA concentration was inappropriately low, an additional extraction was carried out using the salt precipitation method (DTAB/CTAB; Sigma-Aldrich, Merck, St. Louis, MO, USA) (50). The DNA samples underwent spectrophotometric evaluation to assess yield and purity. SNVs were investigated by real-time PCR with the TaqMan® Genotyping Master Mix assay and the corresponding SNV-specific primers in the StepOnePlus platform (Applied Biosystems, Thermo Fisher Scientific, Foster City, CA, USA). The investigated SNPs included *IL1B* −31 rs1143627 T>C, *IL6* −174 rs1800795 C>G, *IL17A* −152 rs2275913 G>A, *IL18* −137 rs187238 C>G, and *IL18* −607 rs1946518 C>A.

Serum IL-18 Quantification

IL-18 levels were measured using commercial ELISA Kits (R&D Systems, Minneapolis, MN, USA) according to the manufacturer's instructions. Sera from 43 patients, 15 HIV-infected and 28 non-infected, were stored at −70°C. Twenty-four of such patients had cardiac disease. At the time of blood collection, the median viral load in the 15 HIV-infected patients was 0.0 DNA copies/µl. In 14 of them the median of CD4 count was 873.5 (769.8–974.0) cells/mm^3. Three of the 15 HIV-infected patients were not on regular antiretroviral therapy. Two had detectable viremia, with one of them displaying a CD4 count below 350 cells/mm^3. The third is an HIV-1-infected patient with an undetectable viral load and high CD4 level despite the absence of HAART therapy, belonging to the rare group named as "elite suppressor" (51).

Statistical Analyses

The calculations of Hardy-Weinberg equilibrium (HWE) were performed using chi square tests in MS Excel 365 (Microsoft Corporation, Redmond, WA). Multiple contingency analyses were performed to investigate potential associations among elected dependent variables and covariates. Fisher's exact test was used for 2x2 contingency tables; otherwise the chi-square test was applied. When chi square test was used and was applicable, we performed a *post-hoc* test using standardized and adjusted residues with the Bonferroni correction. The P values obtained with single association tests (Fisher exact test or Pearson chi square test) were used as triage to elect candidate variables for multivariable analyses. We included in the logistic regression all variables that reached $P < 0.2$ in the single variable association test with the dependent variable. In the genetic models, when more than one model reached $P < 0.2$, we assumed the model with lower P value as the best-fit model and included it in the logistic regression analysis. To increase the modeling performance, continuous variables were categorized using a ROC (receiving operator characteristic) curve and clinical/biological criteria. Some variables presented missing values in 1–20% of cases and displayed a non-monotone missing pattern. In such cases, we performed multiple imputations including 100 imputed values for each missing one (52). This step was accomplished using MCMC (Markov chain-Monte Carlo simulation) for value imputation. The genotypes were clustered according to four possible models of genetic effects: additive (each genotype was analyzed separately), dominant (the presence of at least one SNV allele is associated with the effect), heterozygous (the heterozygous genotype is associated with the effect on phenotype), and recessive (the presence of SNV homozygosity is associated with the effect on phenotype). We adopted the best-fit model in the chi-square/Pearson exact test analyses, defined by the most significant P-value.

Since rs1946518 and rs187238 are just 470 bp apart from each other in the *IL18* promoter, we investigated linkage disequilibrium between these two SNVs using the Haploview software (53) and evaluated potential associations involving the haplotypes.

Chagas cardiopathy, NYHA (New York Heart Association) score, LVEF, and parasitemia were selected upfront as dependent variables for the multiple logistic regressions. Since there was potential interference of the clinical form in the analyzed endpoints, we considered the digestive form as an independent variable in addition to traditional potential confounding factors. To address this point, such a variable was included in the triage as a potential predictor in the model applied to the logistic regression analysis.

Continuous variables were tested for normality with the Shapiro-Wilk test. Continuous parametric variables were analyzed using *t* test to compare two groups, with the Welch correction if the Levine test pointed to unequal variance between the groups. Continuous non-parametric variables were analyzed using the Mann-Whitney U test when comparing two groups, or Kruskal-Wallis test when comparing more than two groups, followed by *post-hoc* analysis with the Bonferroni correction. Categorical variables were compared using the chi-square or Fisher exact test. Categorical variables are expressed as the number of cases and percentages while continuous variables as mean ± standard deviation when parametric, and median (25–75% range) when non-parametric. We accepted an α risk of 5% in this exploratory research. The statistical analyses were run in SPSS 24.

RESULTS

Single Nucleotide Variant Genotype and Allele Distribution in the Analyzed Patient Population and Potential Implications

The studied Chagas disease patient population presented a balanced gender composition, predominance of whites and a median age of 50 (42-60) years (**Table 1**). Notably, 49 patients

TABLE 1 | Patient distribution according to demographic features, HIV status, parasitemia, cardiac phenotypes, and single nucleotide variant (SNV) genotypes.

Patient characteristics	n/median	%/25–75%
Age (years)	50.62	42.0–60.0
Age Range		
<35	23	11.2
35–50	88	42.7
>50	95	46.1
Skin color		
White	152	73.8
Non-white	54	26.2
Sex		
Female	103	50
Male	103	50
HIV		
HIV infection	49	23.8
No HIV infection	157	76.2
Parasitemia		
Positive	90	43.7
Negative	112	54.4
Missing	4	1.9
Chagas cardiopathy		
No	83	40.3
Yes	123	59.7
Clinical forms		
Indeterminate form	51	24.8
Cardiac form	96	46.6
Digestive form	32	15,5
Cardio-digestive form	27	13.1
NYHA		
NYHA < 2/no CA	79	38.3
NYHA ≥ 2	112	54.4
Missing	15	7.3
LVEF (%)	60	28–67
LVEF < 45%		
Negative	115	55.8
Positive	69	33.5
Missing	22	10.7
IL1B –31 rs1143627 T>C		
TT	68	33.0
TC	92	44.7
CC	46	22.3
IL6 –174 rs1800795 C>G		
CC	12	5.8
CG	65	31.6
GG	129	62.6
IL17A –152 rs2275913 G>A		
GG	131	63.6
GA	62	30.1
AA	13	6.3
IL18 –607 rs1946518 C>A		
CC	74	35.9
CA	93	45.1
AA	39	18.9
IL18 –137 rs187238 C>G		
CC	111	53.9
CG	77	37.4
GG	18	8.7

HIV, human immunodeficiency virus; LVEF, left ventricular ejection fraction; NYHA, New York Heart Association score; no CA, without cardiopathy. n = 206 patients, except of IL18 levels (n = 43). When missing values were not shown those values are zero.

(23.8%) had HIV co-infection. The distribution of SNV-related genotypes, additional clinical features and the Brazilian state of birth are shown in **Supplementary Table 1**.

The entire study population was in Hardy-Weinberg equilibrium (HWE) (**Supplementary Table 2**). The genotype frequencies were also in HWE in whites and non-whites (**Supplementary Table 2**). Interestingly, HWE equilibrium was not present in some disease conditions. We detected HWE violation in *IL6* –174 rs1800795 C>G in patients with detectable *T. cruzi* DNA in peripheric blood; in patients without cardiopathy (*IL17* rs2275913 G>A and *IL18* –137 rs187238 C>G) and in patients with cardiopathy (*IL1B* rs1143627 T>C); in individuals with NYHA < 2 (NYHA 1) or without heart failure (*IL17* rs2275913 G>A and *IL18* –607 rs1946518 C>A); and in subjects with NYHA ≥ 2 (*IL1B* rs1143627 T>C) (**Supplementary Table 2**). Those data suggest that the mentioned disease conditions could be influenced by the allelic composition in the selected *loci*.

We analyzed self-declared/documented ancestry as a potential confounding factor for all dependent variables. The P values are mentioned in **Supplementary Table 3** and the comparisons can be appreciated in **Supplementary Table 4**, which comprises the frequencies of self-declared/documented ancestry for each of the dependent variables. The P values show that there was no significant interference of self-declared/documented ancestry in the analyzed comparisons carried out in this study.

IL1B, IL17A, and *IL18* Polymorphic Genotypes Decrease the Risk or Attenuate Progression of Cardiomyopathy in Chagas Disease

Preliminary univariate analyses showed potential associations between cardiomyopathy and sex (P = 0.023), *IL18* –607 rs1946518 C>T applying the recessive model (P = 0.011), *IL18* –137 rs187238 C>G using the recessive model (P = 0.078), *IL17* rs2275913 G>A based on the recessive model (P = 0.039), and digestive involvement (P = 0.012) (**Supplementary Table 3**).

These initial analyses also predicted potential associations between NYHA score ≥ 2 and gender (p = 0.019), *IL1B* rs1143627 T>C using the heterozygous model (P = 0.008), *IL18* –607 rs1946518 C>A applying the recessive model (P = 0.009), *IL18* –137 rs187238 C>G applying the recessive model (P = 0.194), and digestive involvement (P = 0.001) (**Supplementary Table 3**). LVEF-based analyses, in turn, showed potential associations between LVEF < 45% and sex (P = 0.128), *IL18* –607 rs1946518 C>A applying the recessive model (P = 0.003), *IL18* –137 rs187238 C>G applying the recessive model (P = 0.052), *IL1B* rs1143627 T>C using the heterozygous model (P = 0.033), *IL6* rs 1800795 C>G applying the recessive model (P = 0.028), *IL17* rs2275913 G>A using the recessive model (P = 0.157), and digestive involvement (P < 0.001) (**Supplementary Table 3**).

As for Parasitemia, potential associations were shown with LVEF < 45% (P = 0.031), NYHA score ≥ 2 (P = 0.180), and *IL6* rs1800795 heterozygous model (P = 0.023) (**Supplementary Table 3**).

In this scenario, we performed multiple logistic regression analyses for each of the elected dependent variables. This assessment revealed that males with Chagas disease had an OR of 2.22 (P = 0.011, 95% CI 1.20–4.09) to develop cardiomyopathy

(**Table 2**). Interestingly, homozygosity for the *IL17* rs2275913 A allele carried a heart protective effect, being associated with an OR of 0.27 (P = 0.044, 95% CI 0.07–0.97) (**Table 2**). A similar effect was detected for homozygosity of the *IL18* −607 rs1946518 A allele (OR = 0.35; P = 0.023, 95% CI 0.14–0.87).

Our analyses also established a positive association between NYHA score ≥ 2 and male gender (OR = 2.62, P = 0.007, 95% CI 1.30–5.27) and a negative association between this NYHA score range and the *IL18* −607 rs1946518 AA genotype (OR = 0.21, P = 0.009, 95% CI 0.06–0.68) and *IL1B* rs1143627 T>C using the heterozygous model (OR = 0.48, P = 0.036, 95% CI 0.24–0.95) and digestive involvement (OR = 0.20, P < 0.001, 95% CI 0.09–0.47) (**Table 3**). A similar effect was observed for the *IL18* −607 rs1946518 AA genotype with respect to LVEF < 45% (OR = 0.22, P = 0.034, CI 0.05–0.89), and digestive involvement (OR = 0.24, P = 0.004, 95% CI 0.09–0.62) (**Table 4**).

TABLE 2 | Multiple logistic regression for cardiopathy.

	OR	95% CI	P
Sex (male)	2.22	1.20–4.09	**0.011**
HIV	0.48	0.23–0.96	**0.039**
IL17A −152 rs2275913 G>A recessive	0.27	0.07–0.97	**0.044**
IL18 −607 rs1946518 C>A recessive	0.35	0.14–0.87	**0.023**
IL18 −137 rs187238 C>G recessive	1.04	0.29–3.71	0.953
Digestive Involvement	0.55	0.28–1.05	0.069

95% CI, 95% confidence interval; HIV, human immunodeficiency virus; OR, odds ratio; P values ≤ 0.05 in bold.

TABLE 3 | Multiple logistic regression for New York Heart Association (NYHA) ≥ 2.

	OR	95% CI	P
Sex (male)	2.620	1.30–5.27	**0.007**
HIV	0.153	0.06–0.39	**<0.001**
IL1B −31 rs1143627 T>C heterozygous	0.476	0.24–0.95	**0.036**
IL18 −607 rs1946518 C>A recessive	0.208	0.06–0.68	**0.009**
IL18 −137 rs187238 C>G recessive	2.567	0.52–12.76	0.249
Parasitemia	0.801	0.39–1.63	0.539
Digestive Involvement	0.204	0.09–0.47	**<0.001**

95%, CI 95% confidence interval; HIV, human immunodeficiency virus; NYHA, New York Heart Association score; OR, odds ratio; P values ≤ 0.05 in bold.

TABLE 4 | Multiple logistic regressions for left ventricular ejection fraction (LVEF) < 45%.

	OR	95% CI	P
Sex (male)	1.967	0.82–4.70	0.128
HIV	0.033	0.00–0.25	**0.001**
IL1B −31 rs1143627 T>C heterozygous	0.631	0.29–1.35	0.237
IL6 −174 rs1800795 C>G recessive	13.082	0.40–431.30	0.149
IL17A −152 rs2275913 G>A recessive	0.578	0.05–7.41	0.673
IL18 −607 rs1946518 C>A recessive	0.221	0.05–0.89	**0.034**
IL18 −137 rs187238 C>G recessive	2.213	0.28–17.40	0.450
Parasitemia	0.581	0.26–1.30	0.186
Digestive involvement	0.235	0.09–0.62	**0.004**

95% CI, 95% confidence interval; HIV, human immunodeficiency virus; LVEF, left ventricular ejection fraction; OR, odds ratio; P values ≤ 0.05 in bold.

When investigating linkage disequilibrium between rs1946518 and rs187238, we found D` of 0.89 and r^2 of 0.43, indicating strong linkage disequilibrium between the two *loci*. Our analysis also revealed that the haplotype *IL18* −607 C/*IL18* −137 C was associated with Chagas cardiopathy (P = 0.0186) and LVEF < 45% (P = 0.0149) (**Supplementary Table 5**). This same haplotype also reached a marginal P value for association with NYHA ≥ 2 (P = 0.0554). No haplotype involving these two SNVs showed significant association with the parasitemia status.

A Specific *IL6* Polymorphism Profile Modulates the Risk of *Trypanosoma cruzi* Parasitemia

Based on univariate analyses, potential associations were predicted to occur between positive *T. cruzi* parasitemia and *IL6* rs1800795 C>G applying the heterozygous model (P = 0.023), NYHA ≥ 2 (P = 0.180) and HIV infection (P = 0.008) (**Supplementary Table 3**).

Notably, multiple logistic regression analyses uncovered a negative association between parasitemia and the *IL6* rs1800795 CG genotype (OR = 0.45, P = 0.015, 95% CI 0.24 −0.86) and a positive association between parasitemia and HIV infection (OR = 2.18, P = 0.039, 95% CI 1.04–4.58) (**Table 5**).

HIV Infection Is Protective Against Development and Progression of Cardiomyopathy in Chagas Disease

Our preliminary univariate analyses suggested a protective cardiac effect of HIV infection in patients with Chagas disease, based on the development of cardiomyopathy (P = 0.045), the NYHA score (P < 0.001), and the LVEF values (P < 0.001) (**Supplementary Table 3**).

To evaluate the potential effect of HIV infection on the cardiac form of Chagas disease, we initially compared the HIV population with the non-HIV patients with respect to potentially interfering parameters (**Table 6**). This analysis showed no differences in age, sex, groups (white x non white), and the SNV genotypes analyzed in the current study.

Remarkably, multiple logistic regression analyses revealed a protective effect of HIV infection against the development of cardiomyopathy, displaying an OR of 0.48 (P = 0.039, 95% CI 0.23–0.96) (**Table 2**). In the same line, negative associations were shown for NYHA score ≥ 2 and HIV infection (OR = 0.15, P < 0.001, 95% CI 0.06–0.39) (**Table 3**) as well as for LVEF < 45%

TABLE 5 | Multiple logistic regressions for parasitemia.

	OR	95% CI	P
HIV	2.18	1.04–4.58	**0.039**
IL6 −174 rs1800795 C>G heterozygous model	0.45	0.24–0.86	**0.015**
NYHA ≥ 2	1.06	0.43–2.58	0.900
LVEF < 45%	0.65	0.24–1.72	0.385

95% CI, 95% confidence interval; HIV, human immunodeficiency virus; LVEF, left ventricular ejection fraction; NYHA, New York Heart Association score; OR, odds ratio; P values ≤ 0.05 in bold.

TABLE 6 | Comparisons between Chagas disease patients with and without HIV infection.

	HIV n(%)/median (25–75%)	Non-HIV n(%)/median (25–75%)	P
Age[a]	49 (39–60.5)	50 (42–60)	0.379
Age range[b]			0.062
<35	10 (20.4)	13 (8.3)	
35-50	19 (38.8)	69 (43.9)	
>50	20 (40.8)	75 (47.8)	
Sex[c]			0.326
Male	28 (57.1)	75 (47.8)	
Female	21 (42.9)	82 (52.2)	
White[c]	37 (75.5)	115(73.2)	0.853
Non-white	12 (24.5)	42 (26.8)	
Chagas cardiopathy[c]			**0.045**
No	26 (53.1)	57 (36.3)	
Yes	23 (46.9)	100 (63.7)	
NYHA ≥ 2[c]			**<0.001**
No			
Yes	8 (16.3)	71 (50.0)	
Missing	0	15	
Left ventricular ejection fraction[a]	0.67 (0.62–0.71)	0.43 (0.25–0.65)	**<0.001**
Ejection fraction ≥ 45%[c]	45 (97.8)	70 (50.7)	**<0.001**
Ejection fraction < 45%	1 (2.2)	68 (49.3)	
Missing	3	19	
Parasitemia: negative[c]	18 (38.3)	94 (60.6)	**0.008**
Parasitemia: positive	29 (61.7)	61 (39.4)	
Missing	2	2	
Clinical form[b]			**0.001**
Indeterminate form	20 (40.8)	31 (19.7)	
Cardiac form	11 (22.4)	85 (54.1)	
Digestive form	8 (16.3)	24 (15.3)	
Cardio-digestive form	10 (20.4)	17 (10.8)	
Genotypes			
IL1B –31 rs1143627 T>C[b]			0.168
TT	11 (22.4)	57 (36.3)	
TC	24 (49.0)	68 (43.3)	
CC	14 (28.6)	32 (20.4)	
IL6 –174 rs1800795 C>G[b]			0.984
CC	3 (25.0)	9 (5.7)	
CG	15 (6.1)	50 (31.8)	
GG	31 (63.3)	98 (62.4)	
IL17A –152 rs2275913 G>A[b]			0.559
GG	33 (67.3)	98 (62.4)	
GA	12 (24.5)	50 (31.8)	
AA	4 (8.2)	9 (5.7)	
IL18 –607 rs1946518 C>A[b]			0.814
CC	16 (32.7)	58 (36.9)	
CA	24 (49.0)	69 (43.9)	
AA	9 (18.4)	30 (19.1)	
IL18 –137 rs187238 C>G[b]			0.180
CC	22 (44.9)	89 (56.7.)	
CG	20 (40.8)	57 (36.3)	
GG	7 (14.3)	11 (7.0)	

NYHA, New York Heart Association score. HIV patients, (n = 49), non-HIV patients, (n = 157). Comparisons: [a]Student t test, [b]Pearson chi square test, [c]Fisher exact test. Percentual distributions considered only valid cases. When missing values were not shown those values are zero. P values ≤ 0.05 in bold.

and positive HIV status (OR = 0.03, P < 0.001, 95% CI 0.00–0.25) (**Table 4**).

IL18 Levels, Cardiopathy, New York Heart Association, Left Ventricular Ejection Fraction, and HIV

IL18 levels were analyzed in 43 patients and assessed with respect to the genotypes/alleles and the presence of cardiopathy, HIV infection, NYHA score, and LVEF (**Table 7**). The IL18 levels did not significantly vary among *IL18* −607 or *IL18* −137 SNV genotypes/alleles. No significant differences in this interleukin levels were detected either between patients with and without cardiopathy or HIV infection as well as among the different NYHA score or LVEF-related groups. Three patients without HAART therapy displayed serum levels of 737.49, 739.87, and 744.29 pg/ml. These last two were viremic and only one had a CD4 count below 350 cells/mm^3. The 13 aviremic individuals under HAART therapy presented a median value of 308.24 pg/ml and all of them had CD4 cells higher than 350 cell/mm^3.

TABLE 7 | IL18 serum levels in Chagas disease patients according to the HIV status, cardiac phenotypes, parasitemia, and *IL 18* –607 and *IL 18* –137 genotypes.

	N	Serum level IL-18 (pg/ml)Median (25–75%)	P
HIV[a]			0.212
Negative	28	268.0 (190.3–736.0)	
Positive	15	736.6 (194.7–747.2)	
Cardiopathy[a]			0.903
No	22	301.3 (215.7–737.4)	
Yes	21	308.2 (176.4–753.4)	
NYHA[a]			0.508
NYHA <2/no CA	28	311.2 (215.0–753.2)	
NYHA ≥ 2	15	250.8 (176.7–739.5)	
LVEF[a]			0.782
LVEF ≥ 45%	28	298.3 (199.7–743.2)	
LVEF < 45%	14	284.9 (174.5–740.6)	
Missing	1		
Parasitemia[a]			0.131
Negative	20	247.2 (183.4–732.2)	
Positive	22	722.4 (214.209.7–751.5)	
Missing	1		
IL18 –607 rs1946518 C>A[b]			0.897
CC	17	314,1 (185.6–740.9)	
CA	16	313.7 (221.0–742.3)	
AA	10	275.2 (182.4–741.8)	
IL18 –607 rs1946518 C>A[a]			0.944
CC+CA	33	275.2 (182.4–741.8)	
AA	10	314.2 (204.7–740.8)	
IL18 –137 rs187238 C>G[b]			0.878
CC	24	316.6 (185.3–742.6)	
CG	15	308.2 (216.1–744.0)	
GG	4	275.2 (206.6–623.8)	
IL18 –137 rs187238 C>G[a]			0.702
CC+CG	39	314.2 (194.7–744.0)	
GG	4	275.2 (206.6–623.8)	

HIV, human immunodeficiency virus; LVEF, left ventricular ejection fraction; NYHA, New York Heart Association score; no CA, without cardiopathy. Tests: [a]Mann Whitney U test, [b]Kruskal Wallis test. Total number of patients = 43. Percentual distributions considered only valid cases. When missing values were not shown those values are zero.

DISCUSSION

IL6, IL1B, IL17A, and *IL18* Single Nucleotide Variants and Parasitemia in Chagas Disease

In a still largely unclear scenario relating cytokines and pathogenesis of Chagas disease, our study seeked for potential associations between strategic cytokine-related SNVs and key Chagas phenotypes restricted to the disease or combined with immune dysregulation.

T. cruzi parasitemia has been recognized as an element that accelerates chronic Chagas cardiopathy (19, 20, 22), although some reports question this effect (23–25). PCR-based *T. cruzi* detection in human biopsies supports that parasite persistence in the heart favors the progression of cardiomyopathy (19, 21). Identification of *T. cruzi* DNA in human blood, moreover, has been associated with a higher risk of development and deterioration of cardiomyopathy (20, 22).

IL6 is a key cytokine in mouse-induced *T. cruzi* myocarditis, triggering protection mechanisms in cardiomyocytes but favoring a higher parasite load (29). Acute *T. cruzi* experimental infection in mice with high inoculum, in fact, was followed by increased IL-6, high parasite load in tissue and marked inflammation (54, 55) while *IL6*-KO mice developed different levels of parasite load in the blood and myocardium depending on the *T. cruzi* strain (29, 54). These animals, however, presented increased mortality (29, 54). Such findings suggest that avoidance of high IL6 levels may play a role in lowering the parasite load whereas a certain tissue level of IL6 must be reached to allow a protective response against the parasite-induced lesion. A balanced level of IL6, therefore, is expected to reduce tissue damage and cardiomyocyte death, mitigating the disease. Of note, our data revealed that *IL6* −174 CG heterozygosity is protective against *T. cruzi* parasitemia. This original finding raises an enticing mechanistic hypothesis for the relationship between IL6 and parasitemia. This SNV is located in the *IL6* promoter, having the G allele been associated with higher IL6 blood levels than the C allele (33, 34, 56, 57). It is likely, therefore, that the low IL6 levels associated with the CC genotype lead to a lack of immune-mediated protection against parasitemia, while the high IL6 levels observed in GG individuals create a relatively severe inflammatory background that also favors *T. cruzi* replication. On the other hand, a balanced scenario of protection and controlled inflammation, displayed by heterozygous patients, would provide the best setting to fight parasitemia.

Facing the possible role of IL18 in reducing parasitic load in *IL18*-KO mice (26), we investigated the influence of *IL18* SNVs on *T. cruzi* parasitemia. The *IL18* human gene harbors several SNVs in its promoter. *IL18* −607 C>A and *IL18* −137 C>G are located in nuclear factor binding sites for CREB (cyclic AMP-responsive element binding protein) and H4TF-1 (human histone H4 gene specific transcription fator-1), respectively. Variants of these two sites can not only affect *IL18* transcription but also IFNγ expression (58). The −607 A allele and AA genotype have been associated with lower *IL18* transcriptional rate and/or protein levels than the C allele and CC genotype in different clinical and physiological settings (59–63), whereas the haplotype C-607/G-137 is associated with higher expression of IL18. Our analyses, however, did not identify a significant impact of *IL18* −607 or *IL18* −137 alleles/genotypes on the *T. cruzi* parasitemic status.

The observation of increased parasitemia in *IL17A*-KO mice infected by *Leishmania infantum* supports a role of IL17A in controlling parasitemia (64). IL17A and IFNγ activate macrophages to phagocyte *T. cruzi* for further killing in the endosomal/lysosomal compartment (65). This finding is not a surprise, since association between higher levels of IL17A and resistance to *Leishmania donovani* had been previously reported (66).

The *IL17A* −152 G>A SNV is a critical regulator of the *IL17A* promoter, being located within a binding motif for NFAT (nuclear factor activated T cells) (67). The A allele is more often associated with higher IL17A serum levels (40, 41, 67). Despite these observations, our analysis did not show association between *IL17A* −152 G>A and *T. cruzi* parasitemia, not supporting a protective role of the A allele against parasitemia in human Chagas disease.

Effects of *IL1B, IL17A, IL18, and IL6* Single Nucleotide Variants on Cardiomyopathy in Chagas Disease

Previous studies showed direct correlation between IL-6 serum levels and cardiomyopathy (7–9) and an inverse correlation between IL-6 levels and LVEF in the setting of cardiopathy (7). Based on these observations and the association of *IL6* −174 C with lower IL6 levels (33, 34, 56, 57), we hypothesized that this allele might be protective. Our findings, however, did not reveal such an impact, corroborating results from Colombia and Peru obtained in an ethnically distinct population affected by different parasite lineages (32, 68). It is possible, therefore, that other factors may also play a role in determining IL6 levels that modulate the cardiac phenotype in Chagas disease.

IL1β triggers an inflammation cascade, leads to generation of reactive free radicals, and may promote IFNγ production (69) and facilitate the differentiation of pro-inflammatory cells such as human Th17 (70). The assessed *IL1B* −31 T>C transition causes disruption of a TATA-box, potentially changing the binding site affinity to regulatory proteins (36). We showed association between the *IL1B* −31 TC genotype and lower NYHA in Chagas disease. It is known that IL1β promotes inflammatory activity in acute experimental myocarditis induced by *T. cruzi* (71) and induces hypertrophy in primary cultures of cardiomyocytes infected by this parasite (72). Based on these data and because the *IL1B* −31 T allele is associated with increased *IL1B* transcription (36), heterozygosity may attenuate inflammation and cardiomyocyte hypertrophy in Chagas myocarditis, still allowing enough IL1β to fight *T. cruzi* infection. This balanced response likely explains the observed protective effect of the *IL1B* −31 TC genotype against cardiac disease severity. Interestingly, the CT haplotype for *IL1B* −31 T>C and +3,954 C>T was more prevalent in patients with Chagas cardiomyopathy in a Colombian population (35).

Higher frequencies of CD4+ IL-17A+ T-cells, lower levels of IL10 and IL10, and higher levels of IFNγ and TNFα are observed in individuals with more severe cardiomyopathy (6, 7). These findings are in agreement with the observation of lower lymphocyte IL17A expression in chronic Chagas cardiomyopathy than in seronegative individuals and patients with the indeterminate form (6). In addition, high IL17A levels were also associated with better heart function in Chagas disease (11). Based on these observations, IL17A was expected to potentially modulate inflammation in cardiac tissue and protect against *T. cruzi* infection (27, 28). A study in Brazil, however, unexpectedly revealed associations between the *IL17A* −152 A allele and the AA genotype with chronic cardiomyopathy (42). In contrast, another study in a Colombian cohort reported a protective effect of the C Allele of *IL17A* rs 8193036 C>T in seronegative individuals in comparison with cardiac seropositive patients (38), in a context of previously established association between the C allele and lower IL 17A mRNA expression (39). These data were *a priori* not expected, since previous reports showed a role for IL17A in mouse resistance to *T. cruzi* infection (27) and/or higher IL17A levels in patients without cardiopathy (11, 12). This study also found no association between the *IL17A* G>A 3' UTR rs7747909 SNV, other two *IL17A* promoter SNVs (rs4711998 and rs3819024) or *IL17A* rs2275913 and Chagas cardiopathy.

In agreement with the expected role of IL17A, but in contrast to most clinical results, we found association between *IL17A* rs2275913 G>A and cardiac protection following a recessive model. Indeed, carriers of the A allele and the AA genotype were found to have a lower risk to develop cardiomyopathy. Since A allele has been found in association with higher IL17A serum levels (40, 41, 67), our data are in accordance with reports that show association between better cardiac function and higher IL17 A levels (11, 12). Our findings suggest that IL17A modulates the host inflammatory response to parasites in the myocardium, impacting the risk of developing cardiac dysfunction. Additional studies are necessary, however, to establish the effect of the AA genotype on IL17A serum levels in Chagas disease patients. It must be pointed out that our study differs from the previous ones (38, 42) with respect to patient geographical origin, ethnicity, classification, sample size, subgroup design, and possibly parasite lineage (68). Given the significant ethnical differences among Brazilian, Colombian, and Bolivian populations, genetic background may be a major determinant for the different results.

Since IL18 induces pathological cardiac remodeling (16), cardiomyocyte hypertrophy (73) and increased fibronectin expression (74), high levels of IL18 are expected to lead to cardiac hypertrophy and fibrosis, with a deleterious impact on heart function. IL18 is expressed in myocardium early in the course of experimental myocarditis induced by *T. cruzi* (15), leading to production of IFNγ. IL18 upregulation and correlation between IL18 mRNA and IFNγ expression have been shown in human Chagas heart tissue (18). Standing as a novel observation, we showed association between the *IL18* −607 AA genotype and decreased risk of developing cardiomyopathy, progressing to NYHA ≥ 2, and progressing to LVEF < 45%. These data are in accordance to previously reported association between this AA genotype and low IL18 production in the presence and in the absence of mitogen stimuli (60–66). Unlike these studies, however, our data did not reveal significant associations between IL18 levels and any of the *IL18* −607 or *IL18* −137 genotypes/alleles. Such differences may rely on the nature and size of the studied populations (55–101 patients), including other diseases, and/or the nature the biological samples and/or experimental conditions, including plasma and mucosal biopsies and peripheral blood cells under mitogen stimuli (58–63). The lack of association between IL18 serum levels and *IL18* −607 C>A or *IL18* −137 C>G genotypes/alleles observed in our study does not allow a straight association between the mentioned cardiac findings and IL18 serum levels. This finding raises the hypothesis that IL18 serum levels may not significantly correlate with IL18 heart tissue levels in Chagas disease. However, since our study did not reproduce the association between IL18 levels and the *IL18* −607 SNV in other contexts, more representative patient samples should be evaluated under different conditions to more conclusively investigate this relationship in this disease. It must be noted that a previous study conducted in Colombian and Latin American Chagas patients did not detect significant frequency differences of *IL18* −607 A allele and AA genotype between asymptomatic patients and ones with cardiac dysfunction (43, 44). Data from an Argentinian population, on the other hand, display a trend similar to our study (44). Our data strengthens the potential benefit of targeting IL18 as a therapy in Chagas cardiomyopathy. IL18 levels have indeed been associated with increased mortality and are inversely correlated with LVEF in heart failure (75). Moreover, neutralization of IL18 has been proposed in heart failure (76), Fabry cardiomyopathy (77) and sepsis-induced cardiac dysfunction (78). Our data also revealed association of the *IL18* −607 C/*IL18* −137 C haplotype with Chagas cardiopathy and LVEF < 45%. Our results on *IL18* −137, however, do not support an additive susceptibility status linking such SNVs.

Our study revealed that men have higher risks for cardiopathy and NYHA ≥ 2. These findings are in line with previous data that report male gender as one of the six independent variables that constitute risk factors for death in Chagas heart disease (3, 79). Male sex, therefore, appears as a robust risk factor for worse prognosis in Chagas cardiomyopathy. As a novel finding, digestive involvement associated negatively with NYHA ≥ 2 and LVEF < 45%, suggesting that such patients may develop a milder cardiopathy than affected individuals without digestive disease. This observation has never been reported (1, 31, 80). Alternative explanations for this finding may comprise a potential inclusion of more severely affected cardiac patients in our study and a potentially smaller than real proportion of patients with the indeterminate form due to underdiagnosis and/or loss of follow-up, raising the cardiac form/indeterminate form ratio. The relatively high proportion of cardio-digestive cases previously reported (1, 31), however, adds further support to the influence of digestive involvement in NYHA and LVEF.

Impact of HIV Infection on Development and Progression of Cardiomyopathy in Chagas Disease

In immunosuppressed patients with HIV infection, elevated IL18 serum concentrations have been shown to favor the development

of Aids and associated infections (30). In addition, Chagas disease reactivation does not occur in immunocompetent subjects, while in HIV-infected patients this illness has been associated with increased morbidity and mortality (31). Based on a severe combined immunodeficient (SCID) animal model (81), this observation may be explained by dissociation between a high parasite load and lower tissue inflammation, which is associated with decreased IFNγ levels and early mortality. Interestingly, *T. cruzi* inhibits HIV replication in macrophage-derived monocyte culture (82). In our study the HIV infected and non-infected groups did not differ with respect to the evaluated SNV profiles, age or gender. In the HIV-infected group, 53.1% of the patients were not on HAART therapy. Our findings revealed higher parasitemia in HIV-infected Chagas individuals, confirming previous data (83). Of note, in *T. cruzi*/HIV coinfection a Th2 response likely contributes to the impairment of parasite control (84). Altogether, our data suggest that antiretroviral therapy interferes positively in the host-HIV-*T. cruzi* interaction.

To our surprise, our analyses revealed a previously not described finding: HIV infection exerts a strong protective effect on Chagas disease cardiomyopathy. HIV infection was associated with lower risks to develop cardiopathy and to progress to NYHA ≥ 2 and LVEF < 45%. This *a priori* unexpected effect may be based on actions of the HAART regimens, reported to decrease the prevalence of HIV-associated cardiomyopathy in about 30% of the HIV-infected patients (85). In contrast, HAART failure was associated with continued IL18 elevation (86).

IL18 contributes to Aids pathogenesis by increasing viral replication, death of endothelial cells, and cardiomyocyte proliferation (30). A previous study from our service showed that Chagas reactivation occurred only in patients not in HAART therapy, and progression to a more severe chronic disease and death were observed in 35 and 30% of them, respectively (31). Moreover, progression to severe chronic forms was verified in less than 10% of patients on HAART. In those under HAART therapy, we detected high levels of IL18 (>700 pg/ml) in two of viremic cases and a median of 308.24 pg/ml in 13 aviremic individuals. The small number of analyzed patients, however, did not allow statistical evaluation with respect to IL18 levels and viral load, and no differences in IL18 levels were detected between HIV and non-HIV patients. A previous report did not find difference between 32 HIV viremic and 15 aviremic patients either (87). While our data suggest that IL18 serum levels may not correlate with IL18 levels in cardiac tissue in Chagas disease, a larger future study should address a still possible IL18-reducing effect of HAART on Chagas cardiomyopathy.

Another potential explanation for this positive impact of HIV infection on Chagas disease could be a growth-reduction effect of antiretroviral drugs on *T. cruzi*. HIV protease inhibitors have in fact been reported to restrain epimastigote, trypomastigote, and amastigote growth (88–90). Pretreatment of trypomastigotes with nelfinavir and lopinavir inhibited their association with LLC-MK_2 epithelial cells and RAW macrophages and decreased the number of intracellular amastigotes (88). In addition, interaction of ritonavir, lopinavir and nelfinavir and *T. cruzi* epimastigotes showed potent anti-proliferative effects and led to changes in differentiation (89).

Nelfinavir and lopinavir target vital cellular structures of trypomastigotes, leading to irreversible, lethal metabolic injuries in the size and structure (90). A trypanocidal effect of HIV proteinase inhibitors on the *T. cruzi* aspartyl peptidase intracellular target was also reported using a docking simulation model (91), showing a great affinity of ritonavir and lopinavir to bind to this active enzyme intracellular site. In this setting, saquinavir has been integrated to the computer-guided drug repositioning as a potentially new treatment for Chagas disease (92).

A synergistic interaction between a Th2 predominant response in *T. cruzi*-HIV infected patients and HAART could also potentially lead to reduction in IL18 levels (30). This combined effect might decrease the predominant Th1 response in myocardium (5) and reduce inflammatory cardiac lesions. Other cardiovascular actions of antiretrovirals are unlikely to contribute to the cardioprotective effect, since HAART has been linked to increased risk of cardiovascular illness (30).

While the scientific relevance and possible clinical applications raised by the HIV-related cardioprotective effect on Chagas cardiomyopathy are potentially remarkable, its underlying mechanisms remain unclear. Future studies with larger and more diverse coinfected patient populations, expansion of cardiac function/lesion markers, detailed characterization of the cardiac microenvironment associated this coinfection, and deep characterization of cardiac tissue response to HAART should bring significant contributions to this elucidation.

Our study brought novel and meaningful data to field of Chagas disease, but it also carries some limitations. Such limitations comprise the inclusion of a single center, Brazilian heterogeneous ethnicity, limited analyses of interleukin levels and respective functional impact, and lack of data integration involving the use of HAART, CD4+ count, HIV load, and molecular genetics assessment. The appropriate statistical model employed for small samples and the level of significance detected in key analyses, however, strongly support our conclusions and provide a robust platform for sequential future studies.

In conclusion, our findings revealed a novel association between the *IL6* −174 C>G SNV and parasitemia in Chagas disease, expressed as a decreased risk of its detection in patients with the CG genotype. As additional original findings, our data showed that the *IL17A* −152 AA and the *IL18* −607 AA genotypes are associated with a reduced risk of developing cardiomyopathy in individuals affected by this illness. The *IL18* −607 AA and *IL1B* TC genotypes were also found to associate with a lower risk of manifesting severe cardiac dysfunction. Most of our findings are consistent with previously reported clinical data on Chagas disease and data on cytokine expression. Unexpectedly, our results uncovered a novel protective effect of HIV infection in Chagas disease patients, translated into a decreased risk of developing cardiomyopathy. Available information suggests that a synergistic effect of HIV and HAART may mitigate a Th1-mediated response in the myocardium. The findings revealed by this report not only expand the understanding of Chagas disease pathogenesis and its relationship with other clinical scenarios but also add pieces of information to the field that can be potentially employed in the development of therapeutic interventions.

DATA AVAILABILITY STATEMENT

The datasets generated for this study can be found in the DRYAD Digital Repository (doi: 10.5061/dryad.wstqjq2hn).

AUTHOR CONTRIBUTIONS

MS-Y, VF, LO: conception and design. AG, EW, DF, JO, EN, CO, EB, AP, CN, FC, NC, PS, EY-K, VF, LO, MS-Y: analysis and interpretation. AG, EW, LO, MS-Y: drafting the manuscript for important intellectual content. All authors contributed to the article and approved the submitted version.

FUNDING

This work was supported by São Paulo Research Foundation (FAPESP) [#12/50273-0]; and by Conselho Nacional de Desenvolvimento Científico e Tecnológico - Programa Institucional de Bolsas de Iniciação Científica (CNPq - PIBIC) [AGS #100793/2016-9 from January to July 2016], and JOR # 157966/2015-1 from September to December 2015]; and by FAPESP (Technical Training Scholarship [CSO # 2014/07100-3 from May of 2014 to March 2015] and Secretary of Administration of São Paulo State Secretary [DTF # from March of 2014 to February of 2016], and for IL18 analyses by São Paulo Research Foundation (FAPESP) [#19/06363-4].

ACKNOWLEDGMENTS

The authors acknowledge Expedito Luna for revising the epidemiological design of this manuscript.

SUPPLEMENTARY MATERIAL

The Supplementary Material for this article can be found online at: https://www.frontiersin.org/articles/10.3389/fimmu.2020.521409/full#supplementary-material

REFERENCES

1. Dias JC, Ramos ANJr, Gontijo ED, Luquetti A, Shikanai-Yasuda MA, Coura JR, et al. 2nd Brazilian Consensus on Chagas Disease, 2015. *Rev Soc Bras Med Trop* (2016) 49:3–60. doi: 10.1590/0037-8682-0505-2016
2. Bocchi EA, Bestetti RB, Scanavacca MI, Cunha Neto E, Issa VS. Chronic Chagas Heart Disease Management: From Etiology to Cardiomyopathy Treatment. *J Am Coll Cardiol* (2017) 70:1510–24. doi: 10.1016/j.jacc.2017.08.004
3. Rassi AJr, Rassi A, Little WC, Xavier SS, Rassi SG, Rassi AG, et al. Development and validation of a risk score for predicting death in Chagas' heart disease. *N Engl J Med* (2006) 355:799–808. doi: 10.1056/NEJMoa053241
4. Dutra WO, Gollob KJ. Current concepts in immunoregulation and pathology of human Chagas disease. *Curr Opin Infect Dis* (2008) 21:287–92. doi: 10.1097/QCO.0b013e3282f88b80
5. Abel LC, Rizzo LV, Ianni B, Albuquerque F, Bacal F, Carrara D, et al. Chronic Chagas' disease cardiomyopathy patients display an increased IFN-gamma response to *Trypanosoma cruzi* infection. *J Autoimmun* (2001) 17:99–107. doi: 10.1006/jaut.2001.0523
6. de Araújo FF, Corrêa-Oliveira R, Rocha MO, Chaves AT, Fiuza JA, Fares RC, et al. Foxp3+CD25 (high) CD4+ regulatory T cells from indeterminate patients with Chagas disease can suppress the effector cells and cytokines and reveal altered correlations with disease severity. *Immunobiology* (2012) 217:768–77. doi: 10.1016/j.imbio.2012.04.008
7. Sousa GR, Gomes JA, Fares RC, Damásio MP, Chaves AT, Ferreira KS, et al. Plasma cytokine expression is associated with cardiac morbidity in Chagas disease. *PloS One* (2014) 9:e87082. doi: 10.1371/journal.pone.0087082
8. Reis MM, Higuchi M de L, Benvenuti LA, Aiello VD, Gutierrez PS, Bellotti G, et al. An *in situ* quantitative immunohistochemical study of cytokines and IL-2R+ in chronic human chagasic myocarditis: correlation with the presence of myocardial *Trypanosoma cruzi* antigens. *Clin Immunol Immunopathol* (1997) 83(2):165–72. doi: 10.1006/clin.1997.4335
9. Keating SM, Deng X, Fernandes F, Cunha-Neto E, Ribeiro AL, Adesina B, et al. NHLBI Retrovirus Epidemiology Donor Study-II (REDS-II), International Component. Inflammatory and cardiac biomarkers are differentially expressed in clinical stages of Chagas disease. *Int J Cardiol* (2015) 199:451–9. doi: 10.1016/j.ijcard.2015.07.040
10. López L, Arai K, Giménez E, Jiménez M, Pascuzo C, Rodríguez-Bonfante C, et al. C-reactive protein and interleukin-6 serum levels increase as Chagas disease progresses towards cardiac failure. *Rev Esp Cardiol* (2006) 59:50–6. doi: 10.1016/S1885-5857(06)60048-0
11. Magalhaes LM, Villani FN, Nunes M do C, Gollob KJ, Rocha MO, Dutra WO. High interleukin 17 expression is correlated with better cardiac function in human Chagas disease. *J Infect Dis* (2013) 207:661–5.9. doi: 10.1371/journal.ppat.1005902
12. Sousa GR, Gomes JA, Damasio MP, Nunes MC, Costa HS, Medeiros NI, et al. The role of interleukin 17-mediated immune response in Chagas disease: High level is correlated with better left ventricular function. *PloS One* (2017) 12:e0172833. doi: 10.1371/journal.pone.0172833
13. Guedes PM, Gutierrez FR, Silva GK, Dellalibera-Joviliano R, Rodrigues GJ, Bendhack LM, et al. Deficient regulatory T cell activity and low frequency of IL-17 – producing T cells correlate with the extent of cardiomyopathy in human Chagas' disease. *PloS Negl Trop Dis* (2012) 6:e1630. doi: 10.1371/journal.pntd.0001630
14. Cai CW, Blase JR, Zhang X, Eickhoff CS, Hoft DF. Th17 Cells Are More Protective Than Th1 Cells Against the Intracellular Parasite *Trypanosoma cruzi*. *PloS Pathog* (2016) 12(10):e1005902. doi: 10.1371/journal.ppat.1005902
15. Muller U, Kohler G, Mossmann H, Schaub GA, Alber G, Di Santo JP, et al. IL-12- Independent IFN-gamma production by T cells in experimental Chagas' disease is mediated by IL-18. *J Immunol* (2001) 167(6):3346–53. doi: 10.4049/jimmunol.167.6.3346
16. Xiao H, Li H, Wang JJ, Zhang JS, Shen J, An XB, et al. IL-18 cleavage triggers cardiac inflammation and fibrosis upon β-adrenergic insult. *Eur Heart J* (2018) 39:60–9. doi: 10.1093/eurheartj/ehx261
17. Meyer Zum Büschenfelde C, Cramer S, Trumpfheller C, Fleischer B, Frosch S. *Trypanosoma cruzi* induces strong *IL-12* and *IL-18* gene expression in vivo: correlation with interferon-gamma (IFN-gamma) production. *Clin Exp Immunol* (1997) 110:378–85. doi: 10.1046/j.1365-2249.1997.4471463.x
18. Nogueira LG, Santos RH, Fiorelli AI, Mairena EC, Benvenuti LA, Bocchi EA, et al. Myocardial gene expression of T-bet, GATA-3, Ror-γt, FoxP3, and hallmark cytokines in chronic Chagas disease cardiomyopathy: an essentially unopposed TH1-type response. *Mediators Inflamm* (2014) 2014(914326):9. doi: 10.1155/2014/914326
19. Zhang L, Tarleton RL. Parasite persistence correlates with disease severity and localization in chronic Chagas' disease. *J Infect Dis* (1999) 180:480–6. doi: 10.1016/j.micinf.2014.03.007
20. Basquiera AL, Sembaj A, Aguerri AM, Omelianiuk M, Guzman S, Moreno Barral J, et al. Risk progression to chronic Chagas cardiomyopathy: influence of male sex and of parasitaemia detected by polymerase chain reaction. *Heart* (2003) 89:1186–90. doi: 10.1136/heart.89.10.1186
21. Benvenuti LA, Roggerio A, Freitas HF, Mansur AJ, Fiorelli A, Higuchi ML. Chronic American trypanosomiasis: parasite persistence in endomyocardial

biopsies is associated with high-grade myocarditis. *Ann Trop Med Parasitol* (2008) 102:481–7. doi: 10.1179/136485908X311740
22. Sabino EC, Ribeiro AL, Lee TH, Oliveira CL, Carneiro-Proietti AB, Antunes AP, et al. Detection of *Trypanosoma cruzi* DNA in blood by PCR is associated with Chagas cardiomyopathy and disease severity. *Eur J Heart* (2015) 17:416–23. doi: 10.1002/ejhf.220
23. Norman FF, Perez-Ayala A, Perez-Molina JA, Flores-Chavez M, Canavate C, Lopez-Velez R. Lack of association between blood-based detection of *Trypanosoma cruzi* DNA and cardiac involvement in a non-endemic area. *Ann Trop Med Parasitol* (2011) 105:425–30. doi: 10.1179/1364859411Y.0000000033
24. Apt W, Arribada A, Zulantay I, Saavedra M, Muñoz C, Toro B. Vega, Rodríguez J.Chronic Chagas cardiopathy in Chile. Importance of *Trypanosoma cruzi* burden and clinical evaluation. *Acta Trop* (2016) 162:155–66. doi: 10.1016/j.actatropica.2016.06.025
25. D'Ávila DA, Galvão LMC, Sousa GR, Britto C, Moreira OC, Chiari E. Monitoring the parasite load in chronic Chagas disease patients: comparison between blood culture and quantitative real time PCR. *PloS One* (2018) 13(11):e0208133. doi: 10.1371/journal.pone.0208133
26. Esper L, Utsch L, Soriani FM, Brant F, Esteves Arantes RM, Campos CF, et al. Regulatory effects of IL-18 on cytokine profiles and development of myocarditis during *Trypanosoma cruzi* infection. *Microb Infect* (2014) 16:481–90. doi: 10.1016/j.micinf.2014.03.007
27. Miyazaki Y, Hamano S, Wang S, Shimanoe Y, Iwakura Y, Yoshida H. IL-17 is necessary for host protection against acute-phase *Trypanosoma cruzi* infection. *J Immunol* (2010) 185:1150–7. doi: 10.4049/jimmunol.0900047
28. da Matta Guedes PM, Gutierrez FR, Maia FL, Milanezi CM, Silva GK, Pavanelli WR, et al. IL-17 produced during *Trypanosoma cruzi* infection plays a central role in regulating parasite-induced myocarditis. *PloS Negl Trop Dis* (2010) 4:e604. doi: 10.1371/journal.pntd.0000604
29. Sanmarco LM, Ponce NE, Visconti LM, Eberhardt N, Theumer MG, Minguez Á. R. Aoki MP. L-6 promotes M2 macrophage polarization by modulating purinergic signaling and regulates the lethal release of nitric oxide during *Trypanosoma cruzi* infection. *Biochim Biophys Acta Mol Basis Dis* (2017) 1863:857–69. doi: 10.1016/j.bbadis.2017.01.006
30. Samarani S, Allam O, Sagala P, Aldabah Z, Jenabian MA, Mehraj V, et al. Imbalanced production of IL-18 and its antagonist in human diseases, and its implications for HIV-1 infection. *Cytokine* (2016) 82:38–51. doi: 10.1016/j.cyto.2016.01.006
31. Sartori AM, Ibrahim KY, Nunes Westphalen EV, Braz LM, Oliveira OCJr, Gakiya E, et al. Manifestations of Chagas disease (American trypanosomiasis) in patients with HIV/AIDS. *Ann Trop Med Parasitol* (2007) 101:31–50. doi: 10.1179/136485907X154629
32. Torres OA, Calzada JE, Beraún Y, Morillo CA, González A, González CI, et al. Lack of association between *IL6*-174G/C gene polymorphism and Chagas disease. *Tissue Antigens* (2010) 76:131–4. doi: 10.1111/j.1399-0039.2010.01478.x
33. Lorente L, Martín MM, Pérez-Cejas A, Barrios Y, Solé-Violán J, Ferreres J, et al. Association between interleukin-6 promoter polymorphism (-174 G/C), serum interleukin-6 levels and mortality in severe septic patients. *Int J Mol Sci* (2016) 17:E1861. doi: 10.3390/ijms17111861
34. Fishman D, Faulds G, Jeffery R, Mohamed-Ali V, Yudkin JS, Humphries S, et al. The effect of novel polymorphisms in the interleukin-6 (IL-6) gene on IL-6 transcription and plasma IL-6 levels, and an association with systemic-onset juvenile chronic arthritis. *J Clin Invest* (1998) 102:1369–76. doi: 10.1172/JCI2629
35. Flórez O, Zafra G, Morillo C, Martín J, González CI. Interleukin-1 gene cluster polymorphism in Chagas disease in a Colombian case-control study. *Hum Immunol* (2006) 67:741–8. doi: 10.1016/j.humimm.2006.06.004
36. El-Omar EM, Carrington M, Chow WH, McColl KE, Bream JH, Young HA, et al. *Interleukin-1* polymorphisms associated with increased risk of gastric cancer. *Nature* (2000) 404:398–402. doi: 10.1038/35006081
37. Hall SK, Perregaux DG, Gabel CA. Correlation of poly-morphic variation in the promoter region of the interleukin-1 β gene with secretion of interleukin-1β protein. *Arthritis Rheum* (2004) 50:1976. 2004. doi: 10.1002/art.20310
38. Leon Rodriguez DA, Echeverría LE, González CI, Martin J. Investigation of the role of *IL17A* gene variants in Chagas disease. *Genes Immun* (2015) 16:536–40. doi: 10.1038/gene.2015.42
39. Kim SW, Kim ES, Moon CM, Park JJ, Kim TI, Kim WH, et al. Genetic polymorphisms of IL-23R and IL-17A and novel insights into their associations with inflammatory bowel disease. *Gut* (2011) 60:1527–36. doi: 10.1136/gut.2011.238477
40. Zidan HE, Rezk NA, Alnemr AA, Moniem MI. Interleukin-17 and leptin genes polymorphisms and their levels in relation to recurrent pregnancy loss in Egyptian females. *Immunogenetics* (2015) 67:665–73. doi: 10.1007/s00251-015-0876-8
41. Correa JD, Madeira MF, Resende RG, Correia-Silva JF, Gomez RS, Souza DG, et al. Association between polymorphisms in interleukin-17 A and -17 F genes and chronic periodontal disease. *Mediators Inflammation* (2012) 2012:846052. doi: 10.1155/2012/846052
42. Reis PG, Ayo CM, de Mattos LC, Brandão de Mattos CC, Sakita KM, de Moraes AG, et al. Genetic Polymorphisms of *IL17* and Chagas disease in the south and southeast of Brazil. *J Immunol Res* (2017) 2017(1017621):7. doi: 10.1155/2017/1017621
43. Leon Rodriguez DA, Carmona FD, Echeverría LE, González CI, Martin J. IL18 Gene Variants Influence the Susceptibility to Chagas Disease. *PloS Negl Trop Dis* (2016) 10:e0004583. doi: 10.1371/journal.pntd.0004583
44. Strauss M, Acosta-Herrera M, Alcaraz A, Casares-Marfil D, Bosch-Niccolau P, Lo Presti MS, et al. Association of IL18 genetic polymorphisms with Chagas disease in Latin American populations. *PloS Negl Trop Dis* (2019) 13(11): e0007859. doi: 10.1371/journal.pntd.0007859
45. Sanchez E, Palomino-Morales RJ, Ortego-Centeno N, Jimenez-Alonso J, Gonzalez-Gay MA, López-Nevot MA, et al. Identification of a new putative functional IL18 gene variant through an association study in systemic lupus erythematosus. *Hum Mol Genet* (2009) 18:3739–48. doi: 10.1093/hmg/ddp301 PMID: 19584085
46. Nogueira LG, Frade AF, Ianni BM, Laugier L, Pissetti CW, Cabantous S, et al. Functional IL18 polymorphism and susceptibility to chronic Chagas disease. *Cytokine* (2015) 73:79–83. doi: 10.1016/j.cyto.2015.01.037
47. Furuchó CR, Umezawa ES, Almeida I, Freitas VL, Bezerra R, Nunes EV, et al. Inconclusive results in conventional serological screening for Chagas' disease in blood banks: evaluation of cellular and humoral response. *Trop Med Int Health* (2008) 13:1527–33. doi: 10.1111/j.1365-3156.2008.02172.x
48. Bennett JA, Riegel B, Bittner V, Nichols J. Validity and reliability of the NYHA classes for measuring research outcomes in patients with cardiac disease. *Heart Lung* (2002) 31:262–70. doi: 10.1067/mhl.2002.124554
49. Britto C, Cardoso MA, Wincker P, Morel CM. A simple protocol for the physical cleavage of *Trypanosoma cruzi* kinetoplast DNA present in blood samples and its use in polymerase chain reaction (PCR)-based diagnosis of chronic Chagas disease. *Mem Inst Oswaldo Cruz* (1993) 88:171–2. doi: 10.1590/s0074-02761993000100030
50. Gustincich S, Manfioletti G, Del Sal GS, Schneider G, Carninci PA. Fast method for high quality genomic DNA extraction from whole human blood. *Biotechniques* (1991) 11(3):298–300.
51. Sedaghat AR, Rastegar DA, O'Connell KA, Dinoso JB, Claus O, Wilke CO, et al. T Cell dynamics and the response to HAART in a cohort of HIV-1-infected elite suppressors. *Clin Inf Dis* (2009) 49(11):1763–6. doi: 10.1086/648081
52. Collins LM, Schafer JL. Kam CM. A comparison of inclusive and restrictive strategies in modern missing data procedures. *Psychol Methods* (2001) 6 (4):330–51. doi: 10.1037/1082-989X.6.4.330
53. Barrett JC, Fry B, Maller J, Daly MJ. Haploview: analysis and visualization of LD and haplotype maps. *Bioinformatics* (2005) 21(2):263–5. doi: 10.1093/bioinformatics/bth457
54. Borges DC, Araújo NM, Cardoso CR, Lazo Chica JE. Different parasite inocula determine the modulation of the immune response and outcome of experimental *Trypanosoma cruzi* infection. *Immunology* (2013) 138:145–56. doi: 10.1111/imm.12022
55. Gao W, Pereira MA. Interleukin-6 is required for parasite specific response and host resistance to *Trypanosoma cruzi*. *Int J Parasitol* (2002) 32:167–70. doi: 10.1016/s0020-7519(01)00322-8
56. Giannitrapani L, Soresi M, Giacalone A, Campagna ME, Marasà M, Cervello M, et al. IL-6 -174G/C polymorphism and IL-6 serum levels in patients with liver cirrhosis and hepatocellular carcinoma. *OMICS* (2011) 15:183–6. doi: 10.1089/omi.2010.0093

57. Talar-Wojnarowska R, Gasiorowska A, Smolarz B, Romanowicz-Makowska H, Kulig A, Malecka-Panas E. Clinical significance of interleukin-6 (IL-6) gene polymorphism and IL-6 serum level in pancreatic adenocarcinoma and chronic pancreatitis. *Dig Dis Sci* (2009) 54:683–9. doi: 10.1007/s10620-008-0390-z
58. Giedraitis V, He B, Huang W-X, Hillert J. Cloning and mutation analysis of the human IL-18 promoter: a possible role of polymorphisms in expression regulation. *J Neuroimmunol* (2001) 112:146–52. doi: 10.1016/s0165-5728(00)00407-0
59. Hasan FT, Naif HM. Association of Gene Polymorphisms and Serum Levels of IL-18 with the Susceptibility to Infection with Hepatitis B Virus. *J Infect Dis Med* (2017) 2:117. doi: 10.4172/2576-1420.1000117
60. Chen DY, Hsieh CW, Chen KS, Chen YM, Lin FJ, Lan JL. Association of interleukin-18 promoter polymorphisms with WHO pathological classes and serum IL-18 levels in Chinese patients with lupus nephritis. *Lupus* (2009) 18:29–37. doi: 10.1177/0961203308094559
61. Dziedziejko V, Kurzawski M, Paczkowska E, Machalinski B, Pawlik A. The impact of IL-18 gene polymorphism on mRNA levels and interleukin-18 release by peripheral blood mononuclear cells. *Postepy Hig Med Dosw (Online)* (2012) 66:409–14. doi: 10.5604/17322693.1000980
62. Jurecekova J, Babusikova E, Sivonova MK, Drobkova H, Petras M, Kliment J, et al. Association between interleukin-18 variants and prostate cancer in Slovak population. *Neoplasma* (2017) 64:148–55. doi: 10.4149/neo_2017_119. 2017.
63. Sakai K, Kita M, Sawai N, Shiomi S, Sumida Y, Kanemasa K, et al. Levels of interleukin-18 are markedly increased in *Helicobacter pylori*-infected gastric mucosa among patients with specific IL18 genotypes. *J Infect Dis* (2008) 197:1752–61. doi: 10.1086/588196
64. Nascimento MS, Carregaro V, Lima-Junior DS, Costa DL, Ryffel B, Duthie MS, et al. Interleukin 17A Acts Synergistically With Interferon gamma to Promote Protection Against *Leishmania infantum* Infection. *J Infect Dis* (2015) 211:1015–26. doi: 10.1093/infdis/jiu531
65. Erdmann H, Rossnagel C, Bohme J, Iwakura Y, Jacobs T, Schaible UE, et al. IL-17A promotes macrophage effector mechanisms against *Trypanosoma cruzi* by trapping parasites in the endolysosomal compartment. *Immunobiology* (2013) 218:910–23. doi: 10.1016/j.imbio.2012.10.005
66. Pitta MG, Romano A, Cabantous S, Henri S, Hammad A, Kouriba B, et al. IL-17 and IL-22 are associated with protection against human kala azar caused by *Leishmania donovani*. *J Clin Invest* (2009) 119:2379–87. doi: 10.1172/JCI38813
67. Espinoza JL, Takami A, Nakata K, Onizuka M, Kawase T, Akiyama H, et al. A genetic variant in the IL-17 promoter is functionally associated with acute graft-versus host disease after unrelated bone marrow transplantation. *PloS One* (2011) 6:e26229. doi: 10.1371/journal.pone.0026229
68. Zingales B, Miles MA, Campbell DA, Tibayrenc M, Macedo AM, Teixeira MM, et al. The revised *Trypanosoma cruzi* subspecific nomenclature: rationale, epidemiological relevance and research applications. *Infect Genet Evol* (2012) 12:240–53. doi: 10.1016/j.meegid.2011.12.009
69. Luft T, Jefford M, Luetjens P, Hochrein H, Masterman KA, Maliszewski C, et al. IL-1 beta enhances CD40 ligand-mediated cytokine secretion by human dendritic cells (DC): a mechanism for T cell-independent DC activation. *J Immunol* (2002) 168(2):713–22. doi: 10.4049/jimmunol.168.2.713
70. Acosta-Rodriguez EV, Napolitani G, Lanzavecchia A, Sallusto F. Interleukins 1 beta and 6 but not transforming growth factor-beta are essential for the differentiation of interleukin 17-producing human T helper cells. *Nat Immunol* (2007) 8(9):942–9. doi: 10.1038/ni1496
71. Chandrasekar B, Melby PC, Troyer DA, Colston JT, Freeman GL. Temporal expression of pro-inflammatory cytokines and inducible nitric oxide synthase in experimental acute Chagasic cardiomyopathy. *Am J Pathol* (1998) 152 (4):925–34.
72. Petersen CA, Burleigh BA. Role for interleukin-1 beta in *Trypanosoma cruzi*-induced cardiomyocyte hypertrophy. *Infect Immun* (2003) 71:4441–7. doi: 10.1128/IAI.71.8.4441-4447.2003
73. Chandrasekar B, Mummidi S, Claycomb WC, Mestril R. Nemer M.Interleukin-18 is a pro-hypertrophic cytokine that acts through a phosphatidylinositol 3-kinase-phosphoinositide-dependent kinase-1-Akt-GATA4 signaling pathway in cardiomyocytes. *J Biol Chem* (2005) 280 (6):4553–67. doi: 10.1074/jbc.M411787200
74. Reddy VS, Harskamp RE, van Ginkel MW, Calhoon J, Baisden CE, Kim IS, et al. Interleukin-18 stimulates fibronectin expression in primary human cardiac fibroblasts via PI3K. *J Cell Physiol* (2008) 215(3):697–707. doi: 10.1002/jcp.21348
75. Eslick GD, Thampan BV, Nalos M, McLean AS, Sluyter R. Circulating interleukin-18 concentrations and a loss-of-function P2X7 polymorphism in heart failure. *Int J Cardiol* (2009) 137(1):81–3. doi: 10.1016/j.ijcard.2008.05.017
76. O'Brien LC, Mezzaroma E, Van Tassell BW, Marchetti C, Carbone S, Abbate A, et al. Interleukin-18 as a therapeutic target in acute myocardial infarction and heart failure. *Mol Med* (2014) 12:221–9. doi: 10.2119/molmed.2014.00034
77. Chien Y, Chien CS, Chiang HC, Huang WL, Chou SJ, Chang WC, et al. Interleukin-18 deteriorates Fabry cardiomyopathy and contributes to the development of left ventricular hypertrophy in Fabry patients with GLA IVS4 +919 G>A mutation. *Oncotarget* (2016) 7(52):87161–79. doi: 10.18632/oncotarget.13552
78. Okuhara Y, Yokoe S, Iwasaku T, Eguchi A, Nishimura K, Li W, et al. *Interleukin-18* gene deletion protects against sepsis-induced cardiac dysfunction by inhibiting PP2A activity. *Int J Cardiol* (2017) 243:396–403. doi: 10.1016/j.ijcard.2017.04.082
79. Fae KC, Drigo SA, Cunha-Neto E, Ianni B, Mady C, Kalil J, et al. HLA and β-myosin heavy chain do not influence susceptibility to Chagas' disease cardiomyopathy. *Microb Infect* (2000) 2:745–51. doi: 10.1016/s1286-4579(00)00501-3
80. Matos CS , dos Santos JE Jr., Medeiros FAC, Furtado E, Dias JCP. Current situation and perspectives regarding human Chagas disease in midwestern of the state of Minas Gerais, Brazil. *Mem Inst Osw Cruz* (2014) 109:374–8. doi: 10.1590/0074-0276130385. Rio de Janeiro.
81. Silva JS, Barral-Netto M, Reed SG. Aggravation of both *Trypanosoma cruzi* and murine leukemia virus by concomitant infections. *Amer J Trop Med Hyg* (1997) 49:589–97. doi: 10.4269/ajtmh.1993.49.589
82. Andreani G, Celentano AM, Solana ME, Cazorla S, Malchiodi EL, Martínez Peralta LA, et al. Inhibition of HIV-1 replication in human monocyte-derived macrophages by parasite. *Trypanosoma Cruzi PloS One* (2009) 4(12):e8246. doi: 10.1371/journal.pone.0008246
83. de Freitas VL, da Silva SC, Sartori AM, Bezerra RC, Westphalen EV, Molina TD, et al. Real-time PCR in HIV/*Trypanosoma cruzi* coinfection with and without Chagas disease reactivation: association with HIV viral load and CD4 level. *PloS Negl Trop Dis* (2011) 5(8):e1277. doi: 10.1371/journal.pntd.0001277
84. Rodrigues DBR, Correia D, Marra MD, Giraldo LER, Silva EL, Silva-Vergara ML, et al. Cytokine serum levels in patients infected by human immunodeficiency virus with and without *Trypanosoma cruzi* coinfection. *Rev Soc Bras Med Trop* (2005) 38:483–7. doi: 10.1590/s0037-86822005000600007
85. Barbaro G. Reviewing the cardiovascular complications of HIV infection after the introduction of highly active antiretroviral therapy. *Curr Drug Targets Cardiovasc Haematol Disord* (2005) 5:337–43. doi: 10.2174/1568006054553444
86. Balagopal A, Gupte N, Shivakoti R, Cox AL, Yang WT, Berendes S, et al. Continued Elevation of Interleukin-18 and Interferon-γ After Initiation of Antiretroviral Therapy and Clinical Failure in a Diverse Multicountry Human Immunodeficiency Virus Cohort. *Open Forum Infect Dis* (2016) 3(3):ofw118. doi: 10.1093/ofid/ofw118
87. Iannello A, Boulassel M-R, Suzanne Samarani S, Tremblay C, Toma E, Routy J-P, et al. HIV-1 Causes an Imbalance in the Production of Interleukin-18 and Its Natural Antagonist in HIV-Infected Individuals: Implications for Enhanced Viral Replication. *J Infect Dis* (2010) 201:608–17. doi: 10.1086/650314
88. Sangenito LS, d'Avila-Levy CM, Branquinha MH, Santos ALS. Nelfinavir and lopinavir impair *Trypanosoma cruzi* trypomastigote infection in mammalian host cells and show anti-amastigote activity. *Int J Antimicrob Agents* (2016) 48 (6):703–11. doi: 10.1016/j.ijantimicag.2016.09.017
89. Sangenito LS, Menna-Barreto RF D, Avila-Levy CM, Santos AL, Branquinha MH. Decoding the anti-*Trypanosoma cruzi* action of HIV peptidase inhibitors using epimastigotes as a model. *PloS One* (2014) 9(12):e113957. doi: 10.1371/journal.pone.0113957
90. Sangenito LS, Menna-Barreto RFS, Oliveira AC, d'Avila-Levy CM, Branquinha MH, Santos ALS. Primary evidence of the mechanisms of action of HIV aspartyl peptidase inhibitors on *Trypanosoma cruzi* trypomastigote forms. *Int J Antimicrob Agents* (2018) 52(2):185–94. doi: 10.1016/j.ijantimicag.2018.03.021

91. Castilho VVS, Gonçalves KCS, Rebello KM, Baptista LPR, Sangenito LS, Santos HLC, et al. Docking simulation between HIV peptidase inhibitors and *Trypanosoma cruzi* aspartyl peptidase. *BMC Res Notes* (2018) 11(1):825. doi: 10.1186/s13104-018-3927-z
92. Bellera CL, Balcazar DE, Vanrell MC, Casassa AF, Palestro PH, Gavernet L, et al. Computer-guided drug repurposing: identification of trypanocidal activity of clofazimine, benidipine and saquinavir. *Eur J Med Chem* (2015) 93:338–48. doi: 10.1016/j.ejmech.2015.01.065

Conflict of Interest: The authors declare that the research was conducted in the absence of any commercial or financial relationships that could be constructed as a potential conflict of interest.

The reviewers FD and CM-J declared a shared affiliation, with no collaboration, with the authors to the handling editor at the time of the review.

frontiers in Immunology

ORIGINAL RESEARCH
published: 06 November 2020
doi: 10.3389/fimmu.2020.575076

Structural Modeling and Molecular Dynamics of the Immune Checkpoint Molecule HLA-G

*Thais Arns[1], Dinler A. Antunes[2], Jayvee R. Abella[2], Maurício M. Rigo[2], Lydia E. Kavraki[2], Silvana Giuliatti[3] and Eduardo A. Donadi[1]**

[1] Department of Basic and Applied Immunology, Ribeirão Preto Medical School, University of São Paulo, Ribeirão Preto, Brazil, [2] Department of Computer Science, Rice University, Houston, TX, United States, [3] Department of Genetics, Ribeirão Preto Medical School, University of São Paulo, Ribeirão Preto, Brazil

HLA-G is considered to be an immune checkpoint molecule, a function that is closely linked to the structure and dynamics of the different HLA-G isoforms. Unfortunately, little is known about the structure and dynamics of these isoforms. For instance, there are only seven crystal structures of HLA-G molecules, being all related to a single isoform, and in some cases lacking important residues associated to the interaction with leukocyte receptors. In addition, they lack information on the dynamics of both membrane-bound HLA-G forms, and soluble forms. We took advantage of *in silico* strategies to disclose the dynamic behavior of selected HLA-G forms, including the membrane-bound HLA-G1 molecule, soluble HLA-G1 dimer, and HLA-G5 isoform. Both the membrane-bound HLA-G1 molecule and the soluble HLA-G1 dimer were quite stable. Residues involved in the interaction with ILT2 and ILT4 receptors (α3 domain) were very close to the lipid bilayer in the complete HLA-G1 molecule, which might limit accessibility. On the other hand, these residues can be completely exposed in the soluble HLA-G1 dimer, due to the free rotation of the disulfide bridge (Cys42/Cys42). In fact, we speculate that this free rotation of each protomer (i.e., the chains composing the dimer) could enable alternative binding modes for ILT2/ILT4 receptors, which in turn could be associated with greater affinity of the soluble HLA-G1 dimer. Structural analysis of the HLA-G5 isoform demonstrated higher stability for the complex containing the peptide and coupled β2-microglobulin, while structures lacking such domains were significantly unstable. This study reports for the first time structural conformations for the HLA-G5 isoform and the dynamic behavior of HLA-G1 molecules under simulated biological conditions. All modeled structures were made available through GitHub (https://github.com/KavrakiLab/), enabling their use as templates for modeling other alleles and isoforms, as well as for other computational analyses to investigate key molecular interactions.

Keywords: HLA-G, HLA-G1 soluble dimer, HLA-G5 isoform, molecular dynamics, structural bioinformatics

OPEN ACCESS

Edited by:
Ursula Grohmann, University of Perugia, Italy

Reviewed by:
Aifen Lin, Zhejiang Taizhou Hospital, China
Kenneth Beaman, Rosalind Franklin University of Medicine and Science, United States

****Correspondence:***
Eduardo A. Donadi
eadonadi@usp.br

Specialty section:
This article was submitted to Microbial Immunology, a section of the journal Frontiers in Immunology

Received: *22 June 2020*
Accepted: *13 October 2020*
Published: *06 November 2020*

Citation:
Arns T, Antunes DA, Abella JR, Rigo MM, Kavraki LE, Giuliatti S and Donadi EA (2020) Structural Modeling and Molecular Dynamics of the Immune Checkpoint Molecule HLA-G. Front. Immunol. 11:575076. doi: 10.3389/fimmu.2020.575076

INTRODUCTION

The Human Leukocyte Antigen G (HLA-G) is a nonclassical Major Histocompatibility Complex class I (MHC-I) molecule that possesses immunomodulatory properties (1). Its presence is tissue-restricted, being expressed in fetal tissues [trophoblast cells (2)] and constitutively expressed in adult thymic medulla (3), cornea (4), pancreatic islets (5), erythroid, and endothelial cell precursors (6). However, the expression of HLA-G can be induced in several conditions (1), including cancer (7, 8), transplantation (9), viral infections (10, 11), and autoimmune and inflammatory diseases (12, 13).

A well-recognized function of the HLA-G molecule in these pathological and physiological conditions is the inhibition of the cytotoxic activity of Natural Killer (NK) and $CD8^+$ T lymphocytes. This function is mediated by interaction with leukocyte receptors, particularly with the Leukocyte Ig-like Receptors (LILRs), also known as Immunoglobulin-like Transcripts (ILT2, ILT4). ILT2 and ILT4 interact with several classical class I HLA molecules, but have higher affinity for HLA-G (14). ILT2 is expressed by B cells, some subtypes of T cells and NK cells, and all monocytes/dendritic cells (15). It is also described as a receptor for HLA-G associated with β2-microglobulin. On the other hand, ILT4 is myeloid-specific and only expressed by monocytes/dendritic cells (16), being capable of recognizing HLA-G free heavy chains (17, 18). Through these differentially expressed receptors, HLA-G can interact with all these different cell types, primarily inhibiting their functions. In addition, HLA-G may also generate regulatory/suppressor cells. For instance, human tolerogenic dendritic cells (DC-10) express high levels of membrane-bound HLA-G1 and are potent inducers of adaptive allospecific Type 1 regulatory T (Tr1) cells (19). The *HLA-G* gene is located within the MHC region, presenting low polymorphism, in contrast with the highly polymorphic classical class I genes, i.e., *HLA-A*, *-B*, *-C* (20). Geragthy et al. (21) first described the *HLA-G* gene in 1987, and its structure is homologous to other HLA class I genes. The *HLA-G* primary transcript may generate at least seven alternative splicing mRNAs that encode membrane-bound (HLA-G1, G2, G3, G4) and soluble (HLA-G5, G6, G7) protein isoforms (22–25). HLA-G1 may also be detected in plasma after proteolytic cleavage by metalloproteases, and presents the same domains (α1, α2, and α3) of classical class I molecules, being also associated with a β2-microglobulin. HLA-G2 is devoid of the α2 domain encoded by exon 3. HLA-G3 does not have the α2 and α3 domains encoded by exons 3 and 4, and HLA-G4 lost the α3 domain. The soluble HLA-G5 and HLA-G6 isoforms have the same extra globular domains as HLA-G1 and HLA-G2, respectively, and are generated by transcripts retaining intron 4, which block translation of the transmembrane domain (exon 5). The 5' region of the intron, in the reading phase with exon 4, is translated into a stop codon and generates the HLA-G5 and HLA-G6 isoforms. These isoforms contain a specific 21 residues long tail involved in molecule solubility. The soluble HLA-G7 isoform is limited to the α1 domain and retains two intron 2 specific amino acids. All alternative transcripts are devoid of exon 7 (26, 27).

Sequence comparison of the HLA-G molecule to other HLA class I proteins reveals some interesting particularities. First, HLA-G has an unusually long half-life on the cell surface, resulting from the absence of an endocytosis motif in its truncated cytoplasmic domain (28). Second, HLA-G sequences have two unique Cysteine residues located at positions 42 and 147. Dimerization of HLA-G occurs through the creation of disulfide bonds between the two unique Cysteine residues at position 42 (Cys42-Cys42 bonds). Since all isoforms carry Cys42, all translated isoforms could potentially form membrane-bound homodimers, soluble homodimers, β2-microglobulin-free homodimers, and possibly homotrimers (associated or not to β2-microglobulin) (29, 30). Noteworthy, HLA-G dimers: *i)* do not induce significant structural changes to the main backbone of the protomers (i.e., chains forming the dimer) (17); *ii)* may exhibit distinct inhibitory functions as compared to monomers [e.g., dimers bind to ILT receptors with higher affinity *in vitro* (29) and *in vivo* (31)]; and *iii)* exhibit slower dissociation rates than monomers (17). ILT recognition of HLA-G dimers has a pivotal role on immune suppression at the maternal-fetal interface, possibly contributing to the prevention of pregnancy complications such as pre-eclampsia and recurrent miscarriages (17, 20).

Since HLA-G5 isoform has the same extra globular domains as HLA-G1, it could potentially be recognized by the same receptors. In fact, it has been reported that ILT2 can interact with β2-microglobulin-associated HLA-G5, while ILT4 could be able to recognize isoforms that are not associated to β2-microglobulin (17, 32). Such β2-microglobulin-free heavy chain has been detected in cell culture supernatants expressing HLA-G5 (33). It has also been shown that the expression of soluble HLA-G5 could inhibit the cytotoxicity of NK cells, and that the degree of inhibition was more evident when induced by HLA-G5, as compared to the membrane-bound HLA-G1. Most importantly, it was shown that the combination of HLA-G1 and HLA-G5 leads to significantly greater suppression than the effects of HLA-G1 or HLA-G5 alone (34). The direct involvement of HLA-G5 in inducing graft acceptance *in vivo* after human transplantation was provided by the observation that HLA-G5 purified from the plasma of transplanted HLA-G-positive patients suppressed alloproliferation of T cells *in vitro* (35).

Considering all the aforementioned structural diversity of known HLA-G isoforms, and the multiple roles of HLA-G in different immunological pathways, it is astonishing how little is known about the structure and dynamics of these molecules. As of today, there are only seven crystal structures of HLA-G receptors in the Protein Data Bank (PDB) (36). Note that these structures are limited to HLA-G1, and that even for this particular isoform they do not capture the full molecule (see **Supplementary Table 1**). In addition, there is only so much that can be understood from a static crystal structure in which relates to the dynamic behavior of these molecules. For instance, previous analysis of the membrane-bound HLA-G1 has

indicated an oblique orientation of the protomers. Such orientation makes the ILT2 and ILT4 binding sites slightly more accessible to the interaction with these receptors (17). However, it does not tell us if this oblique orientation is stable in the soluble HLA-G1 dimer, or if other arrangements are possible. Finally, available structural data cannot inform us about the structure and dynamics of all other HLA-G alleles and isoforms.

As a step forward in addressing all these open questions, the present work reports for the first time the complete structure and dynamic behavior of the membrane-bound HLA-G1 model. In addition, it also characterizes the dynamics of the soluble HLA-G1 dimer. These efforts allowed for the first time the observation of a tilting movement of the membrane-bound HLA-G1 monomer, and the total rotational freedom of the HLA-G1 dimer in solution (**Figure 1**). Finally, it investigates the stability of three different proposed structures for the soluble HLA-G5 isoform.

MATERIAL AND METHODS

Molecular Modeling

To obtain the complete HLA-G1 model for the molecule encoded by the *HLA-G**01:01 allele group, homology modeling was performed using Modeller 9.15 software (37) and the PDB_ID: 1YDP structure as a template (38). The selected template structure was obtained by X-ray diffraction crystallography with a 1.9 Å resolution (38), is encoded by the *HLA-G**01:04 allele group, and exhibits 275 resolved residues. It includes the nonapeptide RIIPRHLQL in the binding cleft, and the coupled β2-microglobulin chain. The Rosetta cyclic coordinate descent algorithm (CCD) *ab initio* modeling (39) was applied to unresolved extracellular and intracellular regions in the crystallographic template. Two thousand models were generated in each *ab initio* modeling step. For the transmembrane portion, the GPCR-ITASSER online server was used (40). The complete membrane-bound HLA-G1 model was then applied as template for three possible HLA-G5 isoform structures: monomer, monomer containing the nonapeptide in the cleft, and monomer containing the nonapeptide in the cleft coupled to β2-microglobulin. Isoform residues not included in the membrane-bound HLA-G1 model were resolved using the Rosetta CCD *ab initio* modeling. The existing structural gaps in the HLA-G1 soluble dimer template (PDB_ID: 2D31) were completed by homology modeling using PDB_ID: 1YDP structure as template. All models were evaluated using several validation software, including QMEAN (41), MODFOLD (42), Verify 3D (43, 44), ERRAT (45), and PROCHECK (46). Images and structure visualization were performed using PyMOL software (47). The BioPython package (48) was applied to identify the interacting residues. The Cα Root Mean Square Deviation (RMSD) and Root Mean Square Fluctuations (RMSF) values were calculated using the initial structures as reference. All structures and simulation movies are available in the **Supplementary Material** and at GitHub (https://github.com/KavrakiLab/).

Lipid Bilayer Insertion

The complete HLA-G1 model was inserted into a phospholipid bilayer (DLPA, *1,2-Dilauroyl-sn-glycero-3-phosphate*). This step was performed with the CHARMM-GUI online server (49, 50).

Molecular Dynamics (MD) Simulations

Three simulations of 100 ns were performed for the complete HLA-G1 inserted into the lipid bilayer, using GROMACS v5.1.4 (51) and CHARMM36m force field (52). MD simulations were also performed in triplicate using GROMACS v4.6.5 package and the G54a7 force field, for a total of 600 ns for the soluble HLA-G1 dimer and a total of 2.1 μs for the HLA-G5 isoform. A cubic box was defined with at least 9 Å of liquid layer around the protein (exact dimensions were different for each protein), using single-point charge water model and periodic boundary conditions. An appropriate number of sodium (Na^+) and chloride (Cl^-) counter-ions were added to neutralize the system at the final concentration of 0.15 mol/L. Besides the complete membrane-bound HLA-G1, the dynamic system contained 32,560 DLPA molecules, 184,197 water molecules and 380 counter-ions. As for the soluble dimer, it contained 383,325 water molecules and 470 counter-ions. The HLA-G5 monomer dynamic system contained 90,375 water molecules and 187 counter-ions; the monomer containing the nonapeptide in the cleft system had 90,135 water molecules and 185 counter-ions; and the monomer containing the nonapeptide in the cleft coupled to β2-microglobulin had 83,676 water molecules and 179 counter-ions. The algorithms *v*-

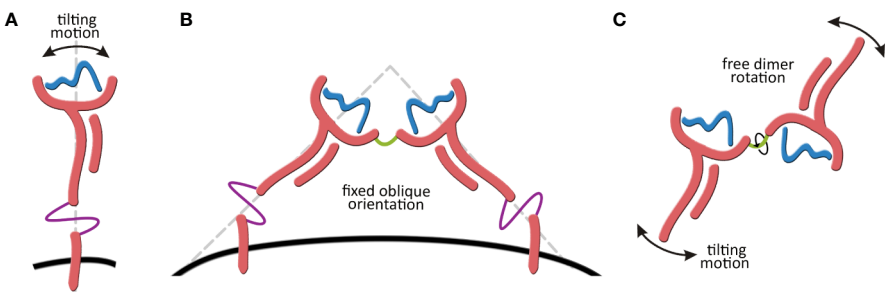

FIGURE 1 | **(A)** Tilting motion of the membrane-bound HLA-G1structure. **(B)** Membrane-bound HLA-G1 dimer representation, showing the oblique orientation (~45° angle) observed by X-ray crystallography. **(C)** Representation of the complete rotational freedom of the soluble HLA-G1 dimer in solution.

rescale (τt = 0.1 ps) and *parrinello-rhaman* (τp = 2 ps) were used for temperature and pressure coupling, respectively. Cutoff values of 1.2 nm were used for both van der Waals and Coulomb interactions, with Fast Particle-Mesh Ewald (PME) electrostatics. For all MD simulations, the production stage was preceded by: *i)* three steps of Energy Minimization (alternating steepest-descent and conjugate gradient algorithms), and *ii)* eight steps of Equilibration as previously described (53). Briefly, the Equilibration stage started with position restraints for all heavy atoms (5,000 $kJ^{-1}mol^{-1}nm^{-1}$) and a temperature of 310 K, for a period of 300 ps, to allow for the formation of solvation layers. The temperature was then reduced to 280 K and the position restraints were gradually reduced. This process was followed by a gradual increase in temperature (up to 300 K). Together, these Equilibration steps represented the first 500 ps of each simulation. During the production stage, the system was held at constant temperature (310 K) without restraints.

Dimensionality Reduction Analysis

Principal component analysis (PCA) was performed using the Python libraries MDTraj (54) and PyEmma (55). PCA is a dimensionality reduction method used to analyze the sampling done by the MDs. PCA maximizes the variance of the transformed coordinates, which is ideal for finding conformations that are geometrically diverse. The residue-residue distances (defined as the distance between the nearest two heavy atoms) between one copy of the dimer and the other were extracted. Only every tenth residue in the system was considered to save memory, resulting in 1,444 features for the dimensionality reduction analysis.

Peptide-Bound Ensemble Modeling and Stability Analysis

A structure-based stability analysis was performed to compare two different HLA-G binders, RIIPRHLQL and RLPKDFRIL. The aforementioned complete model of HLA-G1 (HLA-G*01:01), after removed the bound peptide structure, was used as input to the Anchored Peptide-MHC Ensemble Generator (APE-Gen) (56). Generated ensembles of peptide conformations were later minimized with OpenMM (57), and the lowest energy conformation for each peptide was selected using the Vinardo scoring function (58). All these steps were performed using a customized workflow from the HLA-Arena modeling environment (59). Finally, selected conformations (i.e., lowest energy) were used as input for a structure-based random forest classifier trained on a large dataset of immunopeptidomics experiments (60). This analysis predicted the stability of both complexes, and the individual contribution of each peptide residue toward peptide-MHC complex stability.

Protein-Protein Docking With ILT4

A protein-protein docking study was conducted with the ClusPro webserver (61). A crystal structure of ILT4 was obtained from PDB (PDB_ID: 6AED), and gaps (residues 134 to 143) were filled with loop refinement algorithm from Modeller 9.15 software (37) using UCSF Chimera software (62). This structure was used for protein-protein docking against *(i)* HLA-G monomer and *(ii)* HLA-G dimer structures. The best output structure was chosen considering the frequency of members inside each cluster and the Lowest Energy score.

RESULTS

Membrane-Bound HLA-G1 Molecule Displays Tilting Motion in Solution

A complete model of the mature protein encoded by the *HLA-G*01:01* allele group was generated, containing all 314 residues (**Figure 2A**). The complete modeled system included the HLA-G molecule, sodium (Na^+) and chloride (Cl^-) counter-ions, and a phospholipid bilayer (**Figure 2B**). During the MD simulations, the average cleft width was 23.2 Å, ranging from 19.4 Å to 25.6 Å (measured at each 10 ns), and the peptide cleft depth was 15.8 Å (**Figure 2A**). The RIIPRHLQL peptide remained stable during the simulations, as observed by the low Root Mean Square Fluctuation (RMSF) (data not shown). The RMSD values for the MD simulations did not exceed 11.46 Å for any of the replicated trajectories, oscillating in the range from 4 Å to 10 Å (**Supplementary Figure 1**). Note that the observed RMSD variation does not reflect unfolding or large conformational changes in the protein, but it relates to oscillations on the angle of the transmembrane region and its impact on the orientation of the extracellular domain (**Figure 2C**). In fact, the RMSD value calculated between the initial and final conformations of the protein is of only 3.13 Å. This conformational stability can also be observed by the PCA analysis, which demonstrates great overlap of sampled conformations among all three simulations. Taken together, these results point to the stability and compactness of the complete membrane-bound HLA-G1 model generated (**Figure 2D**). The transmembrane region extended for 32.7 Å and, alongside the cytoplasmic tail, presented an all direction swinging movement, spanning 22.5 Å.

ILT2 and ILT4 Interacting Residues Are Not Fully Accessible in the Membrane-Bound HLA-G1 Molecule

According to previous studies, ILT2 binds to HLA-G residue F195, while ILT4 binds to F195 and Y197 (17, 38). All these residues are located at the end of the α3 domain, and our model shows that these binding sites are very close to the lipid bilayer (**Figure 3**). Limited access to these residues could explain the lower overall affinity of the HLA-G1 monomer to ILT2/ILT4, when compared to the soluble dimer, as previously demonstrated by *Shiroishi* and collaborators (17). Locations of other potential binding sites are also depicted. CD8α/α contacts the α3 domain of HLA-G1 at residues 223 to 229 (63, 64). Q79 and M76 are candidate interacting residues for KIR2DL4 (26, 65, 66).

Soluble HLA-G1 Dimer Displays Full Rotational Freedom of Protomers

Three simulations of 200 ns were performed for the soluble HLA-G1 dimer, starting from the oblique orientation (~45° angle) observed by X-ray crystallography (**Figure 4A**) for the disulfide-linked HLA-G1 dimer. The RMSD values for the MD simulations

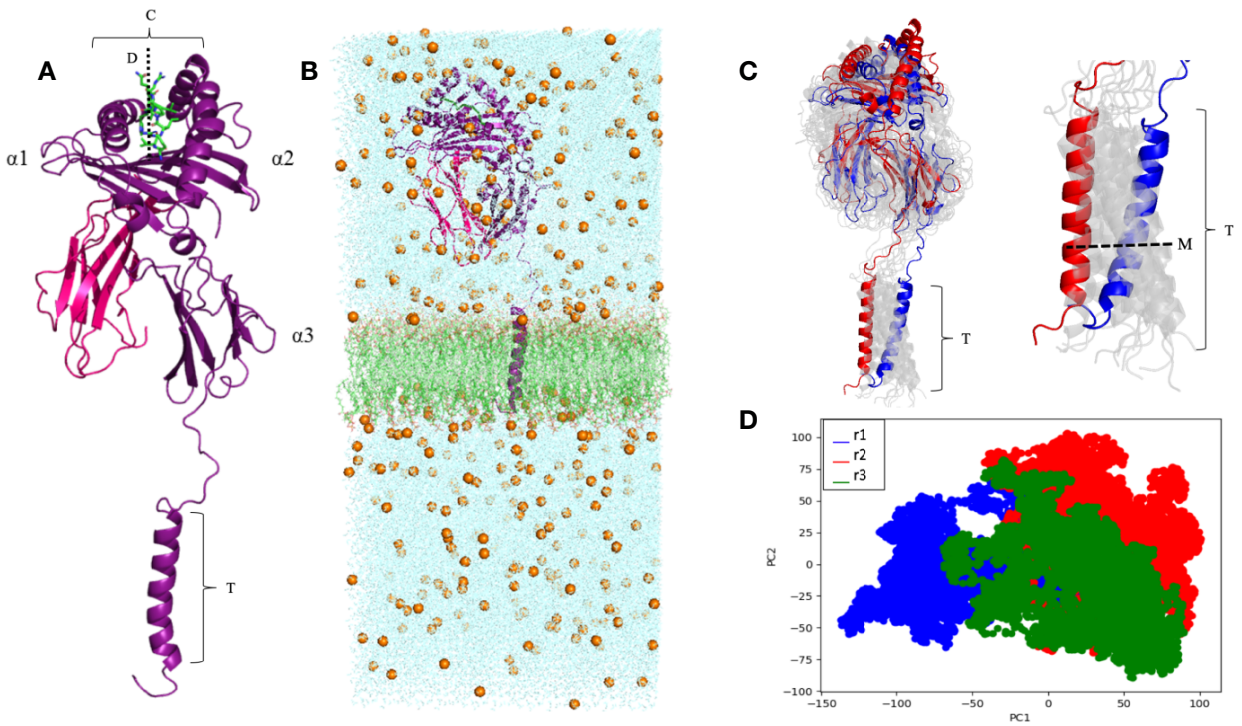

FIGURE 2 | **(A)** Complete membrane-bound HLA-G1 protein encompassing the α1, α2, α3, transmembrane (T), and intracytoplasmic (I) domains (purple), coupled with β2-microglobulin (pink) and the RIIPRHLQL peptide (green). W (average cleft width) = 23.2 Å, and D (cleft depth) = 15.8 Å; T = 32.7 Å. **(B)** Complete membrane-bound HLA-G1 molecular dynamics simulation system, including: *i)* water molecules seen in the blue background, *ii)* Na^+ and Cl^- ions (golden spheres), and *iii)* phospholipid bilayer (green). **(C)** Initial (blue) and final (red) conformations of the 100 ns complete membrane-bound HLA-G1 dynamics (left) and for the transmembrane portion (right). Intermediate conformations obtained at 10ns intervals are displayed in light gray, showing the molecular movement inside the lipid bilayer. M, transmembrane swinging movement over 100 ns. **(D)** Principal component analysis (PCA) depicting the distribution of conformations extracted from three independent MD trajectories (r1, r2, and r3).

oscillated between 9 Å and 25 Å, depending on the simulation (**Supplementary Figure 2**). Once again, these high RMSD values do not reflect conformational changes of the protomers (**Figures 4B, C**). Instead, they reflect the great conformational freedom of the protomers during the MD simulation, as enabled by the rotation of the disulfide bond (**Figure 4C**). Although the dimer as a whole is very flexible, the folding of the protomers is very stable, and the RIIPRHLQL peptide remained stably bound in the cleft; data consistent with the low Root Mean Square Fluctuation (RMSF) obtained (**Supplementary Figure 3**).

Interestingly, the PCA analysis revealed that each soluble dimer simulation described a different trajectory, exploring different regions of the conformational space (**Figure 4D**). In our PCA analysis, PC1 is most correlated with the distance between LEU81 in one copy and ILE214 in the other copy (**Figure 5A**), while PC2 is most correlated with the distance between GLN141 in one copy and SER91 in the other copy (**Figure 5B**).

HLA-G5 Is More Stable When Associated With β2-Microglobulin and a Peptide Ligand

In this work, we evaluated three HLA-G5 structural possibilities: (*i*) monomer (**Figure 6A**), (*ii*) monomer containing the nonapeptide in the cleft (**Figure 6B**), and (*iii*) monomer containing the nonapeptide in the cleft coupled to β2-microglobulin (**Figure 6C**). Considering Cα residue fluctuation of all the HLA-G5 structural possibilities, the most stable structure was the monomer containing the nonapeptide in the cleft coupled to β2-microglobulin, which suffered minimal structural deformations during the MD simulation (**Figure 6D**). As seen in (**Supplementary Material**—HLA-G5 Monomer, nonapeptide, and coupled β2-microglobulin Simulation Video; **Supplementary Figure 4**), the stability is mainly due to the interaction of the tail from intron 4 and the coupled β2-microglobulin, which prevents the tail from reaching up and destabilizing the peptide cleft. In fact, this disruptive behavior was observed in the absence of β2-microglobulin, leading to complete dissociation of the nonapeptide from the HLA-G5 cleft (**Figure 6D** and **Supplementary Material**—HLA-G5 Monomer and nonapeptide Simulation Video). Specifically, the interaction with the tail from intron 4 (last 21 residues) resulted in an increase of the cleft's width, causing the peptide's anchor residues to lose important interactions with residues in the cleft's β-sheet floor and surrounding α-helices (**Supplementary Figure 4**). At the beginning of the simulation

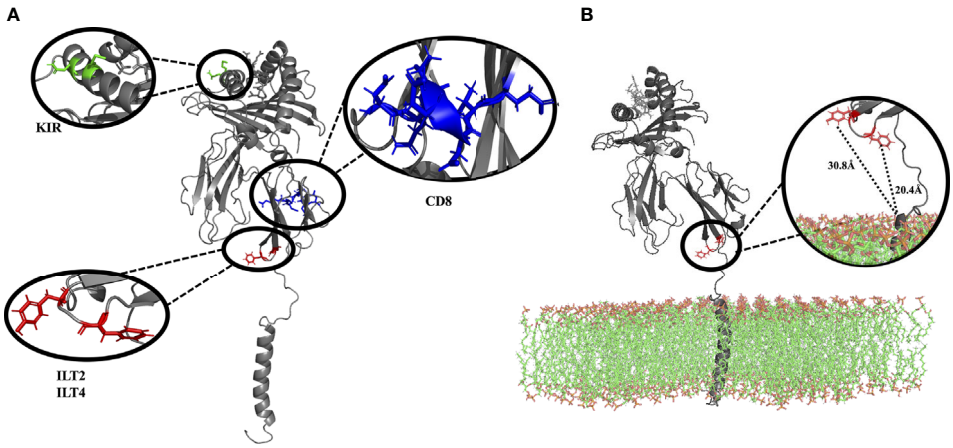

FIGURE 3 | **(A)** Complete membrane-bound HLA-G1 protein (without lipid bilayer), indicating the interacting residues for CD8 receptor (blue: residues D223, Q224, T225, Q226, D 227, V228, E229), ILT2 receptor (red: residues F195), and ILT4 receptor (red: residues F195, Y197). Residues suggested to interact with KIR2DL are also depicted (green: residues Q79, M76) **(B)** Complete membrane bound HLA-G1 protein (including the lipid bilayer), emphasizing the localization and distance of the ILT2 (red: residues F195, 20.4 Å to the membrane) and ILT4 receptors (red: residues F195, Y197, 30.8 Å to the membrane), both of which are close to the lipid bilayer. (D, Aspartic acid; E, Glutamic acid; F, Phenylalanine; M, Methionine; Q, Glutamine; T, Threonine; and V, Valine).

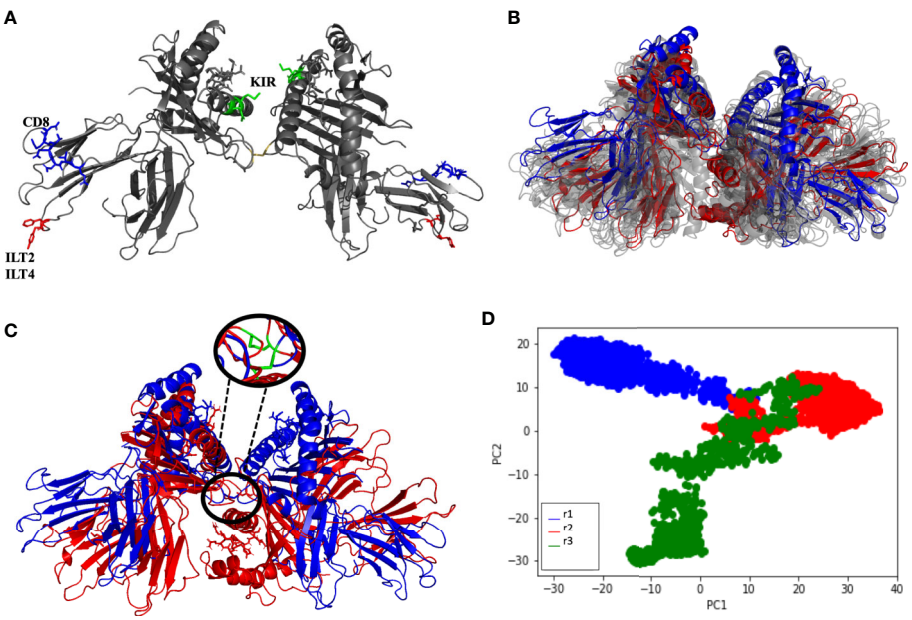

FIGURE 4 | **(A)** Soluble HLA-G1 protein indicating the interacting for CD8 receptor (blue: residues D223, Q224, T225, Q226, D 227, V228, E229), ILT2 receptor (red: residue F195) and ILT4 receptor (red: residues F195, Y197). Residues suggested to interact with KIR2DL are also depicted (green: residues Q79, M76) **(B)** Initial (blue) and final (red) conformations of the 200 ns soluble HLA-G1 dimer dynamics. Twenty-nanosecond intervals (light gray) showing the significant dimer rotation. **(C)** Initial (blue) and final (red) conformations of the 200-ns soluble HLA-G1 dimer dynamics, depicting the zoomed area showing the disulfide bridge. **(D)** Principal component analysis (PCA) depicting the distribution of conformations extracted from three independent MD trajectories (r1, r2, and r3).

the cleft width measured 15.6 Å (**Figure 7A**), increasing its size up to 17.4 Å around 200 ns of the simulation, when the peptide escapes the cleft (**Figure 7B**). The cleft width reduces to about 14.6 Å after the unbinding of the peptide (**Figure 7C**). The superimposed images reveal the variation in cleft's width during the simulated time (**Figure 7D**).

Some structural instability was also observed for the soluble HLA-G5 monomer alone (**Figure 6D**). Both monomer and

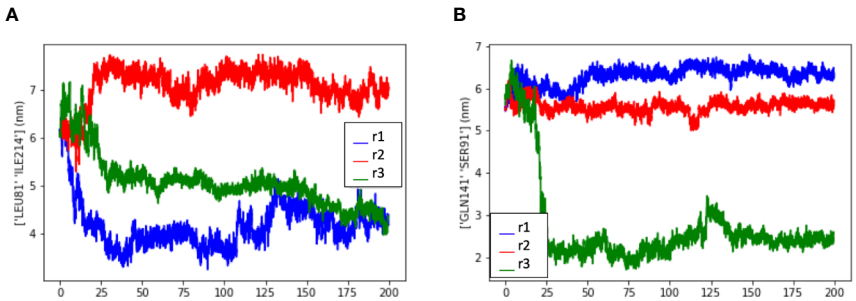

FIGURE 5 | Measurement of the distance between residues to evaluate the dimer flexibility at the disulfide bridge. Measurement data extracted from three dimer simulations (r1, r2, and r3) showed that the residues exhibited similar spatial behavior in all simulations, depending on the residue-residue distance that is observed. **(A)** Measurement data from LEU81 and SER91, **(B)** Measurement data from LEU81 and ILE214. (LEU, Leucine; ILE, Isoleucine; GLN, Glutamine; SER, Serine).

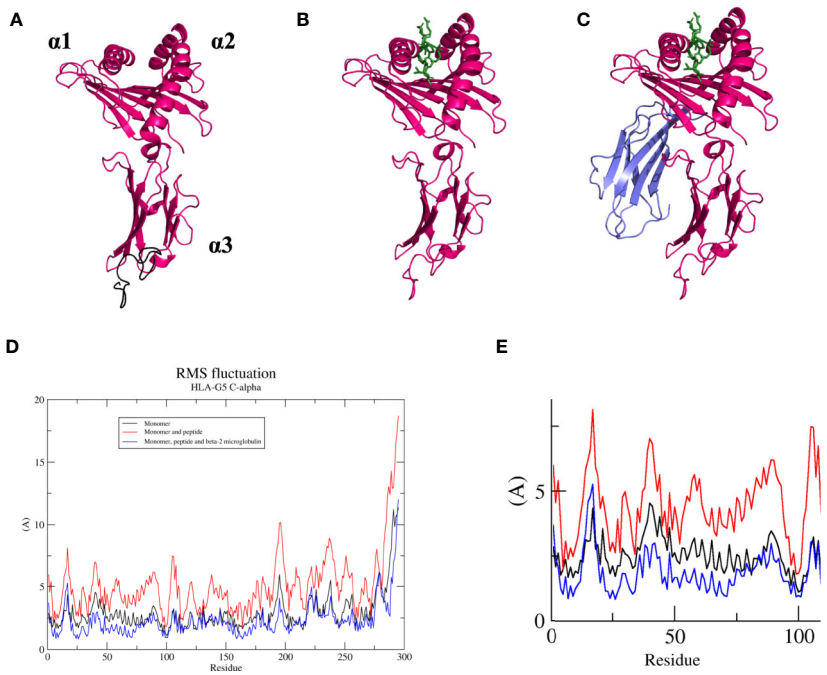

FIGURE 6 | **(A)** Soluble HLA-G5 isoform (pink) and 21 amino acid tail from intron 4 (black, but represented in the following figures in pink). Domain location (α1, α2, and α3) shown. **(B)** Soluble HLA-G5 isoform (pink) and nonapeptide RIIPRHLQL (green). **(C)** Soluble HLA-G5 isoform (pink), nonapeptide RIIPRHLQL (green) and β2-microglobulin (lavender). **(D)** RMSF of all three HLA-G5 structural possibilities: monomer (black), monomer containing the nonapeptide in the cleft (red), and monomer containing the nonapeptide in the cleft coupled to β2-microglobulin (blue). **(E)** Zoomed α-1 domain residues (residue number 1–100), taken from RMSF plot **(D)**, showing HLA-G5 monomer (black), monomer containing the nonapeptide in the cleft (red), and monomer containing the nonapeptide in the cleft coupled to β2-microglobulin (blue).

monomer containing the nonapeptide in the cleft showed much higher RMSF values for the α1-domain region, which constitutes residues 1 to 100. Such residues were extremely important in order to keep the peptide cleft folded, and suffered the majority of the destabilizing interactions induced by the movement of the portion relative to the tail from intron 4 (**Figure 6E** and **Supplementary Material**—HLA-G5 Monomer Simulation Video, **Supplementary Material**—HLA-G5 Monomer and nonapeptide Simulation Video).

Produced Models Can Be Used for Additional Structural Analysis

All produced 3D models were made available through GitHub (github.com/KavrakiLab/hla-g-models) and can now be used as input for additional structural analysis. To demonstrate this point, we conducted a *(i)* peptide-docking analysis comparing two different HLA-G peptide-binders, and a *(ii)* protein-protein docking analysis of binding modes for ILT4.

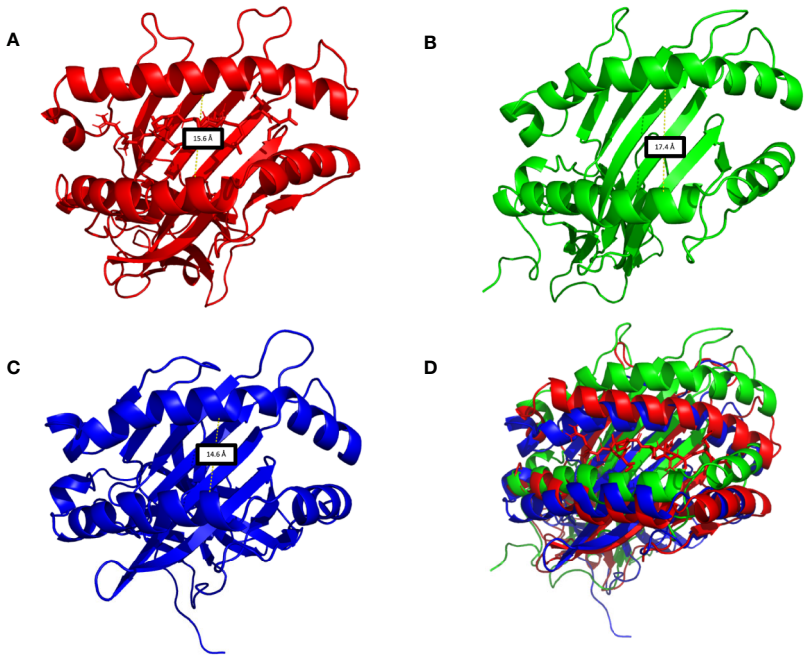

FIGURE 7 | **(A)** HLA-G5 cleft in the absence of the β2-microglobulin, demonstrating the nonapeptide RIIPRHLQL in the initial moments of the simulations. **(B)** Around 200 ns of simulation, due to structural instability, the cleft widens and the nonapeptide RIIPRHLQL loses all interactions with the surrounding structures, escaping the cleft. **(C)** As there is no peptide left in the cleft, its width is diminished. **(D)** Superimposition of **Figures 6A–C**.

Our structural analysis of the peptide-ligands indicated a similar overall contribution to complex stability. A structure-based machine learning method predicted a ~70% probability of stable binding for both peptides (**Supplementary Figure 5**). Moreover, the decomposition of the individual contributions of peptide residues indicated the dominant role of the conserved Leucine in p9 toward complex stability in both systems. As expected, there were differences in secondary interactions with other peptide's residues, with a slight advantage toward RLPKDFRIL. Therefore, our analysis suggests that RLPKDFRIL would provide similar or slightly better stability to the tested HLA-G systems. This prediction is in agreement with recent experimental data showing no significant differences between these peptides regarding the binding of HLA-G1 to ILT2/ILT4 (67).

Our protein-protein docking analysis further corroborated the findings that better interaction with ILT4 is possible when using conformations of the soluble HLA-G1 dimer, as compared to the the membrane-bound HLA-G1 monomer. The putative ILT4-binding site is formed by a relatively hydrophobic patch formed by F195/Y197 residues. This is conserved in HLA-G molecules, but not in other classical HLAs (30). Indeed, our best HLA-G1 dimer/ILT4 interaction models are represented by hydrophobic-favored interactions involving these two HLA residues. Moreover, the ILT4 domains involved in this interaction were domains 1 and 2, which is in accordance to previous binding experiments (30) (**Supplementary Figure 6**). The best interaction model between the monomer of HLA-G and ILT4 was favored by electrostatic interactions and it is depicted in **Supplementary Figure 6A**. Note that the best results indicated a binding mode in which ILT4 approaches HLA-G1 from the "bottom" (**Supplementary Figure 6C**). This binding mode is different from that previously described by Wang et al. (67), and might only be possible for the soluble forms of HLA-G.

DISCUSSION

HLA-G plays an important role on the suppression of immune responses, and both membrane-bound and soluble isoforms may exert this function. As of September 2020, the IMGT-HLA database includes 80 *HLA-G* alleles, encoding 21 complete and 4 truncated proteins (*HLA-G*1*01:05N, G*01:13N, G*01:21N and G*01:25N) (68, 69). All alleles encoding the complete protein have the potential to *i)* form dimers through the conserved Cysteine at position 42, *ii)* form the seven commonly described HLA-G isoforms (HLA-G1 to HLA-G7), and *iii)* interact with the leukocyte receptors (26). This remarkable structural diversity must be studied in detail in order to clarify the diverse roles played by HLA-G molecules in both physiological and pathological conditions. Unfortunately, many questions remain unanswered about the structure, dynamics, expression and interaction patterns of different HLA-G alleles and isoforms. For instance, previous experimental studies have provided structures for the membrane-bound HLA-G1, and HLA-G1 dimer, either alone or interacting with other receptors. However, even in these cases

the structures were incomplete. In addition, there was no available information on the dynamics of membrane-bound and soluble isoforms. Our goal was to conduct accurate structural modeling and molecular dynamics analysis of *i)* the complete membrane bound HLA-G1, *ii)* the soluble HLA-G1 dimer, and the soluble HLA-G5 monomer. This work moves the field forward, providing both insights on the dynamics of these complexes and complete 3D models that can now be used by other groups for further analysis.

Our complete model of HLA-G1 encompasses the heavy-chain (α1, α2, and α3 domains), connecting peptide, transmembrane portion and cytoplasmic tail of the most frequently observed *HLA-G**01:01 molecule. The *HLA-G**01:01 allele group encompasses 25 synonymous substitutions, as reported for the *HLA-G**01:01:01:01 to *HLA-G**01:01:25 alleles (68, 69). The associated light-chain (β2-microglobulin) was also included in our complete model. Finally, the RIIPRHLQL peptide, derived from histone H2A, was selected to be used in this study since (*i)* it is known to confer stability to the HLA-G molecule (64), (*ii)* is one of the most abundant peptides displayed by HLA-G (70), and (*iii)* was present in the cell cultures used for previous HLA-G X-ray diffraction studies (70). Note that an additional structural analysis comparing the binding of RIIPRHLQL with another HLA-G-binder, RLPKDFRIL, suggested that both peptides should provide similar level of stability to HLA-G complexes.

As expected, the MD simulations (**Figure 2B**) showed a stable membrane-bound HLA-G1 molecule, without evidence of unfolding of secondary structures (i.e., α-helices and β-sheets) (**Figure 2D**). In addition, both the β2-microglobulin and the coupled peptide ligand remained stably-bound during all simulations. Interestingly, we observed for the first time the natural "tilting" movement of the membrane-bound HLA-G1 in solution (**Supplementary Figure 1**). This motion, in addition to the lateral swinging movement of the transmembrane portion in the lipid bilayer (spanning 22.5 Å), is reflected on the observed RMSD values. However, the PCA analysis shows great agreement between simulations in terms of sampled conformations. The superposition of frames from the beginning and end of the simulation (**Figure 2D**) also shows that all secondary and tertiary structures were preserved during MD. These results confirms the stability and compactness of the complete membrane-bound HLA-G1 model generated (**Figure 2C**), which could now be used for additional structural analyses.

We also report for the first time the complete model of the soluble HLA-G1 dimer (**Figure 4A**), and the great conformational flexibility of this molecule in solution (**Figure 4B**). While the disulfide-linked dimer is locked into a 45° angle between the protomers (**Figure 1**), our simulations demonstrate that the soluble dimer is able to explore the full rotational flexibility enabled by the disulfide bridge (**Figure 4C**). Note that the secondary and tertiary structures of each protomer were very stable in solution (**Figure 4D**), despite overall dimer flexibility. The peptide-ligands also remained stably-bound to the respective clefts (**Figures 4A, B**). The PCA analysis of the three independent simulations of the soluble HLA-G1 dimer (**Figure 4B**) demonstrated that every dimer explored a different region of the conformational space, while still presenting similar collective motions, as demonstrated by the residue-residue distance comparisons (**Figures 5A, B**). A direct comparison between the PCAs for the membrane-bound HLA-G1 monomer and soluble HLA-G1 dimer is not possible, since the principal components used in each case reflect features that better capture the movements observed in each system. However, it is possible to observe that the soluble HLA-G1 dimer PCA captures a much greater conformational freedom.

Our HLA-G1 dimer model includes residues located at positions 195, 196, 197, 266, and 267, which were missing in the available crystal structure of the disulfide-linked dimer (17). All these residues are located in the α3 domain, where major leukocyte receptor binding sites are located. For instance, they include the putative binding sites for ILTs (residues 195 and 197) and CD8 (residues 223-229 residues). Note that these sites are very close to membrane in the membrane-bound HLA-G1 monomer (**Figure 3B**), which might limit interaction with these protein-ligands. It has indeed been observed that HLA-G1 dimers display higher affinity for leukocyte receptors than monomers (17, 20). This advantage has been associated with the 45° angle of the protomers in the disulfide-linked dimer, which can help exposing these sites for interaction (17, 67). Note that the free rotation of the protomers in the HLA-G1 soluble dimer, as observed in our simulations, would enable even greater exposure of these biding sites. In order to further explore our models and investigate the interaction with ILT4, we decided to conduct a protein-protein docking experiment with ClusPro. As expected, ClusPro successfully identified binding modes in which the D1 domain of ILT4 interacts with the α3 domain of HLA-G1, specifically involving F195 and Y197. Some of the predicted binding modes displayed ILT4 approaching HLA-G from the "top," as previously described by Wang et al. (67). The authors of that study discuss the limited flexibility of ILT4 in terms of bending between Ig-like domains, and describe this "top-down" binding mode as the only interaction possible for membrane-bound forms of HLA-G1. Interestingly, in the absence of the membrane, ClusPro predicted better binding modes in which ILT4 approaches HLA-G1 from the "bottom," while still preserving interactions between D1 and F195/Y197. Based on these results, we can speculate that higher affinity of soluble HLA-G1 dimer for ILT2/ILT4 ligands could be explained by the possibility of using this alternative "bottom-up" binding mode. Further computational and experimental studies would be necessary to investigate the occurrence and stability of alternative binding modes involving ILT2 and ITL4.

The interaction of HLA-G with T $CD8^+$ cells may induce FasL up-regulation, soluble FasL secretion and $CD8^+$ cell apoptosis by Fas-FasL interaction, whose binding sites have not been determined yet (71). Compared to classical class I molecules (e.g., HLA-A, -B, -C), HLA-G binds to CD8α/α loop (residues 223-229) with medium affinity (63, 64), thus inhibiting the T $CD8^+$ cytotoxic function. Although little is known regarding the HLA-G dimer interaction with CD8, it is possible that the interaction confers increased avidity in a proper structural

orientation, permitting an efficient signaling to CD8 as well as it does for ILT2/ILT4 (17, 38). The freedom of rotation reported in this study for the soluble HLA-G1 dimer, exposing two easily accessible binding sites for ILTs/CD8 receptors, corroborates the potential for multiple orientations of the dimer. Considering that these major leukocyte receptors are adjacent to each other, it is possible the formation of complexes containing multiple combinations of one HLA-G dimer and two leukocyte receptors (ILT2/ILT2, ILT4/ILT4; ILT2/ILT4, ILT2/CD8, ILT4/CD8, CD8/CD8).

It has been proposed that HLA-G could interact with the killer cell immunoglobulin-like receptor KIR2DL4 (25), and that such interaction could induce both inhibitory as well as activating signals (28, 72, 73). Although the inhibition of the innate and adaptive immune response is the most accepted role of HLA-G, activating responses have also been reported (74). The soluble form of HLA-G could be the natural KIR2DL4 ligand, since it accumulates in KIR2DL4^{+} endosomes and induces endosome signaling (75). In fact, structural representations (17) indicate that steric constraints would prevent KIR2DL4 from interacting with HLA-G dimers (65, 66, 75). Considering that KIR2DL binding residues are located in the α1 domain of the HLA-G molecule, and considering the HLA-G1 dimer rotation presented here, it is possible that the KIR2DL4 binding area would be more accessible in the soluble HLA-G1 dimer as opposed to the membrane-bound HLA-G1 dimer. However, it is important to stress that we have not tested this interaction in our study, and that recent studies have not found evidence of HLA-G/KIR2DL4 interaction. Once again, the models produced in this work can now be used to further investigate this potential interaction.

Contrary to what was observed for the aforementioned systems, greater instability was observed in two of our HLA-G5 models. Specifically, the only stable system was the one containing both the nonapeptide RIIPRHLQL and ß2-microglobulin (**Figure 6** and **Supplementary Material** – HLA-G5 Monomer, nonapeptide, and coupled β2-microglobulin Simulation Video). Previous studies have reported HLA-G5 isoforms both with and without β2-microglobulin (33, 76). However, our results suggest that the monomeric form of HLA-G5 would not be stable without these other chains (**Supplementary Material** – HLA-G5 Monomer Simulation Video). On the other hand, it is possible that HLA-G5 dimers could be stable in the β2-microglobulin-free form, which was not tested here. For instance, the intronic tails of both protomers could interact with each other, not causing the effect of cleft deformation observed in our simulations (**Supplementary Material** – HLA-G5 Monomer and nonapeptide Simulation Video). Such dimeric structures for HLA-G5 without β2-microglobulin could be similar to the dimers composed by the α1–α3: α1–α3 domains, as in the work published by Kuroki et al., in which HLA-G2 isoform (membrane bound α1–α3) naturally formed a β2-microglobulin-free homodimer which did not have disulfide bridges keeping the structures in place (77). Electron microscopy revealed that the general structure and domain organization of such HLA-G2 homodimers resembled those of class II HLA heterodimers (α1–α2: β1–β2) (20). Published data (77) described the binding of β2-microglobulin and β2-microglobulin-free forms of HLA molecules to members of ILT receptor family and demonstrated that, in addition to ILT4, β2-microglobulin-free structures are recognized by several other members of this receptor family. In fact, the "activating" members of the ILT family showed a preference for such structures. Therefore, it is possible that this could also be the case for HLA-G. This would support the notion that structural variations of HLA-G may be relevant in the modulation of biological function (32). It's also intriguing to consider that, similar to classic class I HLA molecules, HLA-G may have activating receptors. In fact, it is possible that there are other receptors for HLA-G, specific for isoforms or not, and the study of HLA-G structures other than HLA-G1 and HLA-G5 may allow us to identify them (32).

In conclusion, the present study describes for the first time the complete membrane-bound HLA-G1 3D structure and its dynamic behavior in solution. Our study also described the dynamics of the soluble HLA-G1 dimer. Our simulations highlighted the great flexibility enabled by the disulfide bridge, which could even promote alternative binding modes with ILT2/ILT4 receptors. Our study of the HLA-G5 isoform and its structural alternatives demonstrated greater structural instability when the peptide or β2-microglobulin were absent. More comprehensive structural studies will be necessary to verify the existence of other structural conformations for HLA-G5. This work produced insights on the structure, dynamics, and interaction patterns of important HLA-G variants. It also produced 3D models that can now be used to further investigate these and other HLA-G molecules, to identify new HLA-G ligands, and to design potential pharmacological interventions.

DATA AVAILABILITY STATEMENT

The datasets presented in this study can be found in online repositories. The names of the repository/repositories and accession number(s) can be found in the article/**Supplementary Material**.

AUTHOR CONTRIBUTIONS

TA, DA and ED contributed to the conception and design of the study. TA generated all structural models. TA and DA performed simulations. TA, DA, MR and JA performed the analysis. SG and LK supervised the analysis. TA, DA and ED wrote the article. All authors contributed to the article and approved the submitted version.

FUNDING

This work was supported in part by Coordenação de Aperfeiçoamento de Pessoal de Nível Superior (CAPES). This work was also partially supported by the Cancer Prevention & Research Institute of Texas (CPRIT), through award number RP170508, and through a fellowship from the Gulf Cost Consortia on the Computational Cancer Biology Training

Program (grant number RP170593). Finally, this work was also partially supported by a training fellowship from the National Library of Medicine Training Program in Biomedical Informatics (grant number T15LM007093), and by Rice University funds.

SUPPLEMENTARY MATERIAL

The Supplementary Material for this article can be found online at: https://www.frontiersin.org/articles/10.3389/fimmu.2020.575076/full#supplementary-material

REFERENCES

1. Carosella ED, Favier B, Rouas-Freiss N, Moreau P, Lemaoult J. Beyond the Increasing Complexity of the Immunomodulatory HLA-G Molecule. *Blood* (2008) 111(10):4862–70. doi: 10.1182/blood-2007-12-127662
2. Kovats S, Main EK, Librach C, Stubblebine M, Fisher SJ, DeMars R. A Class I Antigen, HLA-G, Expressed in Human Trophoblasts. *Sci (N Y NY)* (1990) 248 (4952):220–23. doi: 10.1126/science.2326636
3. Mallet V, Blaschitz A, Crisa L, Schmitt C, Fournel S, King A, et al. HLA-G in the Human Thymus: A Subpopulation of Medullary Epithelial but Not CD83 (+) Dendritic Cells Expresses HLA-G as a Membrane-Bound and Soluble Protein. *Int Immunol* (1999) 11(6):889–98. doi: 10.1093/intimm/11.6.889
4. Le Discorde M, Moreau P, Sabatier P, Legeais J-M, Carosella ED. Expression of HLA-G in Human Cornea, an Immune-Privileged Tissue. *Hum Immunol* (2003) 64(11):1039–44. doi: 10.1016/j.humimm.2003.08.346
5. Cirulli V, Zalatan J, McMaster M, Prinsen R, Salomon DR, Ricordi C, et al. The Class I HLA Repertoire of Pancreatic Islets Comprises the Nonclassical Class Ib Antigen HLA-G. *Diabetes* (2006) 55(5):1214–22. doi: 10.2337/db05-0731
6. Menier C, Rabreau Michèle, Challier J-C, Le Discorde M, Carosella ED, Rouas-Freiss N. Erythroblasts Secrete the Nonclassical HLA-G Molecule from Primitive to Definitive Hematopoiesis. *Blood* (2004) 104(10):3153–60. doi: 10.1182/blood-2004-03-0809
7. Paul P, Rouas-Freiss N, Khalil-Daher I, Moreau P, Riteau B, Le Gal FA, et al. HLA-G Expression in Melanoma: A Way for Tumor Cells to Escape from Immunosurveillance. *Proc Natl Acad Sci U States America* (1998) 95(8):4510–15. doi: 10.1073/pnas.95.8.4510
8. Rouas-Freiss N, Moreau P, Ferrone S, Carosella ED. HLA-G Proteins in Cancer: Do They Provide Tumor Cells with an Escape Mechanism? *Cancer Res* (2005) 65(22):10139–44. doi: 10.1158/0008-5472.CAN-05-0097
9. Lila N, Carpentier A, Amrein C, Khalil-Daher I, Dausset J, Carosella ED. Implication of HLA-G Molecule in Heart-Graft Acceptance. *Lancet (London England)* (2000) 355(9221):2138. doi: 10.1016/S0140-6736(00)02386-2
10. Lozano JM, González R, Kindelán JM, Rouas-Freiss N, Caballos R, Dausset J, et al. Monocytes and T Lymphocytes in HIV-1-Positive Patients Express HLA-G Molecule. *AIDS (London England)* (2002) 16(3):347–51. doi: 10.1097/00002030-200202150-00005
11. Lafon M, Prehaud C, Megret F, Lafage M, Mouillot G, Roa M, et al. Modulation of HLA-G Expression in Human Neural Cells after Neurotropic Viral Infections. *J Virol* (2005) 79(24):15226–37. doi: 10.1128/JVI.79.24.15226-15237.2005
12. Wiendl H, Feger U, Mittelbronn M, Jack C, Schreiner B, Stadelmann C, et al. Expression of the Immune-Tolerogenic Major Histocompatibility Molecule HLA-G in Multiple Sclerosis: Implications for CNS Immunity. *Brain: A J Neurol* (2005) 128(Pt 11):2689–704. doi: 10.1093/brain/awh609
13. Khosrotehrani K, Le Danff C, Reynaud-Mendel B, Dubertret L, Carosella ED, Aractingi S. HLA-G Expression in Atopic Dermatitis. *J Invest Dermatol* (2001) 117(3):750–52. doi: 10.1046/j.0022-202x.2001.01487.x
14. Boyson JE, Erskine R, Whitman MC, Chiu M, Lau JM, Koopman LA, et al. Disulfide Bond-Mediated Dimerization of HLA-G on the Cell Surface. *Proc Natl Acad Sci U States America* (2002) 99(25):16180–85. doi: 10.1073/pnas.212643199
15. Colonna M, Navarro F, Bellón T, Llano M, García P, Samaridis J, et al. A Common Inhibitory Receptor for Major Histocompatibility Complex Class I Molecules on Human Lymphoid and Myelomonocytic Cells. *J Exp Med* (1997) 186(11):1809–18. doi: 10.1084/jem.186.11.1809
16. Colonna M, Samaridis J, Cella M, Angman L, Allen RL, O'Callaghan CA, et al. Human Myelomonocytic Cells Express an Inhibitory Receptor for Classical and Nonclassical MHC Class I Molecules. *J Immunol (Baltimore Md: 1950)* (1998) 160(7):3096–100.
17. Shiroishi M, Kuroki K, Ose T, Rasubala L, Shiratori I, Arase H, et al. Efficient Leukocyte Ig-like Receptor Signaling and Crystal Structure of Disulfide-Linked HLA-G Dimer. *J Biol Chem* (2006) 281(15):10439–47. doi: 10.1074/jbc.M512305200
18. Gonen-Gross T, Achdout H, Arnon TII, Gazit R, Stern N, Horejsí V, et al. The CD85J/Leukocyte Inhibitory Receptor-1 Distinguishes between Conformed and Beta 2-Microglobulin-Free HLA-G Molecules. *J Immunol (Baltimore Md: 1950)* (2005) 175(8):4866–74. doi: 10.4049/jimmunol.175.8.4866
19. Amodio G, Comi M, Tomasoni D, Emma Gianolini M, Rizzo R, LeMaoult J, et al. HLA-G Expression Levels Influence the Tolerogenic Activity of Human DC-10. *Haematologica* (2015) 100(4):548–57. doi: 10.3324/haematol.2014.113803
20. Kuroki K, Maenaka K. Immune Modulation of HLA-G Dimer in Maternal-Fetal Interface. *Eur J Immunol* (2007) 37(7):1727–29. doi: 10.1002/eji.200737515
21. Geraghty DE, Koller BH, Orr HT. A Human Major Histocompatibility Complex Class I Gene That Encodes a Protein with a Shortened Cytoplasmic Segment. *Proc Natl Acad Sci U States America* (1987) 84 (24):9145–49. doi: 10.1073/pnas.84.24.9145
22. Fujii T, Ishitani A, Geraghty DE. A Soluble Form of the HLA-G Antigen Is Encoded by a Messenger Ribonucleic Acid Containing Intron 4. *J Immunol (Baltimore Md: 1950)* (1994) 153(12):5516–24.
23. Ishitani A, Geraghty DE. Alternative Splicing of HLA-G Transcripts Yields Proteins with Primary Structures Resembling Both Class I and Class II Antigens. *Proc Natl Acad Sci U States America* (1992) 89(9):3947–51. doi: 10.1073/pnas.89.9.3947
24. Paul P, Cabestre FA, Ibrahim EC, Lefebvre S, Khalil-Daher I, Vazeux G, et al. Identification of HLA-G7 as a New Splice Variant of the HLA-G MRNA and Expression of Soluble HLA-G5, -G6, and -G7 Transcripts in Human Transfected Cells. *Hum Immunol* (2000) 61(11):1138–49. doi: 10.1016/s0198-8859(00)00197-x
25. Carosella ED, Moreau P, Le Maoult J, Le Discorde M, Dausset J, Rouas-Freiss N. HLA-G Molecules: From Maternal-Fetal Tolerance to Tissue Acceptance. *Adv Immunol* (2003) 81:199–252. doi: 10.1016/s0065-2776(03)81006-4
26. Donadi EA, Castelli EC, Arnaiz-Villena A, Roger M, Rey D, Moreau P. Implications of the Polymorphism of HLA-G on Its Function, Regulation, Evolution and Disease Association. *Cell Mol Life Sci: CMLS* (2011) 68(3):369–95. doi: 10.1007/s00018-010-0580-7
27. Carosella ED, Moreau P, Lemaoult J, Rouas-Freiss N. HLA-G: From Biology to Clinical Benefits. *Trends Immunol* (2008) 29(3):125–32. doi: 10.1016/j.it.2007.11.005
28. Diehl M, Münz C, Keilholz W, Stevanović S, Holmes N, Loke YW, et al. Nonclassical HLA-G Molecules Are Classical Peptide Presenters. *Curr Biol: CB* (1996) 6(3):305–14. doi: 10.1016/s0960-9822(02)00481-5
29. Gonen-Gross T, Achdout H, Gazit R, Hanna J, Mizrahi Sa'ar, Markel G, et al. Complexes of HLA-G Protein on the Cell Surface Are Important for Leukocyte Ig-like Receptor-1 Function. *J Immunol (Baltimore Md: 1950)* (2003) 171(3):1343–51. doi: 10.4049/jimmunol.171.3.1343
30. Shiroishi M, Tsumoto K, Amano K, Shirakihara Y, Colonna M, Braud VM, et al. Human Inhibitory Receptors Ig-like Transcript 2 (ILT2) and ILT4 Compete with CD8 for MHC Class I Binding and Bind Preferentially to HLA-G. *Proc Natl Acad Sci U States America* (2003) 100(15):8856–61. doi: 10.1073/pnas.1431057100
31. Apps R, Gardner L, Sharkey AM, Holmes N, Moffett A. A Homodimeric Complex of HLA-G on Normal Trophoblast Cells Modulates Antigen-Presenting Cells via LILRB1. *Eur J Immunol* (2007) 37(7):1924–37. doi: 10.1002/eji.200737089
32. HoWangYin K-Y, Loustau M, Wu J, Alegre E, Daouya M, Caumartin J, et al. Multimeric Structures of HLA-G Isoforms Function through Differential Binding to LILRB Receptors. *Cell Mol Life Sci: CMLS* (2012) 69(23):4041–49. doi: 10.1007/s00018-012-1069-3
33. Juch H, Blaschitz A, Daxböck C, Rueckert C, Kofler K, Dohr G. A Novel Sandwich ELISA for Alpha1 Domain Based Detection of Soluble HLA-G

Heavy Chains. *J Immunol Methods* (2005) 307(1–2):96–106. doi: 10.1016/j.jim.2005.09.016
34. Zhang W-Q, Xu D-P, Liu D, Li Y-Y, Ruan Y-Y, Lin A, et al. HLA-G1 and HLA-G5 Isoforms Have an Additive Effect on NK Cytolysis. *Hum Immunol* (2014) 75(2):182–89. doi: 10.1016/j.humimm.2013.11.001
35. Le Rond S, Azéma C, Krawice-Radanne I, Durrbach A, Guettier C, Carosella ED, et al. Evidence to Support the Role of HLA-G5 in Allograft Acceptance through Induction of Immunosuppressive/Regulatory T Cells. *J Immunol (Baltimore Md: 1950)* (2006) 176(5):3266–76. doi: 10.4049/jimmunol.176.5.3266
36. Berman HM, Westbrook J, Feng Z, Gilliland G, Bhat TN, Weissig H, et al. The Protein Data Bank. *Nucleic Acids Res* (2000) 28(1):235–42. doi: 10.1093/nar/28.1.235
37. Webb B, Sali A. Comparative Protein Structure Modeling Using MODELLER. *Curr Protoc Bioinf* (2016) 54(20 2016):5.6.1–5.6.37. doi: 10.1002/cpbi.3
38. Clements CS, Kjer-Nielsen L, Kostenko L, Hoare HL, Dunstone MA, Moses E, et al. Crystal Structure of HLA-G: A Nonclassical MHC Class I Molecule Expressed at the Fetal-Maternal Interface. *Proc Natl Acad Sci U States America* (2005) 102(9):3360–65. doi: 10.1073/pnas.0409676102
39. Wang C, Bradley P, Baker D. Protein-Protein Docking with Backbone Flexibility. *J Mol Biol* (2007) 373(2):503–19. doi: 10.1016/j.jmb.2007.07.050
40. Yang J, Zhang Y. I-TASSER Server: New Development for Protein Structure and Function Predictions. *Nucleic Acids Res* (2015) 43(W1):W174–181. doi: 10.1093/nar/gkv342
41. Benkert P, Biasini M, Schwede T. Toward the Estimation of the Absolute Quality of Individual Protein Structure Models. *Bioinf (Oxford England)* (2011) 27(3):343–50. doi: 10.1093/bioinformatics/btq662
42. Maghrabi AHA, McGuffin LJ. ModFOLD6: An Accurate Web Server for the Global and Local Quality Estimation of 3D Protein Models. *Nucleic Acids Res* (2017) 45(W1):W416–21. doi: 10.1093/nar/gkx332
43. Bowie JU, Lüthy R, Eisenberg D. A Method to Identify Protein Sequences That Fold into a Known Three-Dimensional Structure. *Sci (N Y NY)* (1991) 253(5016):164–70. doi: 10.1126/science.1853201
44. Lüthy R, Bowie JU, Eisenberg D. Assessment of Protein Models with Three-Dimensional Profiles. *Nature* (1992) 356(6364):83–5. doi: 10.1038/356083a0
45. Colovos C, Yeates TO. Verification of Protein Structures: Patterns of Nonbonded Atomic Interactions. *Protein Sci: A Publ Protein Soc* (1993) 2(9):1511–19. doi: 10.1002/pro.5560020916
46. Laskowski RA. PDBsum: Summaries and Analyses of PDB Structures. *Nucleic Acids Res* (2001) 29(1):221–22. doi: 10.1093/nar/29.1.221
47. Holec PV, Hackel BJ. PyMOL360: Multi-User Gamepad Control of Molecular Visualization Software. *J Comput Chem* (2016) 37(30):2667–69. doi: 10.1002/jcc.24489
48. Biopython: Freely Available Python Tools for Computational Molecular Biology and Bioinformatics. Available at: https://www.ncbi.nlm.nih.gov/pubmed/?term=Biopython%3A+freely+available+Python+tools+for+computational+molecular+biology+and+bioinformatics (Accessed January 29, 2020).
49. Wu EL, Cheng X, Jo S, Rui H, Song KC, Dávila-Contreras EM, et al. CHARMM-GUI Membrane Builder toward Realistic Biological Membrane Simulations. *J Comput Chem* (2014) 35(27):1997–2004. doi: 10.1002/jcc.23702
50. Lee J, Patel DS, Ståhle J, Park S-J, Kern NR, Kim S, et al. CHARMM-GUI Membrane Builder for Complex Biological Membrane Simulations with Glycolipids and Lipoglycans. *J Chem Theory Comput* (2019) 15(1):775–86. doi: 10.1021/acs.jctc.8b01066
51. Abraham MJ, Murtola T, Schulz R, Páll S, Smith JC, Hess B, et al. GROMACS: High Performance Molecular Simulations through Multi-Level Parallelism from Laptops to Supercomputers. *SoftwareX* (2015) 1–2:19–25. doi: 10.1016/j.softx.2015.06.001
52. Huang J, Rauscher S, Nawrocki G, Ran T, Feig M, de Groot BL, et al. CHARMM36m: An Improved Force Field for Folded and Intrinsically Disordered Proteins. *Nat Methods* (2017) 14(1):71–3. doi: 10.1038/nmeth.4067
53. Devaurs D, Antunes DA, Papanastasiou M, Moll M, Ricklin D, Lambris JD, et al. Coarse-Grained Conformational Sampling of Protein Structure Improves the Fit to Experimental Hydrogen-Exchange Data. *Front Mol Biosci* (2017) 4:13:13. doi: 10.3389/fmolb.2017.00013
54. McGibbon RT, Kyle A. B, Harrigan MP, Klein C, Swails JM, Hernández CX, et al. MDTraj: A Modern Open Library for the Analysis of Molecular Dynamics Trajectories. *Biophys J* (2015) 109(8):1528–32. doi: 10.1016/j.bpj.2015.08.015
55. Scherer MK, Trendelkamp-Schroer B, Paul F, Pérez-Hernández G, Hoffmann M, Plattner N, et al. PyEMMA 2: A Software Package for Estimation, Validation, and Analysis of Markov Models. *J Chem Theory Comput* (2015) 11(11):5525–42. doi: 10.1021/acs.jctc.5b00743
56. Abella JR, Dinler A.A, Clementi C, Kavraki LE. APE-Gen: A Fast Method for Generating Ensembles of Bound Peptide-MHC Conformations. *Mol (Basel Switzerland)* (2019) 24(5):881–94. doi: 10.3390/molecules24050881
57. Eastman P, Swails J, Chodera JD, McGibbon RT, Zhao Y, Beauchamp KA, et al. OpenMM 7: Rapid Development of High Performance Algorithms for Molecular Dynamics. *PloS Comput Biol* (2017) 13(7):e1005659. doi: 10.1371/journal.pcbi.1005659
58. Quiroga R, Villarreal MA. Vinardo: A Scoring Function Based on Autodock Vina Improves Scoring, Docking, and Virtual Screening. *PloS One* (2016) 11(5):e0155183. doi: 10.1371/journal.pone.0155183
59. Antunes DA, Abella JR, Hall-Swan S, Devaurs D, Conev A, Moll M, et al. HLA-Arena: A Customizable Environment for the Structural Modeling and Analysis of Peptide-HLA Complexes for Cancer Immunotherapy. *JCO Clin Cancer Inf* (2020) 4:623–36. doi: 10.1200/CCI.19.00123
60. Abella JR, Antunes DA, Clementi C, Kavraki LE. Large-Scale Structure-Based Prediction of Stable Peptide Binding to Class I HLAs Using Random Forests. *Front Immunol* (2020) 11:1583:1583. doi: 10.3389/fimmu.2020.01583
61. Kozakov D, Hall DR, Xia B, Porter KA, Padhorny D, Yueh C, et al. The ClusPro Web Server for Protein-Protein Docking. *Nat Protoc* (2017) 12(2):255–78. doi: 10.1038/nprot.2016.169
62. Pettersen EF, Goddard TD, Huang CC, Couch GS, Greenblatt DM, Meng EC, et al. UCSF Chimera–a Visualization System for Exploratory Research and Analysis. *J Comput Chem* (2004) 25(13):1605–12. doi: 10.1002/jcc.20084
63. Gao GF, Willcox BE, Wyer JR, Boulter JM, O'Callaghan CA, Maenaka K, et al. Classical and Nonclassical Class I Major Histocompatibility Complex Molecules Exhibit Subtle Conformational Differences That Affect Binding to CD8alphaalpha. *J Biol Chem* (2000) 275(20):15232–38. doi: 10.1074/jbc.275.20.15232
64. Estibaliz A, Rizzo R, Bortolotti D, Fernandez-Landázuri S, Fainardi E, González A. Some Basic Aspects of HLA-G Biology. *J Immunol Res* (2014) 2014):657625. doi: 10.1155/2014/657625
65. Hsu KC, Chida S, Geraghty DE, Dupont B. The Killer Cell Immunoglobulin-like Receptor (KIR) Genomic Region: Gene-Order, Haplotypes and Allelic Polymorphism. *Immunol Rev* (2002) 190:40–52. doi: 10.1034/j.1600-065x.2002.19004.x
66. Apps R, Gardner L, Moffett A. A Critical Look at HLA-G. *Trends Immunol* (2008) 29(7):313–21. doi: 10.1016/j.it.2008.02.012
67. Wang Q, Song H, Cheng H, Qi J, Nam G, Tan S, et al. Structures of the Four Ig-like Domain LILRB2 and the Four-Domain LILRB1 and HLA-G1 Complex. *Cell Mol Immunol* (2020) 17(9):966–75. doi: 10.1038/s41423-019-0258-5
68. Robinson J, Barker DJ, Georgiou X, Cooper MA, Flicek P, Marsh SGE. IPD-IMGT/HLA Database. *Nucleic Acids Res* (2020) 48(D1):D948–55. doi: 10.1093/nar/gkz950
69. Robinson J, Soormally AR, Hayhurst JD, Marsh SGE. The IPD-IMGT/HLA Database - New Developments in Reporting HLA Variation. *Hum Immunol* (2016) 77(3):233–37. doi: 10.1016/j.humimm.2016.01.020
70. Ishitani A, Sageshima N, Lee N, Dorofeeva N, Hatake K, Marquardt H, et al. Protein Expression and Peptide Binding Suggest Unique and Interacting Functional Roles for HLA-E, F, and G in Maternal-Placental Immune Recognition. *J Immunol (Baltimore Md: 1950)* (2003) 171(3):1376–84. doi: 10.4049/jimmunol.171.3.1376
71. Contini P, Ghio M, Poggi A, Filaci G, Indiveri F, Ferrone S, et al. Soluble HLA-A,-B,-C and -G Molecules Induce Apoptosis in T and NK CD8+ Cells and Inhibit Cytotoxic T Cell Activity through CD8 Ligation. *Eur J Immunol* (2003) 33(1):125–34. doi: 10.1002/immu.200390015
72. Selvakumar A, Steffens U, Dupont B. NK Cell Receptor Gene of the KIR Family with Two IG Domains but Highest Homology to KIR Receptors with Three IG Domains. *Tissue Antigens* (1996) 48(4 Pt 1):285–94. doi: 10.1111/j.1399-0039.1996.tb02647.x

73. Faure M, Long EO. KIR2DL4 (CD158d), an NK Cell-Activating Receptor with Inhibitory Potential. *J Immunol (Baltimore Md: 1950)* (2002) 168(12):6208–14. doi: 10.4049/jimmunol.168.12.6208
74. Fu B, Zhou Y, Ni X, Tong X, Xu X, Dong Z, et al. Natural Killer Cells Promote Fetal Development through the Secretion of Growth-Promoting Factors. *Immunity* (2017) 47(6):1100–13.e6. doi: 10.1016/j.immuni.2017.11.018
75. Rajagopalan S, Long EO. KIR2DL4 (CD158d): An Activation Receptor for HLA-G. *Front Immunol* (2012) 3:258. doi: 10.3389/fimmu.2012.00258
76. Morales PJ, Pace JL, Platt JS, Langat DK, Hunt JS. Synthesis of β2-Microglobulin-Free, Disulphide-Linked HLA-G5 Homodimers in Human Placental Villous Cytotrophoblast Cells. *Immunology* (2007) 122(2):179. doi: 10.1111/j.1365-2567.2007.02623.x
77. Kimiko K, Mio K, Takahashi A, Matsubara H, Kasai Y, Manaka S, et al. Cutting Edge: Class II–like Structural Features and Strong Receptor Binding of the Nonclassical HLA-G2 Isoform Homodimer. *J Immunol (Baltimore Md: 1950)* (2017) 198(9):3399–403. doi: 10.4049/jimmunol.1601296

Conflict of Interest: The authors declare that the research was conducted in the absence of any commercial or financial relationships that could be construed as a potential conflict of interest.

frontiers in Immunology

ORIGINAL RESEARCH
published: 23 December 2020
doi: 10.3389/fimmu.2020.608016

Susceptibility to *Plasmodium falciparum* Malaria: Influence of Combined Polymorphisms of IgG3 Gm Allotypes and Fc Gamma Receptors IIA, IIIA, and IIIB

Abdou Khadre Dit Jadir Fall[1], *Celia Dechavanne*[1], *Audrey Sabbagh*[1], *Evelyne Guitard*[2], *Jacqueline Milet*[1], *André Garcia*[1], *Jean-Michel Dugoujon*[2], *David Courtin*[1†] *and Florence Migot-Nabias*[1*†]

[1] Université de Paris, Institut de Recherche pour le Développement (IRD), UMR 261 MERIT, Paris, France, [2] CNRS UMR 5288 Laboratoire d'Anthropologie Moléculaire et d'Imagerie de Synthèse (AMIS), Université Paul Sabatier Toulouse III, Toulouse, France

OPEN ACCESS

Edited by:
Julio Aliberti,
National Institutes of Health (NIH), United States

Reviewed by:
Marita Troye Blomberg, Stockholm University, Sweden
Karl Seydel, Michigan State University, United States

***Correspondence:**
Florence Migot-Nabias
florence.migot-nabias@ird.fr

[†]These authors have contributed equally to this work

Specialty section:
This article was submitted to Microbial Immunology, a section of the journal Frontiers in Immunology

Received: 18 September 2020
Accepted: 13 November 2020
Published: 23 December 2020

Citation:
Fall AKDJ, Dechavanne C, Sabbagh A, Guitard E, Milet J, Garcia A, Dugoujon J-M, Courtin D and Migot-Nabias F (2020) Susceptibility to Plasmodium falciparum Malaria: Influence of Combined Polymorphisms of IgG3 Gm Allotypes and Fc Gamma Receptors IIA, IIIA, and IIIB. Front. Immunol. 11:608016. doi: 10.3389/fimmu.2020.608016

The binding of immunoglobulin (Ig) to Fc gamma receptors (FcgR) at the immune cell surface is an important step to initiate immunological defense against malaria. However, polymorphisms in receptors and/or constant regions of the IgG heavy chains may modulate this binding. Here, we investigated whether polymorphisms located in FcgR and constant regions of the heavy chain of IgG are associated with susceptibility to *P. falciparum* malaria. For this purpose, a clinical and parasitological follow-up on malaria was conducted among 656 infants in southern Benin. G3m allotypes (from total IgG3) were determined by a serological method of hemagglutination inhibition. FcgRIIA 131R/H and FcgRIIIA 176F/V genotypes were determined using the TaqMan method and FcgRIIIB NA1/NA2 genotypes were assessed by polymerase chain reaction using allele-specific primers. Association analyses between the number of malaria infections during the follow-up and polymorphisms in IgG G3m allotypes and FcgR were studied independently by zero inflated binomial negative regression. The influence of combinations of G3m allotypes and FcgRIIA/FcgRIIIA/FcgRIIIB polymorphisms on the number of *P. falciparum* infections, and their potential interaction with environmental exposure to malaria was assessed by using the generalized multifactor dimensionality reduction (GMDR) method. Results showed that individual carriage of G3m24 single allotype and of G3m5,6,10,11,13,14,24 phenotype was independently associated with a high risk of malaria infection. A risk effect for G3m6 was observed only under high environmental exposure. FcgRIIIA 176VV single genotype and combined carriage of FcgRIIA 131RH/FcgRIIIA 176VV/FcgRIIIB NA1NA2, FcgRIIA 131HH/FcgRIIIA 176FF/FcgRIIIB NA1NA1, FcgRIIA 131HH/FcgRIIIA 176VV/FcgRIIIB NA2NA2 and FcgRIIA 131HH/FcgRIIIA 176VV/FcgRIIIB NA1NA2 genotypes were related to a high number of malaria infections. The risk was accentuated for FcgRIIIA 176VV when considering the influence of environmental exposure to malaria. Finally, the GMDR analysis including environmental exposure showed strengthened associations with a malaria risk when

FcgRIIA/FcgRIIIA/FcgRIIIB genotypes were combined to G3m5,6,11,24 and G3m5,6,10,11,13,15,24 phenotypes or G3m10 and G3m13 single allotypes. Our results highlight the relevance of studying IgG heavy chain and FcgR polymorphisms, independently as well as in combination, in relation to the individual susceptibility to *P. falciparum* infection. The intensity of individual exposure to mosquito bites was demonstrated to impact the relationships found.

Keywords: malaria, IgG polymorphism, Gm allotypes, Fc gamma receptor, Benin, generalized multifactor dimensionality reduction

INTRODUCTION

Malaria remains the most lethal parasitic disease in the world. According to the latest world malaria report in 2019, 228 million estimated cases of malaria occurred in 2018 while the estimated number of deaths remained a concern, 429 000 in 2017 and 405 000 in 2018 (1). Data for the 2015–2018 period highlight that no significant progress in reducing global malaria cases was made. Therefore, it seems urgent to identify new targets and new tools to fight the disease.

The pioneering work of Cohen et al. in 1960 demonstrated that IgG from malaria immune Gambian adults contributed to diminish the *P. falciparum* parasitemia when transferred to non-immune African infected children (2). Since then, there has been an increased interest in exploring the role of IgG in malaria immunity. Namely, the same experimentation was made with IgG from malaria immune African adults passively transferred to Thai patients, demonstrating that efficacy was independent of the type of infecting isolate (3). Further studies established that firstly, cytophilic IgG1 and IgG3 isotypes were mostly associated with *P. falciparum* malaria protection (4–6) including protection of the newborn partly conferred by transplacental transfer of malaria-specific IgG3 (7). Secondly, they showed that it was crucial to investigate the functionality, and not only the levels of IgG directed to asexual stages of *P. falciparum* when evaluating malaria protection parameters (8).

IgG can act on *P. falciparum* in two ways: directly by agglutinating the parasites and therefore preventing their reinvasion of red blood cells and indirectly by binding to Fc gamma receptors (FcgR) expressed at the surface of immune cells such as monocytes, macrophages, or neutrophils (9). This fixation triggers cell activation signals and immune response (opsonization, phagocytosis, reactive oxygen species-ROS, and nitric oxide-NO production). FcgR are important in providing a significant link between the humoral and cellular immunity by bridging the interaction between specific antibodies and effector cells. Nevertheless, genetic variability in constant regions of IgG heavy chains (10) and in FcgR (11) could modulate the susceptibility to malaria infections.

Indeed, most of the interactions between FcgR and IgG involve constant regions (CH1, CH2, and CH3) of the heavy IgG chains. Allelic variations found in the CH1, CH2, and CH3 IgG chains can lead to variations in the amino acid sequences of IgG subclasses and therefore in their efficiency to bind to their receptors. These amino acid changes are responsible for antigenic determinants named human immunoglobulin Gm (gamma markers) allotypes. There are four allotypes for IgG1 in the CH1 and CH3 constant domains called G1m [1, 2, 3, 17], one allotype for IgG2 in the CH2 constant domain called G2m23 and thirteen allotypes for IgG3 in the CH2 and CH3 constant domains called G3m [5, 6, 10, 11, 13, 14, 15, 16, 21, 24, 26, 27, 28] (12, 13). The most polymorphic G3m allotypes are distinguished by variations on nine amino acids (13, 14). Gm allotypes, which are inherited in fixed combinations called haplotypes, vary qualitatively and quantitatively according to human population groups (15).

Facer (16) was the first author to highlight the relationship between Gm allotypes and malaria. She showed, in a sample of Gambian children with past or acute *P. falciparum* malaria, a preferential expression of G3m10, G3m11, and G3m14 allotypes associated with a risk of anemia (16). According to Pandey et al. (17), G3m6 carrying haplotypes may explain the difference in susceptibility to malaria infection between the Fulani and Masaleit ethnic groups in Sudan. Indeed, a lower frequency of G3m6 in Fulani was associated with a lower parasitamia compared to Masaleit. Migot-Nabias et al. (10) demonstrated the existence of an inverse relationship between the carriage of the Gm5,6,13,14; 1,17 phenotype (G3m; G1m) and the presence of uncomplicated malaria in Benin, while for Giha et al. (18) the Gm5,6,13,14; 1,17 phenotype was associated with a higher incidence of malaria in Sudan. Finally, Pandey et al. (19) showed that the carriage of Gm5,13,14; 3; 23 phenotype (G3m; G1m; G2m) was associated with a high level of IgG1 to *P. vivax* *Pv*MSP1-19 and *Pv*AMA-1 antigens, response considered as protective against malaria.

The FcgRs are key components of the immune response, by operating on activation and modulation of the pro-inflammatory and cytotoxic pathways, by influencing the number of white blood cells as well as the transport of circulating antibodies (20, 21). In the family of FcgR receptors, FcgRIIA, FcgRIIIA, and FcgRIIIB appear to play an important role in malaria susceptibility.

FcgRIIA initiates endocytosis, phagocytosis, and the release of inflammatory mediators. There are two variants for FcgRIIA, 131R (Arginine) and 131H (Histidine) firstly described according to their IgG2 binding efficiency, which is more affine for the 131H variant (22). Binding affinity for IgG is more important for IgG3 and IgG1 than for IgG4 and IgG2 (23). Ouma et al. (24) showed that 131R homozygosity confers protection against high parasite densities in contrast to 131H homozygosity.

FcgRIIIA receptor plays an important role in phagocytosis and degranulation and presents two allotypes variants consisting

in either F (Phenylalanine) or V (Valine) in position 176, the 176V variant offering a better affinity for IgG1 (25).

FcgRIIIB is a C-terminus linked glycosylphosphatidylinositol (GPI) receptor expressed at the surface of neutrophils and eosinophils. A strong affinity for IgG1 and IgG3 was described (11). The FcgRIIIB presents a polymorphism named NA1/NA2 that refers to neutrophil antigen (NA) 1 and 2 forms which differ in amino acids at positions 65 and 82 in two extra-glycosylation sites (11, 26, 27). The FcgRIIIB NA1 form is capable of better ingestion of IgG1 or IgG3 opsonized particles than the NA2 form (28). The FcgRIIA and FcgRIIIB receptors play an important role in phagocytosis and degranulation. Indeed, in order of decreasing affinity, we have for FcgRIIA, IgG3 > IgG1 > IgG2 = IgG4, for FcgRIIIA, IgG3 > IgG1 >> IgG4 > IgG2 while FcgRIIIB binds generally IgG1 and IgG3 and not IgG2 and IgG4 (23).

Various studies have investigated the relationships between polymorphisms in FcgRIIA, FcgRIIIA, and FcgRIIIB receptors and malaria immunity. Omi et al. (29) showed an association between the FcgRIIIB NA2 allele and an increased susceptibility to cerebral malaria in Thailand. Those results were strengthened by the study of Adu et al. (30) which described an association between FcgRIIIB NA2 allele and a higher risk of malaria infection. Moreover, the authors showed that the FcgRIIA 131R allele was associated with protection against malaria. The presence of the FcgRIIA 131RH heterozygous polymorphism was associated with malaria protection in some studies (31, 32) while for Maiga et al. (33), a marginal protective effect on parasitemia was observed in a Fulani group from Mali harboring the 131RR genotype. Munde et al. (11) demonstrated that the FcgRIIA 131R-FcgRIIIA 176F-FcgRIIIB NA2 haplotype was important in conditioning susceptibility to malaria anemia (or increased levels of circulating parasites) in West Kenya. Ouma et al. (34) reinforced the results obtained from independent analysis of FcgR (31, 32) by showing a negative association between the FcgRIIA 131H-FcgRIIIB NA1 haplotype and severe malaria anemia and a positive one when considering the FcgRIIA 131H-FcgRIIIB NA2 haplotype.

As presented above, the individual susceptibility to malaria has yet been related to polymorphisms located either in the constant domains of the IgG heavy chain or in several FcgR, considered independently. We can hypothesize that the anchoring of IgG on its cellular receptors can be favored according to the respective variants on both sides. For this purpose, the present study investigated the combination of polymorphisms at both IgG constant domains and FcgR with the aim to evaluate their joint impact on susceptibility to *P. falciparum* malaria. More precisely, the relationships between FcgRIIA 131R/H, FcgRIIIA 176 F/V, FcgRIIIB NA1/NA2, Gm allotypes, and malaria phenotypes were determined in a cohort of Beninese infants.

METHODS

Study Area and Design

The study was conducted in three health centers from the district of Tori Bossito located in southwest Benin, where 656 infants were included at birth (35) and 567 of them followed up from birth to 18 months of age (36). Health workers performed an active follow-up of these infants. It consisted of scheduled home visits every week to detect fever. In case of axillary temperature higher than 37.5°C, a questionnaire was fulfilled and both a *Plasmodium* rapid diagnostic test (RDT) and a thick blood smear examination (TBS) by optical microscopy were performed.

A symptomatic malaria infection was defined by the combined presence of an axillary temperature >37.5°C and a positive RDT and/or a positive TBS. In this case, an antimalarial treatment was administered according to the national guidelines that were applied at the time of the study. It consisted in an artemisinin-based combination therapy (artemether and lumefantrine). TBS were also performed every month to detect asymptomatic malaria infections. In addition, mothers were invited to bring their infants to the health center, at any time, in case of fever (suspected by the mother) or clinical signs, whether or not they were related to malaria, and the same protocol was applied.

Venous blood samples were collected quarterly for hematological and immunological measurements. Venous blood was centrifuged for plasma isolation, and genomic DNA extraction was performed from buffy coat using the QIAamp® DNA blood Mini Kit (QIAGEN) according to the manufacturer's instructions.

To assess the environmental risk of malaria exposure, environmental (information on house characteristics and its immediate surrounding) and geographical data (satellite images, soil type, watercourse nearby, vegetation index, rainfall) were recorded. Throughout the study, every 6 weeks, human landing catches were performed in several points of the villages to evaluate spatial and temporal variations of *Anopheles* density. Altogether, these data allowed modeling, for each child included in the follow-up, an individual risk of exposure to *Anopheles* bites by means of a space- and time-dependent variable (37).

IgG Gm Allotypes

The Gm allotype determination was performed for 501 infants (all singletons) for whom a sufficient quantity of plasma (200 µl) was available at 15 months of age. Indeed, plasma samples collected earlier in the follow-up (3, 6, 9, and 12 months) were not suitable for this determination due 1) to a possible presence of IgG from maternal origin bearing their own Gm allotypes and 2) to an insufficient quantity of infant neo-synthesized IgG.

In order to guarantee a highly reliable result, Gm allotype determinations for infants were confirmed by means of their consistency (inheritance) with those of both biological parents. Thereby, Gm determinations of 71 infants were discarded due to the lack of either the paternal (n = 62) or the maternal sample (n = 9).

From the 430 residual samples for whom trios of Gm determinations could be constituted, inconsistent determinations within the father-mother-child trio were observed for 23 cases (5.3%), leading to Gm data for 407 infants that were retained for further analysis.

G1m [1, 2, 3, 17] and G3m [5, 6, 10, 11, 13, 14, 15, 16, 21, 24, 28] allotypes were determined in plasma samples by a standard hemagglutination inhibition method (38). All infants carried the G1m1,17 allele. Considering G3m allotypes, no child presented G3m16 or G3m21, both on the CH2 domain, and absent in

populations of sub-Saharan Africa (13). Similarly, due to the uncertain location of the Gm28 allotype on either IgG1 or IgG3 sub-classes among sub-Saharan Africans (13), this allotype was discarded from the analysis. Therefore, the differentiation of infants was based on the remaining G3m allotypes combined into four G3m alleles mostly encountered in Africa, that are G3m5,10,11,13,14, G3m5,6,11,24, G3m5,6,10,11,14, and G3m10,11,13,15 (13, 15). The homozygous or heterozygous carriage of these alleles led to the ten following possible G3m phenotypes: G3m5,10,11,13,14; G3m5,6,10,11,14; G3m5,6,10,11,13,14; G3m5,6,11,24; G3m5,6,10,11,13,14,24; G3m5,6,10,11,14,24; G3m10,11,13,15; G3m5,10,11,13,14,15; G3m5,6,10,11,13,14,15; and G3m5,6,10,11,13,15,24.

FcgRIIA, FcgRIIIA, and FcgRIIIB Genotyping

Genomic DNA was available for 369 out of the 407 infants for whom Gm data were retained. Among these 369 infants, 368 Gm data were available, while all were genotyped for FcgRIIA, 365 for FcgRIIIA and 353 for FcgRIIIB. However, multivariate models using the four complete FcgR polymorphisms and G3m phenotypes determinations were done on 350 infants.

FcgRIIA and FcgRIIIA Genotyping

Single nucleotide polymorphisms (SNP) corresponding to FcgRIIA rs1801274 and FcgRIIIA rs396991 were genotyped by the Applied Biosystems TaqMan SNP Genotyping Assay using predesigned primer/probe sets (C_9077561_20 and C_25815666_10). PCR was performed using the 7900HT Real-time PCR System (Applied Biosystems) according to the following conditions: one cycle at 92°C for 10 min, 40 cycles at 92°C for 15 s, and 60°C for 60 s. The results were then analyzed using the SDS software.

FcgRIIIB Genotyping

Two different PCR were performed for the detection of FcgRIIIB NA1 and NA2 alleles, using allele-specific oligonucleotides described previously by Hans and Mehta (39). Regarding NA1, the 5'-CAG TGG TTT CAC AAT GTG AA-3' (forward) and 5' CAT GGA CTT CTA GCT GCA CCG 3' (reverse) primers were used to amplify a DNA fragment of 142 pb. Genomic DNA (100 ng) was added to the reaction mixture containing 100 µM $MgCl_2$, 1X buffer solution, 16 µM dNTPs, 2.8 µM sense and antisense primers and 0.5 unit of Taq polymerase. PCR reaction conditions included 1 cycle at 95°C for 5min, followed by 30 cycles at 95°C for 30 s, 55°C for 30 s, and 72°C for 45 s. For NA2, the 5'-CTTC AAT GGT ACA GCG TGC TT-3' (forward) and 5'-CTG TAC TCT CCA CTG TCG TT-3' (reverse) primers were used to amplify a DNA sequence of 169 pb. Genomic DNA (100 ng) was added to the reaction mixture containing 45 µM $MgCl_2$, 1X buffer solution, 16 µM dNTPs, 1.39 µM sense and antisense primers, and 0.5 unit of Taq polymerase. PCR reaction conditions included one cycle at 95°C for 5min, followed by 30 cycles at 95°C for 30 s, 60°C for 30 s, and 72°C for 45 s. The products of 142 pb and 169 pb were revealed on a 2% agarose gel.

Statistical Analysis

The clinical phenotype of interest was the number of *P. falciparum* infections per individual during the follow-up. No discrimination was made between symptomatic and asymptomatic infections since the total of symptomatic infections was greater than that of asymptomatic infections (597 *versus* 200 out of 797 infections) and there were more infants presenting only symptomatic infections (n = 153) than infants presenting only asymptomatic infections (n = 14).

The Chi-square test was used to examine differences between proportions and the Mann-Whitney *U*-test was used for comparisons of demographic and clinical characteristics between groups. The genotypic frequencies of FcgRIIA 131R/H, FcgRIIIA 176F/V and FcgRIIIB NA1/NA2 were tested for Hardy-Weinberg equilibrium (HWE).

First, association analyses between the number of malaria infections during the 18-month follow-up and polymorphisms in FcgR and IgG G3m allotypes were studied by zero-inflated binomial negative regression with adjustment on covariates (age of mothers in years and of infants in months, number of antenatal visits, bednet use, birthweight, and environmental exposure). Environmental exposure was categorized into low *versus* high exposure, taking the median as the threshold value. Univariate analyzes on each of the covariates were made and only those with a P value < 0.20 in the univariate model were included in the final multivariate model.

The statistical analysis was carried out using the Stata software version 13.

Finally, to evaluate the influence of combinations of G3m allotypes, FcgRIIA, FcgRIIIA, and FcgRIIIB polymorphisms on the number of *P. falciparum* infections during the follow-up, and their potential interaction with mosquito exposure, we performed multivariate analyses by using the generalized multifactor dimensionality reduction (GMDR) method (40). This non-parametric and genetic model-free approach overcomes some of the limitations of the traditional statistical methods (i.e. sample size limitation) to detect and characterize gene-gene and gene-environment interactions. GMDR is very similar to the original MDR method. However, instead of using the counts of individuals, the GMDR method uses a residual-based score in order to classify the individuals, thus allowing adjustment for discrete and continuous covariates.

Since the GMDR software requires a complete dataset with no missing values for analysis, we removed individuals with missing genotype data for at least two polymorphisms and those with unknown number of antenatal visits (n = 21). The remaining missing data for FcgR polymorphisms were imputed using the R package MICE (Multivariate Imputation by Chained Equations) (41), a multivariate imputation approach that takes into consideration patterns in the data such as linkage disequilibrium.

We performed an exhaustive search of all possible genotype combinations of one to four polymorphisms among those studied (G3m allotypes, FcgRIIA 131R/H, FcgRIIIA 176F/V, and FcgRIIIB NA1/NA2), and model selection and evaluation was carried out using ten-fold cross-validation. Briefly, a GMDR model was developed using 9/10th of the data and a classification

error was estimated from this training set. Then, cross-validation methods were used to estimate the prediction error of the selected GMDR model using 1/10th of the data as evaluation data. This procedure was repeated for each of the ten pieces of the data and the classification and prediction errors were averaged across all ten runs. Two parameters were used to evaluate the best models: (a) the testing balanced accuracy (TBA), which is a measure of the degree of accuracy to which the selected interaction correctly predicts the number of malaria infections in the testing sets (value averaged across all ten sets), with 1.00 indicating perfect prediction, and (b) the cross-validation consistency (CVC), which indicates how many times a set of loci is identified across the cross-validation subsets.

Besides TBA and CVC statistics, GMDR also provides a measure of the significance of the identified model, the signal test, a robust nonparametric test implemented in this extension to MDR (40). The model with the highest TBA, the maximum CVC score, and 0.05 or lower P value derived from the sign test was considered as the best model.

In the first round of analysis, the environmental variable quantifying mosquito exposure at individual level was included as a covariate in the GMDR models as well as the following variables: mother and child ages, bednet use, and number of antenatal visits. In the second round of analysis, this environmental variable was tested for its interaction with the gene polymorphisms to detect gene-environment interactions (only four covariates in the GMDR models).

A linear regression analysis was performed for the significant models found in the GMDR analysis to estimate the effect of the combinations on malaria infections.

Ethics

The University of Abomey-Calavi's institutional review board and the IRD's Consultative Ethics Committee approved the study protocol. All women in this study signed an informed consent before enrollment (which also included their infants) with the possibility to withdraw at any time.

RESULTS

Participants Characteristics

As presented in **Table 1**, the study was conducted in a sample of Beninese infants presenting malaria infections (n = 260, 70%) or not (n = 109, 30%). The number of infants who had symptomatic and asymptomatic infections during the follow-up was respectively 245 and 106. A majority of infants presenting malaria infections had less than four infections (n = 201, 77.3%), 51 infants (19.6%) had between five and eight infections and eight infants (3.1%) had more than eight infections during the follow-up.

Infants belonged mostly to the Tori ethnic group and no difference appeared between ethnic groups regarding malaria infection (P = 0.156). There were almost as many girls as boys and infants distributed equally in *P. falciparum* infected and non-infected groups (P = 0.842).

TABLE 1 | Characteristics of the 369 study participants.

Characteristics of mothers and infants	*P. falciparum* infections in infants		P-value
	No (n = 109)	Yes (n = 260)	
Mothers			
Mother age (mean ± SD in years)	30 (6.07)	26 (5.20)	**0.001**[a]
Number of antenatal visits (mean ± SD)	4.20 (2.22)	3.43 (1.58)	0.443[a]
Placental malaria (n, %)			0.189[b]
No	99 (27.0)	224 (61.2)	
Yes	9 (2.5)	34 (9.3)	
Maternal education (n, %)			0.781[b]
No education	94 (25.5)	221 (59.9)	
Partial primary	11 (3.0)	25 (6.8)	
Complete primary or more	4 (1.0)	14 (3.8)	
Primigravidae (n, %)			0.078[b]
No	98 (28.5)	215 (58.3)	
Yes	11 (3.0)	45 (12.2)	
Infants			
Birth weight (mean ± SD in g)	3049 (418)	2976 (392)	0.589[a]
Infant age (mean ± SD in months)	12 (3.54)	14 (3.06)	<**0.001**[a]
Sex (n, %):			
Male	55 (50.4)	129 (49.6)	0.882[b]
Female	54 (49.5)	131 (50.4)	
Ethnic group (n, %)[c]:			
Tori	77 (70.6)	195 (51.9)	0.156[b]
Fon	9 (8.2)	27 (10.4)	
Others	23 (21.1)	34 (13.1)	
Bednet use (mean of use ± SD)	0.77 (0.41)	0.71 (0.45)	**0.023**[a]
Mosquito exposure (mean of exposure ± SD)	0.42 (0.50)	0.53 (0.50)	**0.048**[a]
***P. falciparum* infections in infants (n, %)**			
1 to 4 infections	–	201 (77.3)	
5 to 8 infections		51(19.6)	
9 to 16 infections		8 (3.1)	

[a] *Statistical significance determined using Mann-Whitney U-test.*
[b] *Statistical significance determined by $\chi 2$ analysis.*
[c] *4 missing values.*
In bold: significant P value at the 0.05 threshold.

Interestingly, infants from the non-infected group were younger (P < 0.001), had more bednet use (P = 0.023), and were less exposed to mosquitoes (P = 0.048) and their mothers were older (P = 0.001) than infants from the *P. falciparum* infected group.

G3m Allotypes and Malaria Infection

Distribution of G3m Phenotypes in the Study Group

Nine G3m phenotypes were observed in the study population, among which six presented a frequency above 5% and were G3m5,10,11,13,14 (n = 110, 29.9%), G3m5,6,10,11,13,14,24 (n = 106, 28.8%), G3m5,6,10,11,13,14 (n = 49, 13.3%), G3m5,10,11,13,14,15 (n = 41, 11.1%), G3m5,6,11,24 (n = 26, 7.1%), and G3m5,6,10,11,13,15,24 (n = 19, 5.2%) (**Figure 1**). The three remaining combinations were G3m5,6,10,11,13,14,15 (n = 8, 2.2%), G3m5,6,10,11,14 (n = 8, 2.2%), and G3m5,6,10,11,14,24 (n = 1, 0.3%).

G3m Allotypes and Malaria Infections

Carriage of G3m allotypes both in single form and in combinations was analyzed through a zero-inflated binomial

regression model in order to explain the number of malaria infections per infant during the follow-up. We introduced a term of interaction between the genetic and the environmental variables in the model in order to explore the potential effect of G3m allotypes varying according to the intensity of individual exposure to mosquito bites.

Association Between G3m Allotypes and Malaria Infections

The six most prevalent G3m phenotypes (frequency above 5%) were analyzed.

Only G3m5,6,10,11,13,14,24 was associated with a greater risk of malaria infections (n = 106, IRR = 1.295, 95% CI = 1.093;1.535, P = 0.003, **Table 2**).

The analysis of the carriage of single G3m6, G3m10, G3m13, G3m14, G3m15 and G3m24 allotypes showed that G3m24 is associated with an increased risk of malaria infections (n = 152, IRR = 1.195, 95% CI = 1.016;1.406, P = 0.031, **Table 2**).

To explore the potential role of environmental exposure on this effect, we introduced an interaction term in the analyses.

Interaction Between G3m Allotypes—Environmental Exposure and Malaria Infections

Table 3 confirmed that under conditions of high level of environmental exposure to mosquito bites, G3m5,6,10,11,13,14,24 is associated with an increased risk of malaria infection (n = 56, IRR = 1.648, 95% CI = 1.312;2.070, P < 0.001) as well as the carriage of G3m6 (n = 116, IRR = 1.350, 95% CI = 1.059;1.720, P = 0.015) and of G3m24 (n = 78, IRR = 1.479, 95% CI = 1.183;1.850, P = 0.001).

FcgRIIA 131R/H, FcgRIIIA 176 F/V, and FcgRIIIB NA1/NA2 Polymorphisms

Distribution of FcgR Polymorphisms in the Study Group

The observed distribution of FcgRIIA 131R/H and FcgRIIIA 176F/V genotypes in the whole study group showed consistency with HWE (both P > 0.10). The FcgRIIIB NA1/NA2 genotype distribution revealed significant deviation from HWE

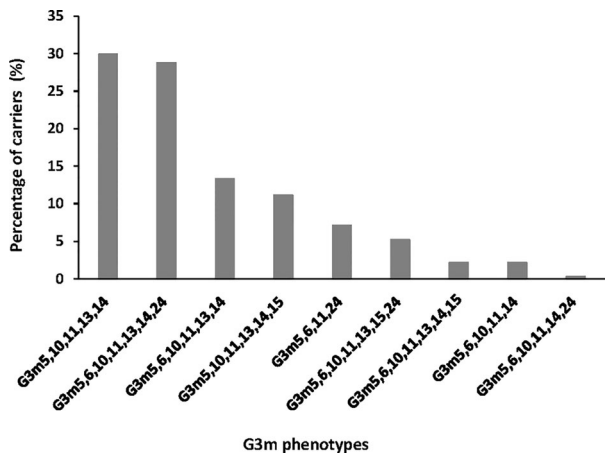

FIGURE 1 | Distribution of G3m phenotypes in the study group.

TABLE 2 | Association between G3m allotypes and malaria infections.

G3m allotypes	n	IRR	CI 95%	P value
G3m phenotypes with frequency at least 5%				
G3m5,10,11,13,14	110	0.952	0.793; 1.149	0.626
G3m5,6,10,11,13,14,24	**106**	**1.295**	**1.093; 1.535**	**0.003**
G3m5,6,10,11,13,14	49	0.821	0.646; 1.043	0.100
G3m5,10,11,13,14,15	41	0.252	0.653; 1.171	0.370
G3m5,6,11,24	26	0.938	0.674; 1.302	0.708
G3m5,6,10,11,13,15,24	19	0.853	0.577; 1.259	0.424
G3m single allotypes				
G3m6	217	1.089	0.918; 1.292	0.323
G3m10	342	1.065	0.765; 1.482	0.708
G3m13	333	1.016	0.777; 1.330	0.903
G3m14	323	1.109	0.858; 1.433	0.426
G3m15	68	0.855	0.684; 1.069	0.171
G3m24	**152**	**1.195**	**1.016; 1.406**	**0.031**

This table presents the zero inflated negative binomial model obtained through the control variables mother age (in years), child age (in months), bednet use, environmental exposure, and number of antenatal visits. The reference groups were the absence of the respective models for each G3m phenotype or single allotype. G3m5 and G3m11 were not analyzed individually because the whole population group carries them.
In bold: significant P value at the 0.05 threshold.

expectations which was also observed by Munde et al. (11) (P < 0.001, **Table 4**).

FcgR Polymorphisms and Malaria Infections

Association between FcgRIIA 131R/H, FcgRIIIA 176F/V, and FcgRIIIB NA1/NA2 polymorphisms and the number of malaria infections was determined using zero-inflated binomial regression models (with and without the interaction between the genetic and environmental variables).

Association Between FcgR Polymorphisms and Malaria Infections

We determined if individual FcgR polymorphisms were associated with malaria infections (**Table 5**). None of the FcgRIIA 131RH, 131RR, nor 131HH genotypes was associated with the number of malaria infections. However, infants carrying FcgRIIIA 176VV compared to FcgRIIIA 176FF had a higher risk of infection (n = 35, IRR = 1.344, 95% CI = 0.303;3.308, P = 0.035) while the FcgRIIIB NA1NA2 was associated with a lower number of infections compared to NA2NA2 (n = 131, IRR = 0.812, 95% CI = 0.670;0.985, P = 0.035).

Finally, we analyzed the influence of FcgRIIA/RIIIA/RIIIB genotype combinations on the occurrence of malaria infections. The distribution of these combinations is shown in **Figure 2**, where 25 out of the 27 possible combinations are present in the study group, the three most prevalent of them being 131RH/176FV/NA2NA2 (10.6%), 131RH/176FV/NA1NA1 (9.1%), and 131RH/176FF/NA1NA1 (8.9%). No individual presented the 131RR/176VV/NA1NA1 and 131RR/176VV/NA2NA2 genotype combinations. Compared to the reference 131RR/176FF/NA2NA2, a higher risk of malaria infection was found for carriers of the following genotype combinations: 131RH/176VV/NA1NA2 (n = 4, IRR = 2.035, 95% CI = 1.126;3.677, P = 0.019), 131HH/176VV/NA1NA2 (n = 9, IRR = 1.842, 95% CI =

TABLE 3 | Interaction between G3m allotypes—environmental exposure and malaria infections.

G3m allotypes*exposure to malaria	n	IRR	95% CI	P value
G3m phenotypes with frequency at least 5%				
Ref. No G3m5,10,11,13,14*low exposure				
G3m5,10,11,13,14*low exposure	61	0.893	0.677; 1.179	0.427
G3m5,10,11,13,14*high exposure	49	1.209	0.927; 1.577	0.160
Ref. No G3m5,6,10,11,13,14,24*low exposure				
G3m5,6,10,11,13,14,24*low exposure	50	1.056	0.803; 1.389	0.693
G3m5,6,10,11,13,14,24*high exposure	**56**	**1.648**	**1.312; 2.070**	**<0.0001**
Ref. No G3m5,6,10,11,13,14*low exposure				
G3m5,6,10,11,13,14*low exposure	19	1.097	0.750; 1.605	0.632
G3m5,6,10,11,13,14*high exposure	30	0.932	0.685; 1.269	0.659
Ref. No G3m5,10,11,13,14,15*low exposure				
G3m5,10,11,13,14,15*low exposure	21	1.042	0.658; 1.651	0.859
G3m5,10,11,13,14,15*high exposure	20	1.018	0.695; 1.491	0.925
Ref. No G3m5,6,11,24*low exposure				
G3m5,6,11,24*low exposure	12	1.095	0.656; 1.828	0.728
G3m5,6,11,24*high exposure	14	1.059	0.682; 1.644	0.797
Ref. No G3m5,6,10,11,13,15,24*low exposure				
G3m5,6,10,11,13,15,24*low exposure	11	0.784	0.420; 1.466	0.448
G3m5,6,10,11,13,15,24*high exposure	8	1.119	0.674; 1.859	0.663
G3m single allotypes				
Ref. No G3m6*low exposure				
G3m6*low exposure	101	1.087	0.837; 1.411	0.529
G3m6*high exposure	**116**	**1.350**	**1.059; 1.720**	**0.015**
Ref. No G3m10*low exposure				
G3m10*low exposure	171	0.895	0.537; 1.491	0.671
G3m10*high exposure	171	1.137	0.685; 1.886	0.618
Ref. No G3m13*low exposure				
G3m13*low exposure	167	0.807	0.540; 1.206	0.297
G3m13*high exposure	166	1.048	0.706; 1.555	0.814
Ref. No G3m14*low exposure				
G3m14*low exposure	160	1.056	0.703; 1.585	0.792
G3m14*high exposure	163	1.336	0.895; 1.993	0.156
Ref. No G3m15*low exposure				
G3m15*low exposure	37	0.897	0.623; 1.241	0.465
G3m15*high exposure	31	1.053	0.775; 1.432	0.737
Ref. No G3m24*low exposure				
G3m24*low exposure	74	1.020	0.789; 1.317	0.878
G3m24*high exposure	**78**	**1.479**	**1.183; 1.850**	**0.001**

This table presents the zero inflated negative binomial model obtained through the control variables mother age (in years), child age (in months), number of antenatal visits, and the use of bednet. The interaction between G3m allotypes and the environmental exposure was studied. The reference groups were indicated in each case.
In bold: significant P value at the 0.05 threshold.

1.016;3.339, P = 0.044), 131HH/176VV/NA2NA2 (n = 5, IRR = 1.933, 95% CI =1.087;3.437, P = 0.025) and 131HH/176FF/NA1NA1 (n = 7, IRR = 2.110, 95% CI = 1.039;4.283, P = 0.039) (**Table 6**). To explore the potential role of environmental exposure on this effect, we introduced an interaction term in the analyses.

Interaction Between FcgR Polymorphisms—Environmental Exposure and Malaria Infections

Results confirmed the higher risk of infection associated with FcgRIIIA 176VV compared to 176FF when exposed to high levels of mosquito bites (n = 17, IRR = 1.722, 95% CI = 1.213;2.445, P = 0.002). A similar pattern, barely significant, was observed for infants carrying FcgRIIIB NA2NA2 compared to FcgRIIIB NA1NA1 (n = 51, IRR = 1.372, 95% CI = 0.998;1.885, P = 0.051) (**Table 7**).

The analysis of the interaction between FcgRIIA/RIIIA/RIIIB combined genotypes and environmental exposure showed that infants carrying 131RH/176FV/NA1NA2 compared to 131RR/176FF/NA2NA2 have a trend towards a lower number of infections when exposed to low environmental risk levels (n = 13, IRR = 0.445, 95% CI = 0.194;1.017, P = 0.055). However, compared to the same reference, the carriage of 131HH/176FF/NA1NA1 was associated with a trend towards a higher risk of infection when exposed to low levels of exposure (n = 2, IRR = 2.622, 95% CI = 0.978;7.029, P = 0.055) (**Table 8**).

Detection of Gene-Gene and Gene-Environment Interactions by Generalized Multifactor Dimensionality Reduction (GMDR)

GMDR was used to screen the potential interactions among G3m and FcgR polymorphisms and to evaluate the impact of gene-exposure interaction on the risk of malaria infection.

Among all possible one- to four-locus models evaluated by the GMDR method, none reached the cut-off significance level of 0.05 when mosquito exposure was included as a covariate in the GMDR models, along with mother and child age, bednet use, and number of antenatal visits (data not shown). In contrast, when the exposure variable was combined with G3m and FcgR polymorphisms to detect potential gene-environment interactions, several models displayed significant results (**Table 9**).

The five-factor interaction model combining G3m, FcgRIIA, FcgRIIIA, FcgRIIIB polymorphisms, and mosquito exposure was the best model identified, with the maximum prediction accuracy of 62.70%, the maximum CV consistency of 10/10, and a sign test P-value of 0.001.

These results only hold for four G3m in single form and in combinations: G3m5,6,11,24, G3m5,6,10,11,13,15,24, G3m10, and G3m13. Models with lower prediction accuracies, though still significant, were obtained for G3m5,10,11,13,14,15 and G3m14 (TBA of 0.5602 and 0.6043, respectively; CVC = 10/10 and P = 0.011 for both). These results suggest significant gene-gene interactions between G3m and FcgR polymorphisms that are only revealed in an environment of high exposure to mosquito bites. The four-factor model including the three FcgR polymorphisms and mosquito exposure was the second best prediction model with a prediction accuracy of 60.82%, a maximum CV consistency of 10/10, and a sign test P-value of 0.001. The two-factor model involving the FcgRIIA 131R/H polymorphism and mosquito exposure (TBA of 0.604) reached an almost identical prediction accuracy.

We also conducted a linear regression analysis for the significant models associating G3m, FcgR and environmental exposure found in the GMDR analysis (**Table 9**, P in bold) in order to estimate the effect of such associations. GMDR analysis is

TABLE 4 | Distribution of FcgR genotypes in the study group.

	FcgRIIA 131 R/H			FcgRIIIA 176 F/V			FcgRIIIB NA1/NA2		
Variations	rs1801274			rs396991					
Genotypes	**HH**	**RH**	**RR**	**FF**	**FV**	**VV**	**NA1NA1**	**NA1NA2**	**NA2NA2**
Number of infants	80	194	95	165	165	35	106	131	116
(%)	(21.7%)	(52.6%)	(25.7%)	(45.2%)	(45.2%)	(9.6%)	(30.0%)	(37.1%)	(32.9%)
Minor allele frequency		0.48			0.32			0.48	
(minor allele)		(H)			(V)			(NA1)	
HWE test [a]		χ^2 = 1.04 (P > 0.10)			χ^2 = 0.46 (P > 0.10)			χ^2 = 23.35 (P < 0.001)	
χ^2 (P-value, df = 2)									

[a]*Hardy-Weinberg equilibrium test.*

TABLE 5 | Association between each FcgRIIA, FcgRIIIA, and FcgRIIIB genotype and malaria infections.

FcgR polymorphisms	n	IRR	95% CI	P value
FcgRIIA 131 R/H model				
131RR (reference)	95			
131RH	194	1.168	0.955; 1.429	0.129
131HH	80	8.435	0.929; 1.523	0.929
FcgRIIIA 176 F/V model				
176FF (reference)	165			
176FV	165	0.948	0.200; 1.069	0.071
176VV	**35**	**1.344**	**0.303; 3.308**	**0.035**
FcgRIIIB NA1/NA2 model				
NA2NA2 (reference)	116			
NA1NA2	**131**	**0.812**	**0.670; 0.985**	**0.035**
NA1NA1	106	0.903	0.735; 1.109	0.332

This table presents the zero inflated negative binomial individual models obtained through the control variables mother age (in years), child age (in months), number of antenatal visits, environmental exposure, and bednet use. The references are indicated for FcgRIIA R/H, FcgRIIIA F/V, and FcgRIIIB NA1/NA2.
In bold: significant P value at the 0.05 threshold.

TABLE 6 | Association between FcgRIIA/FcgRIIIA/FcgRIIIB combined genotypes and malaria infections.

FcgR polymorphisms combination models	n	IRR	95% CI	P value
131RR/176FF/NA2NA2 (reference)	21			
131RR/176FF/NA1NA2	30	1.091	0.684; 1.739	0.713
131RR/176FF/NA1NA1	9	1.456	0.842; 2.520	0.179
131RR/176FV/NA2NA2	12	1.426	0.819; 2.481	0.209
131RR/176FV/NA1NA2	10	0.495	0.214; 1.148	0.102
131RR/176FV/NA1NA1	4	0.980	0.397; 2.415	0.965
131RR/176VV/NA1NA2	1	1.053	0.306; 3.616	0.934
131RH/176FF/NA2NA2	22	1.459	0.934; 2.279	0.096
131RH/176FF/NA1NA2	26	1.036	0.655; 1.639	0.878
131RH/176FF/NA1NA1	31	1.331	0.854; 2.075	0.206
131RH/176FV/NA2NA2	37	1.365	0.879; 2.119	0.165
131RH/176FV/NA1NA2	23	1.014	0.624; 1.649	0.953
131RH/176FV/NA1NA1	32	1.186	0.748; 1.881	0.467
131RH/176VV/NA2NA2	6	0.866	0.295; 2.539	0.795
131RH/176VV/NA1NA2	**4**	**2.035**	**1.126; 3.677**	**0.019**
131RH/176VV/NA1NA1	5	0.684	0.203; 2.307	0.541
131HH/176FF/NA2NA2	5	1.919	0.922; 3.995	0.081
131HH/176FF/NA1NA2	6	0.628	0.214; 1.839	0.397
131HH/176FF/NA1NA1	**7**	**2.110**	**1.039; 4.283**	**0.039**
131HH/176FV/NA2NA2	7	1.064	0.453; 2.496	0.886
131HH/176FV/NA1NA2	20	1.180	0.727; 1.917	0.501
131HH/176FV/NA1NA1	14	0.780	0.436; 1.395	0.403
131HH/176VV/NA2NA2	**5**	**1.933**	**1.087; 3.437**	**0.025**
131HH/176VV/NA1NA2	**9**	**1.842**	**1.016; 3.339**	**0.044**
131HH/176VV/NA1NA1	4	1.838	0.877; 3.851	0.106

This table presents the zero inflated negative binomial model obtained through the control variables age (mother and child), antenatal visits, mosquito exposure, and mosquito net possession for the FcgRIIA/FcgRIIIA/FcgRIIIB genotype models. The reference was the absence of HH/FF/NA2NA2.
In bold: significant P value at the 0.05 threshold.

based on linear regression. Therefore, using linear regression models was perfectly suited to quantify the effect detected by GMDR analysis. Consistent with the GMDR analysis, the linear regression models showed a higher risk of malaria infection in carriers of 131RR/176FF/NA2NA2/G3m5,6,11,24 and 131HH/176VV/NA1NA2/G3m5,6,10,11,13,15,24 combinations, when exposed to a high-risk environment (regression coefficient = 4.804, P = 0.032 and regression coefficient = 5.444, P = 0.015, respectively) (**Supplementary Table 1**). Linear models confirmed, also, a higher risk of malaria infection in carriers of G3m10 and G3m13 combined to 131HH/176FF/NA1NA1 in a low-risk environment with a regression coefficient of 6.160 (P = 0.039) and 6.248 (P = 0.044), respectively (**Supplementary Table 2**). The genotype combination 131HH/176FF/NA1NA1 indeed showed a trend towards a higher risk of infection in a low-risk environment (**Table 8**).

DISCUSSION

We studied the combined impact of FcgRIIA, FcgRIIIA, and FcgRIIIB polymorphisms and IgG G3m allotypes on malaria susceptibility in early life in Benin. First, we studied separately the influence of IgG G3m allotypes and of FcgRs polymorphisms on the number of *P. falciparum* infections during an 18 months clinical and parasitological follow-up of newborns. Second, the influence of combined IgG G3m allotypes and FcgRs polymorphisms was assessed. We identified an increased risk of *P. falciparum* infection in infants carrying particular FcgRIIA 131R/H – FcgRIIIA 176F/V – FcgRIIIB NA1/NA2 genotypes combined to G3m5,6,11,24 or G3m5,6,10,11,13,15,24 phenotypes or to G3m10 or G3m13 single allotypes. These

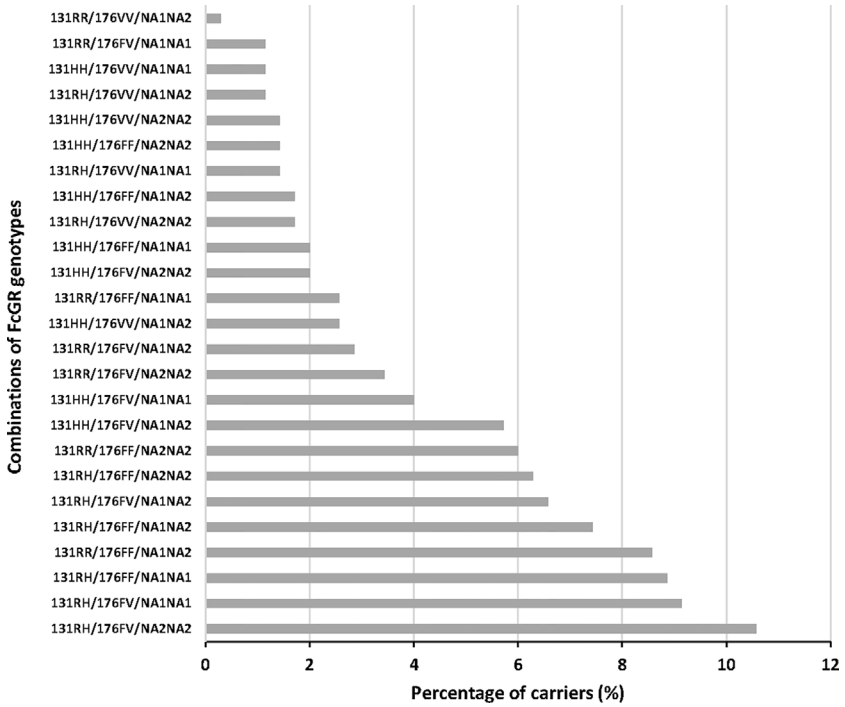

FIGURE 2 | Distribution of FcgRIIA/FcgRIIIA/FcgRIIIB phenotypes in the study group.

observations were reinforced by the application of two complementary statistical approaches (GMDR method and linear regression analysis), allowing to take into account the individual risk of exposure to malaria. **Figure 3** presents a summary of the main results.

No diversity was observed among infants for the G1m allotypes, since all infants were G1m1 and G1m17 positive; therefore, the analysis focused on the G3m diversity present on IgG3. Our results showed an increased risk of malaria infections associated with the carriage of the G3m5,6,10,11,13,14,24 phenotype. It should be pointed out that the presence of G3m24 in this combination could play an important role as it was also associated with a higher risk to be infected by *P. falciparum* when considered as a single allotype. The risk effect of some allotypes was accentuated when infants were highly exposed to mosquito bites. For example, the effect of G3m6 appeared only when the interaction with the exposure variable was considered. These results suggest that the G3m6 effect is accentuated in conditions of high mosquito exposure and the risk associated with G3m5,6,10,11,13,14,24 could be linked to the presence of both G3m6 and G3m24.

The interactions observed between G3m allotypes and mosquito exposure could be related to the quantity of anti-malarial IgG3 that increased following repeated infections with *P. falciparum*. IgG3 antibodies were shown to be protective against malaria and they can act directly by limiting host cell invasion or indirectly *via* their Fc-mediated effector functions (8, 42). Therefore, an increased level of IgG3 harboring specific G3m allotypes, in case of high mosquito exposure, could facilitate the identification of the risk effect linked to these characteristics. Of note, IgG allotypes were found to correlate with serum IgG levels (19, 43) but also with the switching between IgG isotypes suggesting that IgG allotypes may affect the humoral antibody response. Moreover, it was recently demonstrated that allotypic variants within the IgG3 subclass substantially affect FcgRIIIA binding and Antibody-Dependent Cellular Cytotoxicity (44). To our knowledge, no work has previously shown associations between Gm phenotypes comprising G3m24 or G3m24 alone with a higher risk of malaria infections, while G3m24 is prevalent among sub-Saharan African populations (45, 46). In contrast, Gm phenotypes including G3m6 have been already associated with malaria susceptibility (10, 17, 18). Indeed, the G3m5,6,13,14 phenotype was associated with a higher incidence of uncomplicated malaria (18). It is interesting to note that G3m6 allotype is rare among Fulani, who are less susceptible to malaria than other sympatric ethnic groups (17). However, we also demonstrated the existence of an inverse relationship between the carriage of the G3m5,6,13,14 phenotype and the presence of uncomplicated malaria (10) in the Fon ethnic group. Given that both polymorphisms in the IgG3 heavy chain gene and FcgR can influence the IgG binding on immunoglobulin Fc-receptors and impact immunity to malaria through ADCC, ADCI, or phagocytosis of malaria parasites, the interpretation of results coming from separate investigations of these distinct polymorphisms remains challenging.

TABLE 7 | Interaction between FcgRIIA, FcgRIIIA, and FcgRIIIB genotypes—environmental exposure and malaria infections.

FcgR genotypes*exposure to malaria	n	IRR	95% CI	P value
FcgRIIA model				
FcgRIIA 131RR*low exposure (reference)	46			
FcgRIIA 131RR*high exposure	49	0.824	0.587; 1.155	0.263
FcgRIIA 131RH*low exposure	104	0.885	0.668; 1.173	0.399
FcgRIIA 131RH*high exposure	90	1.266	0.970; 1.652	0.081
FcgRIIA 131HH*low exposure	34	0.972	0.656; 1.440	0.890
FcgRIIA 131HH*high exposure	46	1.213	0.892; 1.650	0.218
FcgRIIIA model				
FcgRIIIA 176FF*low exposure (reference)	76			
FcgRIIIA 176FF*high exposure	89	1.072	0.847; 1.357	0.559
FcgRIIIA 176FV*low exposure	78	0.833	0.640; 1.083	0.174
FcgRIIIA 176FV*high exposure	87	1.124	0.884; 1.430	0.337
FcgRIIIA 176VV*low exposure	18	1.022	0.646; 1.616	0.924
FcgRIIIA 176VV*high exposure	**17**	**1.722**	**1.213; 2.445**	**0.002**
FcgRIIIB model				
FcgRIIIB NA2NA2*low exposure (reference)	65			
FcgRIIIB NA2NA2*high exposure	51	1.227	0.932; 1.617	0.144
FcgRIIIB NA1NA2*low exposure	66	0.814	0.610; 1.085	0.161
FcgRIIIB NA1NA2*high exposure	65	0.997	0.764; 1.299	0.983
FcgRIIIB NA1NA1*low exposure	48	0.894	0.649; 1.233	0.497
FcgRIIIB NA1NA1*high exposure	58	1.115	0.847; 1.468	0.436
FcgRIIIB NA1NA1*low exposure (reference)	48			
FcgRIIIB NA2NA2*high exposure	51	1.372	0.998; 1.885	0.051

This table presents the zero inflated negative binomial model obtained through the control variables mother age (in years), child age (in months), number of antenatal visits mosquito, and bednet use. The interaction between FcgR polymorphisms and environmental exposure was studied. The reference was the absence of estimations in FcgRIIA R/H, FcgRIIIA F/V, and FcgRIIIB NA1/NA2.
In bold: significant P value at the 0.05 threshold; underlined: trend of significance at the P value threshold of 0.05.

TABLE 8 | Interaction between FcgRIIA/RIIIA/RIIIB combined genotypes—environmental exposure and malaria infections.

FcgR genotypes combinations*exposure to malaria	n	IRR	95% CI	P value
131RR/176FF/NA2NA2*low exposure (reference)	9			
131RR/176FF/NA2NA2*high exposure	12	0.737	0.356; 1.524	0.411
131RR/176FF/NA1NA2*low exposure	10	0.947	0.498; 1.801	0.869
131RR/176FF/NA1NA2*high exposure	16	0.729	0.354; 1.503	0.393
131RR/176FF/NA1NA1*low exposure	5	1.078	0.508; 2.284	0.844
131RR/176FF/NA1NA1*high exposure	4	1.293	0.573; 2.917	0.535
131RR/176FV/NA2NA2*low exposure	7	1.052	0.513; 2.158	0.889
131RR/176FV/NA2NA2*high exposure	5	1.230	0.486; 3.113	0.662
131RR/176FV/NA1NA2*low exposure	3	0.219	0.028; 1.692	0.146
131RR/176FV/NA1NA2*high exposure	7	0.488	0.185; 1.286	0.147
131RR/176FV/NA1NA1*low exposure	3	0.880	0.284; 2.726	0.825
131RR/176FV/NA1NA1*high exposure	1	0.621	0.138; 2.793	0.535
131RR/176VV/NA1NA2*low exposure	1	0.796	0.224; 2.821	0.724
131RH/176FF/NA2NA2*low exposure	14	1.018	0.536; 1.933	0.955
131RH/176FF/NA2NA2*high exposure	8	1.385	0.728; 2.634	0.320
131RH/176FF/NA1NA2*low exposure	11	0.801	0.403; 1.595	0.529
131RH/176FF/NA1NA2*high exposure	15	0.883	0.464; 1.680	0.706
131RH/176FF/NA1NA1*low exposure	10	0.998	0.478; 2.084	0.997
131RH/176FF/NA1NA1*high exposure	21	1.176	0.638; 2.169	0.602
131RH/176FV/NA2NA2*low exposure	23	0.952	0.504; 1.799	0.881
131RH/176FV/NA2NA2*high exposure	14	1.287	0.685; 2.418	0.431
131RH/176FV/NA1NA2*low exposure	13	0.445	0.194; 1.017	0.055
131RH/176FV/NA1NA2*high exposure	10	1.147	0.598; 2.201	0.679
131RH/176FV/NA1NA1*low exposure	17	0.752	0.381; 1.484	0.412
131RH/176FV/NA1NA1*high exposure	15	1.207	0.629; 2.318	0.571
131RH/176VV/NA2NA2*low exposure	5	0.642	0.206; 2.001	0.445
131RH/176VV/NA1NA2*low exposure	3	1.778	0.720; 4.386	0.211
131RH/176VV/NA1NA2*high exposure	3	1.675	0.761; 3.688	0.200
131RH/176VV/NA1NA1*low exposure	2	0.381	0.049; 2.933	0.355
131RH/176VV/NA1NA1*high exposure	3	0.733	0.164; 3.280	0.685
131HH/176FF/NA2NA2*low exposure	2	1.013	0.286; 3.591	0.983
131HH/176FF/NA2NA2*high exposure	3	1.855	0.746; 4.609	0.183
131HH/176FF/NA1NA2*low exposure	3	0.481	0.134; 1.719	0.260
131HH/176FF/NA1NA2*high exposure	3	0.454	0.058; 3.496	0.449
131HH/176FF/NA1NA1*low exposure	2	2.622	0.978; 7.029	0.055
131HH/176FF/NA1NA1*high exposure	5	1.332	0.498; 3.559	0.567
131HH/176FV/NA2NA2*high exposure	7	0.943	0.375; 2.371	0.901
131HH/176FV/NA1NA2*low exposure	10	1.033	0.504; 2.118	0.927
131HH/176FV/NA1NA2*high exposure	10	0.955	0.486; 1.876	0.895
131HH/176FV/NA1NA1*low exposure	6	0.362	0.103; 1.275	0.114
131HH/176FV/NA1NA1*high exposure	8	0.791	0.381; 1.641	0.530
131HH/176VV/NA2NA2*low exposure	2	1.520	0.535; 4.319	0.431
131HH/176VV/NA2NA2*high exposure	3	1.724	0.835; 3.559	0.140
131HH/176VV/NA1NA2*low exposure	4	0.366	0.047; 2.828	0.336
131HH/176VV/NA1NA2*high exposure	5	1.888	0.922; 3.867	0.082
131HH/176VV/NA1NA1*low exposure	2	1.328	0.430; 4.099	0.622
131HH/176VV/NA1NA1*high exposure	2	1.752	0.673; 4.562	0.251

This table presents the zero inflated negative binomial model, with the interaction between FcgR and environmental exposure obtained through the control variables mother age (in years), child age (in months), number of antenatal visits, and use of bednet.
Underlined: trend of significance at the P value threshold of 0.05.

FcgRs provide a crucial link between the humoral and cellular immune responses. Polymorphisms which alter the affinity of FcgRs in binding IgG subclasses have been described. In human, FcgRII and FcgRIII are known to bind IgG subclasses. Regarding FcgRIIA 131R/H polymorphisms, our results revealed no significant association with malaria infections whether or not the mosquito exposure factor was taken into account. On the other side, a malaria risk associated with the FcgRIIIA 176VV genotype was observed, which was strengthened in conditions of high exposure to mosquitoes. These results differed from those of Omi et al. (47) who found no relation between FcgRIIIA 176F/V polymorphism and the severity of malaria in Thai people (47) and of Munde et al. (11) who showed no relation between FcgRIIIA 176F/V and severe malarial anemia (SMA) (11). The differences in the size of the population groups, the ethnic origin and genetic diversity of the populations and the clinical definition of malaria used, may preclude a rigorous comparison between studies. In other cases, the FcgRIIIA 176V allele was identified as a genetic risk factor for the development of atopic diseases (48) or for generalized aggressive periodontitis (39). It has been shown that the 176V variant improved the FcgRIIIA affinity for IgG1 and IgG2 (49). Regarding our results, this same variant could be associated with a lower affinity to IgG3, thus reducing the effectiveness of the antimalarial response. Finally, our results showed an association between the FcgRIIIB NA1NA2 genotype and protection against malaria when compared to the carriage of NA2NA2, while in conditions of high mosquito exposure, the NA2NA2 genotype was associated with a higher risk compared to NA1NA1. The polymorphic expression of FcgRIIIB NA1/NA2 influences the phagocytic capacity of neutrophils and Salmon et al. (50) already showed a decreased phagocytosis in relation to NA2NA2 compared to NA1NA1 (50). In line with these results, other studies showed a risk for malaria (30) or cerebral malaria (29) associated with the carriage of the FcgRIIIB NA2 variant.

TABLE 9 | Association between FcgR polymorphisms, G3m phenotypes, and malaria infections: Results of the GMDR analysis when considering environmental exposure as an interaction variable.

No. of variables considered	Best model	Testing balanced accuracy(TBA)	Sign test P-value	Cross-validation consistency (CVC)
1	environmental exposure	0.6161	**0.0107**	10/10
2	FcgRIIA, environmental exposure	0.6038	**0.0010**	9/10
3	FcgRIIA, FcgRIIIA, environmental exposure	0.4871	0.6230	5/10
4	FcgRIIA, FcgRIIIA, FcgRIIIB, environmental exposure	0.6082	**0.0010**	10/10
5	G3m[†], FcgRIIA, FcgRIIIA, FcgRIIIB, environmental exposure	0.6270	**0.0010**	10/10

All models are adjusted for mother age (in years), child age (in months), bednet use, and number of antenatal visits.

[†]These results were obtained only for the four following G3m allotypes and allotype combinations: G3m5,6,11,24, G3m5,6,10,11,13,15,24, G3m10, and G3m13 (each considered as presence/absence). The five-factor models were also significant for G3m5,10,11,13,14,15 (TBA = 0.5602; CVC = 10/10) and G3m14 (TBA = 0.6043; CVC = 10/10) although at a lesser degree (sign test P = 0.0107 in both cases).

In bold: significant P value at the 0.05 threshold.

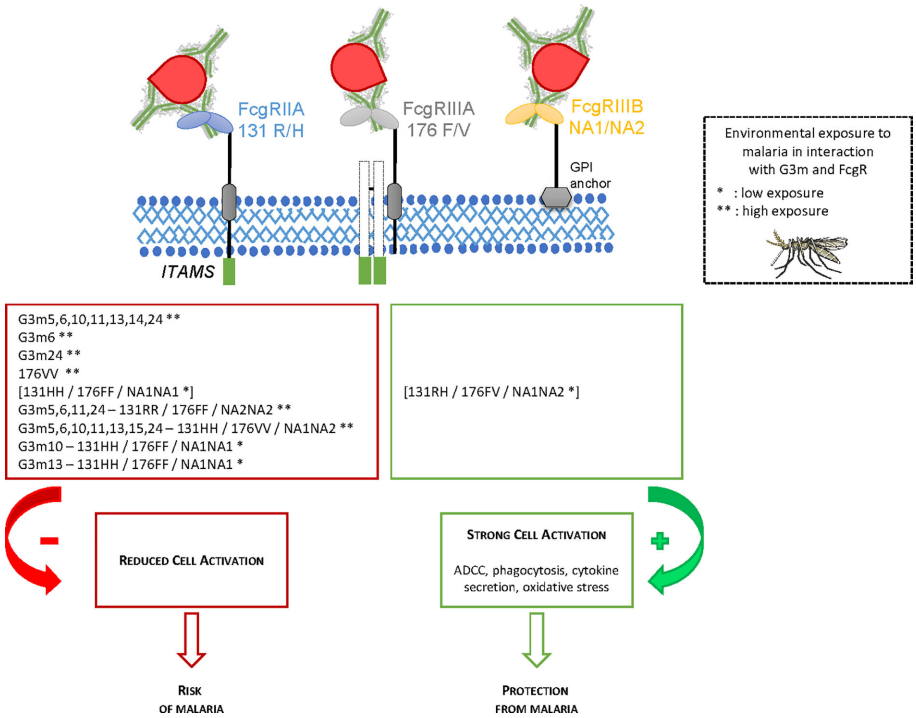

FIGURE 3 | Summary of the main findings of the study.

FcgR receptors act synergistically by crosslinking. The additive effects of the host FcgRIIA/FcgRIIIA/FcgRIIIB genotypes might impact the immune response to *P. falciparum* and therefore affect the outcome of the disease. This synergy function results in phagocytosis of immunoglobulin-opsonized immune complexes and in the stimulation of neutrophils degranulation, which leads to the production of reactive oxygen species (ROS). The absence in our study of relationship with malaria infection involving FcgRIIA/FcgRIIIA genotype combinations compared to FcgRIIA/FcgRIIIA/FcgRIIIB ones may reflect a particular synergy between FcgRIIA and FcgRIIIB receptors (**Table 9**). Indeed, it has been shown that FcgRIIA and FcgRIIIB can interact functionally to trigger neutrophils by means of an IgG mediated response (51–53). Moreover, FcgRIIA is considered essential for the induction of effector functions, and the abundance of FcgRIIIB can guarantee an effective interaction with IgG complexes (54). As already suggested, the HWE deviation observed for FcgRIIIB could be due to unidentified mutations likely resulting from disease-related evolutionary selection pressure exerted by *P. falciparum* and potentially by other infectious diseases occurring in the population (11).

It has been shown that FcgRIIA 131H contributes to an efficient binding to IgG2 and IgG3 as opposed to 131R (23) and also that IgG2 and IgG3 contribute to individual resistance to malaria (8). The 131H variant was found more prevalent in the Fulani people of Daraweesh, a village in eastern Sudan, who are less affected by clinical malaria (55). The same variant was

associated with protection from malaria infection in Indian individuals at least 5 years old (56) and with protection against high parasitemia both in African and Asian people (31). However it was associated with a higher risk in a cohort of Gambian children less than 5 years (57). In comparison, the 131R variant has been shown to play a major role in ADRB (58, 59) and is associated with a low phagocytic activity and poor immune complex clearance (60). In genotype analysis, the higher risk associated with 131RH/176VV/NA1NA2, 131HH/176VV/NA2NA2, 131HH/176VV/NA1NA2 and 131HH/176FF/NA1NA1 carriage compared to 131RR/176FF/NA2NA2 may be explained by the presence of FcgRIIIA 176VV in the three first genotype combinations. Moreover, the joint presence of FcgRIIA 131H variant in all combinations is in line with results from some of the studies reported above, according to which this variant is less protective than the 131R one (57).

Since G3m and FcgR polymorphisms act individually on malaria infections, it is plausible that their combined polymorphisms act in synergy against malaria infections. This aspect has never been studied before and the MDR method was used to precisely explore it. The G3m5,6,11,24 – 131RR/176FF/NA2NA2 and G3m5,6,10,11,13,15,24 – 131HH/176VV/NA1NA2 combinations were the most significant G3m/FcgR ones associated with malaria (at risk according to the linear regressions) when taking into account the interaction with the environmental variable of exposure to mosquito bites, according to the GMDR analysis. This is particularly interesting in view of the preceding results, indicative of a cumulative risk linked to the double carriage of G3m6 and G3m24 joined to either FcgRIIIA 176VV or FcgRIIIB NA2NA2. Moreover, linear regression of these interactions showed high regression coefficients (4.804 and 5.444). Thus, these interactions are at risk under conditions of high exposure to mosquito bites because of the cumulative presence of G3m6 and G3m24 in one hand and of the FcgRIIIA 176VV and FcgRIIIB NA2NA2 genotypes in another hand. The malaria risk under conditions of low exposure involving G3m10 - FcgRIIA 131HH/FcgRIIIA 176FF/FcgRIIIB NA1NA1 and G3m13 - FcgRIIA 131HH/FcgRIIIA 176FF/FcgRIIIB NA1NA1 is interesting to note since at the individual level, G3m10 and G3m13 did not show any significant association. Thus, this result could reflect the fact that the effect found is only due to the influence of the FcgR association. Moreover, the linear regression showed that the FcgR associations concerned were defined at risk in the previous results.

The efficacy of IgG3 response can be explained by FcgR affinity but also by the nature of targeted antigens. High concentrations of AMA1, MSP1, MSP2-FC27, MSP3, GLURP-R2-specific IgG3 were found in infants able to control asymptomatic infections (61). Of course, other key antigens expressed during the different steps of the *P. falciparum* cycle life probably participate to the control of the parasite growth. Functional assays will clarify the mechanisms and antigens involved in malaria protection. These answers can probably also vary depending immune system cells. For example, FcgRIIIB is present on neutrophils and not monocytes, natural killers react more with FcgRIIIA compared to FcgRIIA, while monocytes and macrophages present both FcgRIIA and FcgRIIIA.

This study showed the importance of polymorphisms in both FcgR and IgG in the modulation of the risk of malaria infections in Beninese infants. It would then be interesting to look at the CNV (Copy Number Variations) of these polymorphisms and their influence on risk or protection against malaria. CNV are polymorphisms represented by DNA segments that differ among individuals due to suppression, insertion, inversion, duplication, or complex recombination (62). Recent studies have highlighted the relationship between CNV and disease: FcgRIIIB low CNV was associated with systemic lupus erythematosus risk (63) while for Chen et al. (64) a low FcgRIIIA CNV was positively associated with lupus and rheumatoid arthritis and a low FcgRIIIB CNV, with a risk of lupus but not rheumatoid arthritis (64). It would be interesting, thus, to explore the role of CNV in FcgR receptors in individual variation of malaria susceptibility.

In summary, the current study demonstrates that some combined G3m-FcgR polymorphisms are associated with a malaria risk and that this risk is even more pronounced in case of high mosquito exposure. The results highlight the relevance of studying combined IgG heavy chain/FcgR polymorphisms in relation to *P. falciparum* malaria as one or the other, or both, may influence the individual susceptibility to infection. Understanding the functional diversity within IgG subclasses may shed light on associations found with infectious diseases or auto-immune diseases and potentially initiate new strategies to improve therapeutic antibodies.

DATA AVAILABILITY STATEMENT

The data presented in the study are deposited in the Open Science Framework repository (https://osf.io/), with accession number gmr4s.

ETHICS STATEMENT

The studies involving human participants were reviewed and approved by the Abomey-Calavi's institutional review board and the IRD's Consultative Ethics Committee. Written informed consent to participate in this study was provided by the participants' legal guardian/next of kin.

AUTHOR CONTRIBUTIONS

CD, DC, and FM-N conceived and designed the project. AF, EG, DC, and FM-N performed the laboratory experiments. JM and J-MD brought technical support or result validation. AF, CD, AS, AG, DC, and FM-N performed statistical analysis. AF, CD, DC, and FM-N wrote the paper. All authors contributed to the article and approved the submitted version.

FUNDING

This work was supported by the Agence Nationale de la Recherche (ANR) Santé Environnement Santé Travail (SEST 2006; 040 01). The Université de Paris awarded a PhD scholarship to AF.

ACKNOWLEDGMENTS

The authors are grateful to all women and infants of Tori Bossito who agreed to participate in this project, to field supervisors and community health workers of contributing villages, to midwives, nurses, and health auxiliaries of the three health centers, as well as to laboratory technicians of Tori Bossito for their collaboration. The authors would like to thank the Faculté des Sciences de la Santé (FSS), the Institut des Sciences Biomédicales Appliquées de Cotonou (ISBA), the Programme National de Lutte contre le Paludisme (PNLP) for their institutional support.

SUPPLEMENTARY MATERIAL

The Supplementary Material for this article can be found online at: https://www.frontiersin.org/articles/10.3389/fimmu.2020.608016/full#supplementary-material

REFERENCES

1. World Health Organization. (2019). Available at: https://www.who.int/malaria/publications/world-malaria-report-2018/report/fr/ (Accessed December 2019).
2. Cohen S, Carrington S, McGregor IA. Gamma-globulin and acquired immunity to human malaria. *Nature* (1961) 192:733–7. doi: 10.1038/192733a0
3. Sabchareon A, Burnouf T, Ouattara D, Attanath P, Bouharoun-Tayoun H, Chantavanich P, et al. Parasitologic and clinical human response to immunoglobulin administration in falciparum malaria. *Am J Trop Med Hyg* (1991) 45:297–308. doi: 10.4269/ajtmh.1991.45.297
4. Aribot G, Rogier C, Sarthou JL, Trape JF, Balde AT, Druilhe P, et al. Pattern of immunoglobulin isotype response to Plasmodium falciparum blood-stage antigens in individuals living in a holoendemic area of Senegal (Dielmo, west Africa). *Am J Trop Med Hyg* (1996) 54:449–57. doi: 10.4269/ajtmh.1996.54.449
5. Beck HP, Felger I, Genton B, Alexander N, Al-Yaman F, Anders RF, et al. Humoral and cell-mediated immunity to the Plasmodium falciparum ring-infected erythrocyte surface antigen in an adult population exposed to highly endemic malaria. *Infect Immun* (1995) 63:596–600. doi: 10.1128/IAI.63.2.596-600.1995
6. Ferreira MU, Kimura EAS, Katzin AM, Santos-Neto LL, Ferrari JO, Villalobos JM, et al. The IgG-subclass distribution of naturally acquired antibodies to Plasmodium falciparum, in relation to malaria exposure and severity. *Ann Trop Med Parasitol* (1998) 92:245–56. doi: 10.1080/00034989859807
7. Dechavanne C, Dechavanne S, Sadissou I, Lokossou AG, Alvarado F, Dambrun M, et al. Associations between an IgG3 polymorphism in the binding domain for FcRn, transplacental transfer of malaria-specific IgG3, and protection against Plasmodium falciparum malaria during infancy: a birth cohort study in Benin. *PloS Med* (2017) 14:e1002403. doi: 10.1371/journal.pmed.1002403
8. Courtin D, Oesterholt M, Huismans H, Kusi K, Milet J, Badaut C, et al. The quantity and quality of African children's IgG responses to merozoite surface antigens reflect protection against Plasmodium falciparum malaria. *PloS One* (2009) 4:e7590. doi: 10.1371/journal.pone.0007590
9. Beeson JG, Drew DR, Boyle MJ, Feng G, Fowkes FJ, Richards JS. Merozoite surface proteins in red blood cell invasion, immunity and vaccines against malaria. *FEMS Microbiol Rev* (2016) 40:343–72. doi: 10.1093/femsre/fuw001
10. Migot-Nabias F, Noukpo JM, Guitard E, Doritchamou J, Garcia A, Dugoujon JM. Imbalanced distribution of GM immunoglobulin allotypes according to the clinical presentation of Plasmodium falciparum malaria in Beninese children. *J Infect Dis* (2008) 198:1892–5. doi: 10.1086/593210
11. Munde EO, Okeyo WA, Raballah E, Anyona SB, Were T, Ong'echa JM, et al. Association between Fcg receptor IIA, IIIA and IIIB genetic polymorphisms and susceptibility to severe malaria anemia in children in western Kenya. *BMC Infect Dis* (2017) 17:289. doi: 10.1186/s12879-017-2390-0
12. De Lange GG. Polymorphisms of human immunoglobulins: Gm, Am, Em and Km allotypes. *Exp Clin Immunogenet* (1989) 6:7–17.
13. Lefranc MP, Lefranc G. Human Gm, Km, and Am allotypes and their molecular characterization: a remarkable demonstration of polymorphism. *Methods Mol Biol* (2012) 882:635–80. doi: 10.1007/978-1-61779-842-9_34
14. Lefranc M-P, Giudicelli V, Duroux P, Jabado-Michaloud J, Folch G, Aouinti S. IMGT®, the international ImMunoGeneTics information system® 25 years on. *Nucleic Acids Res* (2015) 43(Database issue):D413–22. doi: 10.1093/nar/gku1056
15. Dugoujon JM, Hazout S, Loirat F, Mourrieras B, Crouau-Roy B, Sanchez-Mazas A. GM haplotype diversity of 82 populations over the world suggests a centrifugal model of human migrations. *Am J Phys Anthropol* (2004) 125:175–92. doi: 10.1002/ajpa.10405
16. Facer CA. Direct antiglobulin reactions in Gambian children with P. falciparum malaria. III. Expression of IgG subclass determinants and genetic markers and association with anaemia. *Clin Exp Immunol* (1980) 41:81–90.
17. Pandey JP, Nasr A, Rocca KM, Troye-Blomberg M, Elghazali G. Significant differences in GM allotype frequencies between two sympatric tribes with markedly differential susceptibility to malaria. *Parasite Immunol* (2007) 29:267–9. doi: 10.1111/j.1365-3024.2007.00938.x
18. Giha HA, Nasr A, Iriemenam NC, Arnot D, Troye-Blomberg M, Theander TG, et al. Antigen-specific influence of GM/KM allotypes on IgG isotypes and association of GM allotypes with susceptibility to Plasmodium falciparum malaria. *Malar J* (2009) 8:306. doi: 10.1186/1475-2875-8-306
19. Pandey JP, Morais GC, Fontes JFC, Braga EM. Immunoglobulin GM 3 23 5,13,14 phenotype is strongly associated with IgG1 antibody responses to Plasmodium vivax vaccine candidate antigens PvMSP1-19 and PvAMA-1. *Malar J* (2010) 9:229. doi: 10.1186/1475-2875-9-229
20. Ravetch J. In vivo veritas: the surprising roles of Fc receptors in immunity. *Nat Immunol* (2010) 11:183–5. doi: 10.1038/ni0310-183
21. Hogarth PM, Pietersz GA. Fc receptor-targeted therapies for the treatment of inflammation, cancer and beyond. *Nat Rev Drug Discovery* (2012) 11:311–31. doi: 10.1038/nrd2909
22. Parren PW, Warmerdam PA, Boeije LC, Arts J, Westerdaal NA, Vlug A, et al. On the interaction of IgG subclasses with the low affinity Fc gamma RIIa (CD32) on human monocytes, neutrophils, and platelets. Analysis of a functional polymorphism to human IgG2. *J Clin Invest* (1992) 90:1537–46. doi: 10.1172/JCI116022
23. Vidarsson G, Dekkers G, Rispens T. IgG subclasses and allotypes : from structure to effector functions. *Front Immunol* (2014) 5:520:520. doi: 10.3389/fimmu.2014.00520
24. Ouma C, Keller CC, Opondo DA, Were T, Otieno RO, Otieno MF, et al. Association of FCgamma receptor IIA (CD32) polymorphism with malarial anemia and high-density parasitemia in infants and young children. *Am J Trop Med Hyg* (2006) 74:573–7. doi: 10.4269/ajtmh.2006.74.573
25. Yoo EM, Morrison S. "Antibody Engineering", in Encyclopedia of Industrial Biotechnology, Bioprocess, Bioseparation, and Cell Technology, ed. John Wiley & Sons. (2010) 1:332–43. doi: 10.1002/9780470054581.eib044
26. Huizinga TW, Kleijer M, Tetteroo PA, Roos D, von dem Borne AE. Biallelic neutrophil Na-antigen system is associated with a polymorphism on the phospho-inositol-linked Fc gamma receptor III (CD16). *Blood* (1990) 75:213–7. doi: 10.1182/blood.V75.1.213.bloodjournal751213
27. Bux J, Kissel K, Hofmann C, Santoso S. The use of allele-specific recombinant Fc gamma receptor IIIb antigens for the detection of granulocyte antibodies. *Blood* (1999) 93:357–62. doi: 10.1182/blood.V93.1.357.401k39_357_362

28. Huizinga TW, Kerst M, Nuyens JH, Vlug A, von dem Borne AE, Roos D, et al. Binding characteristics of dimeric IgG subclass complexes to human neutrophils. *J Immunol* (1989) 142:2359–64.
29. Omi K, Ohashi J, Patarapotikul J, Hananantachai H, Naka I, Looareesuwan S, et al. Fcgamma receptor IIA and IIIB polymorphisms are associated with susceptibility to cerebral malaria. *Parasitol Int* (2002) 51:361–6. doi: 10.1016/s1383-5769(02)00040-5
30. Adu B, Dodoo D, Adukpo S, Hedley PL, Arthur FK, Gerds TA, et al. Fc g receptor IIIB (FcgRIIIB) polymorphisms are associated with clinical malaria in Ghanaian children. *PloS One* (2012) 7:e46197. doi: 10.1371/journal.pone.0046197
31. Zhao J, Ma L, Chen S, Xie Y, Xie L, Deng Y, et al. Association between Fc-gamma receptor IIa (CD32) gene polymorphism and malaria susceptibility: a meta-analysis based on 6928 subjects. *Infect Genet Evol* (2014) 23:169–75. doi: 10.1016/j.meegid.2014.02.011
32. Grant AV, Roussilhon C, Paul R, Sakuntabhai A. The genetic control of immunity to Plasmodium infection. *BMC Immunol* (2015) 16:14. doi: 10.1186/s12865-015-0078-z
33. Maiga B, Dolo A, Toure O, Dara V, Tapily A, Campino S, et al. Fc gamma receptor IIa-H131R polymorphism and malaria susceptibility in sympatric ethnic groups, Fulani and Dogon of Mali. *Scand J Immunol* (2014) 79:43–50. doi: 10.1111/sji.12122
34. Ouma C, Davenport GC, Garcia S, Kempaiah P, Chaudhary A, Were T, et al. Functional haplotypes of Fc gamma (Fcg) receptor (FcgRIIA and FcgRIIIB) predict risk to repeated episodes of severe malarial anemia and mortality in Kenyan children. *Hum Genet* (2012) 131:289–99. doi: 10.1007/s00439-011-1076-8
35. Le Port A, Cottrell G, Martin-Prevel Y, Migot-Nabias F, Cot M, Garcia A. First malaria infections in a cohort of infants in Benin : biological, environmental and genetic determinants. Description Study Site Population Methods Prelim Results *BMJ Open* (2012) 2:e000342. doi: 10.1136/bmjopen-2011-000342
36. Dechavanne C, Sadissou I, Bouraima A, Ahouangninou C, Amoussa R, Milet J, et al. Acquisition of natural humoral immunity to P. falciparum in early life in Benin: impact of clinical, environmental and host factors. *Sci Rep* (2016) 6:33961. doi: 10.1038/srep33961
37. Cottrell G, Kouwaye B, Pierrat C, Le Port A, Bourama A, Fonton N, et al. Modeling the influence of local environmental factors on malaria transmission in Benin and its implications for cohort study. *PloS One* (2012) 7:e28812. doi: 10.1371/journal.pone.0028812
38. Field LL, Dugoujon JM. Immunoglobulin allotyping GM, KM of GAW5 families. *Genet Epidemiol* (1989) 6:31–3. doi: 10.1002/gepi.1370060108
39. Hans VM, Mehta DS. Genetic polymorphism of Fcγ-receptors IIa, IIIa and IIIb in South Indian patients with generalized aggressive periodontitis. *J Oral Sci* (2011) 53:467–74. doi: 10.2334/josnusd.53.467
40. Lou XY, Chen GB, Yan L, Ma JZ, Zhu J, Elston R, et al. A generalized combinatorial approach for detecting gene-by-gene and gene-by-environment interactions with application to nicotine dependence. *Am J Hum Genet* (2007) 80:1125–37. doi: 10.1086/518312
41. Van Buuren S, Groothuis-Oudshoorn K. mice: Multivariate Imputation by Chained Equations in R. *J Stat Software* (2011) 45:1–67. doi: 10.18637/jss.v045.i03
42. Roussilhon C, Oeuvray C, Müller-Graf C, Tall A, Rogier C, Trape JF, et al. Long-term clinical protection from falciparum malaria is strongly associated with IgG3 antibodies to merozoite surface protein 3. *PloS Med* (2007) 13:e320. doi: 10.1371/journal.pmed.0040320
43. Pandey JP, French MA. GM phenotypes influence the concentrations of the four subclasses of immunoglobulin G in normal human serum. *Hum Immunol* (1996) 51:99–102. doi: 10.1016/s0198-8859(96)00205-4
44. De Taeye SW, Bentlage AEH, Mebius MM, Meesters JI, Lissenberg-Thunnissen S, Falck D, et al. FcγR Binding and ADCC Activity of Human IgG Allotypes. *Front Immunol* (2020) 11:740. doi: 10.3389/fimmu.2020.00740
45. Damelang T, Rogerson SJ, Kent SJ, Chung AW. Role of IgG3 in infectious diseases. *Trends Immunol* (2019) 40:197–211. doi: 10.1016/j.it.2019.01.005
46. Dard P, Lefranc MP, Osipova L, Sanchez-Mazas A. DNA sequence variability of IGHG3 alleles associated to the main G3m haplotypes in human populations. *Eur J Hum Genet* (2001) 9:765–72. doi: 10.1038/sj.ejhg.5200700
47. Omi K, Ohashi J, Patarapotikul J, Hananantachai H, Naka I, Looareesuwan S, et al. Absence of association between the Fc gamma receptor IIIA-176F/V polymorphism and the severity of malaria in Thai. *Jpn J Infect Dis* (2002) 55:167–9.
48. Zeyrek D, Tanac R, Altinoz S, Berdeli A, Gulen F, Koksoy H, et al. FcγRIIIa-V/F 158 polymorphism in Turkish children with asthma bronchiale and allergic rhinitis. *Pediatr Allergy Immunol* (2008) 19:20–4. doi: 10.1111/j.1399-3038.2007.00553.x
49. Bruhns P, Iannascoli B, England P, Mancardi DA, Fernandez N, Jorieux S, et al. Specificity and affinity of human Fcgamma receptors and their polymorphic variants for human IgG subclasses. *Blood* (2009) 113:3716–25. doi: 10.1182/blood-2008-09-179754
50. Salmon JE, Edberg JC, Kimberly RP. Fc gamma receptor III on human neutrophils. *Allelic Variants Have Function Distinct Capacities J Clin Invest* (1990) 85:1287–95. doi: 10.1172/JCI114566
51. Salmon JE, Millard SS, Brogle NL, Kimberly RP. Fc gamma receptor IIIb enhances Fc gamma receptor IIa function in an oxidant-dependent and allele-sensitive manner. *J Clin Invest* (1995) 95:2877–85. doi: 10.1172/JCI117994
52. Vossebeld PJ, Homburg CH, Roos D, Verhoeven AJ. The anti-Fc gamma RIII mAb 3G8 induces neutrophil activation via a cooperative action of Fc gamma RIIIb and Fc gamma RIIa. *Int J Biochem Cell Biol* (1997) 29:465–73. doi: 10.1016/s1357-2725(96)00160-4
53. Edberg JC, Kimberly RP. Modulation of Fc gamma and complement receptor function by the glycosyl-phosphatidylinositol-anchored form of Fc gamma RIII. *J Immunol* (1994) 152:5826–35.
54. Van Sorge NM, Van der Pol WL, Van de Winkel JG. FcgammaR polymorphisms: implications for function, disease susceptibility and immunotherapy. *Tissue Antigens* (2003) 61:189–202. doi: 10.1034/j.1399-0039.2003.00037.x
55. Nasr A, Iriemenam NC, Troye-Blomberg M, Giha HA, Balogun HA, Osman OF, et al. Fc gamma receptor IIa (CD32) polymorphism and antibody responses to asexual blood-stage antigens of Plasmodium falciparum malaria in Sudanese patients. *Scand J Immunol* (2007) 66:87–96. doi: 10.1111/j.1365-3083.2007.01947.x
56. Sinha S, Mishra SK, Sharma S, Patibandla PK, Mallick PK, Sharma SK, et al. Polymorphisms of TNF-enhancer and gene for FcgammaRIIa correlate with the severity of falciparum malaria in the ethnically diverse Indian population. *Malar J* (2008) 7:13. doi: 10.1186/1475-2875-7-13
57. Cooke GS, Aucan C, Walley AJ, Segal S, Greenwood BM, Kwiatkowski DP, et al. Association of Fcgamma receptor IIa (CD32) polymorphism with severe malaria in West Africa. *Am J Trop Med Hyg* (2003) 69:565–8. doi: 10.4269/ajtmh.2003.69.565
58. Pleass RJ, Ogun SA, McGuinness DH, Van de Winkel JG, Holder AA, Woof JM. Novel antimalarial antibodies highlight the importance of the antibody Fc region in mediating protection. *Blood* (2003) 102:4424–30. doi: 10.1182/blood-2003-02-0583
59. Shi J, McIntosh RS, Adame-Gallegos J, Dehal PK, Van Egmond M, Van de Winkel J, et al. The generation and evaluation of recombinant human IgA specific for Plasmodium falciparum merozoite surface protein 1-19 (PfMSP1 19). *BMC Biotechnol* (2011) 11:77. doi: 10.1186/1472-6750-11-77
60. Warmerdam PA, van de Winkel JG, Gosselin EJ, Capel PJ. Molecular basis for a polymorphism of human Fc gamma receptor II (CD32). *J Exp Med* (1990) 172:19–25. doi: 10.1084/jem.172.1.19
61. Adamou R, Dechavanne C, Sadissou I, d'Almeida T, Bouraima A, Sonon P, et al. Plasmodium falciparum merozoite surface antigen-specific cytophilic IgG and control of malaria infection in a Beninese birth cohort. *Malar J* (2019) 18:194–204. doi: 10.1186/s12936-019-2831-x
62. Redon R, Ishikawa S, Fitch KR, Feuk L, Scherer SW, Hurles ME, et al. Global variation in copy number in the human genome. *Nature* (2006) 444:444–54. doi: 10.1038/nature05329
63. Molokhia M, Fanciulli M, Petretto E, Patrick AL, McKeigue P, Roberts AL, et al. FCGR3B copy number variation is associated with systemic lupus erythematosus risk in Afro-Caribbeans. *Rheumatol (Oxford)* (2011) 50:1206–10. doi: 10.1093/rheumatology/keq456
64. Chen JY, Wang CM, Chang SW, Cheng CH, Jan Wu YJ, Lin JC, et al. Association of FCGR3A and FCGR3B copy number variations

with systemic lupus erythematosus and rheumatoid arthritis in Taiwanese patients. *Arthritis Rheumatol* (2014) 66:3113–21. doi: 10.1002/art.38813

Conflict of Interest: The authors declare that the research was conducted in the absence of any commercial or financial relationships that could be construed as a potential conflict of interest.

frontiers in Immunology

REVIEW
published: 15 February 2021
doi: 10.3389/fimmu.2021.613468

The Genetics of Human Schistosomiasis Infection Intensity and Liver Disease: A Review

Estelle M. Mewamba[1†] Oscar A. Nyangiri[2†], Harry A. Noyes[3], Moses Egesa[4,5], Enock Matovu[2] and Gustave Simo[1] for the TrypanoGEN+ research group of the H3Africa consortium*

[1] Molecular Parasitology and Entomology Unit, Faculty of Science, University of Dschang, Dschang, Cameroon, [2] College of Veterinary Medicine Animal Resources and Biosecurity, Makerere University, Kampala, Uganda, [3] Centre for Genomic Research, School of Biological Sciences, University of Liverpool, Liverpool, United Kingdom, [4] Medical Research Council/Uganda Virus Research Institute and London School of Hygiene & Tropical Medicine Uganda Research Unit, Entebbe, Uganda, [5] London School of Hygiene and Tropical Medicine, London, United Kingdom

OPEN ACCESS

Edited by:
David Courtin,
Institut de Recherche Pour le Développement (IRD), France

Reviewed by:
Christophe Chevillard,
INSERM U1090 Technologies Avancées pour le Génome et la Clinique, France
Deborah Negrão-Corrêa,
Federal University of Minas Gerais, Brazil

***Correspondence:**
Gustave Simo
gsimoca@yahoo.fr

[†]These authors have contributed equally to this work and share first authorship

Specialty section:
This article was submitted to Microbial Immunology, a section of the journal Frontiers in Immunology

Received: 02 October 2020
Accepted: 22 January 2021
Published: 15 February 2021

Citation:
Mewamba EM, Nyangiri OA, Noyes HA, Egesa M, Matovu E and Simo G (2021) The Genetics of Human Schistosomiasis Infection Intensity and Liver Disease: A Review. Front. Immunol. 12:613468. doi: 10.3389/fimmu.2021.613468

Schistosomiasis remains the fourth most prevalent parasitic disease affecting over 200 million people worldwide. Control efforts have focussed on the disruption of the life cycle targeting the parasite, vector and human host. Parasite burdens are highly skewed, and the majority of eggs are shed into the environment by a minority of the infected population. Most morbidity results from hepatic fibrosis leading to portal hypertension and is not well-correlated with worm burden. Genetics as well as environmental factors may play a role in these skewed distributions and understanding the genetic risk factors for intensity of infection and morbidity may help improve control measures. In this review, we focus on how genetic factors may influence parasite load, hepatic fibrosis and portal hypertension. We found 28 studies on the genetics of human infection and 20 studies on the genetics of pathology in humans. *S. mansoni* and *S. haematobium* infection intensity have been showed to be controlled by a major quantitative trait locus *SM1*, on chromosome 5q31-q33 containing several genes involved in the T_h2 immune response, and three other loci of smaller effect on chromosomes 1, 6, and 7. The most common pathology associated with schistosomiasis is hepatic and portal vein fibroses and the *SM2* quantitative trait locus on chromosome six has been linked to intensity of fibrosis. Although there has been an emphasis on T_h2 cytokines in candidate gene studies, we found that four of the five QTL regions contain T_h17 pathway genes that have been included in schistosomiasis studies: *IL17B* and *IL12B* in *SM1*, *IL17A* and *IL17F* in 6p21-q2, *IL6R* in 1p21-q23 and *IL22RA2* in *SM2*. The T_h17 pathway is known to be involved in response to schistosome infection and hepatic fibrosis but variants in this pathway have not been tested for any effect on the regulation of these phenotypes. These should be priorities for future studies.

Keywords: schistosomiasis, fibrosis, Th17, intensity of infection, QTL, linkage

INTRODUCTION

Schistosomiasis is caused by digenic trematodes of the genus *Schistosoma* with *Schistosoma mansoni* and *Schistosoma haematobium* causing the majority of human infections. Adult parasites live in the veins around the gut and bladder and eggs are excreted in feces or urine and infect snails in fresh water. Parasite numbers are amplified in the snail intermediate host and human infective stages then emerge that can penetrate human skin when people enter the water. Schistosomiasis induces acute, severe, and chronic morbidity among those who are infected and can cause liver and bladder fibrosis and eventually bladder or colorectal cancer (1). Although exposure to water infested with the infective schistosome cercariae is the main risk factor for schistosomiasis there is considerable variation in infection intensity between people with similar exposures and schistosomiasis cases aggregate in families, some of this variation has been attributed to the genetics of the human immune response (2–4).

A review of the genetics of human susceptibility to schistosomiasis related fibrosis has been published recently (5), but there has been no review of the genetics of schistosome infection since 2008 (2).

A fundamental understanding of the genetics of schistosomiasis susceptibility and high worm load may contribute to rational design of interventions, including vaccines (6). For example, it has recently been shown that a set of 32 SNPs in 10 genes can predict susceptibility to severe hepatic disease among Brazilians with 63% sensitivity and 90% specificity (5). In the present review of the genetics of human susceptibility to schistosomiasis we focus on loci associated with egg/worm burden and hepatic fibrosis.

We therefore present an updated review of the genes and variants that have been found associated with schistosomiasis infection intensity and liver disease, together with a review of genes within QTL that could be prioritized for future analyses. We have excluded the HLA region since we have only identified one study of genes in this region since they were was last reviewed (7, 8).

Epidemiology and Treatment

The disease affects almost 240 million people, and 700 million are at risk of infection in 74 countries, the majority being in Africa, Asia and South America (9, 10). Between 3 and 56 million disability-adjusted life years (DALYs) are lost per annum and 280,000 deaths per annum have been attributed to effects of schistosomiasis (11–13). Approximately 85% of infections occur in sub-Saharan Africa and at least 90% of people requiring treatment for schistosomiasis live in Africa (14). Schistosomiasis can also be associated with chronic anemia, childhood growth stunting, protein calorie malnutrition, cognitive disability, and poor school performance (15–20).

Control of schistosomiasis has continued to rely mainly on mass drug administration (MDA) of school-aged children using the anti-schistosomal drug praziquantel (PZQ) (21, 22). Although this strategy has reduced morbidity, the impact on prevalence has been more limited, because praziquantel does not kill immature schistosomes (23, 24), coverage remains restricted and only school age children are routinely treated. Vaccines are in development but phase three trials have not been successful (25).

Immune Responses During Schistosome Infections

Immune responses to penetrating and migrating *Schistosoma* larvae (schistosomula) and maturing adults are predominantly T_h1 (26). Excretory/secretory *Schistosoma* antigens damage host barrier cells which release alarmins, activate innate cells and induce proinflammatory cytokines (IL1B, IL6, IL17, TNF, and IFNG) (27). About 6 weeks after infection, *Schistosoma* eggs are deposited in tissues (the liver and the intestine or the bladder) and trigger an expansion of T_h2 cells (28). *Schistosoma* egg antigens also directly bind receptors on antigen presenting cells inhibiting IL12 production and consequently T_h1 responses (29). T_h2 responses can also be induced independently of egg deposition as infection with single sex schistosomes induce pre-patent IL4 production by CD4 T cells (30). Schistosome specific T_h2 responses are downmodulated in long-standing infections (31) and this is associated with a development of regulatory cells producing IL10 and transforming growth factor beta (TGFB). This not only allows the parasite to survive in the host and minimize host tissue damage but also modulates host immune responses to unrelated antigens including allergens, self-antigens, and vaccines.

Schistosome egg secretions are highly antigenic (31) and typically induce polarized granulomatous T_h2 responses (32). Granulomas form around eggs lodged in tissues to protect tissue cells (33) but persistent host CD4 T_h2 cell mediated responses to parasite eggs cause fibrosis (34). The pro-fibrotic T_h2 cytokine IL13 is associated with periportal fibrosis in humans (35). Beyond T_h2 cytokine responses, intensified hepatic granulomatous inflammation in *S. mansoni* infected mice is associated with high levels of IL17 and controlled by IFNG (36). In human schistosomiasis, IL17 producing CD4 T helper cells are associated with ultrasound textural abnormalities while T regulatory cells are associated with reductions in this pathology (37).

Phenotypes

Schistosomal Fecal Egg Count and Worm Burden

Studies of the human genetics of susceptibility to schistosomiasis have focussed on two classes of phenotype; infection associated phenotypes and pathology related phenotypes. Infection associated phenotypes are usually egg counts or worm burden estimates but sometimes total IgE as a marker of the immune response (38). Eggs counts are obtained by the Kato Katz (KK) method for *S. mansoni* and by urine filtration for *S. haematobium* and worm burdens are estimated by measuring the circulating cathodic antigen (CCA) in urine or circulating anodic antigen (CAA) in plasma (39) that are produced by adult worms.

Approximately 80% of the environmental egg burden from helminths including schistosomes, derives from ∼20% of the cases (40). For example 22 out of 119 Kenyan school children had developed high *S. mansoni* egg burden (>100 eggs per gram of feces) 12 months after treatment, whilst 70 children still had low (<30 epg) egg burdens (41) and this effect was not correlated with

the amount of water contact. This tendency for some people to develop high infections even after treatment has been attributed to variation in genetic risk (42).

Schistosome egg burdens are also highly skewed by age with egg burdens increasing up to the age of puberty and declining thereafter (43–46). A study in Brazil found that children under 19 had egg burdens that were over ten times higher than older adults (42). The higher intensity and frequency of infections in children may be due to the slow development of immunity to schistosomes. Possibly, the antigens that are exposed by dying worms cross react with larval antigens and stimulate a protective anti-larval IgE response. The long life span of adult worms (5–15 years) means that it takes many years for children to be exposed to sufficient dying worms to develop an IgE response to the larvae (47). High anti-parasite IgE levels have been associated with resistance and high specific IgG4 has been associated with susceptibility and it has been proposed that the ratio of these two immunoglobulins controls resistance to schistosomiasis (48–51).

Schistosomiasis Associated Hepatic and Periportal Fibrosis and Portal Vein Hypertension

Although schistosomes cause a wide range of symptoms and fibrotic lesions can form around egg granulomas in many tissues, the main indicator of *S. mansoni* and *S. japonicum* pathology is hepatic fibrosis (HF) and periportal fibrosis (PPF) (52). WHO guidelines provide scoring scales for HF and PPF (53) and both scales are used as phenotypes in genetic research (54). HF and PPF is caused by extracellular matrix forming around schistosome eggs. In the hepatic portal vein this can lead to portal hypertension (PH) (55, 56), ultimately, some patients with PH die of internal bleeding, superinfections, or heart or kidney failure. *S. haematobium* is associated with bladder cancer and *S. mansoni* may be associated with hepatocellular carcinoma (57) but genetic studies of the pathology of schistosomiasis have focussed almost exclusively on hepatic and periportal fibrosis and in this review all references to pathology are to these closely related conditions unless otherwise indicated. Fibrosis can be measured by ultra-sound scan, although there are concerns about the accuracy and reproducibility of ultrasound (58); additional markers and protocols for grading pathology are being developed but are not well-validated (59–61).

GENOME WIDE LINKAGE STUDIES DISCOVER SCHISTOSOMIASIS SUSCEPTIBILITY LOCI

The reviews of linkage and candidate gene studies of schistosomiasis are broken down into two sections by phenotype: (1) studies of infection status, which is usually determined by egg count in urine or feces and (2) studies of pathology which is mainly periportal fibrosis determined by ultra-sound. Relevant publications were identified by searching PubMed using the terms in **Supplementary Table 1**.

Heritability of Schistosomiasis Infection Risk

Heritability, the proportion of risk attributable to genetic variation, must be substantial to be detectable. A summary of heritability estimates for schistosomiasis are shown in **Table 1**. Studies in Brazil (62–64); Kenya (46); and China (65, 66) have each estimated similar proportions of the variance of *S. mansoni* egg count that are attributable to genetic variation, with additive heritability (*h2*) estimates of 23–31%. However, there were striking differences in the two estimates for heritability of infection with *S. japonicum* in China using variance components (VC) (0 & 58%) (**Table 1**), which have been discussed by others (2).

Linkage Studies for *Schistosoma* Egg Count

The initial study of the genetics of human schistosomiasis used segregation analysis, which determines whether the distribution of the disease on family pedigrees is consistent with the presence of a major gene (3). This study demonstrated the presence of a major gene which was subsequently named *SM1* and located on chromosome five by parametric linkage analysis (4). A major gene has alleles that cause a difference in phenotype between family members that is large enough to be able to categorize individuals as carriers or non-carriers on the basis of phenotype alone (67) and parametric linkage analysis requires estimates of the disease allele frequency and penetrance of the phenotype for the three possible genotypes.

The *SM1* quantitative trait locus (QTL) on chromosome 5 5q31-q33 for *S. mansoni* fecal egg count was the first QTL to be mapped in humans for any infectious disease (**Table 2**, **Figure 1**) (4). The great success of this study was partially attributable to the very large effect size of the *SM1* locus (66% of the variance after accounting for water contact, age and sex). This is in striking contrast to the very modest proportions of the variance explained by most loci identified by GWAS in which loci rarely explain more than 10% of the variance of the trait that is not attributable to covariates (96). Three further loci (1p22.2, 7q36 and 21q22–22-qter) had evidence of association and contained genes known to be involved in the response to schistosomes but did not achieve genome wide significance (68). A reanalysis of the same data controlling for *SM1* genotype identified additional genome wide significant loci at 1p21-q23 and 6p21-q21 (**Table 2**, **Figure 1**) (69), since the effect of these loci was small in comparison to the effect of *SM1,* they were only identifiable when using *SM1* genotype as a parameter of the model.

A further study on a Senegalese population, by the same group that conducted the original study in Brazil, confirmed an association at the *SM1* locus. However, the effect was not as strong and the association could only be demonstrated by non-parametric pedigree tests for an effect at the *SM1* locus (70). Non-parametric analysis requires no prior knowledge of the disease allele frequency or the disease penetrance of the different genotypes.

TABLE 1 | Heritability estimates for genetic component of risk of schistosomiasis in different populations.

Parasite	Phenotype	Country and district	Heritability estimate and method eg *h2*	References
S. mansoni	Egg count	Brazil, Minas Gerais	23% (*h2*)	(62)
S. mansoni	Egg count	Brazil, Minas Gerais	27% (VC)	(63)
S. mansoni	Egg count	Brazil, Bahia	31% (VC)	(64)
S. mansoni	IgE	Brazil, Bahia	59% (VC)	(64)
S. haematobium	Egg count	Kenya, Coast	9% (*h2*)	(46)
S. haematobium	Bladder morbidity	Kenya, Coast	14% (*h2*)	(46)
S. japonicum	Infection	China, Jiangxi	58% (VC)	(65)
S. japonicum	Infection	China Sichuan	0% (VC)	(66)

h2 additive heritability, VC variance components.

TABLE 2 | Loci associated with *S. mansoni* infection discovered by linkage studies.

Phenotypes	Locus name	5' Marker (Position)	3'Marker (Position)	References	Candidate genes, Tested (Untested)
Egg count	*SM1* 5q31-q33	D5S642 (128Mb)	D5S412 (158Mb)	(4, 68–70)	***IL4, IL5, IL9, IL13,*** *(IL3, CXCL14, CD14, 1IL17B, IL12B)*
Egg count	1p21-q23	D1S236 (95Mb)	D1S196 (168Mb)	(69)	*(IL6R, CRP)*
Egg count	6p21-q21	D6S271 (43Mb)	D6S283 (67Mb)	(69)	(*VEGFA, IL17A, IL17F*)
Hepatic fibrosis	*SM2* 6q22-q23	D6S1009 (137Mb)	D6S310 (142Mb)	(71)	***CTGF, IFNGR1, IL22RA2***
Egg count	7q35-q36	D7S483 (152Mb)	D7S550 (156Mb)	(69)	(*TRB, NOS3, SHH*)

*Marker positions are shown in GRCh37 co-ordinates. Candidate genes that have been found associated with the phenotype are shown in bold (**Tables 3**, **4**). Other plausible candidates (See **Figure 2**) in the regions are in brackets. Genes associated with the T_h17 response are underlined. These loci are shown graphically in **Figures 1**, **2**.*

Linkage Studies Identify QTL for Pathology That Are Independent of QTL for Parasite Burden

A study in Sudan found that 12% of the study population had moderate or advanced fibrosis and that half of these also had portal hypertension (97). A linkage study of four candidate gene regions in the same population identified a locus (*SM2*) on chromosome six near the interferon-gamma receptor (*IFNGR1*) associated with hepatic fibrosis (**Table 2**, **Figure 1**) (98). Fifty percentage of people with risk alleles at *SM2* had some continuous thickening of periportal vein branches within 19 years of coming to live within the study area. IFNG is strongly anti-fibrogenic and polymorphisms in *IFNGR1* could plausibly regulate fibrosis. No linkage was found with the *SM1* locus suggesting that control of infection and pathology were independent. The *SM2* locus at 6q22-q23 did not overlap either the HLA region on chromosome six or the 6p21-q21 region that was associated with *S. mansoni* worm burden in Brazil (69) (**Table 2**, **Figure 1**).

The *SM2* locus was replicated in a linkage study of 11 candidate gene regions in Egypt where 32.7% of individuals 11 years and older had significant fibrosis and rs1327475 in *IFNGR1* was significantly associated with severe PPF. In contrast to the earlier study in Sudan, this study found a weak association with the T_h2 cytokine cluster (IL4, IL13) in *SM1* (54), suggesting that worm burden does contribute to risk of pathology. There is evidence for a potentially protective role of a high IFNG response to schistosome infection, consistent with the anti-fibrogenic properties of IFNG [reviewed by Abath et al. (99)] and a SNP in *IFNG* has been associated with time to reinfection (**Table 3**) (72). Consequently, it appears that the variation in the IFNG system is involved in both the outcome of infection and pathology. Variation in *IFNGR1* has only been shown to be involved in the development of pathology but it has yet to be tested in a candidate gene study for effect on infection response.

ANNOTATION OF GENES IN QTL REGIONS

Very few genes were known in the 5 QTL regions for schistosomiasis (**Table 2**) at the time that the QTL were discovered, and we are not aware of any attempts to identify the genes that are responsible for the QTL effect. Hundreds of genes are now known in these loci, each of which could potentially regulate the phenotype and we prepared a short list of the most likely candidates in each region. In order to discover which genes in each schistosomiasis QTL region might be involved in the response to schistosomiasis we used a custom Perl script to search

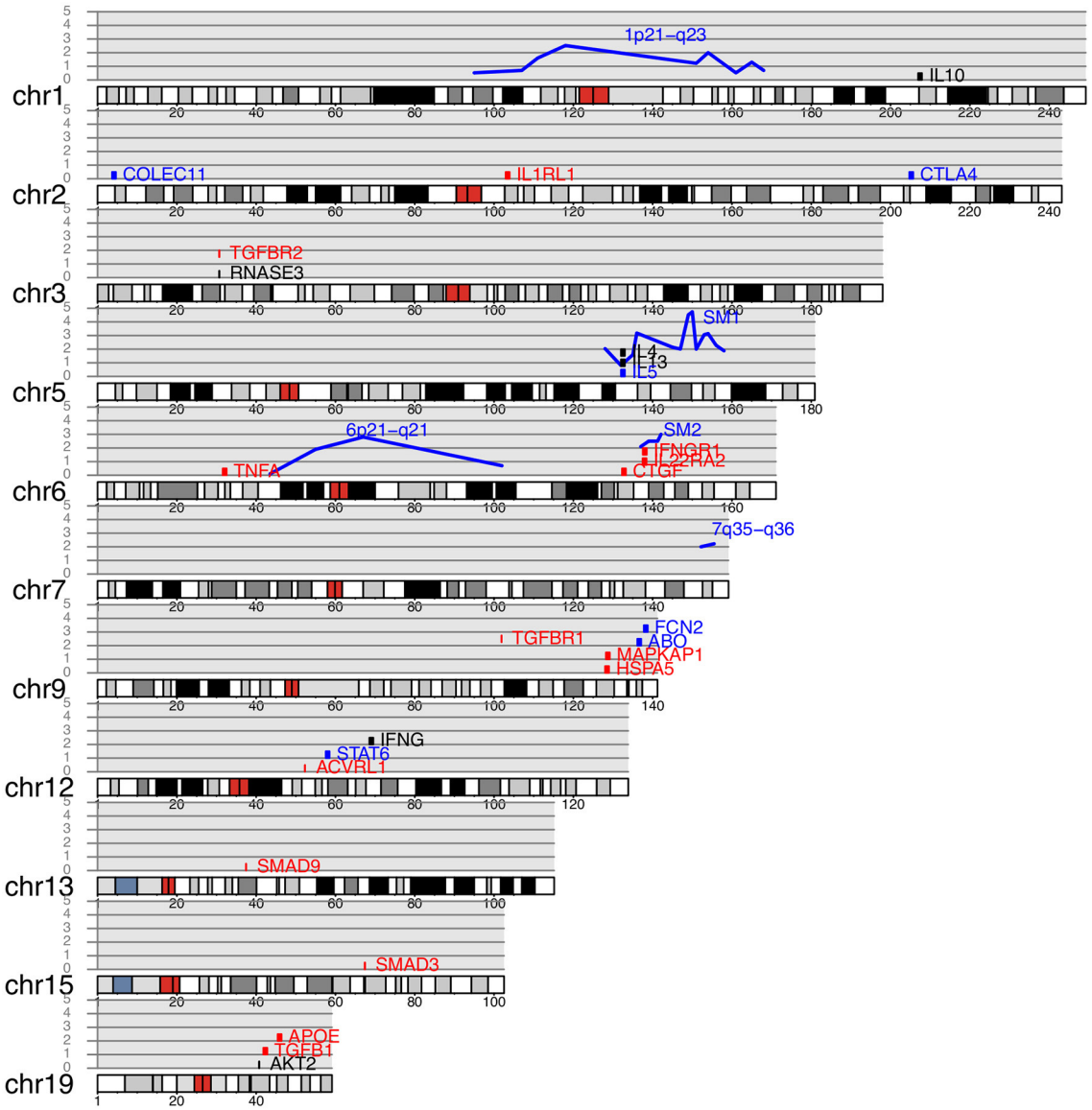

FIGURE 1 | Genes and quantitative trait loci associated with schistosomiasis plotted on a human karyotype. Blue lines indicate QTL, with reported −log *p*-value for association shown on the y axis. Genes containing SNP associated with schistosomiasis infection (**Table 3**) are shown in blue, genes associated with pathology (**Table 4**) are shown in red and genes associated with both pathology and infection are shown in black. Genes are arranged vertically on the plot for clarity and their position on the y axis is arbitrary.

PubMed with terms for schistosomiasis and each gene name and its aliases and obtained a count of the number of publications returned as detailed in **Supplementary Table 4**.

We assumed that the genes that are most likely to be the QTL genes will already have been shown to be involved in the response to schistosome infection. In order to identify these genes, we systematically searched PubMed for papers that included terms for schistosomiasis and each of the gene names in the 5 QTL regions in **Table 2** or their synonyms (**Supplementary Table 4**). The genes that have been mentioned most frequently in the abstract of a paper that also mentions schistosomiasis and that are in one of the QTL are shown in **Figure 2**, **Table 2**. A complete list of all genes that are in the QTL and that have been studied in the context of schistosomiasis is in **Supplementary Table 4**. The number of papers shown in **Figure 2** is an indicator of the genes most commonly associated with schistosomiasis in these regions. The genes with the largest literature were the T_h2 cytokine genes originally identified by Marquet (4) in *SM1* (*IL3, IL4, IL5*, *IL9*, and *IL13*), that each had between 17 and 511 publications associated with schistosomiasis. Only *CSF1* and *TRB*

TABLE 3 | SNP which have been found to be associated with schistosomiasis infection phenotypes in candidate gene studies.

SNP	Gene	Phenotype	Parasite	Neg refs	Pos refs
rs2430561	*IFNG*	T2R	Sm	none	(72)
rs3024495	*IL10*	FEC	Sm	None	(38)*
rs1800896	*IL10*	IgE	Sm	None	(38)
rs1800871	*IL10*	IgE	Sm	None	(38)*
rs1800872	*IL10*	IgE	Sm	None	(38)*
IL10(-1082/-819/-592)	*IL10*	UEC	Sh	(73)	(74)*
rs20541	*IL13*	FEC	Sm	(75, 76)	(77)
rs2066960	*IL13*	FEC	Sm	(78)	(77)
rs7719175	*IL13*	UEC	Sh	(73)	(79)*
rs2069743	*IL13*	UEC	Sh	(78)	(80)
rs1800925	***IL13***	**UEC, FEC, T2R**	**Sh, Sm**	**None**	**(72, 77–79)***
rs2243250	***IL4***	**UEC, T2R**	**Sh**	**(80)**	**(73), (72)***
rs2079103	*IL5*	IF	Sj	None	(75)*
rs2706399	*IL5*	IF	Sj	None	(75)*
rs3024974	*STAT6*	UEC	Sh	None	(73)*
rs324013	*STAT6*	UEC	Sh	None	(78)*
rs733618	*CTLA4*	UEC	Sh	None	(81)
rs11571316	*CTLA4*	UEC	Sh	None	(81)
rs231775	*CTLA4*	UEC	Sh	None	(81)
rs3124952	*FCN2*	UEC	Sh	None	(82)
rs17514136	*FCN2*	UEC	Sh	None	(82)
rs7567833	*COLECC11*	UEC	Sh	None	(83)
COLEC11*TCCA	*COLECC11*	UEC	Sh	None	(83)
Blood group O	*ABO*	FEC,UEC	Sh,Sm	None	(84)
rs746822072	*RNASE3*	FEC	Sm	None	(85)

*Loci that have been found associated with schistosomiasis in more than one study are shown in bold. * Loci that are not significant after Bonferroni correction. IL10 (−1082/−819/−592) = a haplotype of rs1800870, rs1800871 and rs1800872. COLEC11*TCCA is a haplotype of rs1864480 (−676T/C), rs4849953 (−472T/C), rs6714770 (−469C>G), and (−276C>T). Blood Group O is most commonly defined by genotypes at three SNP rs8176719, rs8176746(CC), rs8176747(GG). IF, Infection Frequency; T2R Time to Reinfection; UEC, Urine Egg Count; FEC, Fecal Egg Count: Sh, S. haematobium; Sm, S. mansoni; Sj, S. japonicum. "Pos refs" column contains citations for the studies that showed a significant association with phenotype and "Neg refs" column contains citations of studies that failed to show a significant association at that locus.*

(beta T cell receptor) were identified as candidate genes by the original authors in the 1p21-q23 and 7q35-q36 egg burden loci (69) and *IFNGR1* was the candidate gene that was used for the linkage study at *SM2* (98). The large literature on T_h2 cytokines and schistosomiasis is expected given the important role of this pathway in response to egg antigens and the development of pathology. The T_h2 cytokines in *SM1* are therefore credible candidate genes at this locus.

Our annotation of these QTL also revealed the presence of T_h17 related genes in four of the five QTL: *IL17B* and *IL12B* in *SM1*, *IL22RA2* in *SM2*, *IL17A* and *IL17F* in 6p21-q21 and *IL6R* in1p21-q23. Although *IL12B* (*IL12p40*) in *SM1* is primarily known as a T_h1 cytokine it is also a component of the heterodimeric IL23 cytokine which is important for T_h17 maintenance and expansion (100) and IL6 is important in T_h17 T helper cell differentiation (101). IL17 cytokines are involved in regulation of worm and egg burdens as well as the development of fibrosis and granuloma in response to eggs (102). The presence of T_h17 related cytokines in four of the five QTL suggests that variation in this system may also contribute to variation in outcome of infection in addition to that caused by variation in the T_h2 system.

CANDIDATE GENE STUDIES

Infection Status and Intensity

We have identified 28 candidate gene studies of *Schistosoma* infection or worm burden that reported associations between 24 loci in eleven candidate genes and seven different phenotypes (**Table 3**, **Supplementary Tables 2, 3**). The genes with associations were *IFNG, IL10, IL13, IL4, IL5, STAT6, CTLA4, FCN2, COLECC11, ABO,* and *RNASE3*. These genes were all chosen because their protein products were known to be involved in the response to infection. One study of *MASP2* (103) and one on *LTA* (104) only reported negative results and are not included in **Table 3**. We have not attempted any formal meta-analysis since few loci were replicated and there were important differences in study design and data reporting in the studies of loci that were replicated, making any meta-analysis hard to interpret.

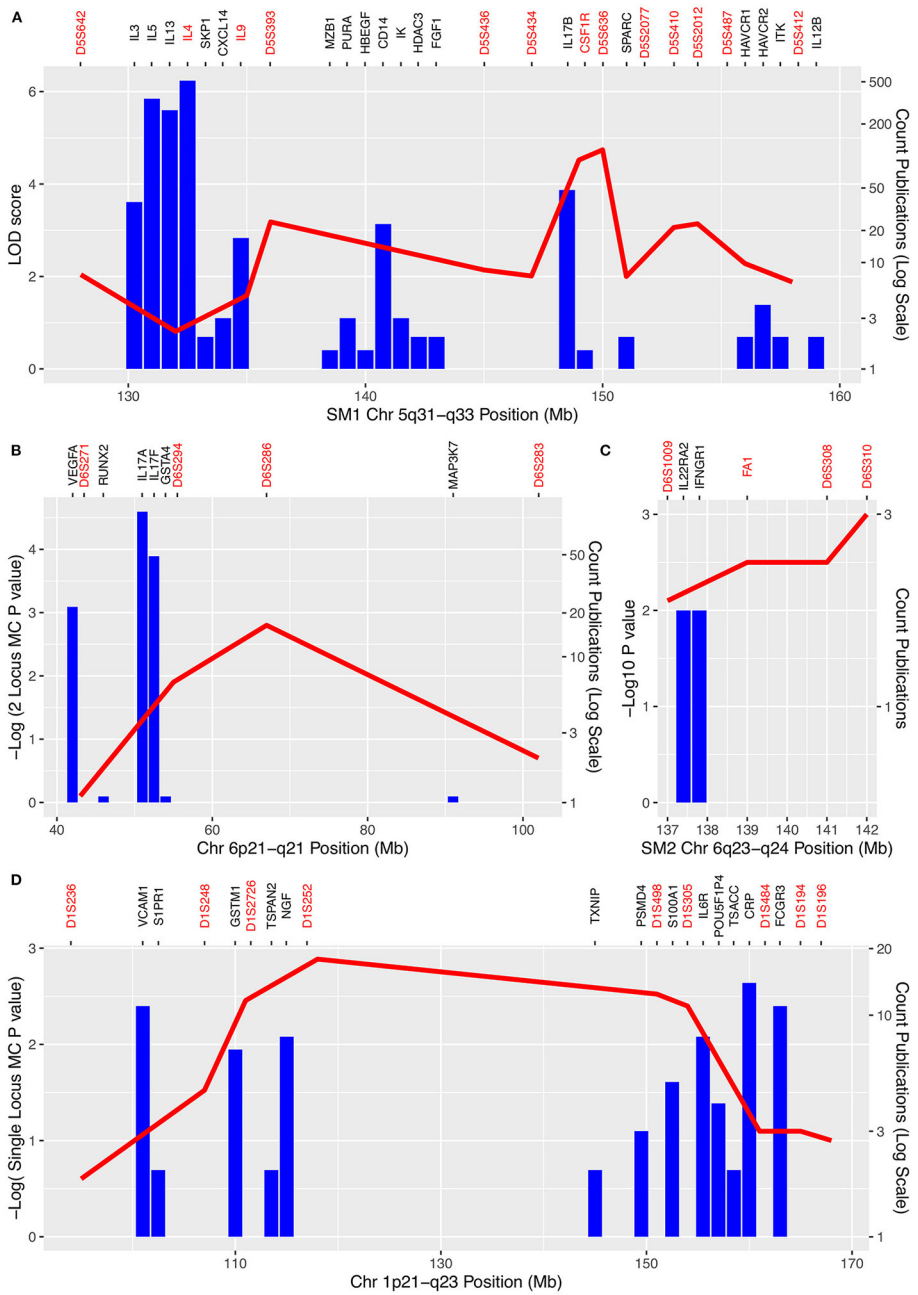

FIGURE 2 | Schistosomiasis QTL and numbers of publications mentioning each gene in each QTL regions. **(A)** *SM1* region 5q31-q33; **(B)** 6p21-q21; **(C)** *SM2* 6q23-q24; **(D)** 1p21-q23. Negative log *p*-values for associations between markers and schistosomiasis are shown on the left-hand axis. Counts of publications which mention both schistosomiasis and genes in the QTL are shown by the blue columns and on a log scale on the right-hand y axis. Markers used in mapping are shown in red on the top axis (including genes used as markers). Genes for which there was only one publication are omitted for clarity and positions of genes and markers have been adjusted by up to 1Mb for clarity. Note the cluster of T_h2 cytokine genes (*IL3, IL4, IL5, IL9, IL13*) in *SM1* with large numbers of publications between 131 and 135 Mb but low LOD scores. However, in a reanalysis of the same data using weighted pairwise correlations the peak of the QTL shifted toward this cytokine cluster (69).

Schistosome eggs induce granulomatous T_h2 responses (*IL4, IL5, IL9, IL10*, and *IL13*) (32) and antigen-specific IgG1, IgG4, and IgE (105). The *SM1* region on chromosome five identified by Marquet et al. (4) (**Figure 1**) included the prototypical T_h2 cytokines *IL4, IL5, IL9*, and *IL13*, these are strong candidates for the QTL gene(s) and SNP and all except *IL9* have been found associated with schistosomiasis in candidate gene studies (**Table 3**). *IL13* and *IL4* regulate *STAT6* expression which in turn

regulates IgE class switching (106) and *STAT6* variants are also associated with schistosomiasis (**Table 3**). *IL13, IL4, IL5*, and *STAT6* are also involved in regulation of the T_h2 response to schistosomiasis (72, 75, 77–80).

T_h1 cytokines and IFNG in particular are involved in the resistance to the immature worms. Studies of mice and *ex vivo* human PBMC have shown that IFNG levels increase in response to schistosome antigens and are correlated with resistance or tolerance to infection (27, 107, 108) and a candidate gene study found an association between the *IFNG* SNP rs2430561 and time to reinfection (72). IL10 and CTLA4 downregulate immune responses in long standing infections (31)**.** *COLECC11* and *FCN2* are involved in the innate immune response, they both bind to specific pathogen-associated molecular patterns (PAMPs) on the pathogen surface and stimulate the complement lectin cascade, thereby clearing the pathogens by opsonization (82, 83). *ABO* regulates blood group and a meta-analysis found evidence for a protective effect for blood group O (84). RNASE3 also known as eosinophil cationic protein (ECP) is a secretory protein of eosinophil granulocytes that efficiently kills the larval stage of *S. mansoni* (85).

The Ensembl Variant Effect Predictor was used to provide functional annotations for these variants (**Supplementary Table 5**). In the functional annotation only rs231775 in *CTLA4* and rs20541 in *IL13* were predicted to have an effect on function. Both of which were non-synonymous variants and were classified as risk factors by ClinVar (109), although SIFT (110), and Polyphen (111) predicted the effect of these SNP would be benign. Other SNP had no predicted effects on function, possibly because they are not functional but are linked to functional SNP nearby. However, the functional annotation cannot detect all functional variants and experimental work has shown that *IL13* expression is regulated by rs1800925 (112). Further detailed studies will be required to determine which of the SNP are truly functional and which are not functional but still potentially useful markers for risk of schistosomiasis.

Pathology: Hepatic and Periportal Fibrosis

It has been noted since at least 1974 that the development of severe fibrosis is clustered in families and is not well-correlated with intensity of infection suggesting that the mechanisms regulating infection intensity and pathology are not closely coupled (5). We found 20 studies which identified associations with schistosomiasis related pathology at 46 candidate SNP or haplotypes in 21 genes outside the HLA complex (**Table 4**, **Supplementary Table 2**). Few of the studies applied any multiple testing corrections and 15 out of the 43 associations would not be significant after a Bonferroni correction (**Table 4**).

There are sixteen genes for which an effect has only been reported for fibrosis and not for infection: *APOE, CCN2, HSPA5, IFNGR1, IL22RA2, MAPKAP1, IL1RL1, TNFA,* mTOR, AKT2, *TGFB1, TGFBR1*, *TGFBR2*, *ACVRL1*, *SMAD9*, and *SMAD3* (**Tables 3**, **4**). Five genes have been associated with both fibrosis and intensity of infection (*RNASE3*, *IL4, IL10, IFNGI,* and *IL13*). Four genes were associated with fibrosis in more than one population: *IFNGR1, IL22RA2, CCN2,* and *MAPKAP1* (**Table 4**), the two former genes are also in the *SM2* QTL (55, 71, 86, 90, 93). Although these sixteen genes have not been tested for associations with infection status or intensity it is plausible that some of them are only associated with pathology. All of these genes except *APOE* and *IL1RL1* have been associated with the regulation of fibrosis (**Table 4**) and variation in these may regulate risk of pathology irrespective of intensity of infection.

The Ensembl Variant Effect Predictor was used to provide functional annotations for the SNP in **Table 4** (**Supplementary Table 5**). Two non-synonymous SNP in *APOE* (rs7412 and rs429358) were predicted by ClinVar to be a risk factor, pathogenic and involved in drug response (109), the rs7412 SNP was also predicted to be deleterious or damaging by SIFT (110) and Polyphen (111). A non-coding SNP in *LTA* (rs1800629) was predicted to be involved in drug response by ClinVar (109) and a non-coding SNP (rs1800872) in *IL10* was predicted to be risk factor by ClinVar. Other SNP in **Table 4** did not have functional annotations, and many may be marker SNP that are linked to functional variants rather than functional themselves.

A recent study found that just 32 SNPs could predict who gets severe hepatic fibrosis in Brazil with 63% sensitivity and 90% specificity (5). This review emphasized the importance of TGFB signaling pathway and IL22. TGFB is also involved in the differentiation of T_h17 cells (113), and together with SMAD regulates T_h17 in response to another worm infection *Echinococus multilocularis* (114) providing further justification for systematic investigation of the role of variants in the T_h17 pathway in differences in response to infection. IL22 and IL17 are co-expressed by T_h17 CD4+ T cells and polymorphisms have been associated with hepatic fibrosis in the *IL22* receptor *IL22RA2* (5, 90). IL22 also has protective effects on the intestinal epithelium against toxic bacterial products (5).

Associations With the HLA Region

The HLA region is associated with response to many communicable and non-communicable diseases. The importance of CD4+ T helper cells in the response to schistosomiasis, and the role of HLA class II alleles in recruiting these, suggests that variation in the HLA region may play an important role in control of schistosome infections. However, associations were not found in this region in the whole genome linkage scans either for worm burden or pathology (4, 68, 71).

Two reviews reported 17 and 18 studies, respectively, of associations of HLA markers with schistosomiasis induced PPF (7, 8), but surprisingly we could not find any studies of HLA genes and worm burden (**Table 3**, **Supplementary Table 3**). We have found only one study of genes in the HLA region and schistosomiasis that has been published in the 9 years since those reviews. A SNP in Major histocompatibility complex class I chain-related A (*MICA*) was associated with liver fibrosis in a Han Chinese population (76).

It has been emphasized that the problems of extensive linkage disequilibrium within the HLA region, the small sizes of the studies reviewed, the allelic diversity and large variations in allele frequencies between populations mean that these studies may not replicate in different populations and need further confirmation

TABLE 4 | SNP which have been found to be associated with schistosomiasis pathology related phenotypes in candidate gene studies.

SNP	Gene	Phenotype	Species	Not associated	Associated	References
rs1327475	*IFNGR1*	HF	Sm	NA	Egypt	(54)
rs2243250§	*IL4*	HF	Sm	NA	Egypt	(54)
rs1056854	*TGFB1*	HF	Sm	NA	Egypt*	(54)
rs373880612	*IFNG*	PPF, HF, PH	Sm	NA	Sudan*	(55)
rs1861494	*IFNG*	PPF, HF, PH	Sm	NA	Sudan*	(55)
IFN-gR1 6q22-q23	*IFNGR1*	HF, PH	Sm	NA	Sudan	(71)
rs3037970	*CCN2(CTGF)*	HF, PH	Sj Sm	China Sudan Brazil	China	(71)
rs1257705	*CCN2(CTGF)*	HF, PH	Sj Sm	Sudan Brazil China	China*	(86)
rs2151532	*CCN2(CTGF)*	HF, PH	Sj Sm	China Egypt	China*	(54, 86)
rs9402373	*CCN2(CTGF)*	HF, PH	Sj Sm	NA	2 China* Sudan Brazil*	(86)
rs9399005	*CCN2(CTGF)*	HF, PH	Sj	China	China*	(86)
rs6918698	*CCN2(CTGF)*	HF, PH	Sj Sm	China Sudan	China* Brazil*	(86)
rs1931002	*CCN2(CTGF)*	HF, PH	Sj	China	China	(86)
rs12526196	*CCN2(CTGF)*	HF, PH	Sj Sm	Sudan Brazil	2 China*	(86)
rs1800925C-rs20541A§	*IL13*	HF, PH	Sj	NA	China	(87)
rs1800925§	*IL13*	HF PH	Sj	NA	China*	(87)
rs12712135	*ST2 (IL1RL1)*	IL1RL1	Sj Sm	NA	China Brazil	(88)
rs1420101	*ST2 (IL1RL1)*	IL1RL1	Sj Sm	NA	China Brazil	(88)
rs6543119	*ST2 (IL1RL1)*	IL1RL1	Sj Sm	NA	China Brazil	(88)
rs7412, rs429358 APOE3	*APOE*	TC, LDL	Sm	Brazil	NA	(89)
rs6570136	*IL22RA2*	HF, PH	Sj Sm	NA	China Brazil* Sudan*	(90)
rs7774663	*IL22RA2*	HF, PH	Sj Sm	China	Sudan Brazil*	(90)
rs2064501	*IL22RA2*	HF, PH, IL22	Sj Sm	NA	China* Brazil* Sudan*	(90)
rs11154915	*IL22RA2*	HF, PH, IL22	Sj Sm	China Brazil	Sudan*	(90)
rs7749054	*IL22RA2*	HF, PH, IL22 level	Sj Sm	China Sudan	Brazil*	(90)
rs1800870	*IL10*	PPF	Sm	NA	Brazil	(91)
IL10 (-1082/-819/-592)§	*IL10*	PPF	Sm	NA	Brazil	(91)
rs1800629	*TNFA*	PPF, TNFA	Sm	NA	Brazil	(92)
rs10118570	*MAPKAP1*	HF, infection	Sj	NA	2 China	(93)
rs391957	*HSPA5*	HF, infection	Sj	NA	China	(93)
rs17025963 rs185882198 rs71093915	*TGFBR2*	HF	Sm	NA	Brazil	(5)

(Continued)

TABLE 4 | Continued

SNP	Gene	Phenotype	Species	Not associated	Associated	References
rs1690215 rs56368010	*ACVRL1(ALK1)*	HF	Sm	NA	Brazil	(5)
rs114046193 rs12345675	*TGFbR1 (ALK5)*	HF	Sm	NA	Brazil	(5)
rs138079455 rs10555873 rs77414361	*SMAD9*	HF	Sm	NA	Brazil	(5)
rs12913547 rs12914140 rs12439500	*SMAD3*	HF	Sm	NA	Brazil	(5)
rs746822072	*RNASE3 (ECP)*	HF	Sm	NA	Uganda	(85)
rs1800629	*TNFA*	PPF regression after treatment	Sm	NA	Brazil	(94)
rs2295080	*mTOR*	HF, infection	Sj	NA	China	(95)
rs7254617	*AKT2*	HF, infection	Sj	NA	China*	(95)

*Loci that have been found associated with schistosomiasis in more than one population are shown in bold. *Loci that are not significant after Bonferroni correction. §SNP which are also associated with infection (**Table 3**). Studies of classical HLA loci have been excluded since they have been fully reviewed elsewhere (7, 8). Sh, S. haematobium; Sm, S. mansoni; Sj, S. japonicum. The "Associated" column shows the locations of studies where a significant association has been found and the "Not Associated" column shows the location of studies that failed to show a significant association. PPF Periportal Fibrosis; PH Portal Hypertension; PT Portal thickness, including portal vein diameter and portal vein branch point thickness, HF Hepatic Fibrosis; AHSD Advanced HepatoSplenic Disease, TC Total Cholesterol, HDL High Density Lipoprotein, TNFA Median levels TNFA higher in patients with PPF, IL22 level of IL22 in plasma, IL1RL1 level of soluble IL1RL1 in plasma. IL-10 (−1082/−819/−592) represents a haplotype of rs1800870, rs1800871, and rs1800872. NA, Not applicable.*

from larger studies (7). However, some alleles of HLA class II loci DQA1, DQB1 and DRB1 and HLA class I HLA-A and HLA-B were associated with PPF in a meta-analysis that combined evidence from 2 to 3 studies for each allele evaluated (8) and these associations may be robust.

DISCUSSION

Replication of Candidate Gene Studies for Infection

Few of the candidate gene studies shown in **Tables 3**, **4** applied correction for testing multiple SNPs and the 32 associations that would not remain significant after such a correction are indicated by asterisks. The lack of Bonferroni corrections suggests that some of these studies will not replicate and, for some of these loci, there are studies that have not replicated the association (**Tables 3**, **4**), although this is often when using a different phenotype. Notably, half of these studies that did not replicate an association were at loci that were significant after a Bonferroni correction.

There are many instances of failures to replicate candidate gene studies. One review found that only 6 out of 166 associations replicated in more than 75% of studies, although 97 of the 166 associations (58%) were reproduced in at least one study (115). Failure to replicate can be due to the initial observation being due to random variation in allele frequencies between test and control samples (a type one error). However, genuine associations can fail to replicate because of linkage between the marker SNP and the functional SNP varying between populations, small study sizes, variable penetrance, population variation at modifier loci, (occult) population stratification within study populations or differences in allele frequencies between populations leading to type two errors. In addition, it is also possible for different SNP in the same gene to be most important in regulating a response in different populations or individuals (116). Therefore, most of these observations should be considered provisional until adequately powered meta-analyses can be conducted.

Associations with infection were replicated at two SNP (*IL13* rs1800925; *IL4* rs2243250), and both of these SNP and also the *IL10* (−1082/−819/−592) haplotype were also found to be associated with pathology (**Tables 3**, **4**), despite the studies using different phenotypes and in one case different parasite species. The *IL13* rs1800925 SNP was associated with schistosomiasis in four infection related studies and one pathology study and all studies that included this SNP found an association with it, despite the association not being significant after a Bonferroni correction in any of these studies. The high level of replication at this SNP suggests that these associations may be robust despite the lack of significance in individual studies. Functional data also supports a role for rs1800925, which is in the promoter of *IL13,* and is associated with increased expression of IL13 from stimulated cells *in vitro* (112). Since IL13 regulates IgE levels via STAT6 (106), there is a plausible mechanism for a role for this SNP in response to infection, increasing the confidence that it is a genuine association. Although *IL4* expression is also associated with IgE levels, the rs2243250 SNP is not (117), so its impact on intensity of infection must be via some other mechanism.

The Th17 Pathway Has Been Neglected in Schistosomiasis Association Studies

Since the Th2 pathway is the dominant response to helminth infections and is the main pathway for response to egg antigens

(28, 30), genes in this pathway have been well-represented in association studies (**Tables 3**, **4**) and these have confirmed the importance of variation in this pathway for outcome of infection. However, the Th1 and Th17 pathways are also important, particularly in the early stages of the infection (26, 29, 36, 37). Variants in *IL17F* and *IL17RA* have been found associated with cerebral malaria (118) and similar variation may contribute to the outcome of schistosome infection. Our annotation of QTL, with the genes that have published associations with schistosomiasis, revealed an excess of Th17 pathway genes in these QTL (**Figures 1**, **2**). There have been no association studies to test candidate gene hypothesis for three out of the five QTL (**Table 2**) and there are Th17 genes in four of the five QTL (underlined in **Table 2**), which could be priorities for future association studies.

It is possible that variation in other Th17 pathway genes outside of the QTL also contribute to variation in response to infection. A KEGG pathway diagram of Th17 cell differentiation and a list of 108 genes in this pathway is shown in **Supplementary Table 6.** We have obtained a list of the 1,742,019 SNP in these genes from dbSNP and kept the 1,052 SNP that were predicted to be "pathogenic" by ClinVar, irrespective of minor allele frequency (**Supplementary Table 7**). We also kept SNP with minor allele frequency > 5% and that had any of the following functional classifications: splice acceptor variant, stop gained, initiator codon variant, stop lost, splice donor variant, missense variant, terminator codon variant, frameshift variant. This left a list of 2,701 SNP in the Th17 pathway which are most likely to have an effect on function and that could be priorities for further testing (**Supplementary Table 7**).

Which Are the Optimal Study Designs to Discover Susceptibility Loci?

Approaches for discovering susceptibility loci for parasitic infections have been reviewed previously (119). The major approaches are association studies in unrelated individuals and linkage studies within families, the merits of which have been evaluated by Abel and Dessein (120). We noted in this review that family based designs were the first to discover QTL loci in schistosomiasis (4), and these were followed up with considerable success by candidate gene studies in these QTL. Schistosomiasis affected communities are frequently geographical clusters of related individuals where case control studies can be confounded by cryptic relatedness. In contrast family-based association studies exploit this relatedness by estimating disequilibrium in transmission of alleles within families.

Schistosomiasis is also an excellent setting for family-based linkage studies of infection intensity because children are the most heavily infected; therefore, parents are often available for genotyping to create complete families, unlike adult onset diseases. However, it is more difficult to collect full families for complications of chronic schistosomiasis such as fibrosis that affect adults. Whole genome linkage studies have only been undertaken on two populations, one in Brazil and one in Senegal, further studies to identify loci regulating intensity of infection in additional populations should be undertaken and could enlarge our understanding of the mechanisms of response to infection. It has already been shown that 32 SNP can be used to identify those at highest risk of developing pathology after *S. mansoni* infection (5). If the 20% of the people that shed 80% of the eggs could also be identified they could be targeted for regular treatment which could dramatically reduce the number of eggs in the environment and the pressure of infection on the whole community.

CONCLUSION

Despite the remarkable success of the early linkage studies that identified major QTL loci, no further whole genome scans for association have been conducted and the QTL genes underlying these loci have not been definitively identified. All subsequent studies have been candidate gene linkage and association studies focussing on genes within the QTL regions *SM1*, *SM2*, and the T_h2 pathway that are hypothesized to play a role in schistosomiasis progression. No candidate gene studies have attempted to identify QTL genes in three of the QTL for *S. mansoni* egg count (**Table 2**). This review has presented evidence that the T_h17 pathway has been overlooked in studies of the genetics of schistosomiasis and should be prioritized in future investigations of susceptibility genes.

The rapid development of genotyping technologies makes large scale genomic studies easier than ever, provided that well-characterized samples can be obtained. The studies of Dessein et al. (86) on populations from China, Sudan and Brazil have demonstrated the value of replicating analyses in multiple populations and similar replication is needed for other candidate SNP and genes.

AUTHOR CONTRIBUTIONS

GS and EMa conceived the review. EMe and ON wrote the draft and collected all the relevant literature. HN significantly reviewed the draft and analyzed QTL data. ME contributed to the draft and revised the manuscript. All authors read and approved the final manuscript.

FUNDING

This study was funded by the African Academy of Sciences grant to the TrypanoGEN+ H3Africa program, Grant no. H3A/18/004. ME received funds from HIC-Vac, a GCRF Network in Vaccines Research and Development which was co-funded by the MRC and BBSRC and is part of the EDCTP2 programme supported by the European Union. Additional support was received through Wellcome Trust grants 215993/Z/19/Z and 218454/Z/19/Z, and through the Makerere University-Uganda Virus Research Institute Centre of Excellence for Infection and Immunity Research and Training (MUII) which was funded by the DELTAS Africa Initiative (Grant no. 107743).

ACKNOWLEDGMENTS

The authors are grateful to Alison Elliott of the London School of Hygiene and Tropical Medicine for helpful discussions and reviewing the manuscript.

THE TRYPANOGEN+ RESEARCH GROUP OF THE H3AFRICA CONSORTIUM

Membership of the TrypanoGEN+ research group is available at http://www.trypanogen.net/.

SUPPLEMENTARY MATERIAL

The Supplementary Material for this article can be found online at: https://www.frontiersin.org/articles/10.3389/fimmu.2021.613468/full#supplementary-material

Supplementary Table 1 | Search strategy: Summary of PubMed search strategy.

Supplementary Table 2 | All included references: Papers included in the review.

Supplementary Table 3 | Details of Refs Populations, study design, phenotypes, and effects from studies.

Supplementary Table 4 | Genes in QTL. List of genes in QTL regions with lists of publications associated with each gene and schistosomiasis.

Supplementary Table 5 | VEP SNP Annotations. Functional annotation of SNP from candidate genes studies with the Ensembl Variant Effect predictor.

Supplementary Table 6 | Th17 genes. List of Genes in Th17 pathway with KEGG pathway diagram.

Supplementary Table 7 | Th17 SNP. List of potentially function SNP in genes in the Th17 pathway.

REFERENCES

1. Ismail HAHA, Hong ST, Babiker ATEB, Hassan RMAE, Sulaiman MAZ, Jeong HG, et al. Prevalence, risk factors, and clinical manifestations of schistosomiasis among school children in the White Nile River basin, Sudan. *Parasites Vectors.* (2014) 7:478. doi: 10.1186/s13071-014-0478-6
2. Bethony JM, Quinnell RJ. Genetic epidemiology of human schistosomiasis in Brazil. *Acta Trop.* (2008) 108:166–174. doi: 10.1016/j.actatropica.2007.11.008
3. Abel L, Demenais F, Prata A, Souza AE, Dessein A. Evidence for the segregation of a major gene in human susceptibility/resistance to infection by *Schistosoma mansoni*. *Am J Hum Genet.* (1991) 48:959–70.
4. Marquet S, Abel L, Hillaire D, Dessein H, Kalil J, Feingold J, et al. Genetic localization of a locus controlling the intensity of infection by *Schistosoma mansoni* on chromosome 5q31-q33. *Nat Genet.* (1996) 14:181–4. doi: 10.1038/ng1096-181
5. Dessein H, Duflot N, Romano A, Opio C, Pereira V, Mola C, et al. Genetic algorithms identify individuals with high risk of severe liver disease caused by schistosomes. *Hum Genet.* (2020) 139:821–31. doi: 10.1007/s00439-020-02160-4
6. Alsallaq RA, Gurarie D, Ndeffo Mbah M, Galvani A, King C. Quantitative assessment of the impact of partially protective anti-schistosomiasis vaccines. *PLoS Negl Trop Dis.* (2017) 11:e0005544. doi: 10.1371/journal.pntd.0005544
7. Blackwell JM, Jamieson SE, Burgner D. HLA and infectious diseases. *CMR.* (2009) 22:370–85. doi: 10.1128/CMR.00048-08
8. Huy NT, Hamada M, Kikuchi M, Lan NTP, Yasunami M, Zamora J, et al. Association of HLA and post-schistosomal hepatic disorder: a systematic review and meta-analysis. *Parasitol Int.* (2011) 60:347–56. doi: 10.1016/j.parint.2011.05.008
9. Colley DG, Bustinduy AL, Secor WE, King CH. Human schistosomiasis. *Lancet.* (2014) 383:2253–64. doi: 10.1016/S0140-6736(13)61949-2
10. Hotez PJ, Kamath A. Neglected tropical diseases in sub-saharan Africa: review of their prevalence, distribution, and disease burden. *PLoS Negl Trop Dis.* (2009) 3:e412. doi: 10.1371/journal.pntd.0000412
11. Steinmann P, Keiser J, Bos R, Tanner M, Utzinger J. Schistosomiasis and water resources development: systematic review, meta-analysis, and estimates of people at risk. *Lancet Infect Dis.* (2006) 6:411–25. doi: 10.1016/S1473-3099(06)70521-7
12. Murray CJL, Vos T, Lozano R, Naghavi M, Flaxman AD, Michaud C, et al. Disability-adjusted life years (DALYs) for 291 diseases and injuries in 21 regions, 1990-2010: a systematic analysis for the Global Burden of Disease Study 2010. *Lancet.* (2012) 380:2197–223. doi: 10.1016/S0140-6736(12)61690-0
13. van der Werf MJ, de Vlas SJ, Brooker S, Looman CWN, Nagelkerke NJD, Habbema JDF, et al. Quantification of clinical morbidity associated with schistosome infection in sub-Saharan Africa. *Acta Trop.* (2003) 86:125–39. doi: 10.1016/S0001-706X(03)00029-9
14. Gbalégba NGC, Silué KD, Ba O, Ba H, Tian-Bi NTY, Yapi GY, et al. Prevalence and seasonal transmission of *Schistosoma haematobium* infection among school-aged children in Kaedi town, southern Mauritania. *Parasites Vectors.* (2017) 10:353. doi: 10.1186/s13071-017-2284-4
15. Ezeamama AE, Friedman JF, Acosta LP, Bellinger DC, Langdon GC, Manalo DL, et al. Helminth infection and cognitive impairment among filipino children. *Am J Trop Med Hyg.* (2005) 72:540–8. doi: 10.4269/ajtmh.2005.72.540
16. Ezeamama AE, Bustinduy AL, Nkwata AK, Martinez L, Pabalan N, Boivin MJ, et al. Cognitive deficits and educational loss in children with schistosome infection—a systematic review and meta-analysis. *PLoS Negl Trop Dis.* (2018) 12:e0005524. doi: 10.1371/journal.pntd.0005524
17. Friedman JF, Kanzaria HK, McGarvey ST. Human schistosomiasis and anemia: the relationship and potential mechanisms. *Trends Parasitol.* (2005) 21:386–92. doi: 10.1016/j.pt.2005.06.006
18. King CH, Dangerfield-Cha M. The unacknowledged impact of chronic schistosomiasis. *Chronic Illn.* (2008) 4:65–79. doi: 10.1177/1742395307084407
19. King CH, Dickman K, Tisch DJ. Reassessment of the cost of chronic helmintic infection: a meta-analysis of disability-related outcomes in endemic schistosomiasis. *Lancet.* (2005) 365:1561–9. doi: 10.1016/S0140-6736(05)66457-4
20. Koukounari A, Gabrielli AF, Toure S, Bosque-Oliva E, Zhang Y, Sellin B, et al. *Schistosoma haematobium* infection and morbidity before and after large-scale administration of praziquantel in Burkina Faso. *J Infect Dis.* (2007) 196:659–69. doi: 10.1086/520515
21. Utzinger J, Raso G, Brooker S, De Savigny D, Tanner M, Ornbjerg N, et al. Schistosomiasis and neglected tropical diseases: towards integrated and sustainable control and a word of caution. *Parasitology.* (2009) 136:1859–74. doi: 10.1017/S0031182009991600
22. Evan Secor W. Water-based interventions for schistosomiasis control. *Pathogens Global Health.* (2014) 108:246–54. doi: 10.1179/2047773214Y.0000000149
23. Ross AGP, Olveda RM, Li Y. An audacious goal: the elimination of schistosomiasis in our lifetime through mass drug administration. *Lancet.* (2015) 385:2220–1. doi: 10.1016/S0140-6736(14)61417-3
24. Gray DJ, McManus DP, Li Y, Williams GM, Bergquist R, Ross AG. Schistosomiasis elimination: lessons from the past guide the future. *Lancet Infect Dis.* (2010) 10:733–6. doi: 10.1016/S1473-3099(10)70099-2
25. Riveau G, Schacht AM, Dompnier JP, Deplanque D, Seck M, Waucquier N, et al. Safety and efficacy of the rSh28GST urinary schistosomiasis vaccine: a phase 3 randomized, controlled trial in Senegalese children. *PLoS Negl Trop Dis.* (2018) 12:e0006968. doi: 10.1371/journal.pntd.0006968
26. Egesa M, Lubyayi L, Tukahebwa EM, Bagaya BS, Chalmers IW, Wilson S, et al. *Schistosoma mansoni* schistosomula antigens induce Th1/Pro-inflammatory cytokine responses. *Parasite Immunol.* (2018) 40:e12592. doi: 10.1111/pim.12592
27. Perrigoue JG, Marshall FA, Artis D. On the hunt for helminths: innate immune cells in the recognition and response to helminth parasites. *Cellular Microbiology.* (2008) 10:1757–1764. doi: 10.1111/j.1462-5822.2008.01174.x

28. Grzych JM, Pearce E, Cheever A, Caulada ZA, Caspar P, Heiny S, et al. Egg deposition is the major stimulus for the production of Th2 cytokines in murine schistosomiasis mansoni. *J Immunol.* (1991) 146:1322–7.
29. Pearce EJ, M Kane C, Sun JJ, Taylor J, McKee AS, Cervi L. Th2 response polarization during infection with the helminth parasite *Schistosoma mansoni*. *Immunol Rev.* (2004) 201:117–26. doi: 10.1111/j.0105-2896.2004.00187.x
30. de Oliveira Fraga LA, Torrero MN, Tocheva AS, Mitre E, Davies SJ. Induction of type 2 responses by schistosome worms during prepatent infection. *J Infect Dis.* (2010) 201:464–72. doi: 10.1086/649841
31. Joseph S, Jones FM, Kimani G, Mwatha JK, Kamau T, Kazibwe F, et al. Cytokine production in whole blood cultures from a fishing community in an area of high endemicity for *Schistosoma mansoni* in Uganda: the differential effect of parasite worm and egg antigens. *IAI.* (2004) 72:728–34. doi: 10.1128/IAI.72.2.728-734.2004
32. Everts B, Perona-Wright G, Smits HH, Hokke CH, van der Ham AJ, Fitzsimmons CM, et al. Omega-1, a glycoprotein secreted by *Schistosoma mansoni* eggs, drives Th2 responses. *J Exp Med.* (2009) 206:1673–80. doi: 10.1084/jem.20082460
33. Kaplan MH, Whitfield JR, Boros DL. Th2 Cells are required for the *schistosoma mansoni* egg-induced granulomatous response. *J Immunol.* (1998) 160:1850–6.
34. Dunne DW, Lucas S, Bickle Q, Pearson S, Madgwick L, Bain J, et al. Identification and partial purification of an antigen (ω1 from *Schistosoma mansoni* eggs which is putatively hepatotoxic in T-cell deprived mice. *Trans R Soc Trop Med Hyg.* (1981) 75:54–71. doi: 10.1016/0035-9203(81)90013-4
35. Alves Oliveira LF, Moreno EC, Gazzinelli G, Martins-Filho OA, Silveira AMS, Gazzinelli A, et al. Cytokine production associated with periportal fibrosis during chronic schistosomiasis mansoni in humans. *Infect Immun.* (2006) 74:1215–21. doi: 10.1128/IAI.74.2.1215-1221.2006
36. Rutitzky LI, Stadecker MJ. Exacerbated egg-induced immunopathology in murine Schistosoma mansoni infection is primarily mediated by IL-17 and restrained by IFN-γ. *Eur J Immunol.* (2011) 41:2677–87. doi: 10.1002/eji.201041327
37. Mbow M, Larkin BM, Meurs L, Wammes LJ, de Jong SE, Labuda LA, et al. T-Helper 17 cells are associated with pathology in human schistosomiasis. *J Infect Dis.* (2013) 207:186–95. doi: 10.1093/infdis/jis654
38. Grant AV, Araujo MI, Ponte EV, Oliveira RR, Cruz AA, Barnes KC, et al. Polymorphisms in IL10 are associated with total Immunoglobulin E levels and *Schistosoma mansoni* infection intensity in a Brazilian population. *Genes Immun.* (2011) 12:46–50. doi: 10.1038/gene.2010.50
39. Corstjens PLAM, De Dood CJ, Kornelis D, Tjon Kon Fat EM, Wilson RA, Kariuki TM, et al. Tools for diagnosis, monitoring and screening of *Schistosoma* infections utilizing lateral-flow based assays and upconverting phosphor labels. *Parasitology.* (2014) 141:1841–55. doi: 10.1017/S0031182014000626
40. Woolhouse MEJ, Dye C, Etard JF, Smith T, Charlwood JD, Garnett GP, et al. Heterogeneities in the transmission of infectious agents: implications for the design of control programs. *PNAS.* (1997) 94:338–42. doi: 10.1073/pnas.94.1.338
41. Butterworth AE, Capron M, Cordingley JS, Dalton PR, Dunne DW, Kariuki HC, et al. Immunity after treatment of human *Schistosomiasis mansoni*. II. Identification of resistant individuals, and analysis of their immune responses. *Trans R Soc Trop Med Hyg.* (1985) 79:393–408. doi: 10.1016/0035-9203(85)90391-8
42. Abel L, Demenais F, Prata A, Souza AE, Dessein A. Evidence for the segregation of a major gene in human susceptibility/resistance to infection by *Schistosoma mansoni*. *Am J Hum Genet.* (1991) 48:959–70.
43. Wilkins HA, Goll PH, Marshall TF, Moore PJ. Dynamics of *Schistosoma haematobium* infection in a Gambian community. III. Acquisition and loss of infection. *Trans R Soc Trop Med Hyg.* (1984) 78:227–32. doi: 10.1016/0035-9203(84)90283-9
44. Bradley DJ, McCullough FS. Egg output stability and the epidemiology of *Schistosoma haematobium*. II. An analysis of the epidemiology of endemic S. haematobium. *Trans R Soc Trop Med Hyg.* (1973) 67:491–500. doi: 10.1016/0035-9203(73)90080-1
45. Warren KS. Regulation of the prevalence and intensity of schistosomiasis in man: immunology or ecology? *J Infect Dis.* (1973) 127:595–609. doi: 10.1093/infdis/127.5.595
46. King CH, Kariuki HC, Kadzo H, Koech DK, Magak P, Ouma JH, et al. Low heritable component of risk for infection intensity and infection-associated disease in urinary schistosomiasis among Wadigo village populations in Coast province, Kenya. *Am J Trop Med Hyg.* (2004) 70:57–62. doi: 10.4269/ajtmh.2004.70.57
47. Fitzsimmons CM, Jones FM, Pinot de Moira A, Protasio AV, Khalife J, Dickinson HA, et al. Progressive cross-reactivity in IgE responses: an explanation for the slow development of human immunity to schistosomiasis? *Infect Immun.* (2012) 80:4264–70. doi: 10.1128/IAI.00641-12
48. Demeure CE, Rihet P, Abel L, Ouattara M, Bourgois A, Dessein AJ. Resistance to *Schistosoma mansoni* in humans: influence of the IgE/IgG4 Balance and IgG2 in immunity to reinfection after chemotherapy. *J Infect Dis.* (1993) 168:1000–8. doi: 10.1093/infdis/168.4.1000
49. Figueiredo JP, Oliveira RR, Cardoso LS, Barnes KC, Grant AV, Carvalho EM, et al. Adult worm-specific IgE/IgG4 balance is associated with low infection levels of *Schistosoma mansoni* in an endemic area. *Parasite Immunol.* (2012) 34:604–10. doi: 10.1111/pim.12001
50. Hagan P, Dunn D, Simpson G, Wilkins HA. Human lgE, lgG4 and resistance to reinfection with *Schistosoma haematobium*. (1991) 349:3. doi: 10.1038/349243a0
51. Ndombi EM, Abudho B, Kittur N, Carter JM, Korir H, Riner DK, et al. Effect of four rounds of annual school-wide mass praziquantel treatment for *Schistosoma mansoni* control on schistosome-specific immune responses. *Parasite Immunol.* (2018) 40:e12530. doi: 10.1111/pim.12530
52. McManus DP, Dunne DW, Sacko M, Utzinger J, Vennervald BJ, Zhou XN. Schistosomiasis. *Nat Rev Dis Primers.* (2018) 4:13. doi: 10.1038/s41572-018-0013-8
53. Richter,J, Hatz,C, Campagne,G, Bequist,N, Jenkins,J. *Ultrasound in Schistosomiasis. A Practical Guide to the Standardized Use of Ultrasonography for the Assessment of Schistosomiasis-Related Morbidity.* Niamey: WHO. (2000).
54. Blanton RE, Salam EA, Ehsan A, King CH, Goddard KA. Schistosomal hepatic fibrosis and the interferon gamma receptor: a linkage analysis using single-nucleotide polymorphic markers. *Eur J Hum Genet.* (2005) 13:660–8. doi: 10.1038/sj.ejhg.5201388
55. Chevillard C, Moukoko CE, Elwali N-EMA, Bream JH, Kouriba B, Argiro L, et al. IFN-gamma polymorphisms (IFN-gamma +2109 and IFN-gamma +3810) are associated with severe hepatic fibrosis in human hepatic schistosomiasis (*Schistosoma mansoni*). *J Immunol.* (2003) 171:5596–601. doi: 10.4049/jimmunol.171.10.5596
56. Hirayama K, Chen H, Kikuchi M, Yin T, Gu X, Liu J, et al. HLA-DR-DQ alleles and HLA-DP alleles are independently associated with susceptibility to different stages of post-schistosomal hepatic fibrosis in the Chinese population. *Tissue Antigens.* (1999) 53:269–74. doi: 10.1034/j.1399-0039.1999.530307.x
57. Palumbo E. Association between schistosomiasis and cancer: a review. *Infect Dis Clin Pract.* (2007) 15:145–8. doi: 10.1097/01.idc.0000269904.90155.ce
58. Asztely MS, Eriksson B, Gabone RM, Nilsson L-Å. Is ultrasonography useful for population studies on schistosomiasis mansoni? An evaluation based on a survey on a population from Kome Island, Tanzania. *Acta Radiol Open.* (2016) 5:2058460116686392. doi: 10.1177/2058460116686392
59. Barreto AVMS, Alecrim VM, Medeiros TB de, Domingues ALC, Lopes EP, Martins JRM, et al. New index for the diagnosis of liver fibrosis in *Schistosomiasis mansoni*. *Arq Gastroenterol.* (2017) 54:51–6. doi: 10.1590/s0004-2803.2017v54n1-10
60. Olveda DU, Inobaya M, Olveda RM, Vinluan ML, Ng S-K, Weerakoon K, et al. Diagnosing schistosomiasis-induced liver morbidity: implications for global control. *Int J Infect Dis.* (2017) 54:138–44. doi: 10.1016/j.ijid.2016.10.024
61. Pereira TA, Syn WK, Pereira FEL, Lambertucci JR, Secor WE, Diehl AM. Serum osteopontin is a biomarker of severe fibrosis and portal hypertension in human and murine *Schistosomiasis mansoni*. *Int J Parasitol.* (2016) 46:829–32. doi: 10.1016/j.ijpara.2016.08.004

62. Pullan RL, Bethony JM, Geiger SM, Correa-Oliveira R, Brooker S, Quinnell RJ. Human helminth co-infection: no evidence of common genetic control of hookworm and *Schistosoma mansoni* infection intensity in a Brazilian community. *Int J Parasitol.* (2010) 40:299–306. doi: 10.1016/j.ijpara.2009.08.002
63. Gazzinelli A, Coelho L, Alves-Fraga L, Soares-Filho B, Williams-Blangero S, Bethony J, et al. Additive host genetic factors influence fecal egg excretion rates during *Schistosoma mansoni* infection in a rural area in Brazil. *Am J Med Hyg.* (2002) 67:336–43. doi: 10.4269/ajtmh.2002.67.336
64. Grant A, Araujo MI, Ponte EV, Oliveira RR, Cruz AA, Barnes KC, et al. High heritability but uncertain mode of inheritance for total serum IgE level and *Schistosoma mansoni* infection intensity in a Schistosomiasis-Endemic Brazilian Population. *J Infect Dis.* (2008) 198:1227–36. doi: 10.1086/591946
65. Ellis MK, McManus DP. Familial aggregation of human helminth infection in the Poyang lake area of China with a focus on genetic susceptibility to schistosomiasis japonica and associated markers of disease. *Parasitology.* (2009) 136:699–712. doi: 10.1017/S003118200900612X
66. Spear RC, Zhong B, Kouch J, Seto EYW, Hubbard A. Genetic and household risk factors for *Schistosoma japonicum* infection in the presence of larger scale environmental differences in the mountainous transmission areas of China. *Am J Trop Med Hyg.* (2005) 73:1145–50. doi: 10.4269/ajtmh.2005.73.1145
67. King, R.C, Stransfield, W.D. *Dictionary of Genetics*. Oxford: Oxford University Press. (1998).
68. Marquet S, Abel L, Hillaire D, Dessein A. Full results of the genome-wide scan which localises a locus controlling the intensity of infection by *Schistosoma mansoni* on chromosome 5q31-q33. *Eur J Hum Genet.* (1999) 7:88–97. doi: 10.1038/sj.ejhg.5200243
69. Zinn-Justin A, Marquet S, Hillaire D, Dessein A, Abel L. Genome search for additional human loci controlling infection levels by *Schistosoma mansoni*. *Am J Trop Med Hyg.* (2001) 65:754–8. doi: 10.4269/ajtmh.2001.65.754
70. Müller-Myhsok B, Stelma FF, Guissé-Sow F, Muntau B, Thye T, Burchard GD, et al. Further evidence suggesting the presence of a locus, on human chromosome 5q31-q33, influencing the intensity of infection with Schistosoma mansoni. *Am J Hum Genet.* (1997) 61:452–4. doi: 10.1086/524851
71. Dessein AJ, Hillaire D, Elwali NE, Marquet S, Mohamed-Ali Q, Mirghani A, et al. Severe Hepatic Fibrosis in *Schistosoma mansoni* Infection Is Controlled by a Major Locus That Is Closely Linked to the Interferon-Gamma Receptor Gene. *Am J Hum Genet.* (1999) 65:709–21. doi: 10.1086/302526
72. Gatlin MR, Black CL, Mwinzi PN, Secor WE, Karanja DM, Colley DG. Association of the gene polymorphisms IFN-gamma +874, IL-13−1055 and IL-4−590 with patterns of reinfection with Schistosoma mansoni. *PLoS Negl Trop Dis.* (2009) 3:e375. doi: 10.1371/journal.pntd.0000375
73. Adedokun SA, Seamans BN, Cox NT, Liou G, Akindele AA, Li Y, et al. Interleukin-4 and STAT6 promoter polymorphisms but not interleukin-10 or 13 are essential for schistosomiasis and associated disease burden among Nigerian children. *Infect Genetics Evol.* (2018) 65:28–34. doi: 10.1016/j.meegid.2018.07.012
74. Adedoja A, Hoan NX, Tong H van, Adukpo S, Tijani DB, Akanbi AA, et al. Differential contribution of interleukin-10 promoter variants in malaria and schistosomiasis mono- and co-infections among Nigerian children. *Trop Med Int Health.* (2018) 23:45–52. doi: 10.1111/tmi.13007
75. Ellis MK, Zhao ZZ, Chen HG, Montgomery GW, Li YS, McManus DP. Analysis of the 5q31 33 locus shows an association between single nucleotide polymorphism variants in the IL-5 gene and symptomatic infection with the human blood fluke, *Schistosoma japonicum*. *J Immunol.* (2007) 179:8366–71. doi: 10.4049/jimmunol.179.12.8366
76. Gong Z, Luo Q-Z, Lin L, Su Y-P, Peng H-B, Du K, et al. Association of MICA gene polymorphisms with liver fibrosis in schistosomiasis patients in the Dongting Lake region. *Braz J Med Biol Res.* (2012) 45:222–9. doi: 10.1590/S0100-879X2012007500024
77. Grant AV, Araujo MI, Ponte EV, Oliveira RR, Gao P, Cruz AA, et al. Functional polymorphisms in IL13 are protective against high *Schistosoma mansoni* infection intensity in a Brazilian population. *PLoS ONE.* (2012) 7:e35863. doi: 10.1371/journal.pone.0035863
78. He H, Isnard A, Kouriba B, Cabantous S, Dessein A, Doumbo O, et al. A STAT6 gene polymorphism is associated with high infection levels in urinary schistosomiasis. *Genes Immun.* (2008) 9:195–206. doi: 10.1038/gene.2008.2
79. Isnard A, Kouriba B, Doumbo O, Chevillard C. Association of rs7719175, located in the IL13 gene promoter, with *Schistosoma haematobium* infection levels and identification of a susceptibility haplotype. *Genes Immun.* (2011) 12:31–9. doi: 10.1038/gene.2010.43
80. Kouriba B, Chevillard C, Bream JH, Argiro L, Dessein H, Arnaud V, et al. Analysis of the 5q31-q33 Locus Shows an Association between IL13-1055C/T IL-13-591A/G Polymorphisms and *Schistosoma haematobium* Infections. *J Immunol.* (2005) 174:6274–81. doi: 10.4049/jimmunol.174.10.6274
81. Idris ZM, Yazdanbakhsh M, Adegnika AA, Lell B, Issifou S, Noordin R. A pilot study on Cytotoxic T Lymphocyte-4 gene polymorphisms in urinary schistosomiasis. *Genetic Testing Mol Biomarkers.* (2012) 16:488–92. doi: 10.1089/gtmb.2011.0209
82. Ouf EA, Ojurongbe O, Akindele AA, Sina-Agbaje OR, Van Tong H, Adeyeba AO, et al. Ficolin-2 Levels and FCN2 genetic polymorphisms as a susceptibility factor in schistosomiasis. *J InfectDis.* (2012) 206:562–70. doi: 10.1093/infdis/jis396
83. Antony JS, Ojurongbe O, Kremsner PG, Velavan TP. Lectin complement protein collectin 11 (CL-K1) and susceptibility to urinary schistosomiasis. *PLoS Negl Trop Dis.* (2015) 9:e0003647. doi: 10.1371/journal.pntd.0003647
84. Tiongco RE, Paragas NA, Dominguez MJ, Lasta SL, Pandac JK, Pineda-Cortel MR. ABO blood group antigens may be associated with increased susceptibility to schistosomiasis: a systematic review and meta-analysis. *J Helminthol.* (2018) 94:e21. doi: 10.1017/S0022149X18001116
85. Eriksson J, Reimert CM, Kabatereine NB, Kazibwe F, Ireri E, Kadzo H, et al. The 434(G>C) polymorphism within the coding sequence of Eosinophil Cationic Protein (ECP) correlates with the natural course of *Schistosoma mansoni* infection. *Int J Parasitol.* (2007) 37:1359–66. doi: 10.1016/j.ijpara.2007.04.001
86. Dessein A, Chevillard C, Arnaud V, Hou X, Hamdoun AA, Dessein H, et al. Variants of CTGF are associated with hepatic fibrosis in Chinese, Sudanese, and Brazilians infected with schistosomes. *J Exp Med.* (2009) 206:2321–8. doi: 10.1084/jem.20090383
87. Long X, Chen Q, Zhao J, Rafaels N, Mathias P, Liang H, et al. An IL-13 promoter polymorphism associated with liver fibrosis in patients with *Schistosoma japonicum*. *PLoS ONE.* (2015) 10:e0135360. doi: 10.1371/journal.pone.0135360
88. Long X, Daya M, Zhao J, Rafaels N, Liang H, Potee J, et al. The role of ST2 and ST2 genetic variants in schistosomiasis. *J Allergy Clin Immunol.* (2017) 140:1416–22.e6. doi: 10.1016/j.jaci.2016.12.969
89. Martins da Fonseca CS, Pimenta Filho AA, dos Santos BS, da Silva CA, Domingues ALC, Owen JS, et al. Human plasma lipid modulation in schistosomiasis mansoni depends on apolipoprotein E polymorphism. *PLoS ONE.* (2014) 9:e101964. doi: 10.1371/journal.pone.0101964
90. Sertorio M, Hou X, Carmo RF, Dessein H, Cabantous S, Abdelwahed M, et al. IL-22 and IL-22 binding protein (IL-22BP) regulate fibrosis and cirrhosis in hepatitis C virus and schistosome infections. *Hepatology.* (2015) 61:1321–31. doi: 10.1002/hep.27629
91. Silva PCV, Gomes AV, de Souza TKG, Coêlho MRCD, Cahu GG de OM, Muniz MTC, et al. Association of SNP (-G1082A) IL-10 with increase in severity of periportal fibrosis in Schistosomiasis, in the Northeast of Brazil. *Genetic Testing Mol Biomarkers.* (2014) 18:646–52. doi: 10.1089/gtmb.2014.0098
92. Silva PCV, Gomes AV, de Britto LRPB, de Lima ELS, da Silva JL, Montenegro SML, et al. Influence of a TNF-α Polymorphism on the severity of schistosomiasis periportal fibrosis in the Northeast of Brazil. *Genet Test Mol Biomarkers.* (2017) 21:658–62. doi: 10.1089/gtmb.2017.0133
93. Zhu X, Zhang J, Fan W, Gong Y, Yan J, Yuan Z, et al. MAPKAP1 rs10118570 polymorphism is associated with anti-infection and anti-hepatic fibrogenesis in schistosomiasis japonica. *PLoS ONE.* (2014) 9:e105995. doi: 10.1371/journal.pone.0105995
94. Oliveira JB, Silva PCV, Vasconcelos LM, Gomes AV, Coêlho MRCD, Cahu GGOM, et al. Influence of polymorphism (-G308A) TNF-α on the periportal fibrosis regression of schistosomiasis after specific treatment. *Genet Test Mol Biomarkers.* (2015) 19:598–603. doi: 10.1089/gtmb.2015.0091

95. Xiao Q, Yu H, Zhu X. The associations of hub gene polymorphisms in PI3K/AKT/mTOR pathway and Schistosomiasis Japonica infection and hepatic fibrosis. *Infect Genet Evol.* (2020) 85:104423. doi: 10.1016/j.meegid.2020.104423
96. Manolio TA, Collins FS, Cox NJ, Goldstein DB, Hindorff LA, Hunter DJ, et al. Finding the missing heritability of complex diseases. *Nature.* (2009) 461:747–53. doi: 10.1038/nature08494
97. Mohamed-Ali Q, Elwali NE, Abdelhameed AA, Mergani A, Rahoud S, Elagib KE, et al. Susceptibility to periportal (Symmers) fibrosis in human *Schistosoma mansoni* infections: evidence that intensity and duration of infection, gender, and inherited factors are critical in disease progression. *J Infect Dis.* (1999) 180:1298–306. doi: 10.1086/314999
98. Dessein AJ, Marquet S, Henri S, El Wali NE, Hillaire D, Rodrigues V, et al. Infection and disease in human *Schistosoma mansoni* are under distinct major gene control. *Microbes Infect.* (1999) 1:561–7. doi: 10.1016/S1286-4579(99)80096-3
99. Abath FGC, Morais CNL, Montenegro CEL, Wynn TA, Montenegro SML. Immunopathogenic mechanisms in schistosomiasis: what can be learnt from human studies? *Trends Parasitol.* (2006) 22:85–91. doi: 10.1016/j.pt.2005.12.004
100. Schön MP, Erpenbeck L. The Interleukin-23/Interleukin-17 axis links adaptive and innate immunity in psoriasis. *Front Immunol.* (2018) 9:1323. doi: 10.3389/fimmu.2018.01323
101. Kimura A, Kishimoto T. IL-6: Regulator of Treg/Th17 balance. *Eur J Immunol.* (2010) 40:1830–5. doi: 10.1002/eji.201040391
102. Wen X, He L, Chi Y, Zhou S, Hoellwarth J, Zhang C, et al. Dynamics of Th17 cells and their role in *Schistosoma japonicum* infection in C57BL/6 Mice. *PLoS Neglected Trop Dis.* (2011) 5:e1399. doi: 10.1371/journal.pntd.0001399
103. Ojurongbe O, Antony JS, Tong HV, Meyer CG, Akindele AA, Sina-Agbaje OR, et al. Low MBL-associated serine protease 2 (MASP-2) levels correlate with urogenital schistosomiasis in Nigerian children. *Trop Med Int Health.* (2015) 20:1311–9. doi: 10.1111/tmi.12551
104. Elsammak MY, Al-Sharkaweey RM, Ragab MS, Amin GM, Kandil MH. In Egyptians, a mutation in the lymphotoxin-alpha gene may increase susceptibility to hepatitis C virus but not that to schistosomal infection. *Ann Trop Med Parasitol.* (2008) 102:709–16. doi: 10.1179/136485908X337599
105. Nutman TB. Looking beyond the induction of Th2 responses to explain immunomodulation by helminths. *Parasite Immunol.* (2015) 37:304–13. doi: 10.1111/pim.12194
106. Goenka S, Kaplan MH. Transcriptional regulation by STAT6. *Immunol Res.* (2011) 50:87–96. doi: 10.1007/s12026-011-8205-2
107. Brito CF, Caldas IR, Filho C, Correa-Oliveira R, Oliveira SC. CD4+ T cells of schistosomiasis naturally resistant individuals living in an endemic area produce interferon-γ and tumour necrosis factor-α in response to the recombinant 14kda *Schistosoma mansoni* fatty acid-binding protein. *Scand J Immunol.* (2000) 51:595–601. doi: 10.1046/j.1365-3083.2000.00710.x
108. Fonseca CT, Oliveira SC, Alves CC. Eliminating schistosomes through vaccination: what are the best immune weapons? *Front Immunol.* (2015) 6:1–8. doi: 10.3389/fimmu.2015.00095
109. Landrum MJ, Lee JM, Benson M, Brown GR, Chao C, Chitipiralla S, et al. ClinVar: improving access to variant interpretations and supporting evidence. *Nucleic Acids Res.* (2018) 46:D1062–7. doi: 10.1093/nar/gkx1153
110. Sim N-L, Kumar P, Hu J, Henikoff S, Schneider G, Ng PC. SIFT web server: predicting effects of amino acid substitutions on proteins. *Nucleic Acids Res.* (2012) 40:W452–7. doi: 10.1093/nar/gks539
111. Adzhubei IA, Schmidt S, Peshkin L, Ramensky VE, Gerasimova A, Bork P, et al. A method and server for predicting damaging missense mutations. *Nat Methods.* (2010) 7:248–249. doi: 10.1038/nmeth0410-248
112. van der Pouw Kraan T, van Veen A, Boeije L, van Tuyl S, de Groot E, Stapel S, et al. An IL-13 promoter polymorphism associated with increased risk of allergic asthma. *Genes Immun.* (1999) 1:61–65. doi: 10.1038/sj.gene.6363630
113. Patel DD, Kuchroo VK. Th17 cell pathway in human immunity: lessons from genetics and therapeutic interventions. *Immunity.* (2015) 43:1040–51. doi: 10.1016/j.immuni.2015.12.003
114. Pang N, Zhang F, Ma X, Zhu Y, Zhao H, Xin Y, et al. TGF-β/Smad signaling pathway regulates Th17/Treg balance during Echinococcus multilocularis infection. *Int Immunopharmacol.* (2014) 20:248–57. doi: 10.1016/j.intimp.2014.02.038
115. Hirschhorn JN, Lohmueller K, Byrne E, Hirschhorn K. A comprehensive review of genetic association studies. *Genet Med.* (2002) 4:45–61. doi: 10.1097/00125817-200203000-00002
116. McClellan J, King M-C. Genetic heterogeneity in human disease. *Cell.* (2010) 141:210–7. doi: 10.1016/j.cell.2010.03.032
117. Choi WA, Kang MJ, Kim YJ, Seo JH, Kim HY, Kwon JW, et al. Gene–gene interactions between candidate gene polymorphisms are associated with total IgE levels in Korean Children with Asthma. *J Asthma.* (2012) 49:243–52. doi: 10.3109/02770903.2012.660294
118. Marquet S, Conte I, Poudiougou B, Argiro L, Cabantous S, Dessein H, et al. The IL17F and IL17RA genetic variants increase risk of cerebral malaria in two African Populations. *Infect Immunity.* (2016) 84:590–7. doi: 10.1128/IAI.00671-15
119. Campino S, Kwiatkowski D, Dessein A. Mendelian and complex genetics of susceptibility and resistance to parasitic infections. *Semin Immunol.* (2006) 18:411–22. doi: 10.1016/j.smim.2006.07.011
120. Abel L, Dessein AJ. Genetic epidemiology of infectious diseases in humans: design of population-based studies. *Emerging Infect Dis.* (1998) 4:593–603. doi: 10.3201/eid0404.980409

Conflict of Interest: The authors declare that the research was conducted in the absence of any commercial or financial relationships that could be construed as a potential conflict of interest.

The handling editor declared a past co-authorship with the authors HN, EMa, and GS.

frontiers in Immunology

ORIGINAL RESEARCH
published: 19 February 2021
doi: 10.3389/fimmu.2020.544548

CCR5 Promoter Polymorphisms Associated With Pulmonary Tuberculosis in a Chinese Han Population

Shuyuan Liu[1†], Nannan Liu[1†], Hui Wang[2], Xinwen Zhang[1], Yufeng Yao[1,3], Shuqiong Zhang[2*] and Li Shi[1*]*

[1] Institute of Medical Biology, Chinese Academy of Medical Sciences & Peking Union Medical College, Kunming, China, [2] The Third People's Hospital of Kunming, Kunming, China, [3] Yunnan Key Laboratory of Vaccine Research and Development on Severe Infectious Diseases, Kunming, China

OPEN ACCESS

Edited by:
Eduardo Antonio Donadi, University of São Paulo, Brazil

Reviewed by:
Celso Teixeira Mendes-Junior, University of São Paulo, Brazil
Henry Hongrong Cai, PAREXEL International, United Kingdom

***Correspondence:**
Yufeng Yao
leoyyf@gmail.com
Shuqiong Zhang
1357626082@qq.com
Li Shi
shili.imb@gmail.com

[†]These authors have contributed equally to this work

Specialty section:
This article was submitted to Microbial Immunology, a section of the journal Frontiers in Immunology

Received: 21 March 2020
Accepted: 21 December 2020
Published: 19 February 2021

Citation:
Liu S, Liu N, Wang H, Zhang X, Yao Y, Zhang S and Shi L (2021) CCR5 Promoter Polymorphisms Associated With Pulmonary Tuberculosis in a Chinese Han Population. Front. Immunol. 11:544548. doi: 10.3389/fimmu.2020.544548

Background: Tuberculosis (TB), an infectious disease caused by *Mycobacterium tuberculosis*, is a major public health concern. Chemokines and their receptors, such as RANTES, CXCR3, and CCR5, have been reported to play important roles in cell activation and migration in immune responses against TB infection.

Methods: To understand the correlations involving *CCR5* gene variations, *M. tuberculosis* infection, and TB disease progression, a case-control study comprising 450 patients with TB and 306 healthy controls from a Chinese Han population was conducted, along with the detection of polymorphisms in the *CCR5* promoter using a sequencing method.

Results: After adjustment for age and gender, the results of logistic analysis indicated that the frequency of rs2734648-G was significantly higher in the TB patient group (P = 0.002, OR = 1.38, 95% CI: 1.123–1.696); meanwhile, rs2734648-GG showed notable susceptibility to TB (P = 6.32E-06, OR = 2.173, 95% CI: 1.546–3.056 in a recessive model). The genotypic frequency of rs1799987 also varied between the TB and control groups (P = 0.008). In stratified analysis, rs2734648-GG significantly increased susceptibility to pulmonary TB in a recessive model (P < 0.0001, OR = 2.382, 95% CI: 1.663–3.413), and the rs2734648-G allele significantly increased susceptibility to TB recurrence in a dominant model (P = 0.0032, OR = 1.936, 95% CI: 1.221–3.068), whereas rs1799987-AA was associated with susceptibility to pulmonary TB (P = 0.0078, OR = 1.678, 95% CI: 1.141–2.495 in a recessive model) but not with extra-pulmonary TB and TB recurrence. A haplotype constructed with the major alleles of the eight SNPs in the *CCR5* promoter (rs2227010-rs2856758-rs2734648-rs1799987-rs1799988-rs41469351-rs1800023-rs1800024: A-A-G-G-T-C-G-C) exhibited extraordinarily increased risk of susceptibility to TB and pulmonary TB (P = 6.33E-11, OR = 24.887, 95% CI: 6.081–101.841).

Conclusion: In conclusion, *CCR5* promoter polymorphisms were found to be associated with pulmonary TB and TB progression in Chinese Han people.

Keywords: tuberculosis, CCR5, polymorphism, susceptibility, Chinese Han

INTRODUCTION

Tuberculosis (TB) is an infectious disease caused by *Mycobacterium tuberculosis* (*M. tuberculosis*). To date, TB remains a major public health concern since approximately one third of the world's population has been infected with *M. tuberculosis* (1). Approximately 5% of the individuals who become infected with *M. tuberculosis* will develop clinical TB disease within 2 years of infection (2). TB is classified as primary TB or latent TB infection (2). Approximately 5–10% of the individuals with latent TB will develop clinical TB disease during their lifetime (2–4).

It was believed that active TB development was probably caused by the failure of host inflammatory responses against the pathogen (5). However, studies have identified complex interactions involving *M. tuberculosis* and the environment, along with the host genetic background playing a critical role in the outcome of *M. tuberculosis* exposure and TB development (4). A number of immunity-related genes have been reportedly associated with susceptibility to TB among different populations, such as human leukocyte antigen (HLA), low molecular weight polypeptide/transporter with antigen processing, natural resistance-associated macrophage protein 1 (NRAMP1), dendritic cell-specific ICAM-3-grabbing non-integrin (DC-SIGN), Toll-like receptors (TLR) 1 and 2, vitamin D receptor (VDR), TNF, interleukin (IL) -1β, IL-6, IL-8, IL-10, interferon γ (IFN-γ), and nucleotide oligomerization binding domain 2 (NOD2) (2, 4, 6, 7). Chemokines such as chemokine (C-C motif) ligand 2 (CCL-2)/monocyte chemoattractant protein 1 (MCP-1), RANTENS (*CCL5*), and chemokine C-X-C motif ligand 10 (CXCL10) have been found to be relevant in *M. tuberculosis* infection (7).

C-C motif chemokine receptor type 5 (CCR5), a transmembrane G-coupled cell-surface chemokine receptor, binds to different kinds of CC-chemokines, including human macrophage inflammatory protein-1α (MIP-1α), MIP-1β, RANTES (regulated on activation normal T cell expressed and secreted factor), monocyte chemotactic protein 1 (MCP-1), MCP-2, MCP-3, and MCP-4 (8). Previous studies report that *CCR5* is highly expressed during activation of T helper 1 (Th1) cells, which play a critical role in host immune responses against TB (9). Moreover, *CCR5* expression is found to be substantially increased during *M. tuberculosis* infection (10–12). Pokkali et al. found that *CCR5* expression is significantly higher in pulmonary TB patients compared to that in healthy controls (10), and Qiu et al. reported that *CCR5* expression levels in rhesus monkeys with severe TB disease exhibit remarkably up-regulated lymphocytes in the lungs, bronchial lymph nodes, and spleen (11). Additionally, CCR5 and its ligand play important roles in T-cell activation and migration during immune responses against TB infection. Galkina et al. observed that $CCR5^{-/-}$ $CD8^+$ T cells exhibit an approximately 50% reduction in effector $CD8^+$ T cell transmigration from pulmonary vascular compartments into interstitial compartments, as compared with CCR5 wild-type $CD8^+$ T cells (13). CCR5 has also been found to possibly regulate effector $CD8^+$ T cell contraction and memory generation after *M. tuberculosis* infection (14). Furthermore, several studies have suggested that CXCR3, CCR5, and CXCR6 potentially mediate *M. tuberculosis*-specific $CD4^+$T cell migration out of the vascular endothelium, and their entry into the lungs during *M. tuberculosis* infection, which is a critical step in host immune responses against *M. tuberculosis* infection (15). Therefore, CCR5 seems to play an important role in the immune response against *M. tuberculosis* infection.

Although CCR5 is reported to be involved in resistance against *M. tuberculosis* infection, a number of studies have reported the association of *CCR5* gene variants with TB infection and progression. In 2014, Carpenter et al. (16) performed an analysis regarding the possible associations between rs1799987 of *CCR5* and clinically active TB phenotypes in three different populations (Peru, Xhosa, and Colored), but found no significant associations. In this study, we examined genetic polymorphisms in the *CCR5* promoter in the Chinese Han population to investigate the association between *CCR5* promoter polymorphisms and *M. tuberculosis* infection, and TB progression.

METHODS AND MATERIALS

Subjects

A total of 450 patients with TB, including 325 cases of pulmonary TB (PTB) and 125 cases of extrapulmonary TB (EPTB, which was defined as TB influencing extrapulmonary sites such as lymph nodes, abdomen, urinary tract, skin, joints, bones, and meninges, exclusively or in combination with PTB), who were enrolled in the Third People's Hospital of Kunming between 2018–2019, were selected as a TB patient group for this study. All subjects were genetically unrelated and belonged to the Chinese Han population from Yunnan province (southwest China).

Diagnoses of TB were based on clinical case definition guidelines for TB issued by the World Health Organization (WHO) (17), Diagnosis for Pulmonary Tuberculosis (WS 288-2017) (18) and Classification of Tuberculosis (WS 196-2017) (19) from the Health Industry Standard of the People's Republic of China. The diagnostic criteria were as follows: (1) *M. tuberculosis* positively confirmed by sputum smear culture bacteriological assessment; (2) clinical symptoms such as cough, fever and weight loss over two weeks, and chest X-ray consistent with TB disease. Usually, Tuberculin skin test (TST) and interferon-γ release assay (IGRA) are also positive. Patients with immunodeficiency, autoimmune diseases, or other acute or chronic infections were excluded from this study.

Over the same period, 306 healthy individuals were recruited as a control group. All the controls had negative history for TB disease and were without any acute or chronic pulmonary disorder, or any bacterial or viral infection or other immune-mediated disorders. All the controls were self-reported Han Chinese.

DNA Extraction and Sequencing

Two to 5 ml of peripheral blood was drawn from each participant, and genomic DNA was extracted from peripheral lymphocytes using the QIAamp Blood Mini Kit (Qiagen, Hilden,

Germany) in a Biosafety Level 2 Laboratory of the Third People's Hospital of Kunming. The *CCR5* promoter region was PCR amplified using primers used in a previously published study (20); CCR5P_F: 5'-gacgagaaagctgagggtaaga-3' and CCR5P_R: 5'-taaccgtctgaaactcattcca-3'. The amplified PCR fragment was 1388 bp in length. PCR for each sample was carried out using the TAKARA PrimeSTAR Max DNA polymerase kit (TAKARA, Dalian, China) in 50 μl reaction volumes containing 10 ng genomic DNA, 10 pmol of each primer, 25 μl 2 × PrimeSTAR Max Premix (TAKARA). Amplification consisted of an initial denaturation step of 5 min at 98°C, followed by: 30 cycles of denaturation for 10 s at 98°C, 5 s of annealing at 55°C, extension at 72°C for 90 s, and a final extension for 5 min at 72°C. Purified PCR fragments were subjected to Sanger DNA sequencing to detect the sites of polymorphism using the Big Dye Terminator Reaction Mix (Applied Biosystems Foster City, CA, USA), along with the same primers used for PCR amplification. Sequencing reaction products were purified using the Big Dye Terminator Purification Kit (Applied Biosystems) and run on an ABI 3730XL sequencer. Sequencing data were analyzed using the DNASTAR Lasergene v.7.1 package. All the *CCR5* promoter region sequencing data in this study have been deposited in the Figshare database named "*CCR5* promoter sequences of TB patients and controls" (DOI: 10.6084/m9.figshare.12015624).

Polymorphic Loci in CCR5 Promoter

In our previous study (20), we found that there are nine identified single nucleotide polymorphisms (SNPs) loci located in the *CCR5* gene promoter. Six SNPs, rs2227010 (A>G), rs2734648 (T>G), rs1799987 (G>A), rs1799988 (T>G), rs1800023 (G>A), and rs1800024 (C>T) were found to be polymorphic in the Chinese Han population sample, whereas the three remaining sites, rs2856758 (AA), rs41469351 (CC), and rs41355345 (CC), were monomorphic in this sample. Thus, we analyzed association between alleles and genotypes of these six SNPs with TB.

Statistical Analysis

The distribution of age and sex between the case and control groups was compared *via* Student's *t*-test and χ^2-tests in SPSS (v.19.0; SPSS Inc., Chicago, IL, USA). Basic statistical analyses for allelic and genotypic frequencies of the six SNPs were carried out using PLINK v.1.9 (http://zzz.bwh.harvard.edu/plink/data.shtml) (21), and risks were estimated using odds ratios (OR) with 95% confidence intervals (95% CI). A goodness-of-fit χ^2-test was used to test for Hardy-Weinberg equilibrium (HWE) for each SNP in the control group, with a threshold of 0.05, which was also assessed using PLINK.

The Linkage disequilibrium (LD) and haplotype frequencies (deduced from the phenotype) among eight SNPs (rs2227010-rs2856758-rs2734648-rs1799987-rs1799988-rs41469351-rs1800023-rs1800024) were calculated based on the genotype results using a standard Expectation Maximization (ignoring missing data) algorithm with a partition-ligation approach for blocks by Haploview v.4.2 software (22). Haploview calculates the LD coefficient D', LOD and r^2 between each pair of genetic markers. *D'* values were defined in the range [-1, 1], with a value of 1 representing perfect disequilibrium. A *D'* value over 0.8 indicated there is a strong linkage disequilibrium among SNPs. The lowest frequency threshold for haplotype analysis was 0.01, and hhaplotype with frequency less than this number will not be considered in analysis. The differences in the haplotypes (with frequencies over 0.01) between the TB and control groups, between PTB and control groups, as well as between EPTB and control groups were determined by χ^2-test. And risks were estimated using ORs and 95%CI. OR and 95% CI were used to estimate associations between SNPs and TB disease by adjusting for age and gender using multivariate logistic regression models. The threshold for statistical significance was $P < 0.05$. Bonferroni correction was applied for multiple comparisons among alleles and genotypes, and the *P*-value was adjusted to 0.05/n. Power-analysis was performed using Power and Sample Size Calculations (v.3.1.2) (23).

RESULTS

Characteristics of Subjects

Table 1 presents participant demographic characteristic data, including gender, age, and clinical type of TB. The mean age of the TB group was 43.76 ± 16.01 years, with the sex ratio (male/female) being 249/201, while the mean age of the control group was 44.68 ± 9.26 years, with a sex ratio (male/female) of 154/152. The distributions of age and gender between the TB and control groups showed no statistical differences ($P > 0.05$). The mean ages were 45.31 ± 15.82 years in the PTB group and 39.75 ± 15.86 years in the EPTB group; whereas the sex ratio (male/female) was 190/135 in the PTB group and 59/66 in the EPTB group. For the initial treatment (IT) and retreatment (RT) groups, the mean ages were 43.20 ± 16.35 years and 44.68 ± 15.46 years, respectively, and sex ratios (male/female) were 144/135 in the IT and 105/66 in the RT group ($P = 0.043$).

Comparisons of Allelic and Genotypic Frequencies of CCR5 Promoter SNPs Between TB Patients and Controls

All six *CCR5* promoter SNPs with polymorphism exhibited HWE in the control group ($P > 0.05$). However, in the TB patient group, rs2734648, rs1799987, and rs1800023 were not in HWE. The allelic and genotypic frequencies of the six *CCR5* promoter SNPs were compared between the TB patient and control groups, after adjusting for age and gender based on the logistic regression model (**Table 2**). The results showed that the frequency of rs2734648-G was significantly higher in the TB patient group compared to that in the control group ($P = 0.002$, OR = 1.380, 95% CI: 1.123–1.696); the genotypic distribution of rs2734648 was significantly different between the TB and control groups ($P = 1.07E-05$). Furthermore, we performed inheritance model analysis and found that rs2734648-GG was significantly associated with TB disease, and exhibited 2-fold susceptibility in a recessive inheritance model ($P = 6.32E-06$, OR = 2.173, 95% CI: 1.546–3.056). The genotypic distribution of rs1799987 also showed significant difference between the TB and control groups ($P = 0.008$).

TABLE 1 | Demographic and clinical data for tuberculosis patients and controls.

Study groups		Num.	Sex, M:F	Age (mean ± SD), years
TB		450	249:201	43.76 ± 16.01
	PTB	325	190:135	45.31 ± 15.82
	Infiltration	146	80:66	45.97 ± 16.92
	Secondary	161	106:55	44.50 ± 14.80
	Cavity	18	4:14	47.17 ± 15.99
	EPTB	125	59: 66	39.75 ± 15.86
	Lymph nodes	13	7:6	36.31 ± 13.68
	Genitourinary tract	31	7:24	40.48 ± 14.66
	bone and joint	24	13:11	41.58 ± 15.20
	cutaneous	5	1:4	42.20 ± 21.81
	celiac	14	8:6	41.00 ± 23.29
	Meningitis	8	8:0	34.13 ± 10.87
	Peritoneal	2	1:1	20.50 ± 6.36
	Pleuritis	1	0:1	47.00
	Multi-site concurrency	17	8:9	39.53 ± 13.01
	others	10	6:4	42.60 ± 18.91
	Initial treatment	279	144:135	43.20 ± 16.35
	Retreatment	171	105:66	44.68 ± 15.46
Healthy control		306	154:152	44.68 ± 9.26

Num., number; M, male; F, female; SD, standard deviation; TB, tuberculosis; PTB, pulmonary tuberculosis; EPTB, extrapulmonary tuberculosis.

TABLE 2 | Comparison of allelic and genotypic frequencies of CCR5 gene between TB patients and controls.

Comparison		Control (n = 306) n (Freq.)	TB (n = 450) n (Freq.)	*P*	OR (95%CI)
rs2227010					
Allelic	**A**	501 (0.819)	734(0.816)		Ref.
	G	111 (0.181)	166(0.184)	0.879	1.021(0.783–1.332)
Genotypic	**A/A**	207 (0.676)	302(0.671)	0.988	Ref.
	G/A	87 (0.284)	130(0.289)		1.024(0.741–1.416)
	G/G	12 (0.039)	18(0.040)		1.028(0.485–2.180)
Dominant	**A/A**	207 (0.676)	302(0.671)		Ref.
	G/G-G/A	99 (0.324)	148 (0.329)	0.877	1.025(0.752–1.397)
Recessive	**A/A-G/A**	294 (0.961)	432 (0.960)		Ref.
	G/G	12 (0.039)	18(0.040)	0.957	1.021(0.484–2.151)
rs2734648					
Allelic	**T**	328 (0.536)	410(0.456)		Ref.
	G	284 (0.464)	490(0.544)	**0.002**	1.380(1.123–1.696)
Genotypic	**T/T**	83 (0.271)	118(0.262)	**1.07E-05**	Ref.
	G/T	162 (0.529)	174(0.387)		0.755(0.531–1.075)
	G/G	61 (0.199)	158(0.351)		1.822(1.212–2.739)
Dominant	**T/T**	83 (0.271)	118(0.262)		Ref.
	G/G-G/T	223 (0.729)	332 (0.738)	0.783	1.048(0.754–1.454)
Recessive	**G/T-T/T**	245 (0.801)	292 (0.649)		Ref.
	G/G	61 (0.199)	158(0.351)	**6.32E-06**	2.173(1.546–3.056)
rs1799987					
Allelic	**G**	365 (0.596)	516 (0.573)		Ref.
	A	247 (0.404)	384 (0.427)	0.372	1.100 (0.893–1.355)
Genotypic	**G/G**	110 (0.359)	174 (0.387)	**0.008**	Ref.
	G/A	145 (0.474)	168 (0.373)		0.732 (0.529–1.015)
	A/A	51 (0.167)	108 (0.240)		1.339 (0.889–2.017)
Dominant	**G/G**	110 (0.359)	174 (0.387)		Ref.
	A/A-A/G	196 (0.641)	276 (0.613)	0.449	0.890 (0.659–1.203)
Recessive	**G/G-A/G**	255 (0.833)	342 (0.760)		Ref.
	A/A	51 (0.167)	108(0.240)	0.015	1.579 (1.090–2.287)
rs1799988					
Allelic	**T**	358 (0.585)	532 (0.591)		Ref.
	C	254 (0.415)	368 (0.409)	0.8117	0.975 (0.791–1.201)
Genotypic	**T/T**	107 (0.350)	157 (0.349)	0.8806	Ref.
	C/T	144 (0.471)	218 (0.484)		1.032 (0.747–1.426)

(Continued)

TABLE 2 | Continued

Comparison		Control (n = 306) n (Freq.)	TB (n = 450) n (Freq.)	*P*	OR (95%CI)
	C/C	55 (0.180)	75 (0.167)		0.929 (0.607–1.423)
Dominant	**T/T**	107 (0.350)	157 (0.349)		Ref.
	C/C-C/T	199 (0.650)	293 (0.651)	0.982	1.003 (0.740–1.361)
Recessive	**T/T-C/T**	251 (0.820)	375 (0.833)		Ref.
	C/C	55 (0.180)	75 (0.167)	0.6401	0.913 (0.622–1.339)
rs1800023					
Allelic	**G**	336 (0.549)	482 (0.536)		Ref.
	A	276 (0.451)	418 (0.464)	0.6061	1.056 (0.859–1.297)
Genotypic	**G/G**	88 (0.288)	119 (0.264)	0.7798	Ref.
	A/G	160 (0.523)	244 (0.542)		1.128 (0.803–1.585)
	A/A	58 (0.190)	87 (0.193)		1.109 (0.720–1.708)
Dominant	**G/G**	88 (0.288)	119 (0.264)		Ref.
	A/A-A/G	218 (0.712)	331 (0.736)	0.4838	1.123 (0.812–1.553)
Recessive	**A/G-G/G**	248 (0.810)	363 (0.807)		Ref.
	A/A	58 (0.190)	87 (0.193)	0.8966	1.025 (0.708–1.483)
rs1800024					
Allelic	**C**	462 (0.755)	687 (0.763)		Ref.
	T	150 (0.245)	213 (0.237)	0.7064	0.955 (0.751–1.214)
Genotypic	**C/C**	170 (0.556)	268 (0.596)	0.1254	Ref.
	T/C	122 (0.399)	151 (0.336)		1.789 (0.911–3.513)
	T/T	14 (0.046)	31 (0.069)		1.405 (0.726–2.717)
Dominant	**C/C**	170 (0.556)	268 (0.596)		Ref.
	T/T-T/C	136 (0.444)	182 (0.404)	0.2742	0.849 (0.633–1.139)
Recessive	**T/C-C/C**	292 (0.954)	419 (0.931)		Ref.
	T/T	14 (0.046)	31 (0.069)	0.1869	1.543 (0.807–2.952)

Co, control; TB, tuberculosis; OR, odds ratio; CI, confidence interval.

The P-value, OR, and 95% CIs of pair-wise comparisons between TB and control groups were calculated based on the logistic regression model adjusted for age and gender. Bonferroni correction was applied, and the P-value was adjusted to 0.008 (0.05/6). And the P-value lower than 0.008 were marked in bold.

This study had powers over 80% to detect ORs of 1.021 for rs2227010, 0.725 for rs2734648, and 0.975 for rs1799988, and had power of 53.8% to detect with an OR of 1.1 for rs1799987, 60.6% to detect with an OR of 1.056 for rs1800023, and 72.6% to detect with a OR of 0.955 for rs1800024, respectively, in 450 TB patients compared with 306 controls.

Stratification Analysis of the Association Between TB and *CCR5* Promoter Polymorphisms

We performed stratification analysis to investigate the association of TB susceptibility with *CCR5* promoter SNPs. We stratified the TB patients into PTB and EPTB patients and compared the distribution of allelic and genotypic frequencies of the six SNPs among the stratification groups and the control group. The associations between SNPs and PTB or EPTB groups were adjusted for age and gender using multivariate logistic regression models. **Table 3** shows comparative results of rs2734648 and rs1799987. The results showed that the frequency of rs2734648-G was significantly higher in PTB patients as compared to controls ($P = 0.0013$, OR = 1.488, 95% CI: 1.192–1.858). Carriers of rs2734648-GG showed a notable increase in susceptibility to PTB in the recessive inheritance model ($P < 0.0001$, OR = 2.382, 95% CI: 1.663–3.413). Carriers of rs1799987-AA also showed a significant association with PTB in the recessive inheritance model ($P = 0.0078$, OR = 1.687, 95% CI: 1.141–2.495). However, significant associations of these two SNPs with EPTB in the recessive inheritance model were not detected (**Table 3**). For other SNPs, no significant differences were found between the PTB and control groups. It should be noted that the results from PTB (**Table 3**) simply reinforce the TB associations observed from **Table 2**, which is not surprising, since PTB represents 72.2% of the TB sample. Finally, no significant difference was found between the EPTB and control groups, and between the EPTB and PTB groups (**Supplementary Table 1**).

Additionally, we stratified the TB patients into IT and RT subgroups according to disease stage at the time of treatment, and analyzed allelic and genotypic distributions of the six SNPs. Associations between SNPs and disease recurrence were adjusted for age and gender using multivariate logistic regression models. We found rs2734648-G and rs2734648-GG to be significantly associated with TB recurrence (**Table 4**). After comparison between IT and control, RT and control, and RT and IT groups, we found that rs2734648-GG was significantly associated with TB recurrence in a dominant inheritance model ($P = 0.0032$, OR = 1.936, 95% CI: 1.221–3.068), while rs1799987 showed no significant association with disease recurrence (**Table 4** and **Supplementary Table 2**).

CCR5 Promoter SNP Combination Analysis and Association With TB

LD among eight SNPs (rs2227010, rs2856758, rs2734648, rs1799987, rs1799988, rs41469351, rs1800023, rs1800024) in the *CCR5* promoter was estimated, where the LD coefficient D (*D'*) was calculated. The *D'* value of these eight SNPs was >0.8,

TABLE 3 | Stratification analysis on the association between CCR5 promoter SNPs and clinical TB phenotypes.

Comparison		Control (n = 306)	PTB (n = 325)	EPTB (n = 125)	PTB vs Co.		EPTB vs Co.		EPTB vs PTB	
		n (Freq.)	n (Freq.)	n (Freq.)	*P*	OR (95%CI)	*P*	OR (95%CI)	*P*	OR (95%CI)
rs2734648										
Allelic	**T**	328(0.536)	284(0.437)	126(0.504)		Ref.		Ref.		Ref.
	G	284(0.464)	366(0.563)	124(0.496)	**1.3E-03**	1.488(1.192–1.858)	0.394	1.137(0.847–1.526)	0.700	0.764(0.570–1.023)
Genotypic	**T/T**	83(0.271)	80(0.246)	38 (0.304)	**5.20E-06**	Ref.	0.076	Ref.	0.256	Ref.
	G/T	162(0.530)	124(0.382)	50 (0.400)		0.794(0.540–1.168)		0.674(0.410–1.109)		0.849(0.511–1.409)
	G/G	61(0.199)	121(0.372)	37 (0.296)		2.058(1.332–3.179)		1.325(0.756–2.321)		0.644(0.378–1.098)
Dominant	**T/T**	83(0.271)	80(0.246)	38 (0.304)		Ref.		Ref.		Ref.
	G/G-G/T	223(0.729)	245(0.754)	87 (0.696)	0.5	1.140(0.798–1.628)	0.730	0.852(0.540–1.346)	0.211	0.748(0.473–1.181)
Recessive	**G/T-T/T**	245(0.801)	204(0.628)	88 (0.704)		Ref.		Ref.		Ref.
	G/G	61(0.199)	121(0.372)	37 (0.296)	**1.64E-06**	2.382(1.663–3.413)	0.049	1.689(1.050–2.717)	0.129	0.709(0.454–1.106)
rs1799987										
Allelic	**G**	365(0.596)	371(0.571)	145(0.580)		Ref.		Ref.		Ref.
	A	247(0.404)	279(0.429)	105(0.420)	0.519	1.111(0.888–1.390)	0.657	1.070(0.794–1.442)	0.802	0.963(0.717–1.294)
Genotypic	**G/G**	110(0.359)	128(0.394)	46 (0.368)	**0.0028**	Ref.	0.740	Ref.	0.353	Ref.
	G/A	145(0.474)	115(0.354)	53 (0.424)		0.682(0.479–0.970)		0.874(0.548–1.393)		1.282(0.803–2.049)
	A/A	51(0.167)	82(0.252)	26 (0.208)		1.382(0.897–2.130)		1.219(0.680–2.187)		0.882(0.506–1.537)
Dominant	**G/G**	110(0.359)	128(0.394)	46 (0.368)		Ref.		Ref.		Ref.
	A/A-A/G	196(0.641)	197(0.606)	79 (0.632)	0.373	0.864(0.626–1.193)	0.990	0.964(0.626–1.485)	0.614	1.116(0.729–1.709)
Recessive	**G/G-A/G**	255(0.833)	243(0.748)	99 (0.792)		Ref.		Ref.		Ref.
	A/A	51(0.167)	82(0.252)	26 (0.208)	**0.0078**	1.687(1.141–2.495)	0.470	1.313(0.776–2.223)	0.324	0.778(0.472–1.282)

Co, control; PTB, pulmonary tuberculosis; EPTB, extra pulmonary tuberculosis; OR, odds ratio; CI, confidence interval.
The P-value, OR, and 95% CIs of pair-wise comparisons between PTB and controls, and EPTB and controls, were calculated based on the logistic regression model adjusted for age and gender. Bonferroni correction was applied, and the P-value was adjusted to 0.008 (0.05/6). And the P-value lower than 0.008 were marked in bold.

indicating that these *CCR5* promoter SNPs were in LD (**Supplementary Figure 1**). Next, we constructed haplotypes of the eight SNPs (rs2227010-rs2856758-rs2734648-rs1799987-rs1799988-rs41469351-rs1800023-rs1800024) and compared haplotypes with frequencies over 0.01 between case and control groups, as listed in **Table 5**. The results revealed that haplotype H1 (A-A-T-G-T-C-G-C) was the most prevalent, both in control (50.3%) as well as TB patient groups (41.1%), and showed a significant resistance to TB disease (P = 1.17E-04, OR = 0.660, 95% CI: 0.535–0.816), with notable resistance to PTB (P = 1.05E-05, OR = 0.599, 95% CI: 0.477–0.753). In contrast, haplotype H5 (A-A-G-G-T-C-G-C) presented an extremely increased risk of susceptibility to TB by over 20-fold (P = 7.84E-10, OR = 21.877, 95% CI: 5.378–88.996), as well as a notably increased risk of susceptibility to PTB and EPTB (P = 6.33E-11, OR = 24.887, 95% CI: 6.081–101.841 and P = 8.35E-06, OR = 14.038, 95% CI: 3.088–63.804, respectively); whereas haplotype H7 (A-A-G-A-T-C-G-C) increased the risk of susceptibility to TB and PTB by 10-fold (P = 0.004, OR = 10.715, 95% CI: 1.421–80.796, and P = 0.002, OR = 12.196, 95% CI: 1.595–93.269, respectively). Additionally, both haplotypes H10 (A-A-T-A-T-C-G-C) and H11 (G-A-G-G-C-C-A-C) appeared only in the case group, mainly in the PTB cohort, and frequency differences between PTB and control groups were remarkable after Bonferroni correction (P = 7.63E-05 and P = 0.003, respectively). However, there was no difference between PTB and EPTB groups (**Supplementary Table 3**).

DISCUSSION

TB is a serious infectious disease caused by *M. tuberculosis*; however, only 5–10% of infected individuals actually develop the active form of disease with clinical symptoms, prompting researchers to identify the factors influencing susceptibility to TB. Understanding host immune responses to *M. tuberculosis* infection is critical in identifying the reasons behind varying outcomes after *M. tuberculosis* exposure (latent or active TB disease), and for the development of effective TB vaccines and immune therapeutics. There is substantial evidence to suggest that the onset of TB is influenced by host genetic factors (2, 9, 15, 24). CCR5 has been reported to play important roles in immune responses against *M. tuberculosis* infection by regulating and activating the recruitment of macrophages, and by further activation of T-cells. In the present study, we investigated

TABLE 4 | Association between CCR5 gene variants and TB recurrence.

Comparison		Co (n = 306)	IT (n = 279)	RT (n = 171)	*P*	IT vs Co	*P*	RT vs Co	*P*	IT vs RT
		n (freq.)	n (freq.)	n (freq.)		OR (95% CI)		OR (95% CI)		OR (95% CI)
rs2734648										
Allelic	T	328(0.536)	269(0.482)	141(0.412)		Ref.		Ref.		Ref.
	G	284(0.464)	289(0.518)	201(0.588)	0.0725	1.241(0.986–1.561)	**1.7E-04**	1.646(1.260–2.151)	0.0471	1.327(1.011–1.741)
Genotypic	T/T	83(0.271)	86(0.308)	32(0.187)	**1.0E-05**	Ref.	**2.0E-04**	Ref.	0.01	Ref.
	G/T	162(0.529)	97(0.348)	77(0.450)		0.578(0.390–0.856)		1.233(0.755–2.012)		2.133(1.289–3.532)
	G/G	61(0.199)	96(0.344)	62(0.363)		1.519(0.978–2.359)		2.636(1.537–4.522)		1.736(1.036–2.909)
Dominant	T/T	83(0.271)	86(0.308)	32(0.187)		Ref.		Ref.		Ref.
	G/G-G/T	223 (0.729)	193 (0.692)	139 (0.813)	0.35	0.835(0.584–1.195)	0.034	1.617(1.021–2.560)	**0.0032**	1.936(1.221–3.068)
Recessive	T/T-G/T	245 (0.801)	183 (0.656)	109(0.637)		Ref.		Ref.		Ref.
	G/G	61(0.199)	96(0.344)	62(0.363)	**1.00E-04**	2.107(1.450–3.062)	**1.00E-04**	2.285(1.502–3.475)	0.58	1.084(0.728–1.614)
rs1799987										
Allelic	G	365(0.596)	322(0.577)	194(0.567)		Ref.		Ref.		Ref.
	A	247(0.404)	236(0.423)	148(0.433)	0.555	1.803(0.858–1.367)	0.3848	1.127(0.862–1.474)	0.6775	1.041(0.793–1.366)
Genotypic	G/G	110(0.359)	115(0.412)	59(0.345)	**9.0E-04**	Ref.	0.51	Ref.	0.045	Ref.
	A/G	145(0.474)	92(0.330)	76(0.444)		0.607(0.419–0.878)		0.977(0.642–1.488)		1.610(1.040–2.492)
	A/A	51(0.167)	72(0.258)	36(0.211)		1.350(0.866–2.105)		1.316(0.774–1.577)		0.975(0.586–1.621)
Dominant	G/G	110(0.359)	115(0.412)	59(0.345)		Ref.		Ref.		Ref.
	A/A-A/G	196 (0.641)	164 (0.588)	112 (0.655)	0.19	0.800(0.573–1.117)	0.73	1.065(0.720–1.577)	0.11	1.331(0.897–1.976)
Recessive	A/G-G/G	255 (0.833)	207 (0.742)	135 (0.789)		Ref.		Ref.		Ref.
	A/A	51(0.167)	72(0.258)	36(0.211)	**7.9E-03**	1.739(1.162–2.602)	0.24	1.333(0.829–2.144)	0.3	0.767(0.486–1.208)

Co, control; IT, initial treatment; RT, retreatment; OR, odds ratio; CI, confidence interval.

The P-value, OR, and 95% CIs of pair-wise comparisons between IT and control, RT and control, and RT and IT groups were calculated on the basis of the logistic regression model adjusted for age and gender. Bonferroni correction was applied, and the P-value was adjusted to 0.008 (0.05/6). And the P-value lower than 0.008 were marked in bold.

associations between *CCR5* promoter polymorphisms and TB and discovered that *CCR5* promoter polymorphisms were significantly associated with PTB and TB progression in the Chinese Han population for the first time.

In this study, we found that the allelic frequency of rs2734648-G was significantly higher in the TB patient group, especially in the PTB group, as compared to the control group, and also that rs2734648-GG carriers had a 2.382-fold increased

TABLE 5 | *CCR5* promoter haplotype frequencies in case and control groups.

Haplotype[a,d]		Haplotype similarity[b]	Co (2n = 612)	TB patients (2n = 900)			PTB (2n = 650)			EPTB patients (2n = 250)		
			N (freq.)	N (freq.)	*P*[c]	OR (95%CI)	N (freq.)	*P*[c]	OR (95%CI)	N (freq.)	*P*[c]	OR (95%CI)
H1:	A A T G T C G C	HHC	307.60 (0.503)	370.30 (0.411)	**1.17E-04**	0.660 (0.535–0.816)	250.99 (0.386)	**1.05E-05**	0.599 (0.477–0.753)	121.5 (0.486)	0.6652	0.947(0.706–1.271)
H2:	A A G A C C A T	HHF*1	126.14 (0.206)	179.78 (0.200)	0.644	0.941 (0.728–1.217)	128.64 (0.198)	0.649	0.938 (0.711–1.237)	47.6 (0.190)	0.5996	0.917(0.633–1.328)
H3:	G A G A C C A C	HHE	97.75 (0.160)	143.12 (0.159)	0.863	0.975 (0.736–1.293)	95.95 (0.148)	0.499	0.899 (0.661–1.223)	45.9 (0.184)	0.3999	1.183(0.804–1.740)
H4:	A A G G T C A C	HHA	29.97 (0.049)	46.68 (0.052)	0.857	1.044 (0.652–1.673)	38.87 (0.060)	0.421	1.223 (0.749–1.997)	9.8 (0.039)	0.5409	0.728(0.340–1.555)
H5:	A A G G T C G C	unknown	2.03 (0.003)	61.78 (0.069)	**7.84E-10**	21.877 (5.378–88.996)	49.95 (0.077)	**6.33E-11**	24.887 (6.081–101.841)	11.2 (0.045)	**8.35E-06**	14.038(3.088–63.804)
H6:	A A G G C C A T	unknown	1.95 (0.003)	14.47 (0.016)	0.019	5.030 (1.124–22.509)	13.46 (0.021)	0.005	6.551 (1.453–29.528)	1(0.004)	0.8396	1.225(0.111–13.570)
H7:	A A G A T C G C	unknown	1.00 (0.002)	15.81 (0.018)	**4.10E-03**	10.715 (1.421–80.796)	12.88 (0.020)	**0.002**	12.196 (1.595–93.269)	3(0.012)	0.0423	7.421(0.768–71.690)
H8:	A A G A C C G T	unknown	7.04 (0.012)	4.36 (0.005)	0.134	0.411 (0.124–1.365)	3.30 (0.005)	0.200	0.435 (0.117–1.614)	1.6 (0.006)	0.4821	0.697(0.144–3.379)
H9:	A A T G C C G C	unknown	7.07 (0.012)	1.01 (0.001)	0.006	0.094 (0.012–0.762)	1.01 (0.002)	0.025	0.131 (0.016–1.063)	0(0.000)	0.46	0.302(0.038–2.426)
H10:	A A T A T C G C	unknown	0.00 (0.000)	20.04 (0.022)	**2.43E-04**	14.612(1.960–108.915)	17.24 (0.027)	**7.63E-05**	17.459(2.324–131.181)	3(0.012)	0.027	9.746(1.095–86.770)
H11:	G A G G C C A C	unknown	0.00 (0.000)	10.48 (0.012)	0.034	7.576(0.976–58.835)	10.51 (0.016)	**0.003**	11.530(1.495–88.938)	0(0.000)	–	–

[a]*Haplotypes were constructed with rs2227010-rs2856758-rs2734648-rs1799987-rs1799988-rs41469351-rs1800023-rs1800024.*

[b]*HHA, HHB, HHC, and HHF were previously reported (25–27).*

[c]*Bonferroni correction was applied, and the P-value was adjusted to 0.004 (0.05/11). And the P-value lower than 0.004 were marked in bold.*

[d]*Haplotypes with frequencies over 0.01 were compared and listed in this table.*

risk of susceptibility to PTB in a recessive inheritance model. Additionally, rs2734648 was found to be significantly associated with TB recurrence. It has been reported that *CCR5* variants may alter the response of CCR5-chemokines, including altered ligand-binding properties (28), and *CCR5* promoter polymorphisms could differentially affect *CCR5* gene transcription. We constructed a predictive model involving potential binding sites of transcription factors in the *CCR5* promoter and discovered that SNPs in the *CCR5* promoter might differentially influence transcription factor binding, based on the nucleotide substitution(s) involved (20). Mummidi et al. demonstrated that G to T substitution in rs2734648 (-2554G>T) is associated with differences in binding avidity of the NF-κB family of transcription factors (the binding avidity of rs2734648-G is greater than that of rs2734648-T), which might affect the transcriptional activity of *CCR5*. rs2856758-G can bind to novel nuclear factor 1 (NF1), which can repress transcription of certain genes (29), whereas rs2856758-A cannot bind to NF1 (26). For another SNP in the *CCR5* promoter, rs1799987-AA, we found an increasing risk of susceptibility to PTB in a recessive inheritance model. McDremott et al. reported that rs1799987 (-2459A>G) influences the expression of *CCR5*, and rs1799987-G has 45% lower promoter activity than rs1799987-A *in vitro* (30). The latter authors also observed that rs1799987-A/rs1799988-C in combination stimulates *CCR5* promoter activity by 45% more than other rs1799987/rs1799988 allelic combinations (30). Li et al. showed that rs1799988 C to T substitution results in reduced expression of *CCR5*, which consequently correlated with slower AIDS progression. Furthermore, rs1799988-CC carriers display increased CCR5 expression on the surface of peripheral blood mononuclear cells (PBMCs), CD4+ cells, and CD4+ monocytes, as compared to two other *CCR5*-rs1799988 genotypes (31). Therefore, we deduced that SNPs in the *CCR5* promoter could influence *CCR5* gene and cell surface CCR5 protein expression by altering the binding of transcription factors, thereby affecting the function of CCR5. Hence, rs2734648-GG and rs1799987-AA were significantly associated with PTB and TB progression by possibly increased expression of CCR5.

We also analyzed the effects of combinations of the 8 *CCR5* promoter SNPs (rs2227010, rs2856758, rs2734648, rs1799987, rs1799988, rs41469351, rs1800023, rs1800024) on TB susceptibility and found that haplotype H1 (A-A-T-G-T-C-G-C)—constructed using the major alleles of the eight SNPs—was significantly associated with resistance to PTB; and haplotype H5 (A-A-G-G-T-C-G-C) increased the susceptibility to PTB by over 20-times. *CCR2-CCR5* haplogroups constructed using CCR2 (V>64I), rs2856758(-2733A>G), rs2734648(-2554G>T), rs1799987(-2459G>A), rs1799988(-2135T>C), rs41469351 (-2132C>T), rs1800023(-2086A>G), rs1800024(-1835C>T), and rs333(CCR5Δ32) have been characterized and described in earlier studies, and the haplogroups are termed HHA, HHB, HHC, HHD, HHE, HHF*1, HHF*2, HHG*1, and HHG*2, respectively (25, 26). CCR2-CCR5 haplogroups are correlated with differences in *CCR5* expression and transcriptional activity. HHA is associated with lower *CCR5* expression, whereas HHF and HHG are associated with higher *CCR5* expression (32). Similarly, K562 cells, HHA and HHC exhibit lower transcriptional activity, whereas in Jurkat T-cells, HHB, and HHD show higher transcriptional activity than HHA (33, 34). In 2011, Mamtani et al. found that the *CCR5* promoter haplogroup HHD was associated with susceptibility to TB, by increasing *CCR5* expression in either activated PBMCs, or surface expression on activated (HLA-DR^+) $CD4^+$ T cells (34). In our study, we constructed haplotypes with eight SNPs in the *CCR5* promoter, and only rs2227010 was not included in the defined CCR2-CCR5 haplogroups. Our results showed that H1 was similar to HHC (which exhibited lower transcriptional activity and lower *CCR5* expression), H2 was similar to HHF*1 (related to higher *CCR5* expression), H3 was similar to HHE, and H4 was similar to HHA. Therefore, the noticeable protection against PTB by the H1 haplotype in this study was likely due to the lower transcriptional activity of H1 (similar to HHC, which was associated with lower CCR5 expression). However, haplotype H5 was different from haplotype H1 at only one locus: rs2734648, which was T in haplotype H1 and G in H5. Note that H5 is a novel haplotype not previously detected in any other population. Based on the significant susceptibility of rs2734648-G to TB, and the extraordinarily high frequency of rs2734648-G in the Han population, rs2734648-G as well as haplotype H5 could provide crucial insights into immune responses to TB in the Chinese Han population. In this study, we also found one haplotype rs2856758A-rs2734648T-rs1799987G-rs1799988T-rs41469531C-rs1800023A-rs1800024C was most similar as HHD. However, the haplotype frequencies were very low (0.5 and 0.5% in control and TB group respectively, and data not showed) and with no difference between TB and control group. In addition, haplotype H1, which presented only two differences loci when compared with HHD (rs41469351-C and rs1800023-G in H1, whereas rs41469351-T and rs1800023-A in HHD), showed significant frequency difference between TB and control groups (P = 2.25E-04, OR = 0.674, 95% CI: 0.547–0.832). But haplotype HHD and H1 showed entirely opposite effects on the susceptibility to TB. The reason of this discrepancy could be the different frequency of rs41469351 and rs1800023. According to the 1000 Genomes database the rs41469351-T is only detected in African and American population with the frequencies of 26 and 2%, respectively, and were monomorphic (rs41469351-CC) in Chinese Han and European people (http://asia.ensembl.org/Homo_sapiens/Variation/Population?db=core;r=3:46370271-46371271;v=rs41469351;vdb=variation;vf=5860779). And for rs1800023, the A-allele frequencies in Chinese Han people is 43%, however, there are 91% in African, 63% in European (http://asia.ensembl.org/Homo_sapiens/Variation/Population?db=core;r=3:46370317-46371317;v=rs1800023;vdb=variation;vf=816197). So rs41469351 and rs1800023 maybe important loci which might affect the susceptibility of TB. Haplotypes H7, H10, and H11, which were unlike any reported haplogroups, also showed significantly higher frequencies in the TB group, as well as the PTB cohort. Hence, the combined functions of *CCR5*

promoter SNPs might play important roles in *CCR5*-mediated immune responses to TB.

Associations of SNPs with diseases have always been inconsistent among different populations. Previous studies indicate that *CCR5* allelic frequencies are remarkably different among different populations (16, 35), which might influence the results of correlative studies. Among most populations in the world (including Africans, Americans, Europeans, Japanese, and South Asians), rs2734648-G is the major allele; however, in Chinese Han populations, rs2734648-T is the predominant allele (Han Chinese in Beijing, and Southern Han Chinese from the 1000 Genomes database, and Chinese Han in Yunnan in this study), indicating that the frequency differences in rs2734648 could account for the specific association with TB in Han Chinese people. However, the function of rs2734648 substitution is still unclear; therefore, functional studies regarding the role of rs2734648 in *M. tuberculosis* infection and TB progression need to be conducted in the future.

Hence, more studies involving more individuals from different populations are needed. Additionally, as discussed above, SNP combinations also play an important role in susceptibility to TB and in its progression. Hence, further studies regarding haplotype structure, especially in terms of combinations of rs2734648 with other SNPs in the *CCR5* promoter, are required.

CONCLUSIONS

SNP rs2734638-G of the *CCR5* promoter, as well as haplotype H5, consistent with rs2734648-G, are significantly associated with susceptibility to PTB and with TB recurrence by affecting the transcriptional activity and expression of *CCR5*.

DATA AVAILABILITY STATEMENT

The data sets presented in this study can be found in online repositories. The names of the repository/repositories and accession number(s) can be found below: https://figshare.com/, 10.6084/m9.figshare.12015624.

ETHICS STATEMENT

The studies involving human participants were reviewed and approved by the institutional review board of the Third Hospital of Kunming (approval number is 2018030720). The patients/participants provided their written informed consent to participate in this study.

AUTHOR CONTRIBUTIONS

SL and LS conceived and designed the research. SL and NL mainly performed experiments and data analysis. HW and SZ did the clinical diagnosis. HW and XZ prepared samples for experiments and performed part of the experiments. SL wrote the manuscript. YY, SZ, and LS wrote parts of the manuscript and reviewed the manuscript. All authors contributed to the article and approved the submitted version.

FUNDING

This work was supported by the National Natural and Science Foundation of China (31401063); and the Special Funds for high-level health talents of Yunnan Province (D-201669, L-201615, and H-2018014). The funders had no role in the design of the study, data collection and analysis, decision to publish, or preparation of the manuscript.

ACKNOWLEDGMENTS

We thank all participants for their cooperation.

SUPPLEMENTARY MATERIAL

The Supplementary Material for this article can be found online at: https://www.frontiersin.org/articles/10.3389/fimmu.2020.544548/full#supplementary-material

REFERENCES

1. Cliff JM, Kaufmann SHE, Mcshane H, Van Helden P, O'garra A. The human immune response to tuberculosis and its treatment: a view from the blood. *Immunol Rev* (2015) 264:88–102. doi: 10.1111/imr.12269
2. Abel L, El-Baghdadi J, Bousfiha AA, Casanova J-L, Schurr E. Human genetics of tuberculosis: a long and winding road. *Philos Trans R Soc Lond B Biol Sci* (2014) 369:20130428–20130428. doi: 10.1098/rstb.2013.0428
3. Pai M, Behr MA, Dowdy D, Dheda K, Divangahi M, Boehme CC, et al. Tuberculosis. *Nat Rev Dis Primers* (2016) 2:16076. doi: 10.1038/nrdp.2016.76
4. Dallmann-Sauer M, Correa-Macedo W, Schurr E. Human genetics of mycobacterial disease. *Mamm Genome Off J Int Mamm Genome Soc* (2018) 29:523–38. doi: 10.1007/s00335-018-9765-4
5. Lyadova IV, Tsiganov EN, Kapina MA, Shepelkova GS, Sosunov VV, Radaeva TV, et al. In mice, tuberculosis progression is associated with intensive inflammatory response and the accumulation of Gr-1 cells in the lungs. *PloS One* (2010) 5:e10469. doi: 10.1371/journal.pone.0010469
6. Aravindan PP. Host genetics and tuberculosis: Theory of genetic polymorphism and tuberculosis. *Lung India* (2019) 36:244–52. doi: 10.1016/j.ejcdt.2013.12.002
7. Azad AK, Sadee W, Schlesinger LS. Innate immune gene polymorphisms in tuberculosis. *Infect Immunity* (2012) 80:3343–59. doi: 10.1128/IAI.00443-12
8. Blanpain C, Migeotte I, Lee B, Vakili J, Doranz BJ, Govaerts C, et al. CCR5 Binds Multiple CC-chemokines: MCP-3 Acts as a Natural Antagonist. *Blood* (1999) 94:1899–905. doi: 10.1182/blood.V94.6.1899
9. Camargo JF, Quinones MP, Mummidi S, Srinivas S, Gaitan AA, Begum K, et al. CCR5 expression levels influence NFAT translocation, IL-2 production, and subsequent signaling events during T lymphocyte activation. *J Immunol (Baltimore Md 1950)* (2009) 182:171–82. doi: 10.4049/jimmunol.182.1.171
10. Pokkali S, Das SD. Augmented chemokine levels and chemokine receptor expression on immune cells during pulmonary tuberculosis. *Hum Immunol* (2009) 70:110–5. doi: 10.1016/j.humimm.2008.11.003
11. Qiu L, Huang D, Chen CY, Wang R, Shen L, Shen Y, et al. Severe tuberculosis induces unbalanced up-regulation of gene networks and overexpression of

IL-22, MIP-1alpha, CCL27, IP-10, CCR4, CCR5, CXCR3, PD1, PDL2, IL-3, IFN-beta, TIM1, and TLR2 but low antigen-specific cellular responses. *J Infect Dis* (2008) 198:1514–9. doi: 10.1086/592448

12. Juffermans NP, Paxton WA, Dekkers PE, Verbon A, De Jonge E, Speelman P, et al. Up-regulation of HIV coreceptors CXCR4 and CCR5 on CD4(+) T cells during human endotoxemia and after stimulation with (myco)bacterial antigens: the role of cytokines. *Blood* (2000) 96:2649–54. doi: 10.1182/blood.V96.8.2649
13. Galkina E, Thatte J, Dabak V, Williams MB, Ley K, Braciale TJ. Preferential migration of effector CD8+ T cells into the interstitium of the normal lung. *J Clin Invest* (2005) 115:3473–83. doi: 10.1172/jci24482
14. Kohlmeier JE, Reiley WW, Perona-Wright G, Freeman ML, Yager EJ, Connor LM, et al. Inflammatory chemokine receptors regulate CD8+ T cell contraction and memory generation following infection. *J Exp Med* (2011) 208:1621–34. doi: 10.1084/jem.20102110
15. Kauffman KD, Sallin MA, Sakai S, Kamenyeva O, Kabat J, Weiner D, et al. Defective positioning in granulomas but not lung-homing limits CD4 T-cell interactions with Mycobacterium tuberculosis-infected macrophages in rhesus macaques. *Mucosal Immunol* (2018) 11:462–73. doi: 10.1038/mi.2017.60
16. Carpenter D, Taype C, Goulding J, Levin M, Eley B, Anderson S. M.-A. Shaw, and J.a.L. Armour. CCL3L1 copy number, CCR5genotype and susceptibility to tuberculosis. *BMC Med Genet* (2014) 15:5. doi: 10.1186/1471-2350-15-5
17. World Health Organization. Global tuberculosis report 2019. Geneva: World Health Organization (2019). Available at: https://apps.who.int/iris/handle/10665/329368.
18. National Health and Family Planning Commission of the People's Republic of China. Diagnosis for pulmonary tuberculosis(WS 288-2017). *Chin J Infect Control* (2018) 17:642–52. doi: 10.19871/j.cnki.xfcrbzz.2018.01.017
19. National Health and Family Planning Commission of the People's Republic of China. Classification of tuberculosis (WS 196-2017). *Chin J Infect Control* (2018) 17:367–8. doi: 10.19871/j.cnki.xfcrbzz.2018.03.018
20. Liu S, Chen J, Yan Z, Dai S, Li C, Yao Y, et al. Polymorphisms in the CCR5 promoter associated with cervical intraepithelial neoplasia in a Chinese Han population. *BMC Cancer* (2019) 19:525–5. doi: 10.1186/s12885-019-5738-6
21. Purcell S, Neale B, Todd-Brown K, Thomas L, Ferreira MA, Bender D, et al. PLINK: a tool set for whole-genome association and population-based linkage analyses. *Am J Hum Genet* (2007) 81:559–75. doi: 10.1086/519795
22. Barrett JC, Fry B, Maller J, Daly MJ. Haploview: analysis and visualization of LD and haplotype maps. *Bioinformatics* (2005) 21:263–5. doi: 10.1093/bioinformatics/bth457
23. Dupont W, Plummer WD Jr. Power and sample size calculations. A review and computer program. *Control Clin Trials* (1990) 11(2):116–28. doi: 10.1016/0197-2456(90)90005-m
24. Kalsdorf B, Skolimowska KH, Scriba TJ, Dawson R, Dheda K, Wood K, et al. Relationship between chemokine receptor expression, chemokine levels and HIV-1 replication in the lungs of persons exposed to Mycobacterium tuberculosis. *Eur J Immunol* (2013) 43:540–9. doi: 10.1002/eji.201242804
25. Martin MP, Dean M, Smith MW, Winkler C, Gerrard B, Michael NL, et al. Genetic acceleration of AIDS progression by a promoter variant of CCR5. *Sci (N Y NY)* (1998) 282:1907–11. doi: 10.1126/science.282.5395.1907
26. Mummidi S, Bamshad M, Ahuja SS, Gonzalez E, Feuillet PM, Begum K, et al. Evolution of human and non-human primate CC chemokine receptor 5 gene and mRNA. Potential roles for haplotype and mRNA diversity, differential haplotype-specific transcriptional activity, and altered transcription factor binding to polymorphic nucleotides in the pathogenesis of HIV-1 and simian immunodeficiency virus. *J Biol Chem* (2000) 275:18946–61. doi: 10.1074/jbc.M000169200
27. Picton AC, Paximadis M, Tiemessen CT. Genetic variation within the gene encoding the HIV-1 CCR5 coreceptor in two South African populations. *Infect Genet Evol J Mol Epidemiol Evolutionary Genet Infect Dis* (2010) 10:487–94. doi: 10.1016/j.meegid.2010.02.012
28. Blanpain C, Lee B, Tackoen M, Puffer B, Boom A, Libert F, et al. Multiple nonfunctional alleles of CCR5 are frequent in various human populations. *Blood* (2000) 96:1638–45. doi: 10.1182/blood.V96.5.1638
29. Rafty LA, Santiago FS, Khachigian LM. NF1/X represses PDGF A-chain transcription by interacting with Sp1 and antagonizing Sp1 occupancy of the promoter. *EMBO J* (2002) 21:334–43. doi: 10.1093/emboj/21.3.334
30. Mcdermott DH, Zimmerman PA, Guignard F, Kleeberger CA, Leitman SF, Murphy PM. CCR5 promoter polymorphism and HIV-1 disease progression. *Lancet* (1998) 352:866–70. doi: 10.1016/S0140-6736(98)04158-0
31. Li C, Lu SC, Hsieh PS, Huang YH, Huang HI, Ying TH, et al. Distribution of human chemokine (C-X3-C) receptor 1 (CX3CR1) gene polymorphisms and haplotypes of the CC chemokine receptor 5 (CCR5) promoter in Chinese people, and the effects of CCR5 haplotypes on CCR5 expression. *Int J Immunogenet* (2005) 32:99–106. doi: 10.1111/j.1744-313X.2005.00498.x
32. Gornalusse GG, Mummidi S, Gaitan AA, Jimenez F, Ramsuran V, Picton A, et al. Epigenetic mechanisms, T-cell activation, and CCR5 genetics interact to regulate T-cell expression of CCR5, the major HIV-1 coreceptor. *Proc Natl Acad Sci U S A* (2015) 112:E4762–71. doi: 10.1073/pnas.1423228112
33. Mummidi S, Ahuja SS, Mcdaniel BL, Ahuja SK. The human CC chemokine receptor 5 (CCR5) gene. Multiple transcripts with 5'-end heterogeneity, dual promoter usage, and evidence for polymorphisms within the regulatory regions and noncoding exons. *J Biol Chem* (1997) 272:30662–71. doi: 10.1074/jbc.272.49.30662
34. Mamtani M, Mummidi S, Ramsuran V, Pham M-H, Maldonado R, Begum K, et al. Influence of Variations in CCL3L1 and CCR5 on Tuberculosis in a Northwestern Colombian Population. *J Infect Dis* (2011) 203:1590–4. doi: 10.1093/infdis/jir145
35. Ometto L, Bertorelle R, Mainardi M, Zanchetta M, Tognazzo S, Rampon O, et al. Polymorphisms in the CCR5 promoter region influence disease progression in perinatally human immunodeficiency virus type 1-infected children. *J Infect Dis* (2001) 183:814–8. doi: 10.1086/318828

Conflict of Interest: The authors declare that the research was conducted in the absence of any commercial or financial relationships that could be construed as a potential conflict of interest.

frontiers in Immunology

ORIGINAL RESEARCH
published: 01 April 2021
doi: 10.3389/fimmu.2021.604975

Single-Nucleotide Variants in the AIM2 – Absent in Melanoma 2 Gene (rs1103577) Associated With Protection for Tuberculosis

Mariana Brasil de Andrade Figueira[1,2], Dhêmerson Souza de Lima[3], Antonio Luiz Boechat[1,2], Milton Gomes do Nascimento Filho[1], Irineide Assumpção Antunes[4], Joycenéa da Silva Matsuda[4], Thaís Rodrigues de Albuquerque Ribeiro[1], Luana Sousa Felix[1], Ariane Senna Fonseca Gonçalves[1], Allyson Guimarães da Costa[2,5], Rajendranath Ramasawmy[2,6,7], Alessandra Pontillo[3], Mauricio Morishi Ogusku[8] and Aya Sadahiro[1,2]**

[1] Laboratório de Imunologia Molecular, Departamento de Parasitologia, Universidade Federal do Amazonas (UFAM), Manaus, Brazil, [2] Programa de Pós-Graduação em Imunologia Básica e Aplicada, Universidade Federal do Amazonas, Manaus, Brazil, [3] Laboratório de Imunogenética, Departamento de Imunologia, Instituto de Ciências Biomédicas (ICB), Universidade de São Paulo (USP), São Paulo, Brazil, [4] Policlínica Cardoso Fontes – Secretaria de Estado da Saúde do Amazonas-SUSAM, Manaus, Brazil, [5] Diretoria de Ensino e Pesquisa, Fundação Hospitalar de Hematologia e Hemoterapia do Amazonas (HEMOAM), Manaus, Brazil, [6] Instituto de Pesquisa Clínica Carlos Borborema, Fundação de Medicina Tropical Dr. Heitor Vieira Dourado, Manaus, Brazil, [7] Faculdade de Medicina Nilton Lins, Universidade Nilton Lins, Manaus, Brazil, [8] Laboratório de Micobacteriologia, Instituto Nacional de Pesquisas da Amazônia (INPA), Manaus, Brazil

OPEN ACCESS

Edited by:
Uday Kishore, Brunel University London, United Kingdom

Reviewed by:
Anthony George Tsolaki, Brunel University London, United Kingdom
Yean Kong Yong, Xiamen University, Malaysia

***Correspondence:**
Mariana Brasil de Andrade Figueira
mariana_brasil@hotmail.com
Aya Sadahiro
asadahiro@ufam.edu.br

Specialty section:
This article was submitted to Microbial Immunology, a section of the journal Frontiers in Immunology

Received: *10 September 2020*
Accepted: *03 March 2021*
Published: *01 April 2021*

Citation:
Figueira MBA, de Lima DS, Boechat AL, Filho MGN, Antunes IA, Matsuda JS, Ribeiro TRA, Felix LS, Gonçalves ASF, da Costa AG, Ramasawmy R, Pontillo A, Ogusku MM and Sadahiro A (2021) Single-Nucleotide Variants in the AIM2 - Absent in Melanoma 2 Gene (rs1103577) Associated With Protection for Tuberculosis. Front. Immunol. 12:604975. doi: 10.3389/fimmu.2021.604975

Tuberculosis (TB) remains a serious public health burden worldwide. TB is an infectious disease caused by the *Mycobacterium tuberculosis* Complex. Innate immune response is critical for controlling mycobacterial infection. NOD-like receptor pyrin domain containing 3/ absent in melanoma 2 (NLRP3/AIM2) inflammasomes are suggested to play an important role in TB. NLRP3/AIM2 mediate the release of pro-inflammatory cytokines IL-1β and IL-18 to control *M. tuberculosis* infection. Variants of genes involved in inflammasomes may contribute to elucidation of host immune responses to TB infection. The present study evaluated single-nucleotide variants (SNVs) in inflammasome genes *AIM2* (rs1103577), *CARD8* (rs2009373), and *CTSB* (rs1692816) in 401 patients with pulmonary TB (PTB), 133 patients with extrapulmonary TB (EPTB), and 366 healthy control (HC) subjects with no history of TB residing in the Amazonas state. Quantitative Real Time PCR was performed for allelic discrimination. The SNV of *AIM2* (rs1103577) is associated with protection for PTB (*p*adj: 0.033, ORadj: 0.69, 95% CI: 0.49-0.97). *CTSB* (rs1692816) is associated with reduced risk for EPTB when compared with PTB (*p*adj: 0.034, ORadj: 0.50, 95% CI: 0.27-0.94). Serum IL-1β concentrations were higher in patients with PTB than those in HCs (p = 0,0003). The SNV rs1103577 of *AIM2* appeared to influence IL-1β release. In a dominant model, individuals with the CC genotype (mean 3.78 ± SD 0.81) appeared to have a higher level of

IL-1β compared to carriers of the T allele (mean 3.45 ± SD 0.84) among the patients with PTB (p = 0,0040). We found that SNVs of *AIM2* and *CTSB* were associated with TB, and the mechanisms involved in this process require further study.

Keywords: tuberculosis, inflammasome, SNV, *AIM2*, *CARD8*, *CTSB*

INTRODUCTION

Tuberculosis (TB) is an infectious disease caused by mycobacteria belonging to the *Mycobacterium tuberculosis* complex (MTBC) (1). The MTBC typically affects the lungs (pulmonary TB (PTB) but can also affect other tissues and organs (extrapulmonary TB (EPTB)) (2). Approximately 25% of the world's population is infected with *M. tuberculosis*, but only approximately 5% to 10% of *M. tuberculosis*-infected individuals subsequently develop TB (3). The complexity of TB is influenced by several factors, such as the immune status and genetic factors of host (4–8).

The innate immune response is the first line of host defense against mycobacteria infection (9, 10). Innate immune system senses pathogens via pattern-recognition receptors (PRRs) to recognize conserved microbial components known as pathogen-associated molecular patterns (PAMPs). PRR also function as innate sensors of host-derived danger signals, the danger-associated molecular patterns (DAMPs) and may assemble in inflammasomes (11). Inflammasomes are intracellular multimeric protein complexes that play key roles in the innate immune response (12, 13). Inflammasomes are essential for controlling bacterial growth through the activation of caspase-1 to process pro-inflammatory IL-1β and IL-18 into active cytokines (14, 15). Caspase-1 also induces a type of inflammatory cell death called pyroptosis (16).

Inflammasomes belonging to the NOD-like receptor (NLR) family are composed of at least three components, a sensor protein (NLRP1, NLRP3, NLRP6, NLRP12, NLRC4; PYHIN family (PYD-like and HIN domain-containing proteins) as AIM2 and TRIM family (Tripartite motif proteins) containing PYRIN), an inflammatory caspase (caspase-1, Caspase-11) and an adapter molecule such as the apoptosis-associated speck-like containing a CARD domain (ASC) (17). NLRP3-inflammasomes is the most studied compared to others (18). NLRP3 and AIM2 inflammasomes play important role in host defense against *M. tuberculosis* (9, 15, 19–22).

The *NLRP3* gene is located on human chromosome 1. Basically, member of NLR family of PRR consists of three domains: a leucine-rich repeat (LRR)-region that interacts with antigens, a central nucleotide-binding NACHT domain and an effector domain PYD or CARD (23). *AIM2* gene is located on human chromosome 1. AIM2 is composed of two domains: a N-terminal pyrin domain (PYD) and a C-terminal hematopoietic interferon-inducible nuclear protein with a 200-amino acid repeat (HIN200) domain. AIM2 is a cytosolic double-stranded DNA receptor (24, 25).

Principles of inflammasome activation in TB involve two signals. The first signal induces the expression of NLRP3 and/or AIM2 inflammasome, pro-IL-1β and pro-IL-IL-18 genes caused by Toll-like receptor (TLR) stimulation. The second signal results to oligomerization domain and formation of inflammasome complex consequent of activating stimuli. After that, the effector domain recruits ASC protein to assemble the inflammasome complex (PRR, ASC protein and procaspase-1). ASC protein recruits procaspase-1 through caspase recruitment domain (CARD) consequently it is cleaved into active caspase-1 (14).

Activating stimuli described for NLRP3 are mitochondrial factors (mitochondrial reactive oxygen species, mitochondrial DNA, cardiolipin), mycobacterial components, cathepsins after lysosomal rupture as Cathepsin B encoded by *CTSB* gene located on human chromosome 8, potassium efflux and extracellular ATP via the P2X7 purinergic receptor (26, 27) and AIM2 is cytosolic dsDNA (25, 28). CTSB is cysteine exo/endopeptidase enzymes pH dependent belonging members of the papain family seems to involvement roles in NLRP3-inflammasome activation as well as degradation or processing of lysosomal proteins (29–31). CARD8 adaptor protein is encoded by *CARD8* gene present on chromosome 19. CARD8 acts as a negative regulator during NLRP3 inflammasome activation for adequate functioning and balanced response (32, 33).

In animal models of TB, NLRP3 (34, 35) and AIM2 (19, 36) inflammasomes have been found to recognize cytosolic DNA. Recently, the importance of inflammasomes in TB (37) as well as the crucial role of IL1β in infection control independent of inflammasome activation have been highlighted (38). TB is complex and multifactorial and identification of genetic variants can improve our understanding of the pathogenesis of TB (39).

Several studies have shown a genetic predisposition to development of TB (40–44). Genetic variant in inflammasomes can change their physiological function and contribute to the susceptibility, severity, and outcomes of TB (45). Single-nucleotide variant (SNV) of *NLRP3* (rs10754558) and SNV of *P2X7* (rs2230911) are associated with TB. SNV of *NLRP3* (rs10754558) is associated with protection against PTB (41). The SNV of *P2X7* (rs2230911) is associated with susceptibility to PTB. SNVs of *CARD8* (rs2043211) and *NLRP3* (rs35829419) are associated with EPTB in Ethiopian population (46).

The important role of inflammasomes in immunity to TB prompted us to evaluate the associations of SNVs in genes encoding the AIM2 inflammasome, CARD8, and CTSB in patients with TB from Amazonas state of Brazil.

MATERIAL AND METHODS

Ethics Statement

This study was approved by Human Research Ethics Committee of Federal University of Amazonas (N°. CAAE: 57978916.3.0000.5020;

August 17, 2016). All patients and controls participating in this study provided written informed consent for collection of blood and sputum samples for analysis.

Study Population

This is a case–control study and is consisted of 401 patients with PTB, 133 patients with EPTB, and 366 healthy controls (HCs). The study population was recruited from Policlínica Cardoso Fontes, a sanitary pneumology center (Manaus, AM, Brazil). The patients with PTB were positive for *M. tuberculosis*, which was determined through a molecular rapid test (TRM, GeneXpert MTB/RIF) (47) or through sputum smears and PKO culture method (47, 48). The diagnosis of EPTB was based on recommendations of Brazilian National Guidelines for the Control of Tuberculosis (49). The patients with EPTB were either sputum MTB-positive or culture-positive and were molecularly characterized for MTBC. The clinical manifestations of EPTB were pleural cutaneous, ganglionic, intestinal, perianal, ocular, bone, and miliary.

HCs participating in study had no history of TB and were contacts of patients with TB. The HCs were devoid of TB symptoms and negative for *M. tuberculosis* in sputum and/or in culture tests. Exclusion criteria comprised current pregnancy, recipients of organ transplants, and presence of other comorbidities, such as cancer, diabetes, HIV positive, hepatitis, and autoimmune diseases.

DNA Isolation and SNV Genotyping

Genomic DNA was extracted from whole human blood (1 mL) using tetramethylammonium bromide salts protocol (50). SNVs were selected according to the minor allele frequency (MAF) of > to 10% in the global population from NCBI database, but also for background information on inflammasome complex in tuberculosis. Three SNVs in inflammasome genes *AIM2* T>C (rs1103577) situated on chromosome 1q15, *CARD8* T>C (rs2009373) on 19q48, and *CTSB* A> C (rs1692816) on 8q11 were selected and genotyped using TaqMan probes for allelic discrimination assay by Real-Time PCR System (Applied Biosystems). The technology is based on hydrolysis fluorescent probes. The fluorescent probes are allele-specific oligonucleotides sequences of target SNV labeled with either VIC or FAM fluorescence to discriminate the alleles. Thermal cycling conditions for PCR were a pre-read stage at 60°C for 30 sec and subsequently a hold stage at 95°C for 10 min followed by 50 cycles of denaturation at 95°C for 15 sec and annealing\ extension at 60°C for 01 sec and finally followed by a post-read stage at 60°C for 30 sec. The reaction mix contained 5 µL TaqMan Genotyping Master Mix 1X; 0,5 µL TaqMan® probes 20X of target SNV, 4,5 µL Milli-Q water and 2 µL DNA (50ng\uL). For each PCR plate, a negative control and three known positive controls of target SNV (rare homozygote, wild-type homozygote and heterozygote) were included to increase the reliability of assay. Of note, the SNV rs35130877 of the *AIM2* gene was previously studied in the same population (41). This was carried out using QuantStudio™ 3 (ThermoFisher Scientific) and Design & Analysis Software v.1.4.2. The probes used in experiment are shown in **Supplementary Table 1**.

Cytokine Measurements

Human IL-1β levels were measured in plasma sample from patients with PTB prior to start of drug therapy and HCs using a commercially available enzyme-linked immunosorbent assay (ELISA) kit (BioLegend ELISA MAX™ Deluxe Sets) following the manufacturer's instructions. 50 µL of plasma samples were added to each well of high binding plate and readings were performed on a BioRad spectrophotometer plate as recommended by kit, using the 450 nm filter. Samples and standards were analyzed in duplicate. The minimal detectable concentration of IL-1β for this kit was 0.5 pg/mL.

Statistical Analysis

For each SNVs analysis, alleles analysis was performed using on the link https://ihg.helmholtz-muenchen.de/ihg/snps.html and the associations between the allelic/genotype frequencies among patients with PTB, EPTB, and HCs were examined using the package "SNPassoc" version 1.9-2 (https://cran.r-project.org/web/packages/SNPassoc/index.html) for R software version 3.4.3 (www.r-project.org). The best genetic model was performed via Akaike information criterion (AIC). The Hardy-Weinberg equilibrium was evaluated for all SNVs. The results were shown as the odds ratio (OR) and 95% confidence intervals (95% CI) from multivariate logistic regression analyses. To control the potential confounding factors, adjusted OR (OR_{adj}) values for age and sex were provided. The multivariate logistic regressions were performed using STATA 15 (StataCorp Texas, USA) after adjusting for age and sex. To compare multiple means of cytokine levels, one-way analysis of variance was applied with the Tukey's post-hoc test adjusted for multiple comparisons. A *p*-value less than 0.05 was considered as statistically significant.

RESULTS

Characteristics of the Study Population

A total of 900 unrelated individuals born in the North of Brazil participated in this study. Of 900 individuals, 534 and 366 were patients with TB and HCs, respectively. Among those with TB, 401 had PTB and 133 had EPTB. The mean ages of patients with PTB, EPTB, and the HCs were 38.1 ± 13.7, 34.6 ± 14.1, and 32.9 ± 12.5, respectively. Of patients with PTB, EPTB, and HCs, 243 (60.6%), 75 (56.4%), and 180 (49.2%) were male, respectively. Patients with EPTB exhibited mostly pleural (55.6%), followed by cutaneous (17.3%) and ganglionic (16.5%). Intestinal, perianal, ocular, bone, and miliary TB accounted for 10.5%.

Analysis of the SNVs in Inflammasome Genes

All SNVs studied *AIM2* rs1103577, *CARD8* rs2009373 and *CTSB* rs1692816 were in the Hardy-Weinberg equilibrium (HWE) in both HCs and patients with TB. The frequencies of alleles and genotypes as well as the different comparisons are shown in **Tables 1–4**. Genotypes and the best inheritance modeling for *AIM2*, *CARD8* and *CTSB* genes are reported in **Supplementary Table 2**.

The distribution of SNV of *AIM2* (rs1103577) genotypes is slightly different between patients with PTB compared with HC (p_{adj}: 0.083). The frequency of genotype CC was slightly higher among patients with PTB (32%) than among HCs (27%). The SNV of *AIM2* (rs1103577) was associated with a reduced risk of developing PTB (p_{adj}: 0.027, OR_{adj}: 0.69, 95% CI: 0.50-0.96) in a dominant model (CC versus CT + TT) when compared with HCs (**Table 1**). Carriers of T allele had 31% less chances of developing PTB compared to individuals homozygous for C allele, suggesting homozygosity for C allele may be a risk factor for PTB.

The SNV of *CARD8* (rs2009373) showed a decrease risk in development of EPTB when compared to PTB in a recessive model (p_{adj}: 0.026, OR_{adj}: 0.48, 95% CI: 0.25-0.96) (**Table 2**). Bearers of C allele had 52% less chance of developing PTB. The frequency of genotype TT was predominant among the patients with PTB (22%) than in the EPTB group (12%). Individuals homozygous for T allele had twice chance of developing PTB than EPTB when compared with individuals homozygous for C allele (TT vs. CC p = 0.05, OR=2.1, 95% CI: 0.99-4.4) (The results of the different alleles were extracted on the link https://ihg.helmholtz-muenchen.de/ihg/snps.html). Of note, the frequencies of genotype were 31%, 49% and 20% for CC, CT and TT respectively, among HCs group (**Supplementary Table 2**). Comparisons between patients with EPTB and HCs revealed that carriers of C allele (CC +CT vs. TT) had 85% risk of developing EPTB (p=0.07, OR = 1.85, 95% CI: 0.94-3.7). No association was revealed when patients with PTB were compared with HCs.

Regarding the SNV of *CTSB* (rs1692816), an overdominant model indicated that heterozygous individuals have a lower risk of developing EPTB compared to patients with PTB (p: 0.022, OR: 0.50, 95% CI: 0.27-0.92) (**Supplementary Table 2**) and when adjusted for sex and age (p: 0.026, OR: 0.50, 95% CI: 0.27-0.94) (**Tables 3** and **4**). The frequencies were 23%, 50% and 27% for

TABLE 1 | Genetic models of association SNV rs1103577 of *AIM2* gene adjusted for sex and age in patients with pulmonary tuberculosis (PTB) and healthy control.

AIM2 Genetic Model	PTB n, %	Controls n, %	p value $_{adj}$	OR $_{adj}$ (95% CI)	AIC
Codominant			0.083	1.00	988.4
CC	124 (0.32)	95 (0.27)		_	
CT	180 (0.47)	180 (0.51)		0.68 (0.48-0.96)	
TT	81 (0.21)	76 (0.22)		0.72 (0.47-1.11)	
Dominant			**0.027**		986.5
CC	124 (0.32)	95 (0.27)		_	
CT-TT	261 (0.68)	256 (0.73)		0.69 (0.50- 0.96)	
Recessive			0.672		991.2
CT-CC	304 (0.79)	275 (0.78)		_	
TT	81 (0.21)	76 (0.22)		0.92 (0.64-1.33)	
Overdominant			0.096		988.6
CC-TT	205 (0.53)	171 (0.49)		_	
CT	180 (0.47)	180 (0.51)		0.78 (0.58-1.05)	
Log-Additive	385 (0.52)	351 (0.48)	0.096	0.84 (0.68-1.03)	988.6
0,1,2					

PTB (pulmonary tuberculosis); adjusted for sex and age (p value $_{adj}$, OR_{adj}); 95% confidence interval (CI); AIC, Akaike information criterion value.
The results statistically significant are highlight in bold characters.

TABLE 2 | Genetic models of association SNV rs2009373 of *CARD8* gene adjusted for sex and age in patients with extrapulmonary tuberculosis (EPTB) and pulmonary tuberculosis (PTB).

CARD8 Genetic Model	EPTB n, %	PTB n, %	p value $_{adj}$	OR $_{adj}$ (95% CI)	AIC
Codominant			0.083	¨1.00	462.3
CC	31 (0.34)	111 (0.30)		_	
CT	50 (0.54)	183 (0.49)		0.98 (0.59-1.64)	
TT	11 (0.12)	82 (0.22)		0.48 (0.23-1.01)	
Dominant			0.444		464.6
CC	31 (0.34)	111 (0.30)		_	
CT-TT	61 (0.66)	265 (0.71)		0.82 (0.50-1.35)	
Recessive			**0.026**		460.3
CT-CC	81 (0.88)	294 (0.78)		_	
TT	11 (0.12)	82 (0.22)		0.48 (0.25-0.96)	
Overdominant			0.322		464.2
CC-TT	42 (0.46)	193 (0.51)		_	
CT	50 (0.54)	183 (0.49)		1.26 (0.80-2.00)	
Log-Additive			0.084		462.2
0,1,2	92 (0.20)	376 (0.80)		0.75 (0.53-1.04)	

PTB (pulmonary tuberculosis); EPTB (extrapulmonary tuberculosis); adjusted for sex and age (p value $_{adj}$, OR_{adj}); 95% confidence interval (CI); AIC, Akaike information criterion value.
The results statistically significant are highlight in bold characters.

TABLE 3 | Genetic models of association SNV rs1692816 of *CTSB* gene adjusted for sex and age in patients with extrapulmonary tuberculosis (EPTB) and healthy control subjects.

CTSB Genetic Model	EPTB n, %	Controls n, %	p value $_{adj}$	OR $_{adj}$ (95% CI)	AIC
Codominant			0.120	1.00	310.8
AA	19 (0.37)	93 (0.27)		_	
AC	17 (0.33)	169 (0.48)		0.49 (0.24-1.00)	
CC	15 (0.29)	89 (0.25)		0.83 (0.39-1.73)	
Dominant			0.120		310.6
AA	19 (0.37)	93 (0.26)		_	
AC-CC	32 (0.63)	258 (0.74)		0.61 (0.33-1.13)	
Recessive			0.545		312.7
AA-AC	36 (0.70)	262 (0.75)		-	
CC	15 (0.30)	89 (0.25)		1.22 (0.64-2.34)	
Overdominant			**0.046**		309.1
AA-CC	34 (0.67)	182 (0.52)		_	
AC	17 (0.33)	169 (0.48)		0.54 (0.29-1.00)	
Log-Additive			0.543		312.7
0,1,2	51 (0.13)	351 (0.87)		0.88 (0.59-1.32)	

EPTB (extrapulmonary tuberculosis); adjusted for sex and age (p value $_{adj}$, OR$_{adj}$); 95% confidence interval (CI); AIC, Akaike information criterion value. The results statistically significant are highlight in bold characters.

TABLE 4 | Genetic models of association SNV rs1692816 of CTSB gene adjusted for sex and age in patients with extrapulmonary tuberculosis (EPTB) and pulmonary tuberculosis (PTB).

CTSB Genetic Model	EPTB n, %	PTB n, %	p value $_{adj}$	OR $_{adj}$ (95% CI)	AIC
Codominant			0.084	1.00	314.9
AA	19 (0.37)	103 (0.27)		_	
AC	17 (0.33)	193 (0.50)		0.50 (0.25-1.01)	
CC	15 (0.29)	89 (0.23)		0.98 (0.47-2.07)	
Dominant			0.177		316.1
AA	19 (0.37)	103 (0.27)		_	
AC-CC	32 (0.63)	282 (0.73)		0.65 (0.35-1.20)	
Recessive			0.269		316.7
AA-AC	36 (0.71)	296 (0.77)		_	
CC	15 (0.29)	89 (0.23)		1.46 (0.76-2.80)	
Overdominant			**0.026**		312.9
AA-CC	34 (0.67)	192 (0.50)		_	
AC	17 (0.33)	193 (0.50)		0.50 (0.27-0.94)	
Log-Additive			0.841		317.8
0,1,2	51 (0.12)	385 (0.88)		0.96 (0.64-1.45)	

PTB (pulmonary tuberculosis); EPTB (extrapulmonary tuberculosis); adjusted for sex and age (p value $_{adj}$, OR$_{adj}$); 95% confidence interval (CI); AIC, Akaike information criterion value. The results statistically significant are highlight in bold characters.

the CC, AC and AA genotypes, respectively among patients with PTB and similar pattern was observed among HCs (CC 25%, AC 48% and AA 27%). In contrast, the frequencies among patients with EPTB were 29%, 33%, and 37% for CC, AC and AA genotypes, respectively. Similarly, comparison between patients and HCs disclosed that heterozygous individuals have lower risk of developing EPTB (*p*: 0.045, p_{adj}: 0.046, OR: 0.54, 95% CI: 0.29-1.0).

Logistic regression analysis, including sex and age variables with SNVs, confirmed the association of *AIM2* rs1103577 (*p*:0.033, OR: 0.69, 95% CI: 0.49-0.97) and *CTSB* rs1692816 with a lower risk for EPTB (*p*: 0.034, OR: 0.50, 95% CI: 0.27-0.94) (**Table 5**).

Cytokine IL-1β in a Dominant Model of *AIM2*, *CARD8*, and *CTSB* Genotypes

IL-1β is an important inflammatory cytokine with major role in host immune response against *M.tuberculosis* infection. Next, we evaluated *in vivo* the plasma IL-1β concentrations in PTB and HCs. Plasma IL-1β was higher in patients with PTB compared to those in HC group (*p* = 0.0003) (**Supplementary Figure 1**). We analyzed the distribution of plasma IL1-β according to genotypes of *AIM2*, *CARD8*, and *CTSB* in a dominant model. *AIM2* rs1103577 appeared to have an effect on plasma cytokine IL-1β when CC carriers were compared to allele T carriers (CC vs. CT+TT) in patients with PTB (*p* = 0.0040). CARD8 rs2009373 and CTSB rs1692816 did not show any influence on levels of plasma IL-β (**Figure 1A**). A QQ plot was used to validate the distribution of IL-1β in genotypes (**Figure 1B**).

DISCUSSION

Genetics and environmental factors are crucial for host immune response against *M. tuberculosis*. The complex network of mechanisms from early infection to development of TB remains

TABLE 5 | Multivariate logistic regression analysis for variables sex and age, including three inflammasomes genes in the studied groups.

Variable	Tuberculosis vs Control		Pulmonary tuberculosis vs Control		Extrapulmonary tuberculosis vs Control		Pulmonary vs Extrapulmonary tuberculosis	
	p value	OR (95% CI)	*p* value	OR (95% CI)	*p* value	OR (95% CI)	*p* value	OR (95% CI)
AIM2 rs1103577	0.053	0.73 (0.53-1.00)	**0.033**	0.69 (0.49-0.97)	0.241	0.68 (0.35-1.29)	0.976	1.00 (0.53-1.90)
CARD8 rs2009373	0.825	0.95 (0.70-1.31)	0.652	0.92 (0.66-1.28)	0.539	1.21 (0.64-2.28)	0.279	1.41 (0.75-2.67)
CTSB rs1692816	0.229	0.83 (0.63-1.11)	0.597	1.08 (0.80-1.46)	0.066	0.55 (0.29-1.03)	**0.034**	0.50 (0.27-0.94)

odds ratio (OR) and 95% confidence interval (CI).
The results statistically significant are highlight in bold characters.

poorly understood. Since the identification of function of various inflammasomes, several studies of genetic variants of genes involved in assembling the multiprotein complex of inflammasomes have attempted to determine the reason of susceptibility of some individuals to develop diseases while others remain asymptomatic. In the early stage of infection, innate immune response is essential to ensure the success of control and elimination of bacilli. Subsequently, upon inflammasomes activation, proinflammatory cytokines are released to keep in check the invading pathogen (45). In this context, we have focus on one SNV in the *AIM2* inflammasome in tuberculosis together with two other SNVs, one in *CARD8* and one in *CTSB*, that are related to NLRP3 pathway.

Studies regarding human genetic variants of *AIM2* are rare in infectious diseases (41, 42, 45). Recently, we investigated another SNV of *AIM2* (rs35130877) in 288 patients with PTB and 288 HCs. None of participants had this SNV (41). In this study, we found that SNV of *AIM2* (rs1103577) was associated with protection against TB. Interestingly, immunological studies involving mice have demonstrated a protective role of AIM2 against *M. tuberculosis* infection (19, 51). Inhibition of inflammasomes decreased the survival of *M. tuberculosis* in mice (37) and suggested that a high level of IL-1β favored the survival of bacteria. Carriers homozygous for C allele have higher IL-1 concentrations compared to T allele carriers, and T allele is associated with protection in our study. Furthermore, modern lineages of MTBC have high multiplication rates, which correlates to high levels of IL-1β (52). However, some individuals are resistant to *M. tuberculosis* infection despite continuous exposure (53, 54), suggesting sterile clearance potentially due to a reflex of genetic background and immunity of individual.

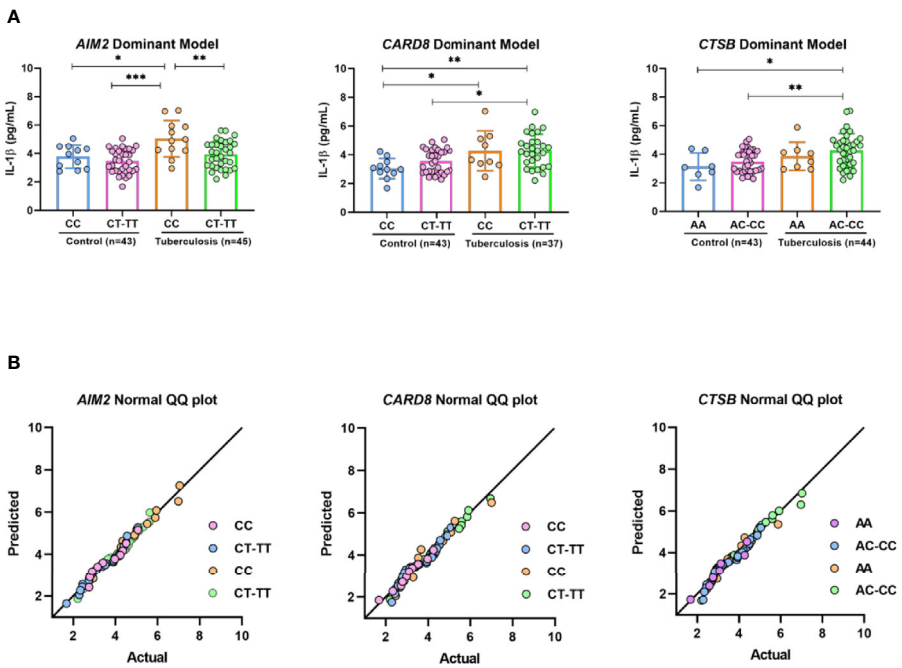

FIGURE 1 | IL-1β profile respective on genotypes of *AIM2*, *CARD8* and *CTSB* from pulmonary tuberculosis patients and control. **(A)** Serum concentrations of IL-1β distributed in *AIM2*, *CARD8* and *CTSB* dominant model genotypes. **(B)** Graphic Normal QQ plot for three SNV studied. Groups were further compared with each other using ANOVA test with Tukey's multiple comparisons test, $^{*}p < 0,05$; $^{**}p < 0,001$; $^{***}p < 0,0001$.

IL-1β is a proinflammatory cytokine and has been suggested to play key role in host protection against *M. tuberculosis* infection (55, 56). The protein ESAT of *M. tuberculosis* is cited as a potent activator of NLRP3\ASC inflammasome to liberate mature IL-1β (9). Patients with PTB also exhibit increased levels of IL-1βcompared to HCs. Patients with PTB also demonstrate higher levels of IL-1β (37, 38, 57), reinforcing an important role in the early innate immune response to control *M. tuberculosis* infection. We found that the serum concentrations of cytokine IL-1β were correlated according to genotypes CC versus CT-TT (*AIM2*) among patients with PTB in a dominant model. The T allele (TT +CT) correlated with low level of IL1 while homozygosity for the C allele with high level of IL-1β. The T allele is associated with protection to development of TB while individuals homozygous for C allele with susceptibility. Interestingly, excessive levels of IL-1β has been associated with severe TB and lung damage (57, 58).

NLRP3 and AIM2-inflammasome are suggested to play important role in host-defense against mycobacteria (19, 59). Recently, Souza de Lima et al. (22) have shown that NLRP3/IL-1ß/IL-18 pathway is strongly activated in a cathepsin-dependent form by virulent strain H37Rv and non-virulent BCG strains of *M. tuberculosis* in human macrophages, in vitro. Interestingly, the response was modulated according to macrophage donor genotype of SNV NLRP3 rs10754558 that correlated to level of IL-1β release (22). Of note, IL-1β is one among key proinflammatory cytokines essential for recruitment of immune cells to the site of *M. tuberculosis* infection (55). Several studies have demonstrated the role of AIM2-inflamasome in mycobacterial infection. Mice macrophages infected with pathogenic strain of *M. bovis* led to activation of AIM2-inflammasome and mature IL-1β release (60). Similarly, another study also demonstrated that THP-1 macrophages exposed to rBCG (Recombinant BCG ΔureC::hly) vaccine results in AIM2-inflammasome activation with increased production of IL-1β and IL-18 and autophagy, corroborating the role of AIM2-inflammasome in innate immune response (61).

AIM2-deficient mice infected with *Mycobacterium bovis* Bacillus Calmette-Guérin (BCG) showed a higher infection burden and developed severe disease due to simultaneous induction of reactive IFN-β and IFN-γ responses compared to wild-type mice (51). The AIM2 inflammasome appears to play a protective role through the induction of IL-1β and negative regulation of type I IFN induction. High production of type I IFNs reduces the IFN-γ response in TB infection (51). Interestingly, we showed that individuals homozygous for C allele had higher level of IL-1β compared to carriers of T allele and T allele is associated with protection to the development of TB. Higher level of IL-1β in the early stage might be important in keeping in check the pathogen but at a later stage might cause tissue damage.

The SNVs of *AIM2* (rs1103577), *CARD8* (rs2009373) and *CTSB* (rs1692816) are located in intronic region of respective gene. Although the functional role of these variants has not been elucidated, non-coding regions can affect gene expression resulting in different responses to presence of pathogens and can serve such as genetic markers (62). In future studies, it will be interesting to quantify the AIM2 messenger RNA (mRNA) from macrophages of different genotypes of *AIM2* (rs1103577) upon mycobacterial infection. Intronic regions have been highlighted for increasing the expression of mRNA in very diverse organisms (mammals, plants). Thus being an important regulator in the expression of proteins (63–66).

In this study, stratification of patients into PTB and EPTB suggested that *CARD8* rs2009373 and *CTSB* rs1692816 were associated with a lower risk of developing PTB. However, multivariate logistic regression analysis showed that only *CTSB* rs1692816 was associated with a reduced risk for EPTB. Indeed, we observed that heterozygosity for the variant provides lower risk for development of EPTB. CTSB is a member of cathepsin family localized in lysosomes and cytosol. CTSB promotes the degradation of protein in lysosomes and controls autophagy (67). Furthermore, the inhibition of CTSB blocks *M. tuberculosis*-induced NLRP3 inflammasome assembly, thereby leading to a decrease in IL-1βrelease, suggesting that the release of lysosomal CTSB and possibly other cathepsins are crucial for activation of NLRP3 to control *M. tuberculosis* infection (22, 30). Although, the function of this *CTSB* rs1692816 is not known, we can speculate that heterozygous individuals have an advantage in modulating the NLRP3 inflammasome in the release of IL-1β that is sufficient to keep in check the bacteria in comparison to homozygotes. Indeed, heterozygosity for some genes variant have been shown to provide an advantage to some infectious diseases. Heterozygosity for hemoglobin S is an advantage in Africa against *Plasmodium falciparum* malaria. Heterozygosity for the MAL/TIRAP variant in the TLRs pathway have been suggested to provide protection against invasive pneumococcal disease, malaria, tuberculosis and chagas disease (68, 69).

The SNV of *CARD8* (rs2009373) was not associated with TB in this study. However, other variants of *CARD8* (rs6509365 and rs2043211) have been associated with susceptibility to TB (41, 46, 70). CARD8 negatively regulates NLRP3 activation, and *CARD8* rs2043211 appears to have a loss of function. Interestingly, *NLRP3* (rs35829419)/*CARD8* (rs2043211) interaction is associated with levels of IL-1β (71).

Another important aspect is the variation in allele frequencies among populations. We found that some alleles were present in high or low frequencies or were entirely absent in specific populations, thereby indicating different evolutionary histories that are assumed are under selective pressure from prevalent diseases.

The distribution of MAF for rs1103577 of *AIM2* (T allele) in HCs (T = 0.47) is comparable to that of a European population (T = 0.40) and different from that of an African population (C = 0.09). The Amazonian population is an admixture of approximately 60% American, 50% European, and 10% African ancestry (72). The MAF of *CARD8* rs2009373 (T allele) in our group (T = 0.45) was similar to frequencies of South Asian (T = 0.46), European (T = 0.47), American (T = 0.41), and African (0.50) populations, but different from those of West Asian populations (C = 0.23). For rs1692816 of *CTSB*, both alleles A and C are frequent in different populations. The frequency of *CTSB* rs1692816 C allele was 0.49 in our population, compared to

African (0.56), American (0.59), and European (0.66) populations. However, the frequency of the rs1692816 C allele was similar to that of East (0.50) and South (0.53) Asian populations. The frequencies of the different alleles were extracted from http://www.ensembl.org/. These frequencies indicate the importance of careful selection of cases and controls from same homogeneous population to avoid spurious associations.

The present study had some limitations. First, the sample size of the cases was small, especially for patients with EPTB. Second, we could not assay IL-1β in patients with EPTB due to a lack of biological samples. Additionally, the *NLRP3* data deviated from the HWE in both cases with TB and HCs; thus, they were excluded.

This result corroborates previous studies carried out by several researchers, both in an experimental model and in human cells infected by mycobacteria, which suggest the critical role of AIM2 in tuberculosis. We suggested *AIM2* rs1103577 was found to be associated with a lower risk of developing PTB and genotypes CC for AIM2 rs1103577 patients with PTB demonstrate higher levels of IL-1β. The *CARD8* and *CTSB* genes were also found to be important targets for TB, and other genetic variants should be investigated. Further studies are needed to confirm the association in other populations. Finally, it is indisputable that tuberculosis is a complex disease with a strong genetic link.

DATA AVAILABILITY STATEMENT

The datasets presented in this study can be found in online repositories. The names of the repository/repositories and accession number(s) can be found in the article/**Supplementary Material**.

ETHICS STATEMENT

The studies involving human participants were reviewed and approved by The Human Research Ethics Committee of the Federal University of Amazonas (N°. CAAE: 57978916.3.0000.5020, August 17th, 2016). The patients/participants provided their written informed consent to participate in this study.

AUTHOR CONTRIBUTIONS

MBAF: realized the experiments, analyzed the data and wrote the paper. DL: analyzed the data and intellectual contribution. AB: analyzed the data and intellectual contribution. MGNF: Sample processing and intellectual contribution. IA: Contributed with samples and patient selection and intellectual contribution. JM: Contributed with samples and patient selection and intellectual contribution and intellectual contribution. TR: Sample processing and intellectual contribution. LF: Sample processing and intellectual contribution. AG: Sample processing and intellectual contribution. AC: intellectual contribution. RR: wrote the paper and intellectual contribution. AP: analyzed the data and intellectual contribution. MO: Sample processing, understanding of genotyping assays and intellectual contribution. AS: Analyzed the data, wrote the paper and intellectual contribution. All authors contributed to the article and approved the submitted version.

FUNDING

This work was supported by FAPEAM (Edital PPSUS, Processo 062.00663/2014).

ACKNOWLEDGMENTS

We thank all subjects involved in the study, incluing pacients and to the staff of Policlínica Cardoso Fontes, Manaus, Amazonas, Brazil; Programa de Apoio à Pós-Graduação-Coordenação de Aperfeiçoamento de Pessoal de Nível Superior (PROAP/CAPES) and Fundação de Amparo à Pesquisa do Estado do Amazonas (FAPEAM).

SUPPLEMENTARY MATERIAL

The Supplementary Material for this article can be found online at: https://www.frontiersin.org/articles/10.3389/fimmu.2021.604975/full#supplementary-material

REFERENCES

1. Galagan JE. Genomic insights into tuberculosis. *Nat Rev Genet* (2014) 15:5. doi: 10.1038/nrg3664
2. Pai M, Behr M, Dowdy D, Dheda K, Divangahi M, Boehme CC, et al. Tuberculosis. *Nat Rev Dis Primers* (2016) 2:16076. doi: 10.1038/nrdp.2016.76
3. World Health Organization. *Global Tuberculosis Report 2019* (2019). Geneva: World Health Organization. Available at: https://apps.who.int/iris/bitstream/handle/10665/329368/9789241565714-eng.pdf?ua (Accessed January 02, 2020).
4. Paramel GV, Sirsjö A, Fransén K. Role of genetic alterations in the NLRP3 and CARD8 genes in health and disease. *Mediators Inflamm* (2015) 2015:10. doi: 10.1155/2015/846782
5. Cadena AM, Fortune SM, Flynn JL. Heterogeneity in tuberculosis. *Nat Rev Immunol* (2017) 17:11. doi: 10.1038/nri.2017.69
6. Torrelles JB, Schlesinger LS. Integrating Lung Physiology, Immunology, and Tuberculosis. *Trends Microbiol* (2017) 25:8. doi: 10.1016/j.tim.2017.03.007
7. Cardona P-J. Pathogenesis of tuberculosis and other mycobacteriosis. *Enferm Infecc Microbiol Clin* (2018) 36:1. doi: 10.1016/j.eimce.2017.10.009
8. Batista LAF, Silva KJS, Silva LMC, Moura YF, Zucchi FCR. Tuberculosis: A granulomatous disease mediated by epigenetic factors. *Tuberculosis* (2020) 123:101943. doi: 10.1016/j.tube.2020.101943
9. Mishra BB, Moura-alves P, Sonawane A, Hacohen N, Griffiths G, Moita LF, et al. Mycobacterium tuberculosis protein ESAT-6 is a potent activator of the NLRP3/ASC inflammasome. *Cell Microbiol* (2010) 12:8. doi: 10.1111/j.1462-5822.2010.01450.x
10. Abdallah AM, Bestebroer J, Savage NDL, Punder K, Zon VM, Wilson L, et al. Mycobacterial secretion systems ESX-1 and ESX-5 play distinct roles in host cell death and inflammasome activation. *J Immunol* (2011) 187:9. doi: 10.4049/jimmunol.1101457

11. Franchi L, Muñoz-Planillo R, Núñez G. Sensing and reacting to microbes through the inflammasomes. *Nat Immunol* (2012) 13:4. doi: 10.1038/ni.2231
12. Martinon F, Burns K, Tschopp J. The Inflammasome: A molecular platform triggering activation of inflammatory caspases and processing of proIL-β. *Mol Cell* (2002) 10:2. doi: 10.1016/S1097-2765(02)00599-3
13. Strowig T, Henao-Mejia J, Elinav E, Flavell R. Inflammasomes in health and disease. *Nature* (2012) 481:7381. doi: 10.1038/nature10759
14. Guo H, Callaway JB, Ting JP-Y. Inflammasomes: mechanism of action, role in disease, and therapeutics. *Nat Med* (2015) 21:7. doi: 10.1038/nm.3893
15. Wawrocki S, Druszczynska M. Inflammasomes in Mycobacterium tuberculosis - Driven Immunity. *Can J Infect Dis Med Microbiol* (2017) 2017:2309478. doi: 10.1155/2017/2309478
16. Xue Y, Tuipulotu DE, Tan WH, Kay C, Man SM. Emerging Activators and Regulators of Inflammasomes and Pyroptosis. *Trends Immunol* (2019) 40:11. doi: 10.1016/j.it.2019.09.005
17. Yu C-H, Moecking J, Geyer M, Masters SL. Mechanisms of NLRP1-Mediated Autoinflammatory Disease in Humans and Mice. *J Mol Biol* (2018) 430:2. doi: 10.1016/j.jmb.2017.07.012
18. Yang Y, Wang H, Kouadir M, Song H, Shi F. Recent advances in the mechanisms of NLRP3 inflammasome activation and its inhibitors. *Cell Death Dis* (2019) 10:128. doi: 10.1038/s41419-019-1413-8
19. Saiga H, Kitada S, Shimada Y, Kamiyama N, Okuyama M, Makino M, et al. Critical role of AIM2 in Mycobacterium tuberculosis infection. *Int Immunol* (2012) 24:10. doi: 10.1093/intimm/dxs062
20. Wassermann R, Gulen MF, Sala C, Perin SG, Lou Y, Rybniker J, et al. Mycobacterium tuberculosis differentially activates cGAS-and inflammasome-dependent intracellular immune responses through ESX-1. *Cell Host Microbe* (2015) 17:6. doi: 10.1016/j.chom.2015.05.003
21. Xu F, Qi H, Li J, Sun L, Gong J, Chen Y, et al. Mycobacterium tuberculosis infection up-regulates MFN2 expression to promote NLRP3 inflammasome formation. *J Biol Chem* (2020) 295:51. doi: 10.1074/jbc.RA120.014077
22. Souza de Lima DS, Bomfim CC, Leal VN, Reis EC, Soares JLS, Fernandes FP, et al. Combining Host Genetics and Functional Analysis to Depict Inflammasome Contribution in Tuberculosis Susceptibility and Outcome in Endemic Areas. *Front Immunol* (2020) 11:550624. doi: 10.3389/fimmu.2020.550624
23. Awad F, Assrawi E, Louvrier C, Jumeau C, Georgin-Lavialle S, Grateau G, et al. Inflammasome biology, molecular pathology and therapeutic implications. *Pharmacol Ther* (2018) 187:133–49. doi: 10.1016/j.pharmthera.2018.02.011
24. Kesavardhana S, Kanneganti T-D. Mechanisms governing inflammasome activation, assembly and pyroptosis induction. *Int Immunol* (2017) 29:5. doi: 10.1093/intimm/dxx018
25. Wang B, Yin Q. AIM2 inflammasome activation and regulation: A structural perspective. *J Struct Biol* (2017) 200:3. doi: 10.1016/j.jsb.2017.08.001
26. Vanaja SK, Rathinam VA, Fitzgerald KA. Mechanisms of inflammasome activation: recent advances and novel insights. *Trends Cell Biol* (2015) 25:5. doi: 10.1016/j.tcb.2014.12.009
27. Jo EK, Kim J, Shin DM, Sasakawa C. Molecular mechanisms regulating NLRP3 inflammasome activation. *Cell Mol Immunol* (2016) 13:148159. doi: 10.1038/cmi.2015.95
28. Jin T, Perry A, Jiang J, Smith P, Curry JA, Unterholzner L, et al. Structures of the HIN domain: DNA complexes reveal ligand binding and activation mechanisms of the AIM2 inflammasome and IFI16 receptor. *Immunity* (2012) 36:4. doi: 10.1016/j.immuni.2012.02.014
29. Mort JS, Buttle DJ. Cathepsin B. *Int J Biochem Cell Biol* (1997) 29:5. doi: 10.1016/S1357-2725(96)00152-5
30. Amaral EP, Riteau N, Moayeri M, Maier N, Mayer-Barber KD, Pereira RM, et al. Lysosomal Cathepsin Release Is Required for NLRP3-Inflammasome Activation by Mycobacterium tuberculosis in Infected Macrophages. *Front Immunol* (2018) 9:1427. doi: 10.3389/fimmu.2018.01427
31. Campden RI, Zhang Y. The role of lysosomal cysteine cathepsins in NLRP3 inflammasome activation. *Arch Biochem Biophys* (2019) 670:32–42. doi: 10.1016/j.abb.2019.02.015
32. Razmara M, Srinivasula SM, Wang L, Poyet JL, Geddes BJ, DiStefano PS, et al. CARD-8 protein, a new CARD family member that regulates caspase-1 activation and apoptosis. *J Biol Chem* (2002) 277(16):13952–8. doi: 10.1074/jbc.M107811200
33. Ito S, Hara Y, Kubota T. CARD8 is a negative regulator for NLRP3 inflammasome, but mutant NLRP3 in cryopyrin-associated periodic syndromes escapes the restriction. *Arthritis Res Ther* (2014) 16:1. doi: 10.1186/ar4483
34. Abdalla H, Srinivasan L, Shah S, Mayer-Barber KD, Sher A, Sutterwala FS, et al. Mycobacterium tuberculosis infection of dendritic cells leads to partially caspase-1/11-independent IL-1β and IL-18 secretion but not to pyroptosis. *PloS One* (2012) 7:7. doi: 10.1371/journal.pone.0040722
35. Dorhoi A, Nouailles G, Jörg S, Hagens K, Heinemann E, Pradl L, et al. Activation of the NLRP3 inflammasome by Mycobacterium tuberculosis is uncoupled from susceptibility to active tuberculosis. *Eur J Immunol* (2012) 42:2. doi: 10.1002/eji.201141548
36. Shah S, Bohsali A, Ahlbrand SE, Srinivasan L, Rathinam VK, Vogel SN, et al. Cutting edge: Mycobacterium tuberculosis but not nonvirulent mycobacteria inhibits IFN-β and AIM2 inflammasome-dependent IL-1β production via its ESX-1 secretion system. *J Immunol* (2013) 191:7. doi: 10.4049/jimmunol.1301331
37. Subbarao S, Sanchez-garrido J, Kri N, Shenoy AR, Robert BD. Genetic and pharmacological inhibition of inflammasomes reduces the survival of Mycobacterium tuberculosis strains in macrophages. *Sci Rep* (2020) 10:3709. doi: 10.1038/s41598-020-60560-y
38. Mayer-Barber KD, Barber DL, Shenderov K, White SD, Wilson MS, Cheever A, et al. Cutting Edge: Caspase-1 Independent IL-1 Production Is Critical for Host Resistance to Mycobacterium tuberculosis and Does Not Require TLR Signaling In Vivo. *J Immunol* (2010) 184:7. doi: 10.4049/jimmunol.0904189
39. Briken V, Ahlbrand SE, Shah S. Mycobacterium tuberculosis and the host cell inflammasome: a complex relationship. *Front Cell Infect Microbiol* (2013) 3:62. doi: 10.3389/fcimb.2013.00062
40. Eklund D, Welin A, Andersson H, Verma D, Söderkvist P, Stendahl O, et al. Human gene variants linked to enhanced NLRP3 activity limit intramacrophage growth of mycobacterium tuberculosis. *J Infect Dis* (2014) 209:5. doi: 10.1093/infdis/jit572
41. Souza de Lima D, Ogusku MM, Sadahiro A, Pontillo A. Inflammasome genetics contributes to the development and control of active pulmonary tuberculosis. *Infect Genet Evol* (2016) 41:240–4. doi: 10.1016/j.meegid.2016.04.015
42. Liu C-W, Lin C-J, Hu H-C, Liu H-J, Chiu Y-C, Lee S-W, et al. The association of inflammasome and TLR2 gene polymorphisms with susceptibility to tuberculosis in the Han Taiwanese population. *Sci Rep* (2020) 10:10184. doi: 10.1038/s41598-020-67299-6
43. Souza de Lima D, Leal VNC, Ogusku MM, Sadahiro A, Pontillo A, Alencar BC. Polymorphisms in SIGLEC1 contribute to susceptibility to pulmonary active tuberculosis possibly through the modulation of IL-1ß. *Infect Genet Evol* (2017) 55:313–7. doi: 10.1016/j.meegid.2017.09.031
44. Barletta-Naveca RH, Naveca FG, de Almeida VA, Porto JIR, da Silva GAV, Ogusku MM, et al. Toll-like receptor-1 single-nucleotide polymorphism 1805T/G is associated with predisposition to multibacillary tuberculosis. *Front Immunol* (2018) 9:1455. doi: 10.3389/fimmu.2018.01455
45. Fernandes FP, Leal VNC, Souza de Lima D, Reis EC, Pontillo A. Inflammasome genetics and complex diseases: a comprehensive review. *Eur J Hum Genet* (2020) 28:13071321. doi: 10.1038/s41431-020-0631-y
46. Abate E, Blomgran R, Verma D, Lerm M, Fredrikson M. Polymorphisms in CARD8 and NLRP3 are associated with extrapulmonary TB and poor clinical outcome in active TB in Ethiopia. *Sci Rep* (2019) 9:3126. doi: 10.1038/s41598-019-40121-8
47. Brasil. Ministério da Saúde. *Secretaria de Vigilância em Saúde. Departamento de Vigilância das Doenças Transmissíveis. Rede de Teste Rápido para Tuberculose no Brasil: primeiro ano da implantação/Ministério da Saúde, Secretaria de Vigilância em Saúde, Departamento de Vigilância das Doenças Transmissíveis* (2015). Brasília: Ministério da Saúde. Available at: http://www.saude.gov.br/images/pdf/2016/janeiro/15/rtr-tb-15jan16-isbn-web.pdf (Accessed March 02, 2020).
48. Salem JI, Carvalho CM, Ogusku MM, Maia R. PKO – Alternative method for isolating mycobacteria from sputum. *Acta Amazonica* (2007) 37:3. doi: 10.1590/S0044-59672007000300013
49. Brasil. Ministério da Saúde *Secretaria de Vigilância em Saúde. Departamento de Vigilância das Doenças Transmissíveis. Manual de recomendações para o controle da tuberculose no Brasil / Ministério da Saúde, Secretaria de*

Vigilância em Saúde, Departamento de Vigilância das Doenças Transmissíveis (2019). Brasília: Ministério da Saúde. Available at: http://bvsms.saude.gov.br/bvs/publicacoes/manual_recomendacoes_controle_tuberculose_brasil_2_ed.pdf (Accessed March 02, 2020).
50. Gustincich S, Manfioletti G, Del Sal G, Schneider C, Carninci P. A fast method for high-quality genomic DNA extraction from whole blood. *Biotechniques* (1991) 11:3.
51. Yan S, Shen H, Lian Q, Jin W, Zhang R, Lin X, et al. Deficiency of the AIM2-ASC Signal Uncovers the STING-Driven Overreactive Response of Type I IFN and Reciprocal Depression of Protective IFN-γ Immunity in Mycobacterial. *J Immunol* (2018) 200:3. doi: 10.4049/jimmunol.1701177
52. Romagnoli A, Petruccioli E, Palucci I, Camassa S, Carata E, Petrone L, et al. Clinical isolates of the modern Mycobacterium tuberculosis lineage 4 evade host defense in human macrophages through eluding IL-1β-induced autophagy. *Cell Death Dis* (2018) 9:624. doi: 10.1038/s41419-018-0640-8
53. Möller M, Kinnear CJ, Orlova M, Kroon EE, Helden PDV, Schurr E, et al. Genetic Resistance to Mycobacterium tuberculosis Infection and Disease. *Front Immunol* (2018) 9:2219. doi: 10.3389/fimmu.2018.02219
54. Simmons JD, Stein CM, Seshadri C, Campo M, Alter G, Fortune S, et al. Immunological mechanisms of human resistance to persistent Mycobacterium tuberculosis infection. *Nat Rev Immunol* (2018) 18:9. doi: 10.1038/s41577-018-0025-3
55. Yamada H, Mizumo S, Horai R, Yoichiro I, Sugawara I, et al. Protective Role of Interleukin-1 in Mycobacterial Infection in IL-1 α/β Double-Knockout Mice. *Lab Invest* (2000) 80(5):759–67. doi: 10.1038/labinvest.3780079
56. Fremond CM, Togbe D, Doz E, Rose S, Vasseur V, Maillet I, et al. IL-1 receptor-mediated signal is an essential component of MyD88-dependent innate response to Mycobacterium tuberculosis infection. *J Immunol* (2007) 179:2. doi: 10.4049/jimmunol.179.2.1178
57. Mishra BB, Rathinam VAK, Martens GW, Martinot AJ, Kornfeld H, Fitzgerald KA, et al. Nitric oxide controls the immunopathology of tuberculosis by inhibiting NLRP3 inflammasome-dependent processing of IL-1beta. *Nat Immunol* (2013) 14:1. doi: 10.1038/ni.2474
58. Zhang G, Zhou B, Li S, Yue J, Yang H, Wen Y, et al. Allele-specific induction of IL-1β expression by C/EBPβ and PU. 1 contributes to increased tuberculosis susceptibility. *PloS Pathog* (2014) 10:10. doi: 10.1371/journal.ppat.1004426
59. Rathinam VAK, Jiang Z, Waggoner SN, Sharma S, Cole LE, Waggoner L, et al. The AIM2 inflammasome is essential for host-defense against cytosolic bacteria and DNA viruses. *Nat Immunol* (2010) 11:5. doi: 10.1038/ni.1864
60. Yang Y, Zhou X, Kouadir M, Shi F, Ding T, Liu C, et al. The AIM2 inflammasome is involved in macrophage activation during infection with virulent Mycobacterium bovis strain. *J Infect Dis* (2013) 208:11. doi: 10.1093/infdis/jit347
61. Saiga H, Nieuwenhuizen N, Gengenbacher M, Koehler AB, Schuerer S, Moura-Alves P, et al. The Recombinant BCG Δ ureC:: hly vaccine targets the AIM2 inflammasome to induce autophagy and inflammation. *J Infect Dis* (2015) 211:11. doi: 10.1093/infdis/jiu675
62. Zou H, Wu LX, Tan L, Shang FF, Zhou HH, et al. Significance of Single-Nucleotide Variants in Long Intergenic Non-protein Coding RNAs. *Front Cell Dev Biol* (2020) 8:347. doi: 10.3389/fcell.2020.00347
63. Chorev M, Carmel L. The function of introns. *Front Genet* (2012) 3:55. doi: 10.3389/fgene.2012.00055
64. Gallegos JE, Rose AB. The enduring mystery of intron-mediated enhancement. *Plant Sci* (2015) 237:8–15. doi: 10.1016/j.plantsci.2015.04.017
65. Shaul O. How introns enhance gene expression. *Int J Biochem Cell Biol* (2017) 91:145–55. doi: 10.1016/j.biocel.2017.06.016
66. Rigau M, Juan D, Valencia A, Rico D. Intronic CNVs and gene expression variation in human populations. *PloS Genet* (2019) 15:1. doi: 10.1371/journal.pgen.1007902
67. Man SM, Kanneganti TD. Regulation of lysosomal dynamics and autophagy by CTSB/cathepsin B. *Autophagy* (2016) 12:12. doi: 10.1080/15548627.2016.1239679
68. Khor CC, Chapman SJ, Vannberg FO, Dunne A, Murphy C, Ling EY, et al. A Mal functional variant is associated with protection against invasive pneumococcal disease, bacteremia, malaria and tuberculosis. *Nat Genet* (2007) 39:4. doi: 10.1038/ng1976
69. Ramasawmy R, Cunha-Neto E, Fae KC, Borba SCP, Teixeira PC, Ferreira SCP, et al. Heterozygosity for the S180L variant of MAL/TIRAP, a gene expressing an adaptor protein in the Toll-like receptor pathway, is associated with lower risk of developing chronic Chagas cardiomyopathy. *J Infect Dis* (2009) 199:12. doi: 10.1086/599212
70. Pontillo A, Carvalho MS, Kamada AJ, Moura R, Schindler HC, Duarte AJS, et al. Susceptibility to Mycobacterium tuberculosis infection in HIV-positive patients is associated with CARD8 genetic variant. *J Acquir Immune Defic Syndr* (2013) 63:2. doi: 10.1097/QAI.0b013e31828f93bb
71. Roberts RL, Van Rij AM, Phillips LV, McCormick SPA, Merriman TR, Jones GT, et al. Interaction of the inflammasome genes CARD8 and NLRP3 in abdominal aortic aneurysms. *Atherosclerosis* (2011) 218:1. doi: 10.1016/j.atherosclerosis.2011.04.043
72. Araujo FJ, Silva LDO, Mesquita TG, Pinheiro SK, Vital WDS, Chrusciak-Talhari A, et al. Polymorphisms in the TOLLIP Gene Influence Susceptibility to Cutaneous Leishmaniasis Caused by Leishmania guyanensis in the Amazonas State of Brazil. *Plos* (2015) 9:6. doi: 10.1371/journal.pntd.0003875

Conflict of Interest: The authors declare that the research was conducted in the absence of any commercial or financial relationships that could be construed as a potential conflict of interest.

frontiers in Cellular and Infection Microbiology

ORIGINAL RESEARCH
published: 01 July 2021
doi: 10.3389/fcimb.2021.587932

Increased PD-1 Level in Severe Cervical Injury Is Associated With the Rare Programmed Cell Death 1 (*PDCD1*) rs36084323 A Allele in a Dominant Model

*Mauro César da Silva[1], Fernanda Silva Medeiros[1], Neila Caroline Henrique da Silva[1], Larissa Albuquerque Paiva[2], Fabiana Oliveira dos Santos Gomes[1], Matheus Costa e Silva[3], Thailany Thays Gomes[1], Christina Alves Peixoto[1], Maria Carolina Valença Rygaard[4], Maria Luiza Bezerra Menezes[5], Stefan Welkovic[6], Eduardo Antônio Donadi[3] and Norma Lucena-Silva[1,4]**

[1] Laboratory of Immunogenetics, Department of Immunology, Aggeu Magalhães Institute, Oswaldo Cruz Foundation, Recife, Brazil, [2] Getúlio Vargas Hospital, Pernambuco Health Department, Recife, Brazil, [3] Clinical Immunology Division, Department of Medicine, School of Medicine of Ribeirão Preto, University of São Paulo (USP), Ribeirão Preto, Brazil, [4] Laboratory of Molecular Biology, IMIP Hospital, Pediatric Oncology Service, Recife, Brazil, [5] Department of Maternal and Child, Faculty of Medical Sciences, University of Pernambuco, Recife, Brazil, [6] Integrated Health Center Amaury de Medeiros (CISAM), University of Pernambuco, Recife, Brazil

OPEN ACCESS

Edited by:
John Hiscott,
Istituto Pasteur Italia Cenci Bolognetti Foundation, Italy

Reviewed by:
Kalichamy Alagarasu,
National Institute of Virology (ICMR), India
Teneema Kuriakose,
St. Jude Children's Research Hospital, United States

***Correspondence:**
Norma Lucena-Silva
norma.lucena@hotmail.com

Specialty section:
This article was submitted to Virus and Host, a section of the journal Frontiers in Cellular and Infection Microbiology

Received: 28 July 2020
Accepted: 21 April 2021
Published: 01 July 2021

Citation:
Silva MC, Medeiros FS, Silva NCH, Paiva LA, Gomes FOdS, Costa e Silva M, Gomes TT, Peixoto CA, Rygaard MCV, Menezes MLB, Welkovic S, Donadi EA and Lucena-Silva N (2021) Increased PD-1 Level in Severe Cervical Injury Is Associated With the Rare Programmed Cell Death 1 (PDCD1) rs36084323 A Allele in a Dominant Model. Front. Cell. Infect. Microbiol. 11:587932. doi: 10.3389/fcimb.2021.587932

The high-risk oncogenic human papillomavirus (HPV) has developed mechanisms for evasion of the immune system, favoring the persistence of the infection. The chronic inflammation further contributes to the progression of tissue injury to cervical cancer. The programmed cell death protein (PD-1) after contacting with its ligands (PD-L1 and PD-L2) exerts an inhibitory effect on the cellular immune response, maintaining the balance between activation, tolerance, and immune cell-dependent lesion. We evaluated 295 patients exhibiting or not HPV infection, stratified according to the location (injured and adjacent non-injured areas) and severity of the lesion (benign, pre-malignant lesions). Additionally, we investigated the role of the promoter region *PDCD1* -606G>A polymorphism (rs36084323) on the studied variables. PD-1 and *PDCD1* expression were evaluated by immunohistochemistry and qPCR, respectively, and the *PDCD1* polymorphism was evaluated by nucleotide sequencing. Irrespective of the severity of the lesion, PD-1 levels were increased compared to adjacent uninjured areas. Additionally, in cervical intraepithelial neoplasia (CIN) I, the presence of HPV was associated with increased (P = 0.0649), whereas in CIN III was associated with decreased (P = 0.0148) PD-1 levels, compared to the uninjured area in absence of HPV infection. The *PDCD1* -606A allele was rare in our population (8.7%) and was not associated with the risk for development of HPV infection, cytological and histological features, and aneuploidy. In contrast, irrespective of the severity of the lesion, patients exhibiting the mutant *PDCD1* -606A allele at single or double doses exhibited increased protein and gene expression when compared to the *PDCD1* -606GG wild type genotype. Besides, the presence of

HPV was associated with the decrease in *PDCD1* expression and PD-1 levels in carriers of the -606 A allele presenting severe lesions, suggesting that other mediators induced during the HPV infection progression may play an additional role. This study showed that increased PD-1 levels are influenced by the -606G>A nucleotide variation, particularly in low-grade lesions, in which the A allele favors increased *PDCD1* expression, contributing to HPV immune system evasion, and in the high-grade lesion, by decreasing tissue PD-1 levels.

Keywords: PD-1, CIN, HPV, polymorphism, inflammation, cancer

INTRODUCTION

Human papillomavirus (HPV) is the most common sexually transmitted biological agent, responsible for causing several types of cancer, particularly in the anogenital region, accounting for about 85% of the cervical tumors (World Health Organization, 2017; De Oliveira et al., 2019). The high-risk oncogenic HPVs have developed immune system evasion mechanisms, favoring viral persistence and chronic inflammation, which play an important role in the progression from cervical injury to cancer (Aggarwal et al., 2006; Grivennikov et al., 2010; Senba and Mori, 2012; Marinelli et al., 2019).

The programmed cell death protein (PD-1), together with its ligands PD-L1 or PD-L2, exerts an inhibitory effect on the cellular immune response, maintaining the balance between activation and tolerance of the immune cell function. The PD-1/PD-L1 signaling pathway has been used by microorganisms and tumor cells to decrease host immune system activity, permitting chronic infection, cell transformation into the tumor, and tumor cell survival (Ishida et al., 1992; Keir et al., 2008). PD-1 protein is mainly expressed on the membrane of T- and B- lymphocytes, NK cells, dendritic cells, activated monocytes, and immature Langerhans cells (Boussiotis, 2016).

Belonging to the immunoglobulin superfamily, PD-1 is a type I transmembrane monomeric protein, which has a cytoplasmic tyrosine-based inhibitory motif (ITIM) and a tyrosine-based switch motif (ITSM) that transmit inhibitory signals to the immune system cells. Once the peptide-MHC complex on the surface of the antigen-presenting cell (APC) binds to the T-cell receptor (TCR), the PD-L1 expressed on APC binds to the PD-1 receptor on T-cells and induces the phosphorylation of ITIM and ITSM motifs. The recruitment of the SHP-1 and SHP-2 phosphatases causes dephosphorylation of other signaling molecules of the cascade, inhibiting phosphatidylinositol 3-kinase (PI3K) and protein kinase B (Akt). These events culminate in immune response inhibition, reflected by i) decreased production of cytokines, such as IFN-γ, IL-2, and TNF-α, ii) inhibition of proliferation and survival of T cells, and iii) re-establishment of the immunological homeostasis, decreasing the expression of co-stimulatory molecules at the immunological synapsis (Muenst et al., 2016; Salmaninejad et al., 2018). Nevertheless, the PD-1/PD-L1 signaling pathway may be used by tumor cells to attenuate or escape anti-tumor immunity, facilitating tumor progression. In human malignancies, high T-cell PD-1 expression has been reported in Hodgkin's lymphoma, chronic lymphocytic leukemia, and breast, bladder, and ovarian cancers, suggesting a state of functional exhaustion of T cells (Muenst et al., 2016; Hollander et al., 2018; Kawahara et al., 2018; Lewinsky et al., 2018; Wieser et al., 2018; Jiang et al., 2019).

The *PDCD1* gene is located at chromosome 2 (2q37.3), presents 5 exons, and encodes a 288 amino acid PD-1 protein. Alternative splicing can generate different isoforms that are expressed at similar levels after T cell activation (Shinohara et al., 1994; Keir et al., 2008); however, genetic variants at *PDCD1* coding and regulatory 5' and 3' untranslated regions (UTR) may influence protein levels and the natural history of cancer development (Tao et al., 2017; Wang et al., 2018). Several *PDCD1* polymorphic sites have been described, including i) 298 single nucleotide polymorphisms (SNPs) at the coding region, of which 213 missense, 112 synonymous, 7 nonsense, and 4 frameshift mutations; ii) 512 SNPs at the extended 5'UTR, iii) 490 SNPs at the extended 3'UTR, and iv) 1,791 intronic sequence mutations. Among these SNPs, 36 at the coding region, 57 at 5'UTR, 56 at 3'UTR and 283 intronic ones have clinical importance (https://www.ncbi.nlm.nih.gov/SNP/). Among all these polymorphic sites, the *PDCD1* promoter region -606G>A polymorphism (rs36084323) has been associated with the oncogenic p53 protein in breast cancer (Hua et al., 2011), in measles-induced autoimmune neurological manifestations (Ishizaki et al., 2010), and the susceptibility to hepatitis B infection (Hou et al., 2017).

Abbreviations: Akt, Protein kinase B; ASC – H, Atypical squamous cells-cannot exclude high-grade squamous intraepithelial lesion; ASC-US, Atypical squamous cells of undetermined significance; CI, Confidence interval; CIN, Cervical intraepithelial neoplasia (I-III); CISAM, Integrated Health Center Amaury de Medeiros; DNA, Deoxyribonucleic acid; DMSO, Dimethyl sulfoxide; GAPDH, Glyceraldehyde phosphate dehydrogenase; HE, Hematoxylin-eosin; HBV, Hepatitis B virus; HIV, Human immunodeficiency virus; *HLA-G*, Human leukocyte antigen G; HPV, Human papillomavirus; HSIL, High-grade squamous intraepithelial lesion; IMIP, Professor Fernando Figueira Institute of Integral Medicine; IHC, Immunohistochemistry; ITIM, Immunoreceptor tyrosine-based inhibitory motif; ITSM, Immunoreceptor tyrosine-based switch motif; LGSIL, Low-grade squamous intraepithelial lesion; NSCLC, Non-small cell lung cancer; OEGE, Online Encyclopedia for Genetic Epidemiology; OR, Odds ratio; *P*, *P*-value; PBMC, Peripheral blood mononucleated cells; PCR, Polymerase chain reaction; PI3K, Phosphatidylinositol 3-kinase; PD-1/*PDCD1*, Programmed cell death 1; PD-L1/PD-L2, Programmed cell death ligand 1 or 2; SNP, Single nucleotide polymorphisms; SSPE, Subacute sclerosing panencephalitis; TAE, Tris-acetate-EDTA buffer; TCR, T-cell receptor; UTR, Untranslated regions.

To study the role of PD-1 on the progression of cervical lesions, we evaluated PD-1 tissue and *PDCD1* gene expression in women infected or not by HPV. To understand the contribution of genetic factors on PD-1 and *PDCD1* expression, we evaluated the *PDCD1* promoter region -606G>A polymorphism (rs36084323) in these patients.

MATERIALS AND METHODS

Study Population and Ethical Consideration

The study population encompassed 295 women, aged 18-71 years (median=37 years). Among the 107 HPV-infected women, 90 were infected by high-risk, 11 by low-risk HPV, and in 6 samples the HPV viral genotype was not identified. Patients attending the Integrated Health Center Amaury de Medeiros (CISAM) and in the Professor Fernando Figueira Institute of Integral Medicine (IMIP), in Pernambuco, Brazil, between April 2016 to October 2018, were invited to participate in this study during the routine gynecological consultations for evaluation of the Papanicolaou smears, which are performed annually in asymptomatic and symptomatic women. This study was approved by the Ethics Committee of the Aggeu Magalhães Institute (CAAE: 51111115.9.0000.5190), and all participants signed an informed consent form after receiving a detailed explanation about the research. HIV-positive patients were not included in this study.

Clinical and laboratory data were obtained from medical records and interviews, using a standard questionnaire (**Table 1**). Venous blood and cervical exfoliative cells and biopsies were obtained during routine colposcopy analysis and evaluated by experienced gynecologists.

For the *PDCD1* gene expression analysis, the reference group was women presenting no atypia in the cytopathological Papanicolaou smear, who were not eligible to be subjected to biopsy due to ethical restriction. Abnormal cytology was classified using the Bethesda system. Cervical abnormalities were stratified as the low-grade squamous intraepithelial lesion (LGSIL) and high-grade squamous intraepithelial lesion (HGSIL). Women presenting abnormal cytology were subjected to cervical biopsies for histological stratification into the benign lesions, low-grade cervical intraepithelial neoplasia (CIN) I, and high-grade CIN II and CIN III. For the immunohistochemistry evaluation of PD-1 protein levels, the reference controls were specimens from the uninjured area adjacent to the lesion.

Histopathology

Biopsies of the cervical lesion and the adjacent area were fixed in formalin (10%) and embedded in paraffin. Four µm tissue sections were cut using a manual microtome (American Optical, Rotary, Leica, Buffalo Grove, IL), placed on silanized glass slides (Agilent-Dako, Santa Clara, CA), stained with hematoxylin-eosin (HE) and mounted with the medium

TABLE 1 | Demographic, clinical, and laboratory features of women exhibiting cervical lesion associated with the HPV-infections [low-grade squamous intraepithelial lesion (LGSIL), the high-grade squamous intraepithelial lesion (HGSIL) and cervical intraepithelial neoplasia (CIN)] or non-associated with the HPV infection [atypical squamous cells of undifferentiated (ASC-US), atypical squamous cells not excluding high-grade squamous intraepithelial lesion (ASC-H)].

Patients characteristics	TOTAL		HPV +		HPV -		
	N = 295	%	N = 107	36.3%	N = 188	63.7%	
Age - years							
Median (minimum - maximum)	37.8 (18-70)		36 (18-66)		38 (19-72)		*P*= 0.3066
Use of oral contraceptives	293		107		188		
Yes	68	23.2	19	17.9	49	26.2	*P*= 0.1152
No	225	76.8	87	82.1	138	73.8	
Data missing	2		1		1		
Cytological alterations	255		107		188		
No atypias	104	40.8	24	25.5	80	49.6	*P*< 0.0001
ASC-US and ASC-H	26	10.2	6	6.4	20	12.4	
LGSIL	51	20.0	22	23.4	29	18.0	
HGSIL	74	29.0	42	44.7	32	19.9	
Data missing	40		13		27		
Histological alterations	267		107		188		
Uninjured (not submitted to biopsy)*	74	27.7	11	11.7	63	36.4	*P*< 0.0001
Benign injury	41	15.4	9	9.6	32	18.5	
CIN I	23	8.6	8	8.5	15	8.7	
CIN II	67	25.1	33	35.1	34	19.6	
CIN III	62	23.2	33	35.1	29	16.8	
Data missing	24		13		15		
Cellular ploidy	122		107		188		
Aneuploidy	27	22.1	10	23.8	63	78.8	*P*< 0.0001
Diploidy	95	77.9	32	76.2	17	21.2	
Data missing	173		65		108		

*To evaluate possible differences between the groups of infected and uninfected by HPV, Mann-Whitney test (age-years), Chi-square test (cytological and histological alterations), and Fisher test (Use of oral contraceptives and Cellular ploidy) were performed. *According to the Brazilian Ministry of Health's screening policy for cervical cancer, there is no indication for colposcopy for these patients, due to the absence of changes in the cytological examination.*

Entellan® (MERCK, Burlington, MA). The sections were visualized with 400x magnification in an inverted microscope (Zeiss, Göttingen, Germany) equipped with a camera and with a 4.7.4 Image Analysis Program (AxionCam MRm Zeiss). HE-stained slides were blindly evaluated by a cervical pathologist.

HPV Detection and Typing

Genomic DNA was extracted from 500µL of a cervical cell suspension, using the Illustra Blood kit (Healthcare®, Little Chalfont, Buckinghamshire, UK), according to the manufacturer's instructions, and quantified using the NanoDrop 2000 spectrophotometer (ThermoScientific, Waltham, MA). The quality of the extracted DNA was also assessed by PCR-amplification using the human constitutive glyceraldehyde phosphate dehydrogenase (*GAPDH*) gene (Martins et al., 2014). HPV infection in cervical samples was diagnosed by amplifying a fragment of the viral *L1* gene with the degenerate MY09 and MY11 primers (Manos et al., 1989), using the L1-fragment encoded plasmid as the positive control. A reaction without adding any sample was used as a negative control. The presence of a band of approximately 450 base pairs (bp) in the 2% agarose gel confirmed the presence of the viral infection. Each amplification product was directly sequenced with the MY11 primer in the Genetic AnalyzerABI 3500 (Applied Biosystems, Foster City, CA) sequencer, using the BigDye terminator v3.1 cycle sequencing kit (Applied Biosystems). The chromatograms were visualized in the Mega 6.0 program (Tamura et al., 2011) to assess the quality of the sequence. Samples with defined peaks and low background in the chromatogram were submitted to Papillomavirus Episteme (https://pave.niaid.nih.gov/) to HPV genotyping.

Determination of Cellular Ploidy

Cervical cells of the uterine cervix (150µL) were ruptured using 2mL of Pharm Lyse lysis buffer (Becton Dickinson, Franklin Lakes, NJ), vigorously homogenized, and incubated in the dark for 10 minutes, and centrifuged for 120 seconds at 1,000 x g. The supernatant was discarded and the pellet resuspended in 2mL of FACs flow buffer, gently homogenized, and recentrifuged for 120 seconds at 1,000 x g. After discarding the supernatant, the pellet was resuspended in 500 µL of propidium iodide plus 10 µL of RNase (100 µg/mL), and incubated at room temperature for 30 minutes at 4°C and then for 10 minutes at 8°C. DNA fluorescence was measured by laser excitation at 488 nm and emission above 600 nm. The DNA index was estimated by comparing the proportion of DNA from the cervical cells analyzed with the diploid blood cells, using the software ModFitLT V3.0 (Verity Software House Inc., Topsham, ME). Aneuploidy was defined by a deviation in the DNA histogram in more than 10% of the cell population analyzed in the area corresponding to G0- G1 of the cell cycle in the sample (Martins et al., 2014).

Cervical Cell PD-1 Levels

Immunohistochemistry (IHC) analysis for cervical biopsies was manually performed using the DAKO EnVision ™ FLEX kit (Agilent-DAKO, Santa Clara, CA). For antigenic recovery, tissue was pretreated with citrate buffer, pH 6.1 (Agilent-DAKO), and heated for 30 minutes. After blocking with endogenous peroxidase, the tissue sample was incubated with the primary monoclonal anti-PD-1 mouse antibody (ABCAM, Cambridge, UK) diluted (1:100) with DAKO antibody diluent for 1h. After washing, the sections were incubated with secondary antibody for 20 minutes and then visualized with the DAB reagent (3,3'-diaminobenzidine tetrahydrochloride, DAKO). After labeling, tissue sections were counterstained with Harris' hematoxylin and assembled with Entellan® (MERCK).

The IHC slides of the cervical lesion and the adjacent uninjured area were independently analyzed by two specialist pathologists. Cell areas showing brown staining were considered to be positive for the expression of PD-1 and quantified in three fields showing the highest labeling per slide, using the Gimp 2.10.18 software (GNU Image Manipulation Program, UNIX platforms, www.gimp.org). To minimize possible reading errors, we measured pixels in areas with an intense and less intense stained area in the same picture; and combined both readings to generate the final PD-1 expression value.

Cervical Cell *PDCD1* Gene Expression

Total RNA was extracted from a 1000 µL of cervical cell suspension, using Trizol® reagent (Invitrogen), and submitted to cDNA synthesis using the MLLV reverse transcriptase (Invitrogen), accordingly to the manufacturer's instructions. For *PDCD1* expression, the qPCR was prepared with 1µL cDNA and 10 pmoles of each PD1F: 5' GAT GGT TCT TAG ACT CCC CAG ACA G 3', and PD1R: 5' GGC TCA TGC GGT ACC AGT TTA GCA C 3' primers, in Power SYBR™ Green PCR Master Mix (Applied Biosystems, Foster City, CA). For the expression of the *GAPDH* constitutive gene, we used also 1 µL cDNA and 10 pmoles of GAPDH2F: 5' AGA AGG CTG GGG CTC ATT TG 3' and GAPDH2R: 5' GTG GTC ATG AGT CCT TCC AC 3' primers in Power SYBR™ Green PCR Master Mix. All primers were designed nearby the exon-intron junction to amplify a fragment that covers two exons, assuring amplification of the cDNA target. The qPCR was performed in a final volume of 20 µL containing 10 µL of 2× Power SYBR® Green PCR Master Mix, 1 µl forward and 1 µl reverse PCR primers (500nM), 1µL cDNA and 7 µL nuclease-free water. The reaction mixtures were processed with an initial holding period at 95°C for 10 min, followed by a two-step PCR program for 40 cycles that consisted of 95°C for 15 sec and 60°C for 1 min. The *PDCD1* and *GAPDH* calibration curves showed similar amplification efficiency, and samples were evaluated in duplicate in Quant Studio 5 (Applied Biosystem). Only samples showing a melting curve with single and specific peaks, and only duplicates showing standard deviation less than 0.5 were considered for analyses. A unique threshold was settled for each gene amplification in all plates, and the sample CTs were annotated. *PDCD1* relative expression was determined by ΔCT-comparative quantification, in which *PDCD1* expression was normalized by the endogenous gene expression ($\Delta CT = CT_{PDCD1} - CT_{GAPDH}$) for each sample, and the final results were expressed in fold-change, using the equation ($\text{Fold-change} = 2^{-\Delta CT}$).

PDCD1 Promoter Region Polymorphism

DNA from peripheral blood mononuclear cells, extracted using DNAzol® Reagent (Invitrogen, Carlsbad, CA) was used for the detection of the -606G>A (rs36084323) SNP. Briefly, DNA was amplified using the *PD-1* PROMO F (5 'GAA AGA TCT GGA ACT GTG GC 3') and PD-1 PROMO R (5 'TGA GAG TGA AAG GTC CCT CC 3') primers. The amplification reaction was performed in a final volume of 20 μL containing 1x of polymerase buffer (Applied Biosystems), 0.5 mM $MgCl_2$, 2% DMSO, 200 μM dNTP's, 1.0 μM of each primer, 1.0 unit of Ampli-Taq Gold (Applied Biosystems) and 80-200 ng of genomic DNA for the amplification of a 962 bp-PD1 fragment. The cycling conditions included an initial stage at 94°C for 10 min; 40 cycles of denaturation at 94°C for 1 min, annealing at 62 °C for 1 min and extension at 72 °C for 1.2 min, and final extension for 7 min at 72°C. The PCR product was visualized using a 1.5% agarose gel and, subsequently, sequenced by the SANGER method, following the BigDye protocol on ABI 3500 sequencer (Applied Biosystems). Polymorphic sites were determined using the Seqman® program (Roche 454, Life ScienceTM, Branford, CT) and individually annotated in an Excel 2016 spreadsheet.

Bioinformatics Analysis

To propose a list of possible microRNAs (miRNA) associated with the *PDCD1* rs36084323 SNP, we took advantage of two separated approaches using: i) the mirDIP Version 4.1.11.1 (Tokar et al., 2018), which integrates 30 different databases of miRNA target prediction, together with a unidirectional search query with *PDCD1* (PD-1 alias), to search for all predicted miRNAs without filtering any specific 'Score class'; ii) the sequence of 100 base pairs that surrounds the SNP, as retrieved from Genome Browser Gateway (http://genome.ucsc.edu/), and blasted using miRBase Release 22.1 (Kozomara et al., 2019). Then, we selected the miRNAs that annealed with the SNP site taking into account the two possible alleles.

Statistical Analysis

Association analyses of allele and genotype frequencies with clinical variables were performed using the two-tailed Fisher's exact and chi-square tests, considering a significance level of $P < 0.05$. The Hardy-Weinberg Equilibrium was assessed by the Online Encyclopedia for Genetic Epidemiology (OEGE). The D'Agostino-Pearson test was used to assess the homogeneity of the PD-1 expression in pixels and fold-change. The central tendency was expressed as a median and the Kruskal-Wallis and Mann-Whitney tests were used to compare numeric variables. The graphics were prepared using GraphPad Prism Software version 5.0 for windows (www.graphpad.com, La Jolla, CA).

RESULTS

PD-1 Detection in Cervical Samples

PD-1 expression was evaluated in samples exhibiting HPV infection and in samples without HPV infection. Irrespective of lesion severity, we observed three patterns of PD-1 staining in cervical samples: i) exclusive labeling of the stratified squamous epithelium, ii) exclusive labeling of stromal cells, and iii) labeling of epithelium and stroma. Considering the uninjured adjacent areas, the expression of PD-1 in epithelium and stroma (n = 50, median = 4,313 pixels) was higher when compared to sections that labeled only the epithelium (n = 48, median = 2,810 pixels, $P = 0.0302$). Considering the injured areas (cervical lesions), the expression of PD-1 in epithelium and stroma (n = 32, median = 21,184 pixels) was also significantly higher when compared to specimens that exclusively labeled the epithelium area (n = 20, median = 6,339 pixels, $P < 0.0001$) (**Figure 1A**).

The evaluation of PD-1 protein level according to the severity of the lesion revealed the following results: i) PD-1 expression in benign lesions, and cervical intraepithelial neoplasia (CIN I, CIN II, and CIN III) was significantly higher when compared to uninjured adjacent tissue ($P<0.0001$, for each comparison, **Figure 1B**); ii) the PD-1 expression in benign lesions did not differ from CIN II ($P = 0.7431$) and CIN III ($P = 0.5854$) and, similarly, CIN II did not differ from CIN III ($P = 0.5122$); and iii) the PD-1 levels in low-grade lesions (CIN I) (n = 12, median = 44,215 pixels) were higher than in those presenting high-grade (CIN II and CIN III) lesions (n = 54, median = 18,942 pixels, $P = 0.0046$); however, the pattern of expression was different. PD-1 labeling in low-grade lesions was higher in infiltrating immune cells of the stroma compared to the epithelium, whereas in high-grade lesions PD-1 expression was observed primarily in the epithelium (**Figure 2**). Additionally, irrespective of the severity of the lesion, PD-1 levels were increased compared to adjacent uninjured areas. Also, in CIN I the presence of HPV was associated with increased PD-1 protein levels ($P = 0.0649$), whereas in CIN III was associated with decreased levels ($P = 0.0148$) compared to correspondent tissue lesion in absence of HPV infection (**Figures 1C, D**).

Polymorphism of the *PDCD1* Promoter Region

Irrespective of the severity of the cervical lesion, the frequency of the wild -606G allele was 91.3%, and the distribution of the GG (83.7%), GA (15.2%), and AA (1.1%) genotypes adhered to the Hardy-Weinberg equilibrium ($\chi^2 = 0.48$). Taking into account the low frequency of the AA genotype, we lumped together the AA and GA genotypes to allow statistical analysis. Women carrying the -606A allele were not at increased risk for i) development of HPV infection, ii) exhibiting cytological and histological HPV and non-HPV changes, and ii) presenting aneuploidy (**Table 2**).

Considering the differential exposure of HPV according to age and the risk for developing cervical lesions, we evaluated the influence of the patient age on the studied variables. Age did not influence the *PDCD1* genotype frequency among patients presenting or not HPV ($P = 0.3066$), and among patients exhibiting benign injury ($P = 0.1692$), CIN I ($P = 0.5698$), CIN II ($P = 0.0746$) or CIN III ($P = 0.7366$) compared to women with normal cytomorphological results.

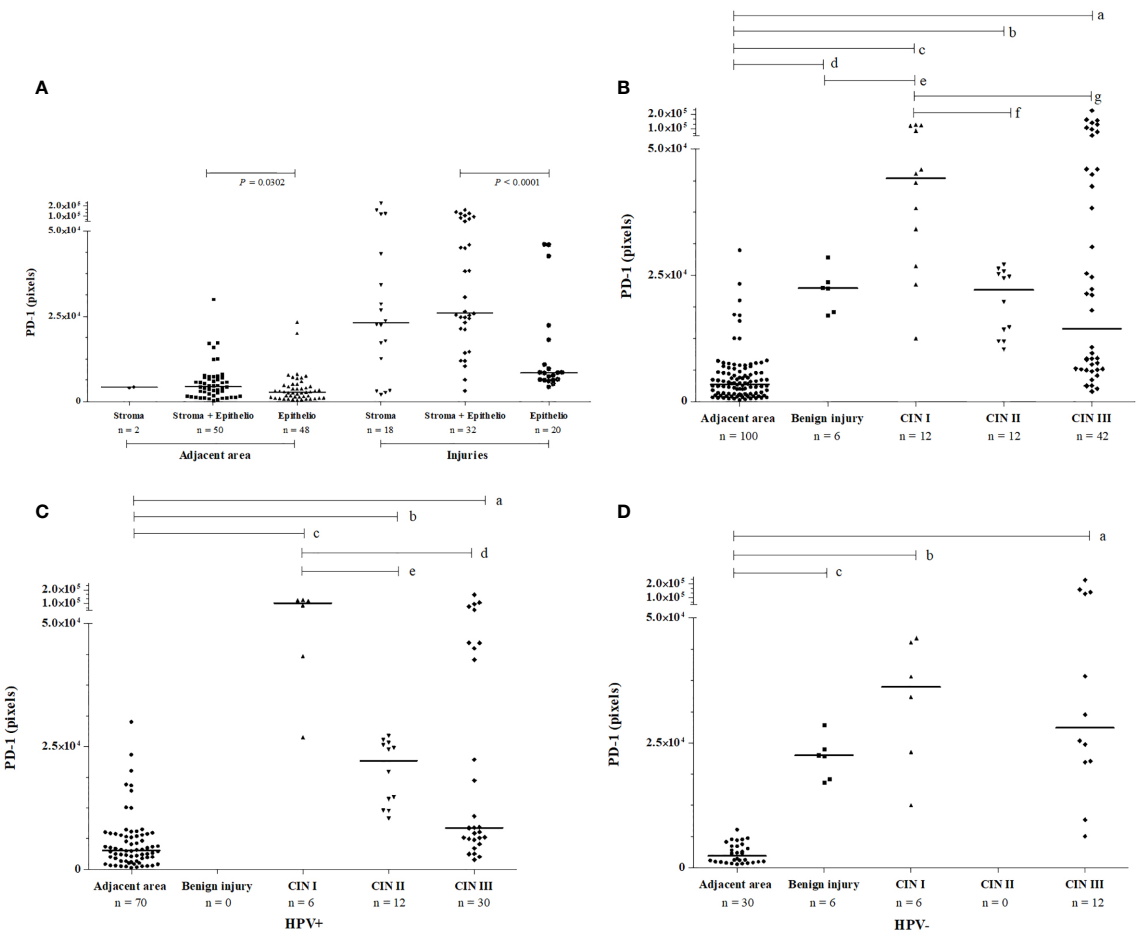

FIGURE 1 | Pattern of PD-1 immunochemistry labeling observed in cervical samples, according to **(A)** the tissue location in injured and uninjured adjacent areas, **(B)** the severity of lesion irrespective to HPV infection, **(C)** in the presence of HPV infection, and **(D)** the absence of HPV infection. PD-1 labeling was analyzed by two independent pathologists, and the intensity of the labeling (pixels) was quantified in three fields per slide. Data were presented as medians, and the comparisons were performed using the Kruskal-Wallis test followed by Mann Whitney U test. In graph B, PD-1 levels were high irrespective of the severity of cervical lesions, CIN III (in a, P<0.0001); CIN II (in b, P<0.0001); CIN I (in c, P<0.0001); and benign lesions (in d, P<0.0001) compared to the uninjured adjacent area; and between benign lesion vs. CIN I (in e, P = 0.0131); however, CIN I lesions showed the highest PD-1 level compared to the CIN II (in f, P = 0.0014) and CIN III (in g, P = 0.0172). In graph C, in presence of HPV the PD-1 levels were high in CIN III (in a, P<0.0001), CIN II (in b, P<0.0001), and CIN I (in c, P<0.0001) compared to uninjured tissue, and lower PD-1 levels were observed in CIN III (in d, P = 0.0048) and CIN II (in e, P = 0.0012) compared to the levels in low-grade lesion CIN I. In graph D, in women non-infected by HPV, high PD-1 levels were also observed in CIN III (in a, P<0.0001), CIN I (in b, P = 0.0001), and benign injury (in c P = 0.0001) compared to the uninjured adjacent area.

Association of the *PDCD1* Gene Expression in the Cervical Lesion With *PDCD1* Polymorphism

The presence of cervical injury was not associated with a greater *PDCD1* expression by exfoliative cervical cells when compared to cervical samples from women with a normal cytomorphological smear (**Figure 3A**). However, considering samples altogether, the mutant -606A allele in single or double dose was associated with higher *PDCD1* gene expression in cervical cells compared to the wild type -606GG genotype (**Figure 3B**). There was no statistical difference (P = 0.4692) between *PDCD1* expression levels in lesions of different severities in carriers of the -606GG genotype (**Figure 3C**). However, among carriers of the -606A allele in homo or heterozygosis, the expression of *PDCD1* was higher in exfoliative cells of patients exhibiting high-grade CIN III lesions compared to those presenting benign (P = 0.0453) or CIN II (P = 0.0233) lesions (**Figure 3D**). Moreover, despite no association of HPV-infection with *PDCD1* expression (P=0.8329) was observed (**Figure 3E**), the presence of HPV increased *PDCD1* expression, particularly in women presenting CIN I lesion (**Figures 3F, G**), a finding that may have been influenced by the -606A allele (**Figure 3H**).

Association Between PD-1 Protein Levels and *PDCD1* Polymorphism

We also evaluated whether the PD-1 tissue levels were associated with the presence of the rare *PDCD1* -606G>A polymorphic sites. Considering the dominant model for the rare allele, women

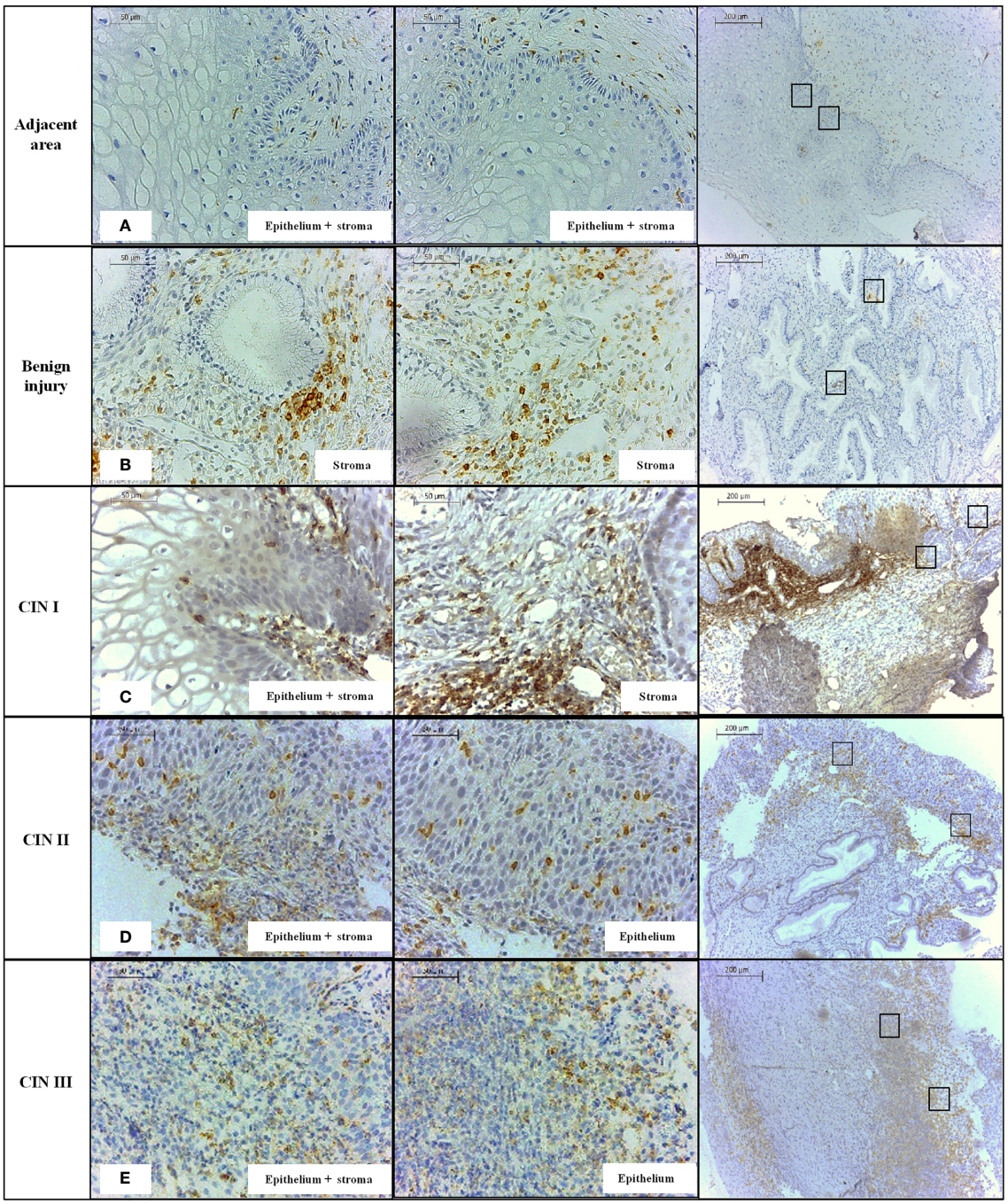

FIGURE 2 | Immunohistochemistry labeling of PD-1 level observed in specimens obtained from the mucosa of the uterine cervix, stratified according to the presence or not of the lesion, and according to the severity of the cervical lesion. **(A)** cervix without lesion, **(B)** benign injury, **(C)** CIN I, **(D)** CIN II, **(E)** CIN III, at 100X and 400X magnifications. PD-1 protein was primarily detected in the stratified epithelium and stroma of the cervical mucosa.

carrying the A allele in homozygosis or heterozygosis (n = 46, median = 7,381 pixels) exhibited increased PD-1 levels in cervical samples when compared to those homozygous for the *G* allele (n = 126, median = 5,697 pixels, $P = 0.0234$) (**Figure 4A**). Besides, the association of *PDCD1* -606A allele with the PD-1 expression was strengthened when we specifically evaluated women with high-grade cervical lesions (CIN III); i.e., women carrying the -606A allele at homo- or heterozygosis exhibited higher PD-1 levels in the cervical lesions when compared to women carrying the homozygous -606G allele (GA + AA with

TABLE 2 | Allelic and genotypic frequency of the promoter region *PDCD1*-606 G>A (rs36084323) polymorphism observed in women exhibiting grades of cervical lesions, stratified according to i) presence or not of the HPV infection, ii) cytological/histological alterations, and iii) cellular ploidy.

Patients characteristics	*PDCD1* (rs36084323)											
	GG		GA+AA		*P*	OR (CI-95%)	G		A		*P*	OR (CI-95%)
	N= 231	83.7%	N=45	16.3%			N= 504	91.3%	N=48	8.7%		
HPV Infection												
Yes	83	35.9	17	37.8	0.8659	0.92 (0.48-1.79)	182	36.1	18	37.5	0.8757	0.94 (0.51-1.74)
No	148	64.1	28	62.2			322	63.9	30	62.5		
Total	231	100.0	45	100.0			504	100.0	48	100.0		
Cytological alterations												
HGSIL	55	27.8	16	40.0	0.3018	n/a	125	28.8	17	40.5	0.2864	n/a
ASC-US, ASC-H and LGSIL	62	31.3	10	25.0			133	30.6	11	26.2		
No atypias	81	40.9	14	35.0			176	40.6	14	33.3		
Total	198	100.0	40	100.0			434	100.0	42	100.0		
Presence of histological alterations												
Presence of CIN	118	56.5	23	56.1	1.0000	1.01 (0.52-1.99)	259	56.8	23	52.3	0.6337	1.20 (0.64-2.23)
Absence of CIN	91	43.5	18	43.9			197	43.2	21	47.7		
Total	209	100.0	41	100.0			456	100.0	44	100.0		
Histological alterations												
CIN III	48	23.0	10	24.4	0.8669	n/a	106	23.2	10	22.7	0.7133	n/a
CIN II	51	24.4	11	26.8			113	24.8	11	25.0		
CIN I	19	9.1	2	4.9			40	8.8	2	4.5		
Benign injury	33	15.8	8	19.5			72	15.8	10	22.7		
Uninjured	58	27.8	10	24.4			125	27.4	11	25.0		
Total	209	100.0	41	100.0			456	100.0	44	100.0		
Cellular ploidy												
Aneuploidy	22	24.2	3	12.0	0.2737	2.34 (0.64-8.57)	47	22.8	3	11.5	0.3092	2.27 (0.65-7.88)
Diploidy	69	75.8	22	88.0			159	77.2	23	88.5		
Total	91	100.0	25	100.0			206	100.0	26	100.0		

Atypical squamous cells of undetermined significance (ASC-US), atypical squamous cells-not excluding high-grade squamous intraepithelial lesion (ASC-H), the low-grade squamous intraepithelial lesion (LGSIL), the high-grade squamous intraepithelial lesion (HGSIL), cervical intraepithelial neoplasia (CIN). N, sample number; P, P-value; G, wild allele; A, variant allele; OR, odds ratio and 95%CI, confidence interval. The frequencies of alleles and genotypes were compared using the two-tailed Fisher's exact and Chi-square tests.

the median of 48,117 pixels *vs*. GG with the median of 8,539 pixels, $P = 0.0010$) (**Figure 4B**). However, PD-1 levels in uninjured adjacent tissue were not associated with the -606G>A variation site (GA + AA with the median of 3,358 pixels *vs*. *GG* with the median of 3,409 pixels, $P = 0.8646$) (**Figure 4C**). In the presence of HPV infection, the high PD-1 levels previously associated with the presence of the -606A allele was not observed anymore (**Figures 4D, E**); however, the influence of HPV infection on PD-1 levels continue to be observed for high-grade CIN III lesions even being in less magnitude (**Figure 4F**).

Predicted miRNA and *PDCD1* rs36084323 SNP Association

Considering the discrepancy regarding the results of the protein (**Figure 4F**) and gene expression (**Figure 3H**) levels, we further evaluated the differential targeting of miRNAs at the *PDCD1* -606 variation site. An in-silico study showed that the hsa-miR-204-3p binds exclusively to the *G* allele, whereas the hsa-miR-6798-5p, hsa-miR-6775-5p, and hsa-miR-4776-5p bind only to the A allele, and the hsa-miR-6771-5p targeted both alleles. Notably, the miRNAs that targeted the -606G>A variation site were included among the 2,586 miRNAs that have been predicted to target the *PDCD1* gene, according to the mirDIP analysis (**Figure 5**).

In summary, our results showed that the -606A allele is rare in our population and, considering the dominant model, women carrying the -606 AX genotype (X= A or G) are more likely to respond to HPV-induced cervical lesions with decreased production of PD-1, and the intensity and pattern of labeling is related to the degree of the cervical injury.

DISCUSSION

Since healthy cervical specimens are not easily available due to ethical reasons, in this study we evaluated PD-1 expression in cervical biopsies obtained from patients presenting several stages of the cervical lesion (injured areas) and used, as controls, the adjacent uninjured cervical areas. Irrespective of the severity of the lesion, injured cervical specimens overexpressed PD-1 when compared to the adjacent uninjured area, and particularly observed in the stromal layer (**Figure 1A**). Notably, samples presenting high-grade (CIN II-III) lesions expressed less PD-1 when compared to low-grade (CIN I) lesions (**Figure 1B**). PD-1 expression predominated in the stroma in low-grade lesions, and the epithelium in high-grade lesions (**Figure 2**). The stroma-rich T cell-infiltrate in low-grade cervical lesions associated with the increased tissue PD-1 (Hemmat and Bannazadeh Baghi, 2019)

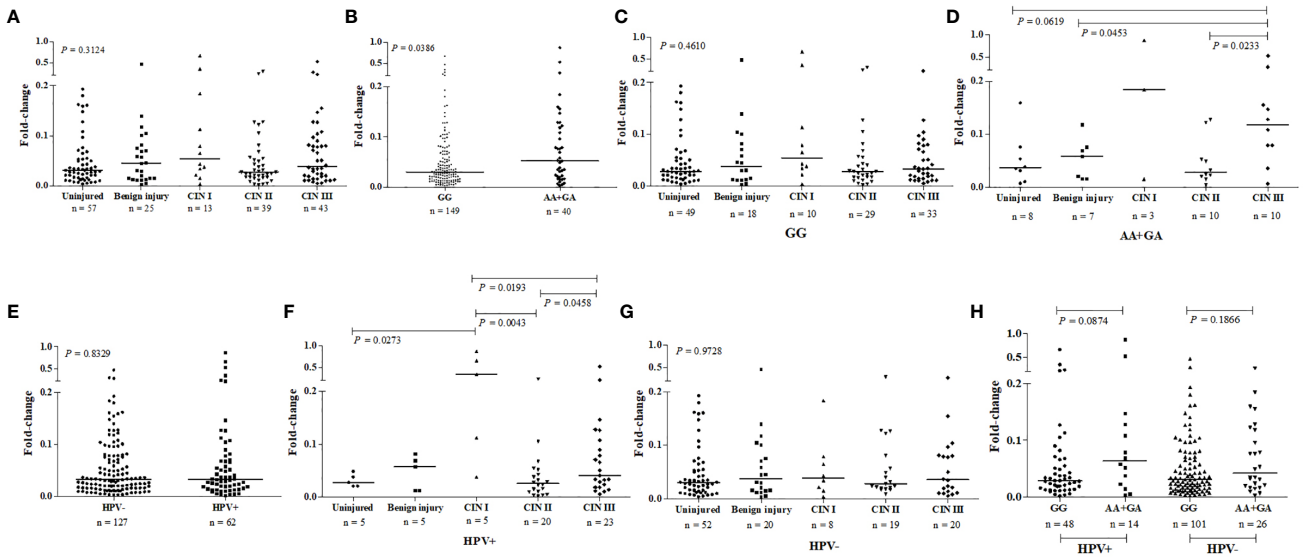

FIGURE 3 | *PDCD1* mRNA expression in exfoliative cervical cells of patients presenting normal (uninjured) and abnormal cytomorphological smear (injured) stratified according to the severity of the lesion, presence or absence of HPV infection, and the nucleotide variability at the promoter region *PDCD1*-606G>A polymorphic site (rs36084323). *PDCD1* expression was calculated by the qPCR comparative method using as reference the *GAPDH* gene and the SYRB green detection system, performed in duplicate. Fold-change differences were estimated by the Kruskal-Wallis or Mann-Whitney U tests. **(A)** *PDCD1* expression stratified according to the severity of the cervical lesion, **(B)** *PDCD1* expression stratified according to the presence of the -606GG and AA/GA genotypes, **(C)** *PDCD1* expression among carries of -606GG genotype, **(D)** and carries of -606 A allele in homo or heterozygosis stratified according to the severity of the cervical lesion, **(E)** *PDCD1* expression among women infected and non-infected by HPV, and stratified according to the severity of the cervical lesion in the presence **(F)** or absence **(G)** of HPV infection, and **(H)** *PDCD1* expression stratified according to the presence of the -606GG and AA/GA genotypes in the presence or absence of HPV infection.

primarily reflect the severity of inflammation associated with HPV infection (Yang et al., 2013), whereas the expression at the epithelium strongly indicates the role of PD-1 on the progression of the cervical lesions (Yang et al., 2017; Chang et al., 2018; Medeiros et al., 2018).

Considering that the magnitude of the *PDCD1* gene expression has been associated with the *PDCD1* -606 G>A polymorphic site (Ishizaki et al., 2010), we further investigated the relationship between alleles/genotypes with the magnitude of PD-1 cervical expression. First, we observed that the *PDCD1* -606AA genotype was rare in our population (1.1%), and according to the data reported at the 1000 Genomes Phase 3 database (The 1000 Genomes Project Consortium, 2015), the promoter region *PDCD1* -606G>A (rs36084323) polymorphic site presents diverse allele frequency distribution in worldwide populations (1000 Genomes Project Phase 3 Allele Frequencies rs36084323 Snp; Auton et al., 2015), being frequent in Asians (1000 Genomes Project Phase 3 Allele Frequencies rs36084323 Snp), particularly in Chinese (21.9%) and Japanese (25%) populations (Hua et al., 2011; Sasaki et al., 2014; Hou et al., 2017). The presence of the -606A allele was not associated with the risk for the development of HPV infection, probably because of the low frequency of the mutant allele in our population. According to the frequency of the -606A in our population, a cohort of 1,834 individuals would be necessary to discriminate susceptibility/protection alleles.

Women carrying the -606A allele in homozygosis or heterozygosis showed a significant increase in the *PDCD1* gene expression and PD-1 protein level when compared to those who carry the -606G allele in homozygosis. In HPV-non-infected women, the *PDCD1* expression was irrespective of the severity of the lesion, but in the presence of HPV infection, the *PDCD1* expression was significantly increased in CIN I lesions, which may suggest a viral attempt to evade immune response against infection, favoring viral persistence (Yang et al., 2013). The PD-1 protein level in CIN I lesions was also high in HPV-infected women compared to non-infected women (P=0.0649). In contrast, HPV decreased the PD-1 protein levels in CIN III (P=0.0148), even though the protein levels remained significantly increased compared to the uninjured adjacent area, indicating that the HPV infection is associated with the cervical transformation (Martins et al., 2014). Noteworthy, the -606G>A variation site did not influence cervical PD-1 protein levels in adjacent uninjured tissue indicating that, besides the genetic background, local microenvironment factors such as local inflammation may have a role

The functional implication of the *PDCD1* -606G>A polymorphism on the magnitude of PD-1 production has been attributed to the target site of the ubiquitin-converting enzyme 2 (UCE-2) transcription regulator (GGCCG in position -610 to -606). The -606G allele was associated with higher relative expression of *PDCD1* mRNA in peripheral blood mononuclear cells of Japanese and Filipino patients exhibiting subacute sclerosing panencephalitis due to measles infection (Ishizaki et al., 2010), and with lower survival in patients with non-small cell lung cancer (Sasaki et al., 2014). Additionally, the -606GG genotype was associated with protection against the development

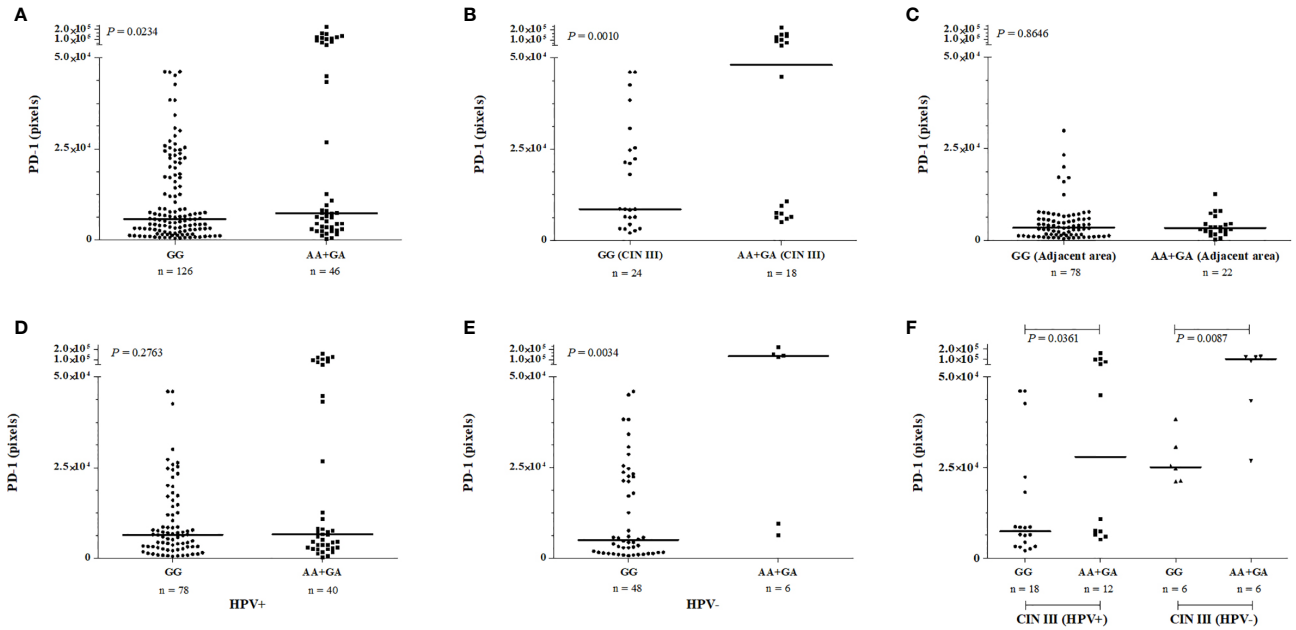

FIGURE 4 | PD-1 levels in cervical mucosa of samples obtained from patients exhibiting cervical lesions, stratified according to the severity of the lesion, presence or absence of HPV infection and according to the *PDCD1* -606G>A (rs36084323) polymorphism. The immunohistochemistry data were analyzed by two pathologists independently, and the intensity of labeling was quantified in three fields per slide. Data were presented as medians. The median differences were calculated using the Mann-Whitney test. **(A)** PD-1 protein levels were increased cervical mucosa of women encompassing the -606AA and -606GA genotypes when compared to the -606GG genotype, the difference is high among severe CIN III injury **(B)**, but not in the uninjured adjacent tissue **(C)**. In the presence of HPV infection **(D)**, the high PD-1 levels previously associated with the presence of the -606A allele **(E)** was not observed anymore; however, the influence of HPV infection on PD-1 levels continue to be observed for high-grade CIN III lesions even being in less magnitude **(F)**.

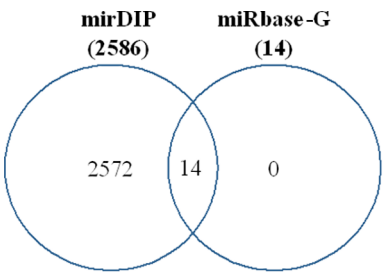

***PDCD1* -606 *G* allele**

miRNA	e-value
has-miR-6771-5p	1.1
has-miR-204-3p	9.1

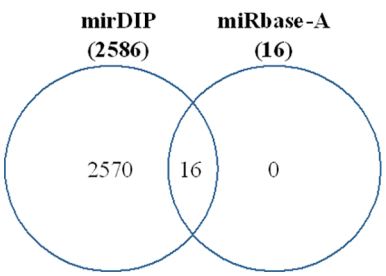

***PDCD1* -606 *A* allele**

miRNA	e-value
has-miR-6798-5p	4.2
has-miR-6775-5p	5.1
has-miR-4776-5p	6.2
has-miR-6771-5p	6.2

FIGURE 5 | Predicted miRNAs that target the *PDCD1* -606G>A (rs36084323) polymorphic site. Binding affinity was evaluated using miRbase and mirDIP software and expressed as e-values, in which high affinity is represented by low e-values and vice-versa.

and progression of breast cancer in women from Northeastern China; however, the A allele and the AA genotype were more frequent in patients exhibiting the p53 protein, a marker of biologically aggressive breast cancer (Hua et al., 2011). The *PDCD1* -606AA genotype was also associated with chronic hepatitis B virus (HBV) infection in the Chinese population, a viral infection that may progress to hepatocarcinoma (Hou et al., 2017). Altogether, these studies indicate a differential role of the *PDCD1* -606G>A polymorphic site according to the major subjacent cancer or viral disorder. In our study, we reported that the *PDCD1* expression and PD-1 protein levels were associated with the -606 A allele, and were modulated by HPV in severe tissue damage, suggesting that other mediators induced during the HPV infection progression may play an additional role.

Among the myriad of transcriptional and post-transcriptional elements that may differentially target gene polymorphic sites, the UCE-2 transcription regulator, which modulates the *PDCD1* -606 G>A polymorphic site (Ishizaki et al., 2010), has not been previously evaluated in the context of the progression of the HPV infection. On the other hand, several miRNAs have been associated with HPV lesion progression (Pardini et al., 2018; Pulati et al., 2019), and little is known regarding miRNA targeting the *PDCD1*-606 G>A region. Considering that virus infection may change the miRNA cell repertoire expression (Park et al., 2017; Chirayil et al., 2018; Del Mar Díaz-González et al., 2019), and that miRNA may also regulate gene expression at the transcriptional level (Lytle et al., 2007; Ørom et al., 2008; Place et al., 2008; Zhang et al., 2014), we conducted a bioinformatics analysis to predict miRNA interaction with the *PDCD1* -606G>A polymorphic site. Three miRNAs were predicted to bind to the mutant A allele: i) the hsa-MiR-6798-5p up-regulates decidual NK cells in recurrent spontaneous abortion (Sfera et al., 2015), ii) the hsa-MiR-6775 is reported to silence the transcription of the alpha 7-cholinergic nicotinic receptor gene (*CHRNA7)* expressed on lymphocyte surface and associated with lymphocyte anergy, T regulatory cell differentiation and immunologic tolerance, which consequently may predispose to cancer development (Li et al., 2018), and iii) the hsa-MiR-4776-5p specifically targets the nuclear factor Kappa B inhibitor beta (NFKBIB) mRNA in Influenza A virus-infected cells, leading to activation of NF-kB, and survival of infected cells (Othumpangat et al., 2017). The hsa-MiR-6771-5p binds to the -606 G alleles with high affinity (e-value = 1.1) and weakly to the mutant *A* allele (e-value = 6.2), and it is involved in ZIKA-associated microcephaly. This miRNA shares the same sequence of the ZIKV genome and human genes associated with microcephaly (McLean et al., 2017). Finally, the hsa-MiR-204-3p targets the wild *PDCD1* -606G allele, and several studies report that this miRNA is a protective factor against cancer development by different cellular mechanisms depending upon the cell origin (Cui et al., 2014; Koga et al., 2018; Li et al., 2019; Xi et al., 2020). Besides targeting the *PDCD1* gene, these miRNAs may also be associated with cell transformation induced by viruses and may share sequences associated with virus infection complications. Therefore, a balance between transcriptional and post-transcription factors together with genetic variability may account for the final result that may halt or permit virus spread and cell transformation.

Concluding, this study showed that PD-1 protein levels are increased in HPV-induced cervical lesions, irrespective of the severity of the injury. In CIN I lesions, the highest PD-1 levels were observed in the inflammatory infiltrating cells of the stroma, whereas in high-grade CIN III lesions, the high PD-1 expression was observed in epithelial cells. In CIN I, the high levels of PD-1 were associated with increased *PDCD1* expression in HPV-infected samples, whereas in CIN III the presence of HPV induced a decrease in *PDCD1* expression and of PD-1 levels in carriers of the -606A allele, suggesting the possible gene regulation by miRNAs. Indeed, we identified some miRNAs specifically targeting the -606A allele region, which may be modulated by the presence of HPV, and may be involved in the progression of the cervical lesion. Future studies are needed to validate the role of these miRNAs in cervical cancer pathogenesis.

DATA AVAILABILITY STATEMENT

The original contributions presented in the study are publicly available in NCBI using accession number PRJNA734653.

ETHICS STATEMENT

The studies involving human participants were reviewed and approved by Ethics Committee of the Aggeu Magalhães Institute (CAAE: 51111115.9.0000.5190). The patients/participants provided their written informed consent to participate in this study.

AUTHOR CONTRIBUTIONS

MS, FM, NL-S, and ED conceived, designed the study, did the formal analysis, and wrote the paper. MS, NS, FG, TG, CP, and MCS conducted the experimental work. LP, MR, MM, and SW followed-up patients and performed cytopathological and coloscopy evaluations. NL-S and ED applied for financial support and managed the project. All authors contributed to the article and approved the submitted version.

FUNDING

This work was supported by grants from i) Brazilian Health Ministry Project DECIT-FINEP, (Grants #1299-13; 401700/2015-1); ii) CAPES (PROCAD grant #88881-068436/2014-09 and Finance code 001); iii) Foundation for Science and Technology of the State of Pernambuco (FACEPE) (Grant #PROEP-APQ16804.01/15 and fellowship #IBPG-0849-4.01/16

to FM); iv) Brazilian National Council for Scientific and Technological Development (CNPq) (grants #310364/2015-9 and #310892/2019-8 to NL-S and #302060/2019.7 to ED). The funders had no role in study design, data collection, and analysis, decision to publish, or preparation of the manuscript.

ACKNOWLEDGMENTS

We thank Viviane Carvalho for invaluable technical assistance and the Program for Technological Development in Tools for Health (PDTIS-FIOCRUZ).

REFERENCES

Ørom, U. A., Nielsen, F. C., and Lund, A. H. (2008). MicroRNA-10a Binds the 5'UTR of Ribosomal Protein mRNAs and Enhances Their Translation. *Mol. Cell* 30 (4), 460–471. doi: 10.1016/j.molcel.2008.05.001

Aggarwal, B. B., Shishodia, S., Sandur, S. K., Pandey, M. K., and Sethi, G. (2006). Inflammation and Cancer: How Hot is the Link? *Biochem. Pharmacol.* 72, 1605–1621. doi: 10.1016/j.bcp.2006.06.029

(2020) *1000 Genomes Project Phase 3 Allele Frequencies rs36084323 Snp*. Available at: http://www.ensembl.org/Homo_sapiens/Variation/Population?db=core;v=rs36084323;vdb=variation (Accessed in April 15, 2020).

Auton, A., Abecasis, G. R., Altshuler, D. M., Durbin, R. M., Bentley, D. R., Chakravarti, A., et al. (2015). A Global Reference for Human Genetic Variation. *Nature* 526, 68–74. doi: 10.1038/nature15393

Boussiotis, V. A. (2016). Molecular and Biochemical Aspects of the PD-1 Checkpoint Pathway. *N Engl. J. Med.* 375, 1767–1778. doi: 10.1056/NEJMra1514296

Chang, H., Hong, J. H., Lee, J. K., Cho, H. W., Ouh, Y. T., Min, K. J., et al. (2018). Programmed Death-1 (PD-1) Expression in Cervical Intraepithelial Neoplasia and its Relationship With Recurrence After Conization. *J. Gynecol. Oncol.* 29, 1–14. doi: 10.3802/jgo.2018.29.e27

Chirayil, R., Kincaid, R. P., Dahlke, C., Kuny, C. V., Dalken, N., Spohn, M., et al. (2018). Identification of Virus-Encoded microRNAs in Divergent Papillomaviruses. *PloS Pathog.* 14 (7), e1007156. doi: 10.1371/journal.ppat.1007156

Cui, Z. H., Shen, S. Q., Chen, Z. B., and Hu, C. (2014). Growth Inhibition of Hepatocellular Carcinoma Tumor Endothelial Cells by miR-204-3p and Underlying Mechanism. *World J. Gastroenterol.* 20 (18), 5493–5504. doi: 10.3748/wjg.v20.i18.5493

Del Mar Díaz-González, S., Rodríguez-Aguilar, E. D., Meneses-Acosta, A., Valadez-Graham, V., Deas, J., Gómez-Cerón, C., et al. (2019). Transregulation of microRNA miR-21 Promoter by AP-1 Transcription Factor in Cervical Cancer Cells. *Cancer Cell Int.* 19, 214. doi: 10.1186/s12935-019-0931-x

De Oliveira, C. M., Fregnani, J. H. T. G., and Villa, L. L. (2019). Hpv Vaccine: Updates and Highlights. *Acta Cytol.* 63, 159–168. doi: 10.1159/000497617

Grivennikov, S. I., Greten, F. R., and Karin, M. (2010). Immunity, Inflammation, and Cancer. *Cell* 140, 883–899. doi: 10.1016/j.cell.2010.01.025

Hemmat, N., and Bannazadeh Baghi, H. (2019). Association of Human Papillomavirus Infection and Inflammation in Cervical Cancer. *Pathog. Dis.* 77, ftz048. doi: 10.1093/femspd/ftz048

Hollander, P., Amini, R. M., Ginman, B., Molin, D., Enblad, G., and Glimelius, I. (2018). Expression of PD-1 and PD-L1 Increase in Consecutive Biopsies in Patients With Classical Hodgkin Lymphoma. *PloS One* 13, 1–16. doi: 10.1371/journal.pone.0204870

Hou, Z., Zhou, Q., Lu, M., Tan, D., and Xu, X. (2017). A Programmed Cell Death-1 Haplotype is Associated With Clearance of Hepatitis B Virus. *Ann. Clin. Lab. Sci.* 47, 334–343.

Hua, Z., Li, D., Xiang, G., Xu, F., Jie, G., Fu, Z., et al. (2011). PD-1 Polymorphisms are Associated With Sporadic Breast Cancer in Chinese Han Population of Northeast China. *Breast Cancer Res. Treat* 129, 195–201. doi: 10.1007/s10549-011-1440-3

Ishida, Y., Agata, Y., Shibahara, K., and Honjo, T. (1992). Induced Expression of PD-1, a Novel Member of the Immunoglobulin Gene Superfamily, Upon Programmed Cell Death. *EMBO J.* 11, 3887–3895. doi: 10.1002/j.1460-2075.1992.tb05481.x

Ishizaki, Y., Yukaya, N., Kusuhara, K., Kira, R., Torisu, H., Ihara, K., et al. (2010). PD1 as a Common Candidate Susceptibility Gene of Subacute Sclerosing Panencephalitis. *Hum. Genet.* 127, 411–419. doi: 10.1007/s00439-009-0781-z

Jiang, C., Cao, S. R., Li, N., Jiang, L., and Sun, T. (2019). PD-1 and PD-L1 Correlated Gene Expression Profiles and Their Association With Clinical Outcomes of Breast Cancer. *Cancer Cell Int.* 19, 1–9. doi: 10.1186/s12935-019-0955-2

Kawahara, T., Ishiguro, Y., Ohtake, S., Kato, I., Ito, Y., Ito, H., et al. (2018). PD-1 and PD-L1 are More Highly Expressed in High-Grade Bladder Cancer Than in Low-Grade Cases: PD-L1 Might Function as a Mediator of Stage Progression in Bladder Cancer 11 Medical and Health Sciences 1112 Oncology and Carcinogenesis. *BMC Urol.* 18, 1–6. doi: 10.1186/s12894-018-0414-8

Keir, M. E., Butte, M. J., Freeman, G. J., and Sharpe, A. H. (2008). PD-1 and Its Ligands in Tolerance and Immunity. *Annu. Rev. Immunol.* 26, 677–704. doi: 10.1146/annurev.immunol.26.021607.090331

Koga, T., Migita, K., Sato, T., Sato, S., Umeda, M., Nonaka, F., et al. (2018). MicroRNA-204-3p Inhibits Lipopolysaccharide-Induced Cytokines in Familial Mediterranean Fever Via the Phosphoinositide 3-Kinase γ Pathway. *Rheumatol. (Oxford).* 57 (4), 718–726. doi: 10.1093/rheumatology/kex451

Kozomara, A., Birgaoanu, M., and Griffiths-Jones, S. (2019). Mirbase: From microRNA Sequences to Function. *Nucleic Acids Res.* 47, D155–D162. doi: 10.1093/nar/gky1141

Lewinsky, H., Barak, A. F., Huber, V., Kramer, M. P., Radomir, L., Sever, L., et al. (2018). CD84 Regulates PD-1/PD-L1 Expression and Function in Chronic Lymphocytic Leukemia. *J. Clin. Invest.* 128, 5479–5488. doi: 10.1172/JCI96610

Li, D., Li, J., Jia, B., Wang, Y., Zhang, J., and Liu, G. (2018). Genome-Wide Identification of microRNAs in Decidual Natural Killer Cells From Patients With Unexplained Recurrent Spontaneous Abortion. *Am. J. Reprod. Immunol.* 80, e13052. doi: 10.1111/aji.13052

Li, X., Zhong, W., Xu, Y., Yu, B., and Liu, H. (2019). Silencing of Lncrna LINC00514 Inhibits the Malignant Behaviors of Papillary Thyroid Cancer Through miR-204-3p/CDC23 Axis. *Biochem. Biophys. Res. Commun.* 508 (4), 1145–1148. doi: 10.1016/j.bbrc.2018.12.051

Lytle, J. R., Yario, T. A., and Steitz, J. A. (2007). Target mRNAs are Repressed as Efficiently by microRNA-binding Sites in the 5' UTR as in the 3' Utr. *Proc. Natl. Acad. Sci. U. S. A.* 104 (23), 9667–9672. doi: 10.1073/pnas.0703820104

Manos, M., Ting, Y., Wright, D., Lewis, A., Broker, T., and Wolinsky, S. (1989). Use of Polymerase Chain Reaction Amplification for the Detection of Genital Human Papillomaviruses. *Cancer Cells: Mol. Diag. of Human Cancer* 7, 209–214.

Marinelli, O., Annibali, D., Aguzzi, C., Tuyaerts, S., Amant, F., Morelli, M. B., et al. (2019). The Controversial Role of PD-1 and Its Ligands in Gynecological Malignancies. *Front. Oncol.* 9:1073. doi: 10.3389/fonc.2019.01073

Martins, A. E. S., Lucena-Silva, N., Garcia, R. G., Welkovic, S., Barbosa, A., Menezes, M. L. B., et al. (2014). Prognostic Evaluation of DNA Index in HIV-HPV Co-Infected Women Cervical Samples Attending in Reference Centers for HIV-AIDS in Recife. *PloS One* 9, 1–8. doi: 10.1371/journal.pone.0104801

McLean, E., Bhattarai, R., Hughes, B. W., Mahalingam, K., and Bagasra, O. (2017). Computational Identification of Mutually Homologous Zika Virus miRNAs That Target Microcephaly Genes. *Libyan. J. Med.* 12:1. doi: 10.1080/19932820.2017.1304505

Medeiros, F. S., Martins, A. E. S., Gomes, R. G., De Oliveira, S. A. V., Welkovic, S., Maruza, M., et al. (2018). Variation Sites At the HLA-G 3' Untranslated Region Confer Differential Susceptibility to HIV/HPV Co-Infection and Aneuploidy in Cervical Cell. *PloS One* 13, 1–14. doi: 10.1371/journal.pone.0204679

Muenst, S., Läubli, H., Soysal, S. D., Zippelius, A., Tzankov, A., and Hoeller, S. (2016). The Immune System and Cancer Evasion Strategies: Therapeutic Concepts. *J. Intern. Med.* 279, 541–562. doi: 10.1111/joim.12470

Othumpangat, S., Bryan, N. B., Beezhold, D. H., and Noti, J. D. (2017). Upregulation of miRNA-4776 in Influenza Virus Infected Bronchial Epithelial Cells Is Associated With Downregulation of NFKBIB and Increased Viral Survival. *Viruses* 9:94. doi: 10.3390/v9050094

Pardini, B., De Maria, D., Francavilla, A., Di Gaetano, C., Ronco, G., and Naccarati, A. (2018). MicroRNAs as Markers of Progression in Cervical Cancer: A Systematic Review. *BMC Cancer.* 18 (1), 696. doi: 10.1186/s12885-018-4590-4

Park, S., Eom, K., Kim, J., Bang, H., Wang, H., Ahn, S., et al. (2017). MiR-9, miR-21, and miR-155 as Potential Biomarkers for HPV Positive and Negative Cervical Cancer. *BMC Cancer* 17 (1), 658. doi: 10.1186/s12885-017-3642-5

Place, R. F., Li, L. C., Pookot, D., Noonan, E. J., and Dahiya, R. (2008). MicroRNA-373 Induces Expression of Genes With Complementary Promoter Sequences. *Proc. Natl. Acad. Sci. U. S. A.* 105 (5), 1608–1613. doi: 10.1073/pnas.0707594105

Pulati, N., Zhang, Z., Gulimilamu, A., Qi, X., and Yang, J. (2019). Hpv16(+) -miRNAs in Cervical Cancer and the Anti-Tumor Role Played by Mir-5701. *J. Gene Med.* 21 (11), e3126. doi: 10.1002/jgm.3126

Salmaninejad, A., Khoramshahi, V., Azani, A., Soltaninejad, E., Aslani, S., Zamani, M. R., et al. (2018). PD-1 and Cancer: Molecular Mechanisms and Polymorphisms. *Immunogenetics* 70, 73–86. doi: 10.1007/s00251-017-1015-5

Sasaki, H., Tatemaysu, T., Okuda, K., Moriyama, S., Yano, M., and Fujii, Y. (2014). PD-1 Gene Promoter Polymorphisms Correlate With a Poor Prognosis in non-Small Cell Lung Cancer. *Mol. Clin. Oncol.* 2, 1035–1042. doi: 10.3892/mco.2014.358

Senba, M., and Mori, N. (2012). Mechanisms of Virus Immune Evasion Lead to Development From Chronic Inflammation to Cancer Formation Associated With Human Papillomavirus Infection. *Oncol. Rev.* 6, 135–144. doi: 10.4081/oncol.2012.e17

Sfera, A., Cummings, M., and Osorio, C. (2015). Non-Neuronal Acetylcholine: The Missing Link Between Sepsis, Cancer, and Delirium? *Front. Med.* 2:56. doi: 10.3389/fmed.2015.00056

Shinohara, T., Tanowaki, M., Ishida, Y., Kawaichi, M., and Honjo, T. (1994). Structure and Chromosomal Localization of the Human Pd-1 Gene (Pdcd1). *Genomics* 23, 704–706. doi: 10.1006/geno.1994.1562

Tamura, K., Peterson, D., Peterson, N., Stecher, G., Nei, M., and Kumar, S. (2011). Mega5: Molecular Evolutionary Genetics Analysis Using Maximum Likelihood, Evolutionary Distance, and Maximum Parsimony Methods. *Mol. Biol. Evol.* 28, 2731–2739. doi: 10.1093/molbev/msr121

Tao, L. H., Zhou, X. R., Li, F. C., Chen, Q., Meng, F. Y., Mao, Y., et al. (2017). A Polymorphism in the Promoter Region of PD-L1 Serves as a Binding-Site for SP1 and is Associated With PD-L1 Overexpression and Increased Occurrence of Gastric Cancer. *Cancer Immunol. Immunother.* 66, 309–318. doi: 10.1007/s00262-016-1936-0

The 1000 Genomes Project Consortium. (2015). A global reference for human genetic variation. *Nature* 526, 68–74. doi: 10.1038/nature15393

Tokar, T., Pastrello, C., Rossos, A. E. M., Abovsky, M., Hauschild, A. C., Tsay, M., et al. (2018). MirDIP 4.1 - Integrative Database of Human microRNA Target Predictions. *Nucleic Acids Res.* 46, D360–D370. doi: 10.1093/nar/gkx1144

Wang, Y., Wang, H., Yao, H., Li, C., Fang, J. Y., and Xu, J. (2018). Regulation of PD-L1: Emerging Routes for Targeting Tumor Immune Evasion. *Front. Pharmacol.* 9:536. doi: 10.3389/fphar.2018.00536

Wieser, V., Gaugg, I., Fleischer, M., Shivalingaiah, G., Sprung, S., Lax, S. F., et al. (2018). BRCA1/2 and TP53 Mutation Status Associates With PD-1 and PD-L1 Expression in Ovarian Cancer. *OncoTargets* 9, 17501–17511. doi: 10.18632/oncotarget.24770

World Health Organization (2017). Human papillomavirus Vaccines: WHO Position Paper, May 2017-Recommendations. *Vaccine* 43, 5753–5755. doi: 10.1016/j.vaccine.2017.05.069

Xi, X., Teng, M., Zhang, L., Xia, L., Chen, J., and Cui, Z. (2020). MicroRNA-204-3p Represses Colon Cancer Cells Proliferation, Migration, and Invasion by Targeting HMGA2. *J. Cell Physiol.* 235 (2), 1330–1338. doi: 10.1002/jcp.29050

Yang, W., Lu, Y. P., Yang, Y. Z., Kang, J. R., Jin, Y. D., and Wang, H. W. (2017). Expressions of Programmed Death (PD)-1 and PD-1 Ligand (PD-L1) in Cervical Intraepithelial Neoplasia and Cervical Squamous Cell Carcinomas are of Prognostic Value and Associated With Human Papillomavirus Status. *J. Obstet. Gynaecol. Res.* 43, 1602–1612. doi: 10.1111/jog.13411

Yang, W., Song, Y., Lu, Y. L., Sun, J. Z., and Wang, H. W. (2013). Increased Expression of Programmed Death (PD)-1 and its Ligand PD-L1 Correlates With Impaired Cell-Mediated Immunity in High-Risk Human Papillomavirus-Related Cervical Intraepithelial Neoplasia. *Immunology* 139, 513–522. doi: 10.1111/imm.12101

Zhang, Y., Fan, M., Zhang, X., Huang, F., Wu, K., Zhang, J., et al. (2014). Cellular microRNAs Up-Regulate Transcription Via Interaction With Promoter TATA-box Motifs. *RNA* 20 (12), 1878–1889. doi: 10.1261/rna.045633.114

Conflict of Interest: The authors declare that the research was conducted in the absence of any commercial or financial relationships that could be construed as a potential conflict of interest.

Advantages of publishing in Frontiers

OPEN ACCESS
Articles are free to read for greatest visibility and readership

FAST PUBLICATION
Around 90 days from submission to decision

HIGH QUALITY PEER-REVIEW
Rigorous, collaborative, and constructive peer-review

TRANSPARENT PEER-REVIEW
Editors and reviewers acknowledged by name on published articles

Frontiers
Avenue du Tribunal-Fédéral 34
1005 Lausanne | Switzerland

Visit us: www.frontiersin.org
Contact us: frontiersin.org/about/contact

REPRODUCIBILITY OF RESEARCH
Support open data and methods to enhance research reproducibility

DIGITAL PUBLISHING
Articles designed for optimal readership across devices

FOLLOW US
@frontiersin

IMPACT METRICS
Advanced article metrics track visibility across digital media

EXTENSIVE PROMOTION
Marketing and promotion of impactful research

LOOP RESEARCH NETWORK
Our network increases your article's readership